Vitamin D and the Molecular Pathogenesis of Non-alcoholic Fatty Liver Disease

Zixuan Zhang

Submitted in accordance with the requirements for the degree of Doctor of Philosophy

The University of Leeds
Faculty of Environment
School of Food Science and Nutrition

March, 2022

Supervised by Dr J. Bernadette Moore and Dr James L. Thorne

School of Food Science and Nutrition, Faculty of Environment,

University of Leeds, Leeds

Declaration:

The candidate confirms that the work submitted is his/her own and that appropriate credit has been given where reference has been made to the work of others.

Acknowledgements

First and foremost, I would like to express my sincere gratitude to my supervisor, Dr J. Bernadette Moore, for allowing me to carry out this PhD. Your excitement and passion for science are inspiring, and I thank you for all of your patience, encouragement and guidance throughout the years. My sincere thanks also to my co-supervisor, Dr James L. Thorne, for all his enthusiasm, support, and intellectual discussions.

I would like to give a special thanks to Dr Sarah Lewis and her team members, Dr Kimberley Burrows and Dr Kushala Abeysekera, from the University of Bristol for providing me with a chance to visit their university and obtain the expertise to perform Mendelian randomisation using the genetic data of the UK Biobank. I would also gratefully acknowledge discussions and professional technical support from Dr Michael Zulyniak and his PhD student Harriett Fuller on the Mendelian randomisation chapter.

I would like to thank all the current and past members of the 2.36 PhD cluster, of the School of Food Science and Nutrition at Parkinson, for making this time such an enjoyable experience to share our life and lab work. A special thank you to Yue Liu, Hang Wu, Dr Lei Xia, Dr Zexi Xu and Dr Priscilia Lianto for being my #1 buddies during my PhD period. I will miss the times of us hanging out and travelling together. As well as my other group members, Alex Websdale, Chrysa Soteriou, Xiaomian Tan and Xiaoying Tian; I'd also like to acknowledge the many BSc and MSc students I have supervised and interacted with, particularly Paula Wasiolek and Rachel Moon, who made contributions to early experiments related to my microRNA work. Also, many thanks to Dr Samantha Hutchinson, Dr Jo Sier and Dr Giorgia Cioccoloni for their support and discussion of lab matters.

Finally, I would like to give a special thanks to my dear mother for being my most critical mental and financial supporter. Last but certainly not least, thanks to my family and friends for sending their love, encouragement and support from overseas.

List of Abbreviations

Abbreviation	Definition
1α,25(OH)2D	1α,25-dihydroxyvitamin D
25(OH)D	25-hydroxyvitamin D
AAP	American Academy of Paediatrics
AASLD	American Association for the Study of Liver Diseases
Ago	Argonaute
ALP	alkaline phosphatase
ALT	alanine aminotransferase
AMDHD1	amidohydrolase domain containing 1
AMPK	AMP-activated protein kinase
AST	aspartate aminotransferase
AUROC	area under the receiver operating characteristic
BCA	bicinchoninic acid
BIC	B-cell integration cluster
BMI	body mass index
BSA	bovine serum albumin
CCl4	carbon tetrachloride
CDS	coding sequence
ChIP	chromatin immunoprecipitation
ChREBP	carbohydrate-responsive element-binding protein
CI	confidence intervals
CK-18	cytokeratin-18
CSM	charcoal-stripped FBS contained medium
Ct	threshold cycle
CV	coefficient of variance
CVD	cardiovascular disease
CYP	cytochrome P450
DAVID	database for annotation, visualization and integrated discovery
ddH_2O	double-distilled water
DEPC	Diethyl pyrocarbonate
DHCR7	dehydrocholesterol reductase-7
DGCR8	DiGeorge syndrome critical region 8
DMEM	Dulbecco's modified Eagle's medium
DMSO	dimethyl sulfoxide
DNL	*de novo* lipogenesis
DPB	vitamin D binding protein
EAF	effect allele frequency
ECM	extracellular matrix
EFSA	European Food Safety Authority
EGF	epidermal growth factor
EMT	epithelial-mesenchymal transition

ER	endoplasmic reticulum
EWAS	exome-wide association study
FA	fatty acid
FAF	fatty-acid free
FAS	fatty acid synthase
FBS	fetal bovine serum
FFA	free fatty acid
FGF2	fibroblast growth factor 2
FIB-4	Fibrosis-4
FLI	fatty liver index
FOXO1	forkhead box protein O1
FXR	farnesoid X receptor
γ-GGT	γ-glutamyl transpeptidase
GC	group-specific component
GCKR	glucokinase regulator
GO	Gene Ontology
GSEA	gene set enrichment analysis
GSK3	glycogen synthase kinase 3
GWAS	genome-wide association study
HbA1C	haemoglobin A1C
HC	healthy control
HCC	hepatocellular carcinoma
HCV	hepatitis C virus
HDAC	histone deacetylation catalyzed by histone deacetylase
HDL-C	high-density lipoprotein cholesterol
HFD	high-fat diet
HMGCR	3-hydroxy-3-methylglutaryl-coenzyme A reductase
HNF4-α	hepatocyte nuclear factor 4 α
HOMA-IR	homeostasis model assessment of insulin resistance
hs-CRP	high sensitive C-reactive protein
HSC	hepatic stellate cell
HSD17B13	17-beta hydroxysteroid dehydrogenase 13
ICD-10	International Classification of Disease version 10
IGF-1	insulin-like growth factor 1
IGFBP-2	insulin-like growth factor-binding protein 2
IKKβ	IkappaB kinase
IL	interleukin
IOM	Institute of Medicine
IQR	interquartile range
IR	insulin resistance
IRR	insulin receptor-related receptor
IRS	insulin receptor substrate
IV	Instrumental Variables
IVW	inverse variance weighted

KEGG	Kyoto Encyclopedia of Genes and Genomes
KL	klotho
LD	linkage disequilibrium
LDL-C	low-density lipoprotein cholesterol
LPI	lysophosphatidylinositol
LXR	liver X receptor
M1	Model 1
M2	Model 2
MAFLD	metabolic associated fatty liver disease
MAPK	mitogen-activated protein kinase
MBOAT7	membrane bond O-acetyltransferase domain containing 7
MeSH	Medical Subject Headings
MetS	metabolic syndrome
MIRHG155	MIR155 host gene
miRNA	microRNA
MR	Mendelian randomisation
mTOR	mammalian target of rapamycin
MTT	3-(4,5-dimethylthiazol-2-yl)-2,5-diphenyltetrazolium bromide
NADSYN1	nicotinamide adenine dinucleotide synthetase-1
NAFL	non-alcoholic fatty liver
NAFLD	non-alcoholic fatty liver disease
NASH	non-alcoholic steatohepatitis
NEAA	non-essential amino acids
NF-κB	nuclear transcription factor-κ B
NFS	NAFLD fibrosis score
NFW	nuclease-free water
NGS	next-generation sequencing
NOAMP	no amplification
OA	oleic acid
OD	optical density
OR	odds ratio
PA	palmitate acid
PBC	primary biliary cholangitis
PBS	phosphate-buffered saline
PDGF α	platelet-derived growth factor α
PDK1	phosphoinositide-dependent protein kinase 1
PGC1-α	PPAR-gamma coactivator 1-α
PI	phosphatidylinositol
PI3K-AKT	phosphatidylinositol 3-kinase-protein kinase B
PIP2	phosphatidylinositol-4,5-bisphosphate
PIP3	phosphatidylinositol-3,4,5-trisphosphate
PNPLA3	patatin-like phospholipase domain-containing protein 3
Pol II	polymerase II

PPAR	peroxisome proliferative active receptor
pri-miRNA	primary miRNA
qPCR	quantitative reverse transcription-polymerase chain reaction
RCT	randomized controlled trial
REC	Research Ethics Committee
RIPA	radio immunoprecipitation assay
RISC	RNA induced silencing complex
RNAseq	RNA sequencing
RXR-α	retinoid X receptor-α
SACN	Scientific Advisory Committee on Nutrition
SAHM	Society for Adolescent Health and Medicine
SCM	serum contained medium
SD	standard deviation
SE	standard error
SEC23A	coat protein complex II component
SEM	standard error of the mean
SFM	serum free medium
SIRT	silent information regulator 2 protein
SLE	systemic lupus erythematosus
SMAD7	mothers against decapentaplegic homolog
SNP	single nucleotide polymorphism
SOCS1	suppressors of cytokine signalling 1
SREBP-1	sterol regulatory element-binding protein 1
STB	syncytiotrophoblast
SV40T	Simian Vacuolating Virus 40 transforming
T2D	type 2 diabetes
TarPmiR	Target Prediction for miRNAs
TE	transient elastography
TG	triglyceride
TGF-β1	transforming growth factor β1
TLDA	TaqMan low-density array
TM6SF2	transmembrane 6 superfamily member 2
TMC4	transmembrane channel-like 4
TNF-α	tumour necrosis factor-α
TRBP	transactivation response element RNA-binding protein
Trypsin-EDTA	Trypsin-ethylenediaminetetraacetic acid
UK	United Kingdom
US	United States
UTR	untranslated region
VLDL	very low-density lipoprotein
WHR	waist-to-hip ratio

Abstract

Evidence from preclinical and clinical studies for the role of vitamin D in non-alcoholic fatty liver disease (NAFLD) pathogenesis is conflicting. Although microRNAs (miRNAs) are critical to the molecular pathogenesis of NAFLD and the cellular response to vitamin D, the role of vitamin D-regulated miRNAs in NAFLD pathogenesis has been relatively unexplored. This project aimed to investigate miRNAs modulated by vitamin D that might contribute to NAFLD progression. In addition to *in vitro* experiments, a two-sample bidirectional Mendelian randomisation (MR) analysis was conducted to determine whether circulating 25-hydroxyvitamin D [25(OH)D] status could be associated with NAFLD.

First, a comprehensive literature review identified six miRNAs (miR-21, miR-30, miR-34, miR-122, miR-146 and miR-200) dysregulated in multiple independent human NAFLD studies. Focusing on miRNAs found dysregulated in more than one vitamin D and NAFLD-related human study, five miRNAs were identified (miR-27, miR-125, miR-146, miR-155 and miR-188). Secondly, the response of immortalised human hepatocytes (HepG2) and hepatic stellate cells (HSCs; LX-2) to fatty acid (FA) and vitamin D [1α,25$(OH)_2$D] treatments was characterised by examining cell viability, intracellular lipid accumulation, vitamin D receptor (VDR) and cytochrome P450 24A1 (CYP24A1) mRNA and protein expression. These *in vitro* cellular models were then used to examine miRNA expression by TaqMan low-density array (TLDA) and bioinformatic analyses. After integrating the bioinformatic data with literature evidence, a subset of candidate miRNAs were followed up for independent verification. However, results were inconclusive, likely because of insufficient miRNA quality. Finally, a two-sample bidirectional MR study indicated no causal relationship between serum 25(OH)D status and NAFLD risk and vice versa.

In conclusion, the modulation of miRNAs by vitamin D in the molecular progression of NAFLD has been understudied. As the TLDA approach has limitations, future work should investigate miRNAs involved in vitamin D metabolism and NAFLD progression using next-generation sequencing (NGS).

Table of Contents

List of Tables

List of Figures

Chapter 1 Overview

1.1 Rationale

Evidence for a role for vitamin D in NALFD pathogenesis is conflicting (Zhang et al., 2019c; Barchetta et al., 2020). Previous work from our group showed low dietary vitamin D intakes and poor vitamin D status in children with NAFLD in the UK (Gibson et al., 2015) and that genetic polymorphisms in the vitamin D metabolic pathway were associated with histological severity in a relatively small cohort (n=103) of children with NAFLD (Gibson et al., 2018). However, preliminary experiments investigating the response to vitamin D treatment at the cellular and RNA levels in immortalised human hepatocytes (HepG2) and HSCs (LX-2) were inconclusive.

The molecular pathogenesis of NAFLD is complex, involving numerous signalling molecules involved in hepatic metabolism, oxidative, inflammatory and fibrotic processes (Moore, 2019a). Furthermore, these include miRNAs that play an essential role in gene expression and regulatory networks involved in lipid and carbohydrate metabolism and cellular stress response pathways (Gjorgjieva et al., 2019a). Dysregulation of miRNA expression is associated with hepatic inflammation, fibrosis, and hepatocellular carcinoma (HCC) (Wang et al., 2020c; Oura et al., 2020). Although miRNAs are also critical to the cellular response to vitamin D, mediating regulation of the VDR and vitamin D's anticancer effects (Zeljic et al., 2017), a role for vitamin D regulated miRNAs in NAFLD pathogenesis has been relatively unexplored.

In addition to exploring the role of vitamin D in NAFLD progression at the molecular level, it is also essential to investigate how genetic polymorphisms may influence the association between vitamin D and NAFLD. MR is an epidemiological approach that uses genetic information as instrumental variables (IVs) to probe the causal relationship between exposure and outcome in an observational setting (Smith and Ebrahim, 2003). MR avoids many limitations of conventional epidemiological studies such as residual confounding and reverse causation, as the populations under investigation are randomised from birth based on their genotype (Sekula et al., 2016).

Although two MR studies to date have explored the causal inference between vitamin D and NAFLD (Wang et al., 2018c; Yuan and Larsson, 2022), these had inconsistent results.

1.2 Overall aim and hypotheses

This project aimed to investigate miRNAs modulated by vitamin D that might contribute to NAFLD progression. In addition to *in vitro* experiments, a two-sample bidirectional MR analysis was conducted to determine whether circulating 25(OH)D status could be associated casually with NAFLD.

The hypotheses tested in this project were: 1) that vitamin D and its regulated miRNAs contribute to NAFLD disease progression at molecular level; and 2). individuals randomly assigned at conception to have lower levels of circulating 25(OH)D levels have a greater likelihood of developing NAFLD.

1.3 Specific objectives

- Critically assess the literature evidence for a potential subset of miRNAs that are both dysregulated in NAFLD and modulated by vitamin D in humans **(Chapter 3)**
- Characterise a lipid loading model in both immortalised human hepatocytes (HepG2) and HSCs (LX-2) to investigate the responses of $1\alpha,25(OH)_2D_3$ treatment **(Chapter 4)**
- Describe the miRNA response in immortalised human hepatocytes and HSCs to vitamin D and/or lipid loading **(Chapter 5)**
- Investigate the causal association between NAFLD and vitamin D in UK Biobank (UKBB) participants utilising a two-sample bidirectional MR study approach (**Chapter 6)**

1.4 Scientific contributions from this PhD

1.4.1 List of abstracts

1. **Zhang, Z.**, Moon, R., Fuller, H., Tan, X., Holmes, M. J., Thorne, J. L., & Moore, J. B. (2021). Characterisation of microRNAs regulated by vitamin D and lipid loading in immortalised hepatic stellate cells. *Proceedings of the Nutrition Society*, *80*(OCE5).

2. **Zhang, Z.**, Moon, R., Fuller, H., Tan, X., Holmes, M. J., Thorne, J. L., & Moore, J. B. (2021). Characterisation of microRNAs regulated by vitamin D and lipid loading in immortalised hepatocytes. *Proceedings of the Nutrition Society*, *80*(OCE2).
3. **Zhang, Z.**, Thorne, J. L., & Moore, J. B. (2020). Serum Choice Influences Lipid Accumulation and Cell Viability in Fatty Acid Treated Immortalised Hepatocytes and Hepatic Stellate Cells. *Proceedings of the Nutrition Society*, *79*(OCE3).
4. **Zhang, Z.**, Thorne, J. L., & Moore, J. B. (2020). Differential Effects of Lipid and Vitamin D treatment on Cell Viability and CYP24A1 Expression in Hepatocytes and Hepatic Stellate Cells. *Proceedings of the Nutrition Society*, *79*(OCE2).

1.4.2 Published peer-reviewed journal articles

1. **Zhang, Z.**, Moon, R., Thorne, J. L., & Moore, J. B. (2021) NAFLD and Vitamin D: Evidence for Intersection of MicroRNA Regulated Pathways. *Nutrition Research Reviews*, 1-52 early online publication.
2. **Zhang, Z.**, Thorne, J. L., & Moore, J. B. (2019). Vitamin D and nonalcoholic fatty liver disease. *Current Opinion in Clinical Nutrition & Metabolic Care*, *22*(6), 449-458.

1.4.3 Supervision of BSc/MSc student projects

1. Role of vitamin D in non-alcoholic fatty liver disease: PCR assay optimisation for characterisation of vitamin D regulated miRNAs expression in hepatic stellate cells (Paula Wasiolek, MSc 2018)
2. Immunoblotting optimisation to measure VDR and CYP24A1 protein expression in immortalised human liver cells (Zhou Wang, BSc 2019)
3. Role of vitamin D in non-alcoholic fatty liver disease: assessment of expression of VDR and CYP24A1 in hepatocytes, in vitro (Utkarshini Nitin Kirtikar, MSc 2019)
4. miRNA expression on vitamin D treated HepG2 and LX2 cells (Ziyuan Wang, MSc 2019)
5. A bioinformatic analysis of microRNA regulation in NALFD and the effect of vitamin D (Rachel Moon, MSci 2021)

Chapter 2 Introduction

2.1 Non-alcoholic fatty liver disease (NALFD)

Rising in parallel with obesity, the dramatic escalation in the prevalence of NAFLD has attracted worldwide attention in the past two decades. NAFLD is now the most common chronic liver disease worldwide, affecting an estimated 25% of the global population and generating remarkable clinical, economic, and societal burdens (Younossi et al., 2018; Younossi et al., 2016). In addition to conferring risk of end stage liver disease, NAFLD is an independent risk factor for type 2 diabetes (T2D) and cardiovascular disease (CVD) (Targher et al., 2020). Given it's close interrelationship with metabolic diseases, a consensus-led expert group has recently proposed NAFLD be re-named as metabolic associated fatty liver disease (MAFLD) (Eslam et al., 2020a; Eslam et al., 2020b). However, at the time of writing, this terminology has not yet been adopted into the International Classification of Diseases (ICD) diagnostic codes, therefore I will use the nomenclature of NAFLD throughout this thesis.

2.1.1 Pathogenesis of NAFLD

Defined physiologically by the excess accumulation of lipids in the liver without excessive alcohol consumption, NAFLD encompasses a broad spectrum of liver conditions. These range from simple steatosis, also known as non-alcoholic fatty liver (NAFL), to non-alcoholic steatohepatitis (NASH), fibrosis, cirrhosis, and even HCC (Moore, 2019a) (**Figure 2.1**). NAFL is defined by the presence of intracellular lipid accumulation in greater than 5% of hepatocytes, with no evidence of hepatocyte injury (Reeder and Sirlin, 2010). Whereas, NASH is defined histologically as the presence of hepatocyte steatosis with accompanying evidence of lobular and portal inflammatory and injury (ballooning), with or without fibrosis (Brown and Kleiner, 2016).

Although clinicopathological records of the fatty liver related to physical inactivity and overnutrition can be dated back to the 1800s (Budd, 1853; Ayonrinde, 2021), the pathogenesis has been only been broadly investigated in the last two decades. The mechanisms underlying the development and

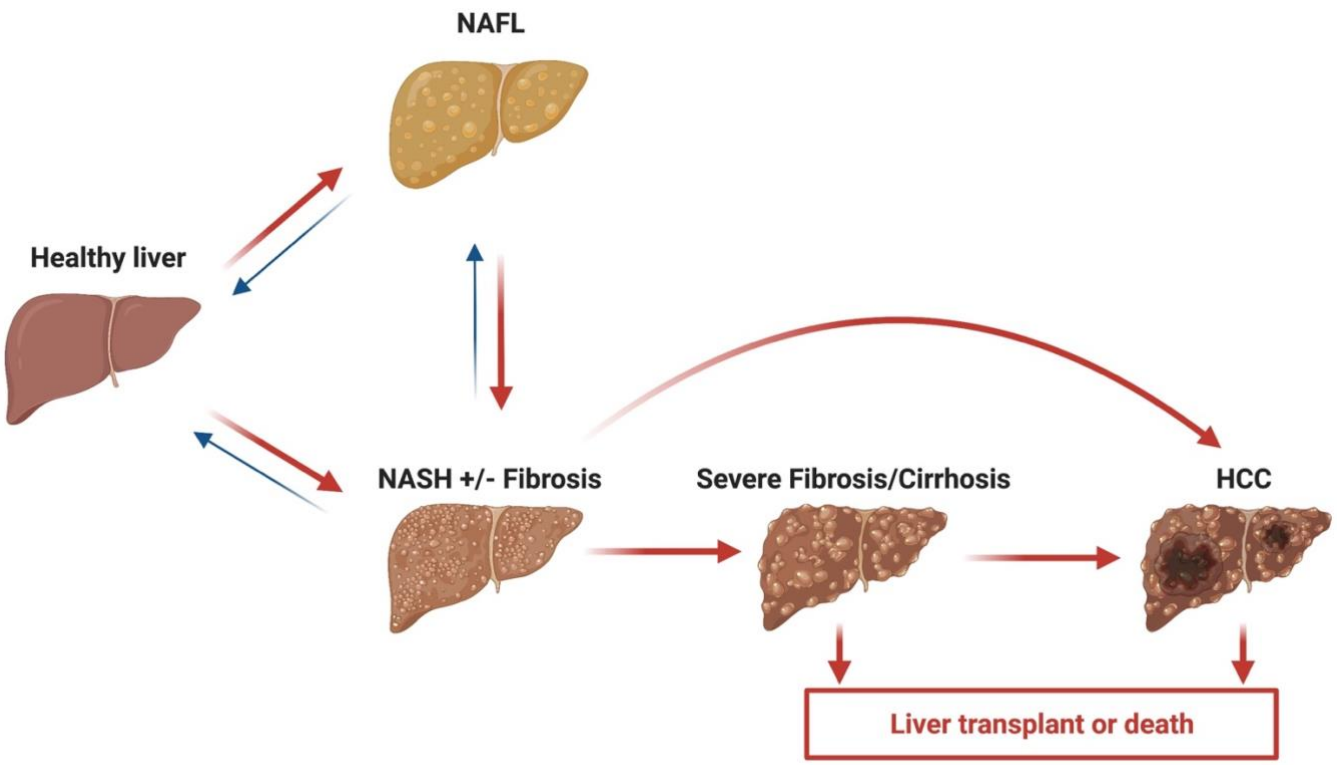

Figure 2.1 The dynamic spectrum of non-alcoholic fatty liver disease (NAFLD) progression. The liver can accumulate fat (nonalcoholic fatty liver; NAFL) in the absence or presence of inflammation (non-alcoholic steatohepatitis; NASH) and fibrosis. These processes are reversible as indicated by the blue arrows. NASH with or with out fibrosis might further advance to severe fibrosis and eventually cirrhosis that can be complicated by hepatocellular carcinoma (HCC). HCC can also develop outside the setting of cirrhosis. This figure was created with BioRender.

progression of NAFLD are complex and still incompletely elucidated. The initial model of NAFLD pathogenesis was envisioned as a “two hit hypothesis”, proposed in 1998 (Day and James, 1998). The first hit was considered the accumulation of triglycerides (TGs) and free fatty acids (FFAs) in hepatocytes caused by insulin resistance (IR), with enhanced dietary influx and increased hepatic lipogenesis. The second hit was hypothesized to involve lipid peroxidation, mitochondrial dysfunction and inflammation, leading to the hepatocyte damage and development of liver fibrosis.

However given our current understanding of the association of NAFLD with metabolic dysfunction, and the interactions between genetic and environmental factors taking part in the disease progression, NAFLD is now described as resulting from parallel ‘multiple hits’, involving crosstalk between multiple organs and the intestinal microbiome (Buzzetti et al., 2016; Moore, 2019a). The multiple parallel-hit model suggests that multiple factors, including genetic and epigenetic determinants, the dysregulation of the lipid and glucose metabolism, IR and gut dysbiosis caused by overnutrition and obesity, drives early development of steatosis. Lipotoxicity, increased oxidative stress, adipokines and inflammatory cytokines [e.g. interleukin (IL)-6, IL-1β, and tumour necrosis factor-α (TNF-α)] secretion, and intestinal barrier disturbance have been suggested to subsequently, or in parallel, contribute to multiple insults, aggravating the hepatic lipid accumulation and triggering inflammation. In the later stage of NASH, sustaining the inflammatory environment in the liver further promotes fibrosis development, including the activation of Kupffer cells and HSCs.

Given the complex and heterogeneous disease features, understanding the pathogenesis and molecular mechanisms of NAFLD is essential for effective diagnosis and treatment.

2.1.2 Factors contributing to the development of NAFLD

NAFLD is a multifactorial disease and disease presentation and progression is highly variable between individuals (Eslam et al., 2018). Complex interactions among multiple factors contribute to high inter-individual variability, determining disease phenotype and progression. In addition to age and ethnicity, NAFLD risk factors include: lifestyle factors (e.g. nutrition and physical activity), the presence of other metabolic disorders [e.g. metabolic

syndrome (MetS), obesity, T2D, hypertension and hyperlipidaemia], and inherited (i.e., genetic/epigenetic) factors (Juanola et al., 2021). A broader discussion of the essential role of genetic and epigenetic risk factors in the pathogenesis of NAFLD will be provided in the following sections.

2.1.2.1 Genetics and NAFLD

There is a wealth of evidence demonstrating the substantial heritability of NAFLD. Findings from family studies have revealed that first-degree relatives of patients with NAFLD are at higher susceptibility of the disease, especially in relation to hepatic fat content (Willner et al., 2001; Schwimmer et al., 2009; Long et al., 2019). Whereas, the heritability of serum liver enzyme levels, such as alanine aminotransferase (ALT) and gamma-glutamyl transpeptidase (γ-GGT), hepatic steatosis and fibrosis have been shown to be high in different twin cohorts (Makkonen et al., 2009; Loomba et al., 2010; Loomba et al., 2015). Specifically, the susceptibility correlations of ALT, steatosis and fibrosis were significantly higher in the monozygotic twins than the dizygotic twins (Makkonen et al., 2009; Loomba et al., 2015). Notably, hepatic steatosis shared up to 0.756 genetic effect with fibrosis, suggesting a similar genetic basis, i.e., sharing regulatory genetic variants, underlying the pathogenesis (Cui et al., 2016). Overall, these data support a significant impact of genotype in the manifestation of NAFLD traits.

In recent years, an accumulating wealth of genome-wide association studies (GWAS), exome-wide association studies (EWAS) and genome sequencing studies have significantly deepened our knowledge of the genetic variants that play vital roles in NAFLD susceptibility, progression and outcomes (Eslam et al., 2018). Summaries of GWAS and genome sequencing studies in European and Asian populations are listed in the **Appendix Table A1-A3**. The most replicated susceptibility genes uncovered by these studies are: patatin-like phospholipase domain-containing protein 3 (PNPLA3), transmembrane 6 superfamily member 2 (TM6SF2), glucokinase regulator (GCKR), membrane bond O-acetyltransferase domain containing 7 (MBOAT7) and 17-β hydroxysteroid dehydrogenase 13 (HSD17B13). The connection of these five genes with NAFLD pathophysiology was summarised in **Figure 2.2**, and their effects and function on NAFLD will be expanded on in brief below.

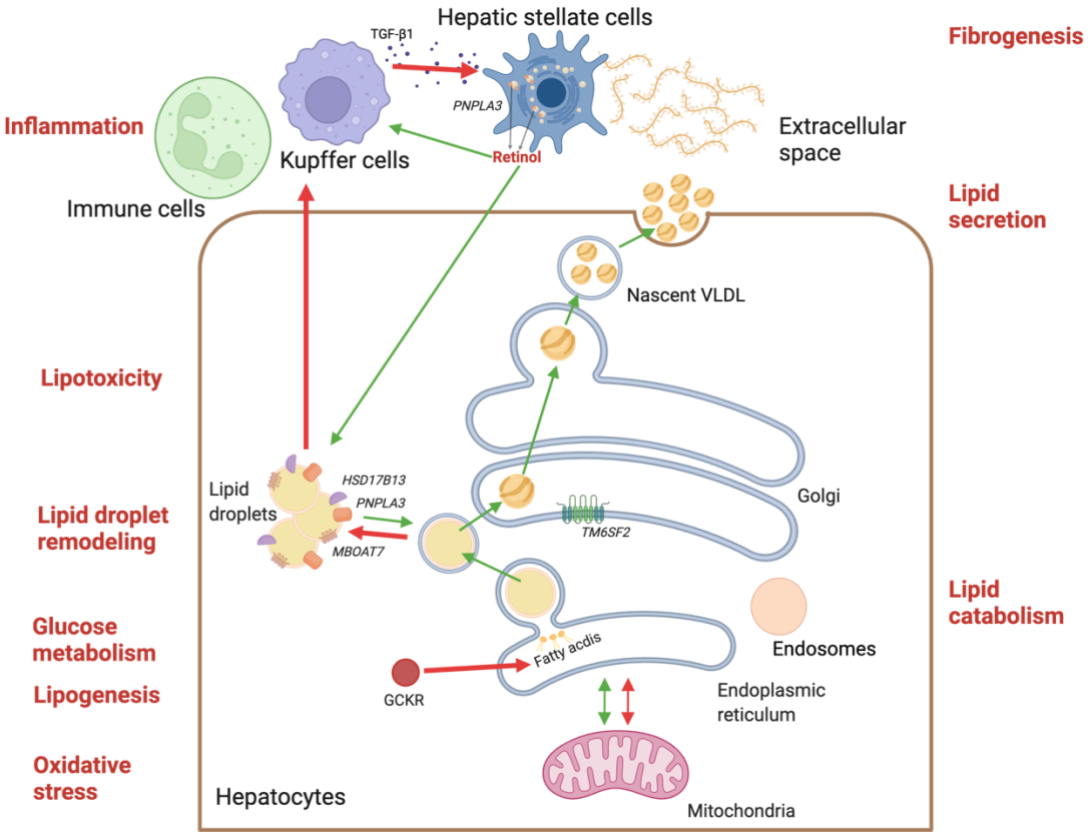

Figure 2.2 Genetic pathophysiology of NAFLD. Genetic determinants of NAFLD, are classified according to the biological processes by which the encoded proteins are thought to contribute to the pathogenesis of the disease in the liver. Red arrows indicate pathological processes/lipid fluxes, while green arrows beneficial pathways. Pathophysiological processes are indicated in red uppercase, gene names in Italics, and cellular and liver compartments in lowercase. GCKR, Glucokinase regulator; HSD17B13, 17-beta hydroxysteroid dehydrogenase 13; NAFLD, non-alcoholic fatty liver disease; MBOAT7, membrane-bound O-acyl transferase 7; PNPLA3, patatin-like phospholipase domain-containing 3; TGF-β1, transforming growth factor β1; TM6SF2, transmembrane 6 superfamily member 2; VLDL, very-low-density lipoproteins. This figure was created with BioRender.

PNPLA3: The PNPLA3 is predominantly expressed in the human liver, adipose tissue, and retina and is a member of the family of patatin-like phospholipase domain-containing proteins with lipid acyl hydrolase activity (Basu Ray, 2019; Pingitore and Romeo, 2019). In the liver, PNPLA3 is predominantly expressed in hepatocytes, stellate cells, and sinusoidal cells, suggesting its vital role in regulating the metabolism of lipids and retinol.

To date, the PNPLA3 gene has been identified as the most critical genetic determinant of NAFLD severity in children and adults (Eslam et al., 2018; Krawczyk et al., 2020). A nonsynonymous point mutation in PNPLA3 rs738409 (C>G, **Figure 2.3A**) caused the substitution of an isoleucine to methionine substitution at position 148 (I148M) of the protein (Romeo et al., 2008). The PNPLA3 I148M variant was first identified in a GWAS (Romeo et al., 2008) and has since been replicated in multiple subsequent GWAS and EWAS (**Appendix Table A1-A2**) (Speliotes et al., 2011; Kawaguchi et al., 2012; Feitosa et al., 2013; Kitamoto et al., 2013; Kozlitina et al., 2014; Chung et al., 2018; Namjou et al., 2019). Furthermore, in NAFLD, carriage of the I148M allele is associated with histological severity and mortality (Rotman et al., 2010; Sookoian and Pirola, 2011; Dongiovanni et al., 2013). The PNPLA3 I148M variant is highly prevalent among the Hispanic population, partly explaining the higher risk of hepatic steatosis and NAFLD in this ethnic group (Browning et al., 2004; Romeo et al., 2008; Rich et al., 2018). In addition, individuals with the homozygous I148M variant have a ~12-fold greater risk of NAFLD-HCC in the general European population (Liu et al., 2014a).

Besides the association between the PNPLA3 risk variant and NAFLD has been repeatedly confirmed by GWAS and EWAS, studies of the underlying pathogenic mechanism have been recently explored. Mice models either overexpressing wild-type PNPLA3 (Li et al., 2012) or with *Pnpla3* knockout (Chen et al., 2010; Basantani et al., 2011) did not have hepatic steatosis. In contrast, knock-in and overexpression of I148M in the liver of mice with excess carbohydrate feeding reproduced hepatic steatosis (Smagris et al., 2015). The 148M substitution appears to disrupt PNPLA3 enzymatic activity as a triacylglycerol hydrolase and acylglycerol transacylase,

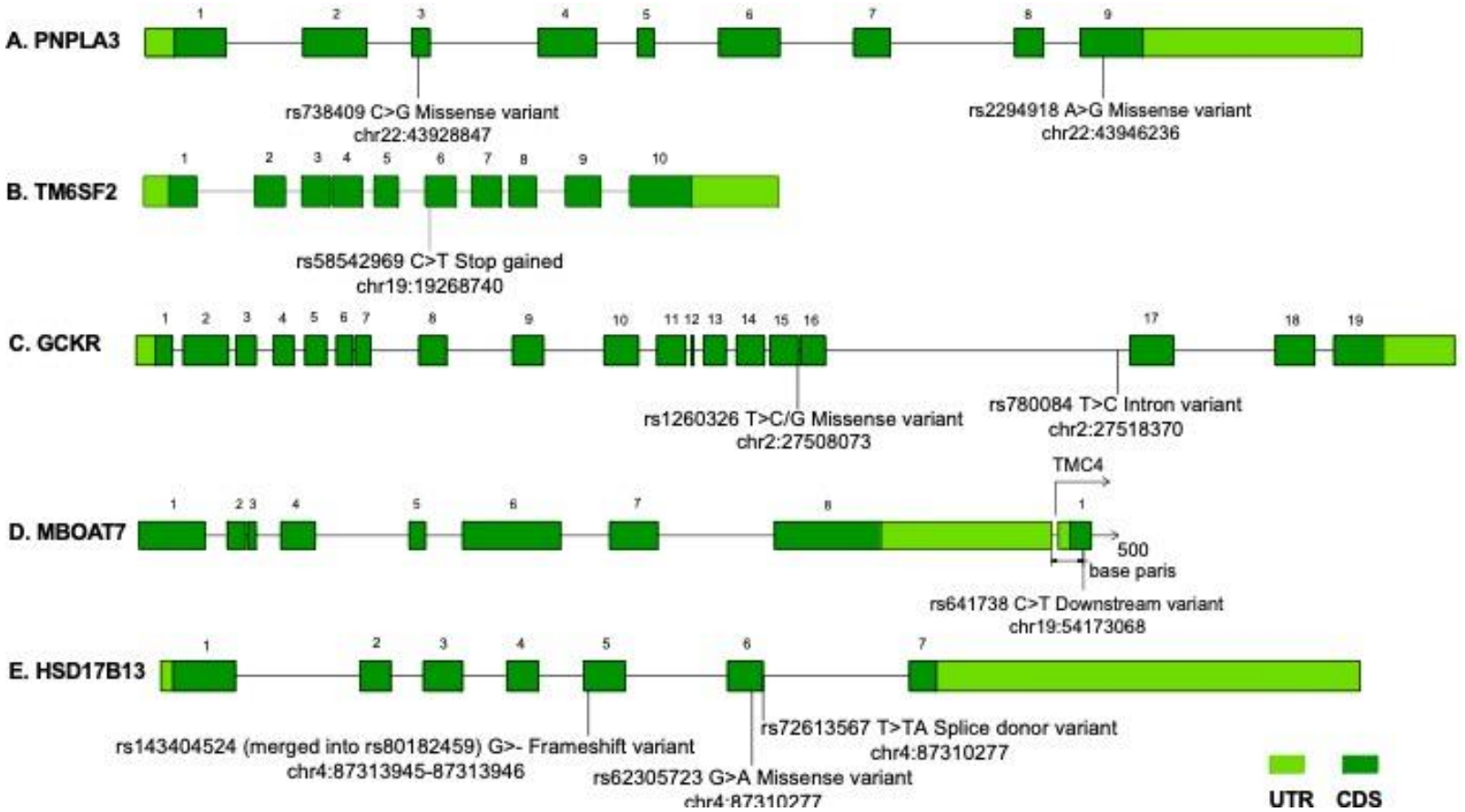

Figure 2.3 Schematic diagram of five NAFLD-related genes with their variant positions. Genes and variants data were extracted from the NCBI database. The light green boxes represent untranslated region (UTR), the dark green boxes represent coding sequence (CDS) and the lines joining boxes represent intronic region. **A.** PNPLA3 gene, **B.** TM6SF2 gene, **C.** GCKR gene, **D.** MBOAT7 gene and **E.** HSD17B13 gene. This figure was created with AutoCAD 2023.

thereby causing hepatic triglyceride and retinol accumulation in hepatocytes and hepatic stellate cells, respectively (Pingitore et al., 2014; Pirazzi et al., 2014). The commonly accepted mechanism of lipid accumulation induced by the I148M variant is that: the I148M mutant protein evaded ubiquitylation and proteasomal degradation, causing an accumulation of the protein on the surface of lipid droplets, which does not allow other lipases to metabolize triglycerides (BasuRay et al., 2017; Luukkonen et al., 2019). On the other hand, the I148M variant also contributes to a heightened, independent risk of fibrosis driven by hepatic stellate cells. The lack of retinyl-palmitate lipase activity driven by I148M appears to disrupt retinol production and release and secretion of matrix-modulating enzymes (Pirazzi et al., 2014; Pingitore et al., 2016), thereby promoting stellate cell fibrogenesis. Interestingly, some data suggested that another variant, rs2294918 (A>G, **Figure 2.3A**), encoding for the glutamic acid to lysine substitution at position 434 (E434K), may attenuate the susceptibility to liver damage and steatosis induced by the 148M mutant (Donati et al., 2016).

TM6SF2: TM6SF2 is a transmembrane protein located in the endoplasmic reticulum (ER) and the ER-Golgi intermediate compartment and is mainly expressed in the liver and small intestine (Mahdessian et al., 2014). The TM6SF2 rs58542926 (C>T; **Figure 2.3B**) is a single nucleotide substitution of a glutamine to lysine substitution at residue 167 (p. Glu167Lys, E167K), leading to a misfolded protein, thus, promoted protein degradation and decreased protein levels (Kozlitina et al., 2014). The rs58542926 (C>T) variant was associated with increased hepatic TG content and higher susceptibility to advanced NAFLD, such as NASH and severe fibrosis (Kozlitina et al., 2014; Liu et al., 2014b; Dongiovanni et al., 2015; Liu et al., 2017). At the same time, patients with NAFLD carrying the E167K variant have a lower risk of cardiovascular disease due to reduced circulating levels of cholesterol and lipids (Dongiovanni et al., 2015).

The molecular function of TM6SF2 needs further investigation, but the available evidence suggests a critical role in hepatocyte secretion of TG and very-low-density lipoprotein (VLDL) (Jonas and Schurmann, 2021). An *in vitro* study indicated overexpression of wildtype TM6SF2 reduced hepatic cell steatosis in HepG2 and Huh-7 cells (Mahdessian et al., 2014). Whereas the

variant TM6FS2 E167K appears to lead to a loss of function as the protein expression of TM6FS2 decreased in E167K transfected Huh-7 cells, compared to wildtype transfection (Kozlitina et al., 2014). Furthermore, Kozlitina et al. (2014) also showed that the E167K variant carriers in mice had increased hepatic TG but reduced circulating lipids levels. Separate work has demonstrated that the incorporation of polyunsaturated fatty acids into hepatic triglycerides, phospholipids, cholesterol esters, and hepatic secretion of large triglyceride-rich VLDL in TM6FSF2 E167K variant carriers was impaired (Luukkonen et al., 2017; Borén et al., 2020). Defective production and secretion of VLDL could lead to aberrant hepatic lipid storage, thereby promoting the progression of NALFD (Sookoian et al., 2015).

GCKR: The GCKR protein acts as an allosteric inhibitor, regulating the activity of the glucokinase to guarantee glucose homeostasis in the liver (Agius, 2008). Variation at the GCKR gene locus has also been associated with NAFLD. Specifically, the intronic rs780094 (T>C) variant (**Figure 2.3C**) was first found associated with hepatic lipid content in an early NAFLD GWAS (**Appendix Table A1**) (Speliotes et al., 2011). Additionally, a recent meta-analysis involving 25 studies evaluated the association between GCKR rs780094 and NALFD. It indicated that an odds ratio (OR) of 1.20 [95% confidence interval (CI) 1.11-1.29] for increased risk of NAFLD in people who carried the rs780094 T allele (Li et al., 2021). However, the effects of GCKR rs780094 polymorphism on its gene expression were not fully understood. Sparsø et al. (2008) speculated that this intronic polymorphism might be in tight linkage disequilibrium (LD) with other genes regulating glucose or triglycerides metabolism. Interestingly, a different variant of GCKR (rs1260326 T>C/G; **Figure 2.3C**) encoding a P446L substitution in GCKR, having LD strongly with rs780094, was most likely the causal variant underlying the association with hepatic lipid accumulation (Beer et al., 2009). While normally GCKR-mediated inhibition of glucokinase was intensified by fructose-6-phosphate, the P446L loss-of-function variant appeared to attenuate this inhibition, thereby increasing hepatic glycogen synthesis and glycolysis (Beer et al., 2009; Valenti et al., 2012). Subsequently, the production of metabolites such as malonyl-CoA likely elevated hepatic

triglyceride storage by serving as a substrate for *de novo* lipogenesis (DNL) and disrupting fatty acid oxidation.

MBOAT7: MBOAT7 is a member of a family of lyso-phosphatidylinositol (LPI) acyltransferases, which participates in phospholipid acyl-chain remodelling of the membranes within the Lands' cycle (Gijon et al., 2008). It specifically catalyses the incorporation of free arachidonic acid, a precursor of pro-inflammatory eicosanoids, into lyso-phosphatidylinositol (PI), thereby achieving an adequate level of desaturation of phospholipids in cell membranes (Gijon et al., 2008; Matsuda et al., 2008).

The rs641738 (C>T) variant of the MBOAT7 gene was initially identified in a GWAS to have an association with alcohol-driven cirrhosis (Buch et al., 2015). The SNP is actually located 500 base pairs downstream of the 3'UTR of the MBOAT7 gene and in exon 1 (p.Gly17Glu) of the transmembrane channel-like 4 (TMC4) gene (**Figure 2.3D**). In NAFLD, this variant was first found to be associated with the risk of hepatic fatty acid accumulation and genetic susceptibility to more severe histology stages, such as inflammation and fibrosis, in a European population (Mancina et al., 2016). Subsequent studies also suggested a role of the rs641738 C>T variant in NAFLD-HCC in individuals of European descent (Luukkonen et al., 2016; Krawczyk et al., 2017). Nevertheless, these findings were not observed in other descents (Sookoian et al., 2018; Koo et al., 2018). Therefore, the association between rs641738 C>T and hepatic fat accumulation and its effects on NAFLD progression is inconclusive. Given the role of the MBOAT7 in inflammatory lipid pathway, the potential mechanism of the genetic impact on hepatic impairment might associate with a lower expression of hepatic MBOAT7 mRNA and protein in rs641738 T allele carriers (Consortium, 2013; Mancina et al., 2016; Donati et al., 2016) and an alteration of serum and hepatic PI composition (Luukkonen et al., 2016; Mancina et al., 2016; Meroni et al., 2020a), resulting in hepatic lipid accumulation and inflammatory mediator secretion.

HSD17B13: The HSD17B13, a protein localised to surfaces of lipid droplets in hepatocytes, has been found to play essential roles in hepatic lipogenesis and the pathogenesis of chronic liver diseases, especially NAFLD (Su et al., 2014; Zhang et al., 2021a). The hepatic HSD17B13 expression was

significantly increased in patients with NAFLD (Su et al., 2014; Ma et al., 2019) and choline-deficient diet-induced NAFLD mice (Mitsumoto et al., 2017). Furthermore, a recent human GWAS study indicated that HSD17B13 gene variations had a robust and replicated association with NAFLD pathogenesis.

The splice rs72613567 (T>TA) variant (**Figure 2.3E**), inserting an A-nucleotide near the splice site of exon 6, generates a truncated loss-of-function enzyme (Abul-Husn et al., 2018). The has been found to protect against advanced NAFLD, especially inflammation and fibrogenesis, more than hepatic fat accumulation (Abul-Husn et al., 2018; Pirola et al., 2019). Interestingly, this protective rs72613567 T>TA variant could attenuate the risk of liver injury in PNPLA3 I148M rs738409 (C>G) variant carriers (Abul-Husn et al., 2018).

Although the roles of the HSD17B13 gene against NAFLD are still not fully characterised, there are indications that the protective effects of HSD17B13 might be through regulating phospholipid and retinol metabolism (Ma et al., 2019; Luukkonen et al., 2020). For example, elevated hepatic phospholipids with downregulation of inflammation-related genes have been observed in rs72613567 T allele carriers (Luukkonen et al., 2020). On the other hand, acting as a retinyl-palmitate lipase, HSD17B13 has also been involved in hepatic retinol metabolism (Ma et al., 2019). Two simultaneously splice variants (exon 6 skipping and a G-nucleotide insertion between exons 6-7 causing a frameshift and premature stop-codon), leading to reduced retinol dehydrogenase activity, were found in the surrounding regions of rs72613567 SNP, which were only found in subjects with the rs72613567 TA allele (Ma et al., 2019). These data are in line with other evidence showing that hepatic vitamin A metabolism is associated with the pathogenesis of hepatic steatosis, fibrosis and insulin resistance (Chen, 2015).

Separate from the protective rs72613567 variant, another two loss-of-function HSD17B13 SNPs, protein-truncating variant rs143404524 (G>-; p.Ala192LeufsTer8; **Figure 2.3E**) (Kozlitina et al., 2018) and missense variant rs62305723 (G>A; P260S; **Figure 2.3E**) (Ma et al., 2019), have been identified related to decreased disease severity of NAFLD. Similar to rs72613567, the retinol oxidation enzymatic activity is abolished in these two variants (Kozlitina et al., 2018; Ma et al., 2019).

2.1.2.2 Epigenetics and NAFLD

In addition to genetic factors, a growing body of evidence supports epigenetic mechanisms contribute to the pathogenesis and progression of NAFLD as well (Lee et al., 2017a; Eslam et al., 2018; Jonas and Schurmann, 2021; Sodum et al., 2021). Epigenetics provides a reversible inheritable phenomenon that affects gene expression at the transcriptional level and phenotypic variation without changing the DNA sequence. The major category of epigenetic mechanisms includes DNA methylation, histone modifications, and non-coding RNAs (e.g. miRNA) (Wang et al., 2012b). In this section, the critical overview of NAFLD epigenetics will be only focused on DNA methylation and chromatin remodelling, as a comprehensive review of non-coding miRNA will be presented in **chapter 3**.

DNA methylation: DNA methylation entails the addition of a methyl group (one-carbon moiety) to a cytosine with guanine as the next nucleotide (CpG islands) catalyzed by DNA methyltransferases (Merlo et al., 1995). The amount of evidence for the effects of DNA methylation in NAFLD has also increased rapidly over the past decade. For example, a microarray analysis investigating the relationship between methylome and transcriptome in a histologically characterized NAFLD cohort indicated that hypomethylation was widely identified in NAFLD regardless of disease severity (Murphy et al., 2013). Indeed, a genome-wide methylation study done in mice with a methyl-deficient diet reported CpG island DNA methylation in 164 genes associated with NAFLD-related processes, such as lipid and glucose metabolism and fibrosis (Tryndyak et al., 2011). Furthermore, transcription-dependent DNA methylation has been identified in several genes that correlated with different stages of NAFLD, especially fibrosis (Murphy et al., 2013; Zeybel et al., 2015). For example, compared to mild NAFLD, CpG hypomethylation of transforming growth factor β1 (TGF- β1) exon (CpG2), collagen 1A1 intron 1 (CpG2) and platelet-derived growth factorα (PDGFα) promoter (CpG3) were detected in NAFLD. Moreover, their expression was upregulated in more severe stages, indicating the possibility of establishing non-invasive markers (Zeybel et al., 2015).

Although most of the effects seen in NAFLD are hypomethylation, several examples of hypermethylated transcription-repressed genes were

found to be involved in essential metabolic functions such as lipid metabolism or belonging to the cytochrome P450 (CYP) family (Murphy et al., 2013). For instance, the promoter hypermethylation of mitochondrial gene NADH dehydrogenase 6 leads to it being transcriptionally silenced, which has been found intensely correlated with the NAFLD severity (Pirola et al., 2013). Another example is the peroxisome proliferative active receptor (PPAR)-gamma coactivator 1-α (PGC1-α) gene, which regulates fatty acid β-oxidation and mitochondria biogenesis (Sookoian et al., 2010). Hepatic PGC-1α methylation levels have been found significantly higher in patients with NAFLD vs controls (Sookoian et al., 2010). In addition, promoter methylation levels of PGC-1α were positively correlated with fasting insulin levels and homeostasis model assessment of insulin resistance (HOMA-IR), but negatively with mitochondrial biogenesis in the patients with NAFLD (Sookoian et al., 2010). Additionally, PGC1-α hypermethylation has been observed in patients with T2D in a study of whole-genome promoter methylation analysis of skeletal muscle (Barrès et al., 2009). Besides PGC-1α, the insulin-like growth factor-binding protein 2 (IGFBP2) has also been found inhibited in patients with NAFLD and NASH via hypermethylation (Ahrens et al., 2013), and correlated with the risk of developing T2D (Wittenbecher et al., 2019). Interestedly, in diet-induced obesity-susceptible mice, IGFBP2 hypermethylation preceded hepatic steatosis development suggesting its potential role to indicate disease development (Kammel et al., 2016).

Histone modifications: Posttranslational modification of histones includes acetylation, methylation, phosphorylation, ubiquitination, ribosylation and sumoylation of histone amino-terminal ends (Chen and Pikaard, 1997). Histone acetylation catalysed by histone acetyltransferase (HAT) enzymes prompts gene transcription activation, whereas histone deacetylation catalyzed by histone deacetylase (HDAC) enzymes leads to gene silencing (Bannister and Kouzarides, 2011). Evidence indicates that the imbalance between both HAT and HDAC activities influences the phenotypic gene expression in NAFLD (Lee et al., 2014b; Sun et al., 2015a).

A member of the HAT family, p300, is an essential transcriptional regulator involved in nuclear transcription factor-κB (NF-κB) dependent inflammatory processes (Chan and La Thangue, 2001). Glycemic

dysregulation and IR increase the activity of NF-κB and pro-inflammatory genes expression through the interaction between NF-κB and p300 (Miao et al., 2004). Additionally, the histone lysine residue 4 repressed by methyltransferase SET7/9 interrupts the assignment of NF-κB p65 to gene promoters, thereby stimulating the release of NF-κB-dependent inflammatory cytokines, such as TNF-α (Li et al., 2008). On the other hand, glucose-activated p300 acetylation stimulates the transcriptional activity of the carbohydrate-responsive element-binding protein (ChREBP), in turn, leads to the progression of hepatic steatosis and IR (Denechaud et al., 2008; Bricambert et al., 2010).

Several HDACs are thought to play a pivotal role developing NAFLD. For example, HDAC3, a member of human class I HDACs, regulates the circadian rhythm of hepatic glucose metabolism and lipogenesis (Gallego-Durán and Romero-Gómez, 2015; Emmett and Lazar, 2019). Animal studies in mice have shown that the disruption of the circadian clock orchestrated by HDAC3 contributes to interfering with lipid metabolism in the liver, resulting in hepatic steatosis and insulin resistance (Feng et al., 2011; Mazzoccoli et al., 2014). In addition, the sirtuins (silent information regulator 2 proteins; SIRTs) are class III HDACs (Schwer and Verdin, 2008). Targeting either histones or non-histone proteins, SIRTs mediate deacetylation reactions to adapt responses to metabolic stress and control insulin secretion and adipogenesis (Lee et al., 2014b). To date, seven sirtuins have been described in humans (SIRT1–7) (Blander and Guarente, 2004). Of these, SIRT1 and SIRT3 in particular have been found related to NAFLD (Hirschey et al., 2011; Mariani et al., 2015; Ding et al., 2017). SIRT1 and SIRT3 are found primarily in the cytoplasmic and mitochondria, respectively (Hirschey et al., 2011). The SIRT1 HDAC mediates hepatic metabolic regulation through direct deacetylation of transcriptional regulators, such as NF-κB and PPARα to protect the progression of fatty liver diseases (Ding et al., 2017; Mukhopadhyay et al., 2017). While Deng et al. (2007) reported that hepatic SIRT1 protein measured by immunoblotting was decreased in HFD induced NAFLD mice, a lower plasma SIRT1 protein expression was observed in patients with severe steatosis and obesity compared to the mild steatosis and obesity (Mariani et al., 2015). Additionally, liver-specific deletion of SIRT1 in mice promoted hepatic steatosis, IR and

inflammation (Purushotham et al., 2009; Yin et al., 2014), while overexpression of SIRT1 attenuated these pathologic conditions (Sun et al., 2007; Herranz et al., 2010). At the same time, SIRT3 plays a role in preserving mitochondrial integrity during oxidative stress (Kim et al., 2010). An *in vivo* study indicated that exposure to a high-fat diet for prolonged periods in mice reduced hepatic SIRT3 mRNA and protein levels and increased hepatic fat content and oxidative stress (Bao et al., 2010). In addition, compared to wild-type, Sirt3-deletion mice fed a high-fat diet showed MetS and NASH phenotypes (Hirschey et al., 2011). Both SIRT1 and SIRT3 are essential for redox state, epigenetic modification, and lipid homeostasis in the liver.

Overall, investigations of the genetic and epigenetic factors in NAFLD have expanded our understanding of pathogenic mechanisms and may also provide prognostic biomarkers and potential therapeutic targets.

MicroRNAs: MicroRNAs are small (~22 nucleotides), single-stranded non-coding RNAs that are involved in the post-transcriptional regulation of gene expression (Bartel, 2004). MicroRNAs bind to complementary sequences of mRNA transcripts, suppressing gene expression through translation repression or mRNA degradation (O'Brien et al., 2018a). Approximately 2300 mature miRNAs have been found in humans (Alles et al., 2019), which regulate at least 60% of human protein-coding genes impacting diverse dynamic biological processes (Friedman et al., 2009; Chipman and Pasquinelli, 2019). Commonly accepted cooperativity and multiplicity principles enable a single miRNA to have multiple mRNA targets, and in addition, a single mRNA can be regulated by multiple miRNAs (Friedman et al., 2009). Present in blood, urine and other body fluids (Weber et al., 2010), miRNA levels are altered in multiple diseases as a result of genomic events or alterations in miRNA biogenesis, which has prompted significant interest in miRNAs as clinical biomarkers and therapeutic targets (Wang et al., 2020c; Ji and Guo, 2019; Rupaimoole and Slack, 2017; Mori et al., 2019).

MicroRNAs are transcribed from DNA by RNA polymerase II (Pol II) to an initial primary miRNA (pri-miRNA) with a hallmark hairpin structure that contains the mature miRNA sequences. In the nucleus, the enzyme Drosha, alongside another protein DiGeorge syndrome critical region 8 (DGCR8) (**Figure 2.4**), cleaves the hairpin structure to release pre-miRNA, exported to

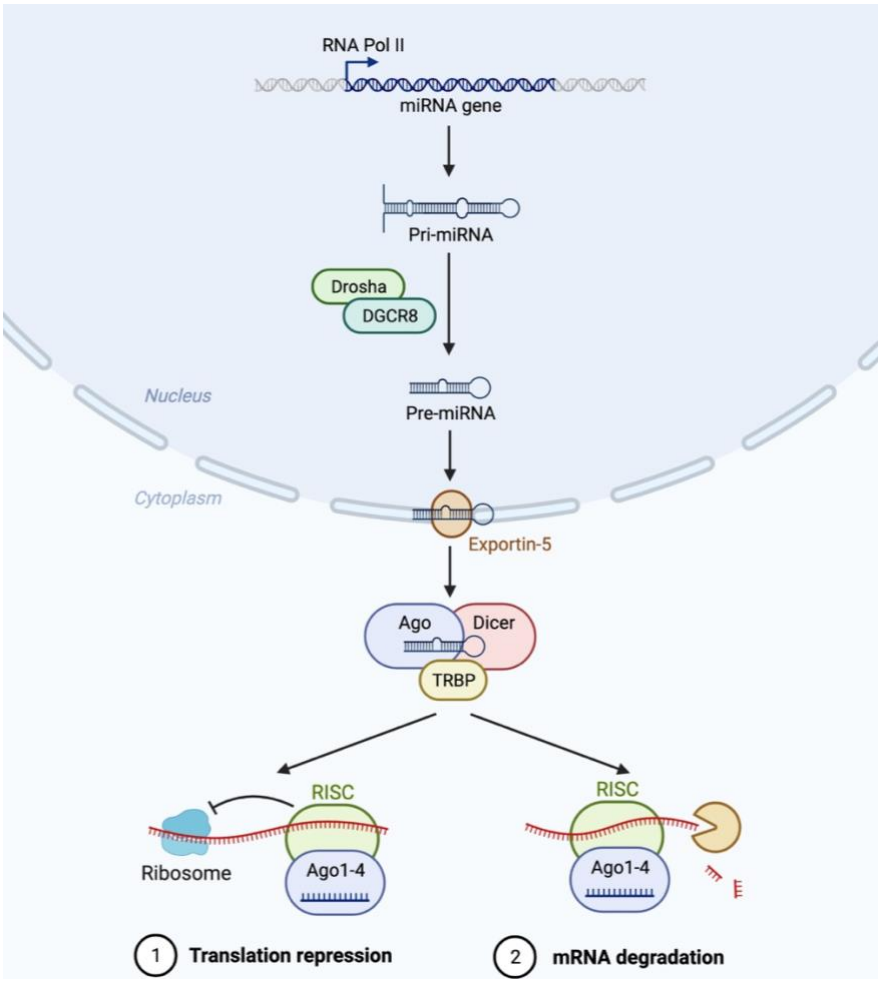

Figure 2.4 MicroRNA biogenesis and function. MicroRNA genes are first transcribed as primary miRNAs (pri-miRNAs) by RNA polymerase II (Pol II) in the nucleus. Then, Microprocessor, including Drosha and DiGeorge syndrome critical region 8 (DGCR8) cleaves the long pri-miRNAs to create the precursor miRNAs (pre-miRNAs). Next, the pre-miRNAs are exported from the nucleus to the cytoplasm by Exportin 5 and further processed by Dicer, a ribonuclease III enzyme that produces the mature miRNAs. One strand of the mature miRNA (the guide strand) is loaded into the miRNA-induced silencing complex (RISC), which contains Dicer1 and Argonaute (Ago) proteins, directs the RISC to target mRNAs by sequence complementary binding and mediates gene suppression by targeted mRNA degradation and translational repression. TRBP, transactivation-responsive RNA-binding protein. This figure was created with BioRender.

the cytoplasm by forming a complex with a protein called exportin 5. Next, Dicer and the transactivation response element RNA-binding protein (TRBP) bind to the pre-miRNA to form a double-stranded mature miRNA in the cytoplasm. During the subsequent multistep assembly of the RNA induced silencing complex (RISC), only one of the miRNA strands of these duplexes (generally called the guide strand) will be retained, becoming the mature miRNA targeting complementary mRNA for degradation and translational repression (Macfarlane and Murphy, 2010).

During the development of NAFLD, hepatic responses to 'multiple hits' lead to the dysregulation of the hepatic transcriptional machinery, altering the activity of transcription factors (Steensels et al., 2020). The abnormal activation or inhibition of transcription regulators further exacerbates lipid accumulation, insulin resistance, inflammation, and fibrosis. Moreover, accumulating evidence indicates that dysregulation of miRNA at the cellular level is involved in each stage of NAFLD progression (Gjorgjieva et al., 2019a). Notably, some of the miRNAs identified as altered in NAFLD play critical roles in hepatic lipid and carbohydrate metabolism and fibrosis; regulating multiple transcription factors such as sterol regulatory element-binding protein 1 (SREBP-1), ChREBP, the PPARs, insulin-like growth factor 1 (IGF-1) and TGF-β (Gjorgjieva et al., 2019a; Fang et al., 2021). Despite the complexity of miRNA involvement in the multiple stages of NAFLD pathogenesis (e.g. steatosis, inflammation, fibrosis), investigating the cell/tissue-specific miRNA or circulating miRNA expression as valuable diagnostic or therapeutic tools for NAFLD is of significant interest (Gjorgjieva et al., 2019a; Wang et al., 2020c; Su et al., 2018). Therefore, in **Chapter 3**, I did a comprehensive review of the literature and examined the data from human serum profiling or mechanistic studies involving human liver tissues to identify miRNAs for involvement in NAFLD progression with good evidence.

2.1.3 Diagnosis

Initially, NAFLD is commonly asymptomatic and is often identified incidentally. Although NAFL is typically benign, patients with NASH and fibrosis are at risk of developing more severe liver complications, including cirrhosis and HCC, and mortality (Moore, 2019a; Reddy et al., 2020). Thus, significant efforts are needed to be made on early diagnosis of NASH and accurate staging of

fibrosis risk for better stratification, monitoring and targeted management of patients at risk.

Screening and diagnosing NAFLD is a multistep procedure. Older age, (>50), Hispanic ethnicity and comorbidities such as obesity, T2D and components of MetS contribute to high-risk of NAFLD when screening (Lonardo et al., 2015). In addition, a 'primary NAFLD' diagnosis can only be made after excluding common secondary causes leading to fatty liver disease. These include alcohol toxicity, viral hepatitis, inherited metabolic disorders, drugs and industrial chemicals (Liebe et al., 2021).

Generally, initial non-invasive assessment involves two aspects: (1) measurement of biochemical biomarkers in serum or plasma (e.g. liver functional tests); and (2) measurement of steatosis and fibrosis via imaging techniques (e.g. ultrasound- or magnetic resonance-based tools) (EASL-EASD-EASO, 2016; Chalasani et al., 2018; Ando and Jou, 2021; National Institute for Health and Care Excellence, 2016). However, the performance of these non-invasive methods are suboptimal for staging NAFLD. Specifically, most NAFLD predictive algorithms that integrate serum or blood biomarkers [e.g. the fatty liver index (FLI), hepatic steatosis index, NASH Score, the NAFLD fibrosis score (NFS), and the Fibrosis-4 (FIB-4) index] have less accuracy in differentiating individuals with NASH (Dorairaj et al., 2021). Furthermore, elastography-based tools may not reliably distinguish NASH from simple steatosis and have less sensitivity and accuracy to patients with confounding factors, including obesity and T2D, in detecting fibrosis and cirrhosis. Therefore, for most accurate staging of NAFLD, histological status requiring a liver biopsy is still needed.

Despite the limitations of liver biopsy, such as high cost, sampling error, procedure-related complications, it is still considered the gold-standard assessment for diagnosis and staging of NASH and fibrosis (Sumida et al., 2014; Berger et al., 2019). In contrasting to non-invasive methods, liver biopsy can identify the presence and location features, including steatosis, lobular inflammation, hepatocyte ballooning, Mallory-Denk bodies, and fibrosis (Boyd et al., 2020).

Beyond the current invasive and noninvasive methods for NAFLD diagnosis, some promising new biomarkers, including genetic markers,

noncoding RNAs and extracellular vesicles, are currently being considered for further development and application (Dorairaj et al., 2021).

2.1.4 Treatment and management

As previously stated, there is tremendous interindividual variation in NAFLD phenotype and risk of progression, which is determined by dynamic interactions between genetic, metabolic and environmental factors that are not entirely understood (Moore, 2019a; Eslam et al., 2020b). Although several genetic variants and epigenetic factors (**2.1.2**) have influenced NAFLD susceptibility, dietary and lifestyle factors strongly influence disease progression (Ullah et al., 2019; Meroni et al., 2020b). There are no approved effective pharmacological treatments for NALFD; lifestyle improvement, involving weight loss, an increase of physical activity and the adoption of a hypocaloric diet, is the mainstay of current clinical management guidelines (Alexander et al., 2018; Cicero et al., 2018). The practical guidance from the American Association for the Study of Liver Diseases (AASLD) concludes that 3-5% of weight loss is necessary to improve steatosis with a more remarkable improvement of the histopathological features of NASH requiring 7-10% weight loss (Chalasani et al., 2018). However, lifestyle modifications are difficult to implement and sustain and need consistent weight loss over 6-12 months (Romero-Gomez et al., 2017).

In recent years, due to the remarkable progress made in understanding the disease pathogenesis, like fat accumulation and injury pathways, increasing studies attempt to explore how specific macronutrients and micronutrients contribute to the development and possible alleviation and treatment of NAFLD (Cicero et al., 2018; Pickett-Blakely et al., 2018). For example, micronutrient deficiencies, such as zinc, copper, retinoic acid and vitamin D, have been associated with NAFLD and a mechanistic basis exists for their therapeutic targeting (Pickett-Blakely et al., 2018). However, only a limited number of intervention trials have assessed nutrient supplements in patients with NAFLD with mixed results (Cicero et al., 2018; Pickett-Blakely et al., 2018). Vitamin D came to scientists' attention because it has antiproliferative, anti-inflammatory and antifibrotic properties that have been shown to attenuate NAFLD progression in preclinical models (Pacifico et al., 2019; Karatayli et al., 2020). Therefore, the following section will

comprehensively discuss the roles of vitamin D in NAFLD progression and its potential therapeutic properties.

2.2 Vitamin D and NAFLD

In the early 20th century, vitamin D was identified by McCollum and Davis (1913) from cod liver oil as a fat-soluble vitamin with the ability of healing rickets. Vitamin D from either the diet or synthesized through sun exposure to skin is metabolized into its biologically active metabolite, 1 α ,25-dihydroxyvitamin D [calcitriol, 1α,25(OH)$_2$D], through two critical hydroxylation steps (Bikle, 2000). The first step occurs in the liver resulting in 25-hydroxyvitamin D [25(OH)D], the more stable circulating form of vitamin D and its most widely used indicator for status assessment. While the second, 1α -hydroxylation step, yielding the active hormone, occurs in the kidneys.

Vitamin D is a misnomer for a family of secosteroid hormones with pleiotropic actions (Demer et al., 2018). The active metabolite of vitamin D, 1α,25(OH)$_2$D$_3$, elicits biological activities through the interaction with VDR, which is a nuclear, ligand-activated transcription factor (Maestro et al., 2016). While vitamin D is well known for its essential role in maintaining mineral homeostasis through regulating calcium/phosphate metabolism, emerging experimental evidence suggests anti-proliferative, anti-inflammatory and anti-fibrotic properties of vitamin D are important factors in chronic liver diseases, including NAFLD (Kitson and Roberts, 2012; Barchetta et al., 2020).

However, clinical and experimental evidence for a role for vitamin D in NAFLD pathogenesis is conflicting (Zhang et al., 2019c; Barchetta et al., 2020). Therefore, the following sections will give insights into the association between NAFLD and vitamin D status, describe vitamin D supplementation trials in patients with NAFLD, and discuss the roles of genetic polymorphisms and the gut microbiome in influencing both vitamin D status and NAFLD pathogenesis.

2.2.1 The association of low-serum vitamin D status and NAFLD

To date, there is no consensus on the optimal circulating 25(OH)D levels and there is debate around the cut-off thresholds to define vitamin D deficiency and insufficiency. A summary of vitamin D thresholds defining vitamin D status

determined by various international agencies is showed in **Table 2.1.** As unfavourable musculoskeletal outcomes are associated with lower vitamin D status (Pludowski et al., 2013), most of the guidelines and thresholds are in relation to bone health.

Table 2.1 Circulating 25-hydroxyvitamin D cut-off thresholds proposed by various international agencies

Agencies	Country/District	25(OH)D cut-off threshold
SACN (SACN, 2016)	UK	Sufficient: >50nmol/L Insufficient: 25-50nmol/L Deficiency: <25nmol/L
EFSA (EFSA Panel on Dietetic Products, 2016)	European	Sufficient: >50nmol/L Deficiency: <30nmol/L
ESPGHAN (Braegger et al., 2013)	European	Sufficient: >50nmol/L Deficiency: <25nmol/L
IOM (Ross, 2011)	North America and Canada	Sufficient: >50nmol/L Insufficient: 30-50nmol/L Deficiency: <30nmol/L
The Endocrine Society (Holick et al., 2011)	US	Insufficient: 52.5-72.5nmol/L Deficiency: <50nmol/L
SAHM (SAHM, 2013)	US	Insufficient: 52.5-72.5nmol/L Deficiency: <50nmol/L
AAP (Wagner et al., 2008)	US	Insufficient: 50-80nmol/L Deficiency: <50nmol/L
National Health Commission of PRC (NHC, 2020)	China	Sufficient: >50nmol/L Insufficient: 30-50nmol/L Deficiency: <30nmol/L

25(OH)D, 25-hydrocyvitamin D; AAP, American Academy of Paediatrics; EFSA, European Food Safety Authority; ESPGHAN, European society for Paediatric Gastroenterology, Hepatology and Nutrition; IOM, Institute of Medicine; PRC, People's Republic of China; SACN, Scientific Advisory Committee on Nutrition; SAHM, Society for Adolescent Health and Medicine; Conversion factors: 1ng/ml 25(OH)D = 2.5nmol/L 25(OH)D;

Generally, a range of below 25 or 30 nmol/L (or 10/12 ng/ml) of serum or plasma 25(OH)D is considered vitamin D deficient by most international agencies (Ross, 2011; Braegger et al., 2013; SACN, 2016; EFSA Panel on Dietetic Products, 2016; NHC, 2020). The agencies agree that a population with circulating 25(OH)D levels below 25-30 nmol/L are at significantly increased risk for rickets and osteomalacia. However, the clinical practice guidelines of the Endocrine Society Task Force on Vitamin D have defined a cut-off level of 50 nmol/L as vitamin D deficient (Holick et al., 2011), similar to the threshold of the Society for Adolescent Health and Medicine (SAHM) (SAHM, 2013) and the American Academy of Paediatrics (AAP) (Wagner et al., 2008). Notably, the Endocrine Society guidelines emphasise the care of

patients at risk of vitamin D deficiency, such as patients with obesity, malabsorption syndromes or those with medication-induced vitamin D metabolism issues. Conversely, the Institute of Medicine (IOM), the European Food Safety Authority (EFSA), the Scientific Advisory Committee on Nutrition (SACN) and the National Health Commission of People's Republic of China emphasize recommendations for the general healthy population.

Low vitamin D status has emerged as a prevalent condition worldwide (Holick, 2017; Amrein et al., 2020). Extensive observational data based on nationally representative populations estimated that the prevalence rates of vitamin D deficiency [25(OH)D<30 nmol/L] was ~13% in Europe (Cashman et al., 2016), ~5.9% in the United States (US) (Schleicher et al., 2016), and ~7.4% in Canada (Sarafin et al., 2015). Whereas, the prevalence of 25(OH)D levels <50 nmol/L has been estimated as approximately 40.4% in Europe, 24.0% in the US, and 36.8% in Canada. Additionally, a recent meta-analysis based on the general population in the Mainland of China indicated that the prevalence of vitamin D deficiency (<30nmol/L) and insufficiency (<50nmol/L) were 20.7% and 63.2%, separately (Liu et al., 2021a). While a study from the National Diet and Nutrition Survey reported that vitamin D status lower than 25nmol/L in the United Kingdom (UK) was about 17% in children and 20% in adults (Bates, 2016). The variation in the prevalence of vitamin D deficiency is likely caused by multi factors, including: sun exposure time, dietary preferences, age and ethnic group (Holick, 2017; Cashman, 2020). Therefore, many international agencies have called for use of vitamin D supplements as a means of correcting low vitamin D intakes and status in the population. Indeed, vitamin D supplement use has been recommended as national policy in certain countries, particularly for at-risk population groups. A summary of dietary reference values for vitamin D by life stages as proposed by international agencies to maintain adequate circulating 25(OH)D concentrations is showed in **Appendix Table A4**.

High prevalence of vitamin D deficiency and insufficiency have been associated with the risk of acute and chronic diseases (Pludowski et al., 2013). Moreover, a growing body of studies suggests an association between vitamin D deficiency and metabolic associated disease, including NAFLD (Kwok et al., 2013; Barchetta et al., 2020). However, whether vitamin D deficiency is a

contributing factor to NAFLD or is symptomatic of associated obesity or impaired liver metabolism capacity in NAFLD remains unclear (Zhang et al., 2019c).

Vitamin D status has been suggested to be associated with NAFLD pathophysiology and progression (Kwok et al., 2013). Early cross-sectional studies done in two Italian cohorts of 120 (Targher et al., 2007) and 262 (Barchetta et al., 2011) adults with and without NAFLD, suggested a lower 25(OH)D was associated with advanced liver steatosis and fibrosis in patients with NAFLD. However, it is essential to note that not all studies are supportive of this. Two recent meta-analyses synthesizing six observational studies in patients with biopsy-proven NAFLD (published before September of 2017) concluded that 25(OH)D level was not associated with either NAFLD activity score (NAS, a measure of histological severity) or fibrosis (Jaruvongvanich et al., 2017; Saberi et al., 2018).

On the other hand, vitamin D deficiency might be associated with an increased prevalence of NAFLD (Eliades and Spyrou, 2015). A meta-analysis of 29 case-control and cross-sectional studies specifically in NAFLD found that adult patients with NAFLD were 26% more likely to be vitamin D deficient than controls (Wang et al., 2015), corroborating an earlier meta-analysis done by Eliades et al. (2013). In addition, lower serum 25(OH)D concentrations were found to be a significant predictor for NAFLD independent of age, gender, body mass index (BMI), lipid profile and fasting blood glucose (FBG) in the multivariate logistic regression analysis model (Gad et al., 2020). This result was consistent with Barchetta and colleagues, who performed a multivariate logistic analysis adjusting for BMI, demonstrating an association between NAFLD and vitamin D (Barchetta et al., 2011).

Contrary to the extensive data from adults with NAFLD, there are less pediatric data regarding vitamin D status and NAFLD. In line with the finding in adults, low serum levels of vitamin D have also been found in children with NAFLD. Manco et al. (2010) and Nobili et al. (2014) reported low serum 25(OH)D concentrations among children with biopsy-proven NASH and NAFLD in Italy (n=64 and n=73, respectively). In comparison, Gibson et al. (2018) demonstrated in the UK that low vitamin D status existed in the majority of paediatric patients (n=103) with NAFLD confirmed by liver biopsy.

Separately, children (n=102) with proven histological NAFLD in the US also had a high prevalence of low vitamin D levels. Notably, only one meta-analysis has investigated the relationship between vitamin D status and NAFLD in children and adolescents in eight studies (Zhu et al., 2019a). Children and adolescents involved in the analysis were NAFLD or NASH diagnosed by biopsy, ultrasound, or elevated ALT levels. The results showed that serum 25(OH)D was significantly lower in patients NAFLD vs controls.

Studies that have examined vitamin D status in NAFLD have been heterogeneous in terms of NAFLD diagnosis, the populations examined, and sample size. A key challenge in NAFLD is the diagnosis of patients. As I mentioned in section **2.1.3**, while liver biopsy is considered the gold standard for staging disease, biopsies are invasive and not practical for large population studies (Moore, 2019a). Elevated liver enzyme levels in the blood are readily measured and are, therefore, often used to define 'suspected NAFLD' in large population studies. However, it is recognized that these are neither sensitive nor specific for NAFLD, and significantly underestimate prevalence (Moore, 2019a). The most extensive population studies in adolescents (n=3,878) (Cho et al., 2019) and adults (n=6,826) (Liangpunsakul and Chalasani, 2011) used elevated serum ALT levels (ALT $\geq$ 30U/l) to diagnose NAFLD.

Furthermore, a recent systematic review included 45 human studies prior to February 2017 exploring the association between vitamin D status and NAFLD/NASH in adults and children indicated that 29 studies reported an inverse association between vitamin D status and NAFLD, while 16 studies did not support this association (Pacifico et al., 2019). Therefore, it is a challenging to draw a conclusion from such heterogeneous studies. In addition, given the observational nature of these studies, a causal relationship between vitamin D deficiency and NALFD cannot be concluded.

2.2.2 Supplementation of vitamin D in NAFLD

While observational studies regarding the link between hypovitaminosis D and NAFLD risk and severity suggest that vitamin D supplementation might be a potential therapeutic option for NAFLD in children and adult populations (Kwok et al., 2013; Eliades and Spyrou, 2015), the results of vitamin D supplementation trials in patients with NAFLD are inconclusive. In 2021, a systematic review with meta-analysis of sixteen randomized controlled trials

(RCT) in patients with NAFLD concluded that vitamin D supplementation had significant effects on anthropometric and biochemical indices (Rezaei et al., 2021). On the other hand, a larger Cochrane review that more broadly focused on chronic liver disease in adults (Bjelakovic et al., 2021) concluded that although vitamin D supplementation appeared to have no effects on liver function or steatosis in patients with NAFLD, the evidence base for this (11 trials) was extremely weak.

It is essential to critically assess the literature and investigate whether vitamin D supplementation could improve NAFLD. The previous literature search was performed from the end of 2017 to the middle of 2019 with the databases including PubMed, Scopus and Cochrane to identify acceptable RCTs published since the end of two census in two meta-analyses (Tabrizi et al., 2017; Bjelakovic et al., 2017). Unfortunately, only four randomised controlled interventions investigating the biochemical and histological benefits of oral vitamin D supplementation in patients with NAFLD were identified (Zhang et al., 2019c). The results were underpowered and inconclusive.

To have an overview of all published clinical trials investing the effects of vitamin D supplementation in patients with NAFLD, in this thesis, the literature search was expanded, and performed up to January 2022 with the database of PubMed, broadly using the terms NAFLD, NASH, MAFLD, MASH, vitamin D and calcitriol, in order to identify RCTs examining vitamin D supplementation in people with NAFLD.

In summary, 23 interventional studies were identified and have investigated the biochemical and histological benefits of vitamin D supplementation in NAFLD patients (**Table 2.2**). These included two studies in children (Namakin et al., 2021; El Amrousy et al., 2021) and three one-arm pilot studies (Kitson et al., 2016; Papapostoli et al., 2016; Dasarathy et al., 2017). Interventions ranged from 8 weeks to 12 months, with outcomes of interest including vitamin D status, principal liver outcomes (including the grade of NAFLD, liver enzymes and lipid profile) (**Table 2.3**) and other metabolic outcomes (such as anthropometric and glycaemic indices, **Appendix Table A5**). Twenty-one trials administered vitamin D orally, and two trials used intramuscular injection (Sakpal et al., 2017; Gad et al., 2021).

Table 2.2 Overall characteristics of randomised controlled intervention trials of vitamin D supplementation in NAFLD.

Randomised controlled intervention trials in children								
Authors (y); Country	**Study design**	**Subjects**				**Other interventions**		
		Population and age	**NAFLD diagnosis**	**Vitamin D assay**	**Vitamin D cut-off**	**Diet**	**Physical activity**	**Sun exposure**
El Amrousy et al. (2021); Egypt	2-arm RCT	Children with obese; **G1:** 7.9 [6.5-17.5]‡, **G2:** 9.6 [7.1-16.2]‡	Biopsy	ECLIA	**Sufficiency:** >50 nmol/L **Insufficiency:** 30-50 nmol/L **Deficiency:** <30 nmol/L	Hypocaloric diet	nr[1]	nr
Namakin et al. (2021); Iran	2-arm RCT	Children with overweight and obesity with vitamin D<75nmol/L; **G1 and G2**: 12-18	Ultrasound	ECLIA	nr	nr	nr	nr
Randomised controlled intervention trials in adults								
Gad et al. (2021); Egypt	2-arm single blinded RCT	Adults with NAFLD; **G1:** 46±10†, **G2:** 47±9†	Ultrasound and TE	ELISA	**Sufficiency:** 75-250 nmol/L **Insufficiency:** 50-75 nmol/L **Deficiency:** <50 nmol/L	nr	nr	nr
Morvaridzadeh et al. (2021); Iran	2-arm RCT	Adults with NAFLD; **G1:** 39.91±7.16†, **G2:** 40.39±6.22†	Ultrasound	ECLIA	**Sufficiency:** >50 nmol/L **Insufficiency:** 30-50 nmol/L **Deficiency:** <30 nmol/L	nr[1,2]	nr[3]	nr[4]
Mahmoudi et al. (2021); Iran	2-arm RCT	Adults with NAFLD with concomitant vitamin D deficiency or insufficiency **G1:** 39.63±8.75†, **G2:** 42.26±11.53†	Ultrasound and ALT	RIA	**Deficiency or insufficiency:** <75 nmol/L	Restriction of high carbohydrates and fat diet	Increase physical activity	nr
Yaghooti et al. (2021); Iran	2-arm RCT	Adults with NAFLD; **G1 and G2**: 18-60	TE	nr	nr	nr	nr	nr
Lukenda Zanko et al. (2020); Croatia	2-arm RCT	Adults with NAFLD and one or more components of MetS; **G1:** 66 [23-83]‡,	Ultrasound and TE	ECLIA	nr	nr[1]	nr[1]	nr

		G2: 64 [20-85]‡						
Hussain et al. (2019); Pakistan	2-arm RCT	Adults with NAFLD and BMI>28; **G1:** 19±19†, **G2:** 27±1.7†	Ultrasound and hepatic enzymes	nr	nr	Restriction of high carbohydrates and fat diet	Increase physical activity	nr
Shidfar et al. (2019b); Iran	3-arm RCT	Adults with NAFLD, BMI 25-35, vitamin D< 37.5nmol/L; **G1:** 44.0±10.8†, **G2:** 39.8±11.0†, **G3:** 38.3±10.1†	Ultrasound	ELISA	nr	Hypocaloric diet[2]	30min moderate walking[3]	Direct sunlight exposure to less than 1 h/day
Geier et al. (2018); Switzerland	2-arm RCT	Adults with NASH; **G1:** 39±16†, **G2:** 50±13†,	Biopsy	ECLIA	**Insufficiency:** <75 nmol/L	nr[1]	nr[1]	nr
Dabbaghmanesh et al. (2018b); Iran	3-arm RCT	Adults with NAFLD and vitamin D< 75nmol/L; **G1:** 45.7±14.8†, **G2:** 44.4±11.1†, **G3:** 44.7±7.6†	Ultrasound	nr	**Insufficiency:** 50-74.75 nmol/L **Deficiency:** <50 nmol/L	nr	nr	nr
Taghvaei (2018); Iran	2-arm RCT	Adults with NAFLD, BMI 25-35, and vitamin D< 75nmol/L; **G1:** 44.00±11.05†, **G2:** 41.20±13.55†	Ultrasound, TE and hepatic enzymes	ELISA	nr	Hypocaloric diet	nr	nr
Sakpal et al. (2017); India	2-arm RCT	Patients with NAFLD; **G1:** 37±10†, **G2:** 40±10†,	Ultrasound	ECLIA	**Deficiency:** <80 nmol/L	Hypocaloric diet	Moderate to vigorous exercise for 45–60 min at least 5 days per week	nr
Dasarathy et al. (2017); US	1-arm RCT	Adults with NAFLD ; **G1:** 50.2±13.3†, **G2:** 53.8±10.5†	Biopsy	ECLIA	**Insufficiency:** <75 nmol/L	nr	nr	nr

Lorvand Amiri et al. (2017); Iran	3-arm RCT	Adults with NAFLD, BMI 25-35, vitamin D< 37.5nmol/L; **G1:** 44.0±10.8†, **G2:** 39.8±11.0†, **G3:** 38.3±10.1†	Ultrasound	ELISA	nr	Hypocaloric diet[2]	30min moderate walking[3]	Direct sunlight exposure to less than 1 h/day
Lorvand Amiri et al. (2016); Iran	2-arm RCT	Adults with NAFLD BMI<35 and vitamin D<37.4nmol/L; **G1:** 39.8±11†, **G2:** 44±10.8†	Ultrasound	ELISA	nr	Hypocaloric diet[2]	Maintain routine physical activity[3]	nr
Barchetta et al. (2016b); Italy	2-arm RCT	Adults with T2D and NAFLD; **G1:** 59.8±9.1†, **G2:** 57.4±10.7†	Ultrasound and MRI	ECLIA	**Deficiency:** <50 nmol/L; **Insufficiency:** <75 nmol/L	nr	nr	nr
Papapostoli et al. (2016); Germany	1-arm RCT	Adults with NAFLD and vitamin D deficiency; **G1:** 54.9 ± 12,1†,	TE	ECLIA	**Deficiency:** <50 nmol/L	nr	nr[3]	nr
Foroughi et al. (2016); Iran	2-arm RCT	Adults with NAFLD; **G1 and G2:** mean age of the participants was 48.5	Ultrasound	ELISA	nr	nr[2]	nr[3]	nr
Sharifi et al. (2016); Iran	2-arm RCT	Adults with NAFLD; **Men:** **G1:** 35 [32,50]§ **G2:** 39 [31.48.5]§ Women: **G1:** 47 [43.5, 52.5]§ **G2:** 41 [35, 46.7]§	Ultrasound and ALT	RIA;	nr	Restriction of high carbohydrates and fat diet[3]	Increase physical activity[3]	nr
Kitson et al. (2016); Australia	1-arm RCT	Adults with NAFLD;	Biopsy	nr	**Deficiency:** <50 nmol/L	nr	nr	nr
Foroughi et al. (2014); Iran	2-arm RCT	Adults with NAFLD; **G1 and G2:** 30-70	Ultrasound	ELISA	nr	nr[2]	nr[3]	nr

Sharifi et al. (2014); Iran	2-arm RCT	Adults with NAFLD; **G1:** 43.92±9.51†, **G2:** 40.33±8.65†	Ultrasound and ALT	RIA	**Sufficiency:** ≥75 nmol/L **Insufficiency:** 50-75 nmol/L **Deficiency:** ≤30 nmol/L	Restriction of high carbohydrates and fat diet[2]	Increase physical activity[3]	nr

ALT, alanine aminotransferase; BMI, body mass index; ECLIA, electro-chemiluminescence binding assay; ELISA, enzyme-linked immunosorbent assay; G, group; nr, not recorded; NAFLD, non-alcoholic fatty liver disease; MetS, metabolic syndrome; MRI, magnetic resonance; RCT, randomised controlled intervention trial; RIA, radioimmunoassay; T2D, type 2 diabetes; TE, transient elastography; † Mean±Standard deviation; ‡ Median [Range]; § Median [25th, 75th percentiles]; * Statistic significant; 1 Patients were instructed not to change their usual diet or physical activity through the study; 2 Dietary intake was assessed by food record questionnaire; 3 Physical activity was assessed using the International Physical Activity Questionnaire; 4 Daily exposure to sunlight was assessed by questionnaire.

Table 2.3 Principal liver outcomes of randomised controlled intervention trails of vitamin D supplementation in NAFLD.

Randomised controlled intervention trials in children					
Authors	**Duration and arms**	**Vitamin D status (Before)**	**Vitamin D status (After)**	**Principal liver outcomes**	**Post-intervention changes related to principal liver outcomes and vitamin D status**
El Amrousy et al. (2021);	6-month; **G1:** placebo (n=50) **G2:** 2,000 IU/day vitamin D (n=50)	**G1:** 31.8 [7.5-50]‡, **G2:** 31.5 [14.8-48.5]‡	**G1:** 12.7 [5-19]‡, **G2:** 42 [51.3-133.5]‡	NAS and fibrosis (biopsy), ALT, AST, TC, TG, LDL-C, HDL-C	**G2 (after vs. before):** NAS↓*, steatosis↓*, lobular inflammation↓*, ALT↓*, AST↓*, TC↓*, TG↓*, LDL-C↓*, HDL-C↓*, 25(OH)D↑*; **G2 vs. G1 (after):** NAS↓*, steatosis↓*, lobular inflammation↓*, ALT↓*, AST↓*, TC↓*, TG↓*, LDL-C↓*, HDL-C↓*, 25(OH)D↑*;
Namakin et al. (2021);	12-week; **G1:** placebo (n=50) **G2:** 5,000 IU/week vitamin D (n=51)	**G1:** 28.2 ± 13.7†, **G2:** 24.5 ± 15.8†	**G1:** 32.8 ± 12.0†, **G2:** 74.9 ± 15.9†	ALT, AST, ALP, TC, TG, LDL-C, HDL-C, hs-CRP, hemoglobin, platelet, albumin	**G2 (after vs. before):** ALT↓*, AST↓*, ALP↓*, TG↓*, LDL-C↓*, HDL-C↑*, hemoglobin↑*, platelet↑*, albumin↑*, 25(OH)D↑*; **G2 vs. G1 (after):** 25(OH)D↑*;
Randomised controlled intervention trials in adults					
Gad et al. (2021)	6-month; **G1:** placebo (ampoule containing 2 ml of normal saline 0.9%; n=40) **G2**: single dose intramuscular 200,000 IU/month cholecalciferol (n=40)	**G1:** 43.4 ± 26.5†, **G2:** 40.8 ± 25.6†	**G1:** 46.9 ± 20.8†, **G2:** 98.4 ± 30.0†	CAP (TE), LSM (TE), FIB4 (TE), NFS(TE), AST, ALT, ALP, TC, TG, LDL-C, HDL-C, platelet, haemoglobin, total plasma protein, INR, total bilirubin, direct bilirubin, albumin, creatinine	**G2 (after vs. before):** CAP↓*, LSM↓*, ALT↓*, AST↓*, HDL-C↑*, 25(OH)D↑*, **G2 vs. G1 (after):** CAP↓*, LSM↓*, ALT↓*, AST↓*, LDL-C↓*, HDL-C↑*, 25(OH)D↑*

Morvaridzadeh et al. (2021);	12-week; **G1:** PY (n=44) **G2:** 1,000IU/day vitamin D in pro-YED (n=44)	**G1:** 51.7 ± 28.6†, **G2:** 51.1 ± 27.4†	**G1:** 60.4 ± 38.3†, **G2:** 75.3 ± 26.6†	nr	**G2 (after vs. before):** 25(OH)D↑*, **G2 vs. G1 (after):** 25(OH)D↑*
Mahmoudi et al. (2021)	8-week; **G1**: 0.25 mcg/day calcitriol (n=27), **G2**: 50,000 IU/week cholecalciferol (n=27)	**G1:** 35.3 ± 15.8†, **G2:** 34.7 ± 14.1†	**G1:** 57.6 ± 38.2†, **G2:** 57.8 ± 38.5†	ALT, AST, ALP, TC, TG, LDL-C, HDL-C	**G1 (after vs. before):** ALT↓*, AST↓*, TC↓*, 25(OH)D↑*; **G2 (after vs. before):** 25(OH)D↑*
Yaghooti et al. (2021);	17-week; **G1**: placebo (n=64), **G2**: 0.25 mcg/day calcitriol (n=64)	**G1:** 43.75 ± 19.25†, **G2:** 47.74 ± 24.00†	nr	ALT, AST, ALP, HSI, APRI, TC, TG, LDL-C, HDL-C, hs-CRP	**G2 vs. G1 (after):** ALP↓*
Lukenda Zanko et al. (2020)	12-month; **G1:** placebo (n=110) **G2:** 1,000 IU/day cholecalciferol drops (n=201)	**G1:** 59.3 [12.3-951]‡, **G2:** 47.3 [8.0-606]‡	nr	CAP (TE), LSM (TE), AST, ALT, ALP, GGT, TG, TC, LDL-C; HDL-C, hs-CRP, haemoglobin, albumin, creatinine	**G2 vs. G1 (after 360 days vs. before):** CAP↓*, LSM↓*, GGT↓*, 25(OH)D↑*
Hussain et al. (2019)	12-week; **G1:** placebo (n=51) **G2:** 50,000 IU/week vitamin D (n=51)	**G1:** 38.5 ± 7.05†, **G2:** 31.3 ± 10.5†	**G1:** 43.8 ± 8.8†, **G2:** 61.3 ± 9.5†	Grade of fatty liver (ultrasound); ALT, AST, TC, TG, LDL-C, HDL-C, hs-CRP	**G2 (after vs. before):** ALT↓*, AST↓*, hs-CRP↓*, 25(OH)D↑* **G2 vs. G1 (after):** ALT↓*, AST↓*, 25(OH)D↑*
Shidfar et al. (2019b)	12-week; **G1:** placebo (25 µg/d lactose, n=36) **G2:** 1,000 IU/d (25g/d calciferol) vitamin D (n=37) **G3:** 500mg calcium carbonate+10,000 IU/d vitamin D (n=37);	**G1:** 25.0 ± 1.6†, **G2:** 24.8 ± 1.6†, **G3:** 24.8 ± 2.3†	**G1:** 27.5 ± 2.0†, **G2:** 53.5 ± 1.8†, **G3:** 67.8 ± 2.8†	ALT, AST, LDL-C/HDL-C, TG/HDL-C, TC/HDL-C, non-HDL-C	**G2 (after vs. before):** ALT↓*, AST↓*, 25(OH)D↑* **G3 (after vs. before):** ALT↓*, AST↓*, 25(OH)D↑* **G2 vs. G1 (after):** ALT↓*, AST↓*, LDL-C/HDL-C↓*, TG/HDL-C↓*, TC/HDL-C↓*, non-HDL-C↓*, 25(OH)D↑* **G3 vs. G1 (after):**

					TG/HDL-C↓*, TC/HDL-C↓*, 25(OH)D↑* **G3 vs. G2 (after):** ALT↓*, LDL-C/HDL-C↓*, 25(OH)D↑*
Geier et al. (2018)	48-week; **G1:** placebo (n=10) **G2:** 2,100 IU/d vitamin D (n=8)	**G1:** 50±25†, **G2:** 52.5±30†	**G1:** 40±23†, **G2:** 98±33†	NAS, ALT, AST, ALP, GGT, TG, LDLD-C, HDL-C, CK-18 M30, hs-CRP, hemoglobin, bilirubin,	**G2 (after vs. before):** CK-18 M30↓*, hemoglobin↓*, 25(OH)D↑*
Dabbaghmanesh et al. (2018b)	12-week; **G1:** placebo (n=31) **G2:** 0.25 mg/d calcitriol (n=28) **G3:** 50,000 IU/week cholecalciferol (n=32)	**G1:** 52.8±13.0†, **G2:** 46.5±13.8†, **G3:** 47.3±15.5†	**G1:** 47.0±17.5†, **G2:** 57.3±49.5†, **G3:** 80.5±35.3†	ALT, AST, ALP, GGT, TC, TG, LDL-C, HDL-C	**G2 (after vs. before):** ALT↓*, ALP↓*, HDL-C↑*, **G3 (after vs. before):** ALP↓*, GGT↓*, 25(OH)D↑*; **G2 or G3 vs. G1 (after):** 25(OH)D↑*; **G3 vs. G1 (after):** 25(OH)D↑*
Taghvaei (2018)	12-week; **G1:** placebo (n=20) **G2:** 50,000 IU/week vitamin D3 (n=20);	**G1:** 49.5±10.9†, **G2**: 47.9 ± 13.7†	**G1:** 52.1 ± 6.2†, **G2:** 86.0 ± 10.7†	CAP (TE), fibrosis (TE), ALT, AST, ALP, TC, TC, LDL-C,	**G2 (after vs. before):** CAP↓*, fibrosis↓*, ALT↓*, AST↓*, ALP↓*, 25(OH)D↑* **G2 vs. G1 (after):** 25(OH)D↑*
Sakpal et al. (2017)	48-week; **G1:** placebo (n=30) **G2:** single dose intramuscular 600,000 IU/month vitamin D (n=51)	**G1:** 32.00±16†, **G2:** 30.75±12†,	nr	LSM (TE), ALT, TG, TC, LDL-C; HDL-C, TNF-α	**G2 (after vs. before):** ALT↓*
Dasarathy et al. (2017)	6-month; **G1:** 2,000IU/d cholecalciferol non-responder[1] (n=26);	**G1:** 46.75±12.5†, **G2:** 56.25±11.5†	**G1:** 50.25±12.25†, **G2:** 97.25±19.5†	NAS, ALT, AST, INR, TG, LDL-C, HDL-C, albumin, creatinine, bilirubin	**G2 vs. G1 (after):** ALT↓*, AST↓*, 25(OH)D↑*

	G2: 2,000IU/d cholecalciferol responder[1] (n=16);				
Lorvand Amiri et al. (2017)	12-week; **G1:** placebo (25 µg/d lactose, n=36) **G2:** 1,000 IU/d (25g/d calciferol) vitamin D (n=37) **G3:** 500mg calcium carbonate+10,000 IU/d vitamin D (n=37);	**G1:** 25.0 ± 1.6†, **G2:** 24.8 ± 1.6†, **G3:** 24.8 ± 2.3†	**G1:** 27.5 ± 2.0†, **G2:** 53.5 ± 1.8†, **G3:** 67.8 ± 2.8†	Grade of fatty liver (ultrasound), ALT, AST, TC, TG, LDL-C, HDL-C	**G2 (after vs. before):** Grade of fatty liver↓*, ALT↓*, AST↓*, TG↓*, HDL-C↑*, 25(OH)D↑* **G3 (after vs. before):** Grade of fatty liver↓*, ALT↓*, AST↓*, TG↓*, HDL-C↑*, 25(OH)D↑* **G2 vs. G1 (after):** Grade of fatty liver↓*, ALT↓*, AST↓*, HDL-C↑*, 25(OH)D↑* **G3 vs. G1 (after):** Grade of fatty liver↓*, 25(OH)D↑* **G3 vs. G2 (after):** ALT↓*, HDL-C↑*, 25(OH)D↑*
Lorvand Amiri et al. (2016)	12-week; **G1:** placebo (25μg/d lactose, n=37) **G2:** 25μg/d calcitriol (n=36);	**G1:** 25.2±9.5†, **G2:** 24.8±9.8†	**G1:** 27.5±11.8†, **G2:** 67.8±18†	Grade of fatty liver (ultrasound), ALT, AST, TC, TG, LDL-C, HDL-C	**G2 (after vs. before):** Grade of fatty liver↓*, ALT↓*, AST↓*, TC↓*, TG↓*, HDL-C↑*, 25(OH)D↑* **G2 vs. G1 (after):** Grade of fatty liver↓*, ALT↓*, TG↓*, HDL-C↑*, 25(OH)D↑*
Barchetta et al. (2016b)	24-week; **G1:** placebo (n=29) **G2:** 2,000IU/d cholecalciferol (n=26)	**G1:** 37.1 [27.3-51.6]‡, **G2:** 43.1 [31.1-58.5]‡	**G1:** 40 [20.8-60.5]‡, **G2:** 85.8 [73-110]‡	Grade of fatty liver (ultrasound), HFF (MRI), ALT, AST, ALP, GGT, TC, TG, FFA, LDL-C, HDL-C, CK-18 M30, hs-CRP, FLI, P3NP	**G2 (after 12-week vs. before):** 25(OH)D↑* **G2 (after 24-week vs. before):** 25(OH)D↑* **G2 vs. G1 (after):** 25(OH)D↑*
Papapostoli et al. (2016)	6-month; **G1:** 20,000IU/week cholecalciferol (n=40)	**G1:** 29.5±12†	**G1:** 86.5±32.25 (4-week), 90.75±25.5 (3-month), 87.0±24.5 (6-month)	CAP (TE), LSM (TE), ALT, AST, ALP, GGT, bilirubin, albumin, creatinine	**G1 (after 4-week vs. before):** CAP↓*, 25(OH)D↑* **G1 (after 6-month vs. before):** CAP↓*
Foroughi et al. (2016)	10-week; **G1:** placebo (n=30)	**G1:** 47±2†, **G2:** 49±1†	**G1:** 44.8±0.44†, **G2:** 117±13†	Grade of fatty liver (ultrasound)	**G2 (after vs. before):** 25(OH)D↑*

	G2: 50,000IU/week vitamin D_3 (n=30)				**G2 vs. G1 (after):** 25(OH)D↑*
Sharifi et al. (2016)	4-month; **G1:** placebo (men n=13, women n=13) **G2:** 50,000IU/14d vitamin D_3 (men n=13, women n=14)	**Men:** **G1:** 38.5 [29.3-58.8]‡, **G2:** 39.3 [26.5-73]‡, **Women:** **G1:** 45.8 [26.5-107.8]‡, **G2:** 25 [19-45.3]‡,	**Men:** **G1:** 43.8 [36.3-62.3]‡, **G2:** 75 [63.5-100.8]‡ **Women:** **G1:** 61 [32.5-83]‡, **G2:** 84 [64-133.2]‡	Grade of fatty liver (ultrasound), ALT, AST, TC, TG, LDL-C, HDL-C, hs-CRP,	**G2 (after vs. before):** **Men:** TC↑*, 25(OH)D↑* **Women:** ALT↓*, 25(OH)D↑* **G2 vs. G1 (after):** **Men:** TC↑*, 25(OH)D↑* **Women:** TC↑*, LDL-C↓*, hs-CRP↓*, 25(OH)D↑*
Kitson et al. (2016)	24-week; **G1:** 25,000 IU/week vitamin D_3	**G1:** 63.3±31.6†	**G1:** 109.8±15.6†	NAS, ALT, AST, GGT, TC	**G1 (after vs. before):** 25(OH)D↑*
Foroughi et al. (2014)	10-week; **G1:** placebo (n=30) **G2:** 50,000IU/week vitamin D_3 (n=30)	**G1:** 47±2†, **G2:** 49.1±1†	**G1:** 45.8±0.44†, **G2:** 117±13†	Grade of fatty liver (ultrasound), AST, ALT, ALP, TG, hs-CRP	**G2 (after vs. before):** TG↓*, hs-CRP↓*, 25(OH)D↑* **G2 vs. G1 (after):** 25(OH)D↑*
Sharifi et al. (2014)	4-month; **G1:** placebo (n=26) **G2:** 50,000IU/14d vitamin D_3 (n=27)	**G1:** 42.1 [29.3-62]‡, **G2:** 28.8 [22-71]‡	**G1:** 48 [36.8-66.8]‡, **G2:** 75 [64.5-116.5]‡	Grade of fatty liver (ultrasound), ALT, AST, ALP, hs-CRP, TNFα, TGFβ1	**G2 (after vs. before):** TNFα ↑*, 25(OH)D↑* **G2 vs. G1 (after):** 25(OH)D↑*

ALP, alkaline phosphatase; ALT, alanine aminotransferase; APRI, AST to platelet ration index; AST, aspartate aminotransferase; CAP, controlled attenuation parameter; CK-18 M30, cytokeratin 18 M30; FFA, free fatty acid; FIB4, fiborisis 4 score; FLI, Fatty Liver Index; HDL-C, high-density lipoprotein cholesterol; HFF, hepatic fat fraction; hs-CRP, high sensitivity C-reactive protein; HSI, hepatic steatosis index; INR, international normalized ratio; G, group; GGT, γ-glutamyl transferase; HS, hepatic steatosis; LDL-C, low-density lipoprotein cholesterol; LSM, liver stiffness measurements; MRI, magnetic resonance; NAS, NAFLD activity score; NFS, NAFLD fibrosis score; nr, not reported; pro-YED, probiotic yogurt fortified with vitamin D; P3NP, N-terminal Procollagen III Propeptide; PY, probiotic yogurt; RCT, randomized controlled trial; TC, total cholesterol; TE, transient elastography; TG, triglyceride; TGF$\boldsymbol{\beta}$1, transforming growth factor $\boldsymbol{\beta}$1; TNF-$\boldsymbol{\alpha}$, tumour necrosis factor-$\boldsymbol{\alpha}$; † Mean±Standard deviation; ‡ Median [Range];* Statistic significant; 1. non-responders were those whose posttreatment plasma 25(OH)D concentration remained <30 ng/mL; responders were patients whose posttreatment plasma 25(OH)D concentration was ≥30 ng/mL

All the trials in **Table 2.3** reported the baseline vitamin D status of participants. In addition, serum 25(OH)D was measured and was significantly increased in all studies after the intervention, except two studies did not report the post-treatment serum 25(OH)D level (Sakpal et al., 2017; Yaghooti et al., 2021).

The studies were heterogeneous in liver-related outcomes measurements (**Table 2.3**). Seventeen studies evaluated the effects of vitamin D supplementation on improving the grade of hepatic steatosis or fibrosis in patients with NAFLD, including four studies examined by biopsy (Kitson et al., 2016; Dasarathy et al., 2017; Geier et al., 2018; El Amrousy et al., 2021), and 13 by ultrasound (Sharifi et al., 2014; Foroughi et al., 2014; Sharifi et al., 2016; Foroughi et al., 2016; Barchetta et al., 2016b; Lorvand Amiri et al., 2016; Lorvand Amiri et al., 2017; Hussain et al., 2019) or FibroScan [ultrasound-based transient elastography (TE)] (Papapostoli et al., 2016; Sakpal et al., 2017; Taghvaei, 2018; Lukenda Zanko et al., 2020; Gad et al., 2021).

The liver-related results of the studies in **Table 2.3** were conflicting. Of the 13 studies that used ultrasound or TE, only 6 reported significant improvement in the grade of steatosis or fibrosis in adults at the postinterventional point (Papapostoli et al., 2016; Lorvand Amiri et al., 2016; Lorvand Amiri et al., 2017; Taghvaei, 2018; Lukenda Zanko et al., 2020; Gad et al., 2021). Only one of the four studies using liver biopsy reported histological improvements post vitamin D intervention. However, it should be noted that in this study of children with NAFLD, biopsies were only taken from the intervention group (n=50) (El Amrousy et al., 2021).

On the other hand, elevated liver enzymes [especially ALT, aspartate aminotransferase (AST) and GTT] are a cheap and non-invasive method to define suspected NAFLD (EASL-EASD-EASO, 2016), and are commonly used as surrogate biomarkers of NAFLD in clinical settings. Therefore, 21 of the 23 independent trials reviewed measured serum concentrations of liver enzymes, although the enzymes measured varied between the studies. With the exception of the studies of Foroughi et al. (2016) and Morvaridzadeh et al. (2021) that focused on evaluating the effects of vitamin D on anthropometric and glycemic indices. All 21 studies measured serum ALT levels but only 13

reported significant decreases, consistent with the meta-analysis study of Rezaei et al. (2021). Only two studies informed a decrease in GGT levels in the cholecalciferol arms: 50,000IU/week for 12 weeks (n=32/arm) (Dabbaghmanesh et al., 2018b) and 1,000 IU/day cholecalciferol for 12 months (n=201/arm) (Lukenda Zanko et al., 2020), respectively. In addition to ALT, AST and GGT, some studies indicated a decreased alkaline phosphatase (ALP) levels (Taghvaei, 2018; Dabbaghmanesh et al., 2018b; Namakin et al., 2021; Yaghooti et al., 2021). ALP is a widely distributed hydrolytic enzyme in the human body and is mainly concentrated in the liver (Kaplan, 1972). Thus, an elevated ALP could be found when liver damage or disease occurs.

Approximately four-fifths (19/23) of the clinical trials investigated the association between supplementation and lipid profile in patients with NAFLD. Similar to liver enzymes, the studies regarding the effect of vitamin D on lipid profiles are contradictory. For example, two studies reported vitamin D intake supplementation significantly reduced the low-density lipoprotein cholesterol (LDL-C) and increased high-density lipoprotein cholesterol (HDL-C) in children (Namakin et al., 2021; El Amrousy et al., 2021). Another three studies found that vitamin D supplementation improved HDL-C, but no significant change was found on LDL-C in adults (Lorvand Amiri et al., 2016; Lorvand Amiri et al., 2017; Dabbaghmanesh et al., 2018b). At the same time, nine studies supplementing with vitamin D found no significant effect on lipid profile (Kitson et al., 2016; Barchetta et al., 2016b; Dasarathy et al., 2017; Sakpal et al., 2017; Taghvaei, 2018; Geier et al., 2018; Hussain et al., 2019; Lukenda Zanko et al., 2020; Yaghooti et al., 2021).

Except for hepatic enzymes and lipid profile, many other serum biomarkers involved in the biochemical measurements have been investigated, such as high sensitive C-reactive protein (hs-CRP), cytokeratin-18 (CK-18), TNF-α and TGFβ1. As an inflammatory marker, hs-CRP has been generally used as a cardiovascular risk factor in MetS but has recently found to be a strong predictor for NAFLD as well (Kogiso et al., 2009). Nine studies in **Table 2.3** assessed hs-CRP. However, only three trials reported a significant decrease after 50,000IU/week vitamin D intervention for 10-week to 4-mouth (Foroughi et al., 2014; Sharifi et al., 2016; Hussain et al., 2019).

Notably, in Sharifi et al. (2016) study, the reduction was only observed in women with NAFLD compared to the placebo at the post-interventional point. On the other hand, the CK-18 has been widely investigated to be a serum biomarker for the NASH diagnosis (Vilar-Gomez and Chalasani, 2018). The M30 enzyme-linked immunosorbent assay measures the caspase-cleaved CK18 fragments (CK-18 M30) and detects apoptosis. Cinical trials that measured the level of CK-18 M30 were done in two smaller European populations [n=26-29/arm in Barchetta et al. (2016b), 2,000IU/day for 24-week; n=8-10/arm in Geier et al. (2018), 2,100IU/day for 24-week]. However, only patients in the vitamin D group of Geier et al. (2018) showed a significant decrease of CK-18 M30 after the intervention. On the other hand, while TNF-α is a proinflammatory cytokine proposed to be a non-invasive marker of the hepatic inflammatory process (Hotamisligil et al., 1993), TGFβ1 is a marker of hepatic fibrosis (Czaja et al., 1989). Sharifi et al. (2014) found that vitamin D intake supplementation for 4-month significantly increased serum TNF-α but had no effect on TGF-β1 in patients with NALFD. Nevertheless, another study using single-dose intramuscular injection of 600,000 IU/month vitamin D for 48-week reported no significant change of serum TNF-α (Sakpal et al., 2017).

While vitamin D has been shown to improve insulin sensitivity and glycemic control in people with prediabetes and type 2 diabetes (Mirhosseini et al., 2018; Li et al., 2018), vitamin D supplementation trials in NAFLD have been typically underpowered and inconclusive (Zhang et al., 2019c). In **Appendix Table A5**, twenty studies were identified that have assessed glycaemic indices, such as fasting blood glucose and insulin level, haemoglobin A1C (HbA1C) and HOMA-IR. Approximately 60% of the studies (12/20) reported a significant improvement of IR-related factors after the intervention, especially fasting blood glucose and HOMA-IR, which were consistent with the results of a previous meta-analysis (Rezaei et al., 2021).

Regarding anthropometric measurements (**Appendix Table A5**), the majority of the studies (21/23) assessed BMI, WHR, or body fat content. Interestingly, all the studies reporting a significant decreased in BMI or WHR had diet and physical activity interventions during the trial procedure as well (**Table 2.2**) (Sharifi et al., 2014; Sharifi et al., 2016; Lorvand Amiri et al., 2016; Lorvand Amiri et al., 2017; Shidfar et al., 2019a; Hussain et al., 2019; El

Amrousy et al., 2021). Therefore, the results on improving anthropometric indices have to be interpreted with caution. On the other hand, the data perhaps suggest that combining vitamin D supplementation with effective lifestyle modification might potentially better manage NAFLD.

In summary, although preclinical studies have shown vitamin D treatment improves NAFLD (Karatayli et al., 2020), clinical trials of vitamin D supplementation in patients with NAFLD have typically been small (n=20-30/arm), single centre trials. In addition, trials have been heterogeneous in terms of populations examined (adolescents, adults, multiple ethnicities, participants with either obesity or T2D), baseline vitamin D status (sufficient, insufficient or deficient), the type of vitamin D supplement (vitamin D versus calcitriol), duration and dosage used, and the modality used for diagnosis of NAFLD.

2.2.2.1 Considerations of type, duration and dosage of vitamin D used for supplementation

Vitamin D supplements could theoretically be provided in multiple different chemical forms; e.g., cholecalciferol (vitamin D_3), ergocalciferol (vitamin D_2), calcidiol [calcifediol, 25-hydroxyvitamin D, 25(OH)D], or calcitriol [1,25-dihydrocyvitamin D, 1,25(OH)D] (Vieth, 2020). In the studies reviewed (**Table 2.3)**, cholecalciferol and calcitriol were generally used in the interventional groups. Because ergocalciferol and its metabolites are less stable and not ordinarily detectable in the circulation; ergocalciferol is less potent per microgram dose than cholecalciferol (Tripkovic et al., 2012; Wilson et al., 2017), and it is better to use cholecalciferol for supplementation or fortification. On the other hand, calcitriol is the hormonally active form of cholecalciferol and is most commonly used as a therapeutic hormone replacement drug for patients with kidney failure (Isakova et al., 2017). However, given the high risk of causing hypercalcemia, the use of calcitriol requires careful monitoring.

Few published reports have compared the cholecalciferol and calcitriol forms of vitamin D in NAFLD patients. In **Table 2.3**, the studies done by Dabbaghmanesh et al. (2018b) and Mahmoudi et al. (2021) were the only two that compared the effects of vitamin D forms of cholecalciferol and high-dose calcitriol in NAFLD. While Mahmoudi et al. (2021) reported a significant

decrease in ALT, AST and total cholesterol in the calcitriol group, calcitriol did not show any beneficial effects in the study of Dabbaghmanesh et al. (2018b). In addition, no significant differences of any parameter were observed in participants who received calcitriol compared with those who received cholecalciferol in these two studies.

On the other hand, current guidelines and recommendations for vitamin D dosing regimens are debated (Hollis, 2011; Holick et al., 2011; Ross, 2011; Korgavkar et al., 2014). To date, no interventional studies testing the efficacy and safety of different oral vitamin D supplementation schedules on NAFLD. Another critical issue involves the baseline circulating 25(OH) vitamin D status differences observed among the trials (**Table 2.3**). Many included vitamin D replete (>50nmol/L) individuals (Kitson et al., 2016; Dasarathy et al., 2017; Dabbaghmanesh et al., 2018b; Geier et al., 2018; Lukenda Zanko et al., 2020; Morvaridzadeh et al., 2021). In this context, it is perhaps not surprising that no benefit of vitamin D supplementation on clinical outcomes was found. Once an optimal balance of nutrients has been restored, no additional effects can be produced (Heaney, 2012; Amrein et al., 2020). Nevertheless, in most intervention studies listed in **Table 2.3** the serum 25(OH)D level of the interventional group reached a normal range from a deficient level after the intervention.

Given that, by far, sun exposure is considered to be the primary source for humans to obtain vitamin D (Nair and Maseeh, 2012); when investigating the effects of vitamin D supplementation, it is essential to restrict or measure and use sun exposure time as a confounder. However, of the twenty-three studies reviewed, only two limited direct sunlight exposure to less than 1 h/day (Lorvand Amiri et al., 2017; Shidfar et al., 2019b). Interestingly, comparing the study of Shidfar et al. (2019b) with an earlier published study done by Lorvand Amiri et al. (2017), it seems that these two studies used the same data from the same population. Namely, they outline the same population size, intervention design and vitamin D status (pre-and post-intervention).

In summary, many of the intervention trials reviewed may be biased by methodological and study design issues, making it impossible to show the potential contributing role of vitamin D supplementation in patients with NAFLD. Although expensive, ideally more extensive studies are needed with

rigorous designs to systematically compare different doses of vitamin D for different durations of treatment to establish a safe, effective treatment strategy in children and adults with NAFLD.

2.2.3 Polymorphisms influencing vitamin D status and NAFLD severity

Both vitamin D status and NAFLD are complex phenotypes that arise from dynamic interactions between dietary, lifestyle and genetic factors (Pacifico et al., 2019; Moore, 2019a). Multiple environmental factors have been implicated in vitamin D status, including reduced dietary intakes, minimal sun exposure related to climate change and modern lifestyles, and age-related impairment of hepatic and renal hydroxylation (Pacifico et al., 2019; Mendes et al., 2019). Equally, hypercaloric diets and sedentary lifestyles are critical contributors to the development and progression of NAFLD (Moore, 2019a). In addition to these environmental factors, both NAFLD and vitamin D status are influenced by genetic polymorphisms.

In addition to the NAFLD genetic polymorphisms mentioned in previous section **2.1.2.2**, several genes involved in vitamin D metabolism have been found by GWAS to have polymorphisms that affect circulating vitamin D concentrations. A summary of GWAS studies exploring the variants that influence circulating 25(OH)D levels is in **Appendix Table A6**. Several genetic variants have been identified repeatedly in the GWAS studies. These include variants in the dehydrocholesterol reductase-7 (DHCR7) gene, which reduces 7-dehydrocholesterol to cholesterol. In addition, DHCR7 is in linkage disequilibrium with nicotinamide adenine dinucleotide synthetase-1 (NADSYN1) that catalyses the final step of NAD biosynthesis (Ahn et al., 2010; Wang et al., 2010b; Jiang et al., 2018). Polymorphisms in the NADSYN1 gene have also been associated with vitamin D status (Ahn et al., 2010; Jiang et al., 2018); along with variants of the group-specific component (GC) gene that encodes the vitamin D binding protein (DPB) responsible for transporting vitamin D in serum (Ahn et al., 2010; Wang et al., 2010b; Anderson et al., 2014; Jiang et al., 2018; O'Brien et al., 2018b; Kampe et al., 2019). Furthermore, polymorphisms in multiple genes encoding for CYP enzymes involved in the formation of 25(OH)D and 1α,25(OH)$_2$D along with the inactivation of 1α,25(OH)$_2$D (CYP2R1, CYP27B1 and CYP24A1 respectively)

have also been associated with vitamin D status (Ahn et al., 2010; Wang et al., 2010b; Anderson et al., 2014; Manousaki et al., 2017; Jiang et al., 2018; O'Brien et al., 2018b; Kampe et al., 2019). Additionally, a recent targeted NGS study of the entire 101kB VDR found rs141114959 was significantly associated with low circulating 25(OH)D level in older Filipino women (Zumaraga et al., 2017).

However, only a few studies have investigated whether vitamin D-related single nucleotide polymorphisms (SNPs) affect the progression and severity of NAFLD and the results are conflicting. A summary of published studies that examined genetic polymorphisms related to vitamin D status and NAFLD is shown in **Table 2.4**. These studies include one RCT, three cross-sectional studies, four case-control studies and two MR studies have examined the relationship between genetic modifiers of vitamin D status and NAFLD.

In the earlier study, Beilfuss et al. (2015b) found in 106 patients with obesity and NAFLD and inadequate vitamin D status that VDR SNPs (rs4516035, rs1544410 and rs757343) were associated with liver fibrosis. A separate cross-sectional study (control patients n=39, patients with biopsy-proven NAFLD n=244) by Patel et al. (2016) reported that polymorphisms in VDR and other vitamin D-related genes did not affect the progression and severity of NAFLD. However, another more recent study done in a large Chinese population (control n=1903, NAFLD n=1123) found that VDR variants (rs2228570-A and rs11168287-A) were significantly reduced the risk of NAFLD (Zhang et al., 2021c). Whereas CYP24A1 (rs2296241 and rs2248359) and CYP27B1 (rs4646536) were associated with an increased risk of NAFLD (control n=1909, NAFLD n=1114) in the Chinese Han population (Wang et al., 2018c).

All three cross-section studies were done in patients with biopsy-proven NAFLD (Arai et al., 2019; Gibson et al., 2018; Liu et al., 2021b). In a Japanese adult population (n=220), a polymorphism in the VDR gene (rs1544410) was significantly associated with advanced liver fibrosis (Arai et al., 2019). Separately in a UK paediatric population (n=103), variants of the NADSYN1/DHCR7 (rs12785878, rs3829251) and VDR (rs2228570) genes were independently associated with increased steatosis (Gibson et al., 2018).

Table 2.4 Studies examining genetic polymorphisms related to vitamin D status and NAFLD

Reference; Country	Design; Sample Size (NAFLD/NN)	Study Population; Age	Diagnosis of NAFLD	Vitamin D Assay; Definition of Inadequacy; Status (nmol/L)	Vitamin D or NAFLD Related Polymorphisms	Summary of Associations
Yuan and Larsson (2022); Europe	Two-sample bidirectional MR; Anstee et al GWAS: 1483/17781, The FinnGen consortium: 894/217898, UKBB: 275/360919	Adults with or without NAFLD; ≥18	nr	nr; nr; nr	**Vitamin D related:** **GC:** rs3755967, **CYP2R1:** rs10741657, rs117913124, **DHCR7:** rs12785878, **AMDHD1:** rs10745742, **SEC23A:** rs8018720, **CYP24A1:** rs17216707 **NAFLD related:** **LEPR:** rs12077210, **ZNF512:** rs2068834, **HSD17B13:** rs13118664, rs88220112, **CILP2:** rs17216588, rs17216588, **PNPLA3:** rs738409, rs738408, **GCKR:** rs1260326, **MARC1:** rs2642438	The FinnGen consortium: **CYP24A1** rs17216707 associated with an decrease risk of NAFLD; The UKBB: **GC** rs3755967 associated with an decrease risk of ALP and AST, **CYP24A1** rs6013897 associated with an decrease risk of ALP, **DHCR7** rs12785878 and **SEC23A** rs8018720 associated with an decrease risk of AST
Liu et al. (2021b); China	Cross-sectional; 531 (531/0)	Adults with NAFLD; 18-75	Biopsy	nr; **Sufficiency:** ≥75 **Insufficiency:** 50-75 **Deficiency:** <50; **A allele:** 58.0±19.1†, **Non-A allele:** 63.5±19.8†	**NAFLD related:** **KL** rs495392	**KL** rs495392 (A allele) had a protective effect on steatosis severity; the patients carrying the A allele had significant higher serum levels of 25(OH)D; the rs495392 A allele attenuated the detrimental impact of

						PNPLA3 rs738409 G allele on the risk of severe hepatic steatosis
Wang et al. (2021); China	Case-control; 3023 (1114/1909)	Adults with or without NAFLD; 18-60	Liver enzymes, biopsy or ultrasound	nr; nr; nr	**Vitamin D related:** **CYP2R1:** rs10741657, rs12794714, rs2060793 and rs1993116 **CYP24A1:** rs2296241, rs2248359, rs927650, and rs6068816 **CYP27B1:** rs703842, rs10877012, and rs4646536	**CYP24A1** rs2296241 and rs2248359, and **CYP27B1** rs4646536 associated with an elevate risk of NAFLD
Zhang et al. (2021c)[1]; China	Case-control; 3023 (1120/1903)	Adults with or without NAFLD; ≥18	Liver enzymes, biopsy or ultrasound	ELISA; **Sufficiency:** ≥75 **Insufficiency:** 50-75 **Deficiency:** <50; **NAFLD:** 40.15 (30.53, 51.95)§ **Control:** 50.00 (42.10, 66.70)§	**Vitamin D related:** **VDR:** rs3782905, rs3847987, rs11574129, rs2228570, rs11568820, rs739837, rs7975232 and rs11168287	**VDR** rs2228570-A and rs11168287-A alleles reduced the risk of NAFLD
Yaghooti et al. (2021); Iran	RCT; 128 (128/0)	Adults with NAFLD; 18-60	TE	nr; nr; **Before RCT: Placebo:** 43.75 ± 19.25†, **Calcitriol group:** 47.74 ± 24.00†, **After RNCT:** nr	**Vitamin D related:** **VDR:** rs2228570	Under calcitriol treatment, patients with the FokI FF and Ff genotypes of **VDR** rs2228570 associated with the ALP level; patients with the Ff genotype had lower ALP activity
Arai et al. (2019); Japan	Cross-sectional; 220 (220/0)	Adults with NAFLD; 18-84	Biopsy	RIA; **Sufficiency:** ≥75 **Insufficiency:** 50-75 **Deficiency:** <50; 45.0 [17.5-97.5]‡	**Vitamin D related:** **CYP2R1**: rs1993116, rs10741657 **DHCR7:** rs7944926, rs12784878,	**CYP2R1** rs1993116 genotype non-AA and **VDR** rs228570 genotype GG associated with VDD; **VDR** rs1544410 genotype CC associated with advanced liver fibrosis

					GC: rs2282670 **CYP27B1:** rs10877012, **VDR:** rs2228570, rs1544410, rs7975232, rs731236	
Gibson et al. (2018); UK	Cross-sectional; 103 (103/0)	Children with NAFLD; 11-16	Biopsy	CLIA reported by season; **Deficiency:** <25 **Insufficiency:** 25-50; **Spring:** 36.6 [30.5-42.1]* **Summer:** 41.8 [36.3-47.2]* **Autumn:** 40.8 [34.2-47.5]* **Winter:** 26.9 [22.7-31.2]*	**Vitamin D related:** **NADSYN1:** rs12785878, rs3829251 **GC:** rs2282670, rs7041, rs4588 **CYP2R1:** rs10741 **VDR:** rs2228570	**NADSYN1** rs3829251, **CYP2R1** rs10741657 and **VDR** rs2228570 associated with increased steatosis; **GC rs4588** associated with increased inflammation in liver biopsies
Wang et al. (2018c); China	One sample bidirectional MR; 9128	General population; 18-93	Ultrasound	CLIA; nr; **VD GRS:** **Quartile 1:** 41.8±12.9† **Quartile 2:** 40.4±12.3† **Quartile 3:** 39.6±12.5† **Quartile 4:** 38.7±11.9† **NAFLD GRS:** **Quartile 1:** 40.2±12.4† **Quartile 2:** 40.3±12.7† **Quartile 3:** 40.0±12.2† **Quartile 4:** 40.0±12.4†	**Vitamin D related:** **DHCR7:** rs12785878, **CYP2R1:** rs10741657 **GC:** rs2282679, **CYP24A1:** rs6013897 **NAFLD related:** **LYPLAL1:** rs12137855 **PPP1R3B:** rs4240624 **TM6SF2:** rs58542926 **PNPLA3:** rs738409 **GCKR:** rs780094 **SAMM50:** rs738491 **PARVB:** rs5764455 **COL13A1:** rs1227756	**GC** rs2282679 and **DHCR7** rs12785878 were significantly associated with 25(OH)D; **GCKR** rs780094, **PNPLA3** rs738409 and **PARVB** rs5764455 associated with NAFLD
Patel et al. (2016); US	Case-control, 263(224/39)	Patients with or without NAFLD; 18-65	Biopsy	CLIA; **Sufficiency:** >75 **Insufficiency:** 50-75 **Deficiency:** <50; **Controls:** 69.8±32.0† **NAFLD:** 69.0±29.5†	**Vitamin D related[2]:** **CYP2R1, CYP3A4, GC, CYP24A1, CYP27A1, CYP28B1, VDR, PTH, RXR, SMAD, NCOA, PPAR**	Polymorphisms in vitamin D-related genes had no effect on the progression and severity of NAFLD

Beilfuss et al. (2015b); German	Case-control, 117(107/10)	Patients with obese with or without NAFLD; 18-65	Biopsy	ELISA; nr; nr	**<u>Vitamin D related:</u>** **VDR:** rs4516035, rs7975232, rs1544410, rs731236, rs757343	**VDR rs4516035**: Compared to patients with AA or AG, homozygous carriers of the GG allele of the had significantly lower VDR mRNA; patients with AA homozygous had significantly lower TGF-β and α-SMA, and correlated with VDR mRNA expression and collagen 1-α; **VDR rs1544410:** Patients with GG allele had significantly lower TGF-β mRNA; **VDR rs757343:** Compared to patients with AG Patients with GG had significantly higher VDR and α-SMA mRNA

ALP, alkaline phosphatase; AST, aspartate aminotransferase; AMDHD1, amidohydrolase domain containing 1; α-SMA, alpha-smooth muscle actin; CILP2, cartilage intermediate layer protein 2; CLIA, chemiluminescent immunoassays; COL13A1, collagen type XIII alpha 1 chain CYP2R1, cytochrome P450 2R1; CYP24A1, cytochrome P450 24A1; CYP27A1, cytochrome P450 27A1; CYP27B1, cytochrome P450 27B1; CYP3A4, cytochrome P450 3A4; DHCR7, 7-dehydrocholesterol reductase; ELISA, enzyme-linked immunosorbent assay; HSD17B13, hydroxysteroid 17-beta dehydrogenase 13; GC, vitamin D binding protein; GCKR, glucokinase regulatory protein; GWAS, genome-wide association study; KL, klotho; LEPR, leptin receptor; LYPLAL1, lysophospholipase-like 1; NADSYN1, adenine dinucleotide synthetase-1; NCOA, nuclear receptor coactivator; NN, Non-NAFLD; nr, not reported; MARC1, mitochondrial amidoxime reducing component 1; MR, Mendelian randomisation; PARVB, parvin beta; PTH, parathyroid hormone; PNPLA3, patatin-like phospholipase domain-containing protein 3; PPAR, peroxisome proliferator-activated receptor; PPP1R3B, protein phosphatase 1 regulatory subunit 3b; RIA, radioimmunoassay; RXR, retinoic X receptor; SAMM50, sorting and assembly machinery component; SEC23A, Sec23 homolog A, COPII coat complex component; TE, transient elastography; TGF-β, transforming growth factor beta; TM6SF2, transmembrane 6 superfamily member 2; UKBB, UK Biobank; VDR, vitamin D receptor; ZNF512, zinc finger protein 512; ‡ Median [Range]; * Mean [95%CI]; † Mean $\pm$ Standard Deviation; § Median (Interquartile range); 1. Serum 25(OH)D levels were measured in 336 NAFLD cases and 336 controls; 2. rs number not available.

In contrast, a GC gene variant (rs4588) was associated with increased inflammation. In addition, in a larger Chinese population (n=531), patients carrying the klotho (KL) rs495392-A had a protective outcome on steatosis and attenuated the detrimental effect of PNPLA3 rs738409-G on the risk of severe hepatic steatosis (Liu et al., 2021b).

On the other hand, in a large Chinese population (n=9128) diagnosed by ultrasound, Wang and colleagues notably used one-sample bidirectional MR to explore the causal relationship between 25(OH)D and NAFLD (Wang et al., 2018c). MR uses SNPs that explain trait variance in the general population to make causal inferences regarding the effect of lifetime exposure to that trait with disease incidence or outcome. MR avoids many limitations of conventional epidemiological studies (such as residual confounding and reverse causation) as the populations under investigation are randomised from birth based on their genotype (Sekula et al., 2016). The authors examined four variants related to vitamin D status and eight associated with NAFLD in this study (**Table 2.4**) (Wang et al., 2018c). The results showed three SNPs (GCKR rs780094, PNPLA3 rs738409 and PARVB rs5764455) were significantly associated with NAFLD, and two SNPs (GC rs2282679 and DHCR7 rs12785878) were significantly associated with serum 25(OH)D status. However, in applying MR utilising polygenetic risk scores (for both vitamin D status and NAFLD), the authors concluded no causal association between vitamin D and NAFLD. In contrast, a two-sample bidirectional MR study released recently in three European populations revealed an inverse genetic association between serum 25(OH)D level and risk of NAFLD (Yuan and Larsson, 2022). Additionally, serum 25(OH)D level was negatively correlated with ALP, but not ALT and AST in the UKBB population.

Only one study to date evaluated the efficiency of vitamin D treatment in NAFLD patients with different genotypes of VDR rs2228570 (Yaghooti et al., 2021). There are four common SNPs in the VDR gene: rs7975232, rs1544410, rs731236, and rs2228570 (Zmuda et al., 2000). Yaghooti et al. (2021) found no significant interactions between the homozygous F and heterozygous VDR rs2228570 and the calcitriol effects on fatty liver. However, patients with the Ff genotype were more responsive to the intervention and had lower ALP activity.

The key limitation of these studies is that the total 25(OH)D levels were measured in serum and bioavailability in the liver cannot be accounted for. Additionally, the hepatic expression of genes responsible for vitamin D metabolism may be altered or switched off in the context of significant liver injury, which could threaten the validity of the results. MR presents a valuable tool to assess the causality of vitamin D status and NAFLD. However, an MR study in a single population may be limited by ethnicity and the potential contribution assessment of rare variants related to vitamin D and NAFLD heritability. Therefore, further MR studies examining rare variants and large multi-ethnic populations are likely warranted.

2.2.4 The crosstalk between the gastrointestinal microbiome and the VDR in NAFLD

The gastrointestinal microbiome is an additional factor that most likely influences the progression of NAFLD, in the first instance through influencing nutrient uptake from the diet, as well as the enterohepatic circulation of nutrients and bile acids (He et al., 2021a; Tilg et al., 2021). In the context of obesity, MetS and NAFLD, dysbiosis or altered gut microflora can result in intestinal permeability and chronic inflammation in patients (Safari and Gerard, 2019; Jayakumar and Loomba, 2019). Approximately 75% of liver blood comes from the intestine via the portal vein, thus exposing the liver to the gastrointestinal microbiome and its endotoxins, such as peptidoglycan and lipopolysaccharides (Schwenger et al., 2018; Safari and Gerard, 2019). Endotoxin exposure can trigger the activation of inflammatory cytokines that contribute to NAFLD pathogenesis. Although murine studies have found associations between NAFLD and certain bacteria, studies in humans reporting differences in the intestinal bacteria between healthy controls and NAFLD have been mainly cross-sectional to date (Schwenger et al., 2018). Therefore, the causal relationships between NAFLD and gastrointestinal microbiome pathology remain uncertain.

On the other hand, the gastrointestinal tract is a leading VDR expression site (Wang et al., 2012c). Most interestingly, a recent GWAS of the gut microbiota in a German population identified significant associations for overall microbial variation and individual taxa at multiple genetic loci, including the VDR gene (Wang et al., 2016a). This is consistent with evidence that

vitamin D and its receptor VDR play a vital role in gut homeostasis by regulating gut microbiota (Sun, 2018). Furthermore, genetic deletion of VDR in mice has been shown to influence the intestinal microbiome at taxonomic and functional levels, resulting in a higher risk of infections, inflammation, cancer and other conditions (Jin et al., 2015). Additionally, in pre-clinical models of NAFLD, a vitamin D deficient, high-fat diet (HFD) led to gut permeability, dysbiosis, endotoxemia, systemic inflammation, insulin resistance and hepatic steatosis; conversely, dietary vitamin D supplementation attenuated steatosis (Su et al., 2016). These results suggest that further studies of vitamin D and VDR signalling at the genetic and functional levels and its microbiome regulation in the gut-liver axis will provide novel mechanistic insights and therapeutic opportunities for NAFLD.

2.2.5 Summary

Experimental research has shown that vitamin D has antiproliferative, anti-inflammatory and anti-fibrotic properties, which might impact disease progression in chronic liver diseases, including NAFLD (**Figure 2.5**). However, epidemiological studies have remained inconclusive, either examining vitamin D status in patients with NAFLD or examining the efficacy of vitamin D supplementation for treating NAFLD. Only a few heterogeneous trials with insufficient participants have been done to date. These were hampered by the challenges of diagnosing NAFLD and the lack of data on clinically meaningful outcomes. The overall quality of evidence is very low. On the basis of current studies, there is limited evidence for a role for the vitamin D-related polymorphisms in NAFLD. In addition, only two MR studies explored the causal inference between vitamin D and NAFLD but have inconsistent results. However, genetic and experimental evidence showed vitamin D and VDR play essential roles in regulating the microbiome in health and disease. Further mechanistic studies of this pathway influencing the gut–liver axis in NAFLD are warranted.

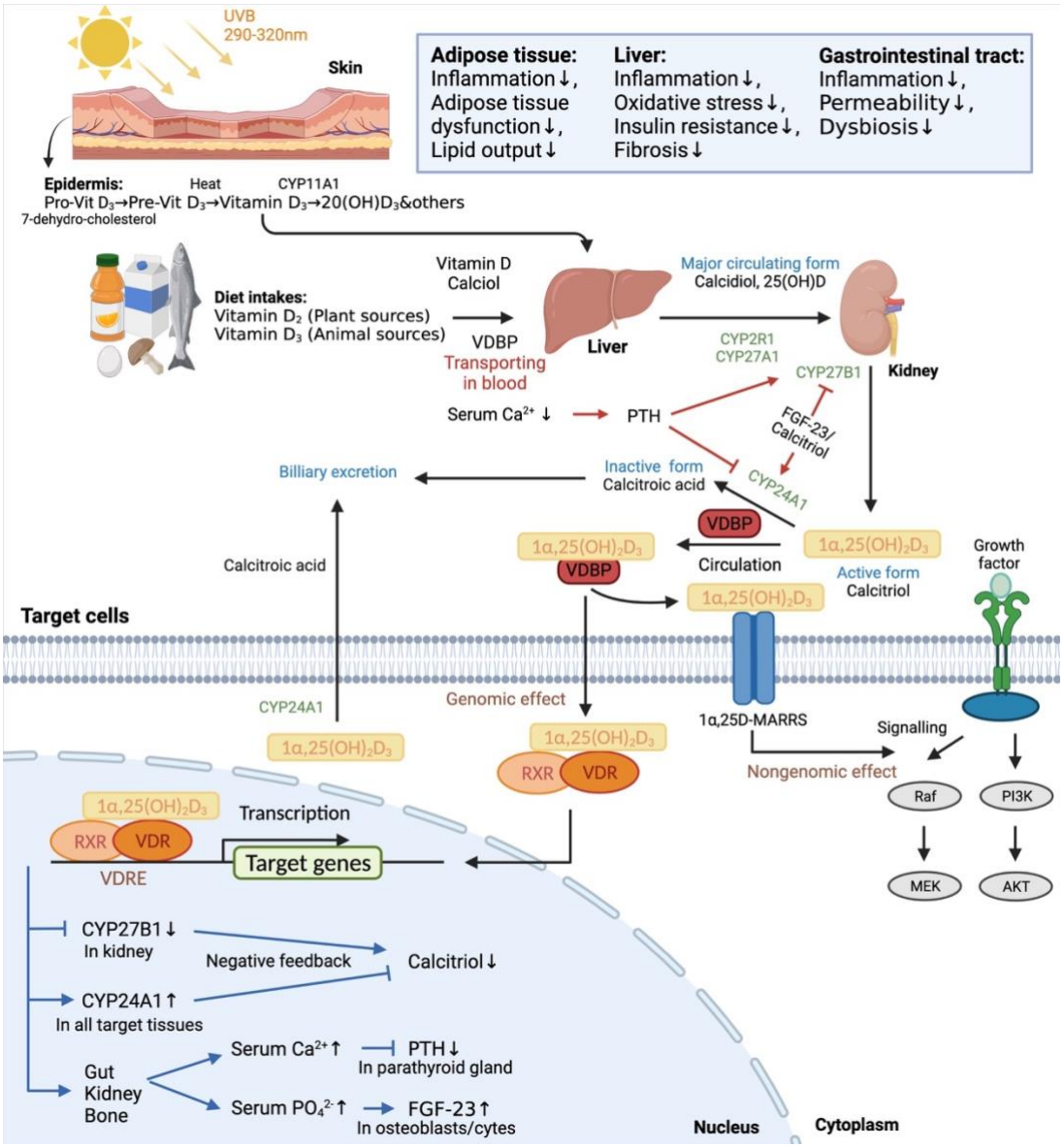

Figure 2.5 Overview of vitamin D metabolism and potential pathways linking vitamin D/vitamin D receptor (VDR) axis to NAFLD. Vitamin D is a misnomer for a family of secosteroid hormones with pleiotropic actions. The active biologically active metabolite of vitamin D, 1α,25(OH)$_2$D$_3$, that bind to their cognate nuclear receptors to regulate diverse physiological processes. The classical and alternative vitamin D metabolic pathways, and hormonal regulation of vitamin D metabolism, are summarised in this figure. The red arrows and inhibitors present hormonal regulation; the blue arrows and inhibitors present feedback regulatory. Additionally, the potential involvement of the vitamin D/VDR axis in the pathogenesis and progression of NAFLD has been suggested by experimental studies linking vitamin D-mediated pathways to critical processes leading to liver steatosis, inflammation, and fibrosis. Indeed, vitamin D may influence NAFLD development directly and indirectly. The blue intersection box summarises potential pathways linking the vitamin D/VDR axis to NAFLD development. This figure was created with BioRender.

Chapter 3
A comprehensive review of microRNA regulation in NAFLD and by vitamin D

3.1 Overview

As reviewed in section **2.1.1**, the molecular pathogenesis of NAFLD is complex, involving numerous signalling molecules involved in hepatic metabolism, oxidative, inflammatory and fibrotic processes (Moore, 2019b). Notably, miRNAs play an essential role in gene expression and regulatory networks involved in lipid and carbohydrate metabolism (Rottiers and Näär, 2012) and cellular stress response pathways (Mendell and Olson, 2012). Moreover, dysregulation of miRNA expression in the liver is associated with hepatic inflammation, fibrosis and the development and progression of multiple liver diseases, including NAFLD (Gjorgjieva et al., 2019b; Wang et al., 2020c).

In addition, a volume of evidence indicates that miRNAs mediate the cellular response of vitamin D, including the post-transcriptional regulation of the VDR (Zenata and Vrzal, 2017) and the anticancer and antifibrotic properties of vitamin D (Zeljic et al., 2017; Udomsinprasert and Jittikoon, 2019). Although the anticancer and antifibrotic effects of vitamin D have been observed in the liver (Wu et al., 2018; Udomsinprasert and Jittikoon, 2019), a potential role for vitamin D regulated miRNAs in NAFLD remains unexplored. Therefore, the aims of this chapter were to first comprehensively review the data from human profiling or mechanistic studies investigating miRNA in NAFLD pathogenesis. Secondly, to examine the evidence for the modulation of human serum miRNAs by vitamin D status or in response to dietary intakes or supplementation, along with any research that has specifically investigated the influence of vitamin D on liver-related miRNAs. Ultimately integrating the data, this chapter finally aims to critically assess the evidence for a potential subset of miRNAs that are both dysregulated in NAFLD and modulated by vitamin D.

Based on current miRNA nomenclature conventions, the prefix ‘miR’ recedes a number that indicates the order of miRNA identification. Lettered suffixes indicate closely related mature miRNAs with nearly identical sequences (e.g. miR-30b and miR-30c). Different precursors or genomic loci leading to the same identical mature miRNA sequences within a species are denoted with an additional suffix number (e.g. miR-30c-1 and miR-30c-2). Lastly, the -3p and -5p suffixes are used to specify mature miRNAs originating from opposite arms of the same pre-miRNA (Budak et al., 2016). Although both the –5p and –3p strands may be functional depending on the context, experimental data suggests the mature -5p strand is more frequently found as a bioactive ‘guide strand’ (Chiang et al., 2010; Alles et al., 2019). The family member and –5p and –3p suffixes of mature miRNAs have not always been consistently reported (Paterson and Kriegel, 2017). Due to the missing detailed information of mature miRNAs in most studies, this notation is not used throughout the text of this chapter. However, the reported family member names and mature form suffixes from the studies reviewed are detailed in the tables.

3.2 MicroRNAs in NAFLD pathogenesis

In light of the aforementioned variables that may confound the reproducibility of miRNA research, I comprehensively surveyed the literature and examined the data from serum profiling or mechanistic studies involving liver tissues to identify miRNAs with good evidence for altered levels in humans with NAFLD. Specifically, ‘good evidence’ was defined as experimentally replicated beyond array or RNA sequencing (RNAseq) profiling, and identified in at least 2 independent studies. The PubMed database was searched from inception through 30th April 2021 using the Medical Subject Headings (MeSH) terms: ‘NAFLD’, ‘NASH’, ‘MAFLD’, ‘MASH’ and ‘microRNAs’ (**Figure 3.1**). In total, there were 548 records according to the retrieval strategy. Literature reviews, systematic reviews, bioinformatic analysis and studies that were not related specifically to NAFLD and miRNA were discarded. Eventually, 81 studies were adopted and summarized.

A close data review identified 67 unique miRNAs (**Figure 3.2A**: 46 in the liver, 41 in serum, and 20 in both). Focusing on miRNAs found dysregulated

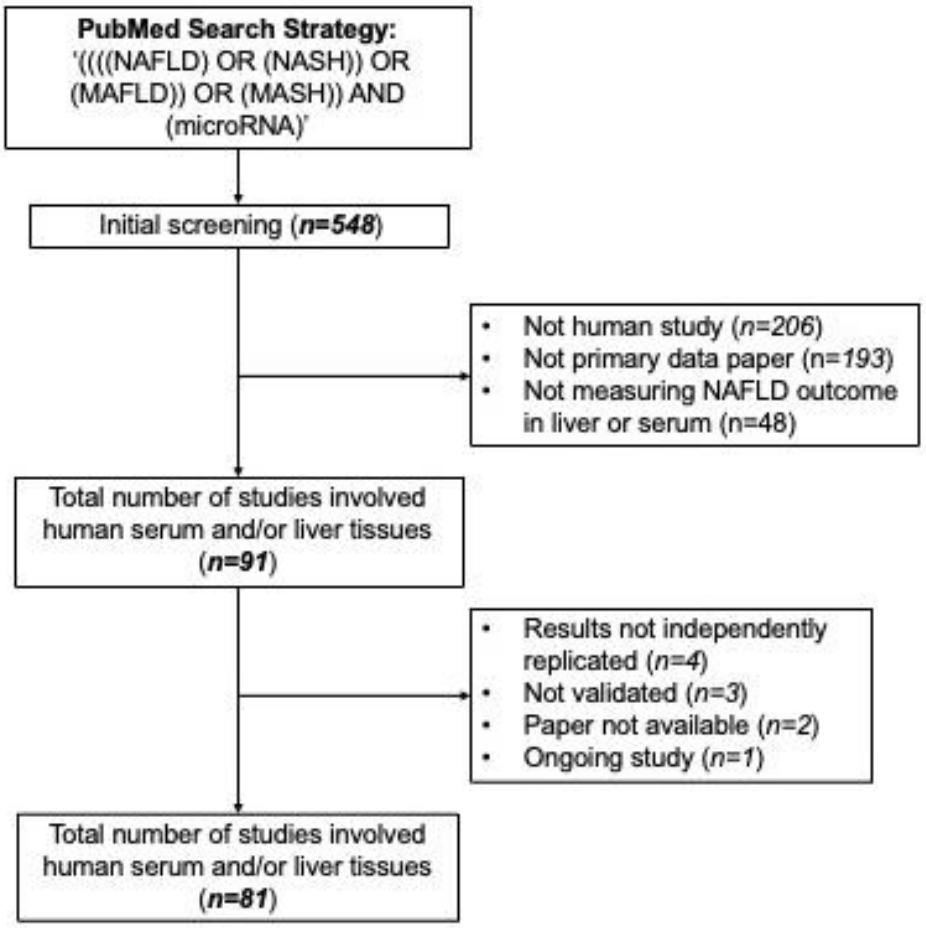

Figure 3.1 Flow chart of studies of NAFLD and miRNA identified in PubMed. PubMed search strategies: '((((NAFLD) OR (NASH)) OR (MAFLD)) OR (MASH)) AND (microRNA)'; search was from PubMed inception through 07/06/2021.

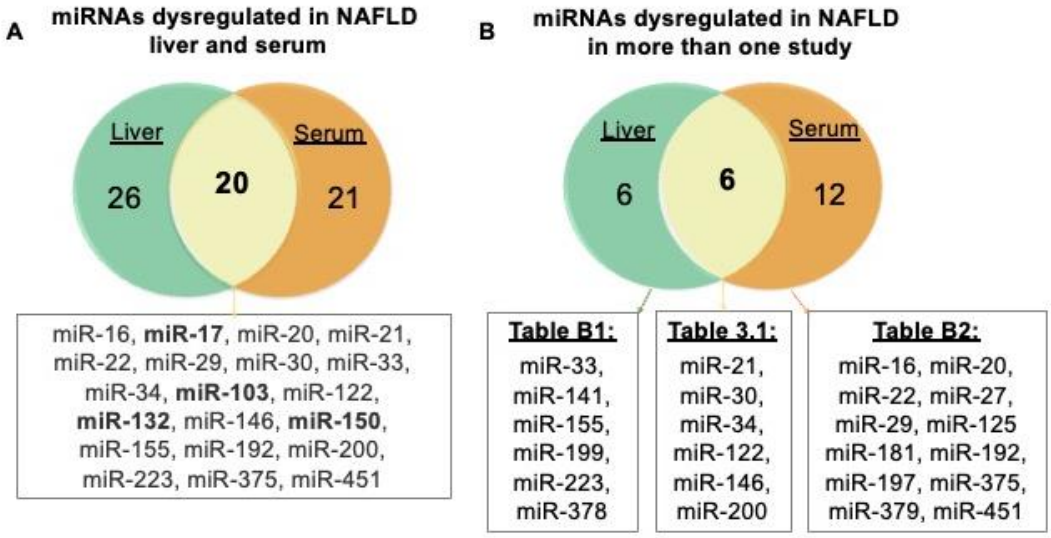

Figure 3.2 Venn Analysis of miRNAs found altered in serum and liver from humans with NAFLD. A. Close data review identified 67 unique miRNAs (46 in the liver, 41 in serum, and 20 in both) validated beyond array or RNASeq profiling. Four miRNAs (miR-17, miR-103, miR-132 and miR-150) were identified in one liver and one serum study (bold in the intersection box). **B.** Focusing on miRNAs found dysregulated in subjects with NAFLD in at least two independent studies identified six miRNAs in liver only (**Appendix B Table B1**) and 12 miRNAs in serum (**Appendix B Table B2**). Six miRNAs were found dysregulated in both liver and serum in at least 2 independent studies (**Table 3.1**)

in subjects with NAFLD from participants with NAFLD in more than one study, 12 miRNAs in the liver and 18 miRNAs in serum were identified. Six miRNAs were found dysregulated in both liver and serum (miR-21, miR-30, miR-34, miR-122, miR-146 and miR-200; **Table 3.1**). While an additional 5 miRNAs (miR-33, miR-141, miR-122, miR-155, miR-199 and miR-378) were identified as only altered in livers (**Appendix Table B1**), and a further 12 (miR-16, miR-20, miR-22, miR-27, miR-29, miR-125, miR-181, miR-192, miR-197, miR-375, miR-379 and miR-451; **Appendix Table B2**) were found altered in serum only.

Potential limitations to the data collection strategy utilized here were: 1) not limiting to studies where the data was adjusted or matched for the relevant confounders, such as age, gender and BMI; and 2) not limiting to studies that only used biopsy for NAFLD. Notably, human NAFLD studies requiring a liver biopsy are typically done in single centres and are often limited in size, similar to miRNA biomarker discovery studies more generally (Keller and Meese, 2016). Therefore, the number of participants in each study group was noted in addition to summarising the direction of expression of the miRNAs and the stages of NAFLD examined. Expectedly, liver sample sizes (n ranged from 3 to 58 per group; **Table 3.1** and **Appendix Table B1**) were smaller than the number of observations in serum (n ranged from 3 to 383 per group **Table 3.1 and Appendix Table B2**). While serum samples typically came from NAFLD case series, liver samples were often from bariatric surgery patients or tissue banks. Only one unusual case (Braza-Boïls et al., 2016b) used post-mortem series. Despite heterogeneous study designs, there was reasonably good concordance between studies in the (generally increased) direction of the miRNAs found dysregulated.

Due to the potential value of diagnostic and therapeutic targets in NAFLD, I briefly outline relevant regulatory functions of the 6 miRNAs found dysregulated in both liver and serum (**Table 3.1**). The functional and pathophysiological effects of these miRNAs are summarized in **Table 3.2** as well. The insights of miRNA-based clinical usages in NAFLD, involving predictive non-invasive biomarkers identification and pharmacological analogues/inhibitors exploitation, are discussed as well.

Table 3.1 miRNAs dysregulated in both liver and serum from NAFLD patients

miRNA	Sample	Summary
miR-21	Liver	**Up** (*miR-21*) in NASH (n=3) vs. controls (n=3) [NIH liver tissue repository] (Dattaroy et al., 2015)
		Up (*miR-21*) in NASH (n=11) vs. steatosis (n=8) and HCs (n=6) [pathology database] (Loyer et al., 2016)
		Up (*miR-21*) in NASH vs. steatosis [N=28, patients with bariatric surgery] (Rodrigues et al., 2017)
		Down (*miR-21-5p*) in NALFD (n=12) vs. non-NALFD (n=15) [postmortem samples, NCSD] (Braza-Boïls et al., 2016b)
	Serum	**Up** (*miR-21*) in NAFLD (n=48) vs. HCs (n=90) [in males but not females (n=44 NAFLD, n=221 HC)] (Yamada et al., 2013)
		Up (*miR-21*) in NASH (n=87) vs. NAFL (n=50) and HCs (n=61); positive correlation with ALT, steatosis and lobular inflammation (Becker et al., 2015)
		Up (*miR-21*) in NASH (n=31) vs. HCs (n=37); positive correlation with hepatic activity† (Liu et al., 2016b)
		Up (*miR-21*) in NASH vs. steatosis [N=24, patients with bariatric surgery] (Rodrigues et al., 2017)
		Up (*miR-21-5p*) in F>2 (n=29) vs. F≤2 (n=46); positive correlation with ALT, AST, APRI (NAFL n=25, NASH n=50, HCs n=17) (López-Riera et al., 2018a)
		Down (*miR-21*) in NAFLD (n=25) vs. HCs (n=12) (Sun et al., 2015b)
miR-30	Liver	**Down** (*miR-30b-5p)* in NAFLD (n=17) and borderline NAFLD (n=24) vs. controls (n=19); negative correlation with NAFLD [patients with bariatric surgery] (Latorre et al., 2017a)
		Down (*miR30b/c*) in >5% steatosis (n=41) vs. <5% steatosis (n=19) [patients with bariatric surgery] (Latorre et al., 2020)
	Serum	**Up** (*miR-30a-3p*) in NAFLD (n=11) vs. HCs (n=10) (Wang et al., 2020b)
		Down (*miR-30c*) in NAFLD (n=18) vs. HCs (n=62) (Zarrinpar et al., 2016)
		Down (*miR-30c-5p*) in SAF≥2 (n=50) vs. SAF<2 (n=25), **down** in NAS≥5 (n=38) vs. NAS<5 (n=37), **down** in F>2 (n=29) vs. F≤2 (n=46); negative correlation with FIB4, BARD, NAFLD_FS (NAFL n=25, NASH n=50, HCs n=17) (López-Riera et al., 2018a)
miR-34	Liver	**Up** (*miR-34a*) in NASH (n=25) vs. normal histology (n=25) [participants with metabolic syndrome] (Cheung et al., 2008)

		Up (*miR-34a*) in NASH (n=13) vs. steatosis (n=15) [patients with bariatric surgery] (Castro et al., 2013)
		Up (*miR34a*) in NASH (n=8) vs. normal histology (n=8) [liver tissue bank] (Xu et al., 2015)
		Up (*miR-34a-5p*) in NASH (n=42) vs. non-NALFD (n=37) [postmortem samples, CSD and NCSD] (Braza-Boïls et al., 2016b)
		Up (*miR-34a-5p*) in NASH (n=11) vs. controls (n=10) and NAFL (n=12) [patients with bariatric surgery] (Guo et al., 2016b)
		Up (*miR-34a*) in steatosis (n=4) vs. non-steatosis (n=4) [liver tissue bank] (Wang et al., 2018b)
	Serum	**Up** (*miR-34a*) in NAFLD (n=34) vs. HCs (n=19), **up** in NASH (NAS>5) vs. steatosis, **up** in steatosis vs. HCs discriminated NASH from steatosis (AUROC=0.764) (Cermelli et al., 2011)
		Up (*miR-34a*) in NAFLD (n=44) vs. HCs (n=221) [adult females], **up** in NAFLD (n=48) vs. HCs (n=90) [adult males] (Yamada et al., 2013)
		Up (*miR-34a*) in NAFLD (n=28) vs. HCs (n=36); discriminated NAFLD from HCs (AUROC=0.781) (Salvoza et al., 2016)
		Up (*miR-34a*) in NAFLD (n=18) vs. HCs (n=62) (Zarrinpar et al., 2016)
		Up (*miR-34a*) in NASH (n=31) vs. NAFL (n=17) and HCs (n=37); positive correlation with histological severity but not fibrosis; discriminated NASH from non-NASH (AUROC=0.811) (Liu et al., 2016b)
		Up (*miR-34a-5p*) in SAF≥2 (n=50) vs. SAF<2 (n=25), **up** in NAS≥5 (n=38) vs. NAS<5 (n=37); positive correlation with ALT, AST, ferritin, APRI, FIB4 and total bilirubin (NAFL n=25, NASH n=50 and HCs n=17); discriminated SAF≥2 from SAF<2 (AUROC=0.76) (López-Riera et al., 2018a)
		Up (*miR-34a*) with inflammation (NALFD N=116, post-transplant protocol biopsy in liver transplant recipients) (Erhartova et al., 2019);
		Up (*miR-34a*) in NAFLD (n=210) vs. HCs (n=90), **up** in NASH (n=86) vs. steatosis (n=124); positive correlation with ALT, AST and histological severity; discriminated NAFLD from HCs (AUROC=0.77) and NASH from steatosis (AUROC=0.84) (Hendy et al., 2019)
		Up (*miR-34a-5p*) with increasing fibrosis severity [N=132, patients with NAFLD]; in multivariate analyses, positive correlation with steatosis, fibrosis, the PNPLA3 I148M and TM6SF2 E167K variants; discriminated fibrosis from no fibrosis (AUROC= 0.75, 73, 0.75 and 0.76 for stages 1, 2, 3 and 4) (Ezaz et al., 2020)
miR-122	Liver	**Up** (*miR-122*) in >33% steatosis vs. <33% steatosis, **down** in severe fibrosis vs. no or mild fibrosis [N=52 patients with NAFLD confirmed by biopsy]; negative correlation with fibrosis, positive correlation with serum miR-122 levels (Miyaaki et al., 2014)

	Up (*miR-122-5p*) in steatosis (n=20) vs. NNL (n=14) and NASH (n=31); negative correlation with AST [patients with liver biopsy] (Pirola et al., 2015)
	Up (*miR-122-5p*) in NAFLD (n=13) vs. controls (n=3) [female patients with bariatric surgery] (Naderi et al., 2017)
	Down (*miR-122*) in NASH (n=25) vs. normal histology (n=25) [participants with metabolic syndrome] (Cheung et al., 2008)
	Down (*miR-122*) in the more severe NASH (n=8) vs. less severe NASH (n=5) and steatosis (n=15) [participants with metabolic syndrome] (Castro et al., 2013)
	Down (*miR-122*) in steatosis vs. non-steatosis [N=14 non-tumour tissue from non-hepatitis B/C HCC resections] (Takaki et al., 2014)
	Down (*miR-122-5p*) in NASH (n=42) vs. non-NALFD (n=37) [postmortem samples, CSD and NCSD]; positive correlation with NAFLD scoring (Braza-Boïls et al., 2016b)
	Down (*miR-122-5p*) in NAFLD (n=17) and borderline NAFLD (n=24) vs. controls (n=19); negative correlation with NAFLD [participants with metabolic syndrome] (Latorre et al., 2017a)
Serum	**Up** (*miR-122*) in NAFLD (n=34) vs. HCs (n=19), **up** in NASH vs. steatosis, **up** in steatosis vs. HCs; discriminated steatosis from HCs (AUROC=0.927) and NASH from steatosis (AUROC=0.698) (Cermelli et al., 2011)
	Up (*miR-122*) in NAFLD (n=44) vs. HCs (n=221) [adults females], **up** in NAFLD (n=48) vs. HCs (n=90) [adult males]; positive correlation with steatosis severity (Yamada et al., 2013)
	Up (*miR-122*) in >33% steatosis vs. <33% steatosis, **down** in severe fibrosis vs. no or mild fibrosis [N=67 patients with NAFLD]; negative correlation with fibrosis, positive correlation with hepatic miR-122 levels; discriminated fibrosis (AUROC=0.82) (Miyaaki et al., 2014)
	Up (*miR-122-5p*) in NAFLD (n=103) vs. HCs (n=80); discriminated NAFLD from HCs (AUROC=0.759) (Tan et al., 2014)
	Up (*miR-122-5p*) in NASH (n=47) vs. steatosis (n=30) and HCs (n=19), **up** with histological severity; positive correlation with ALT, AST, GGT and serum CK-18 levels; discriminated histological severity (AUROC range 0.61-0.71) (Pirola et al., 2015)
	Up (*miR-122*) in NASH (n=87) vs. NAFL (n=50) and HCs (n=61), **up** in NAFL vs. HCs; positive correlation with ALT, steatosis, lobular inflammation and serum CK18-Asp396 (Becker et al., 2015)
	Up (*miR-122*) with histological severity except fibrosis stage 4; positive correlation with ALT, AST, GGT and ferritin [N=305 NAFLD] (Akuta et al., 2016b)
	Up (*miR-122*) in NAFLD (n=28) vs. HCs (n=36); discriminated NAFLD from HCs (AUROC=0.858) (Salvoza et al., 2016)

Up (*miR-122*) in NAFLD (n=18) vs. HCs (n=62) (Zarrinpar et al., 2016)

Up (*miR-122*) in NAFLD (n=40) vs. controls (n=22), **up** in NASH (n=22) vs. steatosis (n=18) [MO women]; discriminated NAFLD from controls (AUROC=0.82) and histological severity from mild disease (AUROC=0.76) (Auguet et al., 2016a)

Up (*miR-122*) in circulating exosomes in advanced stage NAFLD (n=3) vs. early stage NAFLD (n=3) (Lee et al., 2017b)

Up (*miR-122*) in severe NAFLD (n=14) and mild NAFLD (n=36) vs. HCs (n=61), [independent European cohorts of children with obesity]; positive correlation with ALT, AST and serum CK18 (Brandt et al., 2018)

Up (*miR-122)* in NAFLD (n=58) vs. HCs (n=34), **up** in NAS ≥ 4 (n=32) vs. NAS < 4 (n=24) and HC (n=34), up in NAS < 4 (n=24) vs HC (n=34); discriminated NAFLD from HCs (AUROC=0.831) (Jampoka et al., 2018)

Up (*miR-122-5p*) in NAFLD (n=52) vs. controls (n=48); discriminated NAFLD from controls (AUROC=0.774) [adults with T2DM] (Ye et al., 2018b)

Up (*miR-122*) in NAFLD (n=210) vs. HCs (n=90) and **up** in NASH (n=86) vs. steatosis (n=124); positive correlation with ALT, AST and histological severity; discriminated NAFLD vs. HCs (AUROC=0.92) and NASH (AUROC=0.81) (Hendy et al., 2019)

Up (*miR-122*) in NASH (n=31) vs. NAFL (n=17) and HCs (n=37), **up** in NAFL (n=17) vs HCs (n=37); positive correlation with histological severity but not fibrosis (Liu et al., 2016b)

Up (*miR-122-5p*) in SAF≥2 (n=50) vs. SAF<2 (n=25), **up** in NAS≥5 (n=38) vs. NAS<5 (n=37); positive correlation with ALT, AST, ferritin, APRI and BARD (NAFL n=25, NASH n=50 and NL n=17) (López-Riera et al., 2018a)

Up (*miR-122*) with inflammation vs. non-inflammation and ballooning vs. non-ballooning (NALFD N=116, post-transplant protocol biopsy in liver transplant recipients) (Erhartova et al., 2019)

Up (*miR-122-5p*) with increasing fibrosis severity (N=132 patients with NAFLD); in multivariate analyses, positive correlation with steatosis, fibrosis, the PNPLA3 I148M and TM6SF2 E167K variants (Ezaz et al., 2020)

Up (*miR-122*) in NAFLD (n=120) vs. controls (n=60); positive correlation with ALT, AST and GGT [patients with obesity] (Hegazy et al., 2021)

Down (miR-122) with improved histopathological features; positive correlations between serum miR-122 ratio (ratio of level at second biopsy to that at first biopsy) and changes in histological scores as well as ALT, AST, GGT and ferritin [N=36 patients with NAFLD that had repeat biopsies] (Akuta et al., 2016a)

		Down (miR-122) associated with risk of mortality (HR 4.35, P=0.025) in multivariate analyses, and poor cumulative mortality rates over 10 years [N=392 patients with NAFLD confirmed by biopsy that had median 4.7 years follow up] (Akuta et al., 2020)
miR-146	Liver	**Up** (*miR-146b*) in NASH (n=25) vs. normal histology (n=25) [participants with metabolic syndrome] (Cheung et al., 2008)
		Up (*miR-146b-5p*) in NAFLD (n=17) vs. controls (n=19) and borderline NAFLD (n=24); positive correlation with NAFLD [patients with bariatric surgery] (Latorre et al., 2017a)
		Up (*miR-146*) in steatosis (n=4) vs. non-steatosis (n=4) [liver tissue bank] (Wang et al., 2018b)
	Serum	**Down** (miR-146b) in NAFLD (n=20) vs. HCs (n=20); discriminated NAFLD from HCs (AUROC=0.75) (Celikbilek et al., 2014)
		Up (*miR-146b*) in NASH (n=31) vs. HCs (n=37) (Liu et al., 2016b)
miR-200	Liver	**Up** (*miR-200c*) in NASH fatty liver (n=20) vs. NASH non-fatty liver(n=15) and normal histology (n=10) [liver tissue bank] (Tran et al., 2017a);
		Up (*miR-200a/b/c*) in steatosis (n=4) vs. non-steatosis (n=4) [liver tissue bank] (Wang et al., 2018b)
		Down (*miR-200b/c*) in NAFLD (n=11) vs. HCs (n=11) [patients confirmed by biopsy] (Guo et al., 2016a)
	Serum	**Up** (*miR-200a*) with increasing fibrosis severity (N=132 patients with NAFLD); in multivariate analyses, positive correlation with fibrosis and TM6SF2 E167K variants (Ezaz et al., 2020)
		Up (*miR-200*) in NAFLD (n=57) vs. HCs (n=30) (Wang et al., 2020e)

ALT, alanine aminotransferase; AST, aspartate transaminase; APTI, AST to platelet ratio index (fibrosis score); AUROC, the area under the receiver operating characteristic; CHB, chronic hepatitis B; CK18, cytokeratin-18; CSD, cardiac sudden death; CVD, cardiovascular disease; eLP-IR, enhanced lipo-protein insulin-resistance index; F, fibrosis%; FIB4, fibrosis 4; GGT, gamma-glutamyl transpeptidase; HC, healthy control; HCC, hepatocellular carcinoma; HR, hazard ratio; LFTs, liver function tests; MO, morbidly obese, NAFL, non-alcoholic fatty liver; NAFLD, non-alcoholic fatty liver disease; NAS, NAFLD activity score; NASH, non-alcoholic steatohepatitis; NCSD, non-cardiac sudden death; NNL, near normal liver; PBC, primary biliary cirrhosis; PNPLA3, patatin-like phospholipase domain containing protein 3; SAF, steatosis, activity, fibrosis score; T2DM, type 2 diabetes mellitus; TM6SF2, transmembrane 6 superfamily member 2; † Activity is the sum of the score of lobular inflammation and hepatocellular ballooning.

Table 3.2 Serum miRNA profiling studies examining vitamin D status

MicroRNA	Sample type	Summary
miR-21	Liver	*P47phox* mRNA, 3-nitrotyrosine immunoreactivity, NF-κB activation and the immunoreactivity of TGF-β, CTGF, EDAFN, α-SMA and Col1α, and SMAD2/3 and SMAD7 nuclear colocalizations: **up** in NASH (n=3) vs HCs (n=3); SMAD7 protein: **down** in NASH vs HCs (Dattaroy et al., 2015)
		Hepatic PPARα protein: **down** in NASH vs. steatosis [N=28, patients with bariatric surgery] (Rodrigues et al., 2017)
	Serum	Serum *HMGCR* mRNA and protein: **up** NAFLD (n=25) vs. HCs (n=12) (Sun et al., 2015b)
miR-30	Liver	Hepatic *ACSL1*, *Dicer* and *AMPK* mRNA: **down** in >33% steatosis (n=16) vs. <5% steatosis (n=19) (Latorre et al., 2020)
	Serum	Not investigated
miR-34	Liver	Hepatic SIRT1 protein: **down** in NASH (n=13) vs. steatosis (n=15); p53 acetylation: **up** in NASH vs. steatosis; TUNEL-positive cells: **up** in more severe NASH (n=8) vs. less severe NASH (n=5) and steatosis [patients with obesity] (Castro et al., 2013)
		HNF4α mRNA: **down** in NASH vs. HCs [HCs or NASH n=8] (Xu et al., 2015)
		Hepatic circRNA_0046367: **down** in NAFLD (n=5) vs. non-steatosis (n=3); hepatic *PPARα* mRNA and protein, PPARα/β-actin ratio: **down** in NAFLD vs. non-steatosis (Guo et al., 2017)
	Serum	Not investigated
miR-122	Liver	Hepatic *CTDNEP1* mRNA, lipin-1 mRNA and protein: **up** in NAFLD (n=13) vs. controls (n=3) [female obese adults] (Naderi et al., 2017)
	Serum	Not investigated
miR-146	Liver	Not investigated
	Serum	Not investigated
miR-200	Liver	Hepatic SREBP1 and FAS: **up** in NAFLD (n=11) vs. HCs (n=11) [patients confirmed by liver biopsy] (Guo et al., 2016a)
	Serum	Not investigated

ACSL1, acyl-CoA synthetase long chain family member 1; Col1α, collagen α1; CTGF, connective tissue growth factor; CTDNEP1, contactin associated protein 1; EDAFN, extra domain A-fibronectin; HMGCR, 3-hydroxy-3-methylglutaryl-co-enzyme A reductase; HNF4α, hepatocyte nuclear factor 4α; NAFL, non-alcoholic fatty liver; NAFLD, non-alcoholic fatty liver disease; NASH, non-alcoholic steatohepatitis; NNL, near normal liver; NS, not specified; PPARα, peroxisome proliferator-activated receptor α; PRKAA1, AMP-activated protein kinase; SIRT1, sirtuin 1; α-SMA, α-smooth muscle actin; SMAD7, mothers against decapentaplegic homolog 7; SREBP1, sterol regulatory element-binding protein 1; TGF-β, transforming growth factor-β; TUNEL, terminal deoxynucleotidyl transferase dUTP nick end labelling; 3 N-Tyr, 3-nitrotyrosine.

3.2.1 MiR-21

Initially found dysregulated in the development of multiple cancers, miR-21 is considered an 'oncomiR' (Folini et al., 2010). More recently, however, miR-21 has been shown to more broadly play a critical role in various inflammatory and fibrotic diseases, including liver diseases (Kumarswamy et al., 2011). After being found downregulated in ob/ob mice (Li et al., 2009), miR-21 has been further investigated for a functional role in the pathogenesis of NAFLD. Notably, the ob/ob (or obese) mice completely lack functional leptin due to a nonsense mutation on the obese gene (leptin encoding gene, *Lepob*) and the ob/ob mice were generally used as a T2D model (Sparsø et al., 2008). In the context of patients with NAFLD, upregulation of miR-21 has been widely found in both liver (Dattaroy et al., 2015; Loyer et al., 2016; Rodrigues et al., 2017) and serum (Yamada et al., 2013; Becker et al., 2015; Liu et al., 2016b; Rodrigues et al., 2017). In addition, circulating miR-21 has been found to positively correlate with serum levels of liver enzymes such as ALT (Becker et al., 2015; López-Riera et al., 2018b), as well as with steatosis, lobular inflammation (Becker et al., 2015), and hepatic activity (Liu et al., 2016b) (**Table 3.1**). Two studies separately showed lower miR-21 levels measured by real-time reverse transcription-polymerase chain reaction (RT-qPCR) in the liver and serum of patients with NAFLD. One was using post-mortem liver samples from coronary artery disease patients with and without cardiac sudden deaths (Braza-Boïls et al., 2016a); another serum-based study was done in a smaller Chinese population [NAFLD n=25 vs. healthy controls (HCs)], and the diagnosis of NAFLD was not specified (Sun et al., 2015b).

The data reviewed from experimental studies suggests that miR-21 can regulate various signalling pathways in NAFLD, including those mediating IR, steatosis, inflammation and fibrosis (Benhamouche-Trouillet and Postic, 2016; Zhang et al., 2020). Experimental knockdown (Wu et al., 2016) or deletion (Calo et al., 2016) of miR-21 in mice with a HFD distinctly impairs hepatic lipid accumulation and steatosis. Several major transcriptional regulators involved in glucose and lipid metabolism have been shown to be the direct targets of miR-21. These include forkhead box protein O1 (FOXO1), hepatocyte nuclear factor 4 alpha (HNF4-α), SREBP-1c (Wu et al., 2016; Calo et al., 2016), and 3-hydroxy-3-methylglutaryl-coenzyme A reductase (HMGCR) (Sun et al.,

2015b). Additionally, miR-21 is profibrotic and is interestingly the most upregulated miRNA in activated HSCs (Caviglia et al., 2018). Thereby miR-21 contributes critically to the process of hepatic inflammation and fibrosis by regulating the expression of multiple genes, such as PPARα and mothers against decapentaplegic homolog (SMAD) 7 (Noetel et al., 2012; Benhamouche-Trouillet and Postic, 2016; Zhang et al., 2020), and is considered a potential therapeutic target in multiple fibrotic diseases (Liu et al., 2016a). However, the genetic deletion of miR-21 in carbon tetrachloride (CCl4)-induced toxic liver fibrosis mice and $MDR2^{KO}$ cholestatic liver fibrosis mice did not restrain fibrosis (Caviglia et al., 2018).

In summary, while studies to date have illustrated that miR-21 may have potential biomarker or therapeutic applicability in NAFLD, further research is required to fully unravel the complexity of miR-21's different functions during the different stages of NAFLD pathogenesis, as well as for other liver diseases.

3.2.2 MiR-30

In comparison to the other 5 miRNAs summarised in **Table 3.1**, there were relatively fewer human studies that investigated the biological function of miR-30 in NAFLD (**Table 3.1**). One challenge in interpreting the data is that the miR-30 family contains five members (miR-30a through miR-30e). Besides the issues mentioned above of inconsistent specification of a family member and –5p and –3p forms in the literature, miR-30 family members share common seeding sequences, which can interfere with expression profiling and can only be distinguished clearly through high-throughput sequencing (Stokowy et al., 2014). Two studies, which appeared to have used samples from the same group of bariatric surgery patients, reported decreased hepatic miR-30b and/or miR-30c expression (Latorre et al., 2017b; Latorre et al., 2020). On the other hand, two other studies reported a decrease of serum miR-30c in NAFLD (Zarrinpar et al., 2016; López-Riera et al., 2018b), with one of these reporting decreased levels and negative correlations between miR-30c and multiple aspects of disease severity (López-Riera et al., 2018a). However, only a study with fewer participants (NAFLD n=11 vs. HCs n=12) reported increased circulating miR-30a level (Wang et al., 2020b).

Nonetheless, there were some experimental data to suggest a role for miR-30 in NAFLD pathogenesis. A recent review details the anti-fibrotic

properties of miR-30, which notably has been found decreased in the context of HSC activation, hepatic fibrosis and cirrhosis in multiple models of liver injury, as well as human cirrhotic liver (Ezhilarasan, 2020). Indeed, both *in vitro* and *in vivo* studies indicated that overexpression or restoration of miR-30a suppresses HSC activation by inhibiting epithelial-mesenchymal transition (EMT), reducing cell proliferation and migration, consistent with its reported function of tumour suppressor (Zheng et al., 2018). Besides its anti-fibrotic properties, an experimental study reported that miR-30a-3p via targeting PPARα promotes the triglyceride accumulation in hepatocytes induced by fat milk (Wang et al., 2020b). Conversely, another single *in vitro* study indicated that in immortalised human hepatocytes, fatty acid deposition triggered by both AMP-activated protein kinase (AMPK) disruption and DICER knockdown was attenuated by the ectopic recovery of miR-30b and miR-30c (Latorre et al., 2020). Because of limited experimental data, the biological roles of miR-30, especially other family members, in NAFLD have not been fully explored, and more research is undoubtedly required.

3.2.3 MiR-34

Similar to the majority of miRNAs in **Table 3.1**, increased expression of miR-34 have been extensively reported in both liver (6 studies) and serum (9 studies) from patients with NALFD. Higher serum miR-34 levels have been found in more advanced stages of NAFLD (Cermelli et al., 2011; Yamada et al., 2013; Liu et al., 2016b; López-Riera et al., 2018a; Hendy et al., 2019; Ezaz et al., 2020), and shown to correlate with histological severity (Liu et al., 2016b; Hendy et al., 2019; Ezaz et al., 2020) and two common genetic variants associated with hepatic steatosis and accelerated fibrosis, the PNPLA3 I148M and TM6SF2 E167K variants (Ezaz et al., 2020). In addition, moderate diagnostic accuracy has been found in multiple studies for miR-34 in discriminating NAFLD (Salvoza et al., 2016; Hendy et al., 2019), NASH (Cermelli et al., 2011; Liu et al., 2016b; López-Riera et al., 2018a; Hendy et al., 2019), and fibrosis (López-Riera et al., 2018a; Ezaz et al., 2020) with the area under the receiver operating characteristics (AUROCs) ranging from 0.73 to 0.84.

Notably, a recent meta-analysis published in 2020, which examined the utility of miRNAs as non-invasive biomarkers of NAFLD, concluded that miR-

34a had moderate diagnostic accuracy (AUROC=0.85) for NAFLD (Xin et al., 2020). Among the three miRNAs most commonly studied (miR-34a, miR-99a and miR-122), miR-34a had the lowest heterogeneity (I^2 = 5.73% for sensitivity and I^2 = 33.16% for specificity) among the studies meta-analysed. Furthermore, an earlier meta-analysis from 2018 indicated that miR-34 had the best diagnostic accuracy (AUROC=0.7783) for discriminating NASH vs NAFLD (steatosis), while miR-122, discussed in detail below, was best at distinguishing NAFLD from healthy controls (AUROC=0.8174) (Liu et al., 2018). Interestingly, a recent systematic review has determined that both miR-34a and miR-122 may be useful diagnostic biomarkers in obese children with and without NAFLD (Oses et al., 2019).

As direct targets of the tumour suppressor gene p53, the conserved miR-34 family is associated with cell growth arrest and apoptosis promotion, and the repression of miR-34a and miR-34b/c genes is typically observed in cancer with p53 activation (He et al., 2007; Hermeking, 2010). MicroRNA-34a is a transcriptional target gene of p53 and itself targets SRIT1. Therefore, the miR-34a/SIRT1/p53 forms a positive regulatory feedback loop, as p53 triggers the increase of miR-34a and miR-34a increases p53 acetylation by repressing SRIT1 expression (Hermeking, 2010; Rottiers and Näär, 2012). Besides, SIRT1 as a NAD-dependent deacetylase is directly deacetylating multiple metabolic regulators of relevance to NAFLD pathogenesis, including SREBP-1c, the PPARs (alpha and gamma), the farnesoid X receptor (FXR) and liver X receptors (LXR, alpha and beta); as well as NF-κB and p53 itself (Li et al., 2007; Rottiers and Näär, 2012; Kosgei et al., 2020). Thus, a regulatory loop is formed that links cholesterol, lipid and energy homeostasis to inflammation and p53-dependent apoptosis.

Experimental evidence suggests possible benefit from targeting and inhibiting the miR-34 mediated pathway in the more advanced stages of NAFLD, such as fibrosis (Castro et al., 2013; Derdak et al., 2013; Feili et al., 2018), although some conflicting data exist around effects in HSCs (Tian et al., 2016; Feili et al., 2018). Tian et al. (2016) reported that in co-culture of hepatocytes and HSCs, the activation of the miR-34a/SIRT1/p53 pathway in hepatocytes, not in HSCs, leading to its apoptosis, thus promoting HSCs activation and fibrosis. In contrast, Feili et al. (2018) indicated that miR-34a

overexpression in HSCs reduced fibrosis by targeting *Smad4* and inhibiting the TGF-β1/*Smad3* pathway. Interestingly, resveratrol, a naturally occurring dietary polyphenol that activates SIRT1, has been tested in several small clinical trials for benefit in NAFLD and other metabolic diseases (Ding et al., 2017; Kosgei et al., 2020). However, a recent meta-analysis synthesizing data from six RCTs found that, although resveratrol significantly lowered TNF-α and hs-CRP levels, there were no changes in numerous other cardiometabolic risk markers (Rafiee et al., 2021). More potent, synthetic SIRT1 agonists are under development, and some are in early phase clinical trials (Ding et al., 2017).

3.2.4 MiR-122

MicroRNA-122, a highly expressed, liver-specific miRNA, is essential for lipid metabolism and has anti-inflammatory and anti-carcinogenic effects in the liver (Esau et al., 2006; Hsu et al., 2012). Unsurprisingly, miR-122 has been the most explored miRNA in NAFLD, and has been considered as a potential biomarker for pathological changes as well as a therapeutic target for multiple liver diseases, including steatosis, hepatitis and HCC (Jopling, 2012; Bandiera et al., 2015). I identified 22 studies that measured miR-122 levels in serum, and 8 studies that examined hepatic miR-122 expression in NAFLD (**Table 3.1**). Of the 22 serum studies, 20 found increased levels of miR-122 positively correlated with markers of NAFLD severity. Consistent with these findings, serum miR-122 was found decreased with histological improvement on second biopsy in a small number of patients with NAFLD in Japan (Akuta et al., 2016a). Although, other data from the same group suggests that at stage 4 fibrosis miR-122 levels decrease (Akuta et al., 2016b), and that decreased levels of miR-122 (expressed relative to the median of the cohort) may be associated with risk of mortality (Akuta et al., 2020).

Multiple studies found miR-122 to have moderate diagnostic accuracy in discriminating either NAFLD (Cermelli et al., 2011; Tan et al., 2014; Salvoza et al., 2016; Ye et al., 2018b), NASH (Cermelli et al., 2011; Hendy et al., 2019), or histological severity (Miyaaki et al., 2014; Pirola et al., 2015; Auguet et al., 2016a). A diagnostic assay for miR-122 is in pre-clinical development and has been tested in the context of drug-induced liver injury (Rissin et al., 2017). However, miR-122 dysregulation has been found in multiple liver diseases

and other metabolic diseases, including T2D and obesity (Becker et al., 2015; Auguet et al., 2016b; Ye et al., 2018a; Oses et al., 2019). Therefore, any potential utility for miR-122 as a biomarker for NAFLD will most likely be in combination with other miRNAs (e.g. miR-34a and miR-192) or biochemical markers such as transaminases and CK-18 (Becker et al., 2015; Xin et al., 2020). Notably, the limited number of currently available miRNA-based diagnostics for other diseases are panels of 10 or more miRNAs (Bonneau et al., 2019).

On the other hand, the studies of miR-122 hepatic expression were more inconclusive. Sample sizes were typically small, and participants and/or liver samples were heterogenous in origin and variable in disease stage of NAFLD. Of the five studies reporting miR-122 decreased in liver biopsies, three were staged as NASH (Castro et al., 2013; Braza-Boïls et al., 2016b; Cheung et al., 2008), one as NAFLD (Latorre et al., 2017a), and one involved a small number of non-tumour HCC resected liver samples with steatosis (Takaki et al., 2014). Of the three studies reporting increased expression of hepatic miR-122 in steatosis, two found decreased expression in more advanced disease, e.g. NASH (Pirola et al., 2015) and fibrosis (Miyaaki et al., 2014); and the third specifically excluded NASH samples, only examining steatosis in patients with bariatric surgery (Naderi et al., 2017).

The hepatic data perhaps suggest decreased expression of miR-122 in advanced disease, and the possibility of increased expression in steatosis. This fits a hypothesis of an early defensive response (in steatosis) and later causal factor in NASH progression (Wang et al., 2020c), and reconciles with several lines of experimental data highlighting the complexity of the dynamics of miR-122 expression and secretion in the regulation of lipid metabolism. While antisense oligonucleotide inhibition of miR-122 *in vivo* has been shown to have beneficial effects on plasma cholesterol and hepatic steatosis in HFD fed (60% lard, for 19 weeks) mice (Esau et al., 2006); separately, genetic deletion of miR-122 caused steatohepatitis and tumourigenesis (Tsai et al., 2012; Hsu et al., 2012). In addition, free fatty acids have been demonstrated to increase the expression and secretion of miR-122 inhibiting triglyceride synthesis in both liver and muscle (Chai et al., 2017). This mechanism would account for the increased serum levels of miR-122, but underscores that

circulating miRNAs do not always reflect tissue expression or activity (Gjorgjieva et al., 2019a). The question of whether humans with NAFLD might benefit from therapeutic targeting of miR-122 through either antagomirs (anti-miRs) or miRNA mimics, will require considerable more research and development, and larger trials with careful staging of NAFLD.

3.2.5 MiR-146

Along with miR-155, miR-146 is recognized for playing multiple roles in inflammation and is considered as an oncomiR (Testa et al., 2017). However, studies that have investigated the roles of miR-146 in NAFLD pathogenesis are limited. Three clinical studies have suggested hepatic miR-146 expression as significantly increased in: biopsies from participants with metabolic syndrome and NASH (Cheung et al., 2008), bariatric surgery patients with NAFLD (Latorre et al., 2017b), and steatosis tissue bank biopsies (Wang et al., 2018b). However, two studies detecting circulating miR-146 levels were conflicting, possibly relating to the clinical stage of NAFLD or ethnic differences. While a small European cohort study (n=20 in each group) reported a decrease of circulating miR-146 in histologically diagnosed NAFLD patients in comparison to healthy age-matched participants (Celikbilek et al., 2014), a Chinese cohort study found an increase of miR-146 in biopsy-proven NASH patients (n=31) compared to healthy controls (n=37) (Liu et al., 2016b).

In experimental models, the expression of miR-146 was found decreased in dietary-induced NAFLD models (Jin et al., 2017; He et al., 2018), and *in vitro* studies show that miR-146 mimics can suppress lipid accumulation and inflammatory cytokine expressions, such as TNF-α and interleukin-6 (IL-6) (Jiang et al., 2015; He et al., 2018). Additionally, miR-146 is an anti-fibrotic miRNA and regulates fibrosis signalling pathways in HSCs (Ezhilarasan, 2020). In TGF-β stimulated cellular models, overexpression of miR-146 inhibited the proliferation and apoptosis of HSCs and the expression of profibrogenic markers (He et al., 2012; Yuan et al., 2019). Furthermore, in a hepatic fibrosis rat model induced by CCl_4, vein injection of miR-146a-expressing adenovirus increased the level of miR-146 along with the alleviation of fibrogenesis (Zou et al., 2019). The current evidence suggests roles of the miR-146 family in NAFLD pathogenesis, especially in more advanced stages, should be further explored with more attention to the

different isoforms and their unique regulatory functions as previously recommended (Paterson et al., 2017).

3.2.6 MiR-200

Key inhibitors of the EMT, the miR-200 family (miR-200a, miR-200b, miR-200c, miR-141, and miR-429) play critical roles in normal development, as well as cancer metastases (Korpal and Kang, 2008). High expression of miR-200 is associated with an epithelial phenotype, and recent bioinformatic analysis suggests potential binding sites for miR-200b in the 3´ untranslated regions of 60 different mRNAs involved in EMT, the majority of which are associated with a mesenchymal phenotype that miR-200 likely inhibits (Górecki and Rak, 2021). Typically considered tumour suppressors, the miR-200 family have generally been reported down-regulated in multiple cancers, including HCC (Mao et al., 2020). However, this may depend on the tumour stage, with data suggesting the miR-200 family are down-regulated at the primary tumour site permitting intravasation but up-regulated in distal metastases facilitating colonization of metastatic breast cancer cells (Hilmarsdottir et al., 2014).

In the context of NAFLD, to date there are only limited data about the miR-200 family. While two studies have found miR-200a/b/c increased in steatosis and NASH liver samples from tissue banks (Tran et al., 2017b; Wang et al., 2018b); a separate study using biopsies found miR-200b/c decreased in NAFLD compared to healthy controls (Guo et al., 2016a). An additional two studies have found miR-200 increased in the serum from patients with NAFLD (Ezaz et al., 2020; Wang et al., 2020e). Some evidence from animal models supports the idea that inhibition of miR-200 may attenuate steatosis, inflammation and fibrosis. For example, double deletion of miR-141 and miR-200 in mice with methionine and choline deficient diet induced NASH resulted in decreased steatosis and inflammation and alterations in multiple signalling pathways (Tran et al., 2017b). In a similar vein, high fat-fed (20% lard for 4 weeks) mice transduced with an miR-200 inhibitor also evidenced reduced steatosis and fibrosis (Wang et al., 2020e). However, in a separate study of high fat-fed (45% kcal from fat for 10 weeks), miR-200b and miR-200c, but not miR-200a, were found markedly decreased (Guo et al., 2016a). These data may reflect the use of different animal models, but could also relate to

disease stage. While a rationale can be made for increased expression of miR-200 early in NAFLD, and decreased expression later in progression bringing risk of HCC, more data at greater resolution (e.g. single cell discriminating between hepatocytes and HSCs) are required to evidence this.

3.3 MicroRNAs regulated by vitamin D with liver disease

MicroRNAs have multiple essential roles in mediating the cellular response to vitamin D, including the post-transcriptional regulation of VDR (Zenata and Vrzal, 2017). Within the 3'untranslated region of the VDR mRNA are binding sites for four miRNAs (miR-27b, miR-125b, miR-298, miR-346), which have been experimentally verified and shown to decrease VDR protein levels (Pan et al., 2009; Mohri et al., 2009; Essa et al., 2010; Chen et al., 2014). Indeed, miR-125 inhibitors have been demonstrated to increase VDR expression and decrease proliferation and cell viability *in vitro* in HCC cells, while VDR levels were negatively correlated with miR-125 levels in tumour tissue from patients with HCC (Xu et al., 2018). Moreover, multiple genes [CYP27B1, CYP24A1 and retinoid X receptor-alpha (RXRα)] in the vitamin D pathway are regulated by miRNAs (Liu et al., 2012a; Komagata et al., 2009; Ji et al., 2009), and VDR directly regulates the transcription of multiple miRNAs (such as let-7a, miR-26b, miR-182, miR-200b and miR-200c) (Peng et al., 2010). While a large body of pre-clinical research suggests the anti-cancer effects of vitamin D are mediated through miRNA regulation, data from human trials is more limited (Zeljic et al., 2017). Although anti-cancer effects of vitamin D have been observed in the liver (Chiang et al., 2011b; Wu et al., 2018), potential roles for vitamin D regulated miRNAs in the molecular pathogenesis of NAFLD remains largely unexplored.

To investigate whether there is a subset of vitamin D modulated miRNAs that involved in the pathologies of NAFLD, I firstly searched PubMed by using '(((calcitriol) OR (vitamin D)) AND (NAFLD)) AND (microRNA)'. Only a study protocol for an ongoing trial that aims to measure miR-21, miR-34 and miR-122 in response to 12 weeks supplementation of 4000 IU/day vitamin D in patients with NAFLD was found (Ebrahimpour-Koujan et al., 2019). Then, the search strategy changed to looking at miRNA regulation in any liver disease. From searching for '(((calcitriol) OR (vitamin D)) AND (liver)) AND (microRNA)',

there was 13 results: four reviews, one animal study, two studies not related to liver disease; only six studies left using human liver tissues, serum or human hepatic cell lines (including the ongoing RCT).

Besides NAFLD and other metabolic diseases, dysregulation of vitamin D metabolism and functions has been investigated in many types of cancer, such as breast cancer and colon cancer (Deeb et al., 2007; Jeon and Shin, 2018; Negri et al., 2020). This evidence indicate that similar metabolic/pathophysiological signalling pathways might be shared in different diseases. Therefore, I expanded the search strategy to examine all the human research investigating vitamin D-regulated miRNAs regardless of tissue or pathology. A PubMed search was performed using MeSH terms: '((calcitriol) OR (vitamin D)) AND (microRNA)' (**Figure 3.3**).

In total, 251 records were collected up to 7th June 2021. In addition to excluding papers without primary data or irrelevant to vitamin D/miRNA and animal studies, the studies related to skin, muscle, bone or oral health were eliminated. After the screening, 69 studies were identified that had examined miRNAs in human samples or human cell lines. Only 15 of 69 studies were in relation to either vitamin D status (**Table 3.3**; five studies), response to vitamin D supplementation (**Table 3.4**; four studies), or had investigated miRNAs and vitamin D in the context of human liver pathology (**Table 3.5**; six studies). Except for an ongoing clinical trial (Ebrahimpour-Koujan et al., 2019), in the studies related to liver (**Table 3.5)** five characterised miRNAs regulated by vitamin D in a variety of diverse pathologies, including hepatitis C virus (HCV) (Duan et al., 2015), primary biliary cholangitis (PBC) (Kempinska-Podhorodecka et al., 2017), cirrhosis (He et al., 2021b) and HCC (Xu, J. et al., 2018; Provvisiero et al., 2019). While a single study examined the association between miR-27b expression and its targets VDR and cytochrome P450 3A (CYP3A) in normal liver samples from a tissue bank (Ekström et al., 2015).

Next, I reviewed the data from the 54 studies that used human tissues and/or human cell lines to identify dysregulated miRNAs in vitamin D related diseases, predicting the potential mechanical role of these miRNAs in the context of NAFLD. Here 'good evidence' was defined as validation by qPCR

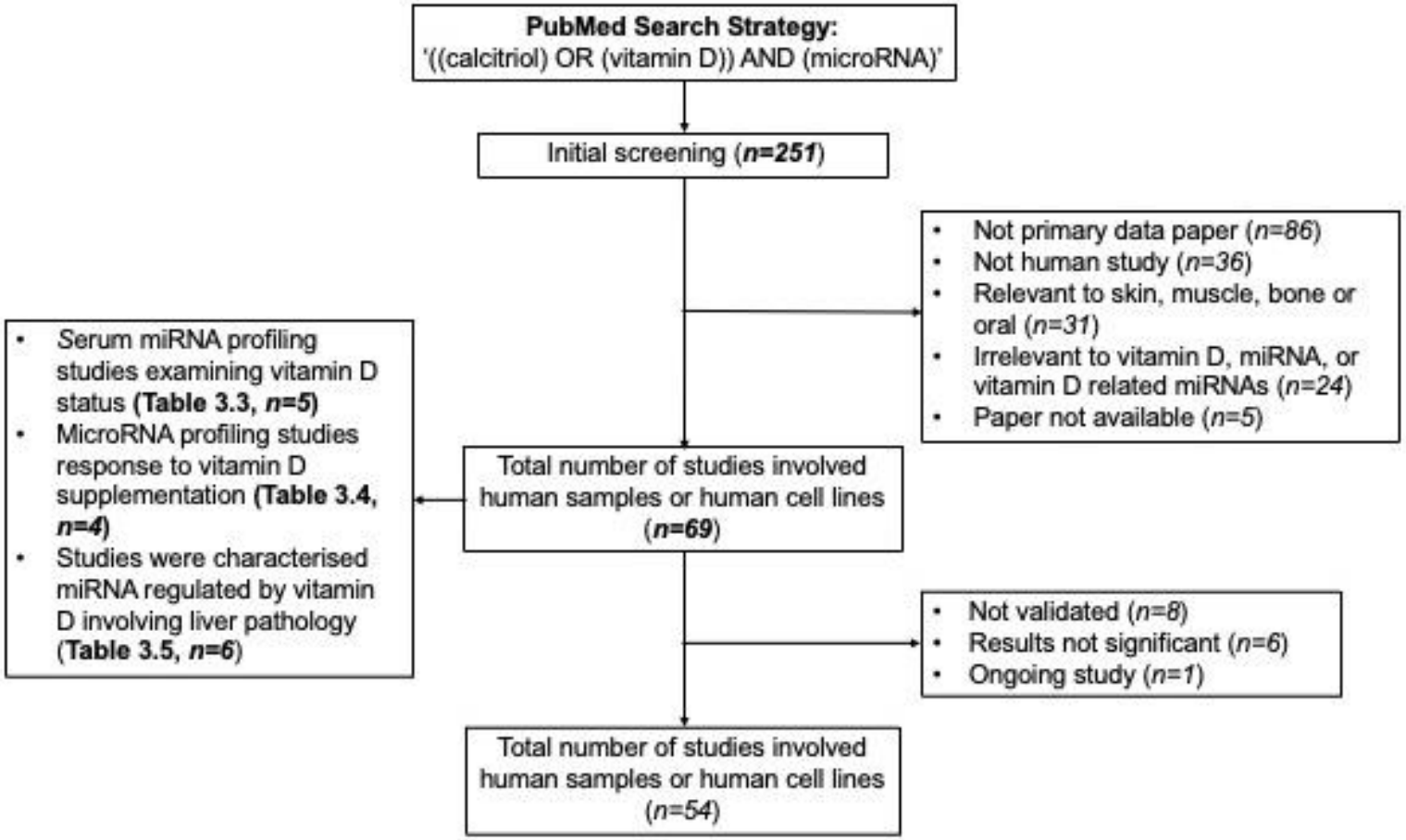

Figure 3.3 Flow chart of studies of vitamin D and miRNA identified in PubMed. PubMed search strategies: '((vitamin D) OR (calcitriol)) AND (microRNAs)'; search was from PubMed inception through 07/06/2021

Table 3.3 Serum miRNA profiling studies examining vitamin D status

Reference	Study design; Group (sample size); 25(OH)D status (nmol/L)	miRNAs related to 25(OH)D status	miRNA related summary
Enquobahrie et al. (2011)	miRNA expression (microarray) in relation to 25(OH)D status† in early (16 weeks' gestation) pregnancy (~34yo women); **High 25(OH)D group (**n=6): 98.05±15.3, **Low 25(OH)D group** (n=7): 57.10±5.0;	Microarray: miR-92b, -93, -138, -196a, -320d, -343-3p, -423-3p, -484, -573, -574-5p, -589, -601	Microarray: **Up** in high 25(OH)D vs. low 25(OH)D: miR-574-5p **Down** in high 25(OH)D vs. low 25(OH)D: miR-92b, -93, -138, -196a, -320d, -343-3p, -423-3p, -484, -573, -589, -601
Lee et al. (2014a)	miRNA expression (microarray and QPCR) in relation to 25(OH)D status in patients with AML (~60yo); **Normal vitamin D** (n=34): >80 **Insufficient vitamin D** (n=34): 50-79.8; **Deficient vitamin D** (n=29): <50;	Microarray: miR-96, -122, -125b-1, -134, -144, -182, -193b, -329, -451, -486-5p, -511, -595, -663, -886-3p -1248 QPCR: Not significant	Microarray: **Up** in <50 (n=10) vs. >50 (n=10): miR-96, -134, -144, -182, -193b, -329, -451, -486-5p, -595, -663, -886-3p **Down** in <50 vs. >50: miR-122, -125b-1, -511, -1248 QPCR (N=58): No miRNAs associated with 25(OH)D levels in validation cohort
Beckett et al. (2014)	Circulation level of let-7 (QPCR) in relation to vitamin D intake in elderly cohort (~75yo); **Adequate intake**‡ (n=23): ns§; **Inadequate intake** (n=177): ns§;	QPCR: let-7b-5p	QPCR: **Down** in adequate vs. inadequate; negative correlation with vitamin D intake
Chen et al. (2017)	miRNA expression (QPCR) in T-cells of patients with SLE with 25(OH)D insufficiency (~36yo); patients with SLE(n=42): 41.7±12.8 **Normal vitamin D** (n=32): NR **Insufficient vitamin D** (n=10): NR;	QPCR: miR-10a, -125a, 342, -374b, -377 and -410	QPCR: All miRNAs d**own** in SLE vs. controls; except miR-377, all miRNAs positive correlated with 25(OH)D level
Ferrero et al. (2020)	Circulating miRNome on healthy volunteers in relation to estimated vitamin D intakes§ (~40yo) **25(OH)D status** (n=120): NR	RNAseq: ~348 miRNAs detected/sample	Microarray: In GLM, miR-361-3p was positive correlation with vitamin D intake and let-7a-5p was negative correlation with vitamin D intake§

AML, acute myeloid leukemia; GLM, generalised linear regression model; NS, not specified; NR, not reported; 25(OH)D, 25-hydroxyvitamin D; QPCR, quantitative polymerase chain reaction; SLE, systemic lupus erythematosus; † 25(OH)D status defined as high: ≥79.25 nmol/l or low: <63.75 nmol/l; ‡ The recommended adequate daily intake for vitamin D intake for vitamin D in Australia is 10ug/day for 51-70 years old and 15ug/day for those aged over 70; §, Intake estimated by food frequency questionnaire 0-65.6g/day.

Table 3.4 Serum miRNA profiling studies examining response to vitamin D supplementation

Reference	Study design; Group (sample size) and vitamin D intake	Serum 25(OH)D status (nmol/L) or 1,25(OH)D status (pmol/L)	miRNAs related to 25(OH)D status§	miRNA related summary
Jorde et al. (2012)	Males with obesity (~50yo) supplemented for 1 year; **Vitamin D** (n=40): 20,000 or 40,000 IU cholecalciferol/week **Placebo(**n=37): placebo/week	**Vitamin D group:** Baseline 50.2±14.2, 12-month 101.7±17.8; **Placebo group:** Baseline 53.0±19.1, 12-month 49.6±16.0	miR-211, miR-532-3p	miR-211: **Down** in 12-month vs. baseline [in the placebo group]; **up** in vitamin D vs. placebo; miR-532-3p: Positive correlated with serum 25(OH)D [at baseline];
Yu et al. (2017)	60 patients with perennial AR and 20 HCs (~35yo) supplemented for 6 months; **Vitamin D** (n=20): 2000IU vitamin D_3/day; **Placebo** (n=20): placebo/day	**All groups:** <75	miR-19a	miR-19a: **Up** in AR with vitamin D_3 vs. HCs
Nunez Lopez et al. (2017)	Adults with prediabetes (~59yo) supplemented for 4 months; **Vitamin D** (n=40): 2,000 IU cholecalciferol/day **Placebo** (n=21): placebo/day	**Vitamin D group:** Baseline 62.0±14.8 4-month: 83.8±18.5 **Placebo group:** Baseline 66.5±20.0 4-month: 43.3±12.3	miR-7, miR-23b miR-107 miR-152, miR-192-5p	miR-7: **Up** in vitamin-D vs. placebo miR-23b: **Up** in post vs. pre [in vitamin D group] miR-107: **Up** in post vs. pre [in vitamin D group] miR-152: **Up** in vitamin-D vs. placebo, **up** in post vs. pre [in vitamin D group]; positive correlated with serum 25(OH)D miR-192-5p: **Down** in vitamin-D vs. placebo down in post vs. pre [in vitamin D group]

Pastuszak-Lewandoska et al. (2020)	20 male UM runners (~38yo) supplemented for 2 weeks; **Vitamin D group** (n=NS): 10,000 IU cholecalciferol/day **Placebo group (**n=NS): placebo/day;	NR;	miR-155, miR-223	<u>miR-155:</u> **Up** in both placebo and vitamin D groups [after UM]; <u>miR-223</u> **Up** in placebo group only [after UM]

AR, allergic rhinitis; HC, healthy control; SLE, systemic lupus erythematosus; NS, not specified; NR, not reported; 25(OH)D, 25-hydroxyvitamin D; 1,25(OH)D, 1,25-dihydroxyvitamin D; PCa, prostate cancer; UM, ultra-marathon; §Jorde (Jorde et al., 2012) used microarrays with quantitative polymerase chain reaction (QPCR) for validation; Yu (Yu et al., 2017), Nunez Lopez (Nunez Lopez et al., 2017) and Pastuszak-Lewandoska (Pastuszak-Lewandoska et al., 2020) used QPCR alone.

Table 3.5 Research studies characterising miRNA regulated by vitamin D involving liver pathology

Reference	Liver pathology; Samples	Vitamin D treatment	Related miRNA	miRNA related summary
Duan et al. (2015)	HCV; Human cell lines: Huh7.5 HCV Con1b replicon Huh7.5.1 infected with HCV J6/JFH1	1M calcitriol for 48h	miR-130a	QPCR: Calcitriol potentiated miR-130a inhibition of HCV RNA replication. But calcitriol did not effect the expression of miR-130a
Ekström et al. (2015)	General population; Serum n=28 Liver n=20;	NR	miR-27b	QPCR: Negative correlation with CYP3A activity* in both liver and serum; no association with mRNA levels of *CYP3A4*, *VDR* and *PPARα* [liver]
Kempinska-Podhorodecka et al. (2017)	PBC; Liver: PBC n=22, PSC n=13 and Controls n=23 PBMCs from human: PBC n=16, PSC n=10 and Controls n=11	Patients with PBC were supplemented with vitamin D/calcium (amount NR) and had normal levels of serum vitamin D	miR-155	QPCR: **Up** in PBC vs. PSC and controls in both liver and PBMCs; Positive correlation with hepatic *VDR* mRNA and SOCS1 protein level [liver];
Xu et al. (2018)	HCC; Liver: HCC n=31 and NL n=10; Human cell lines: HepG2 and SMMC-7221	NR	miR-125a-5p	QPCR: **Up** in HCC vs. NL, negative correlation with hepatic *VDR* mRNA [liver]; Downregulation of miR-125a-5p increased VDR mRNA and protein expression in HepG2, **Target:** *VDR* (luciferase reporter assay) [in cells]
Provvisiero et al. (2019)	HCC; Human cell lines: PLC/PRF/5, and JHH-6	With or without 10^{-7}M $1,25(OH)_2D_3$ for 12h	miR-375	QPCR: **Up** in vitamin D treated vs. untreated; **Target:** *c-MYC* (luciferase reporter assay)
He et al. (2021b)	Liver cirrhosis Liver: cirrhosis n=60 NL=5 Human cell line: 293T	NR	miR-125	QPCR: **Up** in cirrhosis vs. NL [liver]; IHC: **Up** miR-125 expression with reduced VDR staining[liver]; Positive correlation with liver cirrhosis, negative correlation with hepatic VDR protein [liver] **Target:** *VDR* [293T]

CYP3A, cytochrome P450 3A; PBC, primary biliary cholangitis; PBMCs, peripheral blood mononuclear cells; PSC, primary sclerosing cholangitis; HC, healthy control, HCC, hepatocellular carcinoma; HCV, hepatitis C virus; IHC, immunohistochemistry; NAFLD, non-alcoholic fatty liver disease; NL, normal liver; NR, not reported; QPCR, quantitative polymerase chain reaction; RCT, randomized clinical trial; SOCS1, suppressor of cytokine signalling 1; VDR, vitamin D receptor; *CYP3A activity in serum measured by its endogenous marker 4β-hydroxycholesterol; CYP3A activity in liver measured by dextromethorphan N-demethylation.

secondary to microarray or RNAseq profiling alongside other experimental validation [e.g. using luciferase, or chromatin immunoprecipitation (ChIP)], in at least two independent studies.

From 54 nonredundant studies, 57 unique vitamin D related miRNAs were identified for comparison with the 67 miRNAs my previous analyses (**Figure 3.2A**) had identified as NAFLD dysregulated. Venn analysis suggested 23 vitamin D modulated miRNAs potentially relevant to NAFLD (**Figure 3.4A**), including six miRNAs (miR-27, miR-125, miR-155, miR-192, miR-223, and miR-375) described in **Table 3.3-3.5** validated by qPCR. Focusing on miRNAs found dysregulated in more than one study (**Figure 3.4B**), five miRNAs were found potentially altered in NAFLD and vitamin D [miR-27, miR-125, miR-146 (previously discussed in **3.2.5**), miR-155 and miR-181)]. The NAFLD and vitamin D study findings for these five miRNAs are briefly outlined in **Appendix B Table 3** and are expanded on in discussion below.

3.3.1 miR-27

The miR-27 family (contains two homologs: miR-27a and miR-27b) has been shown to regulate adipogenesis (Lin et al., 2009) and relate to hepatic lipid metabolism (Ji et al., 2009). miR-27 has been reported to directly target VDR (Zeljic et al., 2017; Li et al., 2015). However, the only study that examined miR-27b in relation to VDR expression using human liver (N=20) and serum serum (N=28) samples in the general population, found no correlation between miR-27b and the expression of VDR mRNA (Ekström et al., 2015).

To date, no study has evaluated miR-27 in relation to vitamin D status or response to vitamin D supplementary. Only an experimental study reported $1,25(OH)_2D$ inhibited the lung fibroblast differentiation induced by TGF-β1 via miR-27/VDR pathway, concomitant to a decrease of miR-27 expression (Li et al., 2015). Interestingly, Ekström et al. (2015) indicated that CYP3A activity in human serum was negatively correlated to miR-27 but positively associated with circulating 25(OH)D levels. Notably, CYP3A, expressed in the human liver, is (one of many CYP enzymes) responsible for drug metabolism (Guengerich, 1999), including the steroid drugs available for comorbidities of obesity, diabetes and hyperlipidemia (Jamwal et al., 2018). Indeed, besides VDR, miR-27b has been reported to directly target CYP3A4 (Pan et al., 2009).

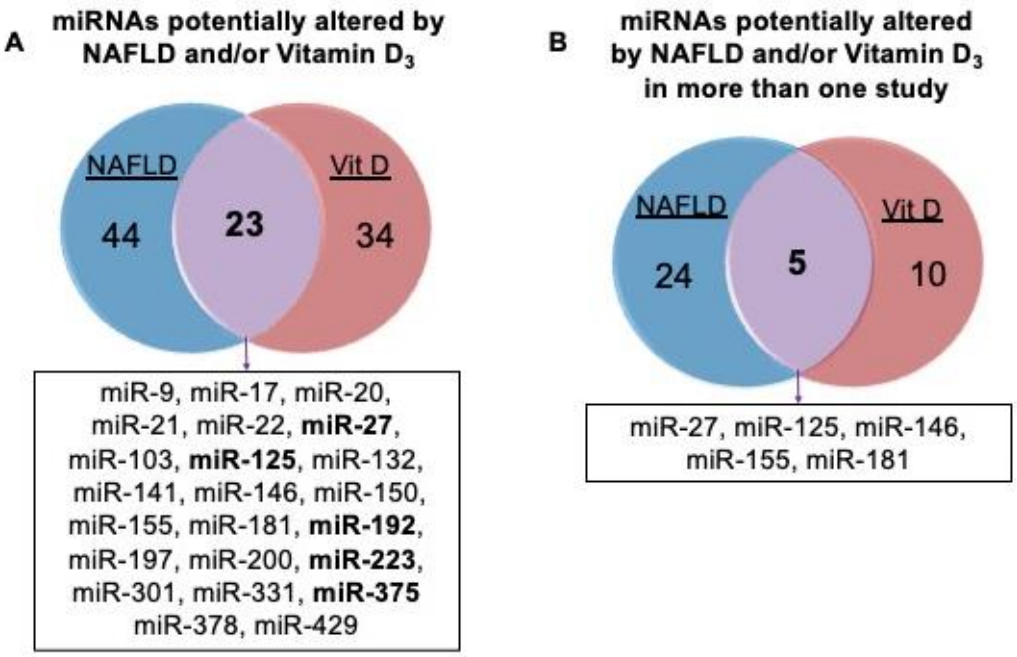

Figure 3.4 Evidence for intersection of microRNA pathways between NAFLD and vitamin D. A. A PubMed search using the terms calcitriol, vitamin D and microRNA, found 54 studies with 57 unique vitamin D related miRNAs. Venn analysis of the 57 vitamin D associated miRNAs with the 67 NAFLD dysregulated miRNAs suggested 23 vitamin D modulated miRNAs potentially relevant to NAFLD. Five miRNAs (bold in intersection box) were identified in Table 3.3-3.5 validated by qPCR. **B.** Focusing on miRNAs found dysregulated in more than one study in both NAFLD (the five bold form Figure 3.2A plus the 24 in Figure 3.2B) and vitamin D, five miRNAs were identified. The detailed information of each miRNA was summarised in Appendix A Table A3.

Furthermore, an *in vivo* study reported a trend of decreasing CYP3A4 protein expression but not mRNA expression with the severity of NAFLD (Fisher et al., 2009). However, to date, no study has investigated the role of the miR-27b/CYP3A axis in patients with NAFLD supplied with vitamin D.

Separately, miR-27 has been found altered in serum from patients with NAFLD in three studies (Tan et al., 2014; López-Riera et al., 2018a; Ando et al., 2019). While Tan et al. (2014) and López-Riera et al. (2018b) reported an increase of miR-27b in patients with NAFLD, a separate study showed downregulation of miR-27a (Ando et al., 2019). Different isoforms of miR-27 may explain these contradictory results. Additionally, circulating miR-27 was considered as a biomarker for NALFD, especially for disease severity like NASH and advanced fibrosis (Tan et al., 2014; López-Riera et al., 2018b). On the other hand, experimental data suggest a critical role of miR-27 in lipid homeostasis. While down-regulation of over-expressed miR-27 restored the accumulation of cytoplasmic lipid in HSCs and suppressed its proliferation (Ji et al., 2009), adenovirus-mediated overexpression of miR-27 blocked fat accumulation in hepatocytes (Zhang et al., 2017). What's more, the expression of the adipogenesis regulator, PPARγ is directly regulated by miR-27 in liver cells (Kida et al., 2011).

3.3.2 miR-125

The miR-125 family (miR-125a, miR-125b-1 and miR-125b-2) play essential roles in haematopoiesis and the normal function of immune cells, and perhaps unsurprisingly, have also been linked to a variety of cancers (Wang et al., 2019). Their effects in cancer are dependent on cell type, and they have been shown to have both oncogenic and tumour suppressive activities. Along with the previously discussed miR-27, miR-125 is of note because it also targets and regulates VDR (Mohri et al., 2009; Zeljic et al., 2017; Xu et al., 2018; He et al., 2021b) and CYP24 (Komagata et al., 2009). I identified ten studies that reported dysregulation of miR-125 in the context of vitamin D. These studies focused on breast cancer (Komagata et al., 2009; Mohri et al., 2009; Klopotowska et al., 2019), prostate cancer (Giangreco et al., 2013) and immune system diseases (Hu et al., 2017; Chen et al., 2017; Zhu et al., 2019b). However, only one study examined miR-125 expression in adipose tissues in obese individuals (Jonas et al., 2019). Two studies reported that miR-125 was

examined in relation to VDR in patients with HCCs (Xu et al., 2018) and liver cirrhosis (He et al., 2021b) (**Table 3.5**). In HCC tissues (n=31), miR-125a was found negatively correlated with VDR expression and was expressed at much higher levels than in non-tumour controls (n=11) (Xu et al., 2018). Similarly, in cirrhotic liver biopsies (n=60), miR-125a expression increased with severity of liver fibrosis associated with a corresponding decrease in VDR expression (He et al., 2021b).

To date, only a single observational study has evaluated miR-125 in relation to vitamin D status. Chen and colleagues reported a positive correlation between miR-125 expression in T cells and serum 25(OH)D levels in patients with systemic lupus erythematosus (SLE) (Chen et al., 2017). Similarly, only an interventional study has identified miRNAs regulated by vitamin D in prostatectomy specimens of patients with prostate cancer (Giangreco et al., 2013). Before the prostatectomy, 66 patients were randomized into three dose groups to orally intake cholecalciferol (400, 10,000 or 40,000 IU/day) for 3–8 weeks. Prostatic miR-125b was found decreased in tumour tissues (n=25) compared to benign tissues (n=23). Additionally, the post-intervention data indicated that prostatic miR-125b level positively correlated with prostatic $1,25(OH)_2D_3$ in both benign and tumour epithelium and positively associated with serum levels of 25(OH)D in tumour tissues. On the other hand, experimental studies substantiate that miR-125b is regulated by vitamin D_3 but with conflicting findings. Downregulation of miR-125b was detected in $1,25(OH)_2D_3$ treated breast cell line (MCF-7) (Mohri et al., 2009; Klopotowska et al., 2019) and leukaemia cell lines (U937 and HL60) (Hu et al., 2017), whereas miR-125b increased in primary prostatic epithelial cells (Giangreco et al., 2013) and THP-1 cells (a human leukaemia monocytic cell line) exposed to lipopolysaccharide (Zhu et al., 2019b). The conflicting findings are possibly related to experimental design and cell line differences.

In the context of NAFLD, only two studies have examined miR-125 in the serum of patients with NAFLD but reported conflicting results (Cai et al., 2020; Zhang et al., 2021b). Whereas Cai and workers found miR-125 decreased in serum from patients with an ultrasound diagnosed NAFLD (n=34) compared to non-NAFLD (n=20) (Cai et al., 2020), a separate study reported the opposite finding miR-125 increased in NAFLD (n=29) compared to healthy

volunteers (n=24) (Zhang et al., 2021b). Differences in NAFLD phenotype and/or qPCR methodologies employed may explain these contradictory findings. Notably, in the later study, the diagnostic modality for NAFLD was unspecified, and SYBR green staining was used for qPCR (Zhang et al., 2021b). However, the associated experimental work of Cai and colleagues (Cai et al., 2020), in combination with previous experimental work demonstrating miR-125 targets fatty acid synthase (Zhang et al., 2015), suggests miR-125 upregulation is likely to be protective for NAFLD and liver fibrosis, and miR-125 in relation to NAFLD is worthy of further investigation.

3.3.3 miR-146

In the context of NAFLD, the potential roles of miR-146 were described in detail in section 3.2.5. Therefore, here, I will focus on the findings in the context of vitamin D. To date there appears that only one interventional study has evaluated miR-146 in response to vitamin D supplements (0.25μg/day calcitriol) in patients with SLE (Wang et al., 2010a). The expression of miR-146 in serum was found to increase after 3/6 months oral intake of calcitriol. Apart from this single clinical study, data from two experimental studies were conflicting. The expression of miR-146 was induced in dendritic cells treated with 1,25(OH)D (Pedersen et al., 2009). However, in human adipocytes pre-treated with 1,25(OH)D downregulation of miR-146 was observed with TNFα incubation in comparison to cells only treated with TNFα (Karkeni et al., 2018). The same study using adipocytes from HFD induced obese mice also showed that 1,25(OH)D suppressed TNFα-induced upregulation of miR-146, and suggested that this may attenuate inflammation in adipose tissues by limiting NF-kB activation. Combining the findings in the context of NAFLD, vitamin D, as an anti-inflammatory reagent, might regulate the expression of miR-146 relevant to the inflammatory response in the progression of NAFLD; however, these potential mechanisms need further investigation.

3.3.4 miR-155

A notorious oncomiR, increased expression of miR-155 has been found in a host of different cancers, including HCC (Tang et al., 2016; Zhang et al., 2016). Transcription of the MIR155 host gene (*MIRHG155)*, historically termed B-cell integration cluster (BIC), is regulated by numerous transcription factors

involved in the inflammatory response, including NF-kB, interferon regulatory factors, TGF-β, and hypoxia inducible factor 1 alpha among others (Mahesh and Biswas, 2019). Therefore, the aberrant expression of miR-155 plays a vital role in multiple inflammatory molecule and signalling pathways. Critical to both innate and adaptive immune responses, miR-155 influences the immune inflammatory response in part through directly targeting suppressors of cytokine signalling 1 (SOCS1) (Yao et al., 2012).

Interestingly, miR-155 is inhibited by VDR, which directly interacts with IκB kinase (IKKβ), preventing NF-kB activation and trans-repression of *MIRHG155* (Chen et al., 2013b). Calcitriol decreases miR-155 expression in human macrophages (Chen et al., 2013a; Arboleda et al., 2019) and adipocytes (Karkeni et al., 2018). Notably, two studies seem to use the same population of patients with SLE (n=40) found after 3/6 months calcitriol supplementary increased serum miR-155 expression (Wang et al., 2010a), but a decrease of miR-155 expression in the urine sediment samples of patients with SLE (Wang et al., 2012a). In mice, vitamin D supplementation ameliorated the increase in miR-155 in adipose tissue in response to HFD feeding, further supporting of an anti-inflammatory role of vitamin D in obesity (Karkeni et al., 2018). Moreover, miR-155 has been observed to decrease in response to both dietary weight loss and bariatric surgery and has been proposed as a biomarker of weight loss (Langi et al., 2019; Catanzaro et al., 2020). In the context of NAFLD, hepatic miR-155 expression was shown to be increased alongside miR-34a and miR-200a-c and other miRNAs in a small number (n=4/group) of tissue bank biopsies from patients with and without steatosis (Wang et al., 2018b). Hepatic expression of miR-155 has also been found elevated in cholestatic liver disease and was related to decreased VDR and SOCS1 protein levels in the peripheral blood mononuclear cells of patients (Kempinska-Podhorodecka et al., 2017). The authors point out the decreased VDR expression was observed despite patients being supplemented with vitamin D and having normal vitamin D status.

Perhaps counterintuitively, in 2016, Wang and colleagues (Wang et al., 2016c) reported significantly decreased circulating levels of miR-155 in 50 participants with NAFLD compared to 50 healthy controls, as well as decreased hepatic miR-155 levels in 11 biopsy samples from patients with

NAFLD compared to 11 control biopsies. However, in accompanying experimental work they showed miR-155 directly targets LXRα, which targets SREBP-1c and fatty acid synthase (FAS) influencing lipid accumulation. In addition, HFD fed mice transfected with miR-155 mimics, had significantly reduced hepatic steatosis, as well as decreased expression of LXRα, SREBP-1c and FAS (Wang et al., 2016c). Apart from the aforementioned study in cholestatic liver disease, only one other study was identified that examined miR-155 response to vitamin D supplementation. Unusually, it involved very high dose vitamin D supplementation (10,000 IU / 250μg cholecalciferol) for 2 weeks prior to a 100km ultra-marathon. In this small study done in a unique population miR-155 levels increased in both groups after the ultra-marathon but there was no difference between groups (Pastuszak-Lewandoska et al., 2020).

Genome-wide analyses have demonstrated miR-155 has many hundreds of gene targets, and furthermore miR-155 binding and miR-155-dependent repression are regulated in a cell-context dependent fashion (Nam et al., 2014; Hsin et al., 2018), which may explain these somewhat disparate results. However, the preclinical data and data from weight loss intervention studies, suggest that the potential interactions between miR-155, vitamin D, hepatic lipid metabolism and inflammation in the molecular pathogenesis of NAFLD are worth pursuing.

3.3.5 miR-181

As a group of highly conserved miRNAs, the miR-181 family contains four different mature forms (miR-181a-d), which have been involved in many pathological processes of neurodegenerative diseases and cancer (Indrieri et al., 2020; Rezaei et al., 2020). Human clinical data on miR-181 expression in NAFLD is sparse and conflicting. While two studies did in the Chinese population reported an upregulation of miR-181 in patients with NAFLD (n=25-30) (Wang et al., 2017; Huang et al., 2019); a Turkish study showed that the miR-181 level was lower in patients with NAFLD (n=20) compared to HCs (n=20) (Celikbilek et al., 2014). In spite of these small numbers, miR-181 was observed as a potential biomarker to distinguish NAFLD from HCs (AUC=0.86) (Celikbilek et al., 2014). To my knowledge, no study has examined hepatic miR-181 expression in patients with NAFLD. On the other hand, the

therapeutic feasibility of miR-181 has been explored in cellular and animal models of NAFLD. The study done by Wang et al. (2017) revealed that silenced miR-181 in HFD induced NAFLD mice led to reductions of hepatic TG level and circulating levels of ALT and AST. At the same time, overexpression of miR-181 was identified to inhibit the expression of SIRT1 and promote steatosis in PA-treated HepG2 cells. In addition, miR-181 was found to negatively regulate the expression of PPARα in human immortalised hepatocyte cell line (L02) and primary mouse hepatocytes and further affected fatty acid β-oxidation and hepatocyte lipid metabolism (Huang et al., 2019).

To date, no study has evaluated miR-181 in relation to vitamin D status or in response to vitamin D supplementation. Only two experimental studies reported that 1,25(OH)D treatment altered the expression of miR-181 in human leukaemia (Wang et al., 2009) and human syncytiotrophoblast (STB) cell lines (Wang et al., 2018a). Only the later study in human STB cells examined miR-181 in relation to VDR (Wang et al., 2018a). Specifically, 1,25(OH)D-VDR signalling stimulated the expression of miR-181 in human STB cells, further leading to post-translational inhibition of corticotropin-releasing hormone. Separately, 1,25(OH)D-induced repression of miR-181 has been proved to contribute to the accumulation of the small protein inhibitors of cyclin-dependent kinase, p27Kip1, and the arrest of the cell cycle progression in the G1 phase in HL60 and U937 cells (Wang et al., 2009). However, the current intersection of miR-181 mediated biological process related to vitamin D regulation and NAFLD progression is insufficient, which might need further investigation.

3.4 Conclusion

This chapter aimed to critically assess the evidence for a potential subset of miRNAs that are both dysregulated in NAFLD and modulated by vitamin D. Comprehensive review of the literature found numerous studies examining dysregulation of miRNA levels in humans with NAFLD. From this, I identified 29 miRNAs found dysregulated in more than one NAFLD study and find six (miR-21, miR-30, miR-34, miR-122, mi R-146 and miR-200) dysregulated in multiple independent NAFLD studies. On the other hand, only a paucity of human studies were identified that had investigated miRNAs in relation to

vitamin D status, response to supplementation, or vitamin D in the context of the liver. This is a notable gap in the evidence base, given that VDR mediates its cellular response in part by directly targeting miRNAs that regulate transcription factors involved in NAFLD pathogenesis and considering that VDR expression is directly regulated by miRNAs likely disrupted in NAFLD.

Thus I expanded the search to other diseases, like breast cancer and colon cancer, that might share similar metabolic/pathophysiological mechanisms to NAFLD. Critical review found evidence from human studies for 23 vitamin D modulated miRNAs likely relevant to NAFLD pathogenesis (overall summary in **Figure 3.5**). Focusing on miRNAs found dysregulated in more than one vitamin D and NAFLD related study, five miRNAs were identified (miR-27, miR-125, miR-146, miR-155 and miR-188). Data presented in this chapter have been published in a peer-reviewed article (Zhang et al., 2021d). The summary tables provide a significant resource to underpin future hypothesis-driven research.

In conclusion, the modulation of miRNAs by vitamin D has been understudied. Based on the evidence to date, a therapeutic benefit for vitamin D supplementation in NAFLD cannot be ruled out. The measurement of serum and hepatic miRNAs in response to vitamin D supplementation in larger trials or biobank samples is warranted.

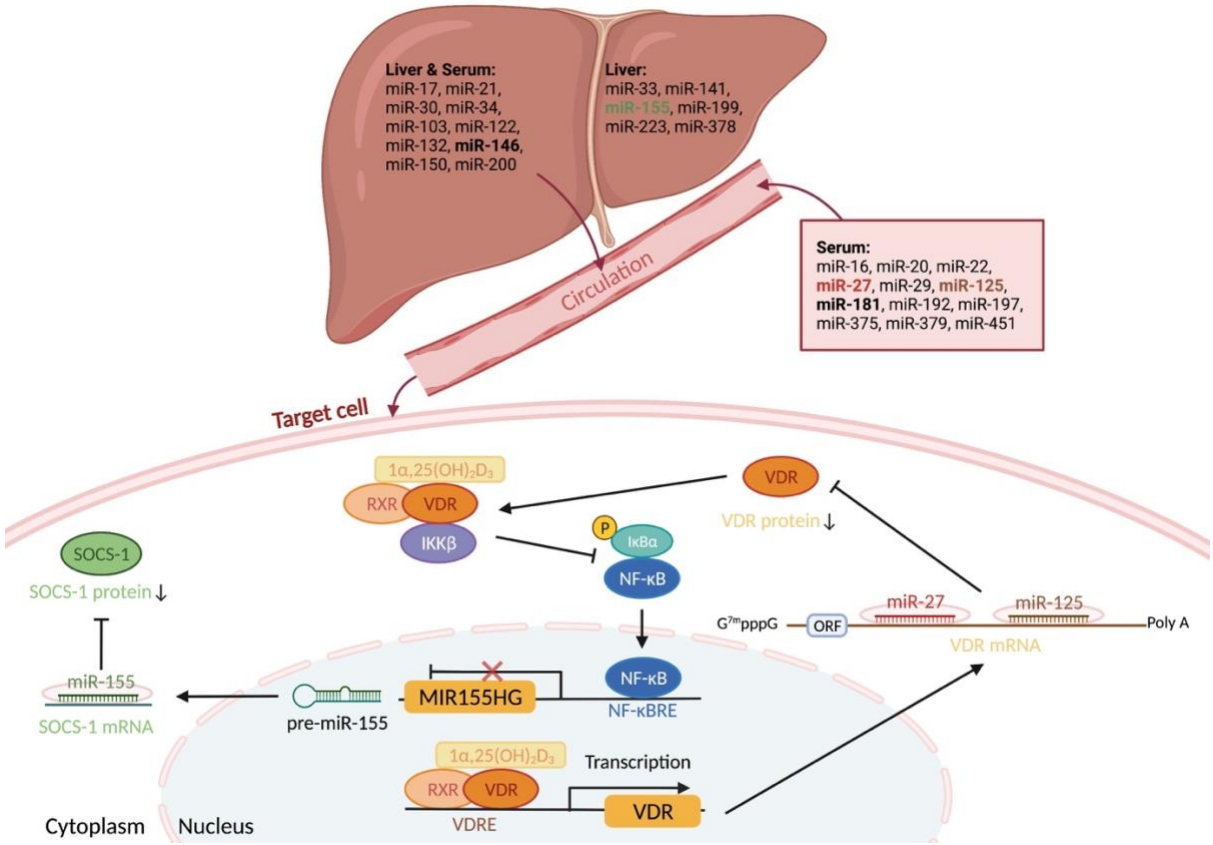

Figure 3.5 Overview of miRNAs altered by NAFLD and vitamin D. Twenty-nine miRNAs were identified as dysregulated in NAFLD in more than one study. Five (bold) were also found in separate studies (more than one study) as vitamin D modulated. Two of these miRNAs, miR-27 and miR-125, target vitamin D receptor (VDR) mRNA and decreased translation. The transcription of a third miRNA, miR-155, is inhibited by VDR, which directly interacts with IB kinase (IKK) preventing nuclear factor-**κ**B (NF**κ**B) activation and transrepression of the MIR155 host gene. Relevant to NAFLD, in the context of low vitamin D/VDR signalling, miR-155 lowers the expression of the suppressor of cytokine signalling 1 (SOCS-1) increasing the expression of proinflammatory cytokines. This figure was created with BioRender.

Chapter 4
Characterisation of lipid loading and vitamin D treatment of liver cells

4.1 Introduction

NAFLD is the hepatic manifestation of obesity and metabolic syndrome, histologically divided into NAFL and NASH (Soret et al., 2020). The molecular mechanisms leading to NASH and more advanced stages of liver disease, such as liver fibrosis and cirrhosis, remain incompletely understood.

To explore the complexity of these molecular mechanisms, *in vitro* models of NAFLD development and progression have been established and improved over the recent decades (Soret et al., 2020). Hepatocytes, accounting for approximately 60% of liver cells and 80% of the liver tissue volume (Ishibashi et al., 2009), play pivotal roles in glucose/lipid metabolism, detoxification, and protein synthesis (Schulze et al., 2019). Therefore, immortalised hepatocyte cell lines have been commonly used to recapitulate liver function *in vitro* (Kunst et al., 2020). Monoculture HepG2 cells treated with fatty acids, such as oleic acid (OA) and palmitic acid (PA), can achieve the NAFLD-relevant downstream consequences of steatosis and apoptosis (Gomez-Lechon et al., 2007; Ricchi et al., 2009).

Besides hepatocytes, non-parenchymal cells including HSCs play essential roles in the progression of NAFLD, especially fibrosis. Under normal physiological conditions, HSCs exhibit a quiescent phenotype and are responsible for retinyl ester storage (Friedman, 2008). Following hepatic injury, HSCs are activated and transdifferentiated to myofibroblasts, which is characterised by loss of retinoid and lipid stores, increasing proliferation, high contractility, pro-inflammation and fibrogenic properties, such as abundant extracellular matrix (ECM) production (Tsuchida and Friedman, 2017). A variety of immortalised HSC lines have been used for mechanistic investigation of their function in hepatic fibrosis and liver pathophysiological processes (Herrmann et al., 2007; Shang et al., 2018). The LX-2 cell line was initially generated by transfection with the Simian Vacuolating Virus 40

transforming (SV40T) antigen and subsequent spontaneous immortalisation under low serum conditions (Xu et al., 2005). LX-2 cells retain vital features of HSCs, such as cytokine signalling, neuronal gene expression, retinoid metabolism and fibrogenesis, and have served as a useful tool in hepatology research (Xu et al., 2005; Herrmann et al., 2007; Shang et al., 2018).

Besides maintaining bone mineral homeostasis, vitamin D has numerous extra-skeletal properties, including anti-proliferative, anti-inflammatory and anti-fibrotic activities (Christakos et al., 2016; Barchetta et al., 2020). A variety of experimental evidence indicates vitamin D might impact disease progression in chronic liver diseases including NAFLD (Kitson and Roberts, 2012; Barchetta et al., 2020). VDR expression has been detected in the liver (Gascon-Barre et al., 2003; Han and Chiang, 2009). Compared to hepatocytes, VDR is more abundantly expressed in non-parenchymal cell types, including HSCs (Gascon-Barre et al., 2003). This differential expression of VDR suggests different cellular functions might be triggered by vitamin D in different liver cells. For example, a causal relationship between induced hepatocyte VDR and increasing hepatic lipid accumulation has been detected in mouse models of NAFLD (Bozic et al., 2016). On the other hand, VDR expression in inflammatory cells has been negatively associated with the severity of liver histology in patients with NASH (Barchetta et al., 2012). Another study has shown that vitamin D mitigated TGF-β-induced fibrogenesis in primary human HSCs via VDR regulation (Beilfuss et al., 2015a). However, the molecular mechanisms underpinning the role of vitamin D in NAFLD pathogenesis are not yet fully understood.

The overall aim of the experiments in this chapter was to characterise a lipid loading model in both immortalised hepatocytes (HepG2) and immortalised HSCs (LX-2) to investigate the responses of 1α,25$(OH)_2D_3$ treatment.

4.2 Methods and materials

4.2.1 Cell culture

HepG2 cells were purchased from European Collection of Authenticated Cell Cultures (ECACC; UK) and routinely cultured in 1.0g/L glucose-containing Dulbecco's modified Eagle's medium (DMEM; GlutaMAX, Gibco®, UK)

supplemented with 10% fetal bovine serum (FBS; Life Science Production, UK), 1% non-essential amino acids (NEAA; Lonza, UK), and penicillin-streptomycin (5,000Units/ml penicillin & 5,000Units/ml streptomycin, Gibco®, UK). LX-2 cells (Merck, US) were cultured in 4.5g/L glucose-containing DMEM medium without sodium pyruvate (Gibco®, UK) supplemented with 2% FBS and penicillin-streptomycin. Both cell lines were maintained at 37°C in a 5% CO_2 air environment. Mycoplasma tests were done routinely by EZ-PCR™ Mycoplasma Detection Kit (BioInd, UK). Phosphate-buffered saline (1X PBS; NaCl 137mM, potassium chloride 2.7mM, disodium hydrogen phosphate 8mM and potassium dihydrogen phosphate 2mM, pH 7.3 ± 0.2 at 25°C) was prepared from tablets (Oxoid, UK), sterilized, and used to wash cells before routine passage or treatment. 10X Trypsin-ethylenediaminetetraacetic acid [Trypsin-EDTA (0.5%); Trypsin 0.1mM, $EDTA_4Na_2H_2O$ 0.9mM, pH 7.1-8.0; Gibco®, UK] was diluted to 1:10 with 1X PBS and used to detach HepG2 cells from flasks (incubated 3-5min at 37°C), while LX-2 cells were detached in Accutase® solution (Sigma, US). Following detachment of cells from the cell culture flask and production of a single-cell suspension using a 19ga needle, 10μl of each cell suspension was mixed with equal volumes of 0.4% w/v trypan blue dye (Sigma, UK) before being read by an automated cell counter (BioRad, Hemel Hempstead, UK) to calculate both the cell amount and the percentage of live cells. Both cell lines were routinely seeded at 30,000cells/cm^2 and cultured for 3-4d to reach approximately 80% confluence in either 75cm^2 or 25cm^2 tissue culture flasks or 6-well plates as needed.

4.2.2 Cell viability

The 3-(4,5-dimethylthiazol-2-yl)-2,5-diphenyltetrazolium bromide (MTT) assay (5mg/ml in 1X PBS; 0.01μM; Sigma, UK) was used to determine cell viability. It works by reducing the MTT salt by a mitochondrial dehydrogenase to insoluble formazan, which can then be dissolved in an organic solvent, DMSO (Carmichael et al., 1987).

To establish typical growth parameters for HpeG2 and LX-2 cells, seeding density experiments were implemented in 96-well plates for 24h with serum contained medium (SCM, with 10% FBS for HepG2 and 2% FBS for LX-2). Based on the establishment of seeding densities, the optimum seeding

density for HepG2 was 100,000cells/cm^2, while LX-2 was 70,000cells/cm^2. The optimum seeding densities were then applied for all treatments of cell viability in this chapter.

To test the cell viability in different vehicles of fatty acid (FA) and vitamin D, cells were treated with SCM or serum free medium (SFM, without FBS) with or without 2% dimethyl sulfoxide (DMSO) or 0.01% absolute ethanol for 6h and 24h.

To test if the interference from lipophilic materials contained in the serum on cell viability with FA treatment, after cell confluent, cells were cultured for 16h in the fresh CSM media prior to treatments. Then, the cells were treated with FA dissolved in SCM, charcoal-stripped FBS contained medium (CSM, Gibco®, UK) or SFM for 6h or 24h.

After washing cells with 1X PBS, 10μl of MTT with 100μl SCM (without phenol red) was added into each well. The plate was then incubated at 37°C for 4h. Absorbance was quantified at 540nm on the CLARIOstar® plate reader (BMG LABTECH, UK) after shaking 2min at 37°C.

4.2.3 Fatty acid treatment and intracellular fatty acid accumulation

Mono-unsaturated OA and saturated PA in equimolar ration were utilized as lipid loading treatments. Briefly, 25mM OA and 25mM PA (1:1, 0-500μM) in DMSO (Sigma, UK) were complexed with 5.56% fatty-acid free (FAF) bovine serum albumin (BSA) in double-distilled water (ddH_2O) at a molar ratio of 3.3:1 while keeping DMSO at 2% maximum at an upper limit of 500μM FA treatment. This method had previously been optimized by the Moore group (Maldonado et al., 2018). When complexing, the stock solutions were incubated in a shaking water bath at 37°C for 1h (all reagents, Sigma, UK). After that, the complexed fatty acid was sterilized by passing through a 0.22μm filter before adding to medium.

To test if there was interference from lipophilic materials contained in the serum, the SCM was either replenished, replaced with CSM, or replaced with SFM, and cells cultured for 16h in the fresh CSM media prior to 6h or 24h fatty acid treatment. After FA treatment, cells were washed with 1X PBS, harvested, and proceed to endpoint measurements.

The fluorescent lipophilic dye Nile red (Sigma, UK) was used to quantitatively assess intracellular lipid accumulation in HepG2 and LX-2 cells. Briefly, an automated cell counter (BioRad, Hemel Hempstead, UK) was used to count and aliquot $5x10^5$ cells after trypsin digestion. Cells were centrifuged at 800x g for 10min and the supernatant was removed. 500µl of 1µM Nile red dissolved in 1X PBS was added to the pelleted cells, mixed thoroughly and incubated at 37°C for a further 10min. Cells were centrifuged again at (800x g for 10min at room temperature) and the supernatant removed before 500µl 1X PBS was used to re-suspend the cells. Cells were passed through 19ga needle 3-5 times, pipetted 100ul per sample with 3 technical replicates into a black 96-well plate (Greiner bio-one, UK) and read at fluorescence excitation 485-20nm and filter emission 520-10nm on the CLARIOstar® plate reader.

4.2.4 Vitamin D treatment

Calcitriol [1α,25-dihydroxy vitamin D_3 or 1α,25$(OH)_2D_3$; Cayman Chemical, UK] was prepared in nitrogen flushed absolute ethanol (Fisher BioReagents, Canada) to make 1mM stock solution and stored at -20°C in tubes covered with foil.

For vitamin D treatment only, 1α,25$(OH)_2D_3$ was prepared in SFM at a concentration of 1µl/ml (1000nM) and serial dilutions were performed for lower concentrations (0nM, 2nM, 10nM and 100nM).

Initial experiments for vitamin D dosing were done using SFM. However, after testing for differential serum effects, subsequent experiments used CSM.

4.2.5 Fatty acid and vitamin D co-treatment

In the initial experiments of FA and vitamin D treatment, LX-2 cells were pre-treated with vehicle (2% DMSO) or 500µM FA wish SFM for 6h, and then treated with vehicle, 10nM or 100nM 1α,25$(OH)_2D_3$ with SFM to collect total RNA samples at different time points (15min, 30min, 1h, 2h, 6h and 24h). However, after testing for differential serum effects, subsequent experiments used CSM and the treatment groups are illustrated in **Table 4.1**. Total RNA samples of both HepG2 and LX-2 cells treated according to **Table 4.1** were collected at different time points (0min, 30min, 1h, 6h and 24h).

Table 4.1 Fatty acid and vitamin D cotreatment experimental design.

Treatment	1	2	3	4	5	6
Fatty acid	vehicle	vehicle	vehicle	500μM	500μM	500μM
Vitamin D	vehicle	10nM	100nM	vehicle	10nM	100nM

After choosing optimal vitamin D concentration and timepoint, in subsequent experiments, both HepG2 and LX-2 cells were treated with or without FA (2% DMSO or 500μM) and with or without vitamin D (0.001% ethanol or 100nM $1\alpha,25(OH)_2D_3$). Total RNA and protein samples from HepG2 and LX-2 cells were collected at different time points (6h and 24h). Cell viability and intracellular lipid accumulation were also measured at 6h and 24h, separately.

4.2.6 RNA isolation

Cells were lysed in TRIzol reagent (ThermoFisher, UK) and stored at -80°C until all samples could undergo RNA extraction simultaneously. RNA was extracted by phase separation using chloroform (Honeywell, UK) and subsequently precipitated by adding 0.5ml isopropanol (Fisher Scientific, UK) per 1ml of TRIzol reagent into the aqueous phase extraction and centrifugation to get RNA pellets. Then, the resulting RNA pellet was washed with 75% ethanol [absolute ethanol: Fisher Scientific, UK; diluted with nuclease-free water (NFW): Promega, UK] and re-suspended in Diethyl pyrocarbonate (DEPC)-treated water (Invitrogen, UK). The concentration of the isolated RNA was determined spectrophotometrically, and purity was evaluated by 260/230nm and 260/280nm optical density. Extracted RNA was stored at -80°C until required. The SuperScript IV First-Strand Synthesis System (Invitrogen, UK) was used to synthesize the first-strand cDNA from 2μg of purified cell RNA samples.

4.2.7 Quantitative reverse transcription-polymerase chain reaction (qPCR)

For mRNA targets, qRT-PCRs with pre-designed TaqMan™ gene expression assays (CYP24A1, Hs00167999_m1; VDR, Hs01045843_m1; 18S Hs03003631_g1) were prepared with TaqMan™ Fast Advanced Master Mix (Applied Biosystems, UK) and run in triplicates as a 5-point standard curve

with MicroAmp Optical 96-well reaction plates (Applied Biosystems, UK) on the Quant Studio 7 according to manufacturer's instructions (**Appendix Figure C12**). The cDNAs used for standard curves were synthesized from 2μg Human Small Intestine Reference RNA (Takarabio, US) and untreated HepG2 RNA mixture (1:1).

The cDNAs synthesised from treated HepG2 and LX-2 cells were used to quantified CYP24A1 and VDR mRNA expression and run in triplicates on MicroAmp Optical 384-well reaction plates (Applied Biosystems, UK). 18S was used as a reference gene. Relative fold changes of mRNA expression in vitamin D, FA or co-treatment compared to the vehicle was then calculated using the ΔΔCt method.

4.2.8 Protein extraction and analysis

Protein samples were collected from HepG2 and LX-2 cells by applying radio immunoprecipitation assay (RIPA) buffer (ready-to-use solution containing 150mM NaCl, 1.0% IGEPAL® CA-630, 0.5% $C_{24}H_{39}NaO_4$, 0.1% SDS, 50mM Tris, pH 8.0.) containing EDTA-free protease inhibitor (Sigma, UK) directly onto the cells in the flask and incubated on ice for 5min. The flask was then rinsed with a cell scraper to remove and lyse residual cells. After that, the cell lysate was transferred to a proteinase-free tube on ice. The lysate was clarified by moving the whole sample into a labelled single use QIAshredder column (Qiagen, UK) for lysing DNA and reducing sample viscosity, and centrifuged at 10,000x g for 2min at 4℃. The spin column was disposed, tube capped and kept on ice prior to quantification.

The bicinchoninic acid (BCA) protein assay kit (Pierce, Thermo Scientific, UK) was used according to manufacturer's guidelines. A standard curve from 0-2000μg/ml was produced using BSA serially diluted in RIPA buffer. Protein samples were diluted 1/10 in RIPA buffer and the absorbance was measured at 562nm on the CLARIOstar® plate reader.

4.2.8.1 Immunoblotting

Appropriate volumes corresponding to 35μg protein of extracts from treated HepG2 and LX-2 cells were combined with 5μl 4X protein sample loading buffer (LI-COR, UK; containing 55% glycerol, 5% SDS, 2% Tris HCl and 0.5% Orange G) and RIPA buffer to equalise sample volumes. Then samples were

heated at 60℃ for 10min and separated in 12% resolving gels [home-made gel: ddH_2O, 12% (w/v) 30% Acrylamide/Bis (Sigma, UK), 0.38M 1.5M Tris pH8.8, 0.1% (w/v) 10% SDS, 0.17% N,N,N',N'-Tetramethylethylenediamine (Sigma, UK) and 0.12% (w/v) 10% ammonium persulfate (Sigma, UK; 100mg/ml)] under reducing conditions, and electro-blotted on to methanol activated polyvinlidene difluoride (PVDF) membranes. The transfer of protein was confirmed by Ponceau staining of the membrane. Subsequently, non-specific binding sites were blocked with 1X TBST [500ml: 20mM Tris, 150mM NaCl, 0.1% (v/v) Tween 20, adjust pH with HCl to pH 7.6)] containing 0.1% (w/v) no-fat milk powder (Marvel, UK). Antibodies specific to either VDR (rabbit monoclonal, Abcam, UK, 0.849mg/ml, Cat No. Ab109234) or CYP24A1 (rabbit polyclonal, invitrogen, UK, 0.4mg/ml, Cat No. PA5-54579), and α-tubulin (mouse monoclonal, Abcam, UK, 1μg/μl, Cat No. Ab7291) were used to probe the membrane overnight at 4℃. Primary antibodies were detected with LI-COR IRDye labeled secondary antibodies (donkey anti-rabbit 680; 1:25,000 concentration, and donkey anti-mouse 800; 1:25,000) for 1h at room temperature. Blots were visualized on an Odyssey CLx Imaging System and quantified using Image Studio Lite version 3.1 (LI-COR biosciences).

Levels of CYP24A1 and VDR protein expression were measured in treated HepG2 and LX-2 cells and normalized to α-tubulin protein levels.

4.2.9 Data analysis

Results are presented as mean +/- the standard error of the mean (SEM) alongside individual data points. All statistical analysis were carried out using GraphPad Prisms version 9.1.1 (California, US). Comparisons between groups were measured through one-way ANOVA with Dunnett test, two-way ANOVA with Holm-Sidak test or three-way ANOVA with Sidak test as appropriate.

4.3 Results

4.3.1 Serum choice alters liver cell line viability

Previous work in the lab had used SFM for lipid loading experiments (Maldonado et al., 2018) to eliminate interferences of lipophilic materials such as albumin and cholesterol contained in FBS on lipid accumulation. However,

the greater sensitivity of LX-2 cells to culture in SFM with different vehicles (**Figure 4.1**) prompted the systematic testing of cell viability in response to lipid loading with either SCM, SFM or CSM. These experiments systematically examined the effects of serum choice on cell viability at 6h and 24h when cultured with different FA doses.

Overall analyses by two-way ANOVA showed that while serum choice influenced the viability of both cell lines at both time points (all $P<0.05$), an effect of FA dose was only observed in HepG2 cells (6h $P=0.0341$, 24h $P=0.0007$) (**Figure 4.2**). In addition, serum accounted for a much greater amount of the total variance (54.6% versus 15.1% at 24h in HepG2, 44.8% versus 3.72% at 24h in LX-2) in viability than did FA dose. There was no significant interaction between serum choice and FA dose in either cell line at 6 or 24h.

In post hoc examination of serum effects, there were no significant differences in HepG2 cell viability between those cultured in SCM and SFM or CSM at 6h (**Figure 4.2A**). However, compared to SCM, at 24h, HepG2 cell viability was significantly reduced by SFM in vehicle-treated, and all doses of FA treated cells (**Figure 4.2B**, all $P<0.05$). In contrast, an effect of CSM was only observed at the highest dose, 500μM, of FA treatment ($P<0.01$). The approximate 20% reduction in viability observed in CSM cultured cells at the highest amount of FA treatment was smaller than the 40% reduction observed in SFM relative to SCM cultured cells (**Figure 4.2B**).

Notably, LX-2 cell viability was reduced by ~15-39% when cultured with FA in SFM (**Figure 4.2C and 4.2D**, except 6h treatment of 400 μM of FA, all $P<0.05$). There were no alterations in cell viability at any dose of FA treatment at either 6 or 24h when LX-2 cells were cultured in CSM (**Figure 4.2C and 4.2D)**. The lowest reduction in viability at 6h was detected in SFM with the highest dose of FA (**Figure 4.2C**, a 23% reduction, $P=0.0024$); however, at 24h, even LX-2 cells treated with vehicle had a 37% reduction of cell viability (**Figure 4.2D**, $P=0.0019$). Data were also examined as raw absorbance (**Appendix Figure C2**) and relative to vehicle (**Appendix Figure C3**). These analyses confirmed that culturing in CSM primarily rescues the adverse effects of SFM and FA dose on the viability of HepG2 and LX2 cells.

4.3.2 Serum choice alters lipid loading in liver cell lines

Next, the effects of serum on lipid accumulation in both cell lines were

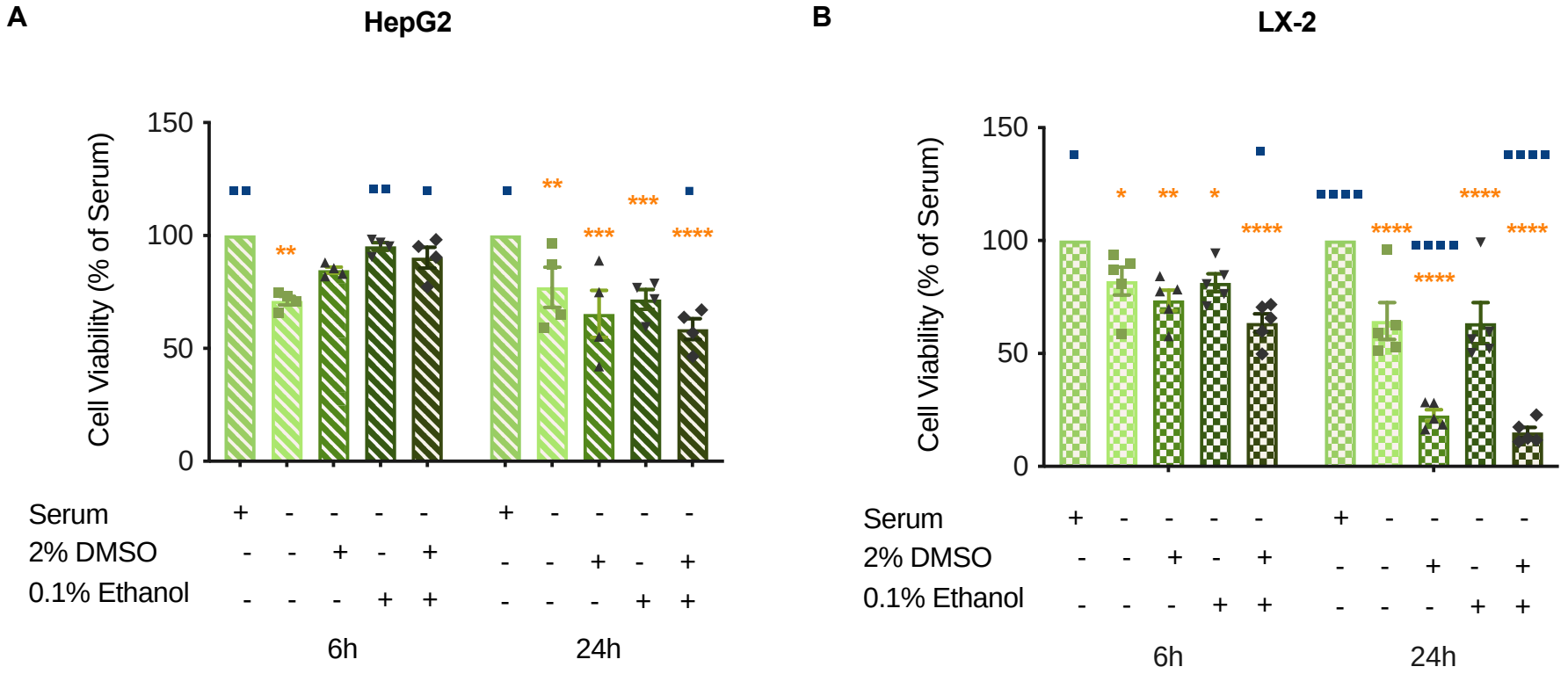

Figure 4.1 Vehicle effects on cell viability. Cell viability was detected by MTT assay of cells cultured in SCM or SFM with or without either 2% DMSO or 0.1% ethanol. Data are shown as mean±SEM and were analysed by two-way ANOVA with Holm-Sidak test for multiple comparisons. **A.** 6h and 24h HepG2 cell viability (n=4, Time: P=0.0002 Treatment: P<0.0001). **B.** 6h and 24h LX-2 cell viability (n=5, Time: P<0.0001, Treatment: P<0.0001). Multiple comparisons examining differences relative to serum (first column) are denoted on the graphs by orange asterisks: *P<0.05, **P<0.01, ***P<0.001 and ****P<0.0001; differences relative to serum-free (second column) are denoted as blue squares: ▪P<0.05, ▪▪P<0.01 and ▪▪▪▪P<0.0001.

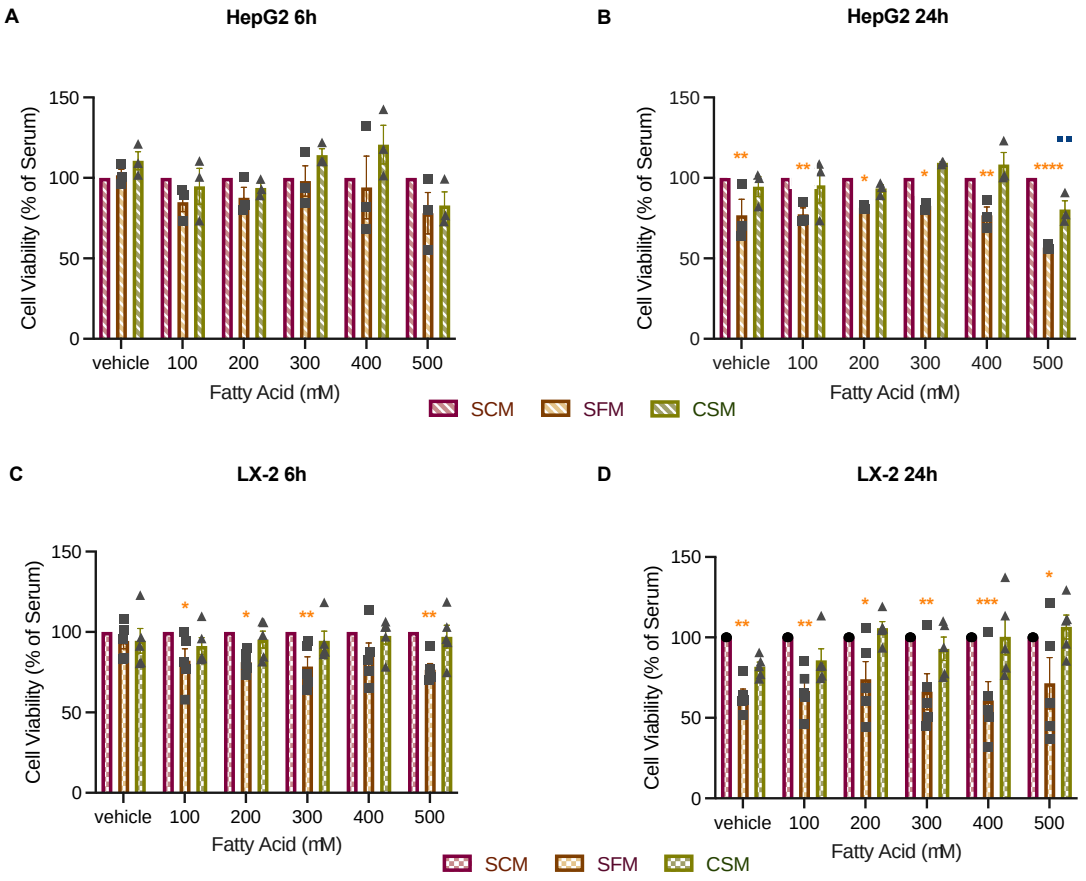

Figure 4.2 Serum effects on cell viability with data presented relative to serum. Cell viability was detected by MTT assay after PA and OA (1:1) treatment (0-500μM) with SCM, SFM and CSM. Data are shown as mean±SEM and were analysed by two-way ANOVA with Holm-Sidak test for multiple comparisons. **A.** 6h HepG2 cell viability (n=3; FA dose: P=0.0341, serum: P=0.0304). **B.** 24h HepG2 cell viability (n=3; FA dose: P=0.0007, serum: P<0.0001). **C.** 6h LX-2 cell viability (n=5; FA dose: P>0.05, serum: P<0.0001). **D.** 24h LX-2 cell viability (n=5; FA dose: P>0.05, serum: P<0.0001). Multiple comparisons examining differences between SCM and SFM denoted are denoted on the graphs by orange asterisks: *P<0.05, **P<0.01, ***P<0.001 and ****P<0.0001; differences between SCM and CSM are denoted as blue squares: ▪▪P<0.01.

assessed. Again data interpretation can be influenced by how the data are expressed; therefore, the data were examined both as raw absorbance (**Appendix Figure C4**) and relative to the vehicle controls for the different mediums (**Figure 4.3**), as well as relative to SCM (**Figure 4.4**). When expressed relative to the appropriate vehicle controls, regardless of the type of medium, the FA treatment induced dose-dependent intracellular lipid accumulation in both cell lines at both time points (**Figure 4.3**, all $P<0.001$). Similar to the cell viability results, overall analyses by two-way ANOVA found effects from serum in both cell lines at both 6h and 24h (**Figure 4.4,** all $P<0.05$). Whereas no effect of FA doses on total variance was detected, no significant interaction was observed between different medium treatments and different FA doses.

In post hoc examination of serum effects, there were no significant differences in HepG2 lipid accumulation between cells cultured in SCM and SFM at 6h (**Figure 4.4A**, except treatment of 100μM of FA with $P=0.0259$). However, compared to SCM, HepG2 intracellular lipid accumulation was significantly reduced by ~33-41% when cultured in CSM with all doses of FA (all $P<0.05$). In contrast with the results of 6h, no significant differences were observed between cells cultured in SCM and SFM or CSM at 24h (**Figure 4.4B**).

Integrating the results of the serum and FA effects on cell viability in HepG2 (**Appendix Figure C3 a and b**) and the serum effects on intracellular lipid accumulation in HepG2 (**Figure 4.3**), we found that, relative to the vehicle, the treatment of 500μM FA could induce the acceptable reduction of cell viability with the highest amount of lipid accumulation. Therefore, to simplify the experiments of LX-2, the serum effects on intracellular lipid accumulation was only examined in cells treated with vehicle and 500μM FA. Compared to SCM, at 6h, the intracellular lipid accumulation of LX-2 was significantly reduced in cells cultured SFM and CSM with the vehicle, as well as 500μM FA (**Figure 4.4C**, all $P<0.001$). However, no significant differences in lipid accumulation were observed between those cultured in SCM and SFM or CSM at 24h (**Figure 4.4D**, except cells treated with 500μM of FA in SFM).

Combined with the results of **Figure 4.4B** and **Figure 4.4D**, no significant differences in lipid accumulation were detected in HepG2 between cells

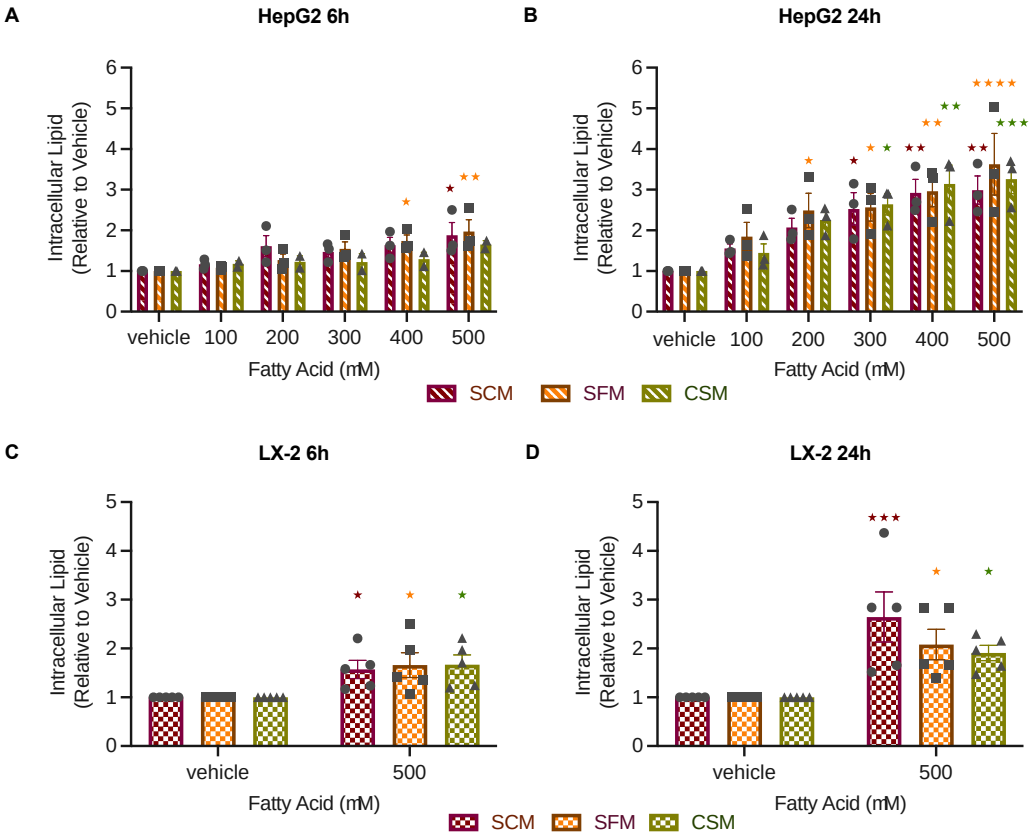

Figure 4.3 Serum effects on lipid accumulation with data presented relative to vehicle. Lipid accumulation was detected by Nile red after PA and OA (1:1, 0-500μM) treatment with SCM, SFM and CSM. Data are shown as mean±SEM and were analysed by two-way ANOVA with Holm-Sidak test for multiple comparisons. **A.** 6h HepG2 intracellular lipid accumulation (n=3; FA dose: P<0.0001, serum: P>0.05). **B.** 24h HepG2 intracellular lipid accumulation (n=3; FA dose: P<0.0001, serum: P>0.05). **C.** 6h LX-2 intracellular lipid accumulation (n=5; FA dose: P<0.0001, serum: P>0.05). **D.** 24h LX-2 intracellular lipid accumulation (n=5; FA dose: P<0.0001, serum: P>0.05). Multiple comparisons examining differences between vehicle and different FA treatments in SCM denoted are denoted on the graphs by red stars: ★P<0.05, ★★P<0.01 and ★★★P<0.001; differences between vehicle and different FA treatments in SFM are denoted as orange stars: ★P<0.05, ★★P<0.01 and ★★★★P<0.0001; differences between vehicle and different FA treatments in CSM are denoted as green stars: ★P<0.05, ★★P<0.01 and ★★★P<0.001.

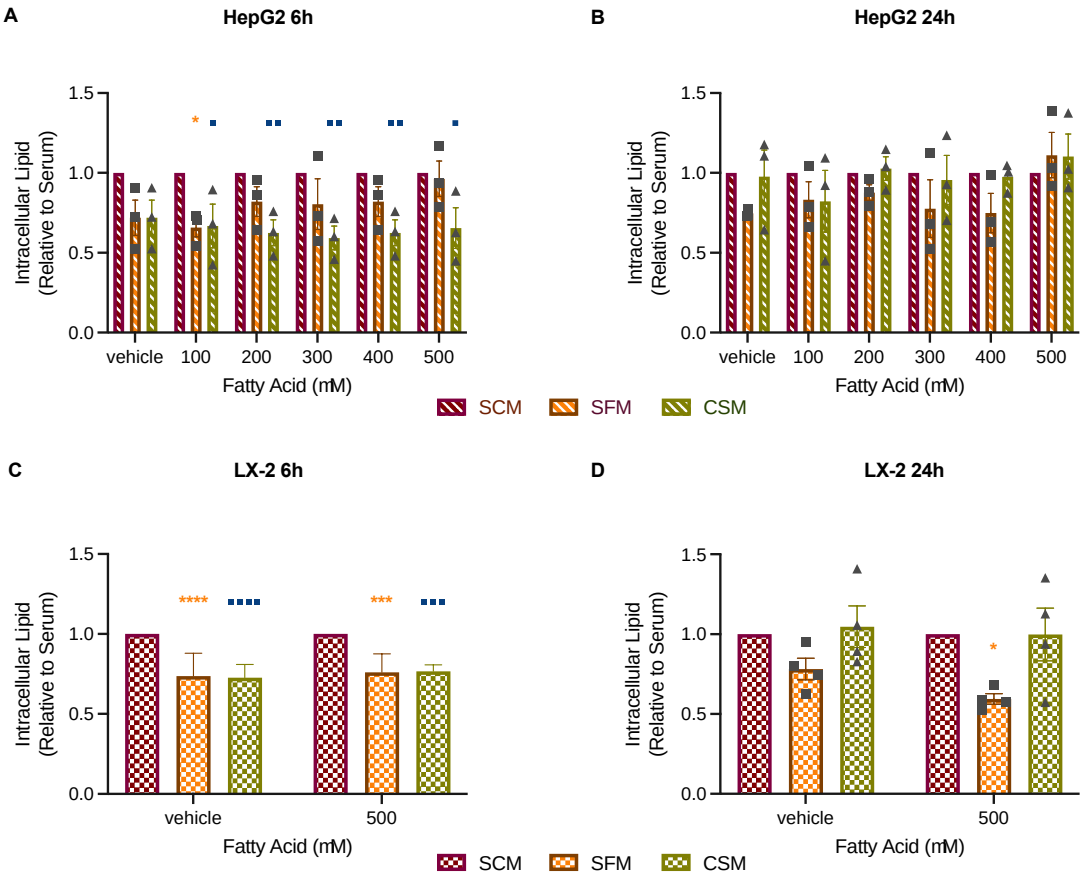

Figure 4.4 Serum effects on lipid accumulation with data presented relative to serum. Lipid was detected by Nile red staining of cells after PA and OA (1:1) treatment (0-500μM) with SCM, SFM and CSM. Data are shown as mean±SEM and were analysed by two-way ANOVA with Holm-Sidak test for multiple comparisons. **A.** 6h HepG2 intracellular lipid accumulation (n=3; FA dose: P>0.05, serum: P<0.0001). **B.** 24h HepG2 intracellular lipid accumulation (n=3; FA dose: P>0.05, serum: P=0.0379). **C.** 6h LX-2 intracellular lipid accumulation (n=5; FA dose: P>0.05, serum: P<0.0001). **D.** 24h LX-2 intracellular lipid accumulation (n=5; FA dose: P>0.05, serum: P<0.0001). Multiple comparisons examining differences between SCM and SFM denoted are denoted on the graphs by orange asterisks: *P<0.05, ***P<0.001 and ****P<0.0001; differences between SCM and CSM are denoted as blue squares: ▪P<0.05, ▪▪P<0.01, ▪▪▪P<0.001 and ▪▪▪▪P<0.0001.

cultured in SCM and SFM or CSM at 24h with 500μM FA. However, a significant reduction was seen in LX-2 cells cultured in SFM with 500μM FA compare to SCM (a 41% reduction, P=0.0164). This suggested that, compared to HepG2 cells, the response of LX-2 cells on lipid accumulation were more sensitive to the serum-free condition when cells treated with 500μM FA. In parallel with the conclusion of cell viability, the CSM culture condition releases the harmful effects of SFM on the cell lipid accumulation treated with FA, especially in LX-2. Therefore, CSM is a better choice for further experiments, which had better cell viability than SFM and a similar amount of FA accumulation to SCM. And 500μM dose of FA was chosen for further investigations to get the highest amount of intracellular lipid loading.

4.3.3 Induction of CYP24A1 and VDR target gene expression is dependent on dose and duration of 1α,25(OH)$_2$D$_3$ exposure in liver cell lines

To examine the bioactivity of vitamin D solution and determine the cell responses to vitamin D, the mRNA expression of two vitamin D responsive genes, CYP24A1 and VDR, was measured in both cell lines. Notably, 1α,25(OH)$_2$D$_3$ induced the expression of CYP24A1; in turn, the increased CYP24A1 promoted the catabolism of 1α,25(OH)$_2$D$_3$ (Jeon and Shin, 2018). On the other hand, 1α,25(OH)$_2$D$_3$ was post-transcriptionally regulated by VDR to perform diverse biologic functions. Before I tested the effects of serum choice on cell viability and made the discission to use CSM for vitamin D and lipid loading experiments, initial vitamin D treatments were done in SFM (**Figure 4.5** and **Appendix Figure C5-9**).

Cells were firstly treated with vehicle (0.1% ethanol) and 1000nM 1α,25(OH)$_2$D$_3$ in SFM for 24h. CYP24A1 was significantly increased in both cell lines after 24h treatment, with an ~22-fold increase in HepG2 and an ~135-fold increase in LX-2 cells, separately (**Figure 4.5A**: all P<0.0001). On the other hand, an ~40% reduction in VDR mRNA levels was observed in both cell lines relative to the vehicle (**Figure 4.5B**: all P<0.0001). Then, both HepG2 and LX2 cells were treated with a series of 1α,25(OH)$_2$D$_3$ doses (0,1, 2, 10, 100 and 1000nM) for 24h (**Figure 4.5 C and D**). Analyses by one-way ANOVA showed that the 1α,25(OH)$_2$D$_3$ treatment induced dose-dependent mRNA expression of CYP24A1 in both cell lines (both P<0.01). This suggested that

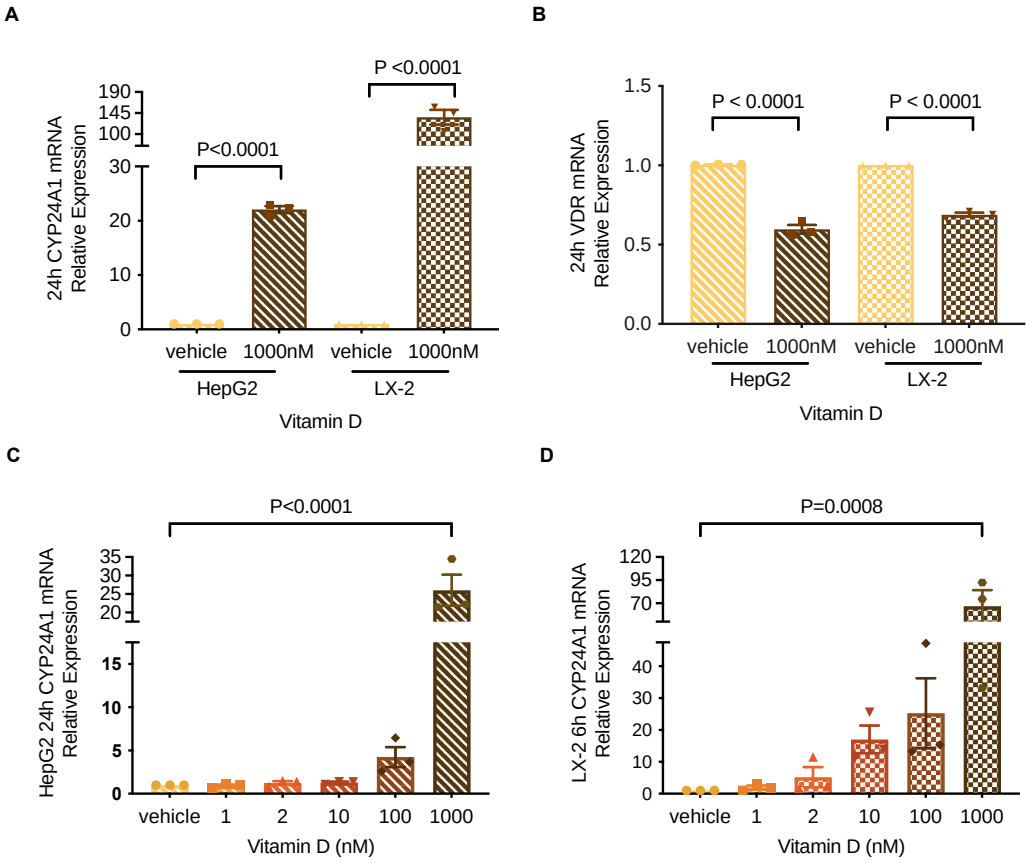

Figure 4.5 CYP24A1 and VDR mRNA expression in response to vitamin D treatment of cells cultured in SFM. Data are normalized 18S rRNA and shown as mean±SEM. Data were analysed by one-way ANOVA with Dunnett test for multiple comparisons. P<0.05 was considered statistically significant. **A.** CYP24A1 mRNA expression in response to 24h vitamin D treatment in HepG2 and LX2 [vehicle (0.1% ethanol) and 1000nM; both HepG2 and LX-2 n=3]. **B.** VDR mRNA expression in response to 24h vitamin D treatment in HepG2 and LX2 [vehicle (0.1% ethanol) and 1000nM; both HepG2 and LX-2 n=3]. **C.** CYP24A1 mRNA expression in response to 24h vitamin D treatment in HepG2 [vehicle (0.1% ethanol), 1nM, 2nM, 10nM, 100nM and 1000nM; HepG2 n=3]. **D.** CYP24A1 mRNA expression in response to 6h vitamin D treatment in LX-2 [vehicle (0.1% ethanol), 1nM, 2nM, 10nM, 100nM and 1000nM; HepG2 n=3, LX-2 n=3].

the mRNA expression of CYP24A1 could be a positive control to assess the cell responses to 1α,25(OH)$_2$D$_3$.

After testing the effects of serum and FA doses on cell viability and lipid accumulation, CSM and 500μM FA were used for further experiments. To establish time points and amounts of vitamin D for the further co-treatment investigations, CYP24A1 and VDR mRNAs were measured in cells cultured with vehicle (2% DMSO) or 500μM FA, and vitamin D [vehicle (0.01% ethanol), 10nM or 100nM 1α,25(OH)$_2$D$_3$] in CSM at several time points (0.5h, 1h, 6h and 24h).

The two-way ANOVA indicated that treatment and time had significant effects on CYP24A1 expression in both cells lines (**Figure 4.6B and 4.7B**: all P<0.0001). The post hoc analyses examined the CYP24A1 mRNA expression response to vitamin D with or without FA at different time points. Compared to the vehicle/vehicle group, the CYP24A1 mRNA expression was only found significantly increased by vehicle/10nM 1α,25(OH)$_2$D$_3$ or vehicle/100nM 1α,25(OH)$_2$D$_3$ at 24h in both cell lines (all P<0.05). In 500μM FA treated groups, both 10nM and 100nM 1α,25(OH)$_2$D$_3$ induced a significant increase of CYP24A1 mRNA expression in HepG2 at 24h (both P<0.001). However, the CYP24A1 was only found to increase by 500μM FA /100nM 1α,25(OH)$_2$D$_3$ at 24h in LX-2 cells (P<0.0001). The highest increase of CYP24A1 expression was detected in the 500μM FA/100nM 1α,25(OH)$_2$D$_3$ group at 24h in both cell lines, with a ~26-fold increase in HepG2 and a ~4.9-fold increase in LX-2, respectively.

For the expression of VDR mRNA, while time influenced the VDR expression in HepG2 cells detected by two-way ANOVA (**Figure 4.6D**, P=0.0148), an effect of treatment was observed in LX-2 cells (**Figure 4.7D**, P=0.00126). There was no significant interaction on the expression of VDR between treatment and time in either cell line. What's more, there were no significant differences between different treatments at any time points tested by the post hoc analyses. Although interestingly, a trend for increased VDR expression was observed from 0.5h to 6h in LX-2 cells treated with 100nM vitamin D, the expression dropped at 24h.

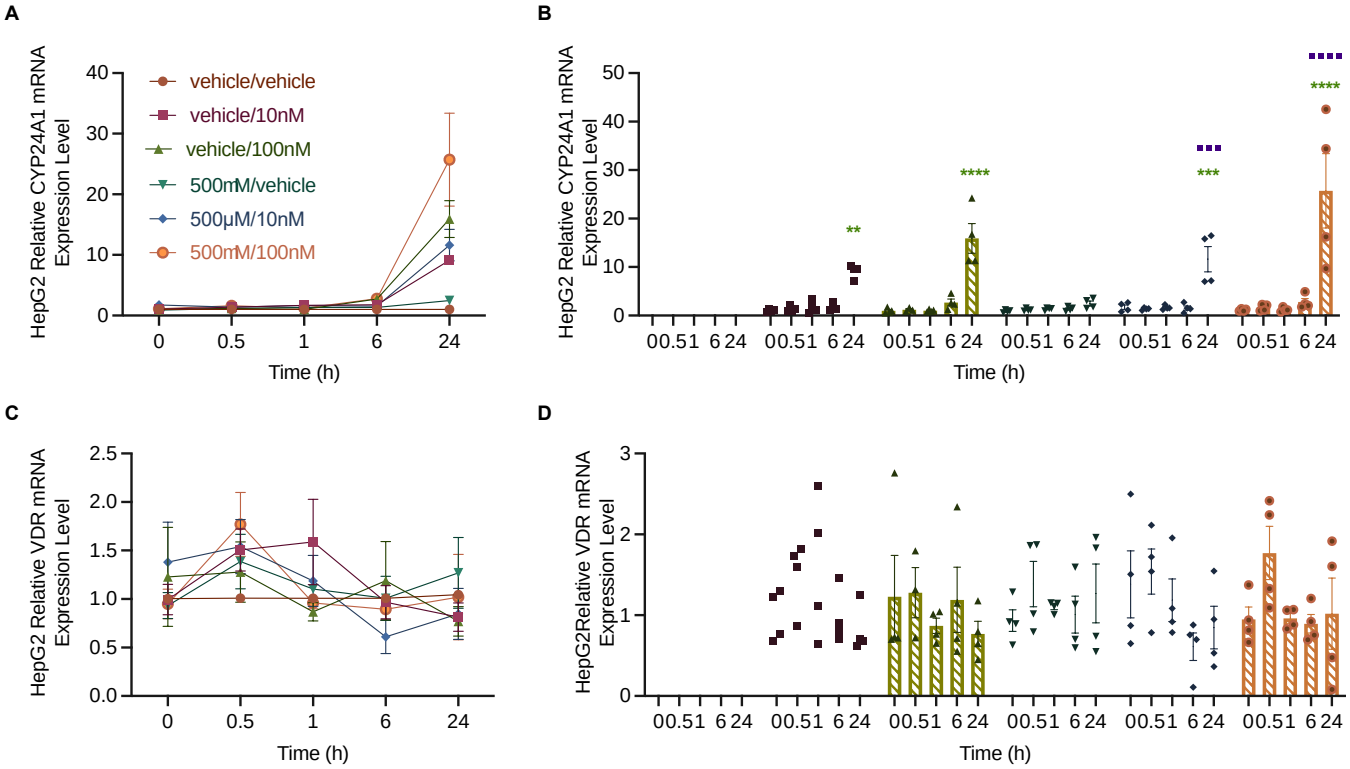

Figure 4.6 CYP24A1 and VDR mRNA expression in response to fatty acid and vitamin D treatment in HepG2 cells. Cells were treated with or without fatty acids [500**μ**M or vehicle (2%DMSO)] and different doses of vitamin D [vehicle (0.01% ethanol), 10nM or 100nM]. Data are *relative* to 18S rRNA and shown as mean±SEM. Data were analysed by two-way ANOVA with Holm-Sidak test for multiple comparisons. **A.** CYP24A1 mRNA expression in response to 24h vitamin D treatment in HepG2 (n=3; Time: P<0.0001, Treatment: P<0.0001). **B.** CYP24A1 mRNA expression in response to 24h vitamin D treatment in HepG2 (based on different treatment group). **C.** VDR mRNA expression in response to 24h vitamin D treatment in HepG2 (n=3; Time: P=0.0148, Treatment: P>0.05). **D.** VDR mRNA expression in response to 24h vitamin D treatment in HepG2 (based on different treatment group). Multiple comparisons examining differences between vehicle/vehicle and 500μM/100nM are denoted on the graphs by green asterisks: **P<0.01, ***P<0.001 and ****P<0.0001; differences between 500μM/vehicle and 500μM/100nM are denoted as purple squares: ▪▪▪▪P<00001.

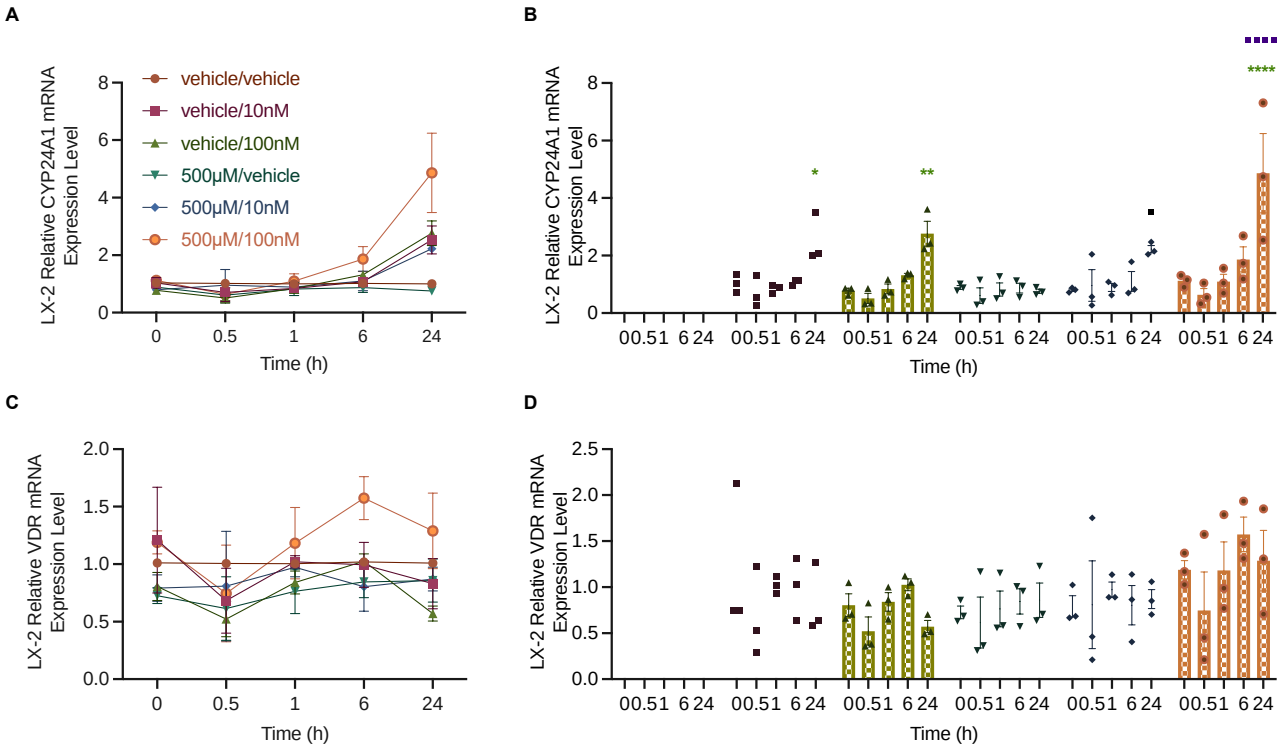

Figure 4.7 CYP24A1 and VDR mRNA expression in response to fatty acid and vitamin D treatment in LX-2 cells. Cells were treated with or without fatty acids [500µM or vehicle (2%DMSO)] and different doses of vitamin D [vehicle (0.01% ethanol), 10nM or 100nM]. Data are *relative* to 18S rRNA and shown as mean±SEM. Data were analysed by two-way ANOVA with Holm-Sidak test for multiple comparisons. **A.** CYP24A1 mRNA expression in response to 24h vitamin D treatment in LX-2 (n=3; Time: P<0.0001, Treatment: P=0.0001). **B.** CYP24A1 mRNA expression in response to 24h vitamin D treatment in LX-2 (based on different treatment group). **C.** VDR mRNA expression in response to 24h vitamin D treatment in LX-2 (n=3; Time P>0.05, Treatment: P=0.0126). **D.** VDR mRNA expression in response to 24h vitamin D treatment in LX-2 (based on different treatment group). Multiple comparisons examining differences between vehicle/vehicle and 500μM/100nM are denoted on the graphs by green asterisks: *P<0.05, **P<0.01 and ****P<0.0001; differences between 500μM/vehicle and 500μM/100nM are denoted as purple squares: ▪▪▪▪P<0.0001.

Therefore, mainly based on the results of CYP24A1 mRNA expression (**Figure 4.6B and 4.7B**), 100nM 1α,25(OH)$_2$D$_3$ would be used in further experiments combined with 500μM FA to get a higher level of CYP24A1 mRNA induction.

4.3.4 Co-treatment with 1α,25(OH)$_2$D$_3$ affects the cell viability induced by fatty acid treatment in liver cell lines

With doses for co-treatment of vitamin D and FA established, the next step was to characterise the lipid loading model to investigate the responses of 1α,25(OH)$_2$D$_3$ treatment in both cell lines. Firstly, cell viability effects were examined in cells cultured with either vitamin D, FA or in combination.

The three-way ANOVA analyses showed a significant FA treatment-dependent effect on cell viability in both cell lines (**Figure 4.8 A and B**: all $P<0.05$). In post hoc multiple comparison analyses, in both HepG2 and LX-2 cells, there were no significant differences between different treatments at any time points. Relative to the control group (2% DMSO and 0.01% ethanol), both HepG2 and LX-2 cells had a ~5.7-12.6% reduction in cell viability responded to fatty acid treatment only, but a ~13.1-26.7% reduction in co-treatment at both time points (all $P>0.05$). Data were also examined as raw absorbance and relative to CSM (**Appendix Figure C11**). The viability results of co-treatment in both cell lines suggested that vitamin D might aggravate the cytotoxicity caused by lipid loading alone.

4.3.5 Co-treatment with 1α,25(OH)$_2$D$_3$ influences the lipid loading induced by fatty acid treatment in liver cell lines

Next, intracellular lipid loading was then examined by Nile red assay in the cotreatment models to investigate whether vitamin D could alleviate intracellular lipid accumulation induced by FA treatment. According to the results of three-way ANOVA, both FA treatment and time contributed to the interaction of lipid accumulation in HepG2 cells (**Figure 4.9A,** both $P<0.0001$). In addition, although vitamin D did not affect lipid loading results in HepG2, there was an interaction between FA and vitamin D treatment on lipid accumulation ($P=0.0121$). In contrast, only FA treatment was found influenced lipid accumulation in LX-2 cells (**Figure 4.9B** $P<0.0001$). The multiple

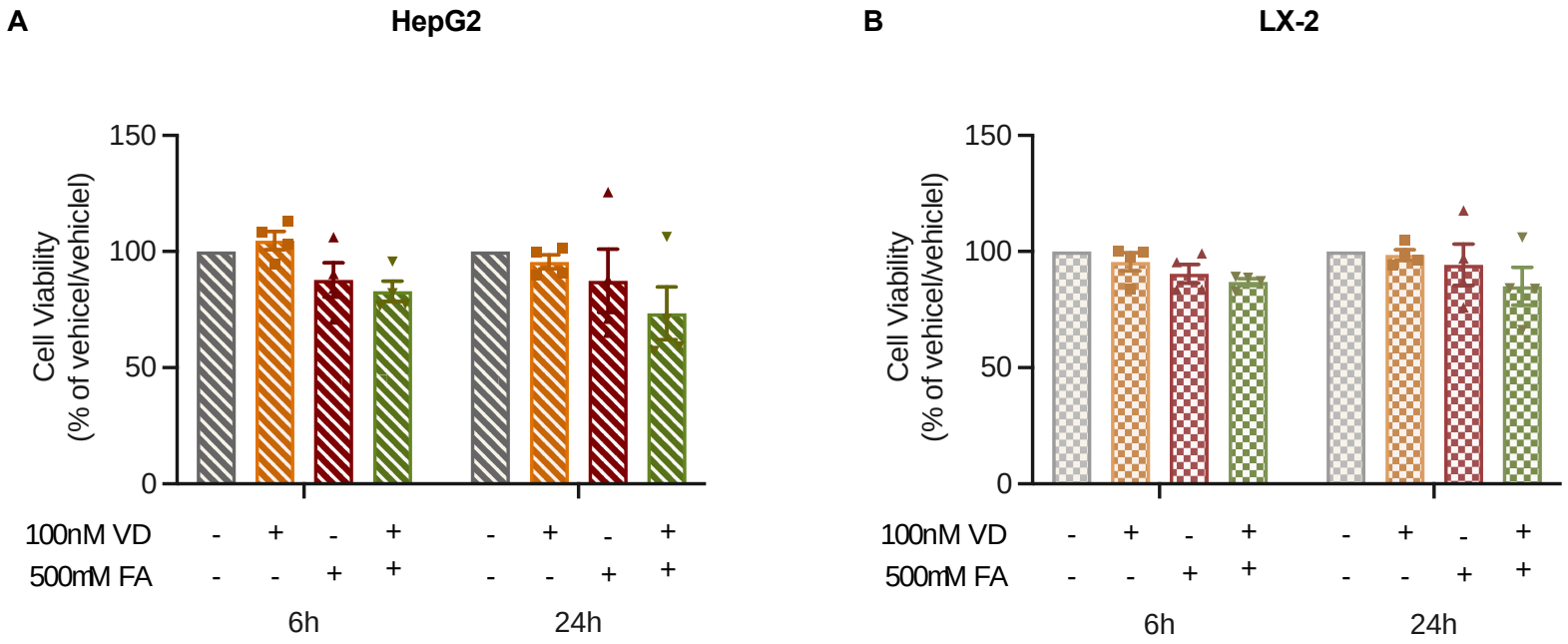

Figure 4.8 Cell viability after cultured either with or without fatty acids or vitamin D with data presented relative to vehicle/vehicle. Cell viability was detected by MTT assay after culturing in CSM, and either with or without PA and OA (1:1) treatment (500μM) or vitamin D treatment (100nM). Data are shown as mean±SEM. Data were analysed by three-way ANOVA with Sidak test for multiple comparisons. **A.** 6h and 24h HepG2 cell viability (n=4, Timepoint: P>0.05, Fatty acid: P=0.0025, Vitamin D: P>0.05). **B.** 6h and 24h LX-2 cell viability (n=4, Timepoint: P>0.05, Fatty acid: P=0.0112, Vitamin D: P>0.05). P<0.05 is considered statistically significant between different groups in multiple comparisons.

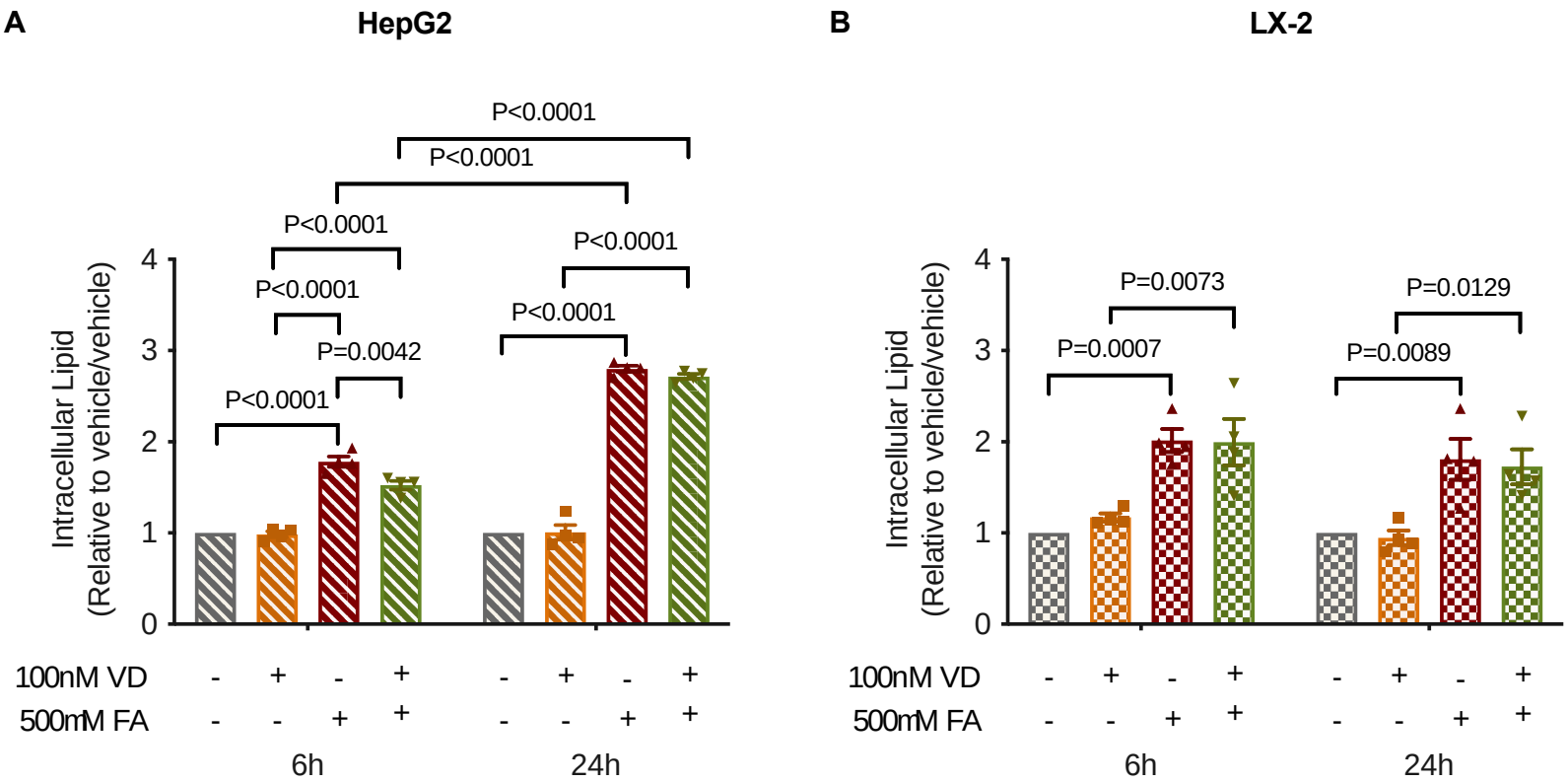

Figure 4.9 Intracellular lipid accumulation after cultured either with or without fatty acids or vitamin D with data presented relative to vehicle/vehicle. Lipid was detected by Nile red staining of cells after either with or without PA and OA (1:1) treatment (500μM) or vitamin D treatment (100nM). Data are shown as mean±SEM. Data were analysed by three-way ANOVA with Sidak test for multiple comparisons. **A.** 6h and 24h HepG2 intracellular lipid accumulation (n=4, Timepoint: P<0.0001, Fatty acid: P<0.0001, Vitamin D: P=0.0098). **B.** 6h and 24h LX-2 intracellular lipid accumulation (n=4, Timepoint: P>0.05, Fatty acid: P<0.0001, Vitamin D: P>0.05). P<0.05 is considered statistically significant between different groups in multiple comparisons.

comparison results indicated that HepG2 cells treated with 500μM FA only at 24h produced more significant intracellular lipid loading than LX-2 cells, with a 2.8-fold increase in HepG2 ($P<0.0001$) and a 1.7-fold increase in LX-2 ($P=0.0089$), separately. Compared to the FA group, a ~14% reduction of lipid accumulation induced by vitamin D was detected in the co-treatment group at 6h in HepG2 cells ($P=0.0042$). Additionally, vitamin D appeared to cause a slight reduction of lipid accumulation in the co-treatment group in HepG2 cells at 24h and in LX-2 cells at both time points; but the results were not statistically significant (HepG2 24h $P>0.05$; LX-2 6h and 24h $P>0.05$). Data were also examined as raw absorbance (**Appendix Figure C12**). Thus, the lipid accumulation results of co-treatment in both cell lines suggested that vitamin D could decrease lipid loading to some extent.

4.3.6 Effects of fatty acid and vitamin D on VDR and CYP24A1 mRNA and protein expression

After investigating the effects of vitamin D and FA treatments on cell viability and intracellular lipid loading, to determine whether vitamin D could induce the expression of two potential control genes, CYP24A1 and VDR, in HepG2 and LX-2 cells, a series of qPCR and immunoblotting experiments were performed in co-treatment models.

The three-way ANOVA analyses showed that while FA treatment affected the VDR mRNA expression of HepG2 cells (**Figure 4.10A,** $P=0.0007$), an effect of time was observed in LX-2 cells (**Figure 4.11A,** $P=0.00177$). In HepG2 cells, compared to vitamin D treated only, the VDR mRNA was significantly decreased at 6h in co-treatment (a 50% reduction, $P=0.0100$). VDR mRNA expression appeared to induce a decrease by FA in HepG2 at both 6h and 24h (all $P>0.05$). When combined with vitamin D, the negative effect seemed to be enhanced (all $P>0.05$). On the contrary, there were no significant differences between treatments at any time point in LX-2 cells. There was appeared to be no fold change detected in LX-2 between FA and cotreatment at 6h ($P>0.05$). However, VDR mRNA seemed to be increased by FA at 24h, and this effect appeared to be inhibited by vitamin D in co-treatment ($P>0.05$).

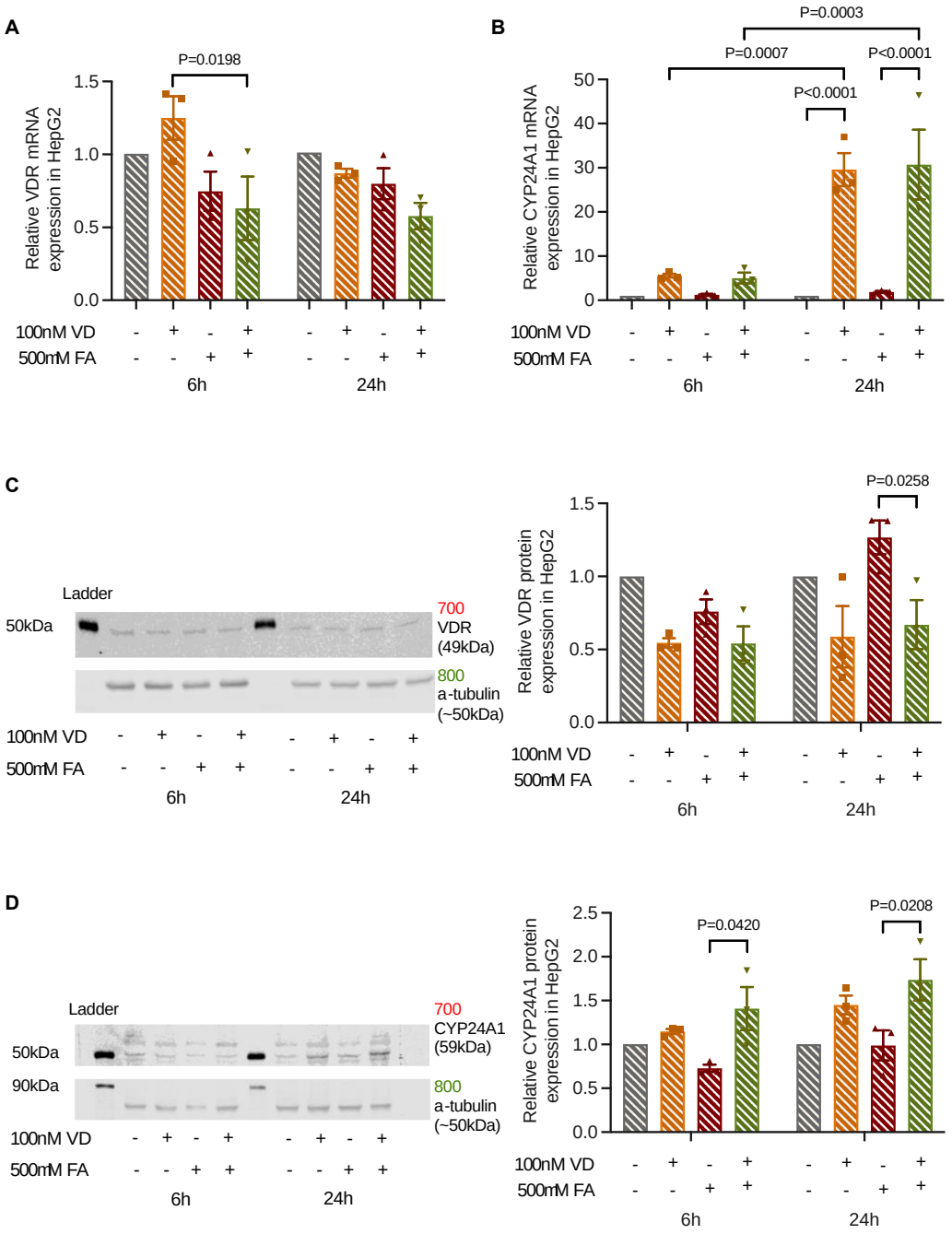

Figure 4.10 CYP24A1/VDR mRNA and protein expression in response to fatty acid and vitamin D co-treatment in HepG2. Cells were treated either with or without PA and OA (1:1) treatment (500 μM) or vitamin D treatment (100nM). Data shown as mean±SEM. Data were analysed by two-way ANOVA with Holm-Sidak test for multiple comparisons. **A.** 6h and 24h VDR mRNA expression in HepG2 (n=3; Timepoint: P>0.05, Fatty acid: P=0.0007, Vitamin D: P>0.05). **B.** 6h and 24h CYP24A1 mRNA expression in HepG2 (n=3; Timepoint: P<0.0001, Fatty acid: P>0.05, Vitamin D: P<0.0001). Data are relative to 18S rRNA. **C.** 6h and 24h VDR protein expression in HepG2 (n=3; Timepoint: P>0.05, Fatty acid: P>0.05, Vitamin D: P<0.0001). **D.** 6h and 24h CYP24A1 protein expression in HepG2 (n=3; Timepoint: P=0.0402, Fatty acid: P>0.05, Vitamin D: P<0.0001). Data are normalised to α-Tubulin. P<0.05 is considered statistically significant between different groups in multiple comparisons.

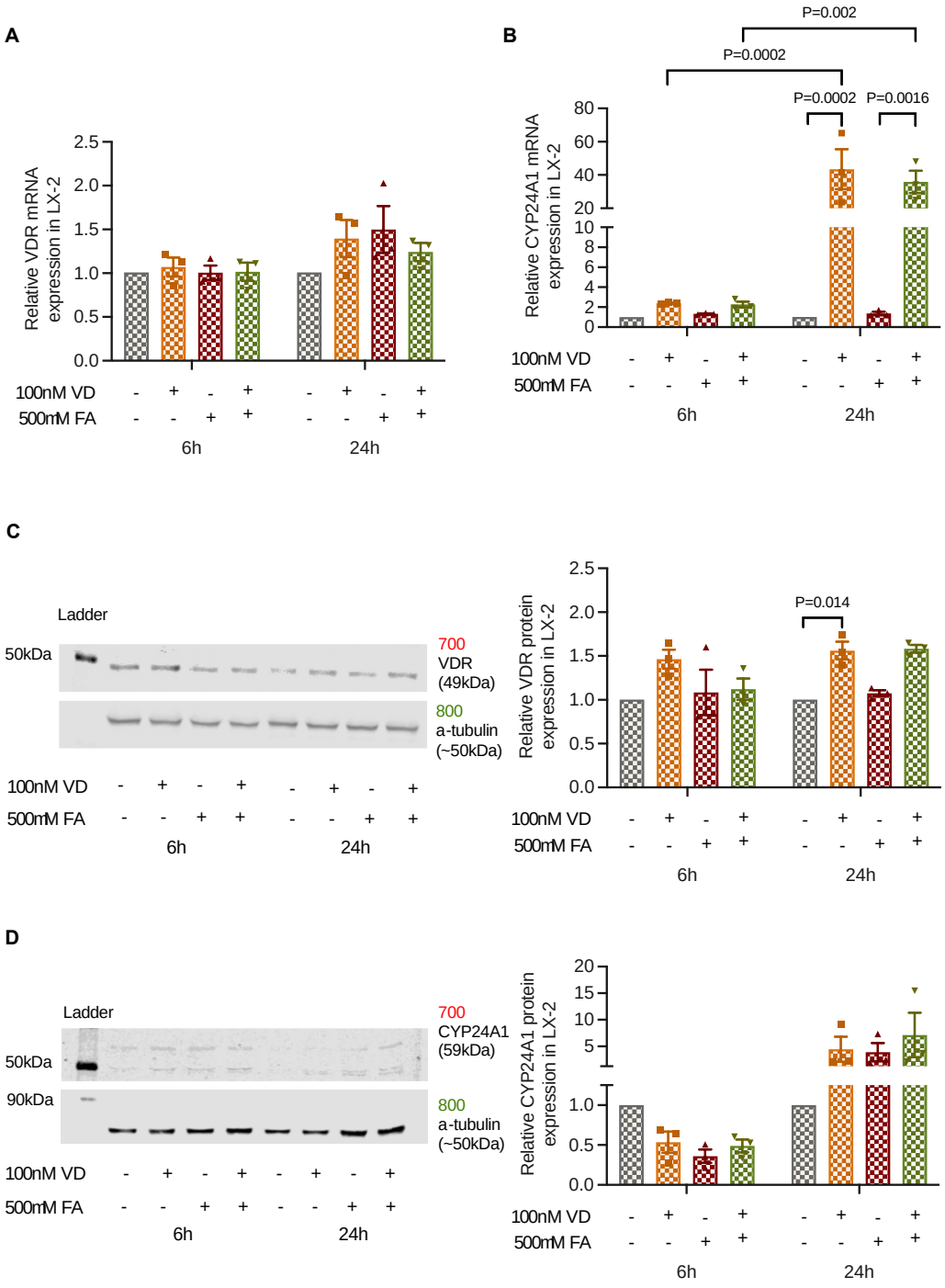

Figure 4.11 CYP24A1/VDR mRNA and protein expression in response to fatty acid and vitamin D co-treatment in LX-2. Cells were treated either with or without PA and OA (1:1) treatment (500μM) or vitamin D treatment (100nM). Data shown as mean±SEM. Data were analysed by two-way ANOVA with Holm-Sidak test for multiple comparisons. **A.** 6h and 24h VDR mRNA expression in LX-2 (n=3; Timepoint: P=0.0177, Fatty acid: P>0.05, Vitamin D: P>0.05). **B.** 6h and 24h CYP24A1 mRNA expression in LX-2 (n=3; Timepoint: P<0.0001, Fatty acid: P>0.05, Vitamin D: P<0.0001). Data are relative to 18S rRNA. **C.** 6h and 24h VDR protein expression in LX-2 (n=3; Timepoint: P>0.05, Fatty acid: P>0.05, Vitamin D: P=0.0002). **D.** 6h and 24h CYP24A1 protein expression in LX-2 (n=3; Timepoint: P=0.014, Fatty acid: P>0.05, Vitamin D: P>0.05). Data are normalised to α-Tubulin. P<0.05 is considered statistically significant between different groups in multiple comparisons.

An effect of vitamin D treatment on VDR protein expression was observed in both HepG2 and LX-2 cells (**Figure 4.11C and Figure 4.11C**, both P<0.01), while FA treatment and time had no effect in both cell lines. In post hoc analyses, in HepG2 cells compared to FA, VDR protein was reduced by ~47% in co-treatment at 24h (P=0.0258). Oppositely, a ~46% increase was seen in co-treatment group compared to FA in LX-2 cells at 24h (P>0.05). Additionally, compared to the control group, FA appeared to increased VDR protein expression in both cells at 24h (both HepG2 and LX-2 P>0.05); however, this effect seemed to be inhibited by vitamin D in HpeG2 (P=0.0258) and promoted in LX-2 (P>0.05). Interestingly, VDR protein was induced by vitamin D treatment only compared to control at 24h in LX-2 cells (P=0.014) but not in HepG2 cells.

The data of VDR mRNA and protein verified that FA inhibits VDR mRNA expression in HepG2 cells, not in LX-2; vitamin D decreases VDR protein expression in HepG2 cells but induced VDR expression in LX-2 cells.

Both vitamin D treatment and time, but not FA treatment, influenced CYP24A1 mRNA expression analysed by three-way ANOVA in both cell lines (**Figure 4.10B and Figure 4.11B**, both P<0.0001). Vitamin D treatment accounted for a greater amount of the total variance (41.08% versus 24.06% in HepG2, 30.33% versus 26.97% in LX-2; all P<0.001) in CYP24A1 mRNA than time. The post hoc analyses showed that, compared to the control, cultured either LX-2 or HepG2 cells with vitamin D increased CYP24A1 mRNA in the absence or presence of FA at 24h (all P<0.0001). The highest level of CYP24A1 mRNA was detected in co-treatment group of HepG2 cells at 24h (~30-fold increase) and in vitamin D group of LX-2 cells at 24h (~36-fold increase).

Analyses by three-way ANOVA showed that both vitamin D treatment and time affect the results of CYP24A1 protein expression in HepG2 cells (**Figure 4.10D**, both P<0.05). However, significant interaction between vitamin D treatment and time was observed in HepG2 (P<0.0001). On the other hand, only an effect of time was detected in LX-2 cells (**Figure 4.11D**, P=0.014). The multiple comparison analyses showed that, compared to FA group, an increase expression of CYP24A1 was observed in co-treatment of HepG2 at both time points (6h: a ~93% increase, 24h: a ~76% increase; both P<0.05).

Contrary to HepG2 cells, there were no significant differences between different treatments at any time points in LX-2 cells.

The data of CYP24A1 mRNA confirmed the conclusion that vitamin D essentially stimulates the mRNA expression of CYP24A1 in both cell lines. Furthermore, in parallel with the results of CYP24A1 mRNA, vitamin D triggers CYP24A1 protein expression in HepG2 cells but not in LX-2.

4.4 Discussion

In this chapter, *in vitro* models of hepatic lipid loading co-treated with vitamin D in both immortalised hepatocytes (HepG2) and immortalised HSCs (LX-2) were evaluated. The importance of serum choice for our co-treatment models, especially in viability, were firstly investigated. The experiments indicate that CSM is a better choice, resulting in better cell viability than SFM and similar lipid loading as SCM in both cell lines after 24h 500μM FA treatment. In addition, 500μM FA was chosen to get the highest amount of intracellular lipid loading. After testing CYP24A1 and VDR mRNA expression in cells cultured in 500μM FA with various vitamin D doses and time points, 100nM 1α,25(OH)$_2$D$_3$ and the 6h and 24h were chosen for co-treatment investigation.

After establishing the treatment conditions and time points, the next step was to characterise the lipid loading model to investigate cellular responses to 1α,25(OH)$_2$D$_3$ treatment in both cell lines. The results of co-treatment suggested that 1α,25(OH)$_2$D$_3$ might aggravate the adverse effects on cell viability caused by FA but attenuate the intracellular lipid accumulation induced by FA in both cell lines. However, the results of CYP24A1 and VDR target gene expression were conflicting. Compared to the vitamin D treatment group, VDR mRNA expression was repressed by FA in HepG2 cells with co-treatment at 6h. Additionally, in comparison to cells treated with FA at 24h, co-treatment with 1α,25(OH)$_2$D$_3$ inhibited VDR protein expression in HepG2 cells, but the contrary results were observed in LX-2. On the other hand, the data of CYP24A1 mRNA confirmed the conclusion that vitamin D essentially stimulates the mRNA expression of CYP24A1 in both cell lines. Furthermore, in parallel with the results of CYP24A1 mRNA, vitamin D triggers CYP24A1 protein expression in HepG2 cells but not in LX-2.

4.4.1 Serum choice influences the viability of liver cell lines in culture

Serum choice significantly affected cell viability and lipid loading in both HepG2 and LX-2 cells when cultured with FAs. In comparison to SCM, SFM reduced cell viability with FA treatments, especially in LX-2 cells. In contrast, no differences in cell viability were found between SCM and CSM in either cell line. In contrast, lipid accumulation was significantly lower in both cell lines at 6h when cultured in CSM with FAs compared to in SCM. No differences were found between SCM and CSM at 24h.

The MTT assay was used to examine serum effects on cell viability in this chapter. Since MTT was first described by Mosmann (1983) for measuring the number of viable cells, it has become a ubiquitous method to measure cellular metabolic activity as an indicator of cell viability, proliferation and drug cytotoxicity (Stockert et al., 2018). Generally, the MTT assay assumes that mitochondrial activity is constant in most viable cells; therefore, a rise or decrease in the number of viable cells is linearly associated with mitochondrial activity (van Meerloo et al., 2011). However, recent studies suggested that the MTT assay is more than a mere representation of mitochondrial activity, as the tetrazolium salt MTT-converted formazan crystals have been located in various other intracellular organelles, such as endoplasmic reticulum, cytosolic lipid droplets, plasma membranes, nucleus, and microsomes (Ghasemi et al., 2021). Additionally, several reducing biomolecules (e.g. ascorbic acid vitamin A and sulfhydryl-containing compounds) could lead to a non-enzymatic reduction of the MTT to formazan, interfering with the results of the MTT assay (Stockert et al., 2018). Therefore, the common claim as a viability assay is often erroneous. Reduction of the tetrazolium relays predominantly on cell metabolism; sometimes, it reflects cell viability, but various confounding factors, such as cell seeding number, culture medium type and experimental treatments, might cause inaccurate results.

Three different types of medium were used to examine serum effects: SCM (containing FBS), SFM (no serum) and CSM (containing CS-FBS). Notably, FBS is essential to stimulate the growth and proliferation of eukaryotic cells cultured *in vitro*, providing various biomolecules, including growth factors, proteins, vitamins and hormones (Puck et al., 1958; Fisher et

al., 1958). Thus, using a medium without serum might cause reduced cell survival and apoptosis. Previous work in the lab had used SFM for lipid loading experiments on HepG2 cells to avoid inducing several variables, such as albumin, cholesterol, and other FAs, to produce extra lipid accumulation (Maldonado et al., 2018). The previous results also indicated that SFM had fewer effects on the viability of HepG2 cells, even with vehicles and experimental treatments.

However, when LX-2 was brought into our lab, the cell viability tests showed that LX-2 cells were more sensitive to vehicle treatments than HepG2 cells without FBS. Although Xu et al. (2005) denoted that LX-2 cells have good viability in serum-free cultured conditions, our results indicated that LX-2 cells cultured in SFM for 24h leaded to ~40% reduction of viability compared to SCM. Furthermore, LX2 viability was lower when combined with vehicle controls, i.e., reduced to just 20% live cells. Thus, the differences in viability found in cells cultured with or without FBS can be explained by a potential protective effect of serum factors in FBS.

To maintain cell viability and set up a lipid loading model on LX-2 cells, charcoal-stripped FBS was induced and systematically tested for cell viability and intracellular lipid accumulation. Compared to FBS, lipophilic materials were removed in charcoal-stripped FBS, but constituents vital to cell growth and viability were preserved (Liang et al., 2020). My results confirmed no differences between SCM and CSM on cell viability when cells were treated with vehicles. On the other hand, significant differences between SCM and CSM on lipid accumulation were only found in both cell lines after 6h FA treatments. However, the differences between SCM and CSM were eliminated in both cell lines after 24h, with a similar amount of FA accumulation.

Considering optimal cell viability in conjunction with achieving the highest intracellular lipid loading, CSM was identified as a better choice than SFM. Remarkably, similar to FBS, the variability of charcoal-stripped FSB also existed (Sikora et al., 2016). Nevertheless, charcoal-stripped FBS has been widely used in studies on steroid hormone-responsive cancers, such as prostate cancer (Tu et al., 2018) and breast cancer (Liang et al., 2020). Notably, as vitamin D is a fat-soluble secosteroid pro-hormone (Cesari et al., 2011), it is crucial to minimise the interferences of lipophilic hormones and

vitamins in FBS is crucial. Therefore, the switch to charcoal-stripped FBS could be more acceptable for vitamin D and FA co-treatment conditions, which has been applied to all other parts of the thesis.

4.4.2 Co-treatment with 1α,25(OH)$_2$D$_3$ may aggravate the decrease of cell viability induced by fatty acid in liver cell lines

The results of co-treatment suggested that 1α,25(OH)$_2$D$_3$ might exacerbate the adverse effects caused by FA on cell viability. Excessive hepatic lipid accumulation could lead to lipotoxicity, responsible for final cell death (Geng et al., 2021). Experimental studies showed that PA alone resulted in more severe cytotoxicity than OA in both hepatocytes (Lee et al., 2010) and hepatic stellate cells (Hu et al., 2020). However, a co-incubation of PA and OA for 24h was shown to restore the viability of HepG2 cells to some extent but demonstrated more lipid accumulation (Ricchi et al., 2009; Zeng et al., 2020). Therefore, our study used a combination of PA and OA to protect cell viability and mimic benign steatosis. Notably, PA and OA are found to be the most abundant free FAs in western diets (Baylin et al., 2002) and hepatic lipids in both normal subjects and patients with NAFLD (Araya et al., 2004). On the other hand, previous experimental data indicated that 1,25(OH)$_2$D$_3$ had an anti-proliferation effect on HCC cells (Cai et al., 2018; Chiang et al., 2011a) and activated HSCs (Abramovitch et al., 2011). Therefore, it is perhaps not surprising that the simultaneous incubation of 1,25(OH)$_2$D$_3$ and FA aggravated the decrease of cell viability in both cell lines.

4.4.3 Co-treatment with 1α,25(OH)$_2$D$_3$ may attenuate the lipid loading induced by fatty acid in liver cell lines

HepG2 cells were found to be more responsive to FA treatment than LX-2 in our models, which was in line with an experimental study (Barbero-Becerra et al., 2015). The lower lipid accumulation in LX-2 cells might be caused by the damage of the lipid storage function of HSCs during activation (Friedman et al., 1993).

Results from clinical showed that vitamin D supplementation had potential benefits to attenuate NAFLD progression to a certain extent, especially for younger people with earlier stages (Barchetta et al., 2020). As we reviewed in **Chapter 2**, **Table 2.3**, there were significant improvements in

liver parameters, including ALT, AST, CAP and LSM, in patients with NAFLD receiving vitamin D treatment. However, no beneficial effects of vitamin D on hepatic fat content were observed (Kitson et al., 2016; Barchetta et al., 2016a). Conversely, 1α,25(OH)$_2$D$_3$ diminished HFD-induced hepatic steatosis in mice and free FA-induced lipid accumulation in HepG2 cells (Li et al., 2017). In my results, 1α,25(OH)$_2$D$_3$ might attenuate the intracellular lipid accumulation induced by FA in liver cell lines but the results were not significant.

4.4.4 The VDR signalling activated by 1α,25(OH)$_2$D$_3$ might play an essential role in attenuating intracellular lipid

Contrary to my HepG2 results, previous work revealed that FA treatment for 24h has been shown to induce a 2-fold change of VDR mRNA in HepG2 cells (Bozic et al., 2016). Additionally, no increase of VDR mRNA was observed in LX-2 cells after 24h FA treatment. On the other hand, the expression of VDR mRNA was only found to be repressed in the cotreatment group of HepG2 cells at 6h when compared with 1α,25(OH)$_2$D$_3$ treated cells.

Overall results showed that, in line with a previous study (Gascon-Barre et al., 2003), the protein expression level of VDR was higher in LX-2 cells than in HepG2. Moreover, hepatic VDR protein was found increased in HFD-induced NAFLD mice and the liver tissues of patients with NAFLD (Bozic et al., 2016). In our lipid loading models, when cells were treated with FAs, an increase of VDR protein was observed in HepG2 cells at 24h and in LX-2 cells at both time points as well. The only reduction of VDR protein was detected in HepG2 cells with 6h FA treatment, which was also observed in a previous study (Li et al., 2017). The expression of VDR protein was found to significantly increase in LX-2 cells treated with 1α,25(OH)$_2$D$_3$ only for 24h, which was consistent with previous findings in LX-2 cells (Potter et al., 2013) and activated primary HSCs (Abramovitch et al., 2011). However, HepG2 cells showed opposite responses of VDR protein expression when treated with vitamin D only. Compared to the FA group, VDR protein expression was significantly induced in LX-2 cells after the cells were co-treated with 1α,25(OH)$_2$D$_3$ at 24h. However, contrary to LX-2 results, a significant decrease of VDR protein was observed in HpeG2 cells at 24h, opposite to the results of Li et al. (2017). Thus, combining the data of lipid loading and VDR expression, my results supported the evidence that the VDR signalling

activated by 1α,25(OH)$_2$D$_3$ might play an essential role in attenuating intracellular lipid accumulation (Li et al., 2017).

4.4.5 1α,25(OH)$_2$D$_3$ induced CYP24A1 target gene expression

As an essential transcriptional target of the 1α,25(OH)D-VDR-RXR complex, CYP24A1 induced by 1α,25(OH)$_2$D$_3$ promotes the catabolism of 1,25(OH)$_2$D$_3$, which accelerates its cellular consumption (Jeon and Shin, 2018). Notably, CYP24A1 induction showed a vitamin D-dependent response to VDR (Bozic et al., 2016). As expected, the expression of CYP24A1 mRNA was found to increase after 100nM vitamin D treatment with either the presence or absence of FA in our models. Therefore, CYP24A1 was commonly chosen as an indicator to assess the effectiveness of vitamin D treatment. However, the increased expression of CYP24A1 protein triggered by vitamin D was found in HepG2 at both time points and only in LX-2 at 24h. This could cause by the differences in transcriptional regulation response to vitamin D in different cell types.

4.4.6 Limitations

The main limitation of my *in vitro* models was the use of 2D monoculture rather than the 3D method to explore the roles of vitamin D in the NAFLD progression. The 2D monoculture models are relatively easy to handle and could scape up to high-throughput reproducible experiments with less time consuming (Müller and Sturla, 2019). The 2D monoculture cell models I used in the project are two different types of human immortalised liver cell lines. HepG2 cells (hepatocytes) are generally obtained from liver tumour tissues (Aden et al., 1979), and LX-2 cells (HSCs) are genetically manipulated primary human liver cells (Xu et al., 2005). Different liver cells have diverse physiological functions (Kmiec, 2001). While hepatocytes play vital roles in metabolism, detoxification and protein synthesis, the primary function of HSCs is to store vitamin A in lipid droplets. Additionally, NAFLD results from a cascade of cellular and signalling events between other liver cells (Loomba et al., 2021). During the progression of NAFD, the exceeded lipid accumulation in hepatocytes results in liver injury with the liberation of proinflammatory and fibrogenic signals. HCSs are activated by these signals and undergo a series of intracellular responses that culminate in enhanced extracellular matrix production,

promoting fibrogenesis (Loomba et al., 2021). Therefore, the 2D monoculture hepatic cell models can't reflect the interactions between cell types to stimulate the NAFLD progression. Compared to the simple 2D monoculture or coculture systems, 3D models provide a dimensionality structure with a medium flow to mimic the interactions between different cell types in the *in vivo* situation of NAFLD progression (Müller and Sturla, 2019). Developing *in vitro* models of NAFLD using 3D coculture and microfluidic techniques could be used to investigate the effects of vitamin D on inflammation and fibrosis in further complicated conditions.

Another limitation is, compared to primary human cells, the immortalised cells have principal advantages of high replicative capacity and stable phenotype for an extended culture period (Soret et al., 2020). However, certain specific functions are limited by the tumour phenotype or the immortalisation process. For example, in HepG2 cells, CYPs that participated in the xenobiotic metabolism were expressed low (Guguen-Guillouzo and Guillouzo, 2010). Therefore, when HepG2 cells are utilised for drug metabolism tests *in vitro*, it is essential to use the transfection method to partially overcome the expression of relevant CYPs (Müller and Sturla, 2019). In contrast, CYPs expression was high in HSCs (Yamada et al., 1997), including LX-2 cells (Haughton et al., 2006; Liu et al., 2013).

Lastly, LX-2 cells are activated HSCs that have already lost their normal physiological function (Xu et al., 2005). VDR has been found highly expressed in quiescent HSCs; however, the activation of HSCs could cause an approximately 40% decrease in VDR expression (Abramovitch et al., 2011), bringing bias on the effects of vitamin D-VDR axis in the current lipid loading models. Therefore, finding out the way to reversion of activated HSCs to a quiescent-like phenotype is vital. For example, El Taghdouini et al. (2015) indicated that synergistic action of epidermal growth factor (EGF), fibroblast growth factor 2 (FGF2), dietary fatty acids (PA and OA) and retinol promoted primary human HSCs to a more quiescent-like phenotype.

4.4.7 Conclusion

In conclusion, the results of this chapter show that both HepG2 and LX-2 cells responded to FA and vitamin D treatment. 1α,25$(OH)_2D_3$ inhibited cell proliferation in both cell lines, and the co-incubation with FA exacerbated

cytotoxicity. The results of intracellular lipid accumulation indicated that 1α,25(OH)$_2$D$_3$ was a positive effect on hepatic steatosis. Additionally, compared to VDR, CYP24A1 could be a better positive control gene to determine the cellular response to vitamin D treatment. The *in vitro* models set up here will be used to examine miRNA expression in response to vitamin D and lipid loading cotreatment in the next chapter.

4.5 Summary

- Serum choice alters liver cell line viability under different doses of FA treatment; specifically, HepG2 and LX-2 cells cultured in CSM rescues the adverse effects of SFM and FA dose on the viability
- Serum choice alters lipid loading in liver cell lines; CSM had a similar amount of intracellular lipid loading to SCM
- Induction of CYP24A1 and VDR target gene expression is dependent on dose and duration of 1α,25(OH)$_2$D$_3$ exposure in liver cell lines; 1α,25(OH)$_2$D$_3$ induced the CYP24A1 mRNA expression by a dose-and-duration manner; thus, CYP24A1 was used a positive control to assess the cell responses to 1α,25(OH)$_2$D$_3$
- The results of co-treatment suggested that 1α,25(OH)$_2$D$_3$ might exacerbate the adverse effects on cell viability caused by FA but attenuate the intracellular lipid accumulation induced by FA in liver cell lines
- Compared to 1α,25(OH)$_2$D$_3$ treated HepG2 cells, FA inhibited VDR mRNA expression in the co-treatment group at 6h
- Compared to the FA group, the VDR protein expression was repressed by co-treatment with 1α,25(OH)$_2$D$_3$ in HepG2 cells, but was promoted by co-treatment with 1α,25(OH)$_2$D$_3$ in LX-2 cells at 24h

Chapter 5
Identification of miRNAs regulated by vitamin D and lipid loading in liver cells

5.1 Introduction

Vitamin D is a molecule with diverse activities, including anti-fibrotic, anti-inflammatory, and insulin-sensitising functions in liver cells (Barchetta et al., 2020; Raza et al., 2021). In addition, epidemiological data show that vitamin D deficiency is associated with the presence of NAFLD (Pacifico et al., 2019). However, results from vitamin D supplementary trials on liver outcomes have been inconclusive and debated (Barchetta et al., 2020; Zhang et al., 2019c).

The molecular pathogenesis of NAFLD is complex and multifactorial, involving numerous signalling molecules, including miRNAs (Wang et al., 2020c; Gjorgjieva et al., 2019a). On the other hand, miRNAs also play essential roles in mediating the cellular response to vitamin D, including the post-transcriptional regulation of the VDR and other genes involved in the vitamin D pathway (Zenata and Vrzal, 2017; Zeljic et al., 2017). However, there is a scarcity of research examining the potential roles for vitamin D regulated miRNAs in the molecular pathogenesis of NAFLD.

TaqMan low-density array (TLDA), a microfluidic card, was designed based on the qPCR technique (Steg et al., 2006). TLDA is an economical and robust method, which can simultaneously detect up to 384 genes for a single sample (Jiang et al., 2006). This technique has been widely applied for gene profiling studies in human cancers (Steg et al., 2006; Lü et al., 2008; Long et al., 2014; Lopez-Campistrous et al., 2021).

Bioinformatics is essential for capturing and interpreting biological data in genomics and proteomics (Bayat, 2002). Bioinformatic analysis plays a vital role in processing large-scale expression profiling studies (Zhang et al., 2009). With the exponential growth in miRNA-related studies, a number of bioinformatics tools and databases have been set up to analyze and manage the miRNA data (Akhtar et al., 2016). Additionally, miRNA bioinformatic tools and databases make it possible to address different aspects of miRNA

research, from miRNA discovery and target prediction to functional implication. In this chapter, I used the miRWalk database (Sticht et al., 2018) along with the database for annotation, visualization and integrated discovery (DAVID) (Huang da et al., 2009) to explore the potential gene targets and regulatory networks of altered miRNAs.

The miRWalk database is a comprehensive open-source integrated online platform for analysing miRNA-mRNA binding, which was first released in 2011 (Dweep et al., 2011). The mRNA and miRNA information of miRWalk is extracted separately from the national centre for biotechnology information (NCBI) and miRBase (Sticht et al., 2018). In order to predict miRNA targets, miRWalk uses a random-forest based approach, the Target Prediction for miRNAs (TarPmiR) algorithm, to search the putative miRNA-binding sites within complete transcript sequences. The binding positions in promoters, coding sequence (CDS), 5'- and 3'- untranslated region (UTR) and mitochondrial genes can be identified using TarPmiR (Sticht et al., 2018; Dweep et al., 2011). Users can filter results by adjusting the binding probability score. In addition, the framework of miRWalk also integrates other datasets, including TargetScan, miRDB and miRTarBases, to let users get results comparison and more accurate predictions.

The Database for Annotation, Visualization, and Integrated Discovery is a web-accessible program, consisting of an integrated biological knowledgebase and analytic tools (Dennis et al., 2003). By systematically combining functionally descriptive data with intuitive graphical displays, investigators can extract biological meaning from large gene/protein lists.

The overall objective of this chapter was to investigate the role of vitamin D regulated miRNAs in NAFLD. Firstly, miRNA expression in immortalised hepatocytes (HepG2 cells) and hepatic stellate cells (LX-2 cells) in response to vitamin D, FA or in combination was measured by TaqMan® low-density miRNA arrays. Then, after determining the target genes of detected miRNAs utilising the miRWalk (v3.0) database, gene set enrichment analysis (GSEA), functional annotation and pathway analyses were processed in the DAVID (v6.8) knowledgebase. Finally, after integrating the *in vivo* data and evidence in the literature (**chapter 3**), a subset of candidate miRNAs was followed up

to verify functional and mechanistic effects in specific metabolic associated signalling pathways independently.

5.2 Methods and materials

5.2.1 Cell culture

HepG2 and LX-2 cells were routinely cultured as described in section **4.2.1 Cell culture.** As detailed in section **4.2.5 Fatty acid and vitamin D co-treatment**, both HepG2 and LX-2 cells were treated with vehicle or FA (2% DMSO or 500μM 1:1 PA:OA), and vehicle or vitamin D (0.001% ethanol or 100nM 1α,25$(OH)_2D_3$). MiRNA samples from HepG2 and LX-2 cells were collected at 24h from T75 flasks.

5.2.2 miRNA isolation

The mirVANA^{TM} miRNA isolation kit (with phenol; Ambion, UK) was initially used to isolate miRNA per the manufacturer's instruction. The isolation procedure in essence includes two major steps: sample lysis and disruption, then organic extraction and RNA purification over glass-fibre filters.

Cells were collected with cell scrapers (VWR, UK) in labelled 1.5ml RNase-free tubes with 1ml 1X PBS after and pelleted at low speed (500x g 3min). After removing the supernatant, the pellet was stored in 500μl RNAlater^{TM} stabilisation solution (Invitrogen, UK) at -80°C until all samples could undergo miRNA extraction simultaneously. The samples were firstly disrupted in a denaturing Lysis/Bind solution [containing 2-mercaptoethanol and thiocyanic acid compound with guanidine (1:1)]. Then, after adding 1/10 volume of miRNA Homogenate Additive, the homogenous lysate was subjected to a volume of acid-phenol: chloroform extraction based on phase separation (all adding volumes based on the original lysate volume). At this stage, there are separate procedures for the purification of either total RNA or for purifying RNA that was highly enriched for small RNA species, including miRNAs.

To isolate RNA that was highly enriched for small RNA species (≤200nt), 100% ethanol (absolute ethanol, Fisher Scientific, UK) was added to the aqueous phase recovered from the organic extraction. Then, the lysate/ethanol mixture was passed through a glass-fiber filter. The filtrate was

collected, and another volume of 100% ethanol was added. The ethanol mixture was then passed through a second glass-fiber filter. At this point, the small RNAs become immobilised. The filter was washed a few times with the Wash Solution provided, and finally eluted in nuclease-free water (NFW; Promega, UK). The concentration of the isolated miRNA was determined spectrophotometrically, and purity was evaluated by 280/260nm optical density (OD). Extracted miRNA was stored at -80°C until required. The TaqMan™ Advanced miRNA cDNA Synthesis Kit (Invitrogen, UK) was used to synthesise the miRNA from 10ng of purified cell small RNA samples.

5.2.3 TapMan low-density array (TLDA)

TaqMan™ human microRNA A+B cards (v2.0 for HepG2 and v3.0 for LX-2; Life Technologies, UK) were used to measure miRNA expression in equally pooled miRNA samples (n=4; sample concentrations were around 35ng/μl for HepG2 and 25ng/μl for LX-2) according to the protocol of the manufacturer (**Figure 5.1**). Firstly, 5μl of each biological replicate of each treatment group were pooled into one tube. Then, the concentration and quality of the pooled samples were measured and finally, 10ng of each pooled sample was used to process cDNA synthesis. Each card contains 384 reactions (primers were already added into each wells by manufacturer) with eight sample reservoirs. Notably, the v2.0 was an older version, with 377 target assays on either card A or card B (754 in total). The v3.0 A+B cards in total contained 752 target assays (376 target assays per card).

For each sample, a 200μl of 1:10 dilution of cDNA prepared with TaqMan™ Fast Advanced Master Mix (Applied Biosystems, UK) and nuclease-free water (NFW) was introduced to each reservoir for both plate A and B. According to the manufacturer's instructions, the plates were run on the Quant Studio 7.

Data analysis was performed using the Applied Biosystems™ Analysis Software (v1.1). According to the manufacturer's instructions, the relative threshold algorithm setting was selected, with the threshold cycle (Ct) cut-off as 32 and the no amplification (NOAMP) flag threshold as 0.3. The global normalisation option was applied prior to the relative fold change calculation. Raw Ct data were normalised to the global median and assessed relative to

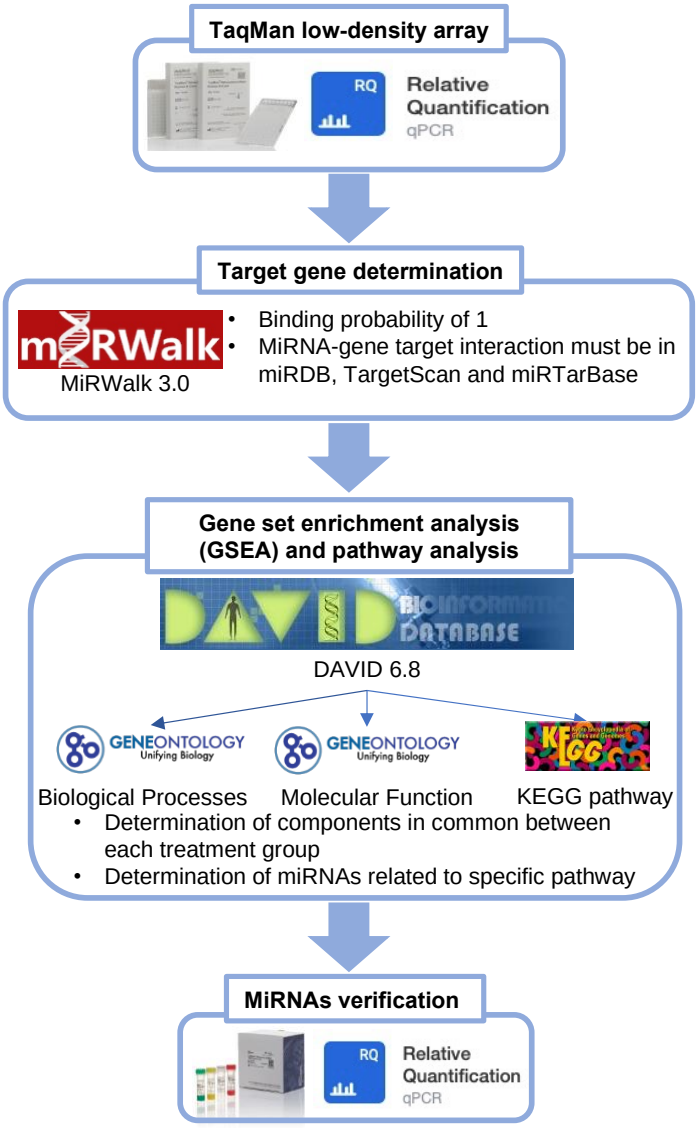

Figure 5.1 Experimental and bioinformatic workflow for identification of miRNAs regulated by vitamin D and lipid loading in liver cells.

the control group (2% DMSO and 0.01% ethanol). When set-up for global normalisation, the algorithm firstly detects assays common to every sample in the analysis; then, the median Ct of those assays is used as a normalisation factor on a per-sample basis. To expand the number of potentially altered miRNAs in different treatment groups, the 'Include maximum Ct values in calculation' was set as on, which means that Ct values over 32 or undetected were replaced into 32 during arithmetic execution. Generally, fold change (FC)>1.33 and FC<0.67 are set as qPCR thresholds (Scientific, 2014). However, as further detailed below in section **5.3.1** plotting all of the miRNA relative FCs to the control group (2% DMSO and 0.01% ethanol) demonstrated clear inflexion points around FCs 2.85 and 0.67. Therefore, the relative FCs>2.85 or FC<0.67 were chosen for the arbitrary thresholds for these experiments and hypothesised to be 'upregulated' or 'downregulated', respectively.

5.2.4 Bioinformatic analyses

In brief, bioinformatic analyses included: the identification of miRNA gene targets, GSEA, and functional annotation and pathway analyses (**Figure 5.1**). The miRWalk v3.0 database (http://mirwalk.umm.uni-heidelberg.de/) was used to retrieve the list of predicted human target genes of miRNA hypothesised as dysregulated from TLDA (Sticht et al., 2018). The miRNA-gene targets were filtered to meet the criteria with a binding probability of 1. Only target genes recognised by three different databases (miRDB, TargetScan and miRTarBase) were considered for further analyses.

After removing duplicate genes, a list of unique genes based on the independent treatment group of each cell line was inputted into the DAVID (v6.8, https://david.ncifcrf.gov/) (Huang da et al., 2009). This knowledge base contains a functional annotation tool that identifies enriched Gene Ontology (GO) terms (Ashburner et al., 2000; Gene Ontology, 2021) and Kyoto Encyclopedia of Genes and Genomes (KEGG) pathways (Kanehisa et al., 2016). Gene ontology analysis of cellular components, biological processes and molecular functions, along with KEGG pathway analysis were performed on potential gene targets of the miRNAs hypothesized to be differentially expressed. GO terms and KEGG pathways having a Benjamini p-value<0.05 were considered significant.

To compare the significant KEGG pathways between different treatment groups and cell lines, Venn diagrams were used to explore the common pathways between groups, using the online Venn analysis tool (https://bioinformatics.psb.ugent.be/webtools/Venn/).

5.2.4 Reverse transcription-polymerase chain reaction (RT-PCR) verification

Pre-designed TaqMan™ Advanced miRNA Assays (**Table 5.1**) were prepared with TaqMan™ Fast Advance Master Mix and run in duplicate on MicroAmp Optical 96-well reaction plates on Quant Studio 7 according to manufacturer's instructions. The serial fold dilutions of cDNAs synthesized from a pooled human reference miRNA mix (Agilent Technologies, UK) were used to generate five-point standard curves, which were used to assess the efficiency of each miRNA assay, as well as deriving the relative quantities of the miRNA in the treatment groups.

Table 5.1 Table of miRNA primers.

Assay Name	Assay ID
hsa-let-7a-5p	478575_mir
hsa-let-7d-5p	478439_mir
hsa-miR-15b-5p	478313_mir
hsa-miR-23a-3p	478532_mir
hsa-miR-27a-3p	478384_mir
hsa-miR-27b-3p	478270_mir
hsa-miR-96-5p	478215_mir
hsa-miR-103-3p	477864_mir
hsa-miR-125a-5p	477884_mir
hsa-miR-200a-3p	478490_mir
hsa-miR-212-3p	478318_mir
hsa-miR-222-3p	477982_mir
hsa-miR-455-3p	478112_mir

5.2.5 Optimisation of mirVana™ miRNA isolation kit

The optimisation of isolation protocols of miRVana™ was made from aspects of sample collection procedure, storage condition and the organic extraction

procedure. All the samples used for optimisation were untreated LX-2 cells cultured in a T75 flask.

Samples collected by Accutase®: After aspirating the medium, Accutase® was added to the flask for cell detachment. Then, the cells were pelleted by centrifugation (300x g for 3min) and discarded the supernatant. In addition, the cells were washed by gently resuspending in 1ml cold 1X PBS and pelleted again at low speed (300x g, 3min) in a 1.5ml tube.

Samples collected by cold 1X PBS: After aspirating the medium, cells in the flask was washed with 3ml cold 1X PBS. Then, the PBS was aspirated, and 1ml of cold PBS was added into the flask. The flask was placed on ice for 3-5min, and the cells were collected with a scraper into a 1.5ml tube and pelleted at 300x g for 3min.

Samples used RNAlater for storage: According to manufacturer's protocol, 500μl RNAlater was added to a cell pellet-containing tube, then the tube was popped at 4℃ overnight. The next morning, the RNAlater was taken out, and the sample was moved to -80℃ for long-term storage.

Samples used liquid nitrogen for storage: the cell pellet-containing tube was snapped in liquid nitrogen and directly stored at -80℃.

The organic extraction procedure modification: The Lysis/Binding buffer volume was increased from 500μl to 600μl, and the lysis time was increased from 5min to 10min. The time and speed of centrifugation at the organic extraction step were modified from 5 min at 10,000x g to 10min 12,000x g. The centrifugation time of small RNAs enrichment procedure was changed from 15s to 1min. Additionally, after the final washes of the spin column, the final centrifugation drying step prior to elution of miRNA was repeated, and an additional 3min air-dry step with column lid open was added.

5.2.6 Data analysis

Results for candidate endogenous control miRNAs identification are presented as raw Ct and the coefficient of variance (CV, %) was assessed across the four treatment groups. Results of miRNA verification assays are presented as mean +/- the SEM alongside individual data points. Comparisons between groups were made using two-way ANOVA with the

Holm-Sidak test as appropriate. All statistical analyses were carried out using GraphPad Prisms version 9.1.1 (California, US).

5.3 Results

5.3.1 MicroRNAs potentially altered by vitamin D and/or fatty acid treatment in miRNA array

After testing the robustness of cellular models in **Chapter 4**, in this chapter, firstly, HepG2 and LX-2 cells treated with or without 100nM 1α,25(OH)$_2$D$_3$ and with or without 500μM FA (1:1 PA:OA) were used to investigate dysregulated miRNAs by using TLDAs.

In total, 754 target miRNA assays in HepG2 and 752 in LX-2 were measured across all four treatment groups. Initially, I used the general qPCR thresholds, FC>1.33 and FC<0.67 (Scientific, 2014); however, using these cut-offs, relative to the control, ~48% of detected miRNAs appeared altered in HepG2, while ~82% were altered in LX-2 cells under the different treatment conditions, which seemed implausible (**Figure 5.2**). Further examining the data by plotting all of the miRNA relative FCs to the control group (2% DMSO and 0.01% ethanol) demonstrated clear inflection points around FCs 2.85 and 0.67 (**Figure 5.3)** and these were chosen for the arbitrary thresholds for these experiments and FC>2.85 hypothesised to be 'upregulated' and FC<0.67 hypothesised to be 'downregulated'. As a result, a more plausible ~17% (129 miRNAs) of detected miRNAs were found potentially different from vehicle-treated HepG2 cells based on the new thresholds. Similarly, ~16% (116 miRNAs) were seen altered in LX-2 (**Figure 5.4**). In addition, the overlap of miRNAs upregulated or downregulated between HepG2 and LX-2 in different treatment groups was shown in **Appendix Figure D2**.

5.3.2 Bioinformatic analyses

It was infeasible to use qPCR to validate all the potentially altered miRNAs (129 miRNAs in HpeG2 and 116 miRNAs) detected from TLDA results. Thus, bioinformatics analyses were conducted sequentially for the subset of miRNAs hypothesised as dysregulated from TLDA to explore the potential gene targets and regulatory networks of altered miRNAs. Specific pathways that are dysregulated in NALFD pathogenesis, contributing significantly to the

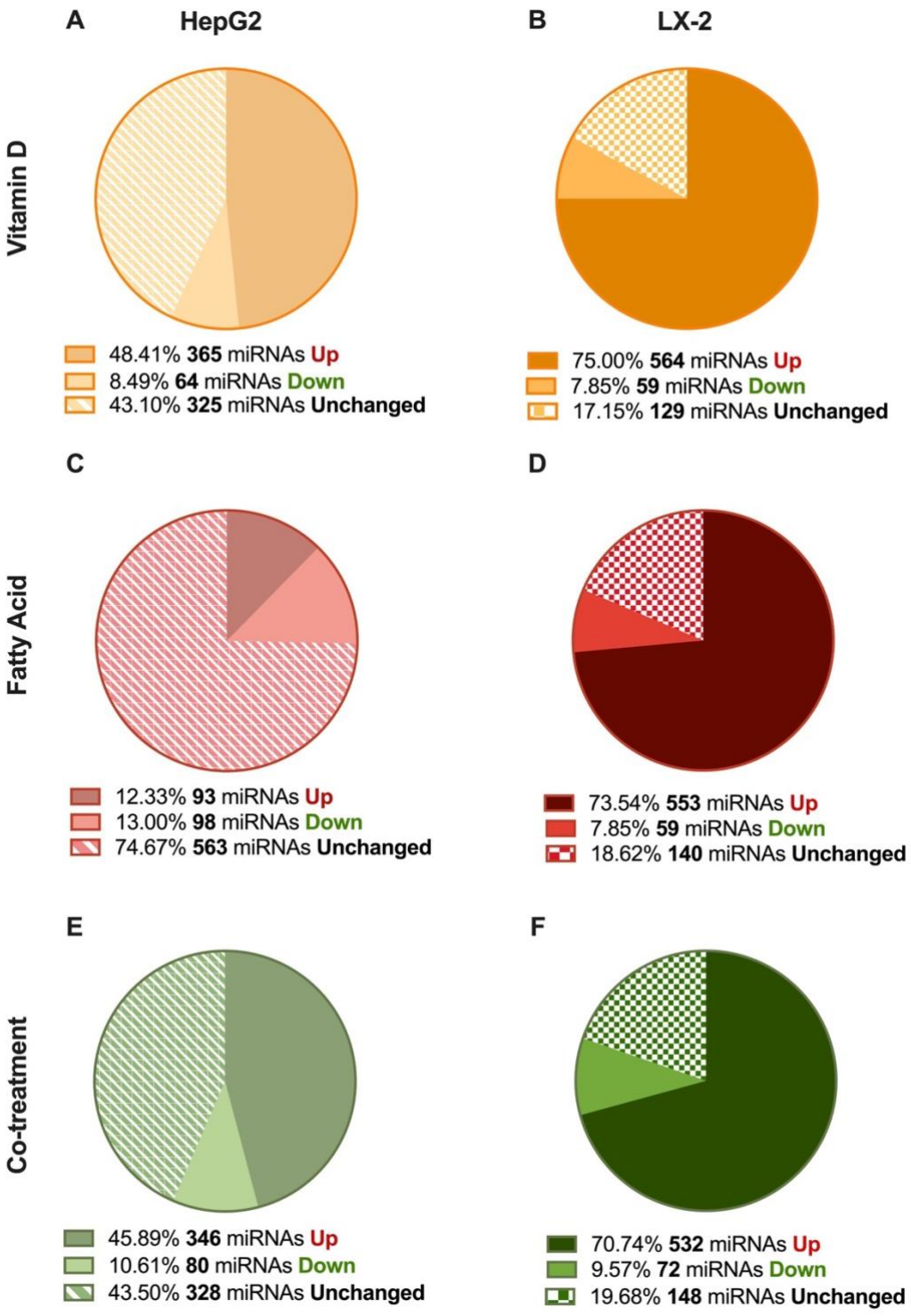

Figure 5.2 Percentage of potentially altered miRNAs in HepG2 and LX-2 using relative fold change (FC) cut-offs of >1.33 and <0.67. Cells were treated with either 100nM $1\alpha,25(OH)_2D_3$, 500μM FA, or both in combination. Raw Ct data were normalised to the global median and assessed relative to the control group (2% DMSO and 0.01% ethanol). A relative FC>1.33 was hypothesised as 'upregulated', and FC<0.67 was 'downregulated'. Data are percentage of miRNAs in: **A.** vitamin D treated HepG2 cells; **B.** vitamin D treated LX-2 cells; **C.** FA treated HepG2 cells; **D.** FA treated LX-2 cells; **E.** vitamin D and FA co-treated HepG2 cells; **F.** vitamin D and FA co-treated LX-2 cells.

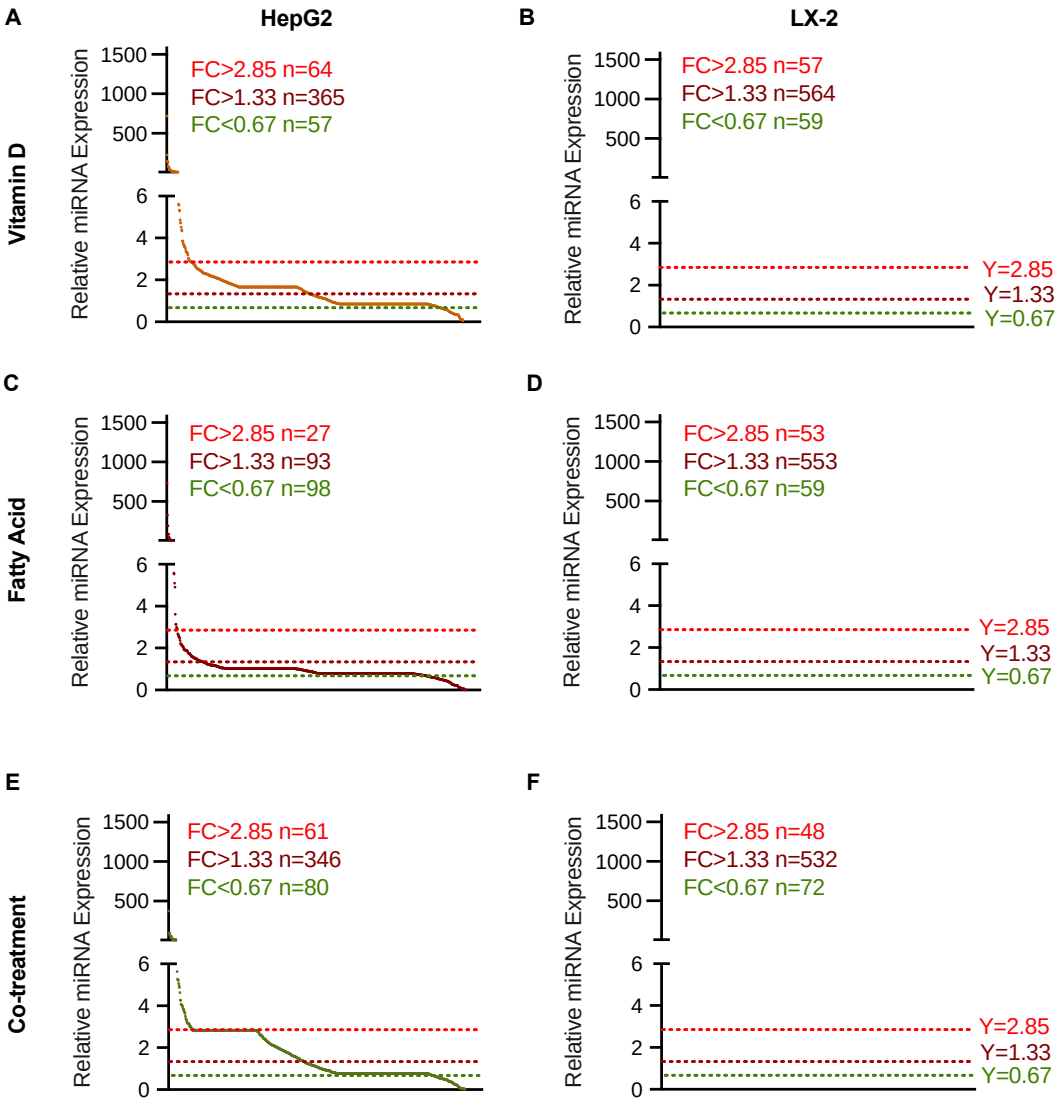

Figure 5.3 Overview of microRNA relative fold changes (FCs) in HepG2 and LX-2. Cells were treated with either 100nM 1α,25(OH)$_2$D$_3$, 500μM FA, or both in combination. Raw Ct data were nomalised to the global median and assessed relative to the control group (2% DMSO and 0.01% ethanol). Data are relative FCs of miRNAs and sorted from the largest to the smallest: **A.** vitamin D treated HepG2 cells; **B.** vitamin D treated LX-2 cells; **C.** Fatty acid treated HepG2 cells; **D.** Fatty acid treated LX-2 cells; **E.** vitamin D and fatty acid co-treated HepG2 cells; **F.** vitamin D and fatty acid co-treated LX-2 cells. **A.C.E.** involved 754 target assays and **B.D.F.** involved 752 target assays.

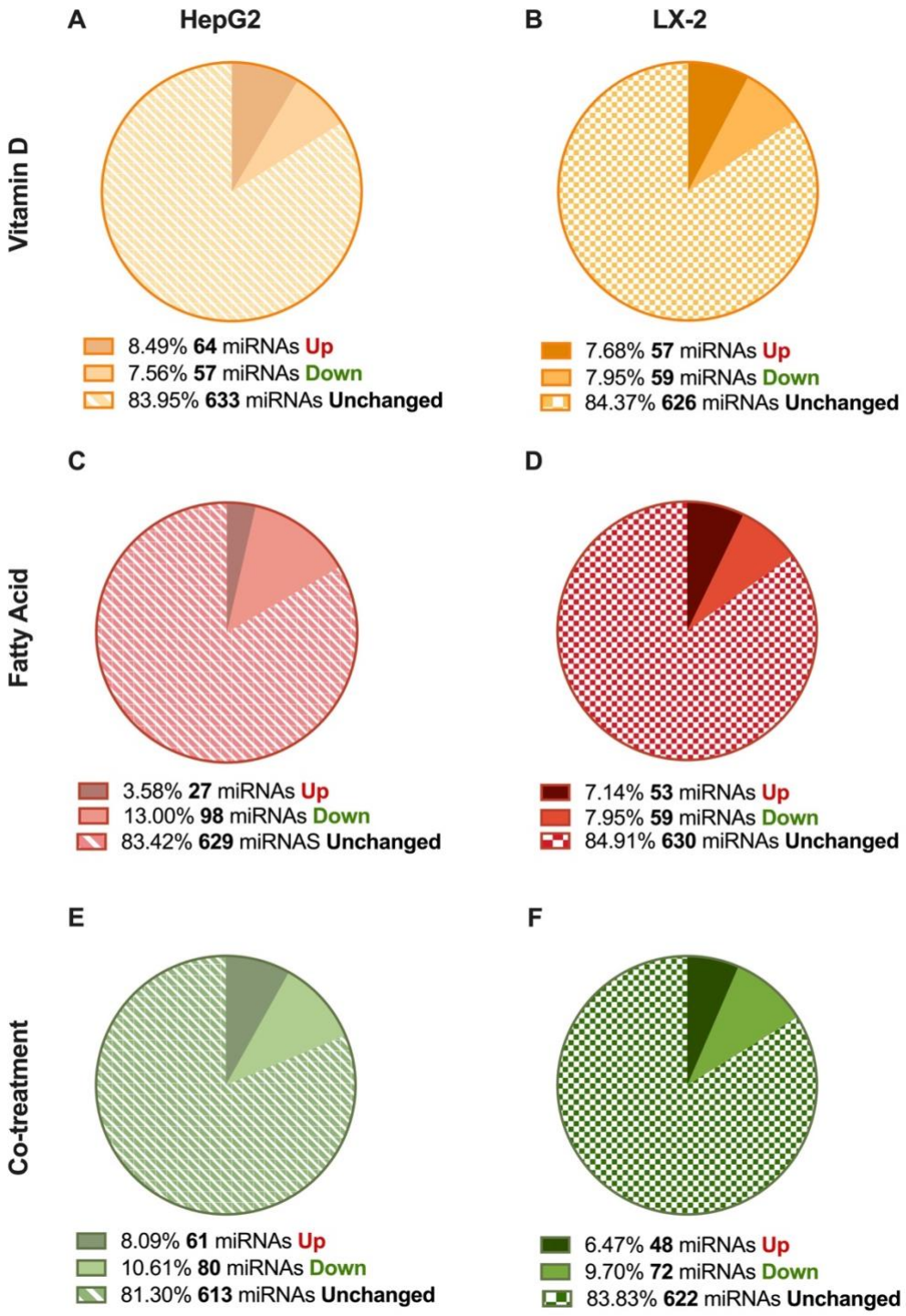

Figure 5.4 Percentage of potentially altered miRNAs in HepG2 and LX-2 using relative fold change (FC) cut-offs of >2.85 and <0.67. Cells were treated with either 100nM 1α,25(OH)$_2$D$_3$, 500μM FA, or both in combination. Raw Ct data were normalised to the global median and assessed relative to the control group (2% DMSO and 0.01% ethanol). A relative FC>2.85 was hypothesized as 'upregulated', and FC<0.67 was 'downregulated'. Data are percentage of microRNAs in: **A.** vitamin D treated HepG2 cells; **B.** vitamin D treated LX-2 cells; **C.** FA treated HepG2 cells; **D.** FA treated LX-2 cells. **E.** vitamin D and FA co-treated HepG2 cells. **F.** vitamin D and FA co-treated LX-2 cells.

disease (Liu et al., 2020a). Therefore, it is crucial to investigate dysregulated miRNA involvement in gene regulation of NAFLD related pathways.

The comparison of significant enriched KEGG pathways between different treatments and cell lines narrowed down to overlapped pathways relative to NAFLD progression for further investigation. Then, the genes involved in the overlapped pathways for each treatment were retrieved from DAVID separately. Next, the original miRWalk data that predicted the miRNAs gene targets were used to compose a list of miRNAs that targeted the genes found in each overlapped KEGG pathway in all treatment groups in both cell lines. After that, the miRNAs involved in each pathway were compared between treatment groups and cell lines to find overlapped miRNAs with their relative fold change. Finally, combining the data of miRNAs dysregulated in the overlapped KEGG pathway with the literature evidence in **chapter 3**, a subset of miRNAs was chosen as potential candidates for further verification.

5.3.2.1 Gene targets of potentially altered miRNAs

Interactions between miRNAs and mRNAs are complex. As miRNAs target multiple genes (Peter, 2010), it is essential to determine the number of mRNAs that are functionally targeted by the same miRNA on a genome-wide scale. By using the miRWalk database, possible miRNA binding sites within the complete sequence (5'-UTR, CDS and 3'-UTR) of a gene could be screened out and further used to explore the significant biological importance.

Six lists of putatively dysregulated miRNAs (from HepG2 or LX-2 cells treated with vitamin D, FA or in combination) were used to identify target genes in miRWalk database. The initial lists from HepG2 cells contained 121 miRNAs from vitamin D treated, 125 miRNAs from FA treated and 141 miRNAs from co-treated cells; LX-2 cells included 116 miRNAs, 112 miRNAs and 120 miRNAs from vitamin D, FA and cotreated, respectively. After fixing the miRNAs not recognized in miRWalk (**Appendix Table D1**), the final number of total nonredundant gene targets for miRNAs suspected dysregulated is shown in **Table 5.2** for each treatment in both cell lines.

The number of unique target genes of the altered miRNAs from different treatment groups ranged from 279-470. Notably, the co-treatment group had the largest number of gene targets in both cell lines (HepG2: 430 genes, LX-2: 470 genes).

Table 5.2 MiRWalk and GSEA results showing the number of miRNA gene targets and significantly enriched components in each treatment for each cell line.

	Vitamin D treatment		***Fatty acid treatment***		***Co-treatment***	
	HepG2	***LX-2***	***HepG2***	***LX-2***	***HepG2***	***LX-2***
Number of miRNAs*****	122	117	124	112	140	122
Total number of gene targets†	279	381	368	374	430	470
Gene Ontology						
Cellular Components	5	7	8	7	10	9
Biological Processes	19	10	17	7	18	14
Molecular Functions	21	8	9	11	24	15
KEGG pathways	38	28	11	47	28	39

KEGG, Kyoto Encyclopedia of Genes and Genomes. *miRNAs with FC>2.85 or FC<0.67 relative to control; †Duplicates removed.

5.3.2.2 Gene set enrichment analysis

In order to gain biological insight, the unique target genes associated with the potentially altered miRNAs for each treatment in each cell line were then examined via the DAVID knowledge base to determine their significant ($P<0.05$) associated GO terms in three domains, namely cellular components, biological processes and molecular functions; as well as their associated KEGG pathways.

An overview of the number of significantly enriched GO terms and KEGG pathways in different cell lines and treatments is shown in **Table 5.2**. Then, integrating the data of HepG2 and LX-2 cells, the specific cellular components, biological processes and molecular functions identified in all three treatments are summarised in the following paragraphs. Data are further detailed in **Figure 5.5-5.7** with -log(P-values) illustrated for the top significant components for each treatment group in both cell lines.

Four cellular components were found in common between all three treatment groups in both cell lines: nucleoplasm, nucleus, cytosol and cytoplasm (**Figure 5.5**). Besides these, two components, membrane and transcription factor complex were specific to LX-2 cells. Notably, nucleoplasm and nucleus had the lowest P-values across treatments in both cell lines, in line with miRNA function.

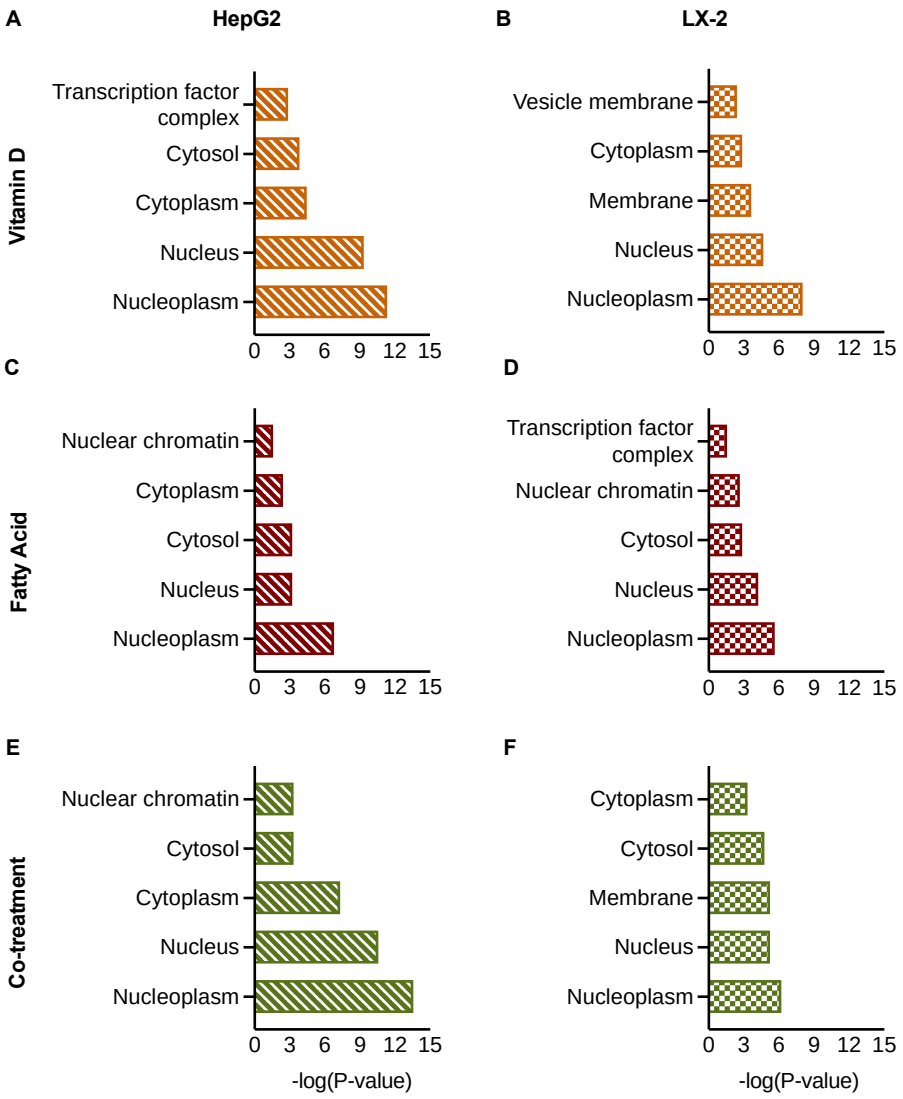

Figure 5.5 Top Five significant cellular components in vitamin D and/or FA treated HepG2 and LX-2 cells. Data are shown as log(P-value). P<0.05 was considered statistically significant. Significant cellular components in vitamin D treated HepG2 (**A**) and LX-2 (**B**) cells, in FA treated HepG2 (**C**) and LX-2 (**D**) cells, and in vitamin D and FA cotreated HepG2 (**E**) and LX-2 (**F**) cells.

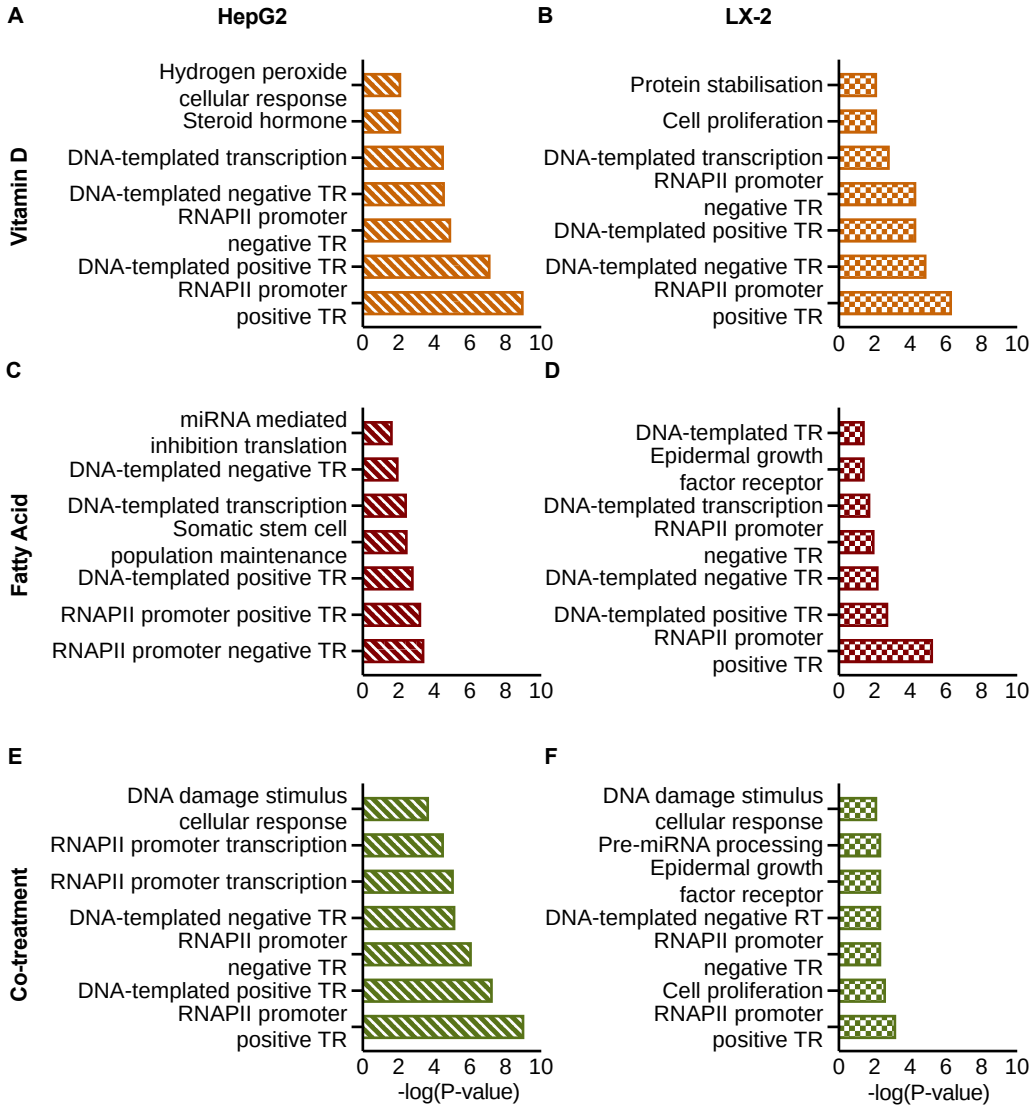

Figure 5.6 Top seven significant biological processes in vitamin D and/or FA treated HepG2 and LX-2 cells. Data are shown as -log(P-value). P<0.05 was considered statistically significant. Significant biological processes functions in vitamin D treated HepG2 (**A**) and LX-2 (**B**) cells, in FA treated HepG2 (**C**) and LX-2 (**D**) cells, and in vitamin D and FA cotreated HepG2 (**E**) and LX-2 (**F**) cells. RNAPII, RNA polymerase II promoter; TR, transcription regulation.

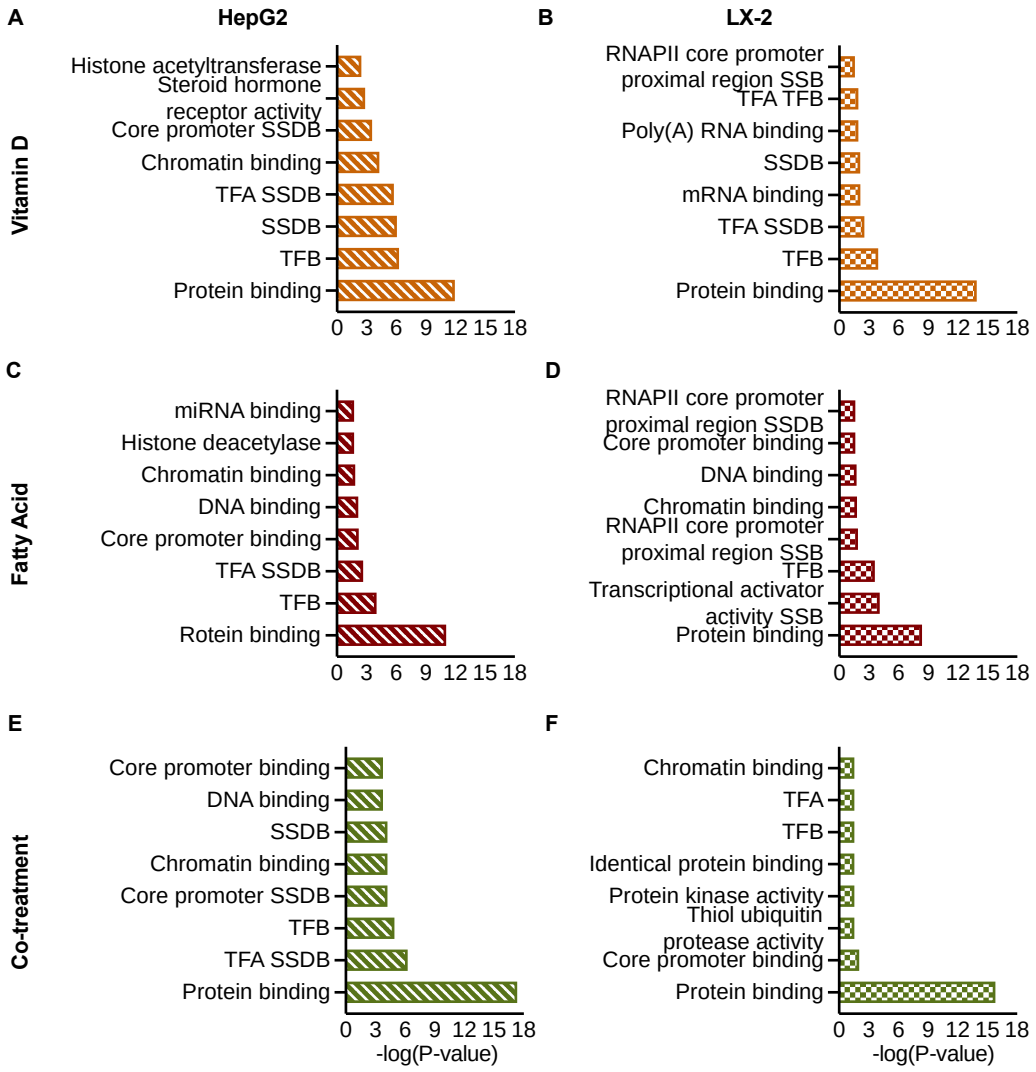

Figure 5.7 Top eight significant molecular functions in vitamin D and/or FA treated HepG2 and LX-2 cells. Data are shown as -log(P-value). P<0.05 was considered statistically significant. Significant molecular functions in vitamin D treated HepG2 (**A**) and LX-2 (**B**) cells, in FA treated HepG2 (**C**) and LX-2 (**D**) cells, and in vitamin D and FA cotreated HepG2 (**E**) and LX-2 (**F**) cells. SSDB, sequence-specific DNA binding; RNAPII, RNA polymerase II; TFA, transcription factor activity; TFB, transcription factor binding.

Eight biological processes were found in common between all treatments in HepG2 cells, with six involved in transcription (**Figure 5.6**). While of the six biological processes found significantly enriched across all three treatments of LX-2, five were related to transcription and in common with HepG2. These included positive and negative regulation of transcription from RNA polymerase II promoter, transcription, and positive and negative regulation of transcription (DNA templated).

While five molecular functions were found significant in all treatments in HepG2 cells, three were associated with LX-2 (**Figure 5.7**), including transcription factor activity (sequence-specific DNA binding), transcription factor binding and protein binding.

5.3.2.3 Significantly Enriched KEGG pathways

Pathway analysis enrichment analysis could provide mechanistic insights into gene lists generated from dysregulated miRNAs identified in HepG2 or LX2 cells treated with vitamin D, FA or in combination. This approach could discover biological pathways that are more enriched in a gene list than is anticipated by chance.

In total, the number of significantly enriched KEGG pathways of HepG2 and LX-2 from different treatment groups ranged from 11-47 (**Table 5.2**). Thirty-eight KEGG pathways were found enriched significantly in vitamin D treated HepG2 cells, whereas 28 were identified in LX-2. On the other hand, there were noticeably fewer identified pathways in FA treated HepG2 cells (n=11) than LX-2 cells (n=47). Additionally, co-treated HepG2 and LX-2 cells had 28 and 39 pathways, respectively. The top ten significant pathways are shown in **Appendix Figure D3**. Among all significantly enriched pathways for each treatment group were multiple pathways of relevance to NAFLD (**Figure 5.8**). These pathways include: phosphatidylinositol 3-kinase-protein kinase B (PI3K-AKT), FOXO, Ras, mitogen-activated protein kinase (MAPK), AMPK, p53, mammalian target of rapamycin (mTOR), TNF, insulin, TGF-β signalling pathways and insulin resistance pathway. The overlapping significant pathways in all three treatment groups from each cell line were identified via a Venn analysis to consider pathways of further interest (**Figure 5.9**; **Appendix Figure D4)**. There were eight pathways in common between all three treatments in HepG2 cells (**Figure 5.9A**) and 22 in LX-2 cells (**Figure**

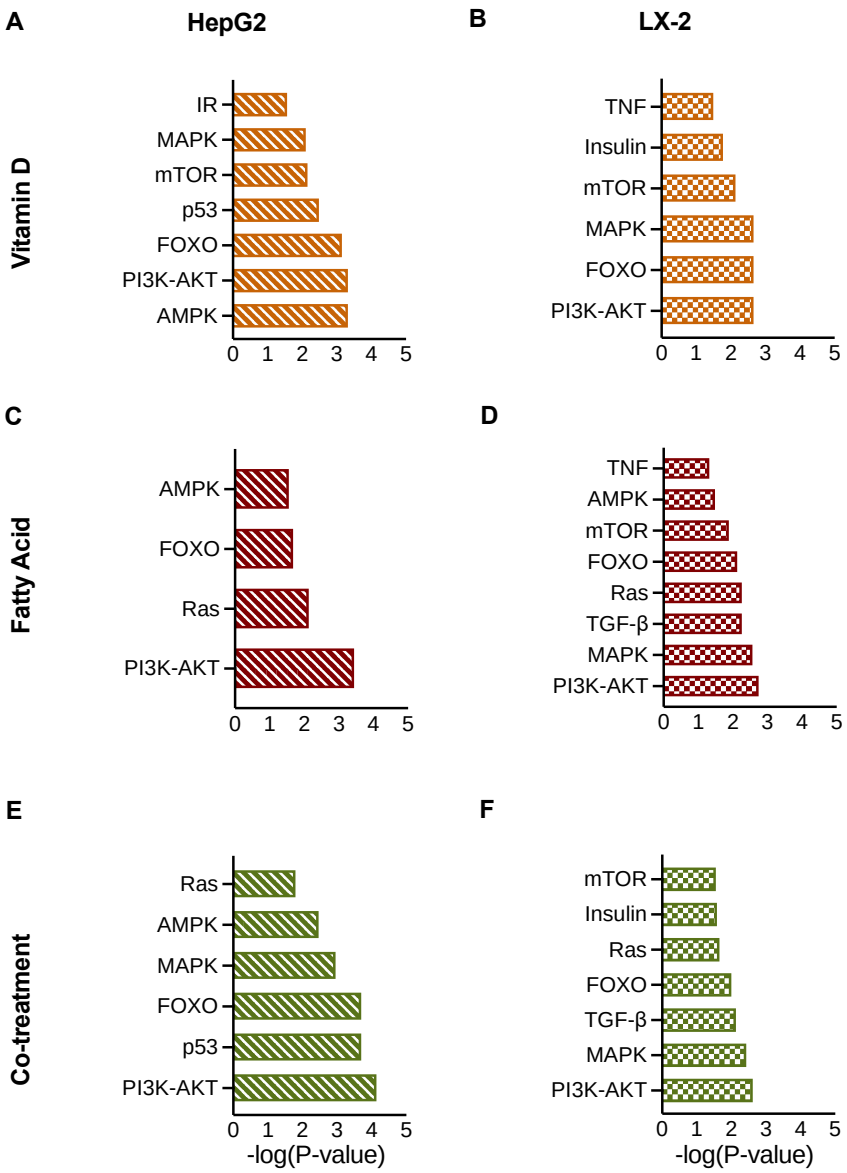

Figure 5.8 The significantly enriched KEGG pathways relevant to NAFLD pathogenesis in vitamin D and/or FA treated HepG2 and LX-2 cells. Data are shown as -log(P-value). P<0.05 was considered statistically significant. KEGG pathways enriched significantly relevance to NAFLD in vitamin D treated HepG2 (**A**) and LX-2 (**B**) cells, in FA treated HepG2 (**C**) and LX-2 (**D**) cell, and in vitamin D and FA cotreated HepG2 (**E**) and LX-2 (**F**) cells. AMPK, AMP-activated protein kinase; FOXO, forkhead box O; IR, insulin resistance; MAPK, mitogen-activated protein kinase; mTOR, mammalian target of rapamycin; PI3K-AKT, phosphatidylinositol 3-kinase-protein kinase B; TGF-β, transforming growth factor beta; TNF, tumour necrosis factor.

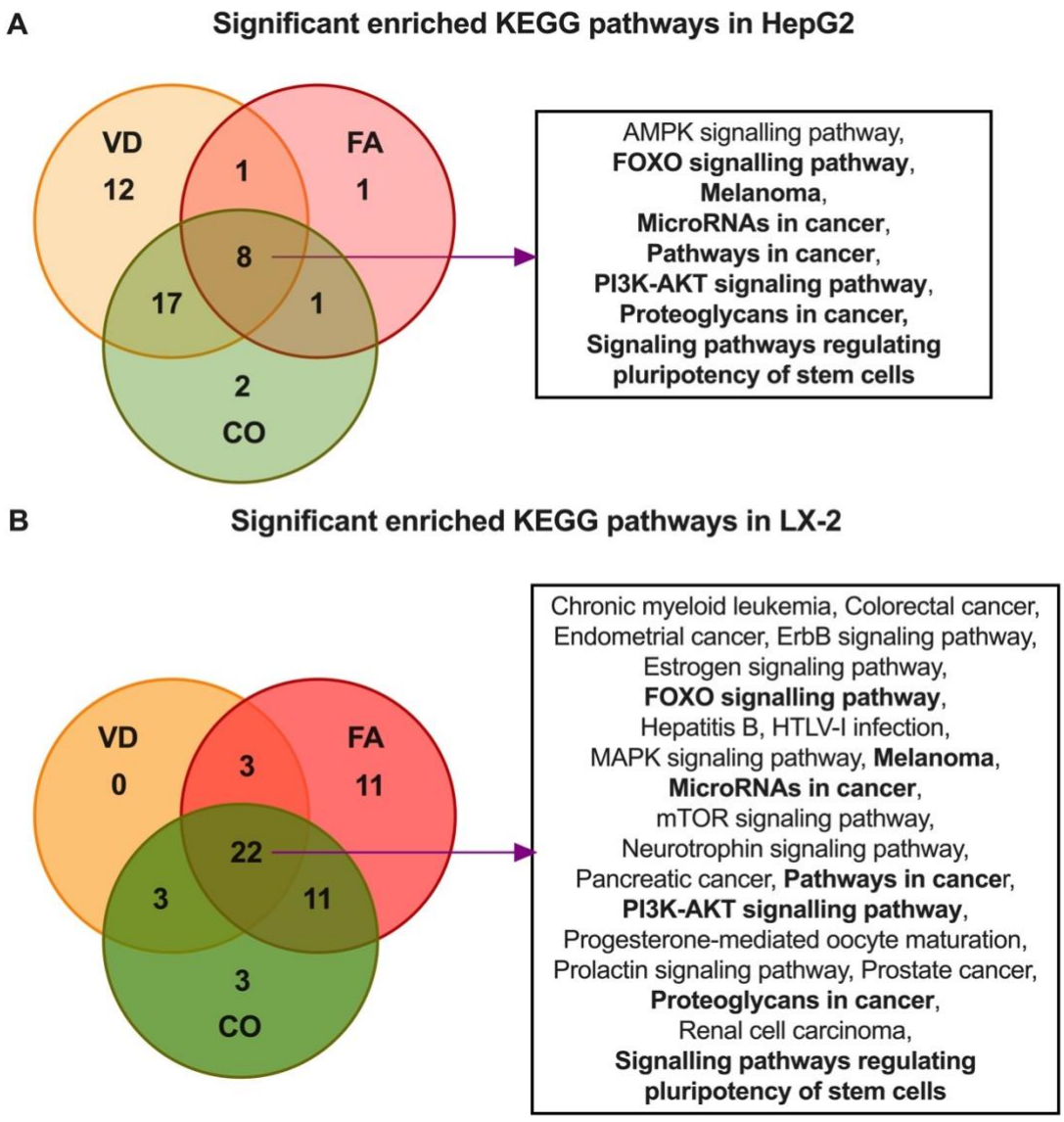

Figure 5.9 Venn diagram illustration of significant KEGG pathways in common between vitamin D and/or FA treated HepG2 and LX-2 cells. P<0.05 was considered statistically significant. Venn diagrams and a list showing significant KEGG pathways in common between all three treatment groups in HepG2 (**A**) and LX-2 (**B**). Note: Seven KEGG pathways significantly enriched in common between all three treatments in both HepG2 and LX-2 are bolded in intersection boxes.

5.9B). However, only seven pathways were in common in both cell lines, including four pathways related to cancers, two signalling pathways and one pathway related to general cellular processes. The two signalling pathways, FOXO and PI3K-AKT, were chosen for further analysis due to previous evidence for their roles in NAFLD cellular pathogenesis (Matsuda et al., 2013; Dong, 2017).

The miRNAs and their target genes found enriched and mapping to the FOXO and PI3K-AKT signalling pathways were assessed and are listed in **Table 5.3** and **Table 5.4** separately. While acknowledging the limitations of these bioinformatic predictions and the limitations of working with cell lines that may not express the target genes in question. However, the FOXO and PI3K-AKT signalling pathways have been shown to be relevant to NAFLD and have been previously examined in HepG2 and LX-2 cells [e.g. PI3K-AKT/FOXO (An et al., 2020) and SIRT1/FOXO/SREBP2 (Shan et al., 2021) pathways in HepG2, and TGF-β/SMAD (Ohara et al., 2018) and FGFR/NF-κB/TNF-α (Wang et al., 2020a) pathways in LX-2]. Interestingly, 13 miRNAs relevant to the FOXO or PI3K-AKT signalling pathways were identified as altered in both HepG2 and LX-2 cells. They were: let-7a-5p, let-7d-5p, miR-15b-5p, miR-18b-5p, miR-20b-5p, miR-23a-3p, miR-27a-3p, miR-27b-3p, miR-96-5p, miR-103a-3p, miR-212-3p, miR-486-5p and miR-490-3p. After integrating the above data and evidence in the literature (**chapter 3**), nine of 13 miRNAs in common in FOXO and PI3K-AKT signalling pathways were followed up for further independent verification in both cell lines. The nine miRNAs included: let-7a-5p, let-7d-5p, miR-15b-5p, miR-23a-3p, miR-27a-3p, miR-27b-3p, miR-96-5p, miR-103a-3p and miR-212-3p. In addition, another miRNA, miR-200a-3p, was chosen for independent verification as well, due to its relative high fold changes in both HepG2 and LX-2 cells treated with vitamin D and co-treatment and upregulated in patients with NAFLD (Wang et al., 2018b; Ezaz et al., 2020).

Overall, gene set enrichment analysis provided evidence of the essential biological roles of miRNAs, especially in transcription. Comparing significantly enriched KEGG pathways between different treatments in HepG2 and LX-2 cells highlighted several pathways relevant to NAFLD, especially FOXO and PI3K-AKT signalling pathways.

Table 5.3 FOXO signalling pathway target genes of candidate dysregulated miRNAs

HepG2		LX-2	
Genes	**miRNAs**	**Genes**	**miRNAs**
NRAS	hsa-let-7a-5p	NRAS	hsa-let-7a-5p
TGFBR1	hsa-let-7d-5p	TGFBR1	hsa-let-7d-5p
SMAD2	hsa-let-7g-5p	FGFR, PIK3R3	hsa-miR-7-5p
SIRT1	hsa-miR-9-5p	AKT3	hsa-miR-15b-5p
AKT3, CCND1	hsa-miR-15b-5p	SMAD2, IGF1	hsa-miR-18b-5p
SMAD2, STK4	hsa-miR-18a-5p	PIK3CA	hsa-miR-19a-3p
IGF1, SMAD2	hsa-miR-18b-5p	BCL2L11	hsa-miR-20b-5p
BCL2L11	hsa-miR-20b-5p	NLK	hsa-miR-23a-3p
NLK	hsa-miR-23a-3p	GRB2, NRAS	hsa-miR-27a-3p
FOXO1, GRB2	hsa-miR-27a-3p	PLK2, TGFBR1	hsa-miR-27b-3p
PLK2, TGFBR1	hsa-miR-27b-3p	BCL2L11, SGK3	hsa-miR-92a-3p
PRKAA1	hsa-miR-33a-5p	IGF1R	hsa-miR-96-5p
IGF1R	hsa-miR-96-5p	PIK3R1	hsa-miR-103a-3p
PIK3R1	hsa-miR-103a-3p	KRAS	hsa-miR-143-3p
PIK3R1	hsa-miR-107	SMAD2	hsa-miR-212-3p
IGF1R	hsa-miR-141-3p	PIK3R1	hsa-miR-486-5p
CCND1	hsa-miR-193a-3p	TGFBR1	hsa-miR-490-3p
CCND1	hsa-miR-193b-3p		
SMAD2	hsa-miR-212-3p		
CCND2	hsa-miR-373-3p		
PIK3R1	hsa-miR-448		
SMAD4	hsa-miR-449b-5p		
PIK3R1	hsa-miR-486-5p		
TGFBR1	hsa-miR-490-3p		
CCND1, CCND2, MAP2K1, PIK3R1	hsa-miR-497-5p		

Note: miRNAs found in both HepG2 and LX-2 cells were underlined.

Table 5.4 PI3K-AKT signalling pathway target genes of candidate dysregulated miRNAs

HepG2		LX-2	
Genes	**miRNAs**	**Genes**	**miRNAs**
ITGB3, NRAS, PPP2R2A, THBS1	hsa-let-7a-5p	ITGB3, NRAS, THBS1	hsa-let-7a-5p
PPP2R2A, THBS1	hsa-let-7d-5p	PPP2R2A, THBS1	hsa-let-7d-5p
AKT3, BCL2, CCND3	hsa-miR-15b-5p	EGFR, PIK3R3	hsa-miR-7-5p
IGF1	hsa-miR-18b-5p	AKT3, BCL2, CCND3	hsa-miR-15b-5p
BCL2L11, GNB5, JAK1	hsa-miR-20b-5p	IGF1	hsa-miR-18b-5p
PPP2R5E	hsa-miR-23a-3p	PIK3CA	hsa-miR-19a-3p
GRB2, PHLPP2	hsa-miR-27a-3p	BCL2L11, GNB5, JAK1	hsa-miR-20b-5p
CREB1, GNG12	hsa-miR-27b-3p	PPP2R5E	hsa-miR-23a-3p
COL4A5, LAMA2, PDGFC	hsa-miR-29b-3p	HGF	hsa-miR-26b-5p
IFNAR2	hsa-miR-30d-5p	GRB2, PHLPP2	hsa-miR-27a-3p
PRKAA1	hsa-miR-33a-5p	CREB1, GNG12	hsa-miR-27b-3p
IGF1R	hsa-miR-96-5p	ITGA6	hsa-miR-29c-3p
FGF2, PIK3R1	hsa-miR-103a-3p	IFNAR2	hsa-miR-30d-5p
BRCA1, CDK6, FGF2, PIK3R1	hsa-miR-107	BCL2L11, PPP2R2A, SGK3, TSC1	hsa-miR-92a-3p
IGF1R	hsa-miR-141-3p	IGF1R	hsa-miR-96-5p
PRKCA, TP53	hsa-miR-150-5p	FGF2, PIK3R1	hsa-miR-103a-3p
PPP2R5E	hsa-miR-181a-5p	KRAS	hsa-miR-143-3p
CCND1, LAMC1, YWHAZ	hsa-miR-193a-3p	MET	hsa-miR-148a-3p
CCND1, KIT, MCL1, TSC1, YWHAZ	hsa-miR-193b-3p	DDIT4	hsa-miR-153-3p
KIT	hsa-miR-199b-5p	BCL2	hsa-miR-182-5p
BRCA1	hsa-miR-212-3p	CREB1, LAMC1	hsa-miR-205-5p
FGF1	hsa-miR-326	BRCA1	hsa-miR-212-3p
CCND2	hsa-miR-373-3p	VEGFA	hsa-miR-302d-3p
LAMC1, PIK3R1	hsa-miR-448	PIK3R1	hsa-miR-486-5p
CCNE2, CDK6	hsa-miR-449b-5p		
PIK3R1	hsa-miR-486-5p		
CCND1, CCND2, CCND3, CDK6, MAP2K1, PIK3R1	hsa-miR-497-5p		

Note: miRNAs found in both HepG2 and LX-2 cells were underlined.

5.3.3 Identification of miRNA candidates for endogenous control for qPCR verification

It has been suggested that normalising target RNA levels using control genes from the same RNA class is desirable. In addition, the endogenous control should, in theory, display consistent expression across the test sample set, as well as storage stability, extraction efficiency, and quantification efficiency comparable to the target nucleic acids (Van Peer et al., 2014). Due to the length and structure different from other small RNAs, such as small nuclear RNA and small nucleolar RNA, in RT-qPCR-based miRNA profiling, using miRNAs as endogenous controls is now the most commonly recommended strategy (Drobna et al., 2018). In order to identify candidate endogenous controls for qPCR verification experiments, the CV of each miRNA detected with four Ct values across treatment groups within each cell line was calculated (**Figure 5.10**). Hypothesizing that a lower CV meant a minimal effect of the different treatments on miRNA expression, first miRNAs with a CV<1.0% were investigated (**Figure 5.11**). Examining miRNAs with the lowest CVs identified 29 and 40 miRNAs in HepG2 and LX2 cells, respectively, with CVs < 1%. Three of these, miR-125a-5p, miR-222-3p and miR-590-3p, were found with CVs < 1% in both cell lines. However, the Ct values of miR-590-3p for all treatments in both HepG2 or LX-2 were around 27, suggesting a lower initial miRNA copy number in comparison to miR-125a-5p and miR-222-3p miRNAs with average Ct's of 23.4 and 23.2, respectively (**Figure 5.11**). Therefore, miRNAs with CVs < 1.1% were examined to expand the options, which raised the number of candidate endogenous controls to six (**Figure 5.12**). After considering the raw Ct values in combination with the CVs across treatment groups, three miRNAs (miR-125a-5p, miR-222-3p and miR-455-3p) were chosen as candidate endogenous controls for miRNA expression confirmation experiments.

5.3.4 MicroRNA expression verification

Before starting the independent verification of ten candidate miRNAs, the raw Cts and the CVs of three candidate endogenous controls (miR-125a-5p, miR-222-3p and miR-455-3p) were first assessed to examine the effects of the different treatments (either vitamin D, FA, or in combination) in both cell lines.

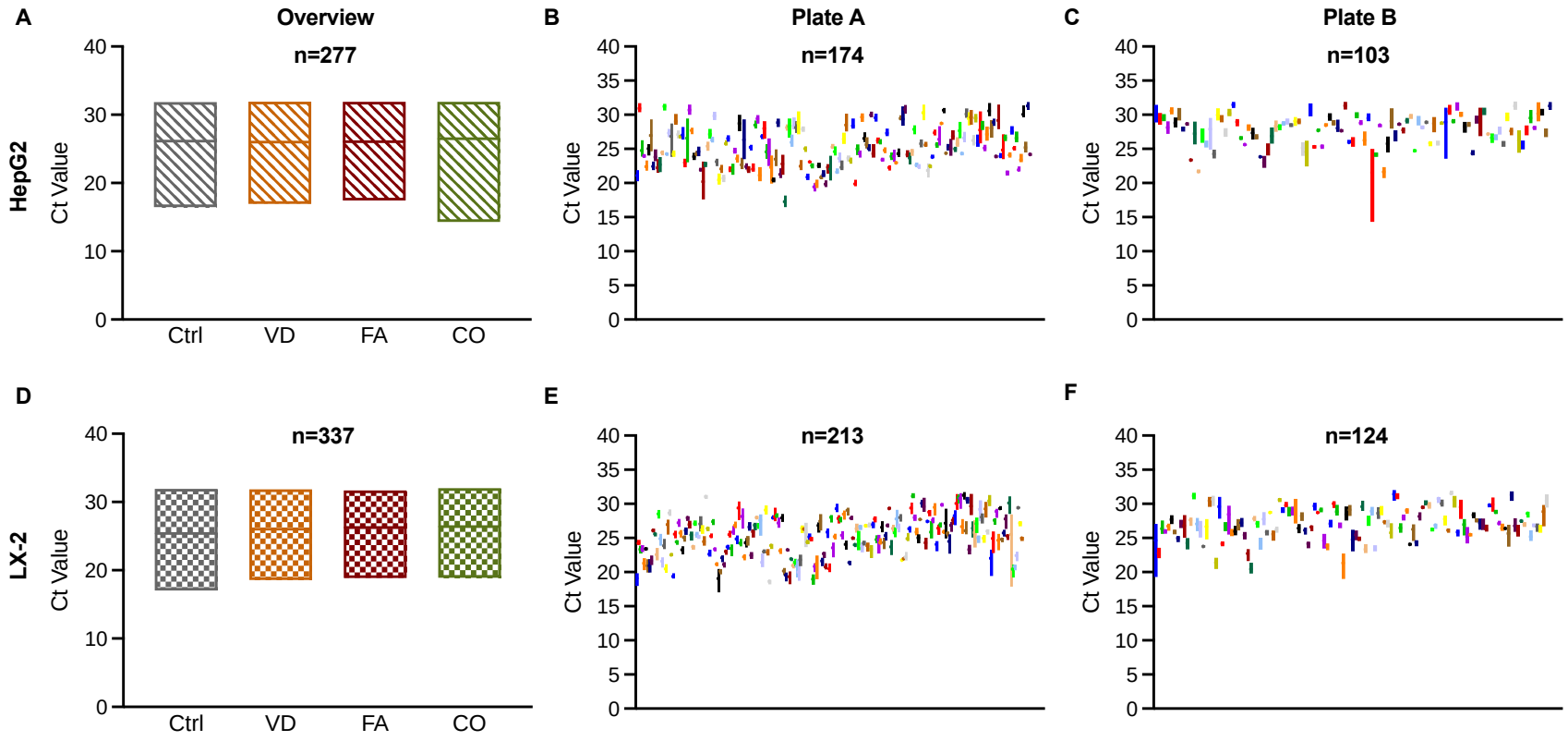

Figure 5.10 Ct values of miRNAs between treatments in HepG2 and LX-2. Cells were treated with vehicle (2% DMSO and 0.01% ethanol, Ctrl) 100nM 1α,25(OH)$_2$D$_3$ (VD), 500μM FA or in combination (CO). Data are shown as raw Ct and analysed by descriptive statistics with CV (%). **A.** (HepG2) **D.** (LX-2) are floating bar charts with a line at the mean; data are shown as a minimum to maximum Ct of all miRNA based on the treatment groups. **B. C. E. F.** are floating bar charts with a line at the mean of four treatment's raw Ct of each miRNA; data are shown based on miRNAs on either plate A or B. **B. C.** are HepG2 cells, **E. F.** are LX-2 cells.

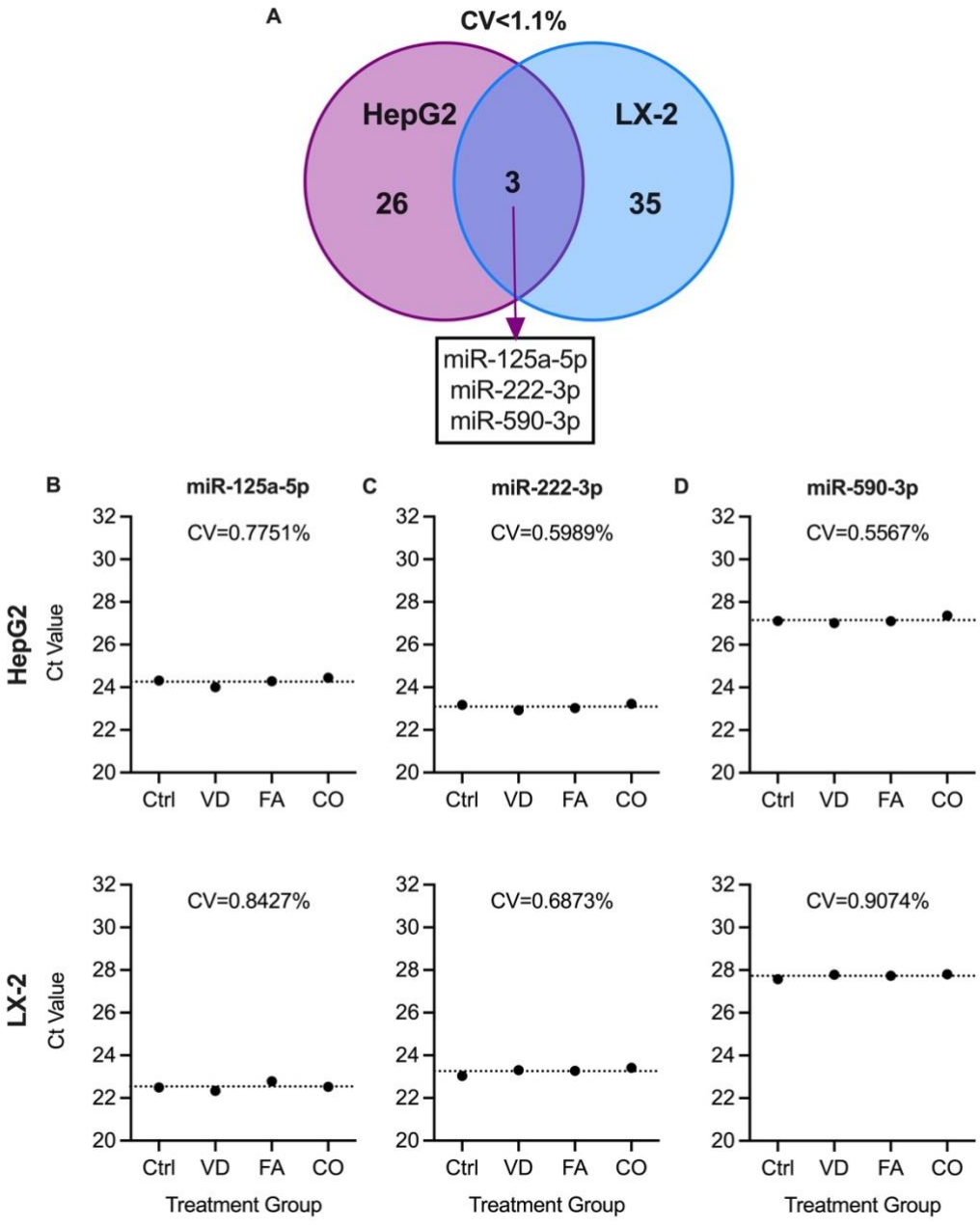

Figure 5.11 Initial assessment of candidate endogenous control miRNAs. A. Venn diagram and table of miRNAs in both HepG2 and LX-2 where the CV<1.0% across treatment groups. **B. C. D.** are plot charts with a dotted line of Ct average of each miRNA in HpeG2 (top graph) or LX-2 cells (bottom graph). **B.** miR-125a-5p, **C.** miR-222-3p, **D.** miR-590-3p.

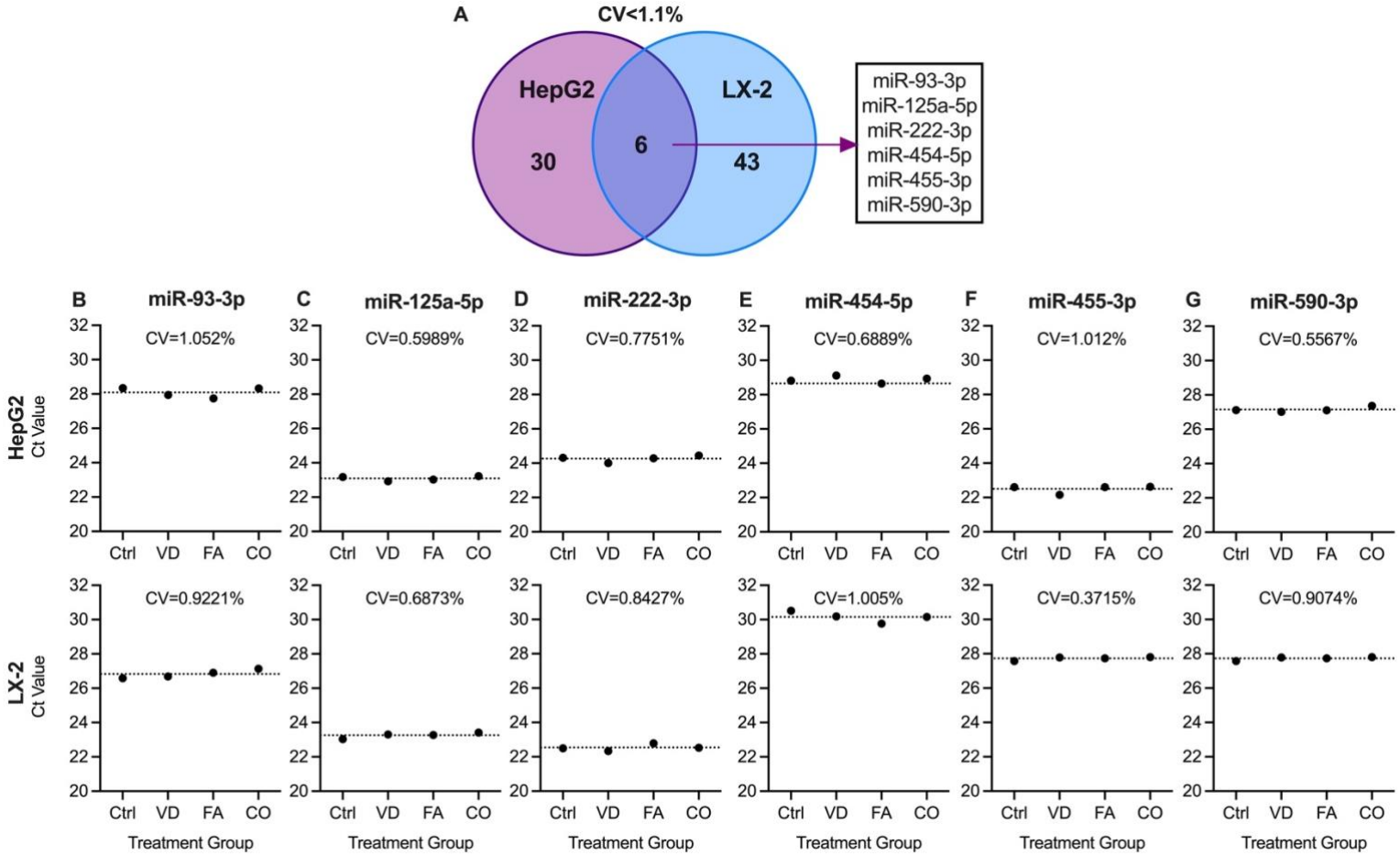

Figure 5.12 Identification of candidate endogenous control miRNAs. A. Venn diagram and table of miRNAs with CV<1.1% in both HepG2 and LX-2 cells. **B. C. D. E. F. G.** are plot charts with a dotted line of Ct average between treatments of each miRNA in HepG2 (top graph) or LX-2 cells (bottom graph). **B.** miR-93-3p.

Then, integrating the results of HepG2 and LX-2, miRNA with the relative minimal effect of the different treatments would be chosen as an endogenous control to process the ddCt analysis.

The results are shown in **Figure 5.13**. Compared to HepG2 cells, the interquartile range (IQR) of each treatment in LX-2 cells were smaller, indicating the central portion of the data spread out closer. In addition, the mean Ct of each treatment group in HepG2 cells was lower than 25, suggesting a greater amount of target miRNA detected in the samples. Whereas the mean Ct of miR-455-3p in all treatment groups of LX-2 cells was around 25.5 in comparison to miR-125a-5p and miR-222-3p miRNAs with average Ct's of 22.5 and 23.3, respectively. Notably, miR-222-3p had the smallest IQR with the lowest CV values in both cell lines. Thus, the decision was made that miRNA-222-3p would be used as the control for further analyses.

As the arrays were done on pooled samples, the top ten miRNAs of interest for follow up were subjected to verification experiments in independent experimental samples to establish variance by qPCR and normalised to miR-222-3p (**Figure 5.14**). The relative FCs derived from qPCR verification analysed by two-way ANOVA with the Holm-Sidak test for multiple comparisons and were compared with array data (**Figure 5.14**).

Overall analyses by two-way ANOVA showed that treatment only influenced the expression of let-7d-5p (P=0.0204) and miR-200a-3p (P=0.0173), while no effect of cell type was observed in the expression of all ten miRNAs. In addition, there was no significant interaction between different treatments and cell types in either miRNA. In post hoc examination of treatment effects on each miRNA expression, there were no significant differences between different treatments in either HepG2 or LX-2 cells.

As these results were surprising, protocols were reviewed for troubleshooting, as well as the initial sample collection information and quality control data. Reviewing the OD data, the 260/280 ratio of the miRNA samples ranged from 1.67-2.04 in HepG2 and LX-2 cells samples, suggesting an acceptable nucleic acids purity with a low amount of protein contamination (**Appendix Table D2 and D3**). However, the 260/230 values were relatively

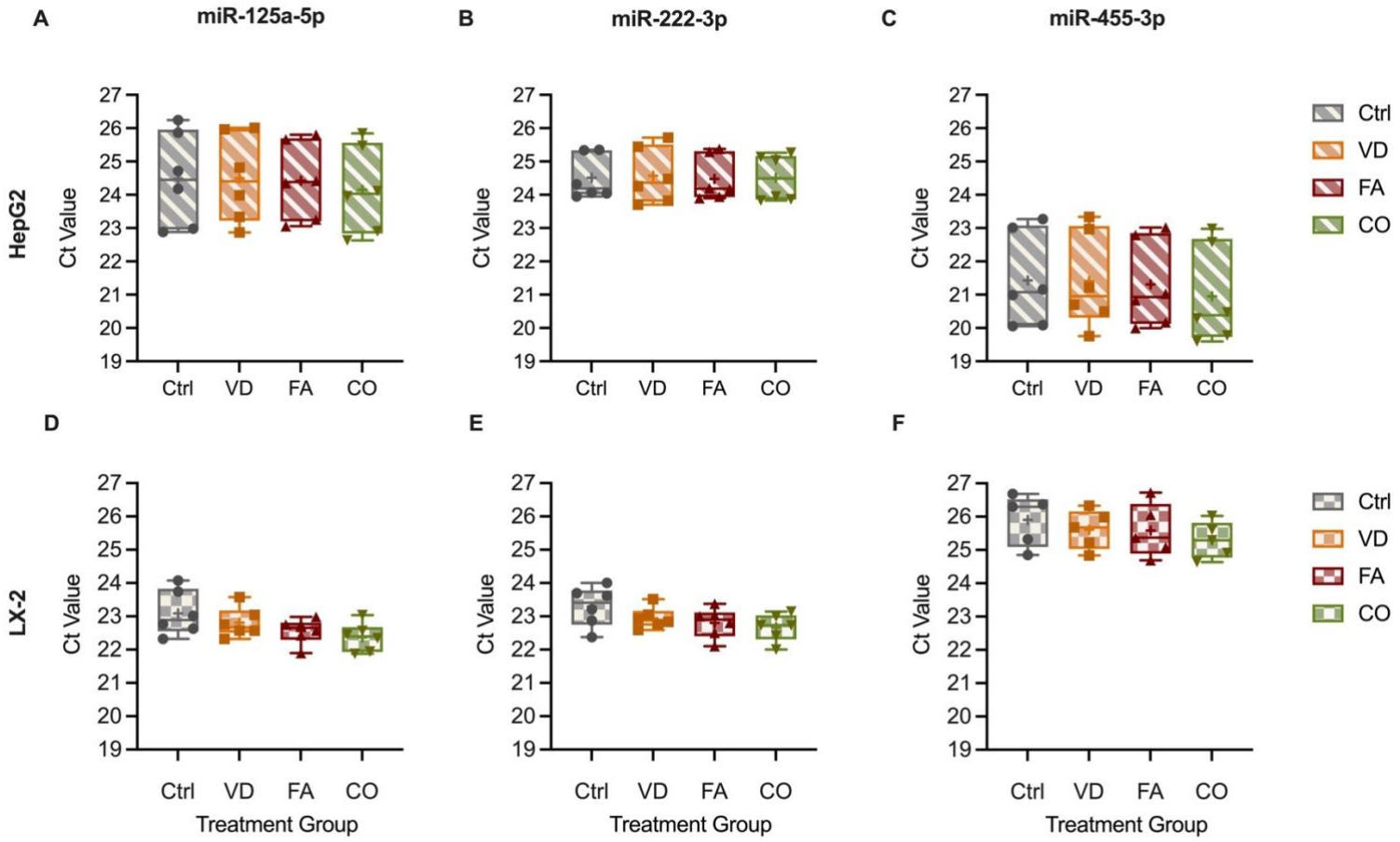

Figure 5.13 Ct value of three endogenous miRNAs between treatments in HepG2 and LX-2. Cells were treated with 100nM 1α,25(OH)D (VD), 500μM FA or in combination (CO). Data are shown as box and whiskers plots (whiskers: minimum to maximum and show all points) with mean shown as '+'. Data are analysed by descriptive statistics with CV (%). The box and whiskers plots of miR-125a-5p (**A**), miR-222-3p (**B**) and miR-455-3p (**C**) in HepG2 cells (n=6). The box and whiskers plots of miR-125a-5p (**D**), miR-222-3p (**E**) and miR-455-3p (**F**) in LX-2 cells (n=6).

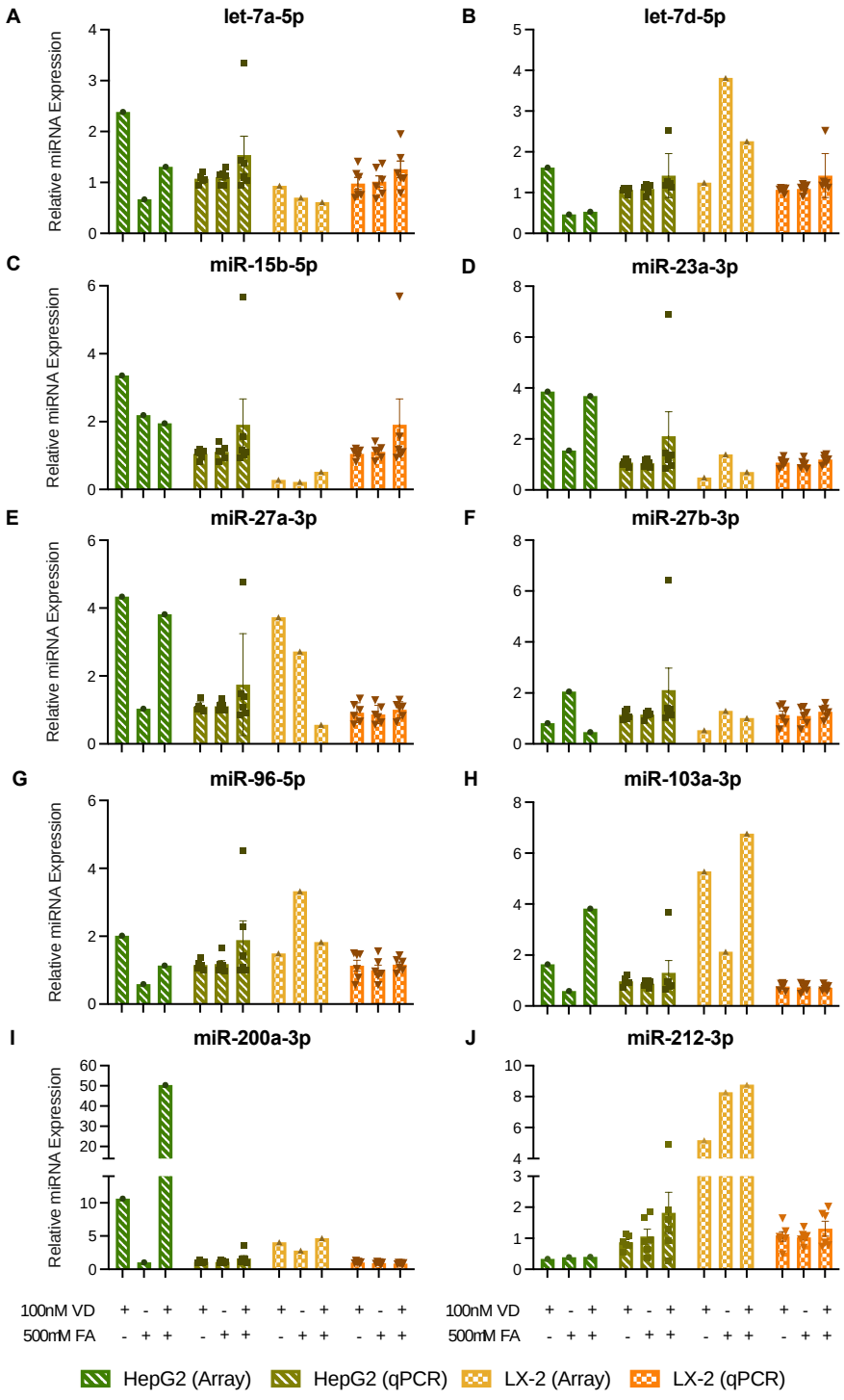

Figure 5.14 Comparison of verification results and array results. Array data were normalised to the global median (both HepG2 and LX-2 n=1 pooled sample from three independent replicates), while qPCR verification data were normalised to miR-222-3p (both HepG2 and LX-2 n=6). Data are shown as mean±SEM. The qPCR data were analysed by two-way ANOVA with Holm-Sidak test for multiple comparisons. **A.** let-7a-5p (both treatment and cell type: P>0.05), **B.** let-7d-5p (treatment: P=0.0204, cell type: P>0.05), **C.** miR-15b-5p (both treatment and cell type: P>0.05), **D.** miR-23a-3p (both treatment and cell type: P>0.05), **E.** miR-27a-3p (both treatment and cell type: P>0.05), **F.** miR-27b-3p (both treatment and cell type: P>0.05), **G.** miR-96-3p (both treatment and cell type: P>0.05), **H.** miR-103a-3p (both treatment and cell type: P>0.05), **I.** miR-200a-3p (treatment: P=0.0173, cell type: P>0.05), **J.** miR-212-3p (both treatment and cell type: P>0.05).

low, with the lowest value as 0.05. Low 260/230 ratios proposed suggested that the miRNA samples were contaminated by phenol, chloroform or guanidine salts included in isolation kits (Desjardins and Conklin, 2010).

5.3.5 Optimisation of RNA isolation protocols

With results of arrays and validation experiments in doubt, the decision was made to repeat these experiments using RNA sequencing rather than arrays. A critical step before this could happen was to improve the quality of miRNAs by optimising isolation protocols. As a first step, with a goal of increasing the 260/230 ratio of isolated miRNAs, I tested aspects of sample collection, storage and miRNA isolation using the same mirVana™ (Thermofisher) kit used in the previous experiments. All the samples used for optimisation were untreated LX-2 cells cultured in T75 flasks, and the final RNA samples were eluted with 50μl NFW. I tested three different sample collection procedures, collecting samples by either Accutase® lysis, cold PBS with a scraper, or lysed directly using Lysis/Binding buffer on fresh cells. In addition, I compared storage conditions, either snap freezing RNA pellets in liquid nitrogen or storing them in RNAlater at -80℃. In addition I modified aspects of the organic extraction procedure, specifically increasing the volume of Lysis/Binding buffer, and maximising lysis time, and the time and speed of centrifugation. Additionally, after the final washes of the spin column, the final centrifugation drying step prior to elution of miRNA was repeated and an additional 3 min air-dry step with column lid open was added.

The results of optimisation of enrichment procedure of small RNAs (**Table 5.5**) showed that samples derived from Accutase® collection had higher concentrations and 260/280 values than cold PBS collection. On the other hand, compared to samples treated with RNAlater, samples snap-frozen in liquid nitrogen had higher concentrations and 260/230 values. Thus, the combination of Accutase® collection and liquid nitrogen frozen appeared to be a better choice for isolation enriched small RNAs.

At the same time, another comparison was made between the small RNAs enrichment and the total RNA isolation by the direct lysis method using mirVana™. The total RNA sample had a much higher concentration (427.18

ng/μl vs. 78.76 ng/μl) and higher 260/280 (2.00 vs 1.90) and 260/230 (1.53 vs 0.84) ratio than the optimised small RNA sample (**Table 5.5**).

Table 5.5 Testing of Thermofisher mirVana™ miRNA isolation kit.

Procedure	**Small RNA enrichment**					**Total RNA**
Collection	Accutase	Accutase	Cold PBS	Cold PBS	Lysis/Binding buffer	Lysis/Binding buffer
Storage	RNAlater	Liquid nitrogen	RNAlater	Liquid nitrogen	Immediate	Immediate
Date of sample collection	08/07/21	08/07/21	08/07/21	08/07/21	12/07/21	12/07/21
Date of sample extraction	09/07/21	09/07/21	09/07/21	09/07/21	12/07/21	12/07/21
Volume of aqueous phase extraction (μl)	400	400	400	400	500	500
Con. (ng/μl)	46.16	51.18	16.92	14.33	78.76	427.18
260/280	1.85	1.87	1.71	1.54	1.90	2.00
260/230	1.38	1.41	0.71	0.82	0.84	1.53

All the samples used for optimisation were untreated LX-2 cells cultured in a T75 flask and eluted with 50μl nuclease-free water.

For RNA-sequencing, I was asked to provide total RNA of high purity sample (both OD260/280 and OD260/230≥2), which even after optimisation the mirVana™ kit did not meet. Therefore I compared two additional RNA isolation kits to the mirVana™, the miRNeasy Tissue/Cells Advanced Mini Kit (QIAGEN) and the ReliaPrep™ RNA Cell Miniprep System (Promega). Both kits are phenol-free and column-based, designed to combine the advantages of organic extraction and solid-phase extraction for total RNA isolation. The OD of the total RNA isolated from a T25 flask of untreated LX-2 cells from the 3 kits were compared (**Table 5.6**), and the ReliaPrep™ RNA isolation kit was chosen to prepare samples for small RNA sequencing. Currently, total RNA samples, derived from HepG2 and LX-2 cells cultured with vitamin D, fatty acid or both, and isolated via the ReliaPrep™ kit, have been sent to the sequencing facility (St. James Hospital) for quality-control tests and library derivation. The OD information for these samples is in **Appendix Table D4**.

Table 5.6 Comparison of 3 total RNA isolation kits recommended for miRNA work.

Kit	mirVana™ (Thermofisher)	miRNeasy (QIAGEN)	ReliaPrep™ (Promega)
Con. (ng/μl)	427.18	218.03	526.91
260/280	2.00	1.94	2.02
260/230	1.53	1.15	1.92

Samples for isolation were untreated LX-2 cells cultured in T25 flasks. Sample isolated by mirVana™ and miRNeasy was used 50µl nuclease-free water (NFW), whereas sample isolated by ReliaPrepTM was eluted by 30µl NFW.

5.4 Discussion

In summary, this chapter aimed to identify miRNAs regulated by vitamin D and lipid loading in immortalised hepatocytes and HSCs. Bioinformatic results provided evidence of the biological roles of miRNAs, especially their vital roles in the transcription of gene expression in biological processes and molecular functions. In line with the study aims, KEGG pathway comparisons between different treatments highlighted FOXO, PI3K-AKT, MAPK and Ras signalling as important, significantly enriched pathways in both cell lines. While AMPK and p53 signalling pathways were found particularly enriched in HepG2 cells, insulin, mTOR, TGF-β and TNF signalling pathways were explicitly involved in LX-2 cells. After integrating the bioinformatic data with literature evidence, a subset of candidate miRNAs (let-7a-5p, let-7d-5p, miR-15b-5p, miR-23a-3p, miR-27a-3p, miR-27b-3p, miR-96-5p, miR-103a-3p, miR-200a-3p and miR-212-3p) were followed up for independent verification by qPCR. However, the results of the array were not reproduced in the validation, and no significant differences were shown in miRNA expression in confirmation experiments between treatments. After identifying miRNA sample quality as potential issue, isolation procedures were optimised, the experiments repeated, and total RNA samples have been sent for RNA sequencing.

5.4.1 The roles of miRNAs involved in signalling pathways

The GSEA notably suggested that miRNAs that regulate the FOXO and PI3K-AKT signalling pathways were found commonly dysregulated in all three treatment groups in both cell lines. Although these results are suspect, given the lack of confirmation in verification experiments and the low OD260/230, accumulating evidence does show that the dysregulation of FOXO and PI3K-

AKT signalling pathways contributes to the progression of NAFLD (Matsuda et al., 2013; Dong, 2017), so I will expand on these pathways briefly here.

The PI3K-AKT signalling pathway is one of the most critical intracellular pathways, regulating various cellular regulatory processes, including cell growth and proliferation, differentiation, apoptosis, metabolism, migration, and secretion (Cantley, 2002; Fruman et al., 2017). Moreover, aberrations in PI3K-AKT signalling contribute to metabolic dysfunctions, including NALFD (Matsuda et al., 2013). For example, an animal study indicated that the protein expression of hepatic PI3K and AKT was significantly lower in high-fat diet-induced NAFLD rats (Liu et al., 2012b).

Generally, the PI3K-AKT signalling transduction pathway contributes to modulating the glucose metabolic actions of insulin in the liver (Pessin and Saltiel, 2000). First, insulin activates tyrosine kinase activity through insulin receptor-related receptors (IRRs), which further triggers the phosphorylation of insulin receptor substrate (IRS) (Cantley, 2002; Taniguchi et al., 2006). Then, phosphorylated IRS combines with the regulatory subunit of PI3K, p85, inducing the catalytic subunit (p110) activation. All these changes in PI3K eventually catalyse the conversion of phosphatidylinositol-4,5-bisphosphate (PIP2) to phosphatidylinositol-3,4,5-trisphosphate (PIP3). Once generated, PIP3 acts as a second messenger, and subsequently recruits a serine-threonine kinase (AKT, also known as protein kinase B) and phosphoinositide-dependent protein kinase 1 (PDK1) through their pleckstrin homology domains (Manning and Toker, 2017). Notably, there are three isoforms of AKT: AKT1, AKT2 and AKT3. In the liver, AKT1 and AKT 2 are the only expression isoforms in healthy situations; AKT2 is the most abundant isoforms expressed in the hepatocytes, accounting for 85% of total hepatic AKT (Easton et al., 2005). The activation of AKT1 requires two essential phosphorylation steps, specifically the threonine 308 and serine 473 of AKT are phosphorylated by PDK1 and mTOR complex 2, respectively. Similar activation also occurs in AKT2 (threonine 309 and serine 474) and AKT3 (threonine 305 and serine 472) (Manning and Toker, 2017).

Downstream effectors, such as glycogen synthase kinase 3 (GSK3) and SREBPs, involved in glucose and lipid metabolism in the liver are regulated by AKTs (Huang et al., 2018). For example, the activation of AKT regulates

glycogen synthesis by inducing the phosphorylation and inactivation of GSK3 (Beurel et al., 2015). Additionally, AKT regulates lipid metabolism through SREBPs (SPEBP-1a/1c/2) (Krycer et al., 2010).

Besides GSK3 and SREBPs, FOXO proteins are direct downstream effectors of AKT (Dong, 2017). The FOXO transcription factors belong to a subfamily of the forkhead protein family, class O; four isoforms of FOXO are found in mammals (FOXO1/3/4/6) (Carlsson and Mahlapuu, 2002). The pleiotropic functional roles of FOXOs in NAFLD development have been comprehensively reviewed by Dong (2017) in several aspects, including maintaining glucose and lipid metabolism and modulating inflammation and fibrosis. For example, generally, FOXOs, through transcriptionally regulating several genes, activate hepatic gluconeogenesis in order to maintain normal blood glucose levels during starvation (Dong et al., 2006; O-Sullivan et al., 2015). However, in the context of IR, FOXOs continuously activate gluconeogenesis without the tight control of insulin signalling and cause further disturb glucose and lipid homeostasis.

In summary, the FOXO and PI3K-AKT signalling pathways play essential roles in maintaining metabolic and cellular homeostasis in the liver, and dysregulation on of these pathways may be contributing to NAFLD development.

5.4.2 miRNA expression

With the growing interest in the value of miRNAs as diagnostic or prognostic biomarkers and/or therapeutic targets, many methodologies have been established to evaluate miRNA expression. These include: bead-based flow cytometry, cloning, in situ hybridisation, northern blotting, qRT-PCR, microarrays, and more recently, NGS (Brown et al., 2018). Although evaluation of miRNA detection methods has received considerable attention (Git et al., 2010; Wang et al., 2011; Jet et al., 2021), the detection of miRNA expression relies on the quality of the input material (Hammerle-Fickinger et al., 2010; Podolska et al., 2011). Therefore, isolating high-quality RNA is critical for successfully performing high quality experiments and the key point is to maximise the yield of contaminant-free and non-degraded RNA (Tan and Yiap, 2009). For example, the contaminants in RNA samples like nucleases, phenol, chloroform or guanidine salts can impede the downstream

applications that are based on enzymatic reactions, like qPCR (Brown et al., 2018).

Currently, there are several standard protocols for miRNA isolation but with challenges of obtaining high quality miRNA from different types of sample (Moldovan et al., 2014; Brown et al., 2018). there is no consensus on the optimal methodologies for miRNA isolation, The existing extraction methods are based on conventional nucleic acid extraction methods, which are divided into solution-based or column-based protocols (Tan and Yiap, 2009). The acid guanidinium thiocyanate-phenol-chloroform extraction is historically the most common and well-established solution-based method (Chomczynski and Sacchi, 1987), and Invitrogen sells the monophasic reagent of phenol and guanidine isothiocyanate subsequently optimised by Chomczynski called TRIzol (Chomczynski, 1993). This method relies on phase separation by centrifugation of a mixture emulsion of sample and phenol-chloroform solution. The hydrophobic (lower) layer and layer interface contain denatured proteins, while the hydrophilic (upper) phase contains nucleic acids. Guanidinium thiocyanate is a chaotropic agent added to the phenol for denaturing proteins. In this single-step method, RNA is separated from DNA and remains in the aqueous layer under an acidic condition. Whereas, solid-phase nucleic acid purification is typically performed with filter-based spin columns (Tan and Yiap, 2009). Compared to solution-based methods, these methods can purify nucleic acid rapidly and are found in most commercial extraction kits available on the market, such as miRVana and miRNeasy. A comparison of different extraction reagents and kits, including TRIzol, mirVana^{TM}, miRNeasy, Isolate II and Norgan total, on target gene expression using mouse tissues was made by Brown et al. (2018). Notably, these reagents and kits were primarily developed to extract long mRNAs and assumed that all RNAs are purified equally. However, the results revealed that the methodologies varied in RNA quantity and quality. For example, the yield results quantified by a Qubit Fluorometer demonstrated that the miRNeasy kit always gave a high yield of RNA across all samples (brain, lung and liver). For miRNA enrichment, the mirVana^{TM} and Norgen total RNA kits consistently yielded higher percentages of miRNA than other methods. But, the mirVana protocol does not include gDNA removal, which could increase the risk gDNA contamination and affect

the reverse transcription. Therefore, choosing a particular RNA extraction method with high quantity, quality and purity and optimising the methods for samples of interest are highly important.

In the previous **chapter 4**, I used TRIzol, followed by alcohol precipitation, to extract total RNA. However, samples isolated by TRIzol are known to reduce recovery of miRNAs with low GC content and stable secondary structure (Kim et al., 2012). Here, I chose the mirVana™ kit (Thermofisher) for miRNA isolation, the most utilised isolation kit for historical reasons (Mraz et al., 2009). In contrast to TRIzol, miRNA isolated from the mirVana™ kit has been shown to perform better in the downstream detection of miRNA (Guo et al., 2014). However, my miRNA samples isolated by mirVana with the small RNA enrichment procedure had poor purity with relative low OD260/230, which suggested contamination of aromatic compounds and salts. This has also been reported in multiple molecular discussion forum (e.g. ResearchGate).

Hence, both the TLDA array and verification experiment results were subject to doubt. Subsequently, troubleshooting and protocol optimisation procedures on mirVana™ isolation were carried on based on three aspects: sample collection, storage and isolation. Firstly, the optimisations were based on getting enriched small RNAs. The results suggested that the combination of Accutase® collection and snap freezing in liquid nitrogen might get comparable better quality of enriched small RNAs. However, the 260/230 ratio was still lower than 1.8. Meanwhile, because both miRVana and Pritchard et al. (2012) suggested that it was not necessary to enrich the miRNA component of the cellular RNA, a comparison of total RNA isolation and enriched small RNA isolation was processed by the direct lysis method. Both samples got acceptable 280/260 ratios, but the 260/230 values were 0.84 and 1.53 in enriched small RNA sample and total RNA sample, respectively. On enquiry, the Thermofisher technicians suggested adding an extra precipitation procedure. However as the re-precipitation might cause sample loss, this was not attempted, rather, I moved on to testing additional phenol-free methods and focused on optimising and standardising the isolation protocols for the cellular samples of interest.

Besides RNA extraction methods, the results of assessing miRNA expression could vary wildly by the choice of the downstream applications. The accurate quantification of miRNAs poses several challenges due to their low amount, short length, low GC content and the high sequence homology with miRNA families (Pritchard et al., 2012). Due to its rapidity, simplicity, and cost-effectiveness than other hybridization or sequencing-based technologies (Git et al., 2010), qRT-PCR is routinely used for determining miRNA expression. In this study, I used qRT-PCR based TLDA array cards, which could simultaneously decide on the expression of multiple miRNA molecules. However, although TLDA is a relatively robust method for gene expression, the reproducibility of low copy genes with high Ct values is limited (Lü et al., 2008). In addition, there is a loss of sensitivity when using relatively small amounts of nucleic acid extract (Heaney et al., 2015). Moreover, because of cost considerations, I used pooled samples without independent and technical replicates thereby eliminating the ability to quantify biological and technical variation.

To repeat the miRNA profiling with more sensitive and robust detection methods, microarray and NGS were considered. Compared to amplification-based qPCR, hybridisation-based microarrays can analyse thousands of miRNAs in one assay. However, qPCR and microarray are mainly limited by detecting known and annotated miRNAs in miRBase (Pritchard et al., 2012). In contrast, NGS has higher discovery power to detect thousands of targets with or without sequence information and precise reading of miRNA sequences. As a sequence-based method, the NGS technologies do not need specific primers and/or probes designed for each targeted miRNA (Jet et al., 2021); its quantification is based on counting sequence tags (Hurd and Nelson, 2009). The digital nature of NGS allows a virtually unlimited fully-quantitative dynamic range, which allows comprehensive detection of all miRNAs in samples, including distinguishing between variants differing by a single nucleotide, as well as isomiRs of varying length (Hurd and Nelson, 2009; Pritchard et al., 2012). Moreover, the problems like background noise and cross-hybridization in microarray are avoided (Dave et al., 2019). As our final aim is to investigate novel miRNAs involved in both vitamin D metabolism and

NAFLD progression, small RNA-sequencing was chosen for further exploration.

Currently, total RNA samples from both HepG2 and LX-2 cells (n=3) treated with either vitamin D, FA, or in combination have completed isolation by ReliaPrep^{TM} RNA Cell Miniprep System (Promega) and sent to the Next Generation Sequencing Facility at St. James for small RNAseq. While waiting for the sequencing results, the expression of several miRNAs, including miR-27, miR-125 and miR-155, will be examined by qPCR. Our published review paper mentioned these three miRNAs (Zhang et al., 2021d). While miR-27 and miR-125 inhibit VDR translation, miR-155 is inhibited by VDR. In the future, a linear bioinformatics analysis will come out with the sequencing results. Afterwards, we could pick up several pathways with potential target genes and relative miRNAs to process verification.

5.4 Summary

- TLDA arrays were processed on immortalised hepatocytes and HSCs treated with either vitamin D, fatty acid, or in combination.
- Bioinformatic analyses were conducted sequentially for the subset of miRNAs hypothesised as dysregulated from TLDA; FC>2.85 was hypothesised to be ‘upregulated’ and FC<0.67 was hypothesised to be ‘downregulated’.
- Bioinformatic results provided evidence of the biological roles of miRNAs, especially their vital roles in the transcription of gene expression in biological processes and molecular functions.
- KEGG pathway comparisons between different treatments in both cell lines highlighted FOXO and PI3K-AKT signalling pathways as important, significantly enriched pathways, which might contribute to NAFLD progression.
- After integrating the bioinformatic data with literature evidence, a subset of candidate miRNAs (let-7a-5p, let-7d-5p, miR-15b-5p, miR-23a-3p, miR-27a-3p, miR-27b-3p, miR-96-5p, miR-103a-3p, miR-200a-3p and miR-212-3p) were followed up for independent verification by qPCR, but the results were not significant.

- After identifying miRNA sample quality as a potential issue, given the low OD26/230, isolation procedures were optimised, the decision was made to repeat experiments using RNA sequencing rather than arrays.
- Optimisation of RNA isolation protocols suggested that the mirVana™ isolation kit (Thermofisher) was not a good choice for miRNA work; comparing the results of three total RNA isolation kits recommended for miRNA work, the ReliaPrep™ RNA Cell Miniprep System (Promega) was chosen to prepare samples for small RNA sequencing.

Chapter 6
Non-alcoholic fatty liver disease and vitamin D in the UK biobank: a two-sample bi-directional Mendelian randomisation study

6.1 Introduction

Understanding the relationships between cause (i.e. exposure) and effect (i.e. outcome) of ill health is essential to informing public health policy and clinical practice. Mendelian randomisation is an epidemiological approach that uses genetic information as IVs to probe the causal relationship between an exposure and outcome in an observational setting (Smith and Ebrahim, 2003). The advantages of MR are that it may be able to overcome the problems in conventional epidemiological studies (observational and interventional) such as residual confounding and reverse causation, as the genomes of each person under investigation were naturally randomised at conception (Smith and Ebrahim, 2003; Sekula et al., 2016).

In recent years, two-sample bidirectional MR has been widely used in epidemiological research (Zheng et al., 2017). Two-sample MR is a method to estimate the causal effect of the exposure on an outcome using genetic instruments (Burgess et al., 2015). Generally, the summary of associations between SNP-exposure and SNP-outcome are obtained from two independent GWASs. In the meantime, in bidirectional MR, the analyses are conducted in both directions to use IVs as proxies for the exposure, thus proxying the causal effect of the actual exposure on the outcome (Davey Smith and Hemani, 2014). The flexible combination of two-sample and bidirectional method greatly increases the scope of MR analysis.

Non-alcoholic fatty liver disease is a major cause of liver disease worldwide, affecting approximately 25% of the worldwide population (Younossi et al., 2018). Despite known multi-systems and genetic contributions, other metabolic comorbidities (such as obesity and diabetes), sedentary lifestyle overnutrition and environment have also been considered as risk factors driving the NAFLD progression (Bence and Birnbaum, 2021). However, the cornerstones of NAFLD management is a healthy lifestyle,

including diet and physical exercise modifications (Rinella and Sanyal, 2016). In addition, individual dietary nutrients have been implicated in NAFLD pathogenesis and may differentially affect disease development and/or progression (Moore, 2019a). Vitamin D is of interest in part because it has antiproliferative, anti-inflammatory and antifibrotic properties that have been shown to improve NAFLD progression, such as inflammation and fibrogenesis in preclinical models (Pacifico et al., 2019; Karatayli et al., 2020). Additionally, increasing observational studies reported inverse correlations between vitamin D deficiency and NAFLD prevalence risk and severity (section **2.2.1**) (Rhee et al., 2013; Liu et al., 2020b). However, as I discussed in **2.2.2**, intervention studies testing the therapeutic effect of vitamin D supplementation on patients with NAFLD have conflicting findings (Pacifico et al., 2019; Zhang et al., 2019c). These inconsistent results, inherent residual confounding of observational studies and possible effects of reverse causality might affect the inference of causal association between vitamin D and NAFLD.

To date, two MR studies explored the causal inference between vitamin D and NAFLD (Wang et al., 2018c; Yuan and Larsson, 2022) but have inconsistent results. For example, while a one-sample MR study performed in a large Chinese population (n=9,128) found no causal association between vitamin D and NAFLD (Wang et al., 2018c), a more recent two-sample MR conducted in the European population revealed an inverse association between serum 25(OH)D level and risk of NAFLD (Yuan and Larsson, 2022).

In this chapter, I conducted a two-sample bidirectional MR analysis to determine whether individuals randomly assigned at conception have lower levels of circulating 25(OH)D levels have a greater likelihood of developing NAFLD and vice versa. The largest meta-GWAS of vitamin D status of European descent was selected to extract genetics instruments (Jiang et al., 2018). Two NAFLD GWAS models, with or without filtering other liver diseases, were conducted using summary-level data from the UKBB. The aims here were to estimate the effect of vitamin D status on NAFLD and vice versa and assess the impact of genetic IVs extracted from various NAFLD GWAS models on the vitamin D outcome.

6.2 Methods

6.2.1 Study design overview

A brief description of the two-samples bidirectional MR design is displayed in **Figure 6.1**. There are three critical assumptions for MR: (1) IVs robustly associated with the exposure of interest (relevance assumption); (2) IVs are not associated with any confounders of the association between the exposure and the outcome (independence assumption), and (3) IVs only affect the outcome via their effect on the exposure of interest (exclusion restriction) (Davey Smith and Ebrahim, 2005; Davies et al., 2018). In addition, if samples used to select IVs associated with the exposures and the outcomes have overlap, it could introduce instrument bias, affecting MR estimation (Burgess et al., 2016). Therefore, the summary-level data from GWAS using independent individuals of European descent circulating 25(OH)D levels and NAFLD were used, respectively. The data sources utilised in the present study are summarised in the following sections.

6.2.2 Data sources and SNPs selection for vitamin D

The summary statistics of the GWAS of circulating 25(OH)D concentrations were downloaded from SUNLIGHT Consortium (URL https://drive.google.com/drive/folders/0BzYDtCo_doHJRFRKR0ltZHZWZjQ). This meta-analysis collected data of 79,366 individuals from 31 cohorts of European ancestry in Europe, Canada and the United States (Jiang et al., 2018). The SUNLIGHT consortium performed genome-wide analyses in each cohort based on a uniform analysis plan. Specifically, additive genetic models were fitted using linear regression on natural log-transformed 25(OH)D. The month of sample collection, sex, age, BMI, and principal components were included as covariates. Then, a fixed-effect inverse variance weighted (IVW) meta-analysis was conducted using the METAL2 software package, controlling for the population structure. SNPs with a minor allele frequency ≤ 0.05, imputation info score ≤ 0.8, Hardy-Weinberg equilibrium $\leq 1\times10^{-6}$, and less than two studies or 10,000 individuals contributing to each reported SNP association were removed.

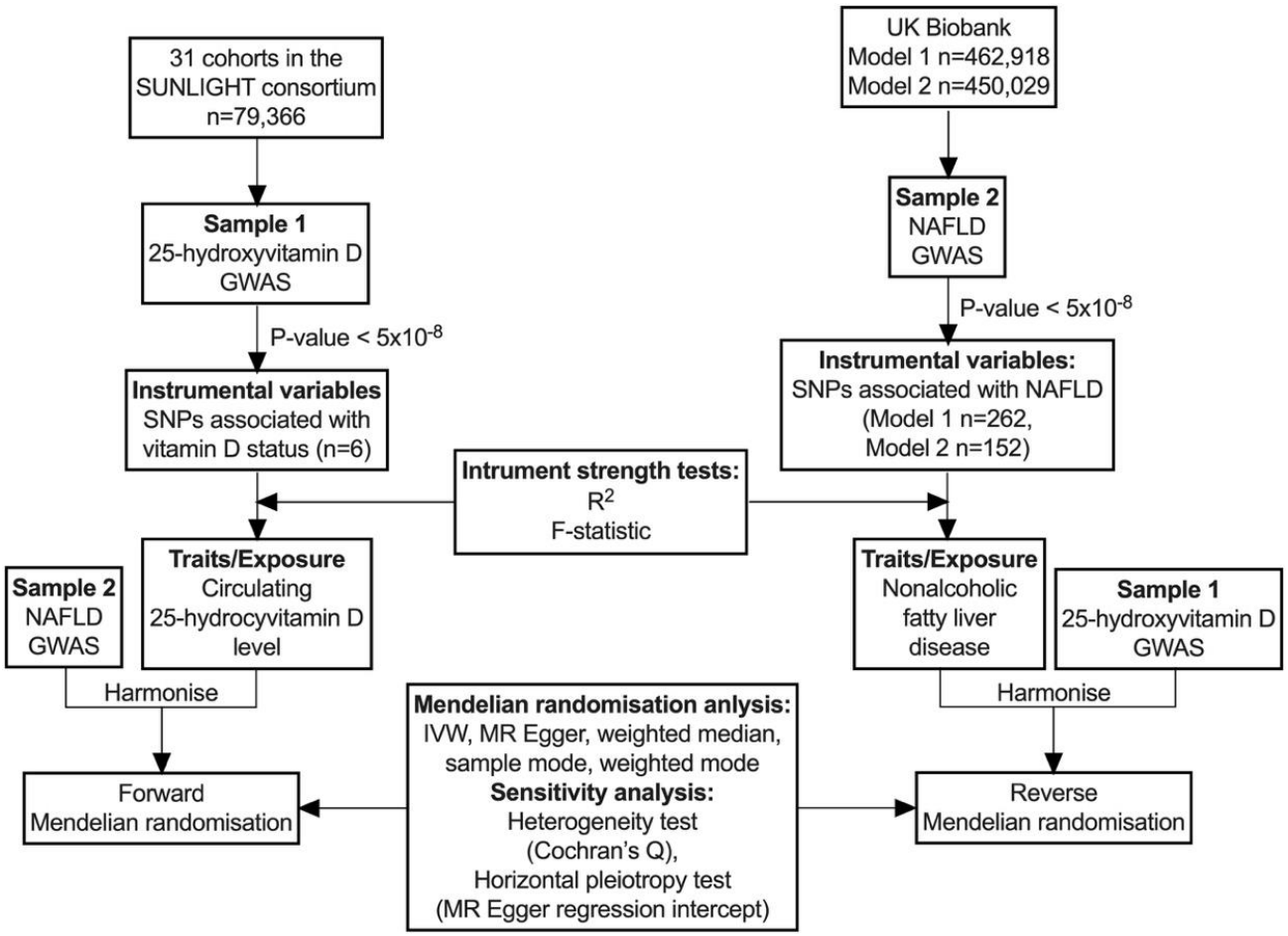

Figure 6.1 Overview of two-sample Mendelian randomisation study on the bidirectional association between circulating 25(OH)D level and NAFLD. GWAS, genome-wide association study; IVW, inverse-variance weighted; MR, Mendelian randomisation; NAFLD, non-alcoholic fatty liver disease; SNP, single-nucleotide polymorphism.

Results from conditional and joint genome-wide association analysis revealed that six susceptibility loci harbouring genome-wide significant SNPs were identified, including GC, NADSYN1/DHCR7, CYP2R1, CYP24A1, amidohydrolase domain containing 1 (AMDHD1) and Sec23 Homolog A, coat protein complex II component (SEC23A) (Jiang et al., 2018). Notably, GC, NADSYN1/DHCR7, CYP2R1 and CYP24A1 are involved in the biological metabolism of vitamin D (Bikle, 2014). Furthermore, while AMDHD1 is an enzyme catabolising several amino acids (Myung et al., 2011), SEC23A is involved in promoting ER-Golgi protein trafficking (Boyadjiev et al., 2006). Then, the analysis was performed using COJO analysis implemented in GCTA software to test whether any other SNPs, in addition to the lead SNP were significantly associated with the serum 25(OH)D concentration (Jiang et al., 2018). Lastly, GC rs3755967, NADSYN1/DHCR7 rs12785878, CYP2R1 rs10741657, CYP24A1 rs17216707, AMDHD1 rs10745742, and SEC23A rs8018720 were identified as the top SNP with the lowest P-value in each locus (all the SNPs P-values $<5\times10^{-8}$); the associations at all six SNPs were confirmed in the two independent in-silico replication cohorts. Therefore, I chose these six SNPs as IVs for vitamin D, and the summary statistics of the SUNLIGHT consortium on 2,579,297 SNPs were downloaded for further MR analysis.

6.2.3 Data sources and SNPs selection for NAFLD

The UKBB is a prospective cohort study that recruited over 500,000 participants aged between 40 and 69 years old between 2006 and 2010 across the UK (Sudlow et al., 2015). This biobank provides invaluable resources of various phenotypical data and with deeply genotyped information, which has been implemented in many genetic studies in the current literature (Bycroft et al., 2018). The UKBB received ethical approval from the Research Ethics Committee (REC reference for UK Biobank is 16/NW/0274).

The case/control status of NAFLD was extracted from UKBB field code 41270. This field summarises the distinct diagnosis codes a participant has recorded across all their hospital inpatient records in either the primary or secondary position. Notably, field code 41270 is an array code, i.e. there are multiple instances present for each participant. Therefore, there may be more than one diagnosis per participant at more than one-time point. For this data,

there are up to 212 instances recorded for the array. The extracted data used in this study is the August 2019 version with 410,320 participants.

Diagnoses are coded according to the International Classification of Disease version 10 (ICD-10). The main ICD10 codes of interest are: K75.8 Other specified inflammatory liver diseases [Nonalcoholic steatohepatitis (NASH)] and K76.0 Fatty (change of) liver, not elsewhere classified [Nonalcoholic fatty liver disease (NAFLD), excluded K75.8]. The cases of NAFLD in the entire UKBB cohort (not subset on genetic data or covariates) were in **Appendix Table E1.**

There were two GWAS models conducted using data from UKBB. Model one (M1) was GWAS of NAFLD cases and controls without filtering other liver diseases; Model two (M2) was GWAS of NAFLD cases and controls after filtering on other liver diseases. In M1, cases were defined as any participant diagnosed with ICD10 codes K75.8 and K76.0 at any point in data collection. Controls were defined as any participant not having a diagnosis of ICD10 codes K75.8 and K76.0 at any point in the data collection. In M2, the whole cohort was first filtered to remove those with any of the ICD 10 codes present in **Appendix Table E2**. Then, the cases and controls were defined as the same as M1. Notably, the analysis exclusions and inclusions used in these two models did not include other measures such as self-report or inclusion of ICD9 codes. Additionally, there could be cases of non-European ancestry in the UKBB not subset on genetic data, however, they are subset to European ancestry once matched with those with genetic data. After filtering for participants with genetic data and covariate data, a brief summary of the number of cases and controls were: M1 involved cases n=2,757 and controls n=460,161; M2 involved cases n=1,747 and controls n=448,282.

The UKBB GWASs were conducted using the BOLT-LMM software (version 2.3.2) (Loh et al., 2015; Loh et al., 2018) and adjusted for sex and genotype chip. As BOLT-LMM association statistics are on the linear scale, test statistics (betas and their corresponding standard errors) need to be transformed to log ODs and their corresponding 95% CI on the liability scale using a Taylor transformation expansion series (Loh et al., 2018). The BOLT-LMM regression coefficients were converted to the log-odds scale in R. Additional filtering on the SNPs removed any SNPs where the minor allele

count in cases was <10. The final number of SNPs in each model is: M1 n=11,324,872 (lambdas=1.05); M2 n=10,788,717 (lambdas=1.00). In addition, the top 1,000 SNPs in M1 (lowest P-values) were taken and compared to Betas with the same SNPs in M2. Of the 1,000 top hits in M1, 969 of those SNPs were also in the top 1000 hits of M2. A scatter plot of the GWAS betas is shown in **Appendix Figure E1**. There is good concordance between the models (r^2=0.95).

Genome-wide significant ($P<5\times10^{-8}$) SNPs associated with NAFLD were extracted from two different models of UKBB GWASs, respectively; in M1, 262 correlated IVs were attained, while 152 in M2 (data not shown).

6.2.4 Statistical analysis

The summary-level data from vitamin D or NAFLD GWAS was obtained, including SNP rs number, β-coefficient, standard errors, effect allele, other allele, effect allele frequency (EAF), P-value and sample size. MR analyses were conducted using the TwoSampleMR package (Hemani et al., 2018b) in R (v4.1.2, R Develop Core Team, Vienna, Austria) (Team, 2014). A P-value less than 0.05 was considered statistically significant for the MR analyses.

To ensure that the IVs for the exposure are independent, the clumping function in TwoSampleMR package (default parameters: LD r^2=0.001, >10000kb) was performed on SNPs either identified for vitamin D or NAFLD when used as the exposure variable (Pritchard and Przeworski, 2001; Hemani et al., 2018b). After clumping, the SNPs that passed the LD threshold with the lowest P-value were retained and used for further MR analysis. All the six SNPs (rs3755967, rs12785878, rs10741657, rs17216707, rs10745742 and rs8018720) identified in the vitamin D GWAS remained. On the other hand, five SNPs (rs10401969, rs9479542, rs10401969, rs429358 and rs3747207) remained in NAFLD M1 after clumping, only three SNPs (rs4351435, rs73001065 and rs3747207) in NAFLD M2.

Notably, a transformation from log scale to standard deviation (SD) scale was performed on the size of effect (β) and standard error (SE) of six serum 25(OH)D related IVs. Thus, the ORs of NAFLD were scaled to per SD increase in genetically predicted serum 25(OH)D level. An approximate SD for serum 25(OH)D was obtained from the population-based Swedish Mammography

Cohort and corresponded to 0.33ln-nmol/L for S-25OHD (Michaelsson et al., 2017).

To match the effect allele of each IV between the exposure and the outcome, harmonising was performed using the harmonise_data function from the TwoSampleMR Package (Hemani et al., 2018b). For example, in the forward MR analysis, additional adjustments were made to the summary statistics of NAFLD M1 GWAS (outcome) to match the effect allele/beta of each SNP identified in vitamin D GWAS (exposure) reflecting Vit D increasing or decreasing. In theory, the MR package automatically harmonises to represent betas for the unit increasing alleles. In addition, there are three actions for the level of strictness in dealing with IVs. The default and conservative ‘action 2’ was chosen here. The 'action 2 ' means trying to infer positive-strand alleles, using allele frequencies for palindromes'.

To identify the strength of instruments, the R^2 of each IV was estimated and summed up to compute the overall R^2 using the data based on the exposure sample. The F-statistic of each IV was assessed, and the overall F-statistic was the average of all the single F-statistic. The formula of R^2 and F-statistic calculation was stated in **Appendix Figure E2**. Additionally, the statistical power of IVs was performed using online tool (https://shiny.cnsgenomics.com/mRnd/).

Five complementary MR methods were applied for MR analysis: Inverse variance weighted (IVW), MR Egger, weighted median, simple mode and weighted mode. IVW was implemented as a primary method in the following analysis. The IVW method estimates the causal relationship between exposure and outcome by using a meta-analysis of the ratio of SNP-exposure effects on SNP-outcome effects weighted by the inverse variance of the outcome effects (Burgess et al., 2013). Notably, the IVW method assumes that all the IVs are valid and could return a precise estimate if the MR core assumptions are met. Remarkably, in the case of a single SNP as IV, the Wald ratio method was applied, which is the gene–outcome association divided by the gene–exposure association (Lawlor et al., 2008).

MR Egger analysis regresses SNP-exposure effects on SNP-outcome effects and estimates the effect of potential pleiotropy on causal estimation (Bowden et al., 2015). Different from the IVW method, MR Egger regression

does not constrain the intercept to pass through the origin, which means the intercept can be used to identify the presence of directional pleiotropy. MR Egger has the lowest power of the five methods used in this chapter to detect a causal effect. As this method requires variation in the SNP effects, the MR Egger is most effective when more SNPs involved to create the instrument.

The weighted median method assumes half of the SNPs are valid instruments for the causal estimate (Bowden et al., 2016). The more heavily weights of SNPs are, the more strongly associated with the exposure. Compared to IVW and MR Egger methods, this approach is more likely to give a robust causal estimate in the presence of up to 50% invalid variants.

The simple mode method, also known as the simple median estimator, calculates causal estimates from each generic variant and finds the median ratio (Bowden et al., 2016). Like the weighted median method, the simple method gives a causal effect estimate when at least 50% of the IVs are valid instrumental variables.

The weighted mode method groups the SNPs and estimates causal effect from the largest group, weighting each SNPs contribution to the group by inverse variance of its outcome (Hartwig et al., 2017). This method supposes that the most common causal effect is consistent with the true causal effect. Hence, the remaining instruments could be invalid without biasing the estimated causal effect.

Several sensitivity analyses were performed to estimate the robustness of the result in R, which including the leave-one-out analysis and heterogeneity and horizontal pleiotropy among SNPs. In addition, the PhenoScanner database V2 (http://www.phenoscanner.medschl.cam.ac.uk/) was searched to investigate potential pleiotropic associations of the IVs (Staley et al., 2016).

6.3 Results

6.3.1 Strengths of IVs

When utilising genetic instruments (IVs), there is typically good previous information on the variation in an exposure variable explained by genetic markers; thus, the IV and power may be established before the investigation begins. To identify the strength of instruments, the R^2, F-statistic, and the

statistical power of IVs was calculated. The R^2 is the proportion of variability in the exposure explained by the IVs (Pierce et al., 2011), while the F-statistic indicates the extent of the relative bias that is likely to occur in estimating a causal association using the IV. In MR analysis, a threshold of F<10 was defined as a weak tool to avoid weak instruments (Burgess and Thompson, 2011; Pierce et al., 2011). Higher R^2 and F statistic values suggest a lower risk of weak instrument bias. In addition, the statistical power calculation could be used to determine a potential putative association from an instrumental variable analysis using asymptotic theory (Brion et al., 2013).

After harmonizing the alleles and effects between SNP associations with exposure traits and GWAS datasets of outcomes, six genome-wide SNPs for the vitamin D trait were remained (**Table 6.1**). However, only three of five SNPs for the NAFLD M1 trait (**Table 6.2**) and one of three SNPs for the NAFLD M2 trait (**Table 6.3**) were left, due to the removing of SNPs for being palindromic with intermediate allele frequencies. The SNPs explained overall 2.78% (range from 0.08-1.89%) of the variance in their corresponding vitamin D traits, while the SNPs explained 0.027% (range from 0.007-0.014%) of the variance in related to NAFLD M1 and 0.008% to NAFLD M2. The mean F-statistic, another parameter for measuring the strength of IVs, was 359.51 (range from 33.56–1504.09) for vitamin D, 41.56 (range from 29.87-62.81) for NAFLD M1, and 36.66 for NAFLD M2, separately. It indicates that weak instrument bias is reduced (the recommended F statistic is >10) for the MR analyses (Stock et al., 2002). For a genetically predicted per SD change in serum levels, I had 14% statistical power to detect an OR of 0.9 (or 1.1) for NAFLD M1 in the analyses of serum 25(OH)D, and had ~11% power to detect an OR 0.9 (or 1.1) for NAFLD in the analyses of serum 25(OH)D.

6.3.2 MR results

Generally, multiple MR methods are used for MR analysis in R. These methods are complementary and make slightly different assumptions about the nature of pleiotropy and instrument strength; therefore, a consistent effect across the multiple methods provides the most robust evidence of causal inference (Hemani et al., 2018a).

The results of the Mendelian randomisation analyses for each method

Table 6.1 Summary of genetic variants used to estimate the effect of serum 25-hydroxyvitamin D concentration on NAFLD.

SNP	Gene	EA/ NEA	EAF	Sample size	Association with vitamin D					Association with NAFLD M1			Association with NAFLD M2		
					Beta	SE	P-value	R^2	F-statistics	Beta	SE	P-value	Beta	SE	P-value
rs3755967	GC	C/T	0.72	78231.8	0.270	0.0070	1.00×10^{-200}*	1.89%	1504.09	-8.12×10^{-3}	2.97×10^{-2}	0.78	1.20×10^{-2}	3.73×10^{-2}	0.75
rs12785878	NADSYN1	T/G	0.75	78328	0.110	0.0067	1.83×10^{-61}*	0.35%	272.25	5.74×10^{-4}	3.28×10^{-2}	0.86	-4.60×10^{-2}	4.11×10^{-2}	0.26
rs10741657	CYP2R1	A/G	0.40	78328	0.093	0.0067	7.79×10^{-45}*	0.29%	196.00	-4.60×10^{-2}	2.75×10^{-2}	0.095	-4.91×10^{-2}	3.45×10^{-2}	0.16
rs17216707	CYP24A1	T/C	0.79	71483.6	0.080	0.0082	1.01×10^{-22}*	0.13%	94.88	-2.79×10^{-2}	3.50×10^{-2}	0.43	-1.30×10^{-2}	4.40×10^{-2}	0.77
rs10745742	AMDHD1	T/C	0.40	69166.6	0.050	0.0067	3.19×10^{-14}*	0.08%	56.26	6.88×10^{-3}	2.79×10^{-2}	0.81	8.88×10^{-3}	3.50×10^{-2}	0.8
rs8018720	SEC23A1	G/C	0.18	68134	0.051	0.0088	3.45×10^{-09}*	0.04%	33.56	7.08×10^{-2}	3.54×10^{-2}	0.045*	8.61×10^{-2}	4.44×10^{-2}	0.053
								2.78% (Sum)	359.51 (Mean)						

AMDHD1, amidohydrolase domain containing 1; CYP2R1, cytochrome P450 2R1; CYP24A1, cytochrome P450 24A1; EA, effect allele; NEA, non-effect allele; EAF, effect allele frequency; GC, vitamin D-binding protein; NADSYN1, nicotinamide adenine dinucleotide synthetase 1; SE, standard error; SEC23A1, SEC homolog A1; SNP, single-nucleotide polymorphism; * means the statistical significance (P-value<0.05).

Table 6.2 Summary of genetic variants used to estimate the effect of NAFLD (model 1) on serum 25-hydroxyvitamin D concentration.

SNP	Gene	EA/NEA	EAF	Sample size	Association with NAFLD M1					Association with vitamin D		
					Beta	SE	P-value	R^2	F-statistics	Beta	SE	P-value
rs10401969	SUGP1	T/C	0.92	462918	-0.405	0.0510	$2.27x10^{-15}$*	0.014%	62.81	-0.002	0.0043	0.5933
rs17321515	RP11-136O12.2	A/G	0.53	462918	0.148	0.0271	$4.63x10^{-8}$*	0.006%	29.87	0.007	0.002	0.0002*
rs9479542	RP11-15GB8.1	A/G	0.76	462918	0.180	0.0319	$1.55x10^{-8}$*	0.007%	31.99	-0.001	0.0024	0.5804
								0.027% (Sum)	41.56 (Mean)			

EA, effect allele; NEA, non-effect allele; EAF, effect allele frequency; NR, nor reported; SE, standard error; SUGP1, SURP and G-patch domain-containing protein 1; * means the statistical significance (P-value<0.05).

Table 6.3 Summary of genetic variants used to estimate the effect of NAFLD (model 2) on serum 25-hydroxyvitamin D concentration.

SNP	Gene	EA/NEA	EAF	Sample size	Association with NAFLD M1					Association with vitamin D		
					Beta	SE	P-value	R^2	F-statistics	Beta	SE	P-value
rs4351435	NR	G/A	0.30	450029	0.224	0.0369	$1.40x10^{-9}$*	0.008%	36.66	-0.0077	0.0041	0.05984
								0.008% (Sum)	36.66 (Median)			

EA, effect allele; NEA, non-effect allele; EAF, effect allele frequency; NR, nor reported; SE, standard error; SNP, single-nucleotide polymorphism; * means the statistical significance (P-value<0.05).

are shown in **Table 6.4**, and graphs showing scatter plots of effect sizes of SNP on exposure and outcome variable are shown in **Figure 6.2**. There was no association of genetically predicted serum 25(OH)D levels with NAFLD. For one SD increment of serum 25(OH)D levels, the OR of NAFLD M1 was 0.95 (95% CIs 0.76 to 1.18; P-value=0.614), and the OR NAFLD M2 was 1.04 (95% CI 0.79 to 1.37; P-value=0.786). On the other hand, no causal association was found between NAFLD and serum 25(OH) levels. The change of S-25(OH)D levels in nmol/L was 1.01 (95% CIs 0.98 to 1.05; P=0.384) and 1.00 (95% CIs 1.00 to 1.07; P=0.060) for a 1-unit increase in the log-transformed OR of NAFLD M1and NAFLD M2, respectively. Additionally, data showing tables and forest plots of single SNP analyses are presented in **Appendix Table E4-5** and **Appendix Figure E3-4.**

6.3.2 Sensitivity analyses

Several sensitivity analyses were performed to estimate the robustness of the results. First, the leave-one-out sensitivity method was conducted to explore the possibility of the causal link driven by individual SNP under the conventional IVW model (Burgess et al., 2013). The fluctuation of the results before and after removing the SNP reflects the stability of the association. Second, heterogeneity among SNPs included in IVW and MR-Egger analysis was estimated using the Cochran's Q test (Cohen et al., 2015). Horizontal pleiotropy, where an exposure SNP influences the outcome by mechanisms other than through the exposure, was estimated by using the MR Egger regression intercept (Bowden et al., 2015).

Sensitivity analyses showed consistent results with the primary IVW estimates for vitamin D trait on either NAFLD M1 or NAFLD M2 (both Cochran Q-derived $P_{IVW}>0.05$, **Table 6.5**). In addition, no horizontal pleiotropy was detected ($P_{intercept} = 0.820$ for NAFLD M1, $P_{intercept} = 0.886$ for NAFLD M2), indicating no robust relationships between circulating 25(OH) level and NAFLD. However, MR association between NAFLD M1 trait and circulating 25(OH) level presented moderate heterogeneity (I^2 =51.85% for IVW, I^2 =31.54% for MR Egger; both Cochran Q-derived $P< 0.01$) and horizontal pleiotropy ($P_{intercept} = 0.010$). Related traits of the IVs associated with 25(OH)D and NAFLD from PhenoScanner V2 were listed in **Appendix Table E6**. In the

Table 6.4 Two-sample bi-directional MR analyses estimates of effect of vitamin D on NAFLD

Exposure	Outcome	Method	Number of SNP	Beta (β)	SE	OR (95% CI)	P-value
Vitamin D	NAFLD M1	IVW	6	-0.0522	0.112	0.95 (0.76-1.18)	0.641
		MR Egger	6	-0.0958	0.218	0.91(0.59-1.39)	0.684
		Weighted median	6	-0.0306	0.101	0.97(0.80-1.18)	0.761
		Weighted mode	6	-0.0310	0.105	0.97(0.79-1.19)	0.780
		Simple mode	6	-0.0119	0.183	0.99(0.69-1.42)	0.951
Vitamin D	NAFLD M2	IVW	6	0.0380	0.140	1.04(0.79-1.37)	0.786
		MR Egger	6	0.0037	0.273	1.00(0.59-1.71)	0.990
		Weighted median	6	0.0285	0.128	1.03(0.80-1.32)	0.824
		Weighted mode	6	0.0362	0.131	1.04(0.80-1.34)	0.793
		Simple mode	6	-0.1296	0.250	0.88(0.54-1.43)	0.626
NAFLD M1	Vitamin D	IVW	3	0.0140	1.61×10^{-2}	1.01 (0.98-1.05)	0.384
		MR Egger	3	-0.0158	4.98×10^{-2}	0.98 (0.89-1.09)	0.804
		Weighted median	3	3.79×10^{-3}	9.49×10^{-3}	1.00 (0.99-1.02)	0.676
		Weighted mode	3	9.54×10^{-4}	9.93×10^{-3}	1.00 (0.98-1.02)	0.932
		Simple mode	3	1.02×10^{-3}	1.05×10^{-2}	1.00 (0.98-1.02)	0.931
NAFLD M2	Vitamin D	Wald ratio	1	0.0344	1.83×10^{-2}	1.00 (1.00-1.07)	0.060

CI, confidence interval; IVW, Inverse variance weighted; M, model; MR, Mendelian randomisation; NAFLD, non-alcoholic fatty liver disease; OR, odds ration; SE, standard error; SNP, single-nucleotide polymorphism; * means the statistical significance (P-value<0.05).

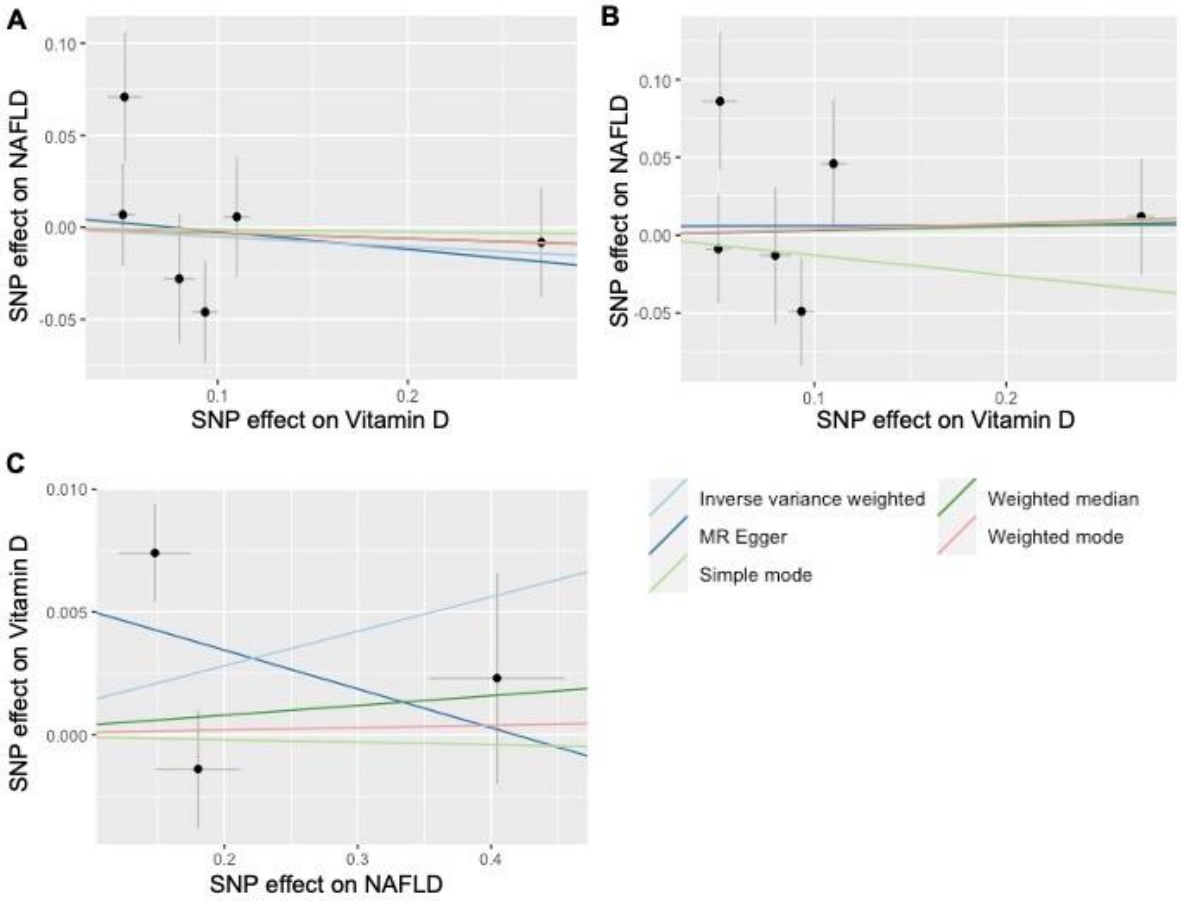

Figure 6.2 Scatter plots of SNP associated with vitamin D and NAFLD different MR methods. The genetic associations with circulating 25(OH)D level against NAFLD model 1 (**A**) and model 2 (**B**) risk. The genetic associations with NAFLD model 1 (**C**) against circulating 25(OH)D level. Vertical and horizontal lines around each SNP show 95% CI. The slopes of each line represent the causal association for each method.

Table 6.5 Sensitivity analyses for Mendelian randomisation analyses in both directions.

Exposure/Outcome	Methods	Test of heterogeneity			Test of pleiotropy		
		Q	P-value	I^2	Intercept	SE	P-value
Vitamin D/NAFLD M1	IVW	7.2798	0.201	31.32%	-	-	-
	MR Egger	7.1745	0.127	30.31%	0.0072	0.0237	0.820
Vitamin D/NAFLD M2	IVW	7.1718	0.208	30.28%	-	-	-
	MR Egger	7.1303	0.129	29.88%	0.0057	0.0371	0.886
NAFLD M1/vitamin D	IVW	7.1719	0.006*	51.86%	-	-	-
	MR Egger	7.3039	0.007*	31.54%	0.0066	0.0102	0.010*
NAFLD M2/vitamin D#	IVW	-	-	-	-	-	-
	MR Egger	-	-	-	-	-	-

IVW, Inverse variance weighted; NAFLD, non-alcoholic fatty liver disease; M, model; MR, Mendelian randomisation; SE, standard error; * means the statistical significance (P-value<0.05); # In this exposure/outcome, only one SNP involved in the MR analysis, the MR was calculated by Wald ratio.

search results, besides TGs and total cholesterol the NAFLD M1 IVs rs10401969 and rs17321515 were both found to be associated with height and coronary artery disease (data not shown). Furthermore, the results from the "leave-one-out" analysis indicated that no single SNP affects the robustness of either direction (**Appendix Table E7** and **Appendix Figure E5**).

6.4 Discussion

Using instruments defined from recently published, large-scale vitamin D GWAS and a self-executed NAFLD GWASs done on UKBB data, and conducting numerous MR methodologies and sensitivity analyses, in the present two-sample bidirectional MR study, no significant causal association between serum 25(OH)D concentration and NAFLD was observed.

As mentioned in the section **2.2.1**, the correlation between vitamin D levels and NAFLD has been controversial in previous studies. For example, a recent comprehensive systematic review investigated the association between vitamin D status and NAFLD/NASH (Pacifico et al., 2019). Of the 45 human studies done prior to February 2017 that were included, 29 reported an inverse association between vitamin D status and NAFLD, while 16 studies did not support an association. However, two recent meta-analyses on the relationship between serum vitamin D and NAFLD histologic severity found no association between serum vitamin D levels and NAFLD activity score and fibrosis among patients with NAFLD (Jaruvongvanich et al., 2017; Saberi et al., 2018). On the other hand, epidemiological data suggest an effect of NAFLD on the risk of low 25(OH)D status. For example, two earlier meta-analyses did by Eliades et al. (2013) and Wang et al. (2015) found that patients with NAFLD were more likely to be vitamin D deficient than controls. Another recently published study reported that compared to the healthy control group, the levels of 25(OH)D in patients with NAFLD were significantly lower (vitamin D deficiency: 35% in the control group vs 70% in the NAFLD group) (Gad et al., 2020). However, small sample sizes and the clinical heterogeneity of NAFLD may explain such heterogeneous results. Therefore, given the difficulty of eliminating bias in observational epidemiological studies, such as the reverse causal association of confounding factors, there are some limitations in etiological interpretation.

An essential difference between MR and epidemiological studies is that the likelihood of inherent bias in observational studies is reduced by the MR study (Smith and Ebrahim, 2003). Two previous studies have used MR analysis to assess the causal relationship between 25(OH)D and NAFLD. The first of these used one-sample bidirectional MR in a Chinese population (Wang et al., 2018c). Using genetic risk score analysis the Wang et al. study did not find clear evidence to support a causal relationship between vitamin D and NAFLD, which aligns with my MR study results. In contrast, the other two-sample bidirectional MR, published while I was completing my write up, found evidence suggestive of a causal effect between higher serum 25(OH)D and a decreased risk of NAFLD in a study based on three genetic cohorts of European descent [the GWAS of Anstee et al. (2020), the FinnGen consortium and their investigation of UKBB], but not vice versa (Yuan and Larsson, 2022). In their meta-analysis of three cohorts, the OR of NAFLD was 0,78 (95% CI, 0.69 to 0.89; P<0.001) for a per SD increase in genetically predicted serum 25(OH)D. However, in their analysis of only the UKBB GWAS data, they reported that genetically predicted higher serum 25(OH)D was not associated with NAFLD (OR per SD increase, 0.74; 95% CI 0.53 to 1.05; P = 0.088), which is consistent with my results. The possible reasons explaining the conflicting findings to current MR might be more robust power caused by a larger variance explained by SNPs using a larger population (meta-GWAS).

However, some limitations should be noted in the present study. First, the GWASs I used to applied in the current two-sample MR were summary level genetic data from two large GWASs that used different covariable adjustments to estimate direct genetic effects on the trait of interest. However, covariable-adjusted summary associations may introduce bias to the MR analyses, especially residual confounding between covariable and outcome (Hartwig et al., 2021). Second, the current summary-level statistics data did not allow me to perform analyses stratified by covariates adjusted by the original GWAS, as lacking detailed demographic information and the clinical characteristics of the subjects. This is important as NAFLD is a multifactorial disease and is strongly associated with obesity, insulin resistance and T2D (Moore, 2010), and previous studies suggest that the relationship between

vitamin D and NAFLD may be age, gender and BMI-dependent (Fraser et al., 2007; Gad et al., 2020).

In addition, two-sample MR depends significantly upon the robustness of the IVs. The current statistical power of vitamin D-related IVs was quite low, which may affect the power of the causal effects. On the other hand, I used a $P<5x10^{-8}$ cut-off for selecting instruments in NAFLD GWAS, which led to only six available SNPs in M1 and one in M2 being used as IV in the causal estimation between the NAFLD and vitamin D status. Fewer IVs can lead to "weak instruments"; thus, it might be possible to use a more flexible instrument selection cut-off (such as $P<1x10^{-5}$ or $P<1x10^{-6}$) to expand the SNP amount, having a greater statistical power (Burgess and Thompson, 2011). In addition, as larger samples become available (e.g. meta-GWAS), the accuracy of SNP effects will improve, making two-sample MR more powerful. Furthermore, the sensitivity analyses of the NAFLD M1 IVs suggested that I cannot rule out that the associations between genetically predicted NAFLD and serum 25(OH)D are driven by pleiotropic effects related to confounders, for example, coronary artery disease. Thus, the lack of evidence for a causal relationship might be due to pleiotropy (Bowden et al., 2018). A final limitation may come from the known selection bias in the UKBB cohort, with participants being more highly educated and likely healthier than the general UK population (Munafò et al., 2018). Because of the lack of representativeness of the UKBB, prevalence and incidence percentages may not reflect original population status and could lead to the potential for collider bias. Thus, replication of the instruments using similar size GWAS is required.

Nonetheless, the current study design had several strengths. First, two NAFLD GWASs were generated using UKBB data, filtering with or without other liver diseases. Different SNPs associated with NAFLD generated from different models could reflect gene pleiotropism of generic variants on other liver diseases, allowing to compare different effects on the vitamin D outcome. Second, the SUNLIGHT Consortium and the UKBB data were generated from two independent European populations, which avoided the potential bias that might be caused by differences in genetic backgrounds and false-positive findings due to participant overlap. Third, the vitamin D IVs used in the current study were chosen from the largest vitamin D GWAS. The biological

plausibility for most of the variants to effect vitamin D levels (i.e gene) were confirmed (Bikle, 2014) and have been replicated in other studies (Ahn et al., 2010; Wang et al., 2010b).

In conclusion, a causal effect between vitamin D status and the risk of NAFLD were not found in this MR study. However, considering the limitations, future studies with larger sample sizes and powerful IVs should be performed to further investigate the nature of the associations.

6.5 Summary

- NAFLD GWASs were conducted using UKBB summary-level data, filtering with or without other liver diseases; 252 genome-wide significant ($P<5\times10^{-8}$) SNPs were extracted from GWAS associated with NAFLD in M1 and 152 SNPs in M2.
- For the forward MR analysis, six independent SNPs ($r^2<0.01$) associated with serum 25(OH)D status at genome-wide significance ($P<5\times10^{-8}$) were selected as IVs from the SUNLIGHT consortium GWAS.
- For the reverse MR analysis, five independent SNPs ($r^2<0.01$) associated with NAFLD M1 and 3 SNPs ($r^2<0.01$) with NAFLD M2 at genome-wide significance ($P<5\times10^{-8}$) were selected as IVs from the UKBB GWASs. However, two SNPs (rs429358 and rs3747207) in NAFLD M1 and two SNPs (rs73001065 and rs3747207) in NAFLD M2 associated with NAFLD were missing in the SUNLIGHT consortium data.
- The statistical power of SNPs was low in the current study, which may affect the power of the causal effects.
- MR association between NAFLD M1 trait and circulating 25(OH) level presented significant effects of heterogeneity and pleiotropy, suggesting that the lack of evidence for a causal relationship could be due to pleiotropy.
- The two-sample bidirectional MR analysis indicated no causal relationship between serum 25(OH)D status and the risk of NAFLD, and vice versa.

Chapter 7
Conclusion

7.1 Conclusion

This PhD project yielded a significant understanding of the role of vitamin D in the progression of NAFLD from epigenetic (i.e. miRNA) and genetic (i.e. MR analysis) aspects. Firstly, a comprehensive literature review was done in PubMed to investigate the mechanisms of miRNAs modulated by vitamin D that contribute to NAFLD disease progression (**chapter 3**). The data from human profiling or mechanistic studies exploring miRNA in NALFD found six miRNAs (miR-21, miR-30, miR-34, miR-122, miR-146 and miR-200) dysregulated in multiple independent human NAFLD studies. Then, the evidence for the modulation of human serum miRNAs by vitamin D status or in response to dietary intakes or supplementation, along with any research that has specifically investigated the influence of vitamin D on liver-related miRNAs, was critically assessed. After integrating the data, a potential subset of miRNAs (miR-27, miR-125, miR-146, miR-155 and miR-188) found both dysregulated in NAFLD and modulated by vitamin D was identified.

Secondly, in **chapter 4**, *in vitro* models of the human hepatocyte and HSC dose responses to FA and 1α,25(OH)$_2$D$_3$ treatments were characterised. Specifically, cell viability, intracellular lipid accumulation and the expression of the vitamin D target genes CYP24A1 and VDR were examined in immortalised HepG2 and LX-2 cells. The results of co-treatment suggested that 1α,25(OH)$_2$D$_3$ might aggravate the adverse effects on cell viability caused by FA but mitigate the intracellular lipid loading induced by FA in liver cell lines. Additionally, 1α,25(OH)$_2$D$_3$ induced CYP24A1 gene expression in HepG2 and LX-2, which was considered an indicator to assess the effectiveness of vitamin D treatment. On the other hand, the data combined with lipid loading and VDR expression suggested that the VDR signalling activated by 1α,25(OH)$_2$D$_3$ might play an essential role in attenuating hepatic steatosis.

Thirdly, these cellular models were then used to examine miRNA expression in response to vitamin D and lipid loading co-treatment by TLDA

and bioinformatic analyses (**chapter 5**). Bioinformatic analyses were conducted sequentially for the subset of miRNAs hypothesised as dysregulated in vitamin D and/or FA treatment from TLDA. Bioinformatic results provided evidence of the biological roles of miRNAs, especially in the transcription of gene expression in biological processes and molecular functions. In addition, KEGG pathway comparisons between different treatment groups in liver cell lines highlighted FOXO and PI3K-AKT signalling pathways as important, significantly enriched pathways, which might contribute to NAFLD progression. Then, integrating the bioinformatic data with literature evidence from **chapter 3**, a subset of candidate miRNAs (let-7a-5p, let-7d-5p, miR-15b-5p, miR-23a-3p, miR-27a-3p, miR-27b-3p, miR-96-5p, miR-103a-3p, miR-200a-3p and miR-212-3p) were followed up for independent verification by qPCR. However, the results were inconclusive.

After identifying miRNA sample quality as a potential issue, given the low OD260/230, miRNA isolation procedures were optimised, and the decision was made to repeat experiments using RNAseq rather than arrays. The results of optimisation of RNA isolation protocols suggested that the mirVana^{TM} isolation kit (Thermofisher) was not a good choice for miRNA work; after comparing the results of three total RNA isolation kits recommended for miRNA work, the ReliaPrep^{TM} RNA Cell Miniprep System (Promega) was chosen to prepare samples for small RNA sequencing.

Lastly, in addition to *in vitro* experiments, a two-sample bidirectional MR analysis was conducted to determine whether circulating 25(OH)D levels could be associated with NAFLD (**chapter 6**). The largest meta-GWAS of serum vitamin D status of European descent from Jiang et al. (2018) was selected to be a sample on and extract vitamin D-related genetics instruments (IVs). Two NAFLD GWAS models, with or without filtering other liver diseases, were conducted using summary-level data from the UKBB; genome-wide significant SNPs from two models were screened out for NAFLD-related as IVs, respectively. The results of the MR analyses indicated that there was no association between genetically predicted serum 25(OH)D levels with NAFLD, and similarly no association between genetically predicted NAFLD and serum 25(OH)D levels. This finding is of interest as it conflicts with the conclusion of the recently published MR paper (Yuan and Larsson, 2022).

7.2 Future work

This PhD project predominantly focused on investigating miRNAs modulated by vitamin D that might contribute to NAFLD progression. In addition to *in vitro* experiments, a two-sample bidirectional Mendelian randomisation (MR) analysis was conducted to determine whether circulating 25-hydroxyvitamin D [25(OH)D] status could be associated with NAFLD.

For the MR study, although the cohort samples used in the recently published MR paper (Yuan and Larsson, 2022) overlapped with my samples, the possibility of publication of the two-sample bidirectional MR done in **chapter 6** has be discussed further and critically assessed. I am currently drafting a manuscript “Non-alcoholic fatty liver disease and vitamin D in the UK Biobank: a two-sample bidirectional Mendelian randomization study” in Frontiers in Nutrition, of which the submission anticipated will be this June.

On the other hand, to further support the findings of miRNAs modulated by vitamin D that might contribute to NAFLD progression in this PhD project, a number of experiments remain. In particular, the results of the small RNAseq need to be investigated. Therefore, the immediate following steps will be:

- Perform bioinformatics analysis on the subset of miRNAs hypothesised as dysregulated from results of small RNAseq to identify enriched GO terms and KEGG pathways
- Based on the results of significant KEGG pathways, using DAVID and miRWalk, investigate several pathways of interest with potential target genes and relative miRNAs will be chosen for further verification

While waiting for the sequencing results, the expression of several miRNAs, including miR-27, miR-125 and miR-155, will be examined by qPCR. These three are of particular interest, as miR-27 and miR-125 inhibit VDR translation and miR-155 is inhibited by VDR (**Figure 3.5**) (Zhang et al., 2021d). Currently, a new PhD of Bernadette, Xiaomian Tan, will carry on my project. First, we will analyse the small RNAseq data in collaboration, and then she will progress the further miRNA experiments.

Appendix A
Supplementary Tables for Chapter 2

Appendix Table A 1 Single nucleotide polymorphisms (SNPs) identified in genome-wide/exome-wide association studies for non-alcoholic fatty liver disease in European descent population.

Reference; country	Design; sample size	Genotyping platform	Study population; age	Replication population	Phenotype or NAFLD diagnosis	NAFLD related polymorphisms	Findings
Romeo et al. (2008); US	**GWAS**; 9,229 nonsynonymous sequence variations from dbSNP and the Perlegen SNP database; 2,111 general population	High-density oligonucleotide arrays (Perlegen Sciences)	Multi-ethnic population (Hispanics, African Americans, European-Americans); 30-65	n/a	H-MRS-measured steatosis	**PNPLA3-I148M** rs738409	Associated with increased hepatic fat levels ($P=5.9x10^{-10}$) and hepatic inflammation ($P=3.7x10^{-4}$) in the three ethnic groups
						PNPLA3-S453I rs6006460	Associated with lower hepatic fat content in African Americans ($P=6.2x10^{-4}$).
Chalasani et al. (2010); US	**GWAS;** 324,623 SNPs from the 22 autosomal chromosomes; 236 women	Infinium HD technology (HumanCNV 370-Quadv3 BeadChips, Illumina)	Non-Hispanic white women with NAFLD; 46-60	n/a	Histologically characterised NAFLD	**FDFT1** rs2645424	Associated with the NAS ($P=6.8\times10^{-7}$)
						PDGFA rs343064	Associated with the degree of fibrosis ($P=2.7\times10^{-8}$)
						COL13A1 rs1227756	Associated with lobular inflammation (P=2.0×10-7)
						LTBP3 rs6591182	Associated with lobular inflammation ($P=8.6\times10^{-7}$)
						EFCAB4B rs887304	Associated with lobular inflammation ($P=7.7\times10^{-7}$)
						ZP4 rs2499604	Associated with serum levels of ALT ($P=2.2\times10^{-6}$)

						PZP rs6487679	Associated with serum levels of ALT ($P = 1.3 \times 10^{-6}$)
						PZP rs1421201	Associated with serum levels of ALT ($P=1.0\times10^{-5}$)
						DDX60L PALLD rs2710833	Associated with serum levels of ALT ($P=6.3\times10^{-7}$)
Speliotes et al. (2011); US	**Fixed-effects meta GWAS**; ~2.4 million imputed or genotyped SNPs, 7,176 individuals from GOLD consortium	AGES: Illumina, Amish: Affymetrix, Family Heart Study: Illumina, Framingham Heart Study: Affymetrix 500K & Affymetrix 50K	Multi-ethnic population; 40-82	CT-hepatic steatosis: 592 biopsy-proven NAFLD patients from NASH CRN and, 1405 healthy controls from MIGen; Histologic NAFLD: 592 biopsy-proven NAFLD patients from NASH CRN and, 3,212 controls from iCONT	CT-measured steatosis	**PNPLA3** rs738409	associated with CT hepatic steatosis ($P=4.3\times10^{-34}$) and histologic NAFLD ($P=3.6\times10^{-43}$)
						NCAN rs2228603	associated with CT hepatic steatosis ($P=1.22\times10^{-18}$) and histologic NAFLD ($P=5.29\times10^{-5}$)
						PPP1R3B rs4240624	associated with CT hepatic steatosis ($P=3.68\times10^{-18}$)
						GCKR rs780094	associated with histologic NAFLD ($P=2.59\times10^{-8}$)
						LYPLAL1 rs12137855	associated with histologic NAFLD ($P=4.12\times10^{-5}$)
Adams et al. (2013); Australia	**GWAS;** 2,078,505 SNPs, 928 adolescents (NAFLD 126/NN 802)	Illumina Human660-W Quad Array	European descent adolescents, 17	n/a Hepatic gene expression: 13 biopsy-proven NAFLD adults and 8 NN adults (biological validation)	Ultrasound-defined NAFLD	**GC** rs222054	Associated with NAFLD adolescents ($P = 1.20 \times 10^{-6}$)
						LCP1 rs7324845	Associated with NAFLD adolescents ($P = 2.96 \times 10^{-6}$)
						LPPR4 rs12743824	Expressed in neurons were also associated with NAFLD ($P = 4.82 \times 10^{-6}$)
						SLC38A8 rs11864146	Expressed in neurons were also associated with NAFLD ($P = 1.86 \times 10^{-6}$)
Feitosa et al. (2013);	**GWAS**;	974 subjects used Illumina	Caucasian, 30-93	n/a	CT-measured steatosis, ALT-	**PNPLA3** rs738409	Associated with fatty liver ($P=2.09 \times 10^{-23}$)

US	~2.5 million imputed SNPs, ALT levels: n= 2,584, CT measured FL: n= 2,597	HumMap 550K chip, 249 subjects used Human 610-Quadv1 Illumina chip, and 1482 subjects used Human 1M-Duov3 Illumina chip.			measured hepatic inflammation	**PPP1R3B** rs2126259, rs4240624	Associated with fatty liver (P = 4.76×10^{-8}), rs4240624 (LD = 1, r2 = 0.80, P = 4.76×10^{-8})
						ERLIN1 rs2862954, rs1408579, rs10883451	Associated with concomitant variation in FL and ALT levels (CMA-p=4.88×10^{-10}, 4.57×10^{-10} and 4.29×10^{-10}, respectively)
						CHUK rs11597086, rs11591741	Associated with concomitant variation in FL and ALT levels (CMA-p=1.46×10^{-9} and 1.84×10^{-9}, respectively)
						CWF19L1 rs17729876, rs17668255, rs17668357, rs12784396	Associated with concomitant variation in FL and ALT levels (CMA-p= 1.82×10^{-9}, 1.82×10^{-9},1.65×10^{-9} and 2.47×10^{-9}, respectively) correlated meta-analysis
Kozlitina et al. (2014) US	**EWAS**; 138,374 sequence variants, 2,736 general population	Illumina Infinium HumanExome BeadChip (genotyping arrays)	Multi-ancestry (non-Hispanic, European Americans, Hispanic and other ancestry groups); 30-65	Dallas Biobank: 8,585 European Americans adults, Copenhagen Study: 73,532 adults	H-MRS-measured steatosis	**PNPLA3** rs738409 rs2281135	Associated with higher liver fat levels ($P=4.0x10^{-16}$ and $P=6.9x10^{-12}$, respectively)
						TM6SF2 rs58542926	Associated with higher liver fat levels ($P=5.9x10^{-8}$), higher circulating levels of ALT (P=0.014), lower levels of LDL-C (P= 0.005), triglycerides (P=0.037) and ALP (P=0.031)
Namjou et al. (2019); US	**GWAS;** 7,263,501 autosomal SNPs, adults: 710 NAFLD/ 7725 NN	High-through SNP genotyping	European ancestry; NAFLD case-control GWAS: paediatrics	n/a	Liver enzyme and histopathologic characterised NAFLD	**PNPLA3** rs738409, rs738408, rs3747207	Associated with NAFLD ($P = 1.70 \times 10^{-20}$, $P = 1.93 \times 10^{-20}$ and $P = 2.63 \times 10^{-20}$, respectively) The effect of rs 738409 was consistent in both paediatric

	paediatric participants: 396 NAFLD/ 846 NN		13.05±5.41, adults 63.50±16.86				($P = 9.92 \times 10^{-6}$) and adult ($P = 9.73 \times 10^{-15}$) cohorts and associated with disease severity and NAS ($P = 3.94 \times 10^{-8}$)
						IL17RA rs5748926	Associated with disease severity (NAS score, $P = 3.80 \times 10^{-8}$)
						ZFP90-CDH1 rs698718	Associated with fibrosis ($P = 2.74 \times 10^{-11}$)
Anstee et al. (2020); UK	**GWAS;** 721078 SNPs, 1,483 European NAFLD cases and 17,781 genetically matched controls	Illumina OmniExpress BeadChip, Illumina HumanCore Exome BeadChip and Illumina OmniExpress Exome BeadChip	European ancestry; European NAFLD: 50.1±13.0	559 NAFLD cases and 945 controls	Histologically characterised NAFLD	**C2ORF16** rs1919127	Case-control analysis: $P=5.61\times 10^{-10}$; not replicated
						GCKR rs1260326	Case-control analysis: $P=1.05\times 10^{-10}$; not replicated
						HSD17B13 rs9992651	Case-control analysis: $P=2.78\times 10^{-8}$
						PNPLA3 rs738409	Case-control analysis: $P=1.45\times 10^{-49}$; Case-only analysis: associated with steatosis, fibrosis and NAS ($P=1\times 10^{-10}$)
						TM6SF2 rs58542926	Case-control analysis: $P=2.05\times 10^{-11}$
						LEPR rs12077210	Case-control analysis: $P=5.62\times 10^{-8}$; Case-only analysis: associated with steatosis, fibrosis and NAS ($P=4.4\times 10^{-9}$)
						IDO2/TC1 rs79137099	Case-control analysis: $P\leq 1\times 10^{-7}$
						PYGO1 rs62021874	Case-only analysis: associated with steatosis, fibrosis and NAS ($P=8.2\times 10^{-8}$)

Park et al. (2020); US	**GWAS;** 1,847,764 genotyped SNPs, 1,709 participants [African Americans (n = 277), Japanese Americans (n = 424), Latinos (n = 348), Native Hawaiians (n = 274), and European Americans (n = 386)]	Illumina MEGA^{EX} array	Multi-ancestry (African Americans, Japanese Americans, Latinos, Native Hawaiians and European Americans); 60-77	n/a	MRI-measured steatosis	**PNPLN3** rs738409	Associated with percent liver fat ($P=3.52\times 10^{-15}$); correlated with the prevalence of NAFLD across the five ethnic groups
						LMBRD1/ COL19A1 rs77249491	Associated with percent liver fat ($P=1.42\times 10^{-8}$); positively correlated with HOMA-IR (P=0.0005), insulin (P=0.0003), TGs (P = 0.01), and negatively correlated with HDK (P=0.04), and sex hormone binding globulin (P=0.0012)
Ghodsian et al. (2021); European	**EHR-based meta-GWAS;** 6,797,908 SNPs; 8,434 NAFLD cases and 770,180 controls (4 cohorts: UKBB, Estonian Biobank, eMERGE, and FinnGen)	Illumina or Affymetrix arrays or imputed using the population specific SISu v3 reference panel	European ancestry; n/a	Mass General Brigham Biobank	HER: ICD9 and ICD10	**GCKR** rs1260326	Associated with NAFLD ($P<5\times 10^{-8}$)
						TR1B1 rs28601761	Associated with NAFLD ($P<5\times 10^{-8}$)
						TM6SF2 rs58542026	Associated with NAFLD ($P=6.90\times 10^{-17}$)
						APOE rs429358	Associated with NAFLD ($P=1.40\times 10^{-8}$)
						PNPLA3 rs738409	Associated with NAFLD ($P=1.23\times 10^{-47}$)
Fairfield et al. (2022); **UK**	**EHR-based GWAS;** 9,723,654 SNPs, 4,761 cases of NAFLD and 373,227 healthy controls (UKBB)	Affymetrix arrays	European ancestry; NALFD: 57.4±7.6, controls: 56.9±7.9	n/a	HER: ICD9 and ICD10	**APOE** rs429358	Associated with NAFLD ($P=2.17\times 10^{-11}$)
						PNPLA3 rs3747207	Associated with NAFLD ($P=6.74\times 10^{-60}$)
						TM6SF2 rs73001065	Associated with NAFLD ($P=1.08\times 10^{-24}$)
						GCKR rs1260326	Associated with NAFLD ($P=2.54\times 10^{-11}$)

						MARC1 rs2642442	Associated with NAFLD ($P=7.67\times 10^{-10}$)
						TRIB1 rs17321515	Associated with NAFLD ($P=1.81\times 10^{-13}$)

AGES, Age, Gene/Environment Susceptibility-Reykjavik study; ALP, alkaline phosphatase; ALT, alanine aminotransferase; APOE, apolipoprotein E; CHUK, conserved helix-loop-helix ubiquitous kinase; C2ORF16, chromosome 2 open reading frame 16; COL13A1, collagen, type XIII, alpha1; COL19A1, collagen type XIX alpha 1 chain; CMA, correlated meta-analysis; CT, computed tomography; CWF19L1, CWF19 like cell cycle control factor 1; DDX60L, DExD/H-Box 60 like; EFCAB4B, EF-hand calcium binding domain 4B; EHR, electronic health record; eMERGE, The Electronic Medical Records and Genomics; ERLIN1, ER lipid raft associated 1; EWAS, exome-wide association study; FDFT1, farnesyl diphosphate farnesyl transferase 1; FL, fatty liver; HDL, high-density lipoprotein; HOMA-IR, homeostasis model assessment of insulin resistance; IDO2/TC1, indoleamine 2,3-Dioxygenase 2/TC1; IL17RA, interleukin 17A receptor; GC, group-specific component; GCKR, glucokinase regulatory protein; GOLD, genetics of obesity-related liver disease; GWAS, genome-wide association study; H-MRS, proton magnetic resonance spectroscopy; HSD17B13, hydroxysteroid 17-beta dehydrogenase 13; iCONT, Illumina Control database; LCP1, lymphocyte cytosolic protein-1; LDL-C, low-density lipoprotein-cholesterol; LEPR, leptin receptor; LMBRD1, limb region 1 domain containing 1; LPPR4, phosphate phosphatase-related protein type 4; LTBP3, latent-transforming growth factor beta-binding protein 3; LYPLAL1, lysophospholipase-like 1; MARC1, mitochondrial amidoxime reducing component 1; MIGen, the Myocardial Genetics Consortium; n/a, not available; MRI, magnetic resonance imaging; NAFLD, non-alcoholic fatty liver disease; NAS, NAFLD activity score; NASH CRN, the Non-alcoholic Steatohepatitis Clinical Research Network; NCAN, neurocan; NN, non-NAFLD; SLC38A8, solute carrier family 38 member 8; SNPs, single nucleotide polymorphisms; TG, triglyceride; TM6SF2, transmembrane 6 superfamily 2; TRIB1, tribbles pseudokinase 1; PDGFA, platelet-derived growth factor subunit A; PNPLA3, patatin-like phospholipase domain-containing protein 3 gene; PPP1R3B, protein phosphatase 1, regulatory subunit 3b; PZP, pregnancy zone protein gene; PYGO1, pgopus family PHD finger 1; UKBB, UK Biobank; ZFP90-CDH1, zinc finger protein 90 homolog-cadherin 1; ZP4, Zona pellucida sperm-binding protein 4.

Appendix Table A 2 Single nucleotide polymorphisms (SNPs) identified in genome-wide/exome-wide association studies for non-alcoholic fatty liver disease in Asian population.

Reference; country	Design; sample size	Study population; age	Phenotype associated with	Diagnosis of NAFLD	NAFLD related polymorphisms	Summary of associations	Genotyping platform	Replication sample size
Kawaguchi et al. (2012); Japan	**GWAS**; 484,751 (SNPs), 529 NAFLD and 932 controls (subjects)	**Japanese**; Type 1 49.7±15.3, Type 2 51.5±15.3 , 49.4±14.0 Type 3 49.4±14.0, Type 4 57.6±14.8, Control 48.8±16.3	Histologically characterized NAFLD	Biopsy	**PNPLA3** rs738409	PNPLA3 rs738409 was significant association with NAFLD ($P=1.4x10^{-10}$) and had a strongest association ($P=3.6\times10^{-6}$) with the histological classifications based on the degree of inflammation, ballooning degeneration, fibrosis and Mallory-Denk body. PNPLA3 rs738409 showed strong associations with three clinical traits related to the prognosis of NAFLD, levels of hyaluronic acid ($P=4.6\times10^{-4}$), HbA1c (P=0.0011) and iron deposition in the liver ($P=5.6\times10^{-4}$).	Illumina Human 610-Quad Bead Chip	ns
Kitamoto et al. (2013); Japan	**GWAS**; 261,540 (SNPs), 392 NAFLD and 934 controls (subjects)	**Japanese**; NAFLD 49.9±14.8, Control ns	Histologically characterized NAFLD	Biopsy	**PNPLA3** rs738409, rs2896019, rs381062; **SAMM50** rs738491, rs3761472, rs2143571; **PARVB** rs6006473, rs5764455, rs6006611	PNPLA3 rs738409 was associated with NAFLD ($P=6.8\times10^{-14}$). PNPLA3 rs2896019, rs381062, SAMM50 rs738491, rs3761472, and rs2143571, PARVB rs6006473, rs5764455, and rs6006611 were found to be in the same linkage disequilibrium block and were associated with decreased serum triglycerides	Illumina Human 660 W-Quad Bead Chip	172 NAFLD and 1012 controls

						and increased AST and ALT in NAFLD patients. These SNPs were associated with steatosis grade and NAS. PNPLA3 rs738409, rs2896019, SAMM50 rs738491, PARVB rs6006473, rs5764455, and rs6006611 were associated with fibrosis.		
Park et al. (2013); Korea	**GWAS;** 747,076 (SNPs), 484 (subjects)	**Korean childhood;** 8-13	Clinical chemistry phenotypes (AST and ALT level)	Liver enzymes	**ST6GALNAC3** rs4949718, **ADAMTS9** rs80311637, **CELF2** rs596406	ST6GALNAC3 rs4949718 ($P=1.87x10^{-7}$), ADAMTS9 rs80311637 ($P=1.85x10^{-6}$), and CELF2 rs596406 ($P=9.18x10^{-6}$) were multiply associated with elevated levels of ALT and AST.	Illumina HumanOmni 1-Quad BeadChip	ns
Kawaguchi et al. (2018); Japan	**GWAS**; 93,606(SNPs), 8,574 [subjects, 902 cases (476 NASH and 58 NASH-HCC patients) and 7,672 controls]	**Japanese;** NAFLD Type 1: 50.7±15.1, NAFLD Type 2: 50.9±14.9, NAFLD Type 3: 52.4±14.1, NAFLD Type 4: 57.9±14.6, NASH-HCC: 71.5±9.8, Control: 52.0±13.4	Histologically characterized NAFLD	Biopsy	**PNPLA3** rs2896019, **GCKR** rs1260326, **GATAD2A** rs4808199, **DYSF** rs17007417	PNPLA3 rs2896019 ($P=2.3x10^{-31}$), GCKR rs1260326 ($P=9.6x10^{-10}$), GATAD2A rs4808199 ($P=2.3x10^{-8}$) were significantly associated with NAFLD; DYSF rs17007417 was significantly associated NASH-HCC.	SNP arrays provided by Illumina	
Chung et al. (2018); Korea	**GWAS**; 584,061 (SNPs), 4,409 (subjects,	**Korean** 50.2±10.5	Ultra-sonographic characterized NAFLD	Ultrasound	**PNPLA3** rs738409, rs12483959, rs2281135; **SAMM50**	PNPLA3 rs738409, rs12483959, rs2281135 were validated in population ($P<8.56\times10^{-8}$) in the same linkage disequilibrium block.	Affymetrix Axiom® Customized Biobank	744 NAFLD patients and 1,137 controls

	NAFLD 1593/NN 2,816)				rs2143571, rs3761472, rs2073080	SAMM50 rs2143571, rs3761472, rs2073080 showed significant associations with NAFLD ($P < 8.56\times10^{-8}$). These six SNPs showed significant associations with the severity of fatty liver (all $P < 2.0\times10^{-10}$ in the discovery set and $P < 2.0\times10^{-6}$ in the validation set) and NAFLD, with elevated levels of alanine aminotransferase (all $P < 2.0\times10^{-10}$ in the discovery set and $P < 2.0\times10^{-6}$ in the validation set).	Genotyping Arrays	

ADAMTS9, ADAM metallopeptidase with thrombospondin type 1 motif 9; ALT, alanine aminotransferase; AST, aspartate aminotransferase; CELF2, CUGBP Elav-like family member 2; CELF2, CUGBP Elav-like family member 2; GATAD2A, the GATA Zinc Finger Domain Containing 2A; HbA1c, haemoglobin A1c; GCKR, glucokinase regulatory protein; GWAS, genome-wide association study; NAFLD, non-alcoholic fatty liver disease; NASH, non-alcoholic steatohepatitis; NASH-HCC, non-alcoholic steatohepatitis-hepatocellular carcinoma; NN, non-NAFLD; PARVB, parvin beta; PNPLA3, patatin-like phospholipase domain-containing protein 3 gene; SAMM50, sorting and assembly machinery component 50 homolog; SNPs, single nucleotide polymorphisms; ST6GALNAC3, ST6 N-acetylgalactosaminide alpha-2,6-sialyltransferase 3.

Appendix Table A 3 Single nucleotide polymorphisms (SNPs) identified in sequencing studies for non-alcoholic fatty liver disease (NAFLD).

Reference; country	Design; sample size	Study population/ discovery cohort; age	Diagnosis of NAFLD	NAFLD related polymorphisms	Replication/ validation sample size	Genotyping platform	Summary of associations
Kitamoto et al. (2014); Japan	**NGS**; genomic region from 44,317,888 to 44,425,903 on chromosome 22, 1552 [subjects, 540 NAFLD (488 NASH and 52 simple steatosis) and 1012 controls]	**Japanese**; simple steatosis 51.4±15.6, NASH 50.5±14.1, control 53.1±15.3	Biopsy	**1-kb LD block 1**: rs738407-rs2006943, **21-kb LD block 2**: rs139051-rs13054885, **48-kb LD block 3:** rs7289329-rs1007863, **2-kb LD block 4:** rs4764455-rs6006611	ns	GeneAmp 9700 PCR System (long-range PCR approach)	HaploView analysis showed that LD block 1 and 2 occurred in PNPLA3, block 3 in SAMM50 and block 4 in PARVB. Variations in LD blocks 1-4 were significantly associated with NAFLD as compared with control subjects ($P<1 \times 10^{-8}$). Variations in LD block 2 were significantly associated with the NAS, ALT and AST. Variations in LD block 1 were significantly associated with the fibrosis stage. The strongest associations were observed for variations in LD block 4, with NASH as compared with simple steatosis ($P=7.1 \times 10^{-6}$) and NAS ($P=3.4 \times 10^{-6}$).
Di Costanzo et al. (2018); Italy	**NGS**; 168 sequence variants, 445 (subjects, 218 NAFLD and 227 controls)	**Caucasian**; NAFLD: 46-60, controls: 41-58	Ultrasound	**PNPLA3** rs738409, **MBOAT7** rs641738 **GCKR** rs1260326, **PPP1R3B** rs61756425, **TM6SF2** rs58542926	ns	Ion Ampliseq Library kit v2.0	GCKR rs1260326 and MBOAT7 rs641738 (recessive), TM6SF2 rs58542926 and PNPLA3 rs738409 (dominant) emerged as associated to NAFLD, with PNPLA3 rs738409 being the strongest predictor ($P < 0.001$); rs61756425 in PPP1R3B and rs641738 in MBOAT7 genes were predictors of NAFLD severity.

Kleinstein et al. (2018); US	**WES**; 4,537 (subjects, 82 NAFLD and 4455 controls)	**Caucasian**; NAFLD protective: (≥50 with T2DM and obesity) 53-61, NAFLD progressor: (50-55, without T2DM and obesity) 37.2-52 Control: ns	Biopsy	**PNPLA3** rs738409, **TM6SF2** rs58542926,	ns	Illumina GAIIx, HiSeq 2000 or 2500 sequencers	Progressors: There was nonsignificant enrichment of the known PNPLA3I148M (rs738409, P= 8.42E-05) and TM6SF2 E167K (rs58542926, P= 4.10E-03) polymorphisms under single-variant allelic models among the NAFLD progressors. Protective: There was nonsignificant enrichment in several NAFLD-associated genes: TM6SF2 E167K (P= $8.88x10^{-4}$ allelic), PARVB and SAMM50.
Pirola et al. (2018); Argentina	**NGS**; 14 chromosomal regions; 96 (subjects; 32 NAFL, 32 NASH and 32 control)	**Argentinea**; NAFL 51.9±9.8, 32 NASH 51.2±11, control 48±7.4	Biopsy	**GCKR** rs149847328	517 (control 139, NAFL 105 and NASH 146; explore the presence of a rare variant in GCKR rs149847328)	NGS was performed using the Ion Torrent Personal Genome Machine; Confirmation of the p.Arg227Ter mutation was performed using a TaqMan genotyping assay	GCKR protein expression was markedly decreased in the liver of the affected patient compared with patients with NAFLD who carry the wild-type allele.
Bale et al. (2019); India	**WES**; ~74,000 (SNPs), 8 (subjects, 6	**Indian**;	ARFI imaging	**PEMT** rs7946, **OSBPL10** rs2290532	Ultrasound detected NAFLD (n = 191) and	Ion Proton™; Ion AmpliSeq™	Variants in genes PEMT and OSBPL10 that have roles in dietary choline intake and regulation of cholesterol

	lean-NAFLD and 2 lean controls)				controls (n = 105)	Exome RDY Kit	homeostasis, respectively, were identified (discovery set). PEMT rs7946 and OSBPL10 rs2290532 revealed that variant in PEMT but not OSBPL10 gene was associated (p = 0.04) with threefold increased risk of NAFLD in lean individuals.

ALT, alanine aminotransferase; AST, aspartate aminotransferase; ARFI, acoustic radiation force impulse; GCKR, glucokinase regulatory protein; LD, linkage disequilibrium; MBOAT7, membrane bound O-acyltransferase domain containing 7; NAFLD, non-alcoholic fatty liver disease; NASH, non-alcoholic steatohepatitis; NAS, NAFLD activity score; NGS, next-generation sequencing; OSBPL10, oxysterol-binding protein-related protein10; PARVB, parvin beta; PEMT, phosphatidylethanolamine N-methyltransferase; PNPLA3, patatin-like phospholipase domain-containing protein 3 gene; ; PPP1R3B, protein phosphatase 1, regulatory subunit 3b; SAMM50, sorting and assembly machinery component 50 homolog; TM6SF2, transmembrane 6 superfamily 2; WES, whole-exome sequencing.

Appendix Table A 4 Dietary reference values for vitamin D (g/d) by life stages as proposed by various international agencies to maintain adequate circulating 25-hydroxy vitamin D concentrations

Agency	Year	Country	Recommended dietary vitamin D intake (μg/d)						25(OH)D Threshold (nmol/L)
			0-12 months	1 to <4 years	4-18 years	19-69 years	>70 years	Pregnancy/ lactation	
SACN[1]	2016	UK	8.5-10 (SI)	10 (SI)	10 (RNI)	10 (RNI)	10 (RNI)	10 (RNI)	25
EFSA	2016	Europe	10 (AI)	15 (AI)	15 (AI)	15 (AI)	15 (AI)	15 (AI)	50
IOM	2011	North America and Canada	10 (AI)	15 (RDA)	15 (RDA)	15 (RDA)	20(RDA)	15 (RDA)	50
The Endocrine Society[2]	2011	US	10-25 (DR)	15-25 (DR)	15-25 (DR)	37.5-50	37.5-50	37.5-50	75
Health Canada	2010	Canada	10 (AI)	15 (RDA)	15 (RDA)	15 (RDA)	20 (RDA)	15 (RDA)	nr
National Health and Medical Research Council	2014	Australia and New Zealand	5 (AI)	5 (AI)	5 (AI)	5-10 (AI)	15 (AI)	5 (AI)	27.5
National Health Commission of RPC	2018	China	10 (AI)	10 (RNI)	10 (RNI)	10-15 (RNI)	15 (RNI)	10 (RNI)	nr
WHO/FAO Joint Expert Consultation[3]	2004	Worldwide	5 (RNI)	5 (RNI)	5 (RNI)	5-15 (RNI)	15 (RNI)	5 (RNI)	27

AI, adequate intake; DR, daily requirement; EFSA, European Food Safety Authority; FAO, Food and Agriculture Organisation; IOM, European Food Safety Authority; nr, not reported; RDA, recommended dietary allowance; RNI, reference nutrient intakes; RPC, People's Republic of China; SACN, Scientific Advisory Committee on Nutrition; SI, safe intake; WHO, World Health Organisation; Conversion factors: 1IU vitamin D =25ng vitamin D, 40IU vitamin D = 1μg vitamin D; 1. SACN did not take into account sunlight exposure in making recommendations because of the number and complexity of factors that affect skin synthesis of vitamin D; 2. Recommended dietary intakes of vitamin D for patients at risk for vitamin D deficiency; 3. Based on maintain normal bone health

Appendix Table A 5 Metabolic and other outcomes of randomised controlled intervention trials of vitamin D supplementation in NAFLD.

Randomised controlled intervention trials in children					
Authors	**Arms**	**Vitamin D status (Before)**	**Vitamin D status (After)**	**Other metabolic outcomes**	**Post-intervention changes related to other metabolic outcomes**
El Amrousy et al. (2021);	**G1:** placebo (n=50) **G2:** 2,000 IU/day vitamin D (n=50)	**G1:** 31.8 [7.5-50]‡, **G2:** 31.5 [14.8-48.5]‡	**G1:** 12.7 [5-19]‡, **G2:** 42 [51.3-133.5]‡	FBG, FBI, HOMA-IR, WC, HC, BMI, serum calcium level	**G2 (after vs. before):** FBG↓*, FBI↓*, HOMA-IR↓*, BMI↓*; **G2 vs. G1 (after):** FBG↓*, FBI↓*, HOMA-IR↓*, BMI↓*;
Namakin et al. (2021);	**G1:** placebo (n=50) **G2:** 5,000 IU/week vitamin D (n=51)	**G1:** 28.2 ± 13.7†, **G2:** 24.5 ± 15.8†	**G1:** 32.8 ± 12.0†, **G2:** 74.9 ± 15.9†	FBS, FBI, CBC, WBC, UC	**G2 vs. G1 (after):** FBI↓*, UC↓*, WBC↓*
Randomised controlled intervention trials in adults					
Gad et al. (2021)	**G1:** placebo (ampoule containing 2 ml of normal saline 0.9%; n=40) **G2:** single dose intramuscular 200,000 IU/month cholecalciferol (n=40)	**G1:** 43.4 ± 26.5†, **G2:** 40.8 ± 25.6†	**G1:** 46.9 ± 20.8†, **G2:** 98.4 ± 30.0†	FBG, HbA1C, BMI, CBC, BUN	ns
Morvaridzadeh et al. (2021);	**G1:** PY (n=44) **G2:** 1,000IU/day vitamin D in pro-YED (n=44)	**G1:** 51.7 ± 28.6†, **G2:** 51.1 ± 27.4†	**G1:** 60.4 ± 38.3†, **G2:** 75.3 ± 26.6†	FBS, FBI, HOMA-IR, WC, WHR, BF, LBM, BMI, SBP, DBP	**G2 (after vs. before):** FBS↓*, FBI↓*, HOMA-IR↓*, SBP↓*
Mahmoudi et al. (2021)	**G1**: 0.25 mcg/day calcitriol (n=27), **G2**: 50,000 IU/week cholecalciferol (n=27)	**G1:** 35.3 ± 15.8†, **G2:** 34.7 ± 14.1†	**G1:** 57.6 ± 38.2†, **G2:** 57.8 ± 38.5†	FPG, FBI, HOMA-IR, BMI	**G1 (after vs. before):** Overweight: FBI↓*; Obese: FBI↓*, HOMA-IR↓*;

Yaghooti et al. (2021);	**G1**: placebo (n=64), **G2**: 0.25 mcg/day calcitriol (n=64)	**G1:** 43.75 ± 19.25†, **G2:** 47.74 ± 24.00†	nr	FBS, FPI, HOMA-IR, QUICKI, WC, BMI, leptin, adiponectin	ns
Lukenda Zanko et al. (2020)	**G1:** placebo (n=110), **G2:** 1,000 IU/day cholecalciferol drops (n=201)	**G1:** 59.3 [12.3-951]‡, **G2:** 47.3 [8.0-606]‡	nr	FBG, FSI, HOMA-IR, HbA1c, BMI, CBC, platelet, ferritin, phosphates, urea, UA	**G2 vs. G1 (after 360 days vs. before):** FSI↓*, HOMA-IR↓*
Hussain et al. (2019)	**G1:** placebo (n=51) **G2:** 50,000 IU/week vitamin D (n=51)	**G1:** 38.5 ± 7.05†, **G2:** 31.3 ± 10.5†	**G1:** 43.8 ± 8.8†, **G2:** 61.3 ± 9.5†	FBS, FSI, HOMA-IR, BMI, adiponectin, SBP, DBP	**G2 (after vs. before):** HOMA-IR↓*, adiponectin↓*, BMI↓* **G2 vs. G1 (after):** HOMA-IR↓*, adiponectin↓*,
Shidfar et al. (2019b)	**G1:** placebo (25 µg/d lactose, n=36) **G2:** 1,000 IU/d (25g/d calciferol) vitamin D (n=37) **G3:** 500mg calcium carbonate+10,000 IU/d vitamin D (n=37);	**G1:** 25.0 ± 1.6†, **G2:** 24.8 ± 1.6†, **G3:** 24.8 ± 2.3†	**G1:** 27.5 ± 2.0†, **G2:** 53.5 ± 1.8†, **G3:** 67.8 ± 2.8†	BF, WHR, BMI	**G2 (after vs. before):** BF↓*, WHR↓* **G3 (after vs. before):** BF↓*, WHR↓*
Geier et al. (2018)	**G1:** placebo (n=10) **G2:** 2,100 IU/d vitamin D (n=8)	**G1:** 50±25†, **G2:** 52.5±30†	**G1:** 40±23†, **G2:** 98±33†	FPG, FPI, HbA1C, WBC, BMI, platelet, adiponectin, calcium, SBP, DBP	ns
Dabbaghmanesh et al. (2018a)	**G1:** placebo (n=31) **G2:** 0.25 mg/d calcitriol (n=28) **G3:** 50,000 IU/week cholecalciferol (n=32)	**G1:** 52.8±13.0†, **G2:** 46.5±13.8†, **G3:** 47.3±15.5†	**G1:** 47.0±17.5†, **G2:** 57.3±49.5†, **G3:** 80.5±35.3†	FPG, BMI, calcium, phosphorus	**G2 (after vs. before):** phosphorus↑*
Taghvaei (2018)	**G1:** placebo (n=20) **G2:** 50,000 IU/week vitamin D3 (n=20);	**G1:** 49.5±10.9†, **G2**: 47.9 ± 13.7†	**G1:** 52.1 ± 6.2†, **G2:** 86.0 ± 10.7†	FBS, BMI, Cr, calcium	**G2 (after vs. before):** BMI↓*
Sakpal et al. (2017)	**G1:** placebo (n=30)	**G1:** 30±15†, **G2:** 30±10†,	nr	FBS, FPI, HOMA-IR, WHR, BMI,	**G2 (after vs. before):** Adiponectin↑*; **G1 (after vs. before):**

	G2: single dose intramuscular 600,000 IU/month (n=51)			adiponectin, SBP, DBP,	FPI↑*, HOMA-IR↑*
Dasarathy et al. (2017)	6-month; **G1:** 2,000IU/d cholecalciferol non-responder (n=26); **G2:** 2,000IU/d cholecalciferol responder (n=16);	**G1:** 46.75±12.5†, **G2:** 56.25±11.5†	**G1:** 50.25±12.25†, **G2:** 97.25±19.5†	FPG, FPI, HOMA-IR, FM, FFM, BMI, BUN	**G2 vs. G1 (after):** FPG↓*, HOMA-IR↓*
Lorvand Amiri et al. (2017)	12-week; **G1:** placebo (25 µg/d lactose, n=36) **G2:** 1,000 IU/d (25g/d calciferol) vitamin D (n=37) **G3:** 500mg calcium carbonate+10,000 IU/d vitamin D (n=37);	**G1:** 25.0 ± 1.6†, **G2:** 24.8 ± 1.6†, **G3:** 24.8 ± 2.3†	**G1:** 27.5 ± 2.0†, **G2:** 53.5 ± 1.8†, **G3:** 67.8 ± 2.8†	FPG, FSI, HOMA-IR, BF, WHR, BMI	**G2 (after vs. before):** FPG↓*, FSI↓*, HOMA-IR↓*, WHR↓* **G3 (after vs. before):** FPG↓*, FSI↓*, HOMA-IR↓*, WHR↓* **G2 vs. G1 (after):** FSI↓*, HOMA-IR↓* **G3 vs. G1 (after):** FPG↓*, FSI↓*, HOMA-IR↓* **G3 vs. G2 (after):** FPG↓*
Lorvand Amiri et al. (2016)	**G1:** placebo (25μg/d lactose, n=37) **G2:** 25μg/d calcitriol (n=36);	**G1:** 25.2±9.5†, **G2:** 24.8±9.8†	**G1:** 27.5±11.8†, **G2:** 67.8±18†	FPG, FSI, HOMO-IR, WC, HC, BF, BW, BMI	**G2 (after vs. before):** FPG↓*, FSI↓*, HOMO-IR↓*, WC↓*, HC↓*, BF↓*, BW↓*, BMI↓*; **G1 (after vs. before):** WC↓*, HC↓*, BF↓*, BW↓*, BMI↓*; **G2 vs. G1 (after):** FSI↓*, HOMO-IR↓*
Barchetta et al. (2016b)	**G1:** placebo (n=29) **G2:** 2,000IU/d cholecalciferol (n=26)	**G1:** 37.1 [27.3-51.6]‡, **G2:** 43.1 [31.1-58.5]‡	**G1:** 40 [20.8-60.5]‡, **G2:** 85.8 [73-110]‡	FGB, FBI, HOMA-IR, HOMA-β, QUICKI, AT, ARIPO-IR, HbA1c, BF,	**G2 vs. G1 (after):** ABI↓*

				distribution (VAT and SAT areas), IMT, FMD, BMI, adiponectin, SBP, DBP, ABI	
Papapostoli et al. (2016)	**G1:** 20,000IU/week cholecalciferol (n=40)	**G1:** 29.5±12†	**G1:** 86.5±32.25 (4-week), 90.75±25.5 (3-month), 87.0±24.5 (6-month)	FFM, FM, VFI, BMI, PTH, calcium, phosphate, urea, urine	ns
Foroughi et al. (2016)	**G1:** placebo (n=30) **G2:** 50,000IU/week vitamin D3 (n=30)	**G1:** 47±2†, **G2:** 49±1†	**G1:** 44.8±0.44†, **G2:** 117±13†	FBG, FSI, HOMA-IR, HOMA-β, calcium	**G2 (after vs. before):** FGB↓*, HOMA-IR↓*, calcium↑*; **G2 vs. G1 (after):** calcium↑*
Sharifi et al. (2016)	**G1:** placebo (male n=13, female n=13) **G2:** 50,000IU/14d vitamin D3 (male n=13, female n=14)	**Men:** **G1:** 38.5 [29.3-58.8]‡, **G2:** 39.3 [26.5-73]‡, **Women:** **G1:** 45.8 [26.5-107.8]‡, **G2:** 25 [19-45.3]‡,	**Men:** **G1:** 43.8 [36.3-62.3]‡, **G2:** 75 [63.5-100.8]‡ **Women:** **G1:** 61 [32.5-83]‡, **G2:** 84 [64-133.2]‡	FBI, HOMA-IR, BW, WC, WHR, BF, BMI, adiponectin, calcium	**G2 (after vs. before):** **Men:** BW↓*, BMI↓*, calcium↑* **Women:** BW↓*, BMI↓*, adiponectin ↑*
Kitson et al. (2016)	24-week; **G1:** 25,000 IU/week vitamin D_3	**G1:** 63.3±31.6†	**G1:** 109.8±15.6†	HOMA-IR, HbA1c, BW, corrected calcium, phosphate, leptin, adiponectin	ns
Foroughi et al. (2014)	**G1:** placebo (n=30) **G2:** 50,000IU/week vitamin D3 (n=30)	**G1:** 47±2†, **G2:** 49.1±1†	**G1:** 45.8±0.44†, **G2:** 117±13†	BMI, calcium	**G2 (after vs. before):** calcium↑*
Sharifi et al. (2014)	**G1:** placebo (n=26) **G2:** 50,000IU/14d vitamin D3 (n=27)	**G1:** 42.1 [29.3-62]‡, **G2:** 28.8 [22-71]‡	**G1:** 48 [36.8-66.8]‡, **G2:** 75 [64.5-116.5]‡	FBG, FBI, HOMA-IR, BW, WC, WHR, BF, BMI, serum MDA, serum TAC	**G2 (after vs. before):** BW↓*, WC↓*, BF↓*, BMI↓*, Serum MDA↓*, serum TAC↑* **G2 vs. G1 (after):** FBG↓*, serum MDA↓*

ABI, ankle-brachial index; AT, adipose tissue; ARIPO-IR, adipose tissue insulin-resistance; BF, body fat; BMI, body mass index; BUN, blood urea nitrogen; BW, body weight; CBC, complete blood count; DBP, diastolic blood pressure; FBG, fasting blood glucose; FBI, fasting blood insulin; FBS, fasting blood sugar; FFM, free-fat mass; FPG, fasting plasma glucose; FM, fat mass; FMD, flow-mediated dilatation; FSI, fasting serum insulin; HbA1C, haemoglobin A1C; HC, hip circumference; HOMA-IR, homeostasis model assessment of insulin resistance; hs-CRP, high-sensitivity C-reactive protein; IMT, intima-media thickness; LBM, lean body mass; MDA, malondialdehyde; ns, not significant; PTH, parathyroid hormone; QUICKI, quantitative insulin sensitivity check index; SAT, subcutaneous adipose tissue; SBP, systolic blood pressure; TAC, total antioxidant capacity; WBC, white blood cell; WC, waist circumference; WHR, waist to hip ratio; UA, uric acid; UC, uric acid; VAT, visceral adipose tissue; VFI, visceral fat index; † Mean±Standard deviation; ‡ Median [Range];* Statistic significant; Ω BMI was calculated and classified according to the World Health Organisation classification into 4 groups of less than 18.5 as underweight, 18.5 to <25 as normal, 25.0 to <30 as overweight, and 30.0 or higher as obese range.

Appendix Table A 6 Single nucleotide polymorphisms identified in genome-wide/exome-wide association studies for 25 hydroxyvitamin D concentration.

Reference; country	Design; sample size (n=); study population; age	Genotyping platform	25(OH)D/1,25(OH)D assay and concentration [25(OH)D, nmol/L; 1,25(OH)D pmol/L]	Findings	Replication population
Revez et al. (2020); UK	**GWAS**; 8,806,780 SNPs; n=417,580; UK Biobank participants; 40-69	Affymetrix UK BiLEVE Axiom array and Affymetrix UK Biobank Axiom® array	**25(OH)D:** CLIA; **25(OH)D:** 33.5-63.2	Identified 143 independent loci (including one on chromosome X; P< 5×10^{-8}) in 112 1-Mb regions associated with 25(OH)D level	The QIMR Brisbane-based twin and family sample (n=1,632); the UKBR (n=1,632) whose PC1 (PC1<0.003) value outside the cut-off for white European; the SUNLIGHT consortium (n=79,366) involved 31 GWAS cohorts of European descent in Europe, Canada and USA
Manousaki et al. (2020); UK	**GWAS**; 20,370,874 SNPs n=401,460; White British UK Biobank participants; 56.8±8†	Affymetrix UK BiLEVE Axiom array and Affymetrix UK Biobank Axiom® array	**25(OH)D:** CLIA; **25(OH)D:** 70.0±34.7†	Observed 138 conditionally independent SNPs (pre- and post-conditioning P<6.6×10^{-9}), identified 63 loci that underline the contribution of genes outside the vitamin D canonical metabolic pathway to the genetic architecture of 25(OH)D	na
Kampe et al. (2019); Finland	**GWAS;** 686,085 SNPs n=761; healthy children; 24-month-old	Illumina Infinium Global Screening array	**25(OH)D:** CLIA; **25(OH)D:** Boys: 84.9±27.5† (at birth) 100.6±27.6† (24 months) Girls: 80.0±24.0† (at birth) 103.0±27.9† (24 months)	GC rs1155563 and CYP2R1 rs10832310 are genome-wide significant associated to 25(OH)D concentration in 2-year-old children	na
O'Brien et al. (2018b); US	**GWAS;** 386,449 SNPs; n=1,829;	Infinium OncoArray	**25(OH)D:** LC-MS; **25(OH)D:** 79.5±26.3†	32 SNPs were associated with 25(OH)D at P< 5×10^{-8}. Top two: GC	1,534 individuals who later developed breast cancer.

	Caucasian women; 55.3±8.9†	genotyping panel		rs1155563 P=6.8×10^{-23}) and CYP2R1 rs117913124 (P=1.3×10^{-10})	
Jiang et al. (2018); US	**Meta-GWAS;** 0.6-4.5 million SNPs; n=79,366; European descent of 31 cohorts; 55.3±8.9†	31 cohorts	ELISA, HPLC, HPLC-MS, RIA, CLIA, LC-MS or ECL; 31 cohorts	GC rs3755967 (P = 4.7×10^{-343}), NADSYN1/DHCR7 rs12785878 (P = 3.8×10^{-62}), CYP2R1 rs10741657 (P = 2.1×10^{-46}), CYP24A1 rs17216707 (P = 8.1×10^{-23}), SEC23A rs8018720 and AMDHD1 rs10745742 genome-wide significantly associated with 25(OH)D concentration.	Two separate replication samples: EPIC study with 40,562 individuals and 2195 individuals from the SOCCS
Manousaki et al. (2017); UK	**Meta-GWAS** ~0.2 billion SNPs; n=42,274; European ancestry of 19 cohorts;	Illumina HiSeq	HPLC-MS, SLC-MS, MS, LCC-MS, or CLIA; 19 cohorts	CYP2R1 rs117913124 (P=1.5 × 10^{-88}), rs116970203 (P= 2.2 × 10^{-90}), rs117361591 (P= 9.1 × 10^{-51}), rs117621176 (P= 8.7 × 10^{-51}), rs142830933 (P= 1.4 × 10^{-48}) and rs117672174 (P= 2.8 × 10^{-45}) were associated with 25(OH) level	8,711 individuals of the effect on vitamin D insufficiency
Sapkota et al. (2016); Indian	**GWAS** 5,904,251SNPs; n=1,387; Punjabi and Sikh Indian adults with or without T2D; Controls: 51.9±13.6†, T2D: 53.9±10.4†	Human 660 W Quad BeadChip	**25(OH)D:** ELISA; **25(OH)D:** Controls: 44.8±34.6†, T2D: 30.5±27.3†	FOXA2/SSTR4 rs2207173 (P=4.47×10^{-9}) was associated with 25(OH)D levels; IVL rs11586313 (P=1.36×10^{-6}) was suggestively associated with 25(OH)D level	An independent replication sample (n=2151) from the same population
Anderson et al. (2014); Australia	**GWAS** 2,461,244SNPs; 6 years old (n=673) and 14 years old (n=1140); Australian children;	Illumina Human660W -Quad BeadChip	**25(OH)D:** ELISA; **25(OH)D:** 6 years old: 101(84-123)‡ 14 years old: 81(68-98)‡	PDE3B/CYP2R1 rs1007392 (age 6, P=3.9 × 10^{-8}), rs11023332 (age14, P=2.2×10^{-10}), GC rs17467825 (age 6, P=4.2 × 10^{-9}), rs1155563 (age14, P=3.9×10^{-9}) and NYP rs156299 (age	na

	5.9±0.19† 14.1±0.21†			6, P=1.3×10^{-6}) were associated with 25(OH)D concentrations	
Engelman et al. (2010); US	**GWAS** 309,200 SNPs; n=229; Hispanic Americans; 41.3±13.9†	Illumina Infinium II HumanHap 300 BeadChips	**25(OH)D and 1,25(OH)D:** RIA; **25(OH)D:** 37.4±15.5† **1,25(OH)D:** 130.8±41.9†	DAB1 rs6680429, rs9970802, and rs10889028 were associated with 1,25(OH)D; none met the threshold for 25(OH)D [the genome-wide significance threshold based on a conservative Bonferroni correction was P <1.62×10^{-7}]	1,190 Hispanic Americans (including those 229 individuals in the discovery sample)
Wang et al. (2010b); US	**Meta-GWAS** SNPs; n=16,125; European descent of 5 cohorts; 55.3±8.9†	5 cohorts	**25(OH)D:** RIA or CLIA or ELISA or MS 5 cohorts	GC rs2282679 (P=1.9×10^{-9}), DHCR7 rs12785878 (P=2.1×10^{-27}), CYP2R1 rs10741657 (P=3.3×10^{-20}) and CYP24A1 rs6013897 (P=6.0×10^{-10}) were associated with 25(OH)D concentrations	An *in-silico* sample of 9,367 individuals and a *de novo* sample of 8,504 individuals
Ahn et al. (2010); US	**Meta-GWAS;** 593,253SNPs; n=4,501 European ancestry of 5 cohorts; na	Illumina 550K or Affymetrix 6.0	**25(OH)D:** CLIA or RIA **25(OH)D:** ATBC: 24.2 (37.3–52.9)‡ CPS-II: 45.2 (57.7–70.0)‡ CLUE II: 44.0 (59.2–76.1)‡ PLCO: 45.0 (56.8–70.0)‡ NHS: 66.6 (49.0–90.0)‡	GC rs2282679 (P=2.0×10^{-30}) was associated with 25(OH)D level; NADSYN1/DHCR7 rs382951 (P=8.8×10^{-7}), C10orf88 rs6599638 (P=3.3×10^{-7}) and CYP2R1 rs2060793 (P=1.4×10^{-5}) were suggestively associated with 25(OH)D levels	2221 individuals with serologic vitamin D levels
Benjamin et al. (2007); US	**GWAS;** 70,987SNPs; n=517; European ancestry; 59±10†	Affymetrix 100K GeneChip	**25(OH)D:** RIA; na	None of the SNPs has passed genome-wide significant p-threshold at 5x10^{-8}; only one suggestive signal in an intron of LOC105377885 (rs10485165, P=1.4×10^{-6}) was identified	na

25(OH)D, 25-hydroxyvitamin D; C10orf88, open-reading frame 88 C10orf88 on chromosome 10q26.13 in the vicinity of acyl-Coenzyme A dehydrogenase; CLIA, chemiluminescent immunoassay; CYP2R1, cytochrome P450 family 2 subfamily R polypeptide 1; DAB1, disabled homolog 1; DBP, vitamin D-binding protein; ELISA, enzyme-linked immunosorbent assay; FOXA2, Forkhead Box A2; GC, gene encoding group-specific component (vitamin D binding) protein; HPLC, high performance liquid chromatography; HPLC-MS, high performance liquid chromatography- tandem mass spectrometry; IVL, involucrin; GWAS, genome-wide associated study; LC-MS, liquid chromatography-tandem mass spectrometry; NPY, neuropeptide Y; PC, principal components; PDE3B, phosphodiesterase 3B, cGMP-inhibited; QIMR, Queensland Institute of Medical Research; RIA, radioimmunoassay; SNP, single nucleotide polymorphism; SSTR4, somatostatin receptor 4; UKBR, UK Biobank replication; WGS, whole-genome sequencing; † Mean±Standard deviation, ‡ median (IQR).

Appendix B
Supplementary Tables for Chapter 3

Appendix Table B 1 Additional miRNAs found dysregulated in liver only from NAFLD patients in more than one study, and their functional and pathophysiological effects

miRNA	Summary	Functional/pathophysiological effects and/or genetic targets of dysregulated miRNA
miR-33	**Up** in NASH (n=22) or SS (n=18) vs. NL(n=22) [MO women]; **up** in NASH (n=12) vs. NL (n=9) [ModO women] (Auguet et al., 2016b)	Hepatic *SREBP2* and *ABCG1* mRNAs: **up** in NASH (n=22) vs. controls (n=22) [MO women]; hepatic *SREBP2*, *ABCG1*, *SREBP1c*, *CPT1a* and *ACC1* mRNAs: **up** in NASH (n=12) vs steatosis (n=9) and NL (n=9) [ModO women] (Auguet et al., 2016b)
	Up *(miR-33a)* in NASH (n=38) vs. normal histology (n=10) [bariatric surgery patients] (Vega-Badillo et al., 2016)	Not investigated
	Down *(miR-33a-5p)* in NAFLD (n=58) vs. non-NAFLD (n=37) [postmortem samples, CSD and NCSD] (Braza-Boïls et al., 2016a)	Not investigated
miR-141	**Up** *(miR-141)* in NASH fatty liver (n=20) vs. NASH non-fatty liver(n=15) and normal histology (n=10) [liver tissue bank] (Tran et al., 2017a)	Not investigated
	Up *(miR-141)* in steatosis (n=4) vs. non-steatosis (n=4) [liver tissue bank] (Wang et al., 2018b)	Not investigated
miR-155	**Up** *(miR-155)* in steatosis (n=4) vs. non-steatosis (n=4) [liver tissue bank] (Wang et al., 2018b)	Not investigated
	Down *(miR-155)* in NAFLD (n=11) vs. HCs (n=11) [biopsy consenting NAFLD and HCs] (Wang et al., 2016b)	Hepatic *SREBP1c*, *FAS* and *ACC1* mRNA: **up** in NAFLD (n=11) vs. HCs (n=11) **Target:** LXRα (Wang et al., 2016b)
miR-199	**Up** (*miR-199a-5p*) in NAFLD (n=5) vs. HCs (n=6); liver steatosis score: **up** in NAFLD vs. HCs [diagnosis and treatment of gallstone disease] (Li et al., 2020)	Hepatic *MST1* mRNA: down in NAFLD (n=5) vs. HCs (n=6) (Li et al., 2020)
	Up (*miR-199a-5p*) in steatosis (n=7) vs. HCs (n=7) [commercial liver tissue bank] (Li et al., 2014)	Hepatic *CAV1* and *PPARα* mRNA: **down** in steatosis (n=7) vs. HCs (n=7)

miRNA	Summary	Functional/pathophysiological effects and/or genetic targets of dysregulated miRNA
		Target: *CAV1* (Li et al., 2014)
miR-223	**Up** *(miR-223)* in NASH (n=10) vs. controls (n=14) [NIH liver tissue repository] (He et al., 2019a)	Hepatic *CXCL10*, *TAZ*, *SERPINB9*, *DOCK11* and *GOLM1* mRNA: **up** in NASH (n=10) vs. HCs (n=14), **up** in steatosis (n=10) vs. HCs; hepatic *GPC3*, *CXCL10* and *TAZ* mRNA: **up** in NASH vs. HCs **Targets:** *CXCL10* and *TAZ* (He et al., 2019a)
	Up *(miR-223)* in steatosis (n=4) vs. non-steatosis (n=4) [liver tissue bank] (Wang et al., 2018b)	Not investigated
miR-378	**Up** *(miR-378)* in NASH (n=24) vs. normal histology (n=19) [liver transplantation biopsies] (Zhang et al., 2019a)	*Ppargc1β* mRNA: **down** in NASH (n=24) vs. HCs (n=19) *LXRα* targets miR-378 promoter (Zhang et al., 2019a)
	Up *(miR-378)* in NASH (n=38) vs. normal histology (n=24) [liver transplantation biopsies] (Zhang et al., 2019b)	*Prkag2* mRNA and protein: **down** in NASH vs. HCs **Targets:** *Prkag2* (Zhang et al., 2019b)
	Down (*miR-378i*) in NAFLD with severe fibrosis or cirrhosis (n=15) vs. NAFLD without fibrosis (n=15) [bariatric surgery patients] (Leti et al., 2015)	Not investigated

ABCG1, ATP binding cassette subfamily G member 1; ACC1, acetyl-CoA carboxylase; CAV, caveolin1; CPT1a, carnitine palmitoyl transferase 1a; CSD, cardiac sudden death; CXCL10, C-X-C motif chemokine 10; DOCK11, dedicator of cytokinesis 11; FAS, fatty acid synthase; GOLM1, Golgi membrane protein 1; GPC3, glypican-3; HCs, healthy controls; LXRα, liver X receptorα; MO, morbidly obese; ModO, moderately obese; MST1, mammalian sterile 20-like kinase 1; NAFLD, non-alcoholic fatty liver disease; NASH, non-alcoholic steatohepatitis; NCSD, non-cardiac sudden death; PPARα; Ppargc1β, peroxisome proliferator-activated receptor γ coactivator 1-beta; Prkag2, protein kinase AMP-activated non-catalytic subunit gamma 2; SREBP1c, sterol regulatory element-binding protein 1c; SREBP2, sterol regulatory element-binding protein 2; SERPINB9, Serpin family B member 9; TAZ, transcriptional coactivator with PDZ-binding motif.

Appendix Table B 2 Additional miRNAs dysregulated in serum only from NAFLD patients, identified in more than one study

miRNA	Summary
miR-16	**Up** *(miR-16)* in NAFLD (n=34) vs. HCs (n=19), **up** in steatosis and NASH vs. HCs; discriminated steatosis from HCs (AUROC=0.962) (Cermelli et al., 2011) **Up** *(miR-16)* in NASH (n=31) vs. HCs (n=37); positive correlation with hepatocellular ballooning and fibrosis (Liu et al., 2016b) **Up** *(miR-16-5p)* in fatty liver infiltration (n=10) vs. no fatty liver infiltration (n=12) [patients with obesity and T2DM] (Pillai et al., 2020) **Down** *(miR-16-5p)* in SAF≥ 2 (n=50) vs. SAF<2 (n=25), **down** in NAS ≥5 (n=38) vs. NAS<5 (n=37), **down** in F>2 (n=29) vs. F≤2 (n=46); negative correlation with AST, APRI, FIB4, BARD and NAFLD fibrosis score (NAFL n=25, NASH n=50 and NL n=17) (López-Riera et al., 2018b)
miR-20	**Up** *(miR-20a-5p/miR-20b-5p)* in NAFLD (n=52) vs. Non-NAFLD (n=48) [adults with T2DM] (Ye et al., 2018a) **Down** (*miR-20a-5p*) in NAFLD (n=14) vs. HCs (n=13) (Wang et al., 2020d) **Down** *(miR-20a)* in NAFLD (n=92) vs. HCs (n=383), **down** in severe NAFLD (n=51) vs. mild NAFLD (n=41) and HCs; in multivariate logistic regression OR=4.09 for severe NAFLD (Ando et al., 2019)
miR-22	**Up** *(miR-22-5p)* in NAFLD (n=32) and NAFLD+fibrate (n=11) vs. HCs (n=10) (López-Riera et al., 2017) **Up** *(miR-22-3p)* in SAF≥ 2 (n=50) vs. SAF<2 (n=25), **up** in NAS≥5 (n=38) vs. NAS<5 (n=37); positive correlation with AST, ALT, Ferritin and APRI (NAFL n=25, NASH n=50 and HC n=17) (López-Riera et al., 2018b)
miR-27	**Up** *(miR-27b-3p)* in NAFLD (n=103) vs. HCs (n=80); discriminated NAFLD from HCs (AUROC=0.693) (Tan et al., 2014) **Up** *(miR-27b-3p)* in SAF≥ 2 (n=50) vs. SAF<2 (n=25), **up** in NAS ≥5 (n=38) vs. NAS <5 (n=37), **up** in F>2 (n=29) vs. F≤2 (n=46); positive correlation with AST, ALT, Ferritin, APRI and FIB4 (NAFL n=25, NASH n=50 and NL n=17); discriminated NAS≥5 from NAS <5 (AUROC=0.73) (López-Riera et al., 2018b) **Down** *(miR-27a)* in NAFLD (n=92) vs. HCs (n=383), **down** in severe NAFLD (n=51) vs. mild NAFLD (n=41) and HCs; in multivariate logistic regression OR=4.09 for severe NAFLD (Ando et al., 2019)

miRNA	Summary
miR-29	**Up** *(miR-29a-3p)* in NAFLD (n=32) and NAFLD+fibrate (n=11) vs. HCs (n=10) (López-Riera et al., 2017); **Up** *(miR-29b-3p but **no change** in miR-29a-3p or miR-29b-3p)* in multivariate logistic regression OR=1.49 for NAFLD [non-T2D NAFLD (n=73) and non-T2D non-NAFLD (n=68)]; positive correlation with intrahepatic lipid content [N=99] (He et al., 2019b) **Down** *(miR-29a)* in NAFLD (n=58) vs. HCs (n=34); discriminated NAFLD from HCs (AUROC=0.679) (Jampoka et al., 2018)
miR-99	**Down** *(miR-99a)* in NAFLD (n=20) vs. HCs (n=20); negative correlation with GGT; discriminated NAFLD from HCs (AUROC=0.76) (Celikbilek et al., 2014) **Down** *(miR-99a)* in NAFLD (n=210) vs. Controls (n=90), **down** in NASH (n=86) vs. steatosis (n=124); negative correlation with ALT, activity, inflammation, ballooning and fibrosis; discriminated NAFLD from HCs (AUROC=0.73) and NASH vs. steatosis (AUROC=0.91) (Hendy et al., 2019)
miR-125	**Up** (*miR-125b-5p*) in NAFLD (n=29) vs. HCs (n=24); ALT: **up** in NALFD vs. HCs; serum TNFAIP3 mRNA: **down** in NAFLD vs. HCs (Zhang et al., 2021b) **Down** (*miR-125b-5p*) in NAFLD (n=34) vs HCs (n=20); serum ITGA8 mRNA: **up** in NAFLD vs. HCs (Cai et al., 2020)
miR-181	**Up** *(miR-181b-3p)* in NAFLD (n=25) vs. HCs (n=21) (Wang et al., 2017) **Up** *(miR-181a-5p)* in NAFLD (n=30) vs. HCs (n=30) (Huang et al., 2019) **Down** *(miR-181d)* in NAFLD (n=20) vs. HCs (n=20); negative correlation with GGT; discriminated NAFLD from HCs (AUROC=0.86) (Celikbilek et al., 2014)

miRNA	Summary
miR-192	**Up** *(miR-192-5p)* in NAFLD (n=103) vs. HCs (n=80); discriminated NAFLD from HCs (AUROC=0.652) (Tan et al., 2014) **Up** *(miR-192)* in NASH (n=87) vs. NAFL (n=50) and HCs (n=61); positive correlation with ALT, steatosis and serum CK18-Asp396 (Becker et al., 2015) **Up** *(miR-192)* in NASH (n=47) vs. steatosis (n=30) and HCs (n=19); positive correlation with AST, GGT; discriminated histological severity (AUROC range 0.676-0.709) (Pirola et al., 2015) **Up** *(miR-192)* in NASH (n=31) vs. NAFL (n=17) and HCs (n=37), **up** in NAFL (n=17) vs HCs (n=37); positive correlation with histological severity but not fibrosis (Liu et al., 2016b) **Up** *(miR-192)* in circulating exosomes in advanced stage NAFLD (n=3) vs. early stage NAFLD (n=3) (Lee et al., 2017b) **Up** *(miR-192-5p)* in SAF≥ 2 (n=50) vs. SAF>2 (n=25), **up** in NAS≥5 (n=38) vs. NAS<5 (n=37); positive correlation with AST, ALT, Ferritin, APRI and BARD (NAFL n=25, NASH n=50 and NL n=17) (López-Riera et al., 2018b) **Up** *(miR-192-5p)* in NASH (n=31) vs. HCs (n=37), **up** in NAFL (n=17) vs. HCs, positive correlation with ALT, AST, steatosis, activity, ballooning and inflammation (Liu et al., 2020c) **Up** *(miR-192-5p)* with increasing fibrosis severity (n=132 NAFLD patients); in multivariate analyses, positive correlation with steatosis, fibrosis, the PNPLA3 I148M and TM6SF2 E167K variants (Ezaz et al., 2020) **Down** *(miR-192-5p)* in NASH (n=60) vs. HCs (n=60); discriminated NAFD vs. HCs (AUROC=0.791) (Hu and Yu, 2020)
miR-197	**Down** *(miR-197)* in NAFLD (n=20) vs. HCs (n=20); negative correlation with inflammation; discriminated NAFLD from HCs (AUROC=0.77) (Celikbilek et al., 2014) **Down** *(miR-197-3p)* in SAF≥ 2 (n=50) vs. SAF<2 (n=25) (López-Riera et al., 2018b)
miR-375	**Up** *(miR-375)* in NASH (n=47) vs. steatosis (n=30) and HCs (n=19); discriminated NAS>5 from NAS<5 (AUROC=0.72) (Pirola et al., 2015) **Up** *(miR-375-3p)* in fatty liver infiltration (n=10) vs. no fatty liver infiltration (n=12) [patients with obesity and T2DM] (Pillai et al., 2020)

miRNA	Summary
miR-379	**Up** *(miR-379)* in NAFLD (n=79) vs. HCs (n=10); discriminated: NAFLD from HC (AUROC= 0.72) (Okamoto et al., 2020) **Up** *(miR-379)* in steatosis (n=10) vs. HCs, **Down** in NASH (n=10) vs. HCs; discriminate steatosis and NASH from HCs(AUROC=0.92) (Okamoto et al., 2016)
miR-451	**Up** *(miR-451)* in NAFLD (n=48) vs. HCs (n=90) [adult males] (Yamada et al., 2013) **Down** *(miR-451)* in NAFLD (n=20) vs. HCs (n=20); serum MIF mRNA: up in NAFLD vs. HCs (Tang et al., 2019)

ALT, alanine aminotransferase; APOE, apolipoprotein E; APTI, AST to platelet ratio index; AST, aspartate transaminase; AUROC, the area under the receiver operating characteristic; CK18, cytokeratin-18; eLP-IR, enhanced lipo-protein insulin-resistance index; F, fibrosis%; FIB4, fibrosis 4; FPG, fasting plasma glucose; GGT, gamma-glutamyl transpeptidase; HC, healthy control; γ-GT, γ-glutamyl transpeptidase; NAFL, non-alcoholic fatty liver; NAFLD, non-alcoholic fatty liver disease; NAS, NAFLD activity score; NASH, non-alcoholic steatohepatitis; NNL, near normal liver; NS, not specified; PNPLA3, patatin-like phospholipase domain containing protein 3; SIRT1, sirtuin 1; SAF, steatosis, activity, fibrosis score; T2DM, type 2 diabetes mellitus; TG, triglyceride.

Appendix Table B 3 Most frequently replicated dysregulated miRNAs relative to both NAFLD and vitamin D and their functional and pathophysiological effects

miRNA	Relative study category	Samples	miRNA related summary
miR-27	NAFLD	Human serum	**Up** *(miR-27b-3p)* in NAFLD (n=103) vs. HCs (n=80); discriminated NAFLD from HCs (AUROC=0.693) (Tan et al., 2014) **Up** *(miR-27b-3p)* in SAF≥ 2 (n=50) vs. SAF<2 (n=25), **up** in NAS ≥5 (n=38) vs. NAS <5 (n=37), **up** in F>2 (n=29) vs. F≤2 (n=46); positive correlation with AST, ALT, Ferritin, APRI and FIB4 (NAFL n=25, NASH n=50 and NL n=17); discriminated NAS≥5 from NAS <5 (AUROC=0.73) (López-Riera et al., 2018b) **Down** *(miR-27a)* in NAFLD (n=92) vs. HCs (n=383), **down** in severe NAFLD (n=51) vs. mild NAFLD (n=41) and HCs; in multivariate logistic regression OR=4.09 for severe NAFLD (Ando et al., 2019)
	Vitamin D	Human liver and serum*	Negative *(miR-27b)* correlation with CYP3A activity§ in both liver and serum; no association with mRNA levels of *CYP3A4*, *VDR* and *PPARα* [liver N=20; serum N=28] (Ekström et al., 2015)
		Human lung fibroblast cell line: MRC-5	**Down** *(miR-27b)* in cells treated with TGF-1β †+1,25(OH)D vs. cells treated with TGF-1β; α-SMA mRNA: **down** in cells treated with TGF-1β †+1,25$(OH)_2D_3$ vs. cells treated with TGF-1β; target: VDR [luciferase assay] (Li et al., 2015)
miR-125	NAFLD	Human serum	**Up** (*miR-125b-5p*) in NAFLD (n=29) vs. HCs (n=24); ALT: **up** in NALFD vs. HCs; serum TNFAIP3 mRNA: **down** in NAFLD vs. HCs (Zhang et al., 2021b) **Down** (*miR-125b-5p*) in NAFLD (n=34) vs HCs (n=20); serum ITGA8 mRNA: **up** in NAFLD vs. HCs (Cai et al., 2020)
	Vitamin D	Human cancer cell lines: MCF-7 and KGN	**Down** (*miR-125b*) in 1,25(OH)D vs. without 1,25(OH)D [MCF-7]; target: VDR [MCF-7 and KGN; luciferase assay] (Mohri et al., 2009)
		Human breast cancer tissue and human cancer cell lines : MCF-7 and KGN	**Down** (*miR-125b*) in cancer tissues vs. adjacent normal tissues [N=14]; CYP24 protein levels negative correlated with the cancer/normal ratios of the miR-125b levels [cancer tissues]; target: CYP24 [MCF-7 and KGN; luciferase assay] (Komagata et al., 2009)
		Human prostatectomy specimens and PrE cells	**Down** (*miR-125b*) in tumuor tissue (n=25) than in benign prostate (n=23) [after 3-8 weeks cholecalciferol supplementation]; positive correlated with serum 25(OH)D [after cholecalciferol supplementation vs. baseline];

			Up (*miR-125b*) in 1,25(OH)D vs. ethanol; E2F3 and PLK1 protein: **down** in 1,25(OH)D vs. ethanol; negative (*miR-125b*) correlated with E2F3 [PrE cells] (Giangreco et al., 2013)
		Human leukaemia cell lines: U937 and HL60	**Down** (*miR-125b*) in 1,25(OH)D vs. without 1,25(OH)D [both U937 and HL60] (Hu et al., 2017)
		Serum and T-cells from SLE patients	**Down** (*miR-125a*) in SLE (n=42) vs. HCs (n=48) [both in serum and T-cells]; positive correlated with 25(OH)D level [T-cells] (Chen et al., 2017)
		Human liver tissues and human cell line: HepG2	**Up** (*miR-125a-5p*) in HCC (n=31) vs. NL (n=10); VDR mRNA: down in HCC vs. NL; negative correlation with hepatic VDR mRNA [liver]; VDR mRNA and protein expression: **up** in miR-125a-5p inhibitor vs. negative control; target: *VDR* (assay) [HepG2] (Xu et al., 2018)
		Human cell line: MCF-7	**Down** (*miR-125b*) in 1,25(OH)D vs. ethanol [at 72h and 96h] (Klopotowska et al., 2019)
		Human cell line: THP-1	**Up** (*miR-125b*) in 1,25(OH)D vs. without 1,25(OH)D [cells exposed to LPS] (Zhu et al., 2019b)
		VAT and SAT from obese individuals	**Down** (*miR-125a-5p/miR-125b-5p*) in SAT-N/VAT-O vs. SAT-O; negative correlated with VDR mRNA [VAT] (Jonas et al., 2019)
		Liver tissues from liver cirrhosis patients and human cell line: 293T	**Up** in cirrhosis (n=60) vs. NL (n=5); VDR : Down in cirrhosis vs. NL [liver]; target: *VDR* [293T, luciferase assay] (He et al., 2021b)
miR-146	NAFLD	Human liver	**Up** *(miR-146b-5p)* in NAFLD (n=17) vs. controls (n=19) and borderline NAFLD (n=24); positive correlation with NAFLD [bariatric surgery patients] (Latorre et al., 2017a) **Up** *(miR-146)* in steatosis (n=4) vs. non-steatosis (n=4) [liver tissue bank] (Wang et al., 2018b)
		Human serum	**Down** (miR-146b) in NAFLD (n=20) vs. HCs (n=20); discriminated NAFLD from HCs (AUROC=0.75) (Celikbilek et al., 2014) **Up** (miR-146b) in NASH (n=31) vs. HCs (n=37) (Liu et al., 2016b)
	Vitamin D	Human DCs	**Up** (miR-146a) in 1,25(OH)D treated mature DCs vs. untreated DCs (Pedersen et al., 2009)
		Serum and urinary of SLE patients	**Down** (*miR-146a*) in SLE (n=40) vs. HCs (n=30) [serum and urinary, baseline]; **Up** (*miR-146a*) 6th/3th month calcitriol treatment vs. 0th month calcitriol; positive correlated to the change of calcium-phosphate [serum of SLE patients] (Wang et al., 2010a)
		Human adipocytes	**Down** (*miR-146a*) in cells treated with pre-treated with1,25(OH)D and incubated with TNFα vs. cells treated with TNFα (Karkeni et al., 2018)
miR-155	NAFLD	Human liver	**Up** *(miR-155)* in steatosis (n=4) vs. non-steatosis (n=4) [liver tissue bank](Wang et al., 2018b) **Down** *(miR-155)* in NAFLD (n=11) vs. HCs (n=11); hepatic SREBP1c, FAS and ACC1 mRNA: **up** in NAFLD vs. HCs [biopsy consenting NAFLD and HCs](Wang et al., 2016b)
		Human serum	**Down** *(miR-155)* in NAFD (n=11) vs. HCs(n=11)(Wang et al., 2016c)

	Vitamin D	Serum of SLE patients	**Down** (*miR-155*) in SLE (n=40) vs. HCs (n=30) [baseline]; **Up** (*miR-155*) 6th/3th month calcitriol treatment vs. 0th month calcitriol [SLE patients] (Wang et al., 2010a)
		Urine sediment of SLE patients	**Up** (*miR-155*) in SLE (n=40) vs. HCs (n=13); positive correlated with proteinuria and SLEDAI; **Down** (*miR-155*) in 6th/3th month calcitriol treatment vs. 0th month calcitriol (n=40) (Wang et al., 2012a)
		Human macrophages: RAW 264.7 and PBMCs	RAW 264.7: **Down** (*miR-155*) in 1,25(OH)D vs. without 1,25(OH)D [cells expose to LPS]; target: bic gene (luciferase reporter assays and ChIP assay) PBMCs: **Down** (*miR-155*) in 1,25(OH)D vs. without 1,25(OH)D; TNF- α IL-6 and bic mRNA: down in 1,25(OH)D vs. without 1,25(OH)D [cells expose to LPS] (Chen et al., 2013a)
		Human adipocytes	**Down** (*miR-155*) in cells treated with pre-treated with1,25(OH)D and incubated with TNFα vs. cells treated with TNFα (Karkeni et al., 2018)
		Human liver and PBMCs	**Up** (*miR-155*) in cirrhotic PBC vs. PSC and controls in both liver and PBMCs; positive correlation with hepatic *VDR* mRNA and SOCS1 protein level [liver] (Kempinska-Podhorodecka et al., 2017)
		Monocyte derived macrophages	**Down** (*miR-155*) in 1,25(OH)D vs. without 1,25(OH)D [cells expose to dengue virus 2]; **down** in 1,25(OH)D vs. without 1,25(OH)D [cells expose to LPS] (Arboleda et al., 2019)
		Human serum	**Up** (*miR-155*) in vitamin D supplementation vs. placebo [after UM]; **up** in after UM vs. before UM [in the placebo group] (Pastuszak-Lewandoska et al., 2020)
miR-181	NAFLD	Human serum	**Up** *(miR-181b-3p)* in NAFLD (n=25) vs. HCs (n=21) (Wang et al., 2017) **Up** *(miR-181a-5p)* in NAFLD (n=30) vs. HCs (n=30) (Huang et al., 2019) **Down** *(miR-181d)* in NAFLD (n=20) vs. HCs (n=20); negative correlation with GGT; discriminated NAFLD from HCs (AUROC=0.86) (Celikbilek et al., 2014)
	Vitamin D	Human leukaemia cell clines: HL60 and U937	HL60: **Down** (miR-181a/b) in cells treated with 1,25(OH)D (1nM, 10nM and 100nM) vs. cells treated without 1,25(OH)D [at 48h]; **down** in 48h/96h 1,25(OH)D treated vs. 0h 1,25(OH)D treated (1nM); U937: **Down** (miR-181a/b) in cells treated with 1,25(OH)D (10nM and 100nM) vs. cells treated without 1,25(OH)D [at 48h]; **down** (miR-181a) in 24h/48h/96h 1,25(OH)D treated vs. 0h 1,25(OH)D treated (10nM) (Wang et al., 2009)
		Primary human STB from placenta cytotrophoblasts of 38-40 weeks' gestation pregnancy healthy women	**Up** (*miR-181b-5p*) in 1,25(OH)D treatment vs. without 1,25(OH)D treatment; CRH mRNA: **down** in 1,25(OH)D treatment vs. without 1,25(OH)D treatment; target: CRH (ChIP and luciferase assay) (Wang et al., 2018a)

ACC1, acetyl-CoA carboxylase; ALT, alanine aminotransferase; AST, aspartate transaminase; APRI, AST to platelet ratio index; AUROC, the area under the receiver operating characteristic; CRH, corticotropin-releasing hormone; ChIP, chromatin immunoprecipitation; CYP3A, cytochrome P450 3A; CYP24, vitamin D_3 hydroxylase; DCs, dendritic cells; F, fibrosis%; FAS, fatty acid synthase; FIB4, fibrosis 4; GFR, glomerular filtration rate; HC, healthy control; HCC, hepatocellular carcinoma; ITGA8, integrin subunit alpha 8; IL-6, interleukin 6; LPS, lipopolysaccharide; NAFLD, non-alcoholic fatty liver disease; NAFL, non-alcoholic fatty liver; NL, normal liver; NAS, NAFLD activity score; NASH, non-alcoholic steatohepatitis; PBMCs, human peripheral blood mononuclear cells; PLK1, polo-like kinase 1; AR, allergic rhinitis; HC, healthy control; SLE, systemic lupus erythematosus; NS, not specified; NR, not reported; 25(OH)D, 25-hydroxyvitamin D; 1,25(OH)D, 1,25-dihydroxyvitamin D; OR, odds ratio; PBS, primary biliary cholangitis; PPARα, peroxisome proliferator-activated receptor α; PrE, primary prostatic epithelial cells; PSC, primary sclerosing cholangitis; SAF, steatosis, activity, fibrosis score; SAT, subcutaneous adipose tissue; SAT-N, SAT- normal weight; SLE, systemic lupus erythematosus; SLEDAI, systemic lupus erythematosus disease activity index; α-SMA, α-smooth muscle actin; SOCS1, suppressor of cytokine signalling 1; SREBP1c, sterol regulatory element-binding protein 1c; STB, syncytiotrophoblast; TGF-1β, transforming growth factor- β1; TNF-α, tumour necrosis factor- α; TNFAIP3, tumour necrosis factor alpha-induced protein 3; UM, ultra-marathon; VAT, visceral adipose tissues; VAT-O, VAT-obese; VDR, vitamin D receptor; * Serum samples collected from general population, liver samples collected form liver bank; § CYP3A activity in liver measured by dextromethorphan N-demethylation and in serum measured by 4β-hydroxycholesterol; † TGF-1β used to induce differentiation of fibroblasts into myofibroblasts.

Appendix C
Supplementary Data Figures for Chapter 4

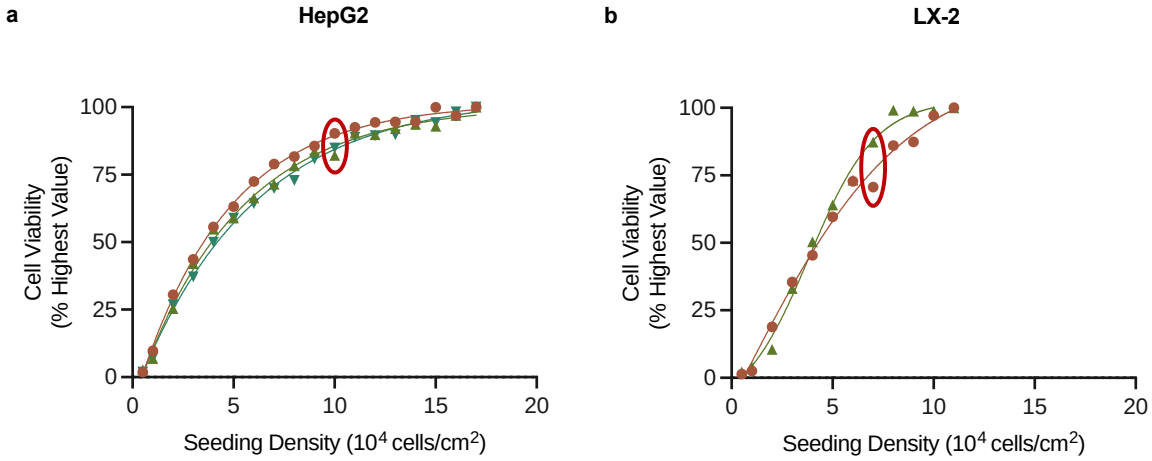

Appendix Figure C 1 Cell viability 24h after seeding at different densities. Cells were seeded at different densities and cultured in 96-well plates (0.96cm^2/well) in FBS containing DMEM medium. Cell viability was measured by MTT assay. **a.** HepG2 seeding density after 24h seeding (from 0.5x10^4 to 1.7x 10^{5}cells/cm^2, n=3). **b.** LX-2 seeding density after 24h seeding (from 0.5x 10^4 to 1.1x 10^{5}cells/cm^2, n=2). Data are shown as mean of four technical replicates. Red circles mark selected density for subsequent 24h set-up experiments (Chapter 4) onwards. Note: Each line represents one biological repeat.

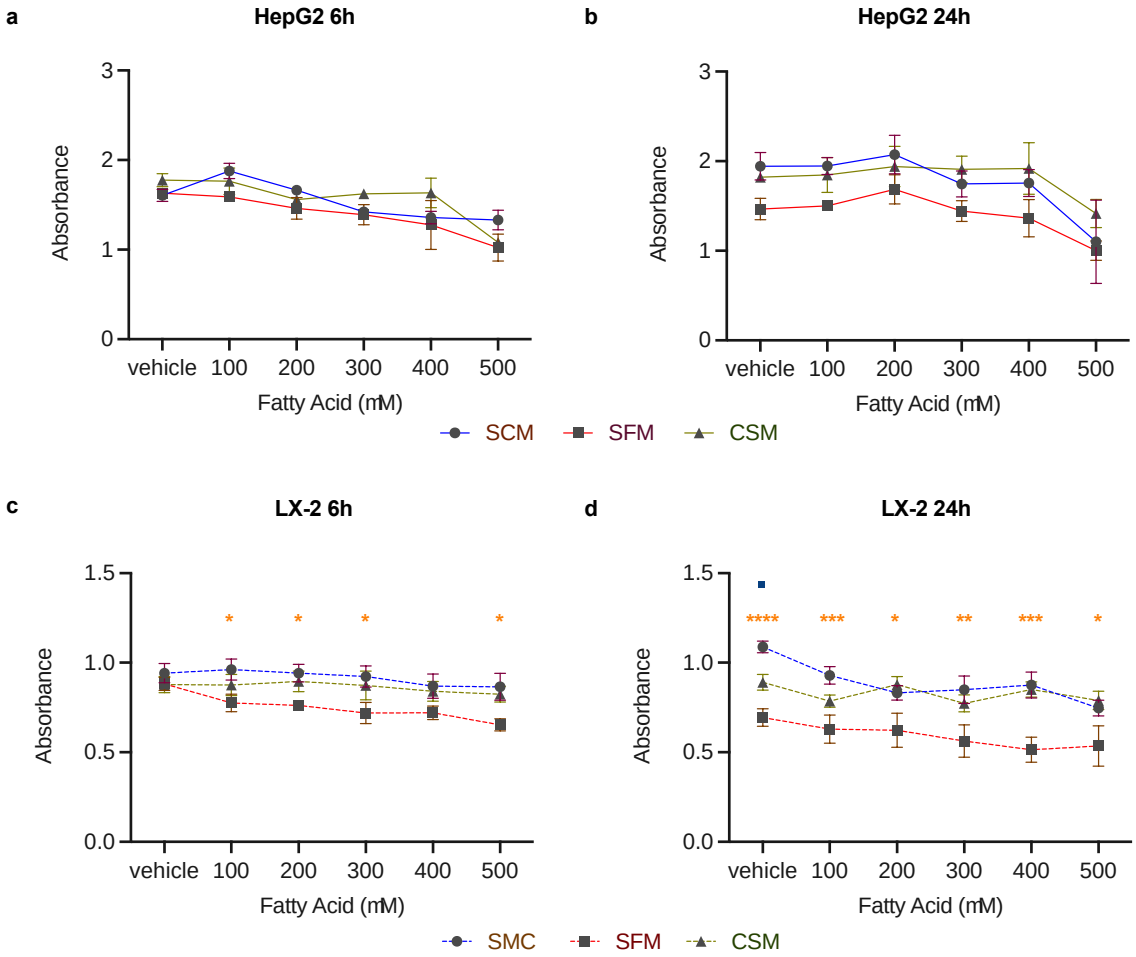

Appendix Figure C 2 Serum effects on cell viability with data presented as raw absorbance. Cell viability was detected by MTT assay after PA and OA (1:1, 0-500μM) treatment with SCM, SFM and CSM. Data are shown as mean±SEM and were analysed by two-way ANOVA with Holm-Sidak test for multiple comparisons. **a.** 6h HepG2 cell viability (n=3; FA dose: P<0.0001, serum: P=0.0185). **b.** 24h HepG2 cell viability (n=3; FA dose: P=0.0012, serum: P=0.0017). **c.** 6h LX-2 cell viability (n=5; FA dose: P>0.05, serum: P<0.0001). **d.** 24h LX-2 cell viability (n=5; FA dose: P=0.0077, serum: P<0.0001). Multiple comparisons examining differences between SCM and SFM are denoted on the graphs by orange asterisks *P<0.05, **P<0.01, ***P<0.001 and ****P<0.0001; differences between SCM and CSM are denoted as blue squares: ▪P<0.05.

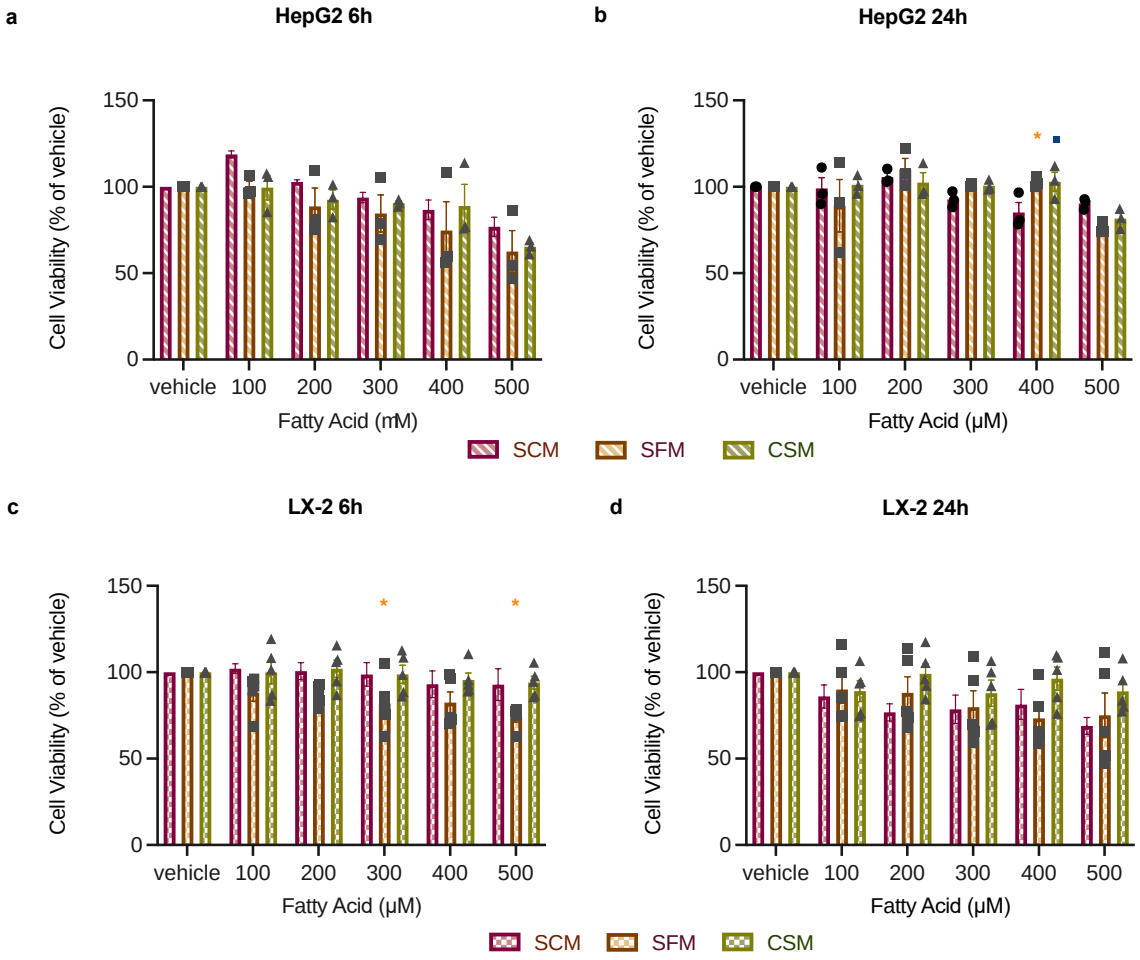

Appendix Figure C 3 Serum effects on cell viability with data presented relative to vehicle. Cell viability was was detected by MTT assay after PA and OA (1:1, 0-500µM) treatment with SCM, SFM and CSM. Data are shown as mean±SEM and were analysed by two-way ANOVA with Holm-Sidak test for multiple comparisons. **a.** 6h HepG2 cell viability (n=3; FA dose: P<0.0001, serum: P=0.0367). **b.** 24h HepG2 cell viability (n=3; FA dose: P=0.0001, serum: P>0.05). **c.** 6h LX-2 cell viability (n=5; FA dose: P=0.0347, serum: P<0.0001). **d.** 24h LX-2 cell viability (n=5; FA dose: P=0.0066, serum: P=0.0144). Multiple comparisons examining differences between SCM and SFM are denoted on the graphs by orange asterisks *P<0.05; differences between SCM and CSM are denoted as blue squares: ▪P<0.05.

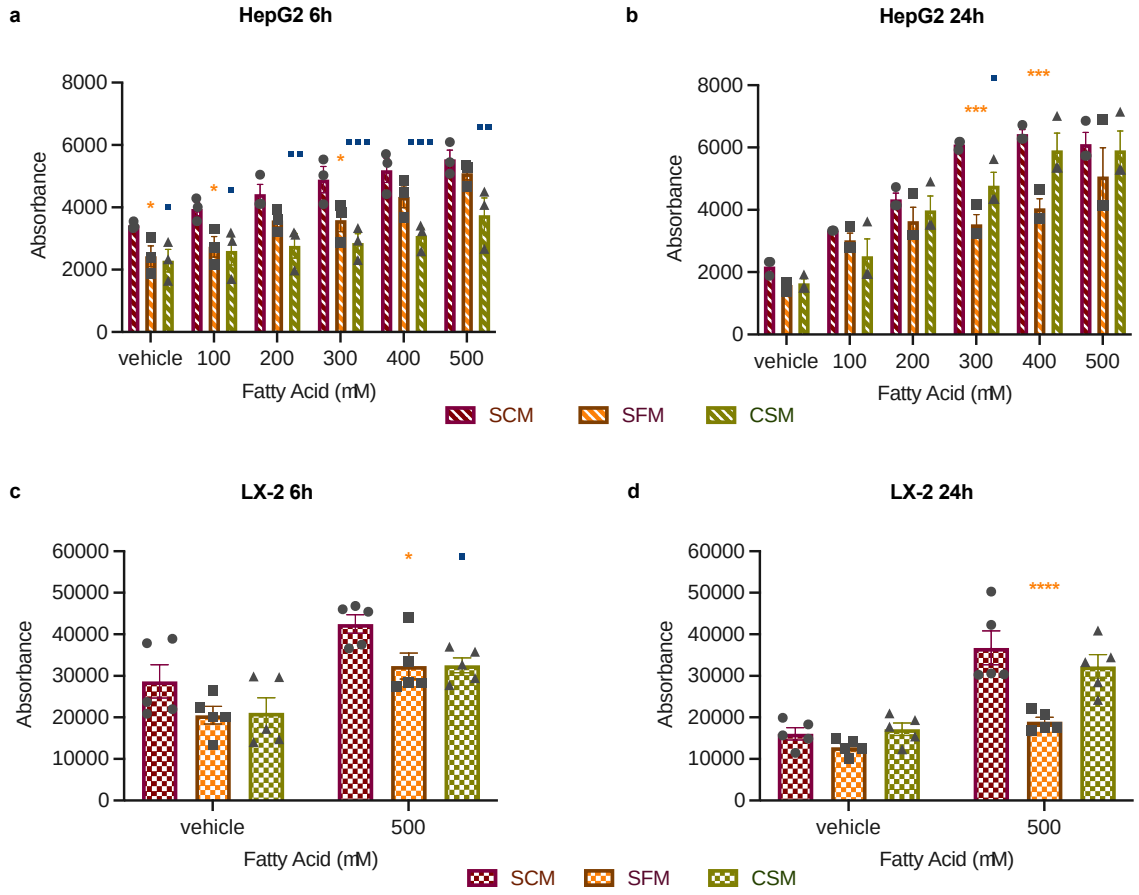

Appendix Figure C 4 Serum effects on lipid accumulation with data presented as raw absorbance. Lipid accumulation was detected by Nile red after PA and OA (1:1, 0-500μM) treatment with SCM, SFM and CSM. Data are shown as mean±SEM and were analysed by two-way ANOVA with Holm-Sidak test for multiple comparisons. **a.** 6h HepG2 intracellular lipid accumulation (n=3; FA dose: P<0.0001, serum: P<0.0001). **b.** 24h HepG2 intracellular lipid accumulation (n=3; FA dose: P<0.0001, serum: P<0.0001). **c.** 6h LX-2 intracellular lipid accumulation (n=5; FA dose: P<0.0001, serum: P=0.0066). **d.** 24h LX-2 intracellular lipid accumulation (n=5; FA dose: P<0.0001, serum: P=0.0002). Multiple comparisons examining differences between SCM and SFM are denoted on the graphs by orange asterisks: *P<0.05, ***P<0.001 and ****P<0.0001; differences between SCM and CSM are denoted as blue squares: ▪P<0.05, ▪▪P<0.01 and ▪▪▪▪P<0.0001.

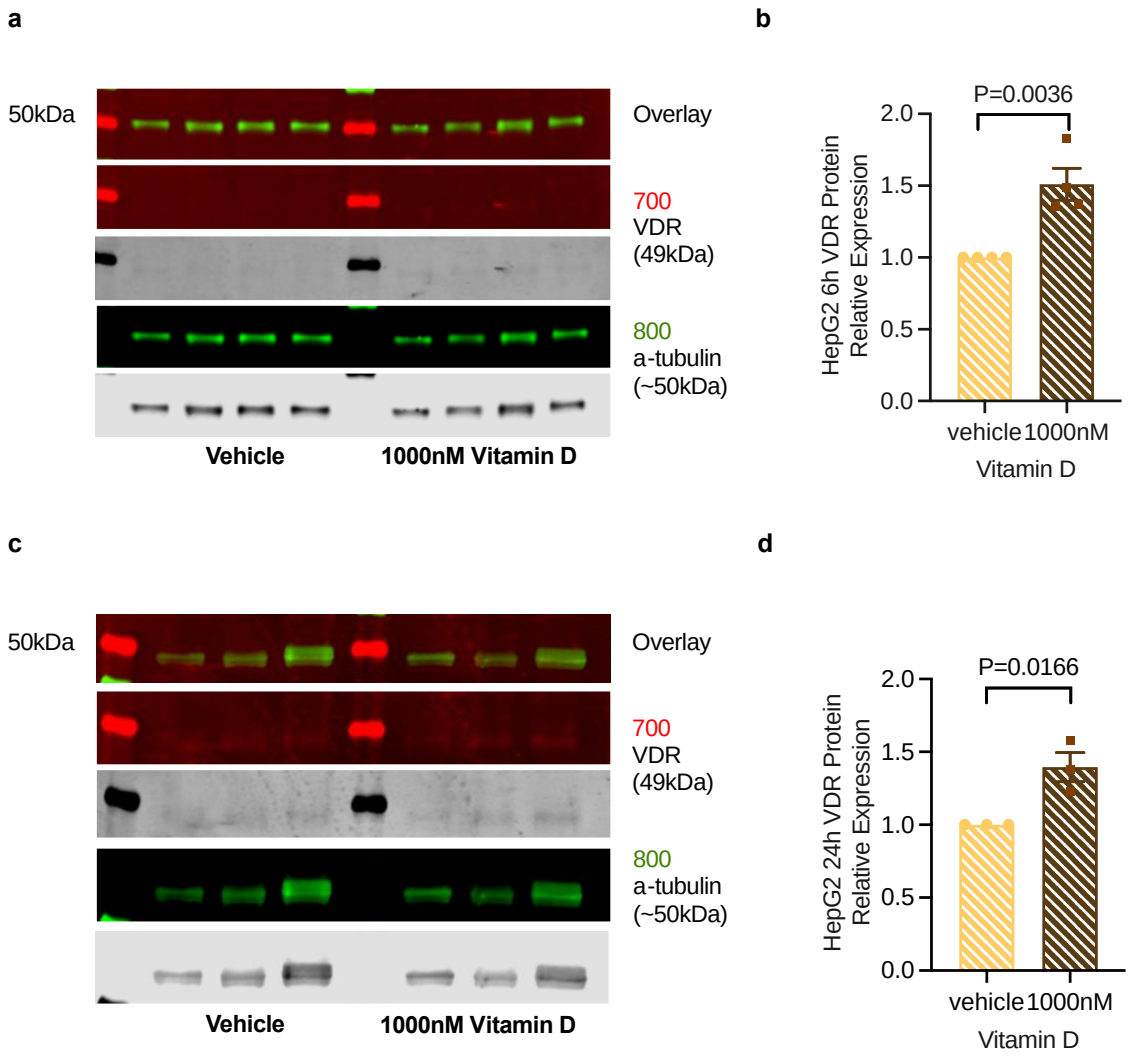

Appendix Figure C 5 VDR protein expression in response to 6h and 24h vitamin D treatment in HepG2 cells cultured in SFM. Data are normalised to α-Tubulin and shown as mean±SEM. Data were analysed by un-paired T-test. P<0.05 was considered statistically significant. **a.** Immunoblot of VDR protein expression with α-Tubulin in HepG2 [6h, vehicle (0.1% ethanol) and 1000nM; HepG2 n=3]. **b.** VDR protein relative expression in HepG2 [6h, vehicle (0.1% ethanol) and 1000nM; HepG2 n=3; related to vehicle]. **c.** Immunoblot of VDR protein expression with α-Tubulin in HepG2 [24h, vehicle (0.1% ethanol) and 1000nM; HepG2 n=3]. **d.** VDR protein relative expression in HepG2 [24h, vehicle (0.1% ethanol) and 1000nM; HepG2 n=3; related to vehicle].

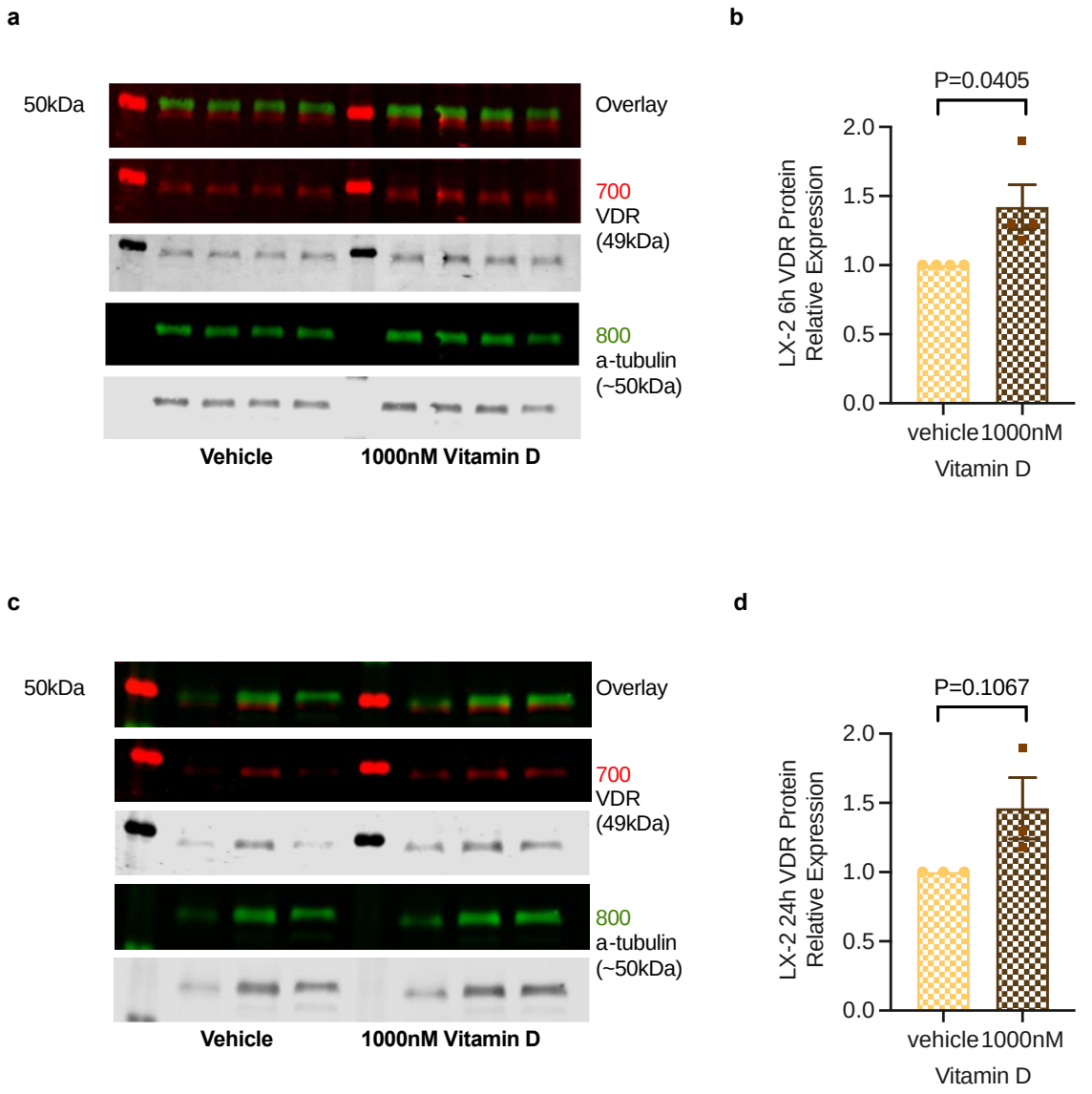

Appendix Figure C 6 VDR protein expression in response to 6h and 24h vitamin D treatment in LX-2 cells cultured in serum-free media. Data are normalised to α-Tubulin and shown as mean ± SEM. Data were analysed by un-paired T-test. P<0.05 was considered statistically significant. **a.** Immunoblot of VDR protein expression with α-tubulin in LX-2 [6h, vehicle (0.1% ethanol) and 1000nM; LX-2 n=3]. **b.** VDR protein relative expression in LX-2 [6h, vehicle (0.1% ethanol) and 1000nM; LX-2 n=3; related to vehicle]. **c.** Immunoblot of VDR protein expression with α-Tubulin in LX-2 [24h, vehicle (0.1% ethanol) and 1000nM; LX-2 n=3]. **d.** VDR protein relative expression in LX-2 [24h, vehicle (0.1% ethanol) and 1000nM; LX-2 n=3; related to vehicle].

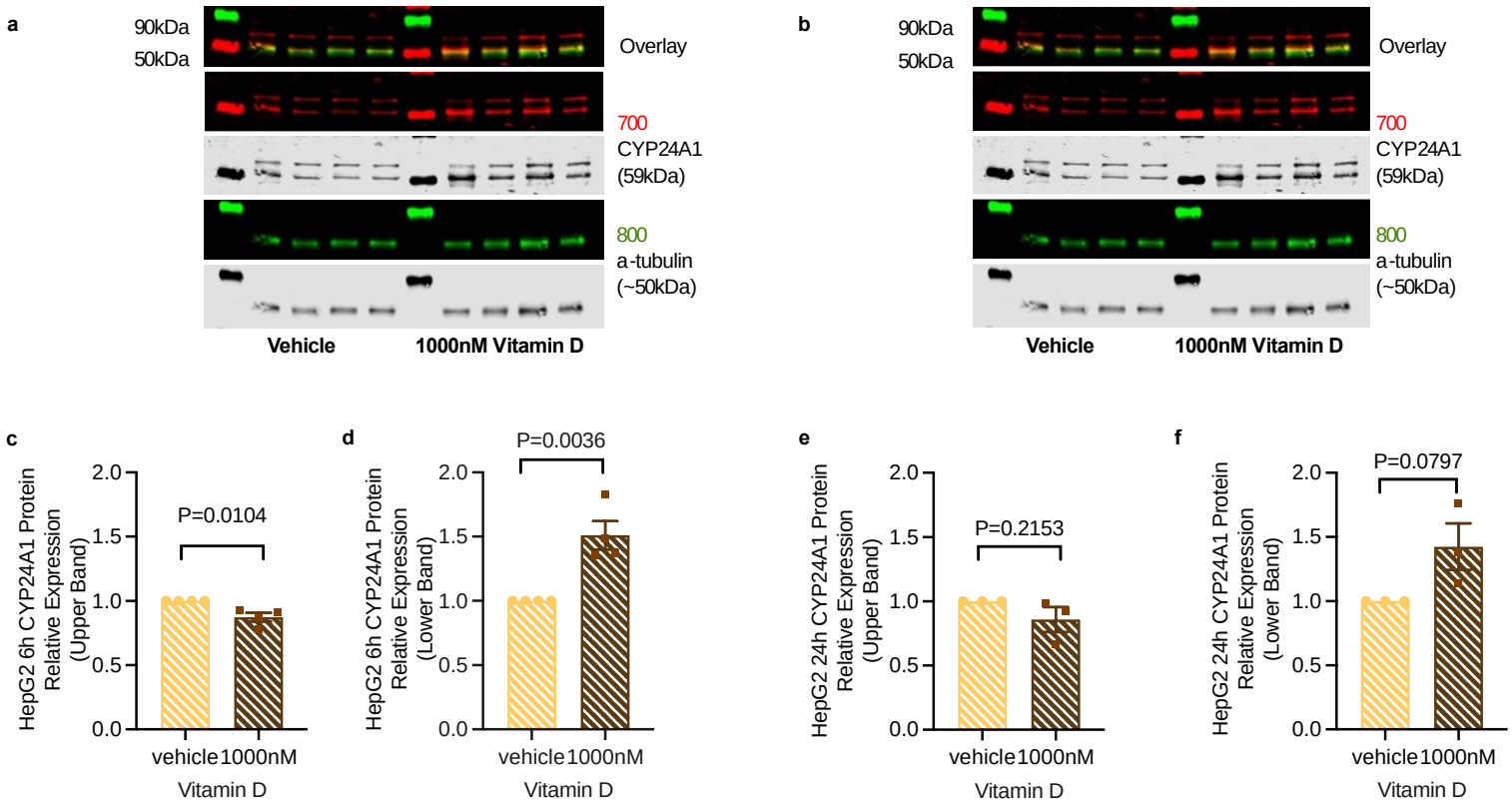

Appendix Figure C 7 CYP24A1 protein expression in response to 6h and 24h vitamin D treatment in HepG2 cells cultured in SFM. Data are normalised to α-Tubulin and shown as mean±SEM. Data were analysed by un-paired T-test. P<0.05 was considered statistically significant. **a.** Immunoblot of CYP24A1 protein expression with α-tubulin in HepG2 [6h, vehicle (0.1% ethanol) and 1000nM; HepG2 n=3]. **b.** Immunoblot of CYP24A1 protein expression with α-Tubulin in HepG2 [24h, vehicle (0.1% ethanol) and 1000nM; HepG2 n=3]. **c.** CYP24A1 protein relative expression in HepG2 (6h upper bands; related to vehicle]. **d.** CYP24A1 protein relative expression in HepG2 [6h lower bands; related to vehicle]. **e.** CYP24A1 protein relative expression in HepG2 (24h upper bands; related to vehicle]. **f.** CYP24A1 protein relative expression in HepG2 (24h lower bands; related to vehicle).

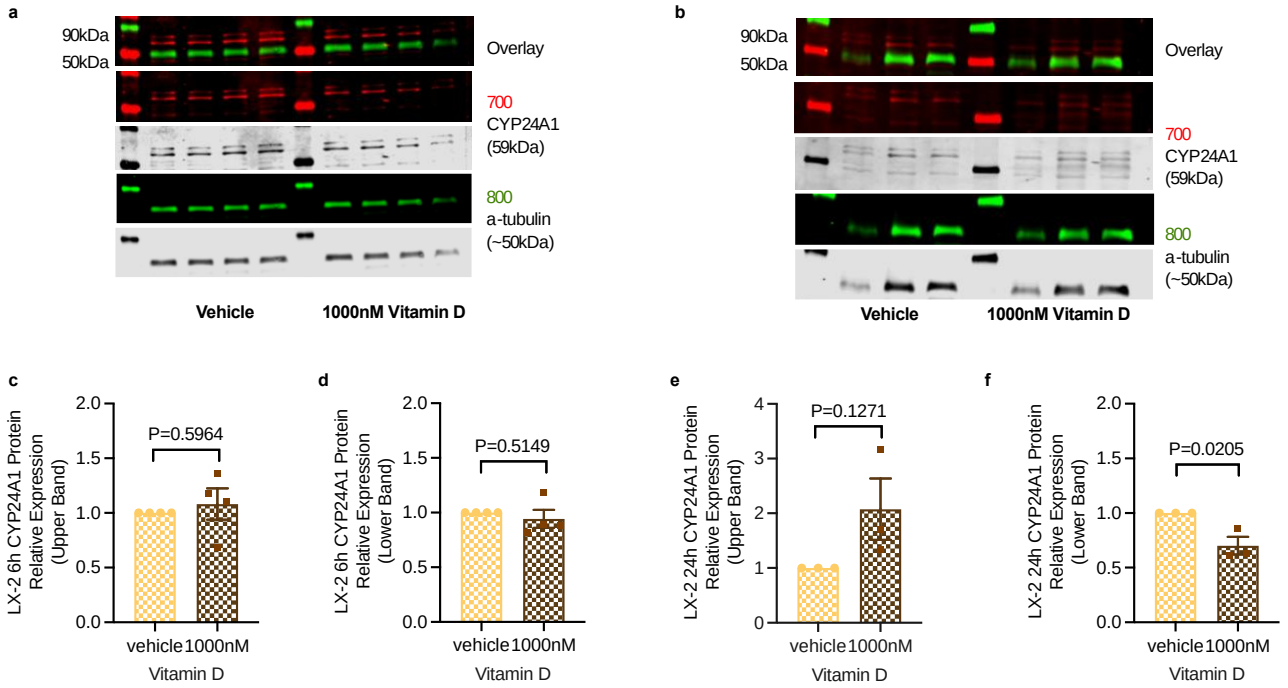

Appendix Figure C 8 CYP24A1 protein expression in response to 6h and 24h vitamin D treatment in LX-2 cultured in SFM. Data are normalised to α-Tubulin and shown as mean±SEM. Data were analysed by un-paired T-test. P<0.05 was considered statistically significant. **a.** Immunoblot of CYP24A1 protein expression with α-tubulin in LX-2 [6h, vehicle (0.1% ethanol) and 1000nM; HepG2 n=3]. **b.** Immunoblot of CYP24A1 protein expression with α-Tubulin in LX-2 [24h, vehicle (0.1% ethanol) and 1000nM; HepG2 n=3]. **c.** CYP24A1 protein relative expression in LX-2 (6h upper bands; related to vehicle]. **d.** CYP24A1 protein relative expression in HepG2 [6h lower bands; related to vehicle]. **e.** CYP24A1 protein relative expression in LX-2 (24h upper bands; related to vehicle]. **f.** CYP24A1 protein relative expression in LX-2 (24h lower bands; related to vehicle).

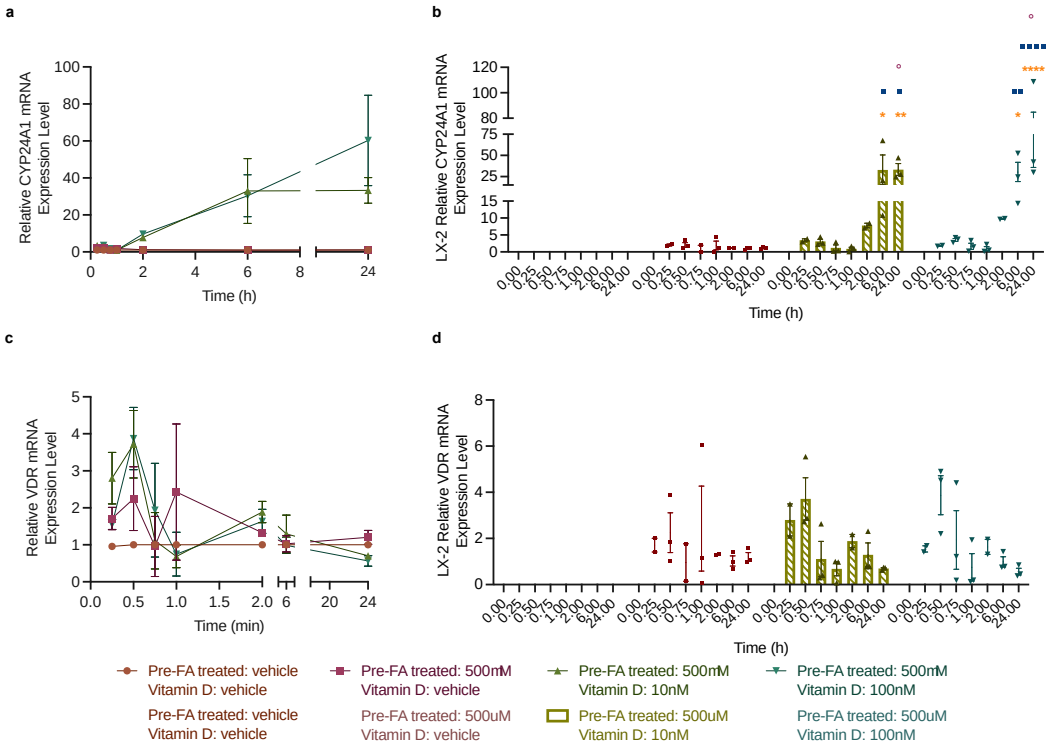

Appendix Figure C 9 CYP24A1 and VDR mRNA expression in response to pre-fatty acid and vitamin D treatment in LX-2 with SFM. LX-2 cells were pre-treated with FA [vehicle (2%DMSO) or 500μM] with SFM for 6h, and then treated with different doses of vitamin D [vehicle (0.01% ethanol), 10nM and 100nM] with SFM. Data are relative to 18S rRNA and shown as mean±SEM. Data were analysed by two-way ANOVA with Holm-Sidak test for multiple comparisons. **a.** CYP24A1 mRNA expression in response to 24h vitamin D treatment in LX2 (n=3; Time: P<0.0001, Treatment: P=0.0005). **b.** CYP24A1 mRNA expression in response to 24h vitamin D treatment in LX2 (based on different treatment group). **c.** VDR mRNA expression in response to 24h vitamin D treatment in LX2 (n=3; Time: P=0.0038, Treatment: P>0.05). **d.** VDR mRNA expression in response to 24h vitamin D treatment in LX2 (based on different treatment group). Multiple comparisons examining differences relative to vehicle/vehicle are denoted on the graphs by orange asterisks: *P<0.05, **P<0.01 and ****P<0.0001; differences relative to 500μM/vehicle are denoted as blue squares: ▪P<0.05, ▪▪P<0.01 and ▪▪▪▪P<0.0001; differences relative to 500μM/10nM are denoted as red circle: ° P<0.05.

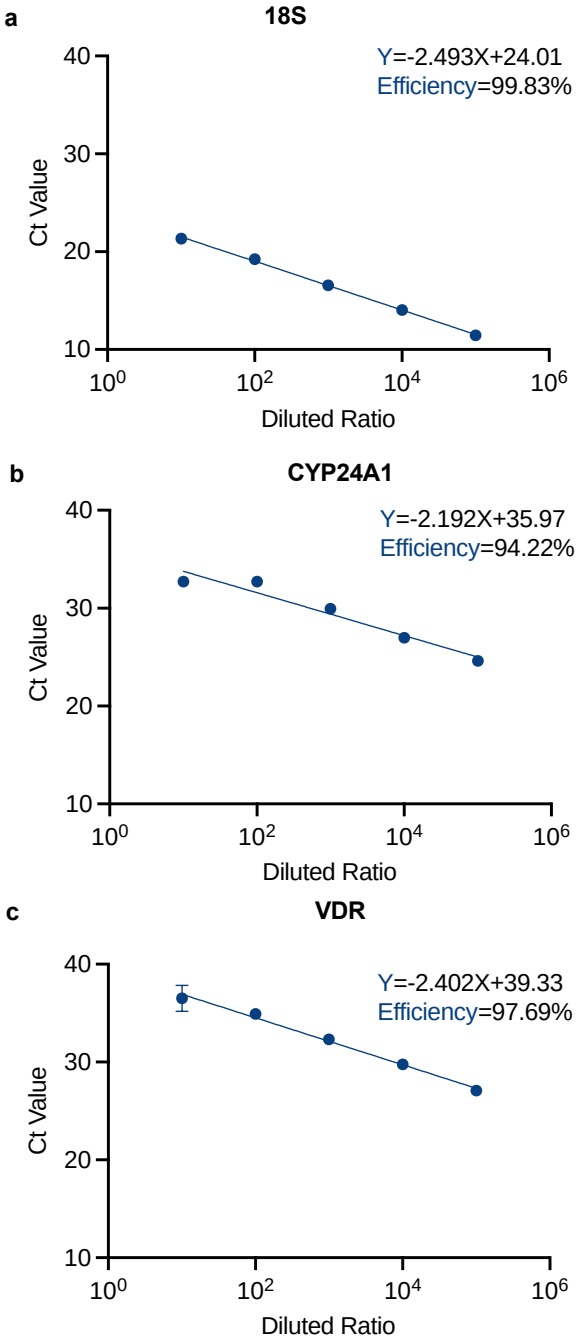

Appendix Figure C 10 mRNA expression assays standard curves. cDNAs synthesized from 2μg human small intestine reference RNA and untreated HepG2 RNA mixture (mixed at 1:1) and diluted at 1:10 from each point. Each point represents a duplicate technical repeats. Standard curve for 18S (**a**), CYP24A1 (**b**) and VDR (**c**).

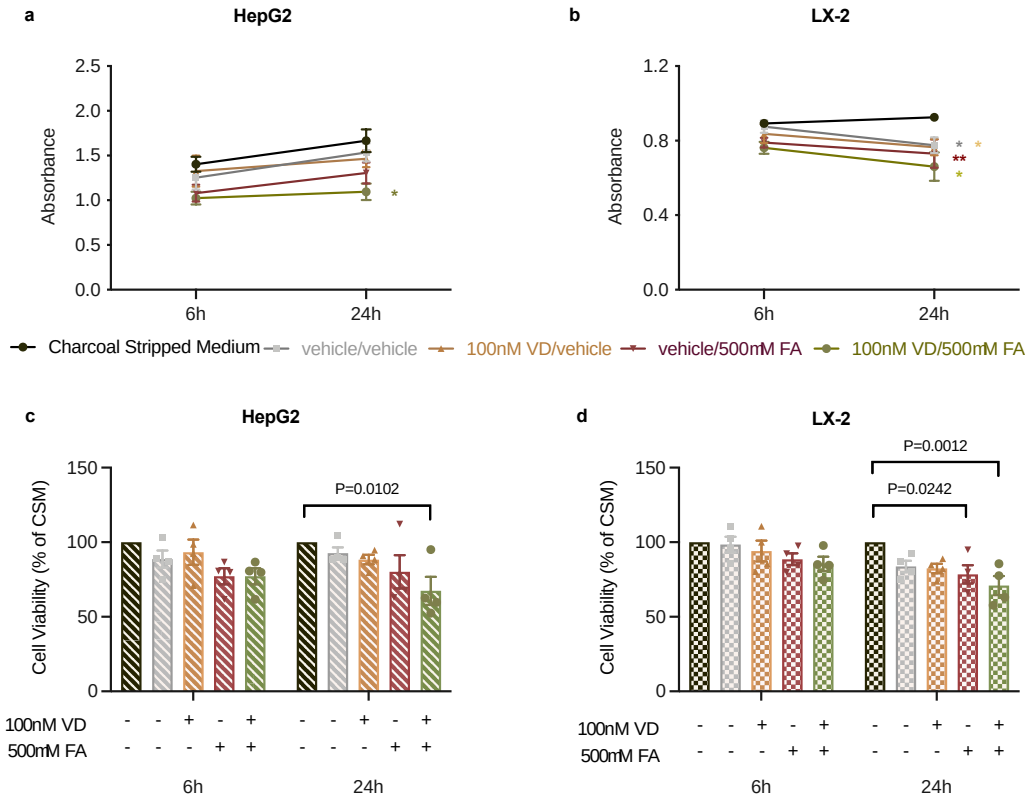

Appendix Figure C 11 Cell viability after cultured either with or without fatty acids or vitamin D with data presented as raw absorbance or relative to CSM. Cell viability was detected by MTT assay after culturing in CSM, and either with or without PA and OA (1:1) treatment (500μM) or vitamin D treatment (100nM). Data are shown as mean±SEM. Data were analysed by two-way ANOVA with Holm-Sidak test for multiple comparisons. **a.** 6h and 24 HepG2 cell viability (n=4; Treatment: P=0.0018, Time: P=0.0101). **b.** 6h and 24h LX-2 cell viability (n=4, Treatment: P=0.0026, Time: P=0.0494). Data are raw absorbance. Multiple comparisons examining differences at 24h relative to CSM is denoted on the graphs by different colours of asterisks: *P<0.05, **P<0.001. **c.** 6h and 24 HepG2 cell viability (Treatment: P=0.0012, Time: P>0.05). **d.** 6h and 24h LX-2 cell viability (Treatment: P=0.0009, Time: P=0.0016). Data are related to CSM. P<0.05 is considered statistically significant between different groups in multiple comparisons.

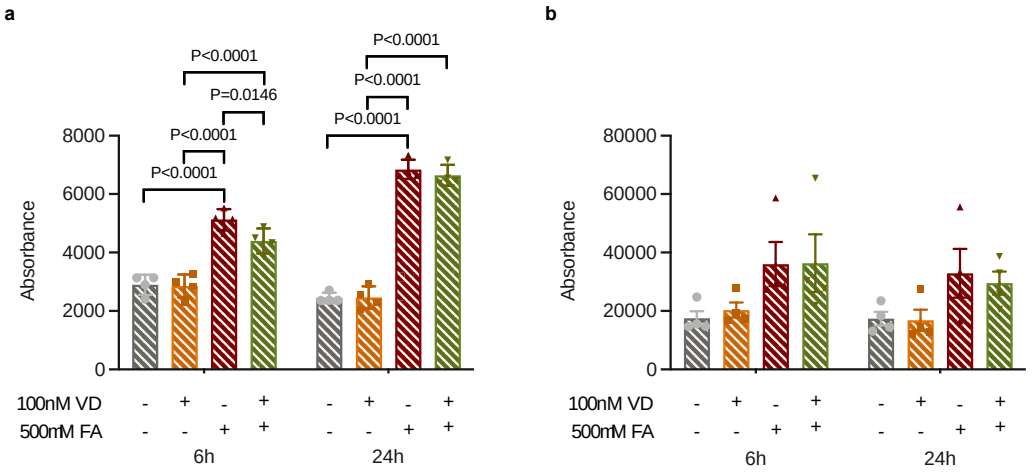

Appendix Figure C 12 Intracellular lipid accumulation after cultured either with or without fatty acids or vitamin D with data presented as raw absorbance. Lipid was detected by Nile red staining of cells after either with or without PA and OA (1:1) treatment (500μM) or vitamin D treatment (100nM). Data are shown as mean±SEM. Data were analysed by two-way ANOVA with Holm-Sidak test for multiple comparisons. **a.** 6h and 24h HepG2 intracellular lipid accumulation (n=4; Treatment: P<0.0001, Time: P<0.0001). **b.** 6h and 24h LX-2 intracellular lipid accumulation (n=4, Treatment: P=0.0084, Time: P>0.05). P<0.05 is considered statistically significant between different groups in multiple comparisons.

Appendix D
Supplementary Data Figures and Tables for Chapter 5

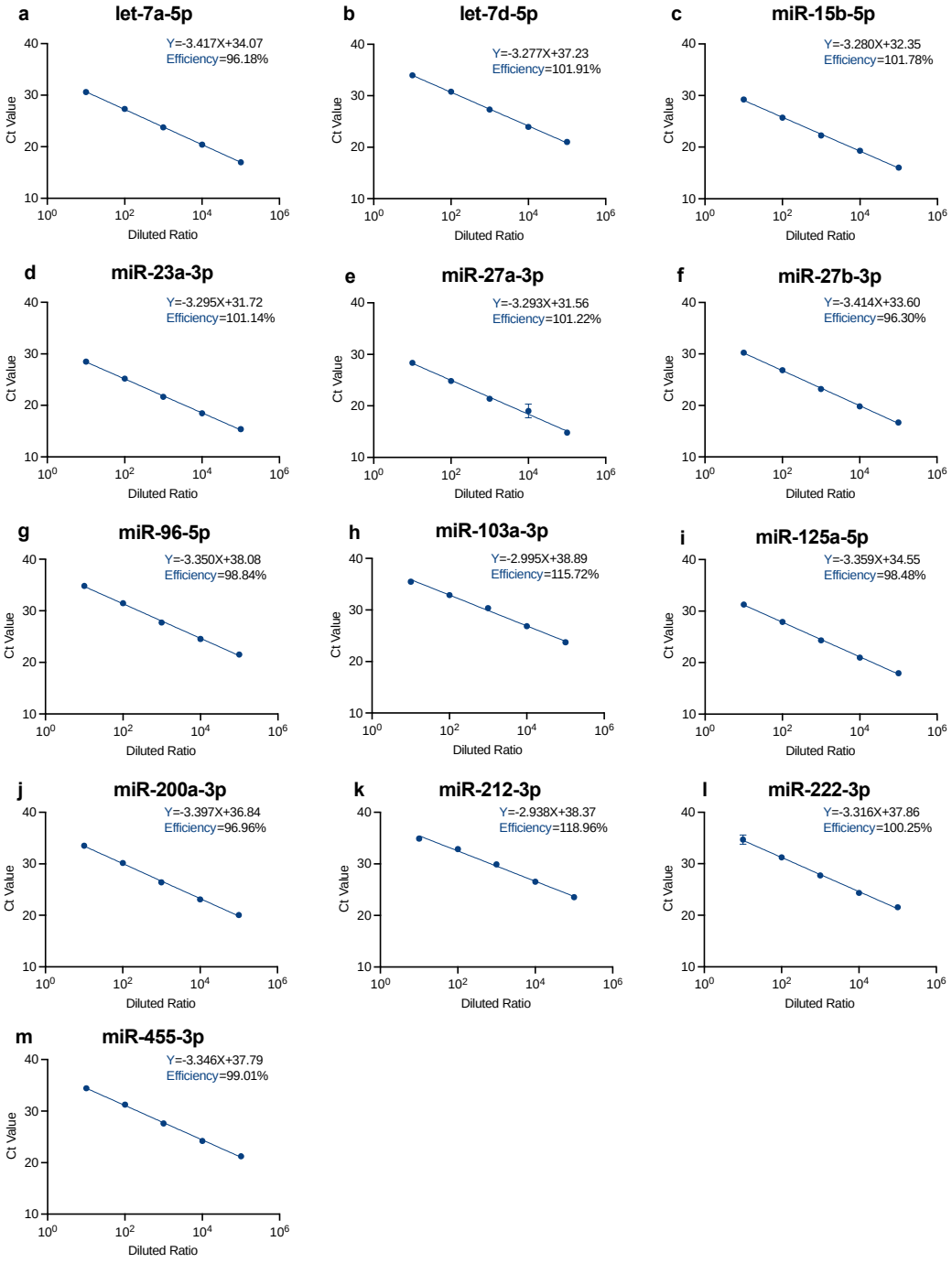

Appendix Figure D 1 Standard curves for miRNA assays. cDNAs were synthesized from 10ng universal human reference total miRNA and serially diluted 1:10. Each point represents duplicate technical repeats. **a.** let-7a-5p, **b.** let-7a-5p, **c.** miR-15b-5p, **d.** miR-23a-3p, **e.** miR-27a-3p, **f.** miR-27b-3p, **g.** miR-96-5p, **h.** miR-103a-3p, **i.** miR-125a-5p, **j.** miR-200a-3p, **k.** miR-212-3p, **l.** miR-22-3p, **m.** miR-455-3p.

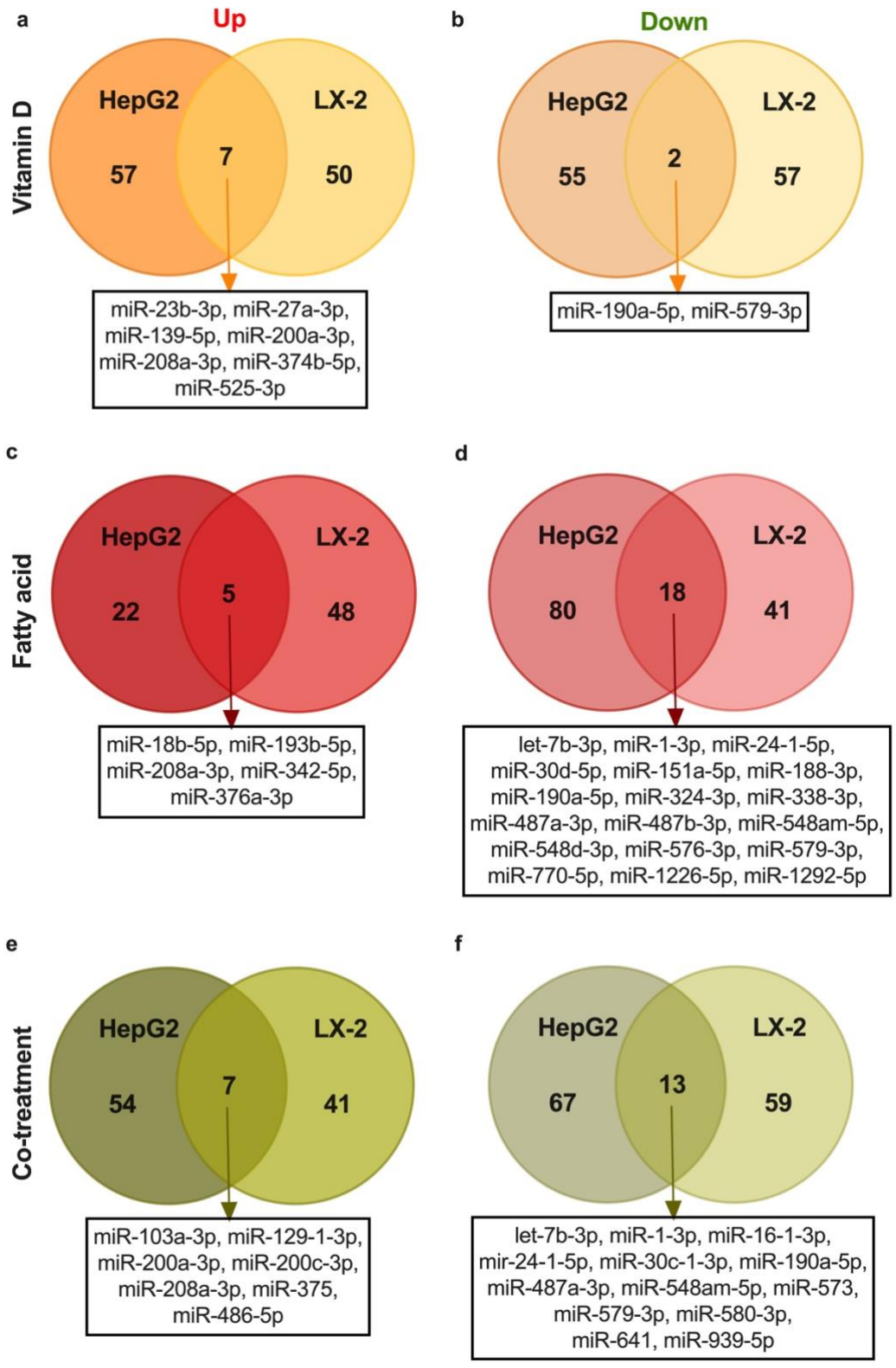

Appendix Figure D 2 Venn diagram illustration of dysregulated miRNAs in common between HepG2 and LX-2 cells in different treatments. A relative FC>2.85 was hypothesised as 'upregulated', and FC<0.67 was 'downregulated'. MicroRNAs upregulated (**a.**) or downregulated (**b.**) in vitamin D treated HepG2 and LX-2 cells; MicroRNAs upregulated (**c.**) or downregulated (**d.**) in FA treated HepG2 and LX-2 cells; MicroRNAs upregulated (**e.**) or downregulated (**f.**) in cotreatment treated HepG2 and LX-2 cells.

Appendix Table D 1 MiRNAs not recognised in miRWalk and adjustments made to name prior to retesting.

miRNA Name	Change	Recognised	Delete
hsa-miR-137	Add 3p and 5p	Yes	
hsa-miR-147b	Add 3p and 5p	Yes	
hsa-miR-190b	Add 3p and 5p	Yes	
hsa-miR-217	Add 3p and 5p	Yes	
hsa-miR-220	Add 3p and 5p	No	Yes
has-miR-220c	Add 3p and 5p	No	Yes
hsa-miR-375	Add 3p and 5p	Yes	
hsa-miR-549a	Add 3p and 5p	Yes	
hsa-miR-672	Add 3p and 5p	No	Yes
hsa-miR-674	Add 3p and 5p	No	Yes
hsa-miR-886-5p	Remove 5p and add 3p	No	Yes
hsa-miR-1254	Add 3p and 5p	No	Yes
hsa-miR-1259	Add 3p and 5p	No	Yes
hsa-miR-1274b	Add 3p and 5p	No	Yes

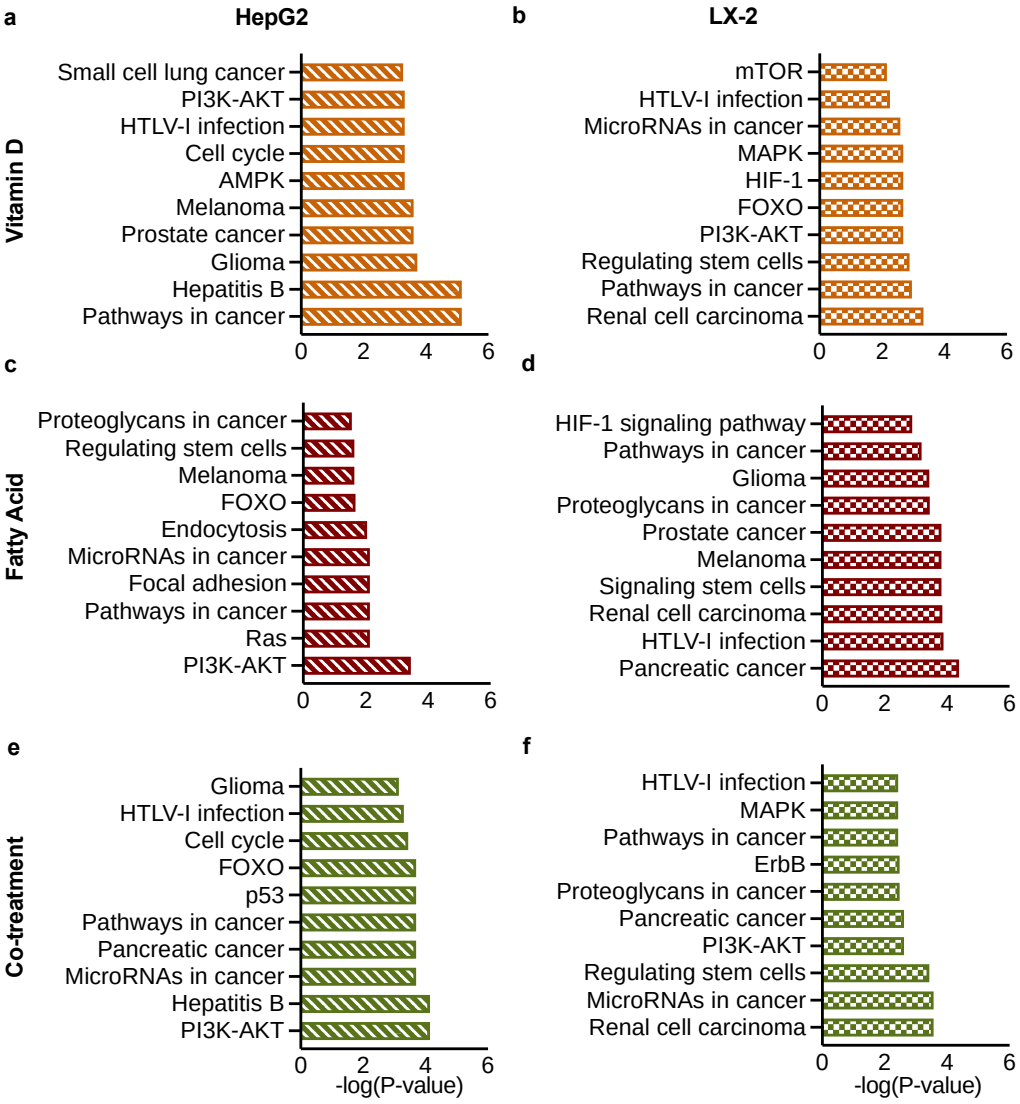

Appendix Figure D 3 Top ten KEGG pathways enriched significantly in vitamin D and/or FA treated HepG2 and LX-2 cells. Data are shown as -log(P-value). P<0.05 was considered statistically significant. The significantly enriched KEGG pathways in vitamin D treated HepG2 (**a**) and LX-2 (**b**) cells, in FA treated HepG2 (**c**) and LX-2 (**d**) cells, and in vitamin D and FA cotreated HepG2 (**e**) and LX-2 (**f**) cells. AMPK, AMP-activated protein kinase; FOXO, forkhead box O; HIF-1, hypoxia inducible factor-1; HTLV-I, human T-lymphotropic virus type 1; MAPK, mitogen-activated protein kinase; mTOR, mammalian target of rapamycin; PI3K-AKT, phosphatidylinositol 3-kinase-protein kinase B.

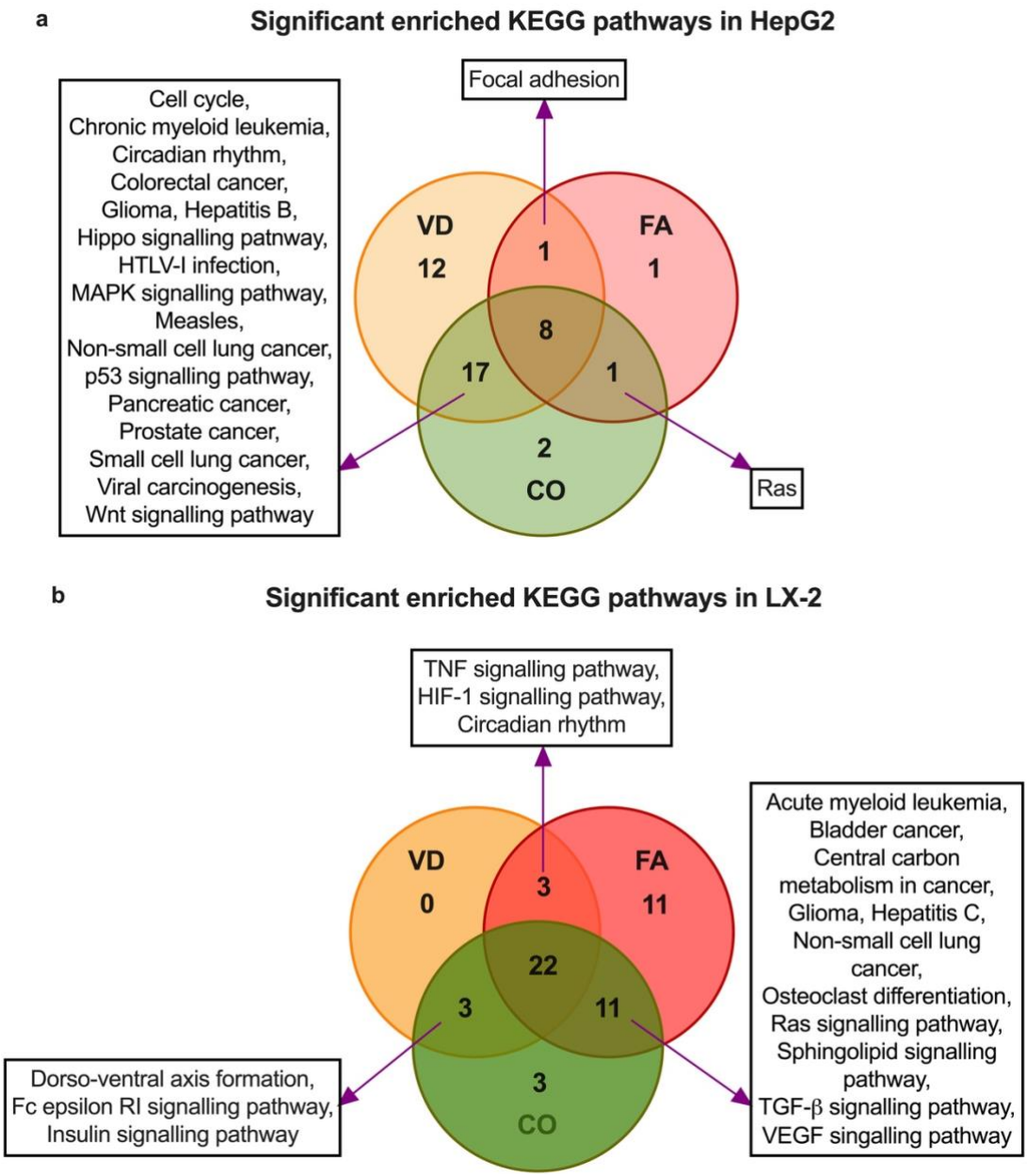

Appendix Figure D 4 Venn diagram illustration of significant KEGG pathways in common between vitamin D and/or FA and/or cotreatment (CO) treated HepG2 and LX-2 cells. P<0.05 was considered statistically significant. Venn diagram and a list showing significant KEGG pathways in common between two treatment groups in HepG2 cells (**a**) and LX-2 cells (**b**).

Appendix Table D 2 HepG2 miRNA sample collection dates and optical density data.

	Lable Name	Passage No.	Treatment	Collected Date	Extracted Date	Con. (ng/ul)	260/230	260/280	Last Quantification Date	cDNA Synthesis Date	Con. (ng/ul)	260/230	260/280
n=1	H1A	p16	vv	04/03/2020	15/03/2020	31.32	0.79	1.84	27/04/2021	27/04/2021	31.8	0.83	1.87
	H1B		v100			41.33	0.63	1.77			37.6	0.77	1.88
	H1C		500v			38.12	1.09	1.89			38.18	1.09	1.89
	H1D		500100			34.52	0.88	1.9			36.01	0.88	1.88
n=2	H2A	p17	vv	07/04/2020	15/03/2020	35.68	0.7	1.85	27/04/2021	27/04/2021	34.44	0.71	1.86
	H2B		v100			28.01	0.47	1.82			28.8	0.47	1.84
	H2C		500v			30.16	0.45	1.83			29.3	0.46	1.83
	H2D		500100			38.24	0.67	1.84			40.54	0.66	1.87
n=3	H3A	p18	vv	10/03/2020	15/03/2020	25.77	0.7	1.83	27/04/2021	27/04/2021	23.64	0.63	1.84
	H3B		v100			29.89	0.7	1.89			27.8	0.61	1.79
	H3C		500v			20.66	0.81	1.8			18.61	0.76	1.69
	H3D		500100			25.63	1	1.83			23.81	0.92	1.82
n=4	H4A	p19	vv	13/03/2020	15/03/2020	27.57	0.57	1.85	27/04/2021	27/04/2021	26.38	0.5	1.78
	H4B		v100			37.14	0.73	1.76			37.31	0.67	1.71
	H4C		500v			36.69	0.99	1.8			32.9	1.06	1.78
	H4B		500100			36.04	0.72	1.74			34.94	0.68	1.7
n=5	H5A	p6	vv	24/10/2020	18/02/2021	24.55	1.2	1.88	27/04/2021	27/04/2021	23.64	1.05	1.84
	H5B		v100			28.02	0.86	1.75			27.8	1.09	1.79
	H5C		500v			20.17	1.37	1.84			18.61	1.23	1.69
	H5D		500100			23.28	1.04	1.86			23.81	0.93	1.82
n=6	H6A	p11	vv	11/11/2020	18/02/2021	24.36	1.28	1.92	27/04/2021	27/04/2021	26.38	1.14	1.78
	H6B		v100			29.66	1.03	1.8			37.31	1.19	1.71
	H6C		500v			21.72	1.51	1.92			32.9	1.11	1.78
	H6D		500100			25.73	1.26	1.89			34.94	1.03	1.7

Appendix Table D 3 LX-2 miRNA sample collection dates and optical density data.

	Lable Name	Passage No.	Treatment	Collected Date	Extracted Date	Con. (ng/ul)	260/230	260/280	Last Quantification Date	cDNA Synthesis Date	Con. (ng/ul)	260/230	260/280
n=1	L3A	P13A	vv	19/11/2020	01/12/2020	28.24	0.1	1.86	27/04/2021	27/04/2021	26.05	0.08	1.9
	L3B		v100			27.23	0.15	1.83			26.68	0.07	1.89
	L3C		500v			27.12	0.09	1.8			23.82	0.83	1.84
	L3D		500100			26.04	0.05	1.9			23.2	1.09	1.93
n=2	L4A	P14A	vv	21/11/2020	01/12/2020	22.99	0.27	1.72	27/04/2021	27/04/2021	21.17	0.21	1.91
	L4B		v100			23.82	0.06	1.9			24.34	0.04	2.04
	L4C		500v			22.38	0.06	1.87			24.04	0.05	1.95
	L4D		500100			22.4	0.16	1.82			21.78	0.12	1.88
n=3	L5A	P15A	vv	25/11/2020	01/12/2020	26.71	0.24	1.6	27/04/2021	27/04/2021	26.28	0.21	1.67
	L5B		v100			27.77	0.48	1.75			26.25	0.41	1.77
	L5C		500v			30.28	0.51	1.74			26.75	0.47	1.78
	L5D		500100			29.39	0.58	1.74			26.12	0.54	1.84
n=4	L8A	P13B	vv	05/12/2020	11/01/2021	28.95	0.69	1.8	27/04/2021	27/04/2021	30.06	0.67	1.87
	L8B		v100			29.51	0.43	1.74			33.12	0.48	1.87
	L8C		500v			30.44	0.38	1.78			31.05	0.39	1.85
	L8D		500100			36.8	0.95	1.81			38.67	0.88	1.84
n=5	L9A	P14B	vv	09/12/2020	11/01/2021	39.18	0.1	1.63	27/04/2021	27/04/2021	41.28	0.09	1.71
	L9B		v100			28.74	0.12	1.82			28.63	0.1	1.91
	L9C		500v			31.37	0.47	1.76			30.88	0.43	1.9
	L9D		500100			32.24	0.99	1.86			31.68	1.02	1.92
n=6	L10A	P15B	vv	12/12/2020	11/01/2021	49	0.33	1.88	27/04/2021	27/04/2021	49.68	0.32	1.88
	L10B		v100			48.87	0.28	1.89			48.78	0.28	1.93
	L10C		500v			42.73	0.17	1.96			43	0.14	2
	L10D		500100			56.52	0.14	1.89			54.85	0.17	1.96

Appendix Table D 4 Total RNA sample collection dates and optical density data for samples sent for RNA-sequencing.

	Lable Name	HepG2	Treatment	Collection Date	Isolation Date	Quantification Date	260/280	260/230	Con. (ng/µl)
n=1	H1A	P6	vv	31/07/2021	04/08/2021	04/08/2021	2.20	2.04	1225.68
	H1B		v100				2.18	2.01	738.72
	H1C		500v				2.19	2.03	737.61
	H1D		500100				2.18	2.02	962.40
n=2	H2A	P8B	vv	31/07/2021	04/08/2021	04/08/2021	2.19	2.02	1116.58
	H2B		v100				2.16	2.02	1255.26
	H2C		500v				2.12	2.00	614.67
	H2D		500100				2.16	2.02	1167.29
n=3	H3A	P9	vv	04/08/2021	06/08/2021	06/08/2021	2.00	2.06	1047.90
	H3B		v100				2.01	2.05	1207.86
	H3C		500v				2.01	2.16	1182.08
	H3D		500100				2.02	2.13	1033.13
		LX-2	Treatment	Collection Date	Isolation Date	Quantification Date	280/260	260/230	Con. (ng/µl)
n=1	L1A	P15	vv	20/08/2021	23/08/2021	23/08/2021	2.02	1.98	264.56
	L1B		v100				2.01	1.96	264.41
	L1C		500v				2.00	2.01	278.24
	L1D		500100				2.02	1.88	279.96
	L2A	P14A	vv	24/08/2021	25/08/2021	25/08/2021	2.02	1.97	333.18
n=2	L2B		v100				2.02	2.04	300.36
	L2C		500v				1.99	1.91	231.44
	L2D		500100				2.02	2.08	316.72
n=3	L3A	P14B	vv	24/08/2021	25/08/2021	25/08/2021	2.02	2.07	315.07
	L3B		v100				2.01	2.03	255.91
	L3C		500v				2.01	1.96	329.41
	L3D		500100				2.00	2.00	252.72

Both HepG2 and LX-2 cells (n=3) were treated with either vitamin D, fatty acid or in combination were used ReliaPrep™ RNA Cell Miniprep System (Promega) to collect total RNA for small RNA sequencing.

Appendix E
Supplementary Data Figures and Tables for Chapter 6

Appendix Table E 1 Cases of NAFLD in entire UKBB cohort

ICD No.	K760 No	K760 Yes	Total
K758 No	0	2696	**2696**
K758 Yes	186	162	**348**
Total	186	2858	**3044 (cases)**

Appendix Table E 2 ICD codes for exclusions for cases and controls of NAFLD.

Exclusion ICD codes or self-reported	Code description in sub-category	Case number show in UKBB showcase
K70 Alcoholic liver disease	K70.0, K70.1, K70.2, K70.3, K70.4, K70.9	1921
K71 Toxic liver disease	K71.0, K71.1, K71.2, K71.3, K71.4, K71.5, K71.6, K71.7, K71.8, K71.9	105
K72 Hepatic failure, not elsewhere classified	K72.0, K72.1, K72.9	617
K73 Chronic hepatitis, not elsewhere classified	K73.0, K73.1, K73.2, K73.8, K73.9	226
K74 Fibrosis and cirrhosis of liver	K74.0, K74.1, K74.2, K74.3, K74.4, K74.5, K74.6	1565
K75 Other inflammatory liver diseases	K75.0, K75.1, K75.2, K75.3, K75.4, K75.9	810
K76 Other diseases of liver	K76.1, K76.2, K76.3, K76.4, K76.5, K76.6, K76.7, K76.8, K76.9	3573
K77 Liver disorders in diseases classified elsewhere	K77.0, K77.8	25
B15 Acute hepatitis A	B15.0, B15.9	97
B16 Acute hepatitis B	B16.0, B16.1, B16.2, B16.9	136
B17 Other acute viral hepatitis	B17.0, B17.1, B17.2, B17.8, B17.9	215
B18 Chronic viral hepatitis	B18.0, B18.1, B18.2, B18.8, B18.9	701
B19 Unspecified viral hepatitis	B19.0, B19.9	47
B94.2 Sequelae of other and unspecified infectious and parasitic diseases	B94.2	2
C22 Malignant neoplasm of liver and intrahepatic bile ducts	C22.0	241
E83 Disorders of mineral metabolism	E83.0	8
E83 Disorders of mineral metabolism	E83.1	973
I85 Oesophageal varices	I85.0	138
I98 Other disorders of circulatory system in diseases classified elsewhere	I98.2	394

G93 Other disorders of brain	G93.7	1
R17 Unspecified jaundice	R17	1294
R18 Ascites	R18	2475
R94 Abnormal results of function studies	R94.5	5505
T86 Failure and rejection of transplanted organs and tissues	T86.4	31
Z94 Transplanted organ and tissue status	Z94.4	146
		Total 21,246

Appendix Table E 3 The number of cases and controls in different GWAS models of UKBB

Model	One	Two
Cases No.	2,757	1,747
Controls No.	460,161	448,282
Total	462,918	450,029

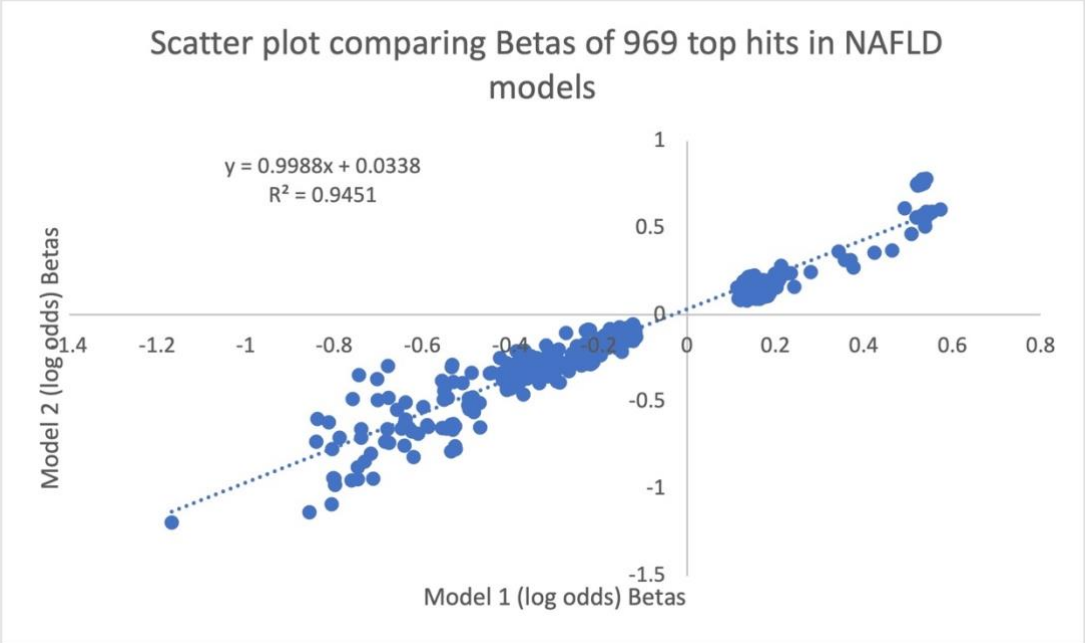

Appendix Figure E 1 A scatter plot of the betas of the top 1,000 SNPs in two GWAS models

a

For each SNP $R^2 = \frac{-2*(b^2)*eaf*(1-eaf)}{(2*(b^2)*eaf*(1-eaf)+(se^2)*(2*n)*eaf*(1-eaf))}$

Note: b= betas of exposure, eaf = effect allele frequency, n=size of exposure GWAS

b

For each SNP $F-statistic = \frac{R^2*(n-(1-1))}{(1-R^2)*1}$

Note: n=size of exposure GWAS

c

$I2 = 100\% * ((Q-df)/Q)$

Note: df=degrees of freedom which is the number of SNPs -1

Appendix Figure E 2 The formula of R^2 and F-statistic calculation.

Appendix Table E 4 Single SNP analyses by using the IVW and MR Egger methods.

Exposure/Outcome	SNP	Beta	SE	P-value
Vitamin D/NAFLD M1	rs10741657	-0.493	0.297	0.097
	rs10745742	0.138	0.558	0.805
	rs12785878	0.052	0.298	0.861
	rs17216707	-0.351	0.441	0.427
	rs3755967	-0.030	0.110	0.785
	rs8018720	1.391	0.736	0.059
	All-IVW	-0.052	0.112	0.641
	All-MR Egger	-0.096	0.218	0.683
Vitamin D/NAFLD M2	rs10741657	-0.526	0.372	0.157
	rs10745742	-0.178	0.700	0.800
	rs12785878	0.418	0.375	0.265
	rs17216707	-0.164	0.552	0.767
	rs3755967	0.044	0.138	0.748
	rs8018720	1.692	0.921	0.066
	All-IVW	0.038	0.140	0.786
	All-MR Egger	0.004	0.273	0.990
NAFLD M1/vitamin D	rs10401969	0.006	0.011	0.594
	rs17321515	0.050	0.016	0.002*
	rs9479542	-0.008	0.013	0.562
	All-IVW	0.014	0.016	0.384
	All-MR Egger	-0.016	0.050	0.804
NAFLD M2/vitamin D#	rs4351435	0.034	0.019	0.072
	All-IVW	NA	NA	NA
	All-MR Egger	NA	NA	NA

IVW, Inverse variance weighted; NA, not available; NAFLD, non-alcoholic fatty liver disease; M, model; MR, Mendelian randomisation; SE, standard error; SNP, single- nucleotide polymorphism; * means the statistical significance (P-value<0.05); # In this exposure/outcome, only one SNP involved in the MR analysis, the MR was calculated by Wald ratio.

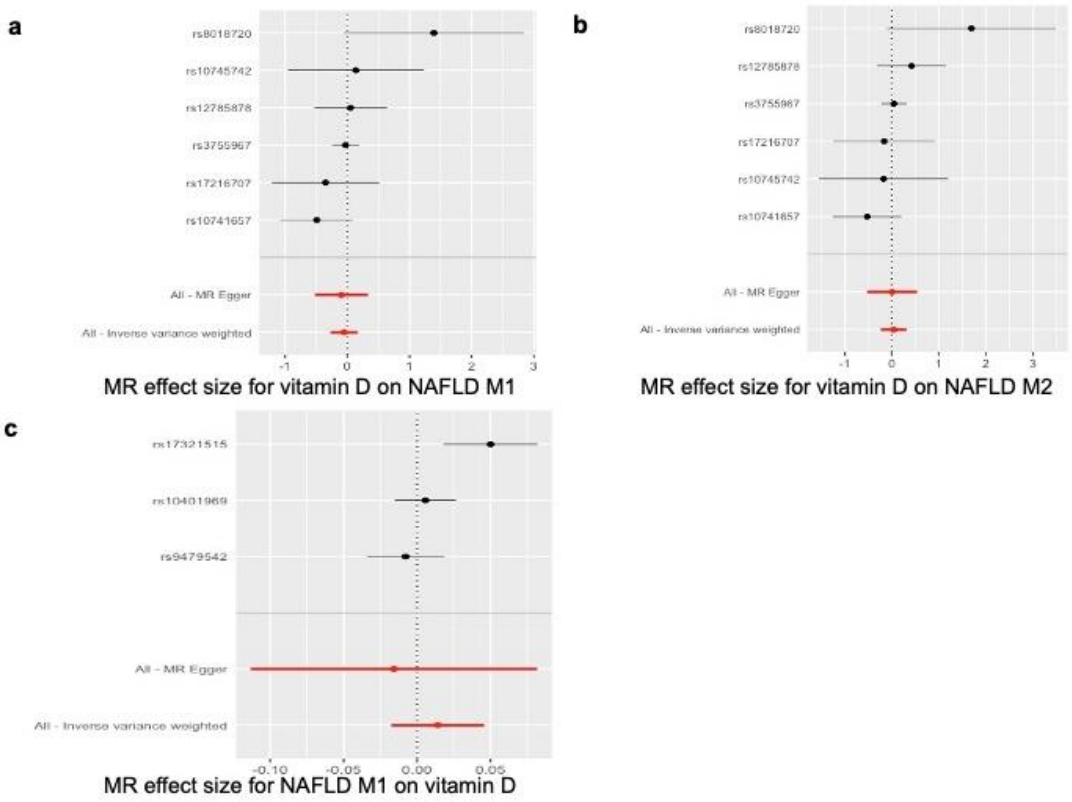

Appendix Figure E 3 Forest plots of single SNP analyses by using the IVW and MR Egger methods. The forest plot shows the association with circulating 25(OH)D level against NAFLD model 1 (**a**) and model 2 (**b**) risk, and the genetic associations with NAFLD model 1 (**c**) against circulating 25(OH)D level. Each black point represents the log odds ratio produced using each of the bipolar disorder SNPs as separate instruments. Red points show the combined causal estimate using all SNPs together in a single instrument, with two different methods (inverse variance weighted and MR-Egger). Horizontal line segments denote 95% confidence intervals of the estimate.

Appendix Table E 5 Single SNP analyses by using the maximum likelihood method.

Exposure/Outcome	SNP	Beta	SE	P-value
Vitamin D/NAFLD M1	rs10741657	-0.493	0.295	0.095
	rs10745742	0.138	0.558	0.805
	rs12785878	0.052	0.298	0.861
	rs17216707	-0.351	0.440	0.425
	rs3755967	-0.030	0.110	0.785
	rs8018720	1.391	0.696	0.045*
	All-Maximum likelihood	-0.051	0.093	0.573
Vitamin D/NAFLD M2	rs10741657	-0.526	0.370	0.155
	rs10745742	-0.178	0.700	0.800
	rs12785878	0.418	0.374	0.264
	rs17216707	-0.164	0.552	0.767
	rs3755967	0.044	0.138	0.748
	rs8018720	1.692	0.873	0.053
	All-Maximum likelihood	0.038	0.117	0.741
NAFLD M1/vitamin D	rs10401969	0.006	0.011	0.593
	rs17321515	0.050	0.014	0.0002*
	rs9479542	-0.008	0.013	0.560
	All-Maximum likelihood	0.016	0.008	0.041*
NAFLD M2/vitamin D#	rs4351435	0.034	0.018	0.060
	All-Maximum likelihood	NA	NA	NA

NA, not available; NAFLD, non-alcoholic fatty liver disease; M, model; MR, Mendelian randomisation; SE, standard error; SNP, single- nucleotide polymorphism; * means the statistical significance (P-value<0.05); # In this exposure/outcome, only one SNP involved in the MR analysis, the MR was calculated by Wald ratio.

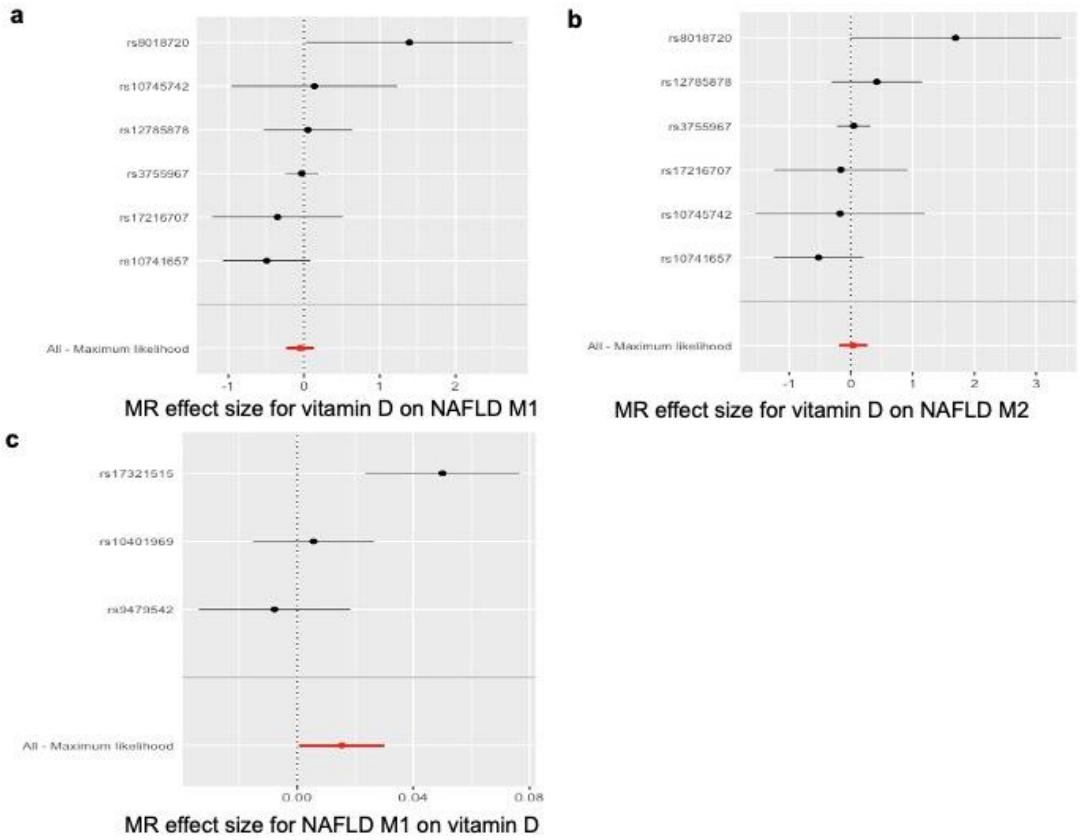

Appendix Figure E 4 Forest plots of single SNP analyses by using the maximum likelihood method. The forest plot shows the association with circulating 25(OH)D level against NAFLD model 1 (**a**) and model 2 (**b**) risk, and the genetic associations with NAFLD model 1 (**c**) against circulating 25(OH)D level. Each black point represents the log odds ratio produced using each of the bipolar disorder SNPs as separate instruments. Red points show the combined causal estimate using all SNPs together in a single instrument, with the maximum likelihood method. Horizontal line segments denote 95% confidence intervals of the estimate.

Appendix Table E 6 Related traits of the IVs associated with 25(OH)D and NAFLD from PhenoScanner V2 (top 10 lowest P-value)

IV (Gene)	Traits	beta	se	p
rs3755967 (GC)	Granulocyte count	-0.02499	0.003943	2.32E-10
	Myeloid white cell count	-0.02569	0.003953	8.05E-11
	Neutrophil count	-0.02473	0.003933	3.22E-10
	Sum basophil neutrophil counts	-0.02511	0.00394	1.85E-10
	Sum neutrophil eosinophil counts	-0.02475	0.003937	3.26E-10
	White blood cell count	-0.02605	0.003935	3.61E-11
	25 hydroxy vitamin D concentrations	NA	NA	2.42E-75
rs12785878 (DHCR7)	25 hydroxy vitamin D concentrations	NA	NA	2.12E-27
	Vitamin D insufficiency	NA	NA	2.00E-27
	Vitamin D	NA	NA	2.00E-27
rs10741657 (CYP2R1)	25 hydroxy vitamin D concentrations	NA	NA	3.27E-20
	25 hydroxy vitamin D concentrations 75 nmolL	NA	NA	9.40E-11
	Vitamin D insufficiency	NA	NA	3.00E-20
	Height	0.00981	0.001756	2.30E-08
	Hip circumference	0.01139	0.002447	3.22E-06
	Leg fat-free mass right	0.007372	0.001627	5.84E-06
	Leg predicted mass left	0.007172	0.001616	9.08E-06
	Leg predicted mass right	0.007235	0.001616	7.57E-06
	Vitamin D	NA	NA	3.00E-20
	log eGFR creatinine in non diabetics	0.0086	0.0012	1.30E-12
	log eGFR creatinine	0.0084	0.0011	6.00E-13
	Serum creatinine	NA	NA	8.90E-06
	Glomerular filtration rate	-0.761	0.1525	6.00E-07
	Glomerular filtration rate creatinine	-0.0077	0.0009932	9.00E-15
	Calculus of kidney and ureter	-0.001223	0.0002669	4.55E-06
	Self-reported kidney stone or ureter stone/bladder stone	-0.001255	0.0002811	8.00E-06
rs10745742 (AMDHD1)	NA	NA	NA	NA
rs8018720 (SEC23A)	NA	NA	NA	NA
rs10401969 (SUGP1)	Cholesterol total	0.137	0.00737	4.00E-77
	Total cholesterol	-0.1369	0.007	4.13E-77
	Total cholesterol levels	-0.137	0.007475	5.00E-75
	Triglyceride levels	-0.121	0.00679	5.00E-71
	Triglycerides	-0.121	0.0065	9.70E-70
	Triglycerides	0.121	0.006855	1.00E-69
	Low density lipoprotein	-0.1184	0.0072	2.65E-54
	LDL cholesterol	0.118	0.007608	3.00E-54
	LDL cholesterol levels	-0.118	0.00786	6.00E-51
	Total cholesterol	NA	NA	4.90E-40
rs9479542 (RP11-15GB8.1)	NA	NA	NA	NA
rs17321515 (RP11-136O12.2)	Triglycerides	0.0724	0.0048	3.18E-53
	Triglycerides	NA	NA	3.18E-53
	Self-reported high cholesterol	0.01222	0.0007969	4.91E-53
	Triglycerides	0.0661	0.0047	2.68E-42
	Triglycerides	NA	NA	1.10E-37
	Red cell distribution width	-0.04484	0.003536	7.42E-37
	Total cholesterol	0.0637	0.0051	6.45E-36
	Total cholesterol	NA	NA	6.45E-36
	Total cholesterol	0.0636	0.0051	2.30E-34
	Medication for cholesterol, blood pressure or diabetes: choleste	0.01759	0.001519	5.20E-31
rs4351435 (RP11-136O12.2)	Self-reported high cholesterol	-0.01154	0.0008681	2.59E-40
	Medication for cholesterol, blood pressure or diabetes: choleste	-0.01765	0.001653	1.26E-26
	Red cell distribution width	0.03925	0.003845	1.86E-24
	Treatment with simvastatin	-0.008071	0.0008399	7.38E-22
	Mean corpuscular hemoglobin concentration	-0.02931	0.003762	6.66E-15
	Treatment with cholesterol lowering medication	-0.009155	0.001208	3.44E-14
	Coronary artery disease	-0.0468	0.0062	4.78E-14
	Triglycerides	-0.0614	0.0087	3.90E-12
	Triglycerides	-0.0782	0.0113	4.05E-12
	Medication for cholesterol, blood pressure or diabetes: none of	0.0124	0.001848	1.98E-11

Appendix Table E 7 Leave-one-out analysis.

Exposure/Outcome	SNP	Beta	SE	P-value
Vitamin D/NAFLD M1	rs10741657	-0.004	0.107	0.972
	rs10745742	-0.058	0.126	0.647
	rs12785878	-0.064	0.131	0.627
	rs17216707	-0.038	0.124	0.757
	rs3755967	-0.108	0.232	0.642
	rs8018720	-0.078	0.094	0.402
	All	-0.052	0.112	0.641
Vitamin D/NAFLD M2	rs10741657	0.100	0.131	0.447
	rs10745742	0.044	0.157	0.779
	rs12785878	-0.003	0.151	0.984
	rs17216707	0.047	0.158	0.765
	rs3755967	0.022	0.291	0.939
	rs8018720	0.008	0.118	0.946
	All	0.038	0.140	0.786
NAFLD M1/vitamin D	rs10401969	0.021	0.029	0.474
	rs17321515	0.0004	0.008	0.957
	rs9479542	0.0239	0.022	0.294
	All	0.014	0.016	0.384
NAFLD M2/vitamin D#	All	NA	NA	NA

NA, not available; NAFLD, non-alcoholic fatty liver disease; M, model; MR, Mendelian randomisation; SE, standard error; SNP, single- nucleotide polymorphism; * means the statistical significance (P-value<0.05); # In this exposure/outcome, only one SNP involved in the MR analysis, the MR was calculated by Wald ratio.

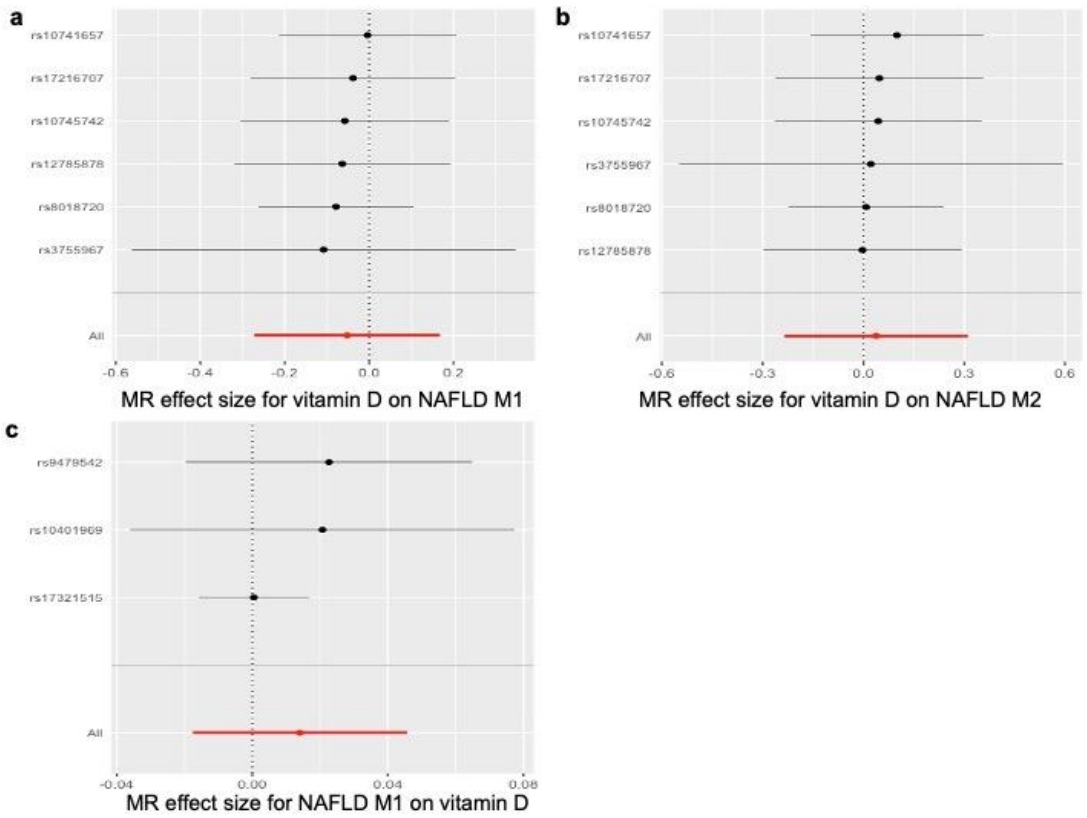

Appendix Figure E 5 Forest plots of leave-one-out analysis. The forest plot shows the association with circulating 25(OH)D level against NAFLD model 1 (**a**) and model 2 (**b**) risk, and the genetic associations with NAFLD model 1 (**c**) against circulating 25(OH)D level. Each black point represents the log odds ratio produced using each of the bipolar disorder SNPs as separate instruments. Red points show the combined causal estimate using all SNPs together in a single instrument, with the maximum likelihood method. Horizontal line segments denote 95% confidence intervals of the estimate.

List of References

References

Abramovitch, S, Dahan-Bachar, L, Sharvit, E, Weisman, Y, Ben Tov, A, Brazowski, E and Reif, S (2011) Vitamin d inhibits proliferation and profibrotic marker expression in hepatic stellate cells and decreases thioacetamide-induced liver fibrosis in rats. *Gut.* 60l, 1728-1737.

Abul-Husn, NS, Cheng, X, Li, AH, Xin, Y, Schurmann, C, Stevis, P, Liu, Y, Kozlitina, J, Stender, S, Wood, GC, Stepanchick, AN, Still, MD, McCarthy, S, O'Dushlaine, C, Packer, JS, Balasubramanian, S, Gosalia, N, Esopi, D, Kim, SY, Mukherjee, S, Lopez, AE, Fuller, ED, Penn, J, Chu, X, Luo, JZ, Mirshahi, UL, Carey, DJ, Still, CD, Feldman, MD, Small, A, Damrauer, SM, Rader, DJ, Zambrowicz, B, Olson, W, Murphy, AJ, Borecki, IB, Shuldiner, AR, Reid, JG, Overton, JD, Yancopoulos, GD, Hobbs, HH, Cohen, JC, Gottesman, O, Teslovich, TM, Baras, A, Mirshahi, T, Gromada, J and Dewey, FE (2018) A protein-truncating hsd17b13 variant and protection from chronic liver disease. *N Engl J Med.* 378l, 1096-1106.

Adams, LA, White, SW, Marsh, JA, Lye, SJ, Connor, KL, Maganga, R, Ayonrinde, OT, Olynyk, JK, Mori, TA, Beilin, LJ, Palmer, LJ, Hamdorf, JM and Pennell, CE (2013) Association between liver-specific gene polymorphisms and their expression levels with nonalcoholic fatty liver disease. *Hepatology.* 57l, 590-600.

Aden, DP, Fogel, A, Plotkin, S, Damjanov, I and Knowles, BB (1979) Controlled synthesis of hbsag in a differentiated human liver carcinoma-derived cell line. *Nature.* 282l, 615-616.

Agius, L (2008) Glucokinase and molecular aspects of liver glycogen metabolism. *Biochem J.* 414l, 1-18.

Ahn, J, Yu, K, Stolzenberg-Solomon, R, Simon, KC, McCullough, ML, Gallicchio, L, Jacobs, EJ, Ascherio, A, Helzlsouer, K, Jacobs, KB, Li, Q, Weinstein, SJ, Purdue, M, Virtamo, J, Horst, R, Wheeler, W, Chanock, S, Hunter, DJ, Hayes, RB, Kraft, P and Albanes, D (2010) Genome-wide association study of circulating vitamin d levels. *Hum Mol Genet.* 19l, 2739-2745.

Ahrens, M, Ammerpohl, O, von Schonfels, W, Kolarova, J, Bens, S, Itzel, T, Teufel, A, Herrmann, A, Brosch, M, Hinrichsen, H, Erhart, W, Egberts, J, Sipos, B, Schreiber, S, Hasler, R, Stickel, F, Becker, T, Krawczak, M, Rocken, C, Siebert, R, Schafmayer, C and Hampe, J (2013) DNA methylation analysis in nonalcoholic fatty liver disease suggests distinct disease-specific and remodeling signatures after bariatric surgery. *Cell Metab.* 18l, 296-302.

Akhtar, MM, Micolucci, L, Islam, MS, Olivieri, F and Procopio, AD (2016) Bioinformatic tools for microrna dissection. *Nucleic Acids Res.* 44l, 24-44.

Akuta, N, Kawamura, Y, Arase, Y, Saitoh, S, Fujiyama, S, Sezaki, H, Hosaka, T, Kobayashi, M, Kobayashi, M, Suzuki, Y, Suzuki, F, Ikeda, K and Kumada, H (2020) Circulating microrna-122 and fibrosis stage predict

mortality of japanese patients with histopathologically confirmed nafld. *Hepatol Commun.* 4l, 66-76.

Akuta, N, Kawamura, Y, Suzuki, F, Saitoh, S, Arase, Y, Fujiyama, S, Sezaki, H, Hosaka, T, Kobayashi, M, Suzuki, Y, Kobayashi, M, Ikeda, K and Kumada, H (2016a) Analysis of association between circulating mir-122 and histopathological features of nonalcoholic fatty liver disease in patients free of hepatocellular carcinoma. *BMC Gastroenterol.* 16l, 141.

Akuta, N, Kawamura, Y, Suzuki, F, Saitoh, S, Arase, Y, Kunimoto, H, Sorin, Y, Fujiyama, S, Sezaki, H, Hosaka, T, Kobayashi, M, Suzuki, Y, Kobayashi, M, Ikeda, K and Kumada, H (2016b) Impact of circulating mir-122 for histological features and hepatocellular carcinoma of nonalcoholic fatty liver disease in japan. *Hepatol Int.* 10l, 647-656.

Alexander, M, Loomis, AK, Fairburn-Beech, J, van der Lei, J, Duarte-Salles, T, Prieto-Alhambra, D, Ansell, D, Pasqua, A, Lapi, F, Rijnbeek, P, Mosseveld, M, Avillach, P, Egger, P, Kendrick, S, Waterworth, DM, Sattar, N and Alazawi, W (2018) Real-world data reveal a diagnostic gap in non-alcoholic fatty liver disease. *BMC Med.* 16l, 130.

Alles, J, Fehlmann, T, Fischer, U, Backes, C, Galata, V, Minet, M, Hart, M, Abu-Halima, M, Grässer, FA, Lenhof, HP, Keller, A and Meese, E (2019) An estimate of the total number of true human mirnas. *Nucleic Acids Res.* 47l, 3353-3364.

Amrein, K, Scherkl, M, Hoffmann, M, Neuwersch-Sommeregger, S, Kostenberger, M, Tmava Berisha, A, Martucci, G, Pilz, S and Malle, O (2020) Vitamin d deficiency 2.0: An update on the current status worldwide. *Eur J Clin Nutr.* 74l, 1498-1513.

An, J, He, H, Yao, W, Shang, Y, Jiang, Y and Yu, Z (2020) Pi3k/akt/foxo pathway mediates glycolytic metabolism in hepg2 cells exposed to triclosan (tcs). *Environ Int.* 136l, 105428.

Anderson, D, Holt, BJ, Pennell, CE, Holt, PG, Hart, PH and Blackwell, JM (2014) Genome-wide association study of vitamin d levels in children: Replication in the western australian pregnancy cohort (raine) study. *Genes Immun.* 15l, 578-583.

Ando, Y and Jou, JH (2021) Nonalcoholic fatty liver disease and recent guideline updates. *Clin Liver Dis (Hoboken).* 17l, 23-28.

Ando, Y, Yamazaki, M, Yamada, H, Munetsuna, E, Fujii, R, Mizuno, G, Ichino, N, Osakabe, K, Sugimoto, K, Ishikawa, H, Ohashi, K, Teradaira, R, Ohta, Y, Hamajima, N, Hashimoto, S and Suzuki, K (2019) Association of circulating mir-20a, mir-27a, and mir-126 with non-alcoholic fatty liver disease in general population. *Sci Rep.* 9l, 18856.

Anstee, QM, Darlay, R, Cockell, S, Meroni, M, Govaere, O, Tiniakos, D, Burt, AD, Bedossa, P, Palmer, J, Liu, YL, Aithal, GP, Allison, M, Yki-Jarvinen, H, Vacca, M, Dufour, JF, Invernizzi, P, Prati, D, Ekstedt, M, Kechagias, S, Francque, S, Petta, S, Bugianesi, E, Clement, K, Ratziu, V, Schattenberg, JM, Valenti, L, Day, CP, Cordell, HJ, Daly, AK and Investigators, EPC (2020) Genome-wide association study of non-alcoholic fatty liver and steatohepatitis in a histologically characterised cohort(). *J Hepatol.* 73l, 505-515.

Arai, T, Atsukawa, M, Tsubota, A, Koeda, M, Yoshida, Y, Okubo, T, Nakagawa, A, Itokawa, N, Kondo, C, Nakatsuka, K, Masu, T, Kato, K, Shimada, N, Hatori, T, Emoto, N, Kage, M and Iwakiri, K (2019) Association of vitamin d levels and vitamin d-related gene

polymorphisms with liver fibrosis in patients with biopsy-proven nonalcoholic fatty liver disease. *Dig Liver Dis.*

Araya, J, Rodrigo, R, Videla, LA, Thielemann, L, Orellana, M, Pettinelli, P and Poniachik, J (2004) Increase in long-chain polyunsaturated fatty acid n - 6/n - 3 ratio in relation to hepatic steatosis in patients with non-alcoholic fatty liver disease. *Clin Sci (Lond).* 106l, 635-643.

Arboleda, JF, Fernandez, GJ and Urcuqui-Inchima, S (2019) Vitamin d-mediated attenuation of mir-155 in human macrophages infected with dengue virus: Implications for the cytokine response. *Infect Genet Evol.* 69l, 12-21.

Ashburner, M, Ball, CA, Blake, JA, Botstein, D, Butler, H, Cherry, JM, Davis, AP, Dolinski, K, Dwight, SS, Eppig, JT, Harris, MA, Hill, DP, Issel-Tarver, L, Kasarskis, A, Lewis, S, Matese, JC, Richardson, JE, Ringwald, M, Rubin, GM and Sherlock, G (2000) Gene ontology: Tool for the unification of biology. The gene ontology consortium. *Nature genetics.* 25l, 25-29.

Auguet, T, Aragonès, G, Berlanga, A, Guiu-Jurado, E, Martí, A, Martínez, S, Sabench, F, Hernández, M, Aguilar, C, Sirvent, JJ, Del Castillo, D and Richart, C (2016a) Mir33a/mir33b* and mir122 as possible contributors to hepatic lipid metabolism in obese women with nonalcoholic fatty liver disease. *International Journal of Molecular Sciences.* 17l.

Auguet, T, Aragonès, G, Berlanga, A, Guiu-Jurado, E, Martí, A, Martínez, S, Sabench, F, Hernández, M, Aguilar, C, Sirvent, JJ, Del Castillo, D and Richart, C (2016b) Mir33a/mir33b* and mir122 as possible contributors to hepatic lipid metabolism in obese women with nonalcoholic fatty liver disease. *Int J Mol Sci.* 17l.

Ayonrinde, OT (2021) Historical narrative from fatty liver in the nineteenth century to contemporary nafld - reconciling the present with the past. *JHEP Rep.* 3l, 100261.

Bale, G, Vishnubhotla, RV, Mitnala, S, Sharma, M, Padaki, RN, Pawar, SC and Duvvur, RN (2019) Whole-exome sequencing identifies a variant in phosphatidylethanolamine n-methyltransferase gene to be associated with lean-nonalcoholic fatty liver disease. *J Clin Exp Hepatol.* 9l, 561-568.

Bandiera, S, Pfeffer, S, Baumert, TF and Zeisel, MB (2015) Mir-122--a key factor and therapeutic target in liver disease. *J Hepatol.* 62l, 448-457.

Bannister, AJ and Kouzarides, T (2011) Regulation of chromatin by histone modifications. *Cell Res.* 21l, 381-395.

Bao, J, Scott, I, Lu, Z, Pang, L, Dimond, CC, Gius, D and Sack, MN (2010) Sirt3 is regulated by nutrient excess and modulates hepatic susceptibility to lipotoxicity. *Free Radic Biol Med.* 49l, 1230-1237.

Barbero-Becerra, VJ, Giraudi, PJ, Chávez-Tapia, NC, Uribe, M, Tiribelli, C and Rosso, N (2015) The interplay between hepatic stellate cells and hepatocytes in an in vitro model of nash. *Toxicol In Vitro.* 29l, 1753-1758.

Barchetta, I, Angelico, F, Del Ben, M, Baroni, MG, Pozzilli, P, Morini, S and Cavallo, MG (2011) Strong association between non alcoholic fatty liver disease (nafld) and low 25(oh) vitamin d levels in an adult population with normal serum liver enzymes. *BMC Med.* 9l, 85.

Barchetta, I, Angelico, F, Del Ben, M, Di Martino, M, Fraioli, A, La Torre, G, Morini, S, Tiberti, C, Del Vescovo, R, Bertoccini, L and et al. (2016a)

Effects of oral high-dose vitamin d supplementation on non-alcoholic fatty liver disease in patients with type 2 diabetes: A randomised, double-blind, placebo-controlled trial. *Journal of hepatology. Conference: 51st annual meeting of the european association for the study of the liver, international liver congress 2016. Barcelona spain. Conference start: 20160413. Conference end: 20160417. Conference publication: (var.pagings).* 64l, S483.

Barchetta, I, Carotti, S, Labbadia, G, Gentilucci, UV, Muda, AO, Angelico, F, Silecchia, G, Leonetti, F, Fraioli, A, Picardi, A, Morini, S and Cavallo, MG (2012) Liver vitamin d receptor, cyp2r1, and cyp27a1 expression: Relationship with liver histology and vitamin d3 levels in patients with nonalcoholic steatohepatitis or hepatitis c virus. *Hepatology.* 56l, 2180-2187.

Barchetta, I, Cimini, FA and Cavallo, MG (2020) Vitamin d and metabolic dysfunction-associated fatty liver disease (mafld): An update. *Nutrients.* 12l.

Barchetta, I, Del Ben, M, Angelico, F, Di Martino, M, Fraioli, A, La Torre, G, Saulle, R, Perri, L, Morini, S, Tiberti, C and et al. (2016b) No effects of oral vitamin d supplementation on non-alcoholic fatty liver disease in patients with type 2 diabetes: A randomized, double-blind, placebo-controlled trial. *BMC medicine.* 14l, 92.

Barrès, R, Osler, ME, Yan, J, Rune, A, Fritz, T, Caidahl, K, Krook, A and Zierath, JR (2009) Non-cpg methylation of the pgc-1alpha promoter through dnmt3b controls mitochondrial density. *Cell Metab.* 10l, 189-198.

Bartel, DP (2004) Micrornas: Genomics, biogenesis, mechanism, and function. *Cell.* 116l, 281-297.

Basantani, MK, Sitnick, MT, Cai, L, Brenner, DS, Gardner, NP, Li, JZ, Schoiswohl, G, Yang, K, Kumari, M, Gross, RW, Zechner, R and Kershaw, EE (2011) Pnpla3/adiponutrin deficiency in mice does not contribute to fatty liver disease or metabolic syndrome. *J Lipid Res.* 52l, 318-329.

Basu Ray, S (2019) Pnpla3-i148m: A problem of plenty in non-alcoholic fatty liver disease. *Adipocyte.* 8l, 201-208.

BasuRay, S, Smagris, E, Cohen, JC and Hobbs, HH (2017) The pnpla3 variant associated with fatty liver disease (i148m) accumulates on lipid droplets by evading ubiquitylation. *Hepatology.* 66l, 1111-1124.

Bates, B, Cox, L., Nicholson, S., Page, P., Prentice, A., Steer, T., & Swan, G. (2016) National diet and nutrition survey results from years 5 and 6 (combined) of the rolling programme (2012/2013–2013/2014). *London: Public Health England.*

Bayat, A (2002) Science, medicine, and the future: Bioinformatics. *BMJ.* 324l, 1018-1022.

Baylin, A, Kabagambe, EK, Siles, X and Campos, H (2002) Adipose tissue biomarkers of fatty acid intake. *Am J Clin Nutr.* 76l, 750-757.

Becker, PP, Rau, M, Schmitt, J, Malsch, C, Hammer, C, Bantel, H, Müllhaupt, B and Geier, A (2015) Performance of serum micrornas -122, -192 and -21 as biomarkers in patients with non-alcoholic steatohepatitis. *PLoS One.* 10l, e0142661.

Beckett, EL, Martin, C, Duesing, K, Jones, P, Furst, J, Yates, Z, Veysey, M and Lucock, M (2014) Vitamin d receptor genotype modulates the

correlation between vitamin d and circulating levels of let-7a/b and vitamin d intake in an elderly cohort. *J Nutrigenet Nutrigenomics.* 7l, 264-273.

Beer, NL, Tribble, ND, McCulloch, LJ, Roos, C, Johnson, PR, Orho-Melander, M and Gloyn, AL (2009) The p446l variant in gckr associated with fasting plasma glucose and triglyceride levels exerts its effect through increased glucokinase activity in liver. *Hum Mol Genet.* 18l, 4081-4088.

Beilfuss, A, Sowa, J-P, Sydor, S, Beste, M, Bechmann, LP, Schlattjan, M, Syn, W-K, Wedemeyer, I, Mathe, Z, Jochum, C, Gerken, G, Gieseler, RK and Canbay, A (2015a) Vitamin d counteracts fibrogenic tgf- beta signalling in human hepatic stellate cells both receptor-dependently and independently. *Gut.* 64l, 791-799.

Beilfuss, A, Sowa, JP, Sydor, S, Beste, M, Bechmann, LP, Schlattjan, M, Syn, WK, Wedemeyer, I, Mathe, Z, Jochum, C, Gerken, G, Gieseler, RK and Canbay, A (2015b) Vitamin d counteracts fibrogenic tgf-beta signalling in human hepatic stellate cells both receptor-dependently and independently. *Gut.* 64l, 791-799.

Bence, KK and Birnbaum, MJ (2021) Metabolic drivers of non-alcoholic fatty liver disease. *Mol Metab.* 50l, 101143.

Benhamouche-Trouillet, S and Postic, C (2016) Emerging role of mir-21 in non-alcoholic fatty liver disease. *Gut.* 65l, 1781-1783.

Benjamin, EJ, Dupuis, J, Larson, MG, Lunetta, KL, Booth, SL, Govindaraju, DR, Kathiresan, S, Keaney, JF, Jr., Keyes, MJ, Lin, JP, Meigs, JB, Robins, SJ, Rong, J, Schnabel, R, Vita, JA, Wang, TJ, Wilson, PW, Wolf, PA and Vasan, RS (2007) Genome-wide association with select biomarker traits in the framingham heart study. *BMC Med Genet.* 8 Suppl 1l, S11.

Berger, D, Desai, V and Janardhan, S (2019) Con: Liver biopsy remains the gold standard to evaluate fibrosis in patients with nonalcoholic fatty liver disease. *Clin Liver Dis (Hoboken).* 13l, 114-116.

Beurel, E, Grieco, SF and Jope, RS (2015) Glycogen synthase kinase-3 (gsk3): Regulation, actions, and diseases. *Pharmacol Ther.* 148l, 114-131.

Bikle, D. 2000. Vitamin d: Production, metabolism, and mechanisms of action. In: Feingold, KR, et al. eds. *Endotext.* South Dartmouth (MA).

Bikle, DD (2014) Vitamin d metabolism, mechanism of action, and clinical applications. *Chem Biol.* 21l, 319-329.

Bjelakovic, G, Nikolova, D, Bjelakovic, M and Gluud, C (2017) Vitamin d supplementation for chronic liver diseases in adults. *Cochrane Database Syst Rev.* 11l, CD011564.

Bjelakovic, M, Nikolova, D, Bjelakovic, G and Gluud, C (2021) Vitamin d supplementation for chronic liver diseases in adults. *Cochrane Database Syst Rev.* 8l, CD011564.

Blander, G and Guarente, L (2004) The sir2 family of protein deacetylases. *Annu Rev Biochem.* 73l, 417-435.

Bonneau, E, Neveu, B, Kostantin, E, Tsongalis, GJ and De Guire, V (2019) How close are mirnas from clinical practice? A perspective on the diagnostic and therapeutic market. *Ejifcc.* 30l, 114-127.

Borén, J, Adiels, M, Björnson, E, Matikainen, N, Söderlund, S, Rämö, J, Ståhlman, M, Ripatti, P, Ripatti, S, Palotie, A, Mancina, RM, Hakkarainen, A, Romeo, S, Packard, CJ and Taskinen, MR (2020)

Effects of tm6sf2 e167k on hepatic lipid and very low-density lipoprotein metabolism in humans. *JCI Insight.* 5l.

Bowden, J, Davey Smith, G and Burgess, S (2015) Mendelian randomization with invalid instruments: Effect estimation and bias detection through egger regression. *Int J Epidemiol.* 44l, 512-525.

Bowden, J, Davey Smith, G, Haycock, PC and Burgess, S (2016) Consistent estimation in mendelian randomization with some invalid instruments using a weighted median estimator. *Genet Epidemiol.* 40l, 304-314.

Bowden, J, Hemani, G and Davey Smith, G (2018) Invited commentary: Detecting individual and global horizontal pleiotropy in mendelian randomization-a job for the humble heterogeneity statistic? *Am J Epidemiol.* 187l, 2681-2685.

Boyadjiev, SA, Fromme, JC, Ben, J, Chong, SS, Nauta, C, Hur, DJ, Zhang, G, Hamamoto, S, Schekman, R, Ravazzola, M, Orci, L and Eyaid, W (2006) Cranio-lenticulo-sutural dysplasia is caused by a sec23a mutation leading to abnormal endoplasmic-reticulum-to-golgi trafficking. *Nat Genet.* 38l, 1192-1197.

Boyd, A, Cain, O, Chauhan, A and Webb, GJ (2020) Medical liver biopsy: Background, indications, procedure and histopathology. *Frontline Gastroenterol.* 11l, 40-47.

Bozic, M, Guzman, C, Benet, M, Sanchez-Campos, S, Garcia-Monzon, C, Gari, E, Gatius, S, Valdivielso, JM and Jover, R (2016) Hepatocyte vitamin d receptor regulates lipid metabolism and mediates experimental diet-induced steatosis. *J Hepatol.* 65l, 748-757.

Braegger, C, Campoy, C, Colomb, V, Decsi, T, Domellof, M, Fewtrell, M, Hojsak, I, Mihatsch, W, Molgaard, C, Shamir, R, Turck, D, van Goudoever, J and Nutrition, ECo (2013) Vitamin d in the healthy european paediatric population. *J Pediatr Gastroenterol Nutr.* 56l, 692-701.

Brandt, S, Roos, J, Inzaghi, E, Kotnik, P, Kovac, J, Battelino, T, Cianfarani, S, Nobili, V, Colajacomo, M, Kratzer, W, Denzer, C, Fischer-Posovszky, P and Wabitsch, M (2018) Circulating levels of mir-122 and nonalcoholic fatty liver disease in pre-pubertal obese children. *Pediatr Obes.* 13l, 175-182.

Braza-Boïls, A, Marí-Alexandre, J, Molina, P, Arnau, MA, Barceló-Molina, M, Domingo, D, Girbes, J, Giner, J, Martínez-Dolz, L and Zorio, E (2016a) Deregulated hepatic micrornas underlie the association between non-alcoholic fatty liver disease and coronary artery disease. *Liver Int.* 36l, 1221-1229.

Braza-Boïls, A, Marí-Alexandre, J, Molina, P, Arnau, MA, Barceló-Molina, M, Domingo, D, Girbes, J, Giner, J, Martínez-Dolz, L and Zorio, E (2016b) Deregulated hepatic micrornas underlie the association between non-alcoholic fatty liver disease and coronary artery disease. *Liver International.* 36l, 1221-1229.

Bricambert, J, Miranda, J, Benhamed, F, Girard, J, Postic, C and Dentin, R (2010) Salt-inducible kinase 2 links transcriptional coactivator p300 phosphorylation to the prevention of chrebp-dependent hepatic steatosis in mice. *J Clin Invest.* 120l, 4316-4331.

Brion, MJ, Shakhbazov, K and Visscher, PM (2013) Calculating statistical power in mendelian randomization studies. *Int J Epidemiol.* 42l, 1497-1501.

Brown, GT and Kleiner, DE (2016) Histopathology of nonalcoholic fatty liver disease and nonalcoholic steatohepatitis. *Metabolism.* 65l, 1080-1086.
Brown, RAM, Epis, MR, Horsham, JL, Kabir, TD, Richardson, KL and Leedman, PJ (2018) Total rna extraction from tissues for microrna and target gene expression analysis: Not all kits are created equal. *BMC Biotechnol.* 18l, 16.
Browning, JD, Szczepaniak, LS, Dobbins, R, Nuremberg, P, Horton, JD, Cohen, JC, Grundy, SM and Hobbs, HH (2004) Prevalence of hepatic steatosis in an urban population in the united states: Impact of ethnicity. *Hepatology.* 40l, 1387-1395.
Buch, S, Stickel, F, Trépo, E, Way, M, Herrmann, A, Nischalke, HD, Brosch, M, Rosendahl, J, Berg, T, Ridinger, M, Rietschel, M, McQuillin, A, Frank, J, Kiefer, F, Schreiber, S, Lieb, W, Soyka, M, Semmo, N, Aigner, E, Datz, C, Schmelz, R, Brückner, S, Zeissig, S, Stephan, AM, Wodarz, N, Devière, J, Clumeck, N, Sarrazin, C, Lammert, F, Gustot, T, Deltenre, P, Völzke, H, Lerch, MM, Mayerle, J, Eyer, F, Schafmayer, C, Cichon, S, Nöthen, MM, Nothnagel, M, Ellinghaus, D, Huse, K, Franke, A, Zopf, S, Hellerbrand, C, Moreno, C, Franchimont, D, Morgan, MY and Hampe, J (2015) A genome-wide association study confirms pnpla3 and identifies tm6sf2 and mboat7 as risk loci for alcohol-related cirrhosis. *Nat Genet.* 47l, 1443-1448.
Budak, H, Bulut, R, Kantar, M and Alptekin, B (2016) Microrna nomenclature and the need for a revised naming prescription. *Brief Funct Genomics.* 15l, 65-71.
Budd, G. 1853. *On diseases of the liver*. Blanchard and Lea.
Burgess, S, Butterworth, A and Thompson, SG (2013) Mendelian randomization analysis with multiple genetic variants using summarized data. *Genet Epidemiol.* 37l, 658-665.
Burgess, S, Scott, RA, Timpson, NJ, Davey Smith, G and Thompson, SG (2015) Using published data in mendelian randomization: A blueprint for efficient identification of causal risk factors. *Eur J Epidemiol.* 30l, 543-552.
Burgess, S and Thompson, SG (2011) Avoiding bias from weak instruments in mendelian randomization studies. *Int J Epidemiol.* 40l, 755-764.
Buzzetti, E, Pinzani, M and Tsochatzis, EA (2016) The multiple-hit pathogenesis of non-alcoholic fatty liver disease (nafld). *Metabolism.* 65l, 1038-1048.
Bycroft, C, Freeman, C, Petkova, D, Band, G, Elliott, LT, Sharp, K, Motyer, A, Vukcevic, D, Delaneau, O, O'Connell, J, Cortes, A, Welsh, S, Young, A, Effingham, M, McVean, G, Leslie, S, Allen, N, Donnelly, P and Marchini, J (2018) The uk biobank resource with deep phenotyping and genomic data. *Nature.* 562l, 203-209.
Cai, L, Luo, L, Tang, Z and Meng, X (2018) Combined antitumor effects of 1,25-dihydroxy vitamin d3 and notch inhibitor in liver cancer. *Oncol Rep.* 40l, 1515-1524.
Cai, Q, Chen, F, Xu, F, Wang, K, Zhang, K, Li, G, Chen, J, Deng, H and He, Q (2020) Epigenetic silencing of microrna-125b-5p promotes liver fibrosis in nonalcoholic fatty liver disease via integrin α8-mediated activation of rhoa signaling pathway. *Metabolism.* 104l, 154140.
Calo, N, Ramadori, P, Sobolewski, C, Romero, Y, Maeder, C, Fournier, M, Rantakari, P, Zhang, FP, Poutanen, M, Dufour, JF, Humar, B, Nef, S

and Foti, M (2016) Stress-activated mir-21/mir-21* in hepatocytes promotes lipid and glucose metabolic disorders associated with high-fat diet consumption. *Gut.* 65l, 1871-1881.
Cantley, LC (2002) The phosphoinositide 3-kinase pathway. *Science.* 296l, 1655-1657.
Carlsson, P and Mahlapuu, M (2002) Forkhead transcription factors: Key players in development and metabolism. *Dev Biol.* 250l, 1-23.
Cashman, KD (2020) Vitamin d deficiency: Defining, prevalence, causes, and strategies of addressing. *Calcif Tissue Int.* 106l, 14-29.
Cashman, KD, Dowling, KG, Skrabakova, Z, Gonzalez-Gross, M, Valtuena, J, De Henauw, S, Moreno, L, Damsgaard, CT, Michaelsen, KF, Molgaard, C, Jorde, R, Grimnes, G, Moschonis, G, Mavrogianni, C, Manios, Y, Thamm, M, Mensink, GB, Rabenberg, M, Busch, MA, Cox, L, Meadows, S, Goldberg, G, Prentice, A, Dekker, JM, Nijpels, G, Pilz, S, Swart, KM, van Schoor, NM, Lips, P, Eiriksdottir, G, Gudnason, V, Cotch, MF, Koskinen, S, Lamberg-Allardt, C, Durazo-Arvizu, RA, Sempos, CT and Kiely, M (2016) Vitamin d deficiency in europe: Pandemic? *Am J Clin Nutr.* 103l, 1033-1044.
Castro, RE, Ferreira, DM, Afonso, MB, Borralho, PM, Machado, MV, Cortez-Pinto, H and Rodrigues, CM (2013) Mir-34a/sirt1/p53 is suppressed by ursodeoxycholic acid in the rat liver and activated by disease severity in human non-alcoholic fatty liver disease. *J Hepatol.* 58l, 119-125.
Catanzaro, G, Filardi, T, Sabato, C, Vacca, A, Migliaccio, S, Morano, S and Ferretti, E (2020) Tissue and circulating microrna as biomarkers of response to obesity treatment strategies. *J Endocrinol Invest.*
Caviglia, JM, Yan, J, Jang, MK, Gwak, GY, Affo, S, Yu, L, Olinga, P, Friedman, RA, Chen, X and Schwabe, RF (2018) Microrna-21 and dicer are dispensable for hepatic stellate cell activation and the development of liver fibrosis. *Hepatology.* 67l, 2414-2429.
Celikbilek, M, Baskol, M, Taheri, S, Deniz, K, Dogan, S, Zararsiz, G, Gursoy, S, Guven, K, Ozbakır, O, Dundar, M and Yucesoy, M (2014) Circulating microrna in patients with non-alcoholic fatty liver disease. *World J Hepatol.* 6l, 613-620.
Cermelli, S, Ruggieri, A, Marrero, JA, Ioannou, GN and Beretta, L (2011) Circulating microrna in patients with chronic hepatitis c and non-alcoholic fatty liver disease. *PLoS One.* 6l, e23937.
Cesari, M, Incalzi, RA, Zamboni, V and Pahor, M (2011) Vitamin d hormone: A multitude of actions potentially influencing the physical function decline in older persons. *Geriatr Gerontol Int.* 11l, 133-142.
Chai, C, Rivkin, M, Berkovits, L, Simerzin, A, Zorde-Khvalevsky, E, Rosenberg, N, Klein, S, Yaish, D, Durst, R, Shpitzen, S, Udi, S, Tam, J, Heeren, J, Worthmann, A, Schramm, C, Kluwe, J, Ravid, R, Hornstein, E, Giladi, H and Galun, E (2017) Metabolic circuit involving free fatty acids, microrna 122, and triglyceride synthesis in liver and muscle tissues. *Gastroenterology.* 153l, 1404-1415.
Chalasani, N, Guo, X, Loomba, R, Goodarzi, MO, Haritunians, T, Kwon, S, Cui, J, Taylor, KD, Wilson, L, Cummings, OW, Chen, YD, Rotter, JI and Nonalcoholic Steatohepatitis Clinical Research, N (2010) Genome-wide association study identifies variants associated with histologic features of nonalcoholic fatty liver disease. *Gastroenterology.* 139l, 1567-1576, 1576 e1561-1566.

Chalasani, N, Younossi, Z, Lavine, JE, Charlton, M, Cusi, K, Rinella, M, Harrison, SA, Brunt, EM and Sanyal, AJ (2018) The diagnosis and management of nonalcoholic fatty liver disease: Practice guidance from the american association for the study of liver diseases. *Hepatology.* 67l, 328-357.

Chan, HM and La Thangue, NB (2001) P300/cbp proteins: Hats for transcriptional bridges and scaffolds. *J Cell Sci.* 114l, 2363-2373.

Chen, DJ, Li, LJ, Yang, XK, Yu, T, Leng, RX, Pan, HF and Ye, DQ (2017) Altered micrornas expression in t cells of patients with sle involved in the lack of vitamin d. *Oncotarget.* 8l, 62099-62110.

Chen, G (2015) The link between hepatic vitamin a metabolism and nonalcoholic fatty liver disease. *Curr Drug Targets.* 16l, 1281-1292.

Chen, W, Chang, B, Li, L and Chan, L (2010) Patatin-like phospholipase domain-containing 3/adiponutrin deficiency in mice is not associated with fatty liver disease. *Hepatology.* 52l, 1134-1142.

Chen, Y, Du, J, Zhang, Z, Liu, T, Shi, Y, Ge, X and Li, YC (2014) Microrna-346 mediates tumor necrosis factor α-induced downregulation of gut epithelial vitamin d receptor in inflammatory bowel diseases. *Inflamm Bowel Dis.* 20l, 1910-1918.

Chen, Y, Liu, W, Sun, T, Huang, Y, Wang, Y, Deb, DK, Yoon, D, Kong, J, Thadhani, R and Li, YC (2013a) 1,25-dihydroxyvitamin d promotes negative feedback regulation of tlr signaling via targeting microrna-155-socs1 in macrophages. *J Immunol.* 190l, 3687-3695.

Chen, Y, Zhang, J, Ge, X, Du, J, Deb, DK and Li, YC (2013b) Vitamin d receptor inhibits nuclear factor κb activation by interacting with iκb kinase β protein. *J Biol Chem.* 288l, 19450-19458.

Chen, ZJ and Pikaard, CS (1997) Epigenetic silencing of rna polymerase i transcription: A role for DNA methylation and histone modification in nucleolar dominance. *Genes Dev.* 11l, 2124-2136.

Cheung, O, Puri, P, Eicken, C, Contos, MJ, Mirshahi, F, Maher, JW, Kellum, JM, Min, H, Luketic, VA and Sanyal, AJ (2008) Nonalcoholic steatohepatitis is associated with altered hepatic microrna expression. *Hepatology.* 48l, 1810-1820.

Chiang, HR, Schoenfeld, LW, Ruby, JG, Auyeung, VC, Spies, N, Baek, D, Johnston, WK, Russ, C, Luo, S, Babiarz, JE, Blelloch, R, Schroth, GP, Nusbaum, C and Bartel, DP (2010) Mammalian micrornas: Experimental evaluation of novel and previously annotated genes. *Genes Dev.* 24l, 992-1009.

Chiang, KC, Yeh, CN, Chen, HY, Lee, JM, Juang, HH, Chen, MF, Takano, M, Kittaka, A and Chen, TC (2011a) 19-nor-2α-(3-hydroxypropyl)-1α,25-dihydroxyvitamin d3 (mart-10) is a potent cell growth regulator with enhanced chemotherapeutic potency in liver cancer cells. *Steroids.* 76l, 1513-1519.

Chiang, KC, Yeh, CN, Chen, MF and Chen, TC (2011b) Hepatocellular carcinoma and vitamin d: A review. *J Gastroenterol Hepatol.* 26l, 1597-1603.

Chipman, LB and Pasquinelli, AE (2019) Mirna targeting: Growing beyond the seed. *Trends Genet.* 35l, 215-222.

Cho, YH, Kim, JW, Shim, JO, Yang, HR, Chang, JY, Moon, JS and Ko, JS (2019) Association between vitamin d deficiency and suspected

nonalcoholic fatty liver disease in an adolescent population. *Pediatr Gastroenterol Hepatol Nutr.* 22l, 233-241.
Chomczynski, P (1993) A reagent for the single-step simultaneous isolation of rna, DNA and proteins from cell and tissue samples. *Biotechniques.* 15l, 532-534, 536-537.
Chomczynski, P and Sacchi, N (1987) Single-step method of rna isolation by acid guanidinium thiocyanate-phenol-chloroform extraction. *Anal Biochem.* 162l, 156-159.
Christakos, S, Dhawan, P, Verstuyf, A, Verlinden, L and Carmeliet, G (2016) Vitamin d: Metabolism, molecular mechanism of action, and pleiotropic effects. *Physiol Rev.* 96l, 365-408.
Chung, GE, Lee, Y, Yim, JY, Choe, EK, Kwak, MS, Yang, JI, Park, B, Lee, JE, Kim, JA and Kim, JS (2018) Genetic polymorphisms of pnpla3 and samm50 are associated with nonalcoholic fatty liver disease in a korean population. *Gut Liver.* 12l, 316-323.
Cicero, AFG, Colletti, A and Bellentani, S (2018) Nutraceutical approach to non-alcoholic fatty liver disease (nafld): The available clinical evidence. *Nutrients.* 10l.
Cohen, JF, Chalumeau, M, Cohen, R, Korevaar, DA, Khoshnood, B and Bossuyt, PM (2015) Cochran's q test was useful to assess heterogeneity in likelihood ratios in studies of diagnostic accuracy. *J Clin Epidemiol.* 68l, 299-306.
Consortium, GT (2013) The genotype-tissue expression (gtex) project. *Nat Genet.* 45l, 580-585.
Cui, J, Chen, CH, Lo, MT, Schork, N, Bettencourt, R, Gonzalez, MP, Bhatt, A, Hooker, J, Shaffer, K, Nelson, KE, Long, MT, Brenner, DA, Sirlin, CB, Loomba, R and For The Genetics Of Nafld In Twins, C (2016) Shared genetic effects between hepatic steatosis and fibrosis: A prospective twin study. *Hepatology.* 64l, 1547-1558.
Czaja, MJ, Weiner, FR, Flanders, KC, Giambrone, MA, Wind, R, Biempica, L and Zern, MA (1989) In vitro and in vivo association of transforming growth factor-beta 1 with hepatic fibrosis. *J Cell Biol.* 108l, 2477-2482.
Dabbaghmanesh, MH, Danafar, F, Eshraghian, A and Omrani, GR (2018a) Vitamin d supplementation for the treatment of non-alcoholic fatty liver disease: A randomized double blind placebo controlled trial. *Diabetes Metab Syndr.* 12l, 513-517.
Dabbaghmanesh, MH, Danafar, F, Eshraghian, A and Omrani, GR (2018b) Vitamin d supplementation for the treatment of non-alcoholic fatty liver disease: A randomized double blind placebo controlled trial. *Diabetes & metabolic syndrome.* 12l, 513-517.
Dasarathy, J, Varghese, R, Feldman, A, Khiyami, A, McCullough, AJ and Dasarathy, S (2017) Patients with nonalcoholic fatty liver disease have a low response rate to vitamin d supplementation. *J Nutr.* 147l, 1938-1946.
Dattaroy, D, Pourhoseini, S, Das, S, Alhasson, F, Seth, RK, Nagarkatti, M, Michelotti, GA, Diehl, AM and Chatterjee, S (2015) Micro-rna 21 inhibition of smad7 enhances fibrogenesis via leptin-mediated nadph oxidase in experimental and human nonalcoholic steatohepatitis. *Am J Physiol Gastrointest Liver Physiol.* 308l, G298-312.
Dave, VP, Ngo, TA, Pernestig, AK, Tilevik, D, Kant, K, Nguyen, T, Wolff, A and Bang, DD (2019) Microrna amplification and detection

technologies: Opportunities and challenges for point of care diagnostics. *Lab Invest.* 99l, 452-469.
Davey Smith, G and Ebrahim, S (2005) What can mendelian randomisation tell us about modifiable behavioural and environmental exposures? *Bmj.* 330l, 1076-1079.
Davey Smith, G and Hemani, G (2014) Mendelian randomization: Genetic anchors for causal inference in epidemiological studies. *Hum Mol Genet.* 23l, R89-98.
Davies, NM, Holmes, MV and Davey Smith, G (2018) Reading mendelian randomisation studies: A guide, glossary, and checklist for clinicians. *BMJ.* 362l, k601.
Day, CP and James, OF (1998) Steatohepatitis: A tale of two "hits"? *Gastroenterology.* 114l, 842-845.
Deeb, KK, Trump, DL and Johnson, CS (2007) Vitamin d signalling pathways in cancer: Potential for anticancer therapeutics. *Nat Rev Cancer.* 7l, 684-700.
Demer, LL, Hsu, JJ and Tintut, Y (2018) Steroid hormone vitamin d: Implications for cardiovascular disease. *Circ Res.* 122l, 1576-1585.
Denechaud, PD, Dentin, R, Girard, J and Postic, C (2008) Role of chrebp in hepatic steatosis and insulin resistance. *FEBS Lett.* 582l, 68-73.
Deng, XQ, Chen, LL and Li, NX (2007) The expression of sirt1 in nonalcoholic fatty liver disease induced by high-fat diet in rats. *Liver Int.* 27l, 708-715.
Dennis, G, Jr., Sherman, BT, Hosack, DA, Yang, J, Gao, W, Lane, HC and Lempicki, RA (2003) David: Database for annotation, visualization, and integrated discovery. *Genome Biol.* 4l, P3.
Derdak, Z, Villegas, KA, Harb, R, Wu, AM, Sousa, A and Wands, JR (2013) Inhibition of p53 attenuates steatosis and liver injury in a mouse model of non-alcoholic fatty liver disease. *J Hepatol.* 58l, 785-791.
Desjardins, P and Conklin, D (2010) Nanodrop microvolume quantitation of nucleic acids. *J Vis Exp.*
Di Costanzo, A, Belardinilli, F, Bailetti, D, Sponziello, M, D'Erasmo, L, Polimeni, L, Baratta, F, Pastori, D, Ceci, F, Montali, A, Girelli, G, De Masi, B, Angeloni, A, Giannini, G, Del Ben, M, Angelico, F and Arca, M (2018) Evaluation of polygenic determinants of non-alcoholic fatty liver disease (nafld) by a candidate genes resequencing strategy. *Sci Rep.* 8l, 3702.
Ding, RB, Bao, J and Deng, CX (2017) Emerging roles of sirt1 in fatty liver diseases. *Int J Biol Sci.* 13l, 852-867.
Donati, B, Motta, BM, Pingitore, P, Meroni, M, Pietrelli, A, Alisi, A, Petta, S, Xing, C, Dongiovanni, P, del Menico, B, Rametta, R, Mancina, RM, Badiali, S, Fracanzani, AL, Craxi, A, Fargion, S, Nobili, V, Romeo, S and Valenti, L (2016) The rs2294918 e434k variant modulates patatin-like phospholipase domain-containing 3 expression and liver damage. *Hepatology.* 63l, 787-798.
Dong, X, Park, S, Lin, X, Copps, K, Yi, X and White, MF (2006) Irs1 and irs2 signaling is essential for hepatic glucose homeostasis and systemic growth. *J Clin Invest.* 116l, 101-114.
Dong, XC (2017) Foxo transcription factors in non-alcoholic fatty liver disease. *Liver Res.* 1l, 168-173.

Dongiovanni, P, Donati, B, Fares, R, Lombardi, R, Mancina, RM, Romeo, S and Valenti, L (2013) Pnpla3 i148m polymorphism and progressive liver disease. *World J Gastroenterol.* 19l, 6969-6978.

Dongiovanni, P, Petta, S, Maglio, C, Fracanzani, AL, Pipitone, R, Mozzi, E, Motta, BM, Kaminska, D, Rametta, R, Grimaudo, S, Pelusi, S, Montalcini, T, Alisi, A, Maggioni, M, Karja, V, Boren, J, Kakela, P, Di Marco, V, Xing, C, Nobili, V, Dallapiccola, B, Craxi, A, Pihlajamaki, J, Fargion, S, Sjostrom, L, Carlsson, LM, Romeo, S and Valenti, L (2015) Transmembrane 6 superfamily member 2 gene variant disentangles nonalcoholic steatohepatitis from cardiovascular disease. *Hepatology.* 61l, 506-514.

Dorairaj, V, Sulaiman, SA, Abu, N and Abdul Murad, NA (2021) Nonalcoholic fatty liver disease (nafld): Pathogenesis and noninvasive diagnosis. *Biomedicines.* 10l.

Drobna, M, Szarzynska-Zawadzka, B, Daca-Roszak, P, Kosmalska, M, Jaksik, R, Witt, M and Dawidowska, M (2018) Identification of endogenous control mirnas for rt-qpcr in t-cell acute lymphoblastic leukemia. *Int J Mol Sci.* 19l.

Duan, X, Guan, Y, Li, Y, Chen, S, Li, S and Chen, L (2015) Vitamin d potentiates the inhibitory effect of microrna-130a in hepatitis c virus replication independent of type i interferon signaling pathway. *Mediators Inflamm.* 2015l, 508989.

Dweep, H, Sticht, C, Pandey, P and Gretz, N (2011) Mirwalk--database: Prediction of possible mirna binding sites by "walking" the genes of three genomes. *J Biomed Inform.* 44l, 839-847.

EASL-EASD-EASO (2016) Easl-easd-easo clinical practice guidelines for the management of non-alcoholic fatty liver disease. *J Hepatol.* 64l, 1388-1402.

Easton, RM, Cho, H, Roovers, K, Shineman, DW, Mizrahi, M, Forman, MS, Lee, VM, Szabolcs, M, de Jong, R, Oltersdorf, T, Ludwig, T, Efstratiadis, A and Birnbaum, MJ (2005) Role for akt3/protein kinase bgamma in attainment of normal brain size. *Mol Cell Biol.* 25l, 1869-1878.

Ebrahimpour-Koujan, S, Sohrabpour, AA, Foroughi, F, Alvandi, E and Esmaillzadeh, A (2019) Effects of vitamin d supplementation on liver fibrogenic factors in non-alcoholic fatty liver patients with steatohepatitis: Study protocol for a randomized clinical trial. *Trials.* 20l, 153.

EFSA Panel on Dietetic Products, NaAN (2016) Dietary reference values for vitamin d. *EFSA Journal.* 14l, e04547.

Ekström, L, Skilving, I, Ovesjö, ML, Aklillu, E, Nylén, H, Rane, A, Diczfalusy, U and Björkhem-Bergman, L (2015) Mirna-27b levels are associated with cyp3a activity in vitro and in vivo. *Pharmacol Res Perspect.* 3l, e00192.

El Amrousy, D, Abdelhai, D and Shawky, D (2021) Vitamin d and nonalcoholic fatty liver disease in children: A randomized controlled clinical trial. *Eur J Pediatr.*

El Taghdouini, A, Najimi, M, Sancho-Bru, P, Sokal, E and van Grunsven, LA (2015) In vitro reversion of activated primary human hepatic stellate cells. *Fibrogenesis Tissue Repair.* 8l, 14.

Eliades, M and Spyrou, E (2015) Vitamin d: A new player in non-alcoholic fatty liver disease? *World J Gastroenterol.* 21l, 1718-1727.

Eliades, M, Spyrou, E, Agrawal, N, Lazo, M, Brancati, FL, Potter, JJ, Koteish, AA, Clark, JM, Guallar, E and Hernaez, R (2013) Meta-analysis: Vitamin d and non-alcoholic fatty liver disease. *Aliment Pharmacol Ther.* 38l, 246-254.

Emmett, MJ and Lazar, MA (2019) Integrative regulation of physiology by histone deacetylase 3. *Nat Rev Mol Cell Biol.* 20l, 102-115.

Engelman, CD, Meyers, KJ, Ziegler, JT, Taylor, KD, Palmer, ND, Haffner, SM, Fingerlin, TE, Wagenknecht, LE, Rotter, JI, Bowden, DW, Langefeld, CD and Norris, JM (2010) Genome-wide association study of vitamin d concentrations in hispanic americans: The iras family study. *J Steroid Biochem Mol Biol.* 122l, 186-192.

Enquobahrie, DA, Williams, MA, Qiu, C, Siscovick, DS and Sorensen, TK (2011) Global maternal early pregnancy peripheral blood mrna and mirna expression profiles according to plasma 25-hydroxyvitamin d concentrations. *J Matern Fetal Neonatal Med.* 24l, 1002-1012.

Erhartova, D, Cahova, M, Dankova, H, Heczkova, M, Mikova, I, Sticova, E, Spicak, J, Seda, O and Trunecka, P (2019) Serum mir-33a is associated with steatosis and inflammation in patients with non-alcoholic fatty liver disease after liver transplantation. *PLoS One.* 14l, e0224820.

Esau, C, Davis, S, Murray, SF, Yu, XX, Pandey, SK, Pear, M, Watts, L, Booten, SL, Graham, M, McKay, R, Subramaniam, A, Propp, S, Lollo, BA, Freier, S, Bennett, CF, Bhanot, S and Monia, BP (2006) Mir-122 regulation of lipid metabolism revealed by in vivo antisense targeting. *Cell Metab.* 3l, 87-98.

Eslam, M, Newsome, PN, Sarin, SK, Anstee, QM, Targher, G, Romero-Gomez, M, Zelber-Sagi, S, Wai-Sun Wong, V, Dufour, JF, Schattenberg, JM, Kawaguchi, T, Arrese, M, Valenti, L, Shiha, G, Tiribelli, C, Yki-Jarvinen, H, Fan, JG, Gronbaek, H, Yilmaz, Y, Cortez-Pinto, H, Oliveira, CP, Bedossa, P, Adams, LA, Zheng, MH, Fouad, Y, Chan, WK, Mendez-Sanchez, N, Ahn, SH, Castera, L, Bugianesi, E, Ratziu, V and George, J (2020a) A new definition for metabolic dysfunction-associated fatty liver disease: An international expert consensus statement. *J Hepatol.* 73l, 202-209.

Eslam, M, Sanyal, AJ, George, J and International Consensus, P (2020b) Mafld: A consensus-driven proposed nomenclature for metabolic associated fatty liver disease. *Gastroenterology.* 158l, 1999-2014 e1991.

Eslam, M, Valenti, L and Romeo, S (2018) Genetics and epigenetics of nafld and nash: Clinical impact. *J Hepatol.* 68l, 268-279.

Essa, S, Denzer, N, Mahlknecht, U, Klein, R, Collnot, EM, Tilgen, W and Reichrath, J (2010) Vdr microrna expression and epigenetic silencing of vitamin d signaling in melanoma cells. *J Steroid Biochem Mol Biol.* 121l, 110-113.

Ezaz, G, Trivedi, HD, Connelly, MA, Filozof, C, Howard, K, M, LP, Kim, M, Herman, MA, Nasser, I, Afdhal, NH, Jiang, ZG and Lai, M (2020) Differential associations of circulating micrornas with pathogenic factors in nafld. *Hepatol Commun.* 4l, 670-680.

Ezhilarasan, D (2020) Microrna interplay between hepatic stellate cell quiescence and activation. *Eur J Pharmacol.* 885l, 173507.
Fairfield, CJ, Drake, TM, Pius, R, Bretherick, AD, Campbell, A, Clark, DW, Fallowfield, JA, Hayward, C, Henderson, NC, Joshi, PK, Mills, NL, Porteous, DJ, Ramachandran, P, Semple, RK, Shaw, CA, Sudlow, CLM, Timmers, P, Wilson, JF, Wigmore, SJ, Harrison, EM and Spiliopoulou, A (2022) Genome-wide association study of nafld using electronic health records. *Hepatol Commun.* 6l, 297-308.
Fang, Z, Dou, G and Wang, L (2021) Micrornas in the pathogenesis of nonalcoholic fatty liver disease. *Int J Biol Sci.* 17l, 1851-1863.
Feili, X, Wu, S, Ye, W, Tu, J and Lou, L (2018) Microrna-34a-5p inhibits liver fibrosis by regulating tgf-β1/smad3 pathway in hepatic stellate cells. *Cell Biol Int.* 42l, 1370-1376.
Feitosa, MF, Wojczynski, MK, North, KE, Zhang, Q, Province, MA, Carr, JJ and Borecki, IB (2013) The erlin1-chuk-cwf19l1 gene cluster influences liver fat deposition and hepatic inflammation in the nhlbi family heart study. *Atherosclerosis.* 228l, 175-180.
Feng, D, Liu, T, Sun, Z, Bugge, A, Mullican, SE, Alenghat, T, Liu, XS and Lazar, MA (2011) A circadian rhythm orchestrated by histone deacetylase 3 controls hepatic lipid metabolism. *Science.* 331l, 1315-1319.
Ferrero, G, Carpi, S, Polini, B, Pardini, B, Nieri, P, Impeduglia, A, Grioni, S, Tarallo, S and Naccarati, A (2020) Intake of natural compounds and circulating microrna expression levels: Their relationship investigated in healthy subjects with different dietary habits. *Front Pharmacol.* 11l, 619200.
Fisher, CD, Lickteig, AJ, Augustine, LM, Ranger-Moore, J, Jackson, JP, Ferguson, SS and Cherrington, NJ (2009) Hepatic cytochrome p450 enzyme alterations in humans with progressive stages of nonalcoholic fatty liver disease. *Drug Metab Dispos.* 37l, 2087-2094.
Fisher, HW, Puck, TT and Sato, G (1958) Molecular growth requirements of single mammalian cells: The action of fetuin in promoting cell attachment to glass. *Proc Natl Acad Sci U S A.* 44l, 4-10.
Folini, M, Gandellini, P, Longoni, N, Profumo, V, Callari, M, Pennati, M, Colecchia, M, Supino, R, Veneroni, S, Salvioni, R, Valdagni, R, Daidone, MG and Zaffaroni, N (2010) Mir-21: An oncomir on strike in prostate cancer. *Mol Cancer.* 9l, 12.
Foroughi, M, Maghsoudi, Z and Askari, G (2016) The effect of vitamin d supplementation on blood sugar and different indices of insulin resistance in patients with non-alcoholic fatty liver disease (nafld). *Iran J Nurs Midwifery Res.* 21l, 100-104.
Foroughi, M, Maghsoudi, Z, Ghiasvand, R, Iraj, B and Askari, G (2014) Effect of vitamin d supplementation on c-reactive protein in patients with nonalcoholic fatty liver. *Int J Prev Med.* 5l, 969-975.
Fraser, A, Longnecker, MP and Lawlor, DA (2007) Prevalence of elevated alanine aminotransferase among us adolescents and associated factors: Nhanes 1999-2004. *Gastroenterology.* 133l, 1814-1820.
Friedman, RC, Farh, KK, Burge, CB and Bartel, DP (2009) Most mammalian mrnas are conserved targets of micrornas. *Genome Res.* 19l, 92-105.
Friedman, SL (2008) Hepatic stellate cells: Protean, multifunctional, and enigmatic cells of the liver. *Physiol Rev.* 88l, 125-172.

Friedman, SL, Wei, S and Blaner, WS (1993) Retinol release by activated rat hepatic lipocytes: Regulation by kupffer cell-conditioned medium and pdgf. *Am J Physiol.* 264l, G947-952.

Fruman, DA, Chiu, H, Hopkins, BD, Bagrodia, S, Cantley, LC and Abraham, RT (2017) The pi3k pathway in human disease. *Cell.* 170l, 605-635.

Gad, AI, Elmedames, MR, Abdelhai, AR and Marei, AM (2020) The association between vitamin d status and non-alcoholic fatty liver disease in adults: A hospital-based study. *Egyptian Liver Journal.* 10l, 25.

Gad, AI, Elmedames, MR, Abdelhai, AR, Marei, AM and Abdel-Ghani, HA (2021) Efficacy of vitamin d supplementation on adult patients with non-alcoholic fatty liver disease: A single-center experience. *Gastroenterol Hepatol Bed Bench.* 14l, 44-52.

Gallego-Durán, R and Romero-Gómez, M (2015) Epigenetic mechanisms in non-alcoholic fatty liver disease: An emerging field. *World J Hepatol.* 7l, 2497-2502.

Gascon-Barre, M, Demers, C, Mirshahi, A, Neron, S, Zalzal, S and Nanci, A (2003) The normal liver harbors the vitamin d nuclear receptor in nonparenchymal and biliary epithelial cells. *Hepatology.* 37l, 1034-1042.

Geier, A, Eichinger, M, Stirnimann, G, Semela, D, Tay, F, Seifert, B, Tschopp, O, Bantel, H, Jahn, D, Marques Maggio, E and et al. (2018) Treatment of non-alcoholic steatohepatitis patients with vitamin d: A double-blinded, randomized, placebo-controlled pilot study. *Scandinavian journal of gastroenterology.* 53l, 1114-1120.

Gene Ontology, C (2021) The gene ontology resource: Enriching a gold mine. *Nucleic acids research.* 49l, D325-D334.

Geng, Y, Faber, KN, de Meijer, VE, Blokzijl, H and Moshage, H (2021) How does hepatic lipid accumulation lead to lipotoxicity in non-alcoholic fatty liver disease? *Hepatol Int.* 15l, 21-35.

Ghasemi, M, Turnbull, T, Sebastian, S and Kempson, I (2021) The mtt assay: Utility, limitations, pitfalls, and interpretation in bulk and single-cell analysis. *Int J Mol Sci.* 22l.

Ghodsian, N, Abner, E, Emdin, CA, Gobeil, E, Taba, N, Haas, ME, Perrot, N, Manikpurage, HD, Gagnon, E, Bourgault, J, St-Amand, A, Couture, C, Mitchell, PL, Bosse, Y, Mathieu, P, Vohl, MC, Tchernof, A, Theriault, S, Khera, AV, Esko, T and Arsenault, BJ (2021) Electronic health record-based genome-wide meta-analysis provides insights on the genetic architecture of non-alcoholic fatty liver disease. *Cell Rep Med.* 2l, 100437.

Giangreco, AA, Vaishnav, A, Wagner, D, Finelli, A, Fleshner, N, Van der Kwast, T, Vieth, R and Nonn, L (2013) Tumor suppressor microrna s, mir-100 and -125b, are regulated by 1,25-dihydroxyvitamin d in primary prostate cells and in patient tissue. *Cancer Prev Res (Phila).* 6l, 483-494.

Gibson, PS, Lang, S, Gilbert, M, Kamat, D, Bansal, S, Ford-Adams, ME, Desai, AP, Dhawan, A, Fitzpatrick, E, Moore, JB and Hart, KH (2015) Assessment of diet and physical activity in paediatric non-alcoholic fatty liver disease patients: A united kingdom case control study. *Nutrients.* 7l, 9721-9733.

Gibson, PS, Quaglia, A, Dhawan, A, Wu, H, Lanham-New, S, Hart, KH, Fitzpatrick, E and Moore, JB (2018) Vitamin d status and associated genetic polymorphisms in a cohort of uk children with non-alcoholic fatty liver disease. *Pediatr Obes.* 13l, 433-441.

Gijon, MA, Riekhof, WR, Zarini, S, Murphy, RC and Voelker, DR (2008) Lysophospholipid acyltransferases and arachidonate recycling in human neutrophils. *J Biol Chem.* 283l, 30235-30245.

Git, A, Dvinge, H, Salmon-Divon, M, Osborne, M, Kutter, C, Hadfield, J, Bertone, P and Caldas, C (2010) Systematic comparison of microarray profiling, real-time pcr, and next-generation sequencing technologies for measuring differential microrna expression. *RNA.* 16l, 991-1006.

Gjorgjieva, M, Sobolewski, C, Dolicka, D, Correia de Sousa, M and Foti, M (2019a) Mirnas and nafld: From pathophysiology to therapy. *Gut.* 68l, 2065-2079.

Gjorgjieva, M, Sobolewski, C, Dolicka, D, Correia De Sousa, M and Foti, M. 2019b. *Mirnas and nafld: From pathophysiology to therapy*. BMJ Publishing Group. 68. pp.2065-2079.

Gomez-Lechon, MJ, Donato, MT, Martinez-Romero, A, Jimenez, N, Castell, JV and O'Connor, JE (2007) A human hepatocellular in vitro model to investigate steatosis. *Chem Biol Interact.* 165l, 106-116.

Górecki, I and Rak, B (2021) The role of micrornas in epithelial to mesenchymal transition and cancers; focusing on mir-200 family. *Cancer Treat Res Commun.* 28l, 100385.

Guengerich, FP (1999) Cytochrome p-450 3a4: Regulation and role in drug metabolism. *Annu Rev Pharmacol Toxicol.* 39l, 1-17.

Guguen-Guillouzo, C and Guillouzo, A (2010) General review on in vitro hepatocyte models and their applications. *Methods Mol Biol.* 640l, 1-40.

Guo, J, Fang, W, Sun, L, Lu, Y, Dou, L, Huang, X, Sun, M, Pang, C, Qu, J, Liu, G and Li, J (2016a) Reduced mir-200b and mir-200c expression contributes to abnormal hepatic lipid accumulation by stimulating jun expression and activating the transcription of srebp1. *Oncotarget.* 7l, 36207-36219.

Guo, XY, Chen, JN, Sun, F, Wang, YQ, Pan, Q and Fan, JG (2017) Circrna_0046367 prevents hepatoxicity of lipid peroxidation: An inhibitory role against hepatic steatosis. *Oxid Med Cell Longev.* 2017l, 3960197.

Guo, Y, Bosompem, A, Zhong, X, Clark, T, Shyr, Y and Kim, AS (2014) A comparison of microrna sequencing reproducibility and noise reduction using mirvana and trizol isolation methods. *Int J Comput Biol Drug Des.* 7l, 102-112.

Guo, Y, Xiong, Y, Sheng, Q, Zhao, S, Wattacheril, J and Flynn, CR (2016b) A micro-rna expression signature for human nafld progression. *J Gastroenterol.* 51l, 1022-1030.

Hammerle-Fickinger, A, Riedmaier, I, Becker, C, Meyer, HH, Pfaffl, MW and Ulbrich, SE (2010) Validation of extraction methods for total rna and mirna from bovine blood prior to quantitative gene expression analyses. *Biotechnol Lett.* 32l, 35-44.

Han, S and Chiang, JY (2009) Mechanism of vitamin d receptor inhibition of cholesterol 7alpha-hydroxylase gene transcription in human hepatocytes. *Drug Metab Dispos.* 37l, 469-478.

Hartwig, FP, Davey Smith, G and Bowden, J (2017) Robust inference in summary data mendelian randomization via the zero modal pleiotropy assumption. *Int J Epidemiol.* 46l, 1985-1998.

Hartwig, FP, Tilling, K, Davey Smith, G, Lawlor, DA and Borges, MC (2021) Bias in two-sample mendelian randomization when using heritable covariable-adjusted summary associations. *Int J Epidemiol.* 50l, 1639-1650.

Haughton, EL, Tucker, SJ, Marek, CJ, Durward, E, Leel, V, Bascal, Z, Monaghan, T, Koruth, M, Collie-Duguid, E, Mann, DA, Trim, JE and Wright, MC (2006) Pregnane x receptor activators inhibit human hepatic stellate cell transdifferentiation in vitro. *Gastroenterology.* 131l, 194-209.

He, L, He, X, Lowe, SW and Hannon, GJ (2007) Microrнas join the p53 network--another piece in the tumour-suppression puzzle. *Nat Rev Cancer.* 7l, 819-822.

He, LH, Yao, DH, Wang, LY, Zhang, L and Bai, XL (2021a) Gut microbiome-mediated alteration of immunity, inflammation, and metabolism involved in the regulation of non-alcoholic fatty liver disease. *Front Microbiol.* 12l, 761836.

He, S, Guo, W, Deng, F, Chen, K, Jiang, Y, Dong, M, Peng, L and Chen, X (2018) Targeted delivery of microrna 146b mimic to hepatocytes by lactosylated pdmaema nanoparticles for the treatment of nafld. *Artif Cells Nanomed Biotechnol.* 46l, 217-228.

He, W, Ni, W, Zhao, L, Wang, X, Liu, L and Fan, Z (2021b) Microrna-125a/vdr axis impaired autophagic flux and contributed to fibrosis in a ccl4-induced mouse model and patients with liver cirrhosis. *Life Sci.* 264l, 118666.

He, Y, Huang, C, Sun, X, Long, XR, Lv, XW and Li, J (2012) Microrna-146a modulates tgf-beta1-induced hepatic stellate cell proliferation by targeting smad4. *Cell Signal.* 24l, 1923-1930.

He, Y, Hwang, S, Cai, Y, Kim, SJ, Xu, M, Yang, D, Guillot, A, Feng, D, Seo, W, Hou, X and Gao, B (2019a) Microrna-223 ameliorates nonalcoholic steatohepatitis and cancer by targeting multiple inflammatory and oncogenic genes in hepatocytes. *Hepatology.* 70l, 1150-1167.

He, Z, Yang, JJ, Zhang, R, Li, HT, Wu, L, Jiang, F, Jia, WP and Hu, C (2019b) Circulating mir-29b positively correlates with non-alcoholic fatty liver disease in a chinese population. *Journal of Digestive Diseases.* 20l, 189-195.

Heaney, J, Rolfe, K, Gleadall, NS, Greatorex, JS and Curran, MD (2015) Low-density taqman® array cards for the detection of pathogens. *Methods in Microbiology.* 42l, 199-218.

Heaney, RP (2012) Vitamin d--baseline status and effective dose. *N Engl J Med.* 367l, 77-78.

Hegazy, MA, Abd, AI, Abuel Fadl, S, Sayed Hassan, M, Ahmed Rashed, L and Hussein, MA (2021) Serum micro-rna-122 level as a simple noninvasive marker of mafld severity. *Diabetes Metab Syndr Obes.* 14l, 2247-2254.

Hemani, G, Bowden, J and Davey Smith, G (2018a) Evaluating the potential role of pleiotropy in mendelian randomization studies. *Hum Mol Genet.* 27l, R195-r208.

Hemani, G, Zheng, J, Elsworth, B, Wade, KH, Haberland, V, Baird, D, Laurin, C, Burgess, S, Bowden, J, Langdon, R, Tan, VY, Yarmolinsky, J, Shihab, HA, Timpson, NJ, Evans, DM, Relton, C, Martin, RM, Davey Smith, G, Gaunt, TR and Haycock, PC (2018b) The mr-base platform supports systematic causal inference across the human phenome. *Elife.* 7l.

Hendy, OM, Rabie, H, El Fouly, A, Abdel-Samiee, M, Abdelmotelb, N, Elshormilisy, AA, Allam, M, Ali, ST, Bahaa El-Deen, NM, Abdelsattar, S and Mohamed, SM (2019) The circulating micro-rnas (-122, -34a and -99a) as predictive biomarkers for non-alcoholic fatty liver diseases. *Diabetes Metab Syndr Obes.* 12l, 2715-2723.

Hermeking, H (2010) The mir-34 family in cancer and apoptosis. *Cell Death Differ.* 17l, 193-199.

Herranz, D, Munoz-Martin, M, Canamero, M, Mulero, F, Martinez-Pastor, B, Fernandez-Capetillo, O and Serrano, M (2010) Sirt1 improves healthy ageing and protects from metabolic syndrome-associated cancer. *Nat Commun.* 1l, 3.

Herrmann, J, Gressner, AM and Weiskirchen, R (2007) Immortal hepatic stellate cell lines: Useful tools to study hepatic stellate cell biology and function? *J Cell Mol Med.* 11l, 704-722.

Hilmarsdottir, B, Briem, E, Bergthorsson, JT, Magnusson, MK and Gudjonsson, T (2014) Functional role of the microrna-200 family in breast morphogenesis and neoplasia. *Genes (Basel).* 5l, 804-820.

Hirschey, MD, Shimazu, T, Jing, E, Grueter, CA, Collins, AM, Aouizerat, B, Stancakova, A, Goetzman, E, Lam, MM, Schwer, B, Stevens, RD, Muehlbauer, MJ, Kakar, S, Bass, NM, Kuusisto, J, Laakso, M, Alt, FW, Newgard, CB, Farese, RV, Jr., Kahn, CR and Verdin, E (2011) Sirt3 deficiency and mitochondrial protein hyperacetylation accelerate the development of the metabolic syndrome. *Mol Cell.* 44l, 177-190.

Holick, MF (2017) The vitamin d deficiency pandemic: Approaches for diagnosis, treatment and prevention. *Rev Endocr Metab Disord.* 18l, 153-165.

Holick, MF, Binkley, NC, Bischoff-Ferrari, HA, Gordon, CM, Hanley, DA, Heaney, RP, Murad, MH, Weaver, CM and Endocrine, S (2011) Evaluation, treatment, and prevention of vitamin d deficiency: An endocrine society clinical practice guideline. *J Clin Endocrinol Metab.* 96l, 1911-1930.

Hollis, BW (2011) Short-term and long-term consequences and concerns regarding valid assessment of vitamin d deficiency: Comparison of recent food supplementation and clinical guidance reports. *Curr Opin Clin Nutr Metab Care.* 14l, 598-604.

Hotamisligil, GS, Shargill, NS and Spiegelman, BM (1993) Adipose expression of tumor necrosis factor-alpha: Direct role in obesity-linked insulin resistance. *Science.* 259l, 87-91.

Hsin, JP, Lu, Y, Loeb, GB, Leslie, CS and Rudensky, AY (2018) The effect of cellular context on mir-155-mediated gene regulation in four major immune cell types. *Nat Immunol.* 19l, 1137-1145.

Hsu, SH, Wang, B, Kota, J, Yu, J, Costinean, S, Kutay, H, Yu, L, Bai, S, La Perle, K, Chivukula, RR, Mao, H, Wei, M, Clark, KR, Mendell, JR, Caligiuri, MA, Jacob, ST, Mendell, JT and Ghoshal, K (2012) Essential

metabolic, anti-inflammatory, and anti-tumorigenic functions of mir-122 in liver. *J Clin Invest.* 122l, 2871-2883.

Hu, J, Zheng, L, Shen, X, Zhang, Y, Li, C and Xi, T (2017) Microrna-125b inhibits aml cells differentiation by directly targeting fes. *Gene.* 620l, 1-9.

Hu, S, Bae, M, Park, YK and Lee, JY (2020) N-3 pufas inhibit tgfbeta1-induced profibrogenic gene expression by ameliorating the repression of ppargamma in hepatic stellate cells. *J Nutr Biochem.* 85l, 108452.

Hu, Y and Yu, Y (2020) Dysregulation of mir-192-5p in acute pancreatitis patients with nonalcoholic fatty liver and its functional role in acute pancreatitis progression. *Biosci Rep.* 40l.

Huang da, W, Sherman, BT, Zheng, X, Yang, J, Imamichi, T, Stephens, R and Lempicki, RA (2009) Extracting biological meaning from large gene lists with david. *Curr Protoc Bioinformatics.* Chapter 13l, Unit 13 11.

Huang, R, Duan, X, Liu, X, Cao, H, Wang, Y, Fan, J and Wang, B (2019) Upregulation of mir-181a impairs lipid metabolism by targeting pparα expression in nonalcoholic fatty liver disease. *Biochem Biophys Res Commun.* 508l, 1252-1258.

Huang, X, Liu, G, Guo, J and Su, Z (2018) The pi3k/akt pathway in obesity and type 2 diabetes. *Int J Biol Sci.* 14l, 1483-1496.

Hurd, PJ and Nelson, CJ (2009) Advantages of next-generation sequencing versus the microarray in epigenetic research. *Brief Funct Genomic Proteomic.* 8l, 174-183.

Hussain, M, Iqbal, J, Malik, SA, Waheed, A, Shabnum, S, Akhtar, L and Saeed, H (2019) Effect of vitamin d supplementation on various parameters in non-alcoholic fatty liver disease patients. *Pakistan journal of pharmaceutical sciences.* 32l, 1343-1348.

Indrieri, A, Carrella, S, Carotenuto, P, Banfi, S and Franco, B (2020) The pervasive role of the mir-181 family in development, neurodegeneration, and cancer. *Int J Mol Sci.* 21l.

Isakova, T, Nickolas, TL, Denburg, M, Yarlagadda, S, Weiner, DE, Gutiérrez, OM, Bansal, V, Rosas, SE, Nigwekar, S, Yee, J and Kramer, H (2017) Kdoqi us commentary on the 2017 kdigo clinical practice guideline update for the diagnosis, evaluation, prevention, and treatment of chronic kidney disease-mineral and bone disorder (ckd-mbd). *Am J Kidney Dis.* 70l, 737-751.

Ishibashi, H, Nakamura, M, Komori, A, Migita, K and Shimoda, S (2009) Liver architecture, cell function, and disease. *Semin Immunopathol.* 31l, 399-409.

Jampoka, K, Muangpaisarn, P, Khongnomnan, K, Treeprasertsuk, S, Tangkijvanich, P and Payungporn, S (2018) Serum mir-29a and mir-122 as potential biomarkers for non-alcoholic fatty liver disease (nafld). *Microrna.* 7l, 215-222.

Jamwal, R, de la Monte, SM, Ogasawara, K, Adusumalli, S, Barlock, BB and Akhlaghi, F (2018) Nonalcoholic fatty liver disease and diabetes are associated with decreased cyp3a4 protein expression and activity in human liver. *Mol Pharm.* 15l, 2621-2632.

Jaruvongvanich, V, Ahuja, W, Sanguankeo, A, Wijarnpreecha, K and Upala, S (2017) Vitamin d and histologic severity of nonalcoholic fatty liver disease: A systematic review and meta-analysis. *Dig Liver Dis.* 49l, 618-622.

Jayakumar, S and Loomba, R (2019) Review article: Emerging role of the gut microbiome in the progression of nonalcoholic fatty liver disease and potential therapeutic implications. *Aliment Pharmacol Ther.*

Jeon, SM and Shin, EA (2018) Exploring vitamin d metabolism and function in cancer. *Exp Mol Med.* 50l, 1-14.

Jet, T, Gines, G, Rondelez, Y and Taly, V (2021) Advances in multiplexed techniques for the detection and quantification of micrornas. *Chem Soc Rev.* 50l, 4141-4161.

Ji, C and Guo, X (2019) The clinical potential of circulating micrornas in obesity. *Nat Rev Endocrinol.* 15l, 731-743.

Ji, J, Zhang, J, Huang, G, Qian, J, Wang, X and Mei, S (2009) Over-expressed microrna-27a and 27b influence fat accumulation and cell proliferation during rat hepatic stellate cell activation. *FEBS Lett.* 583l, 759-766.

Jiang, W, Liu, J, Dai, Y, Zhou, N, Ji, C and Li, X (2015) Mir-146b attenuates high-fat diet-induced non-alcoholic steatohepatitis in mice. *J Gastroenterol Hepatol.* 30l, 933-943.

Jiang, X, O'Reilly, PF, Aschard, H, Hsu, YH, Richards, JB, Dupuis, J, Ingelsson, E, Karasik, D, Pilz, S, Berry, D, Kestenbaum, B, Zheng, J, Luan, J, Sofianopoulou, E, Streeten, EA, Albanes, D, Lutsey, PL, Yao, L, Tang, W, Econs, MJ, Wallaschofski, H, Volzke, H, Zhou, A, Power, C, McCarthy, MI, Michos, ED, Boerwinkle, E, Weinstein, SJ, Freedman, ND, Huang, WY, Van Schoor, NM, van der Velde, N, Groot, L, Enneman, A, Cupples, LA, Booth, SL, Vasan, RS, Liu, CT, Zhou, Y, Ripatti, S, Ohlsson, C, Vandenput, L, Lorentzon, M, Eriksson, JG, Shea, MK, Houston, DK, Kritchevsky, SB, Liu, Y, Lohman, KK, Ferrucci, L, Peacock, M, Gieger, C, Beekman, M, Slagboom, E, Deelen, J, Heemst, DV, Kleber, ME, Marz, W, de Boer, IH, Wood, AC, Rotter, JI, Rich, SS, Robinson-Cohen, C, den Heijer, M, Jarvelin, MR, Cavadino, A, Joshi, PK, Wilson, JF, Hayward, C, Lind, L, Michaelsson, K, Trompet, S, Zillikens, MC, Uitterlinden, AG, Rivadeneira, F, Broer, L, Zgaga, L, Campbell, H, Theodoratou, E, Farrington, SM, Timofeeva, M, Dunlop, MG, Valdes, AM, Tikkanen, E, Lehtimaki, T, Lyytikainen, LP, Kahonen, M, Raitakari, OT, Mikkila, V, Ikram, MA, Sattar, N, Jukema, JW, Wareham, NJ, Langenberg, C, Forouhi, NG, Gundersen, TE, Khaw, KT, Butterworth, AS, Danesh, J, Spector, T, Wang, TJ, Hypponen, E, Kraft, P and Kiel, DP (2018) Genome-wide association study in 79,366 european-ancestry individuals informs the genetic architecture of 25-hydroxyvitamin d levels. *Nat Commun.* 9l, 260.

Jiang, Z, Hu, J, Li, X, Jiang, Y, Zhou, W and Lu, D (2006) Expression analyses of 27 DNA repair genes in astrocytoma by taqman low-density array. *Neurosci Lett.* 409l, 112-117.

Jin, D, Wu, S, Zhang, YG, Lu, R, Xia, Y, Dong, H and Sun, J (2015) Lack of vitamin d receptor causes dysbiosis and changes the functions of the murine intestinal mcrobiome. *Clin Ther.* 37l, 996-1009.e1007.

Jin, X, Liu, J, Chen, YP, Xiang, Z, Ding, JX and Li, YM (2017) Effect of mir-146 targeted hdmcp up-regulation in the pathogenesis of nonalcoholic steatohepatitis. *PLoS One.* 12l, e0174218.

Jonas, MI, Kuryłowicz, A, Bartoszewicz, Z, Lisik, W, Jonas, M, Kozniewski, K and Puzianowska-Kuznicka, M (2019) Vitamin d receptor gene expression in adipose tissue of obese individuals is regulated by mirna

and correlates with the pro-inflammatory cytokine level. *Int J Mol Sci.* 20l.

Jonas, W and Schurmann, A (2021) Genetic and epigenetic factors determining nafld risk. *Mol Metab.* 50l, 101111.

Jopling, C (2012) Liver-specific microrna-122: Biogenesis and function. *RNA Biol.* 9l, 137-142.

Jorde, R, Svartberg, J, Joakimsen, RM and Coucheron, DH (2012) Plasma profile of microrna after supplementation with high doses of vitamin d3 for 12 months. *BMC Res Notes.* 5l, 245.

Juanola, O, Martinez-Lopez, S, Frances, R and Gomez-Hurtado, I (2021) Non-alcoholic fatty liver disease: Metabolic, genetic, epigenetic and environmental risk factors. *Int J Environ Res Public Health.* 18l.

Kammel, A, Saussenthaler, S, Jahnert, M, Jonas, W, Stirm, L, Hoeflich, A, Staiger, H, Fritsche, A, Haring, HU, Joost, HG, Schurmann, A and Schwenk, RW (2016) Early hypermethylation of hepatic igfbp2 results in its reduced expression preceding fatty liver in mice. *Hum Mol Genet.* 25l, 2588-2599.

Kampe, A, Enlund-Cerullo, M, Valkama, S, Holmlund-Suila, E, Rosendahl, J, Hauta-Alus, H, Pekkinen, M, Andersson, S and Makitie, O (2019) Genetic variation in gc and cyp2r1 affects 25-hydroxyvitamin d concentration and skeletal parameters: A genome-wide association study in 24-month-old finnish children. *PLoS Genet.* 15l, e1008530.

Kanehisa, M, Furumichi, M, Tanabe, M, Sato, Y and Morishima, K (2016) Kegg: New perspectives on genomes, pathways, diseases and drugs. *Nucleic Acids Research.* 45l, D353-D361.

Kaplan, MM (1972) Alkaline phosphatase. *Gastroenterology.* 62l, 452-468.

Karatayli, E, Stokes, CS and Lammert, F (2020) Vitamin d in preclinical models of fatty liver disease. *Anticancer Res.* 40l, 527-534.

Karkeni, E, Bonnet, L, Marcotorchino, J, Tourniaire, F, Astier, J, Ye, J and Landrier, JF (2018) Vitamin d limits inflammation-linked microrna expression in adipocytes in vitro and in vivo: A new mechanism for the regulation of inflammation by vitamin d. *Epigenetics.* 13l, 156-162.

Kawaguchi, T, Shima, T, Mizuno, M, Mitsumoto, Y, Umemura, A, Kanbara, Y, Tanaka, S, Sumida, Y, Yasui, K, Takahashi, M, Matsuo, K, Itoh, Y, Tokushige, K, Hashimoto, E, Kiyosawa, K, Kawaguchi, M, Itoh, H, Uto, H, Komorizono, Y, Shirabe, K, Takami, S, Takamura, T, Kawanaka, M, Yamada, R, Matsuda, F and Okanoue, T (2018) Risk estimation model for nonalcoholic fatty liver disease in the japanese using multiple genetic markers. *PLoS One.* 13l, e0185490.

Kawaguchi, T, Sumida, Y, Umemura, A, Matsuo, K, Takahashi, M, Takamura, T, Yasui, K, Saibara, T, Hashimoto, E, Kawanaka, M, Watanabe, S, Kawata, S, Imai, Y, Kokubo, M, Shima, T, Park, H, Tanaka, H, Tajima, K, Yamada, R, Matsuda, F, Okanoue, T and Japan Study Group of Nonalcoholic Fatty Liver, D (2012) Genetic polymorphisms of the human pnpla3 gene are strongly associated with severity of non-alcoholic fatty liver disease in japanese. *PLoS One.* 7l, e38322.

Keller, A and Meese, E (2016) Can circulating mirnas live up to the promise of being minimal invasive biomarkers in clinical settings? *Wiley Interdiscip Rev RNA.* 7l, 148-156.

Kempinska-Podhorodecka, A, Milkiewicz, M, Wasik, U, Ligocka, J, Zawadzki, M, Krawczyk, M and Milkiewicz, P (2017) Decreased expression of

vitamin d receptor affects an immune response in primary biliary cholangitis via the vdr-mirna155-socs1 pathway. *Int J Mol Sci.* 18l.

Kida, K, Nakajima, M, Mohri, T, Oda, Y, Takagi, S, Fukami, T and Yokoi, T (2011) Pparα is regulated by mir-21 and mir-27b in human liver. *Pharm Res.* 28l, 2467-2476.

Kim, HS, Patel, K, Muldoon-Jacobs, K, Bisht, KS, Aykin-Burns, N, Pennington, JD, van der Meer, R, Nguyen, P, Savage, J, Owens, KM, Vassilopoulos, A, Ozden, O, Park, SH, Singh, KK, Abdulkadir, SA, Spitz, DR, Deng, CX and Gius, D (2010) Sirt3 is a mitochondria-localized tumor suppressor required for maintenance of mitochondrial integrity and metabolism during stress. *Cancer Cell.* 17l, 41-52.

Kim, YK, Yeo, J, Kim, B, Ha, M and Kim, VN (2012) Short structured rnas with low gc content are selectively lost during extraction from a small number of cells. *Mol Cell.* 46l, 893-895.

Kitamoto, T, Kitamoto, A, Yoneda, M, Hyogo, H, Ochi, H, Mizusawa, S, Ueno, T, Nakao, K, Sekine, A, Chayama, K, Nakajima, A and Hotta, K (2014) Targeted next-generation sequencing and fine linkage disequilibrium mapping reveals association of pnpla3 and parvb with the severity of nonalcoholic fatty liver disease. *J Hum Genet.* 59l, 241-246.

Kitamoto, T, Kitamoto, A, Yoneda, M, Hyogo, H, Ochi, H, Nakamura, T, Teranishi, H, Mizusawa, S, Ueno, T, Chayama, K, Nakajima, A, Nakao, K, Sekine, A and Hotta, K (2013) Genome-wide scan revealed that polymorphisms in the pnpla3, samm50, and parvb genes are associated with development and progression of nonalcoholic fatty liver disease in japan. *Hum Genet.* 132l, 783-792.

Kitson, MT, Pham, A, Gordon, A, Kemp, W and Roberts, SK (2016) High-dose vitamin d supplementation and liver histology in nash. *Gut.* 65l, 717-718.

Kitson, MT and Roberts, SK (2012) D-livering the message: The importance of vitamin d status in chronic liver disease. *J Hepatol.* 57l, 897-909.

Kleinstein, SE, Rein, M, Abdelmalek, MF, Guy, CD, Goldstein, DB, Mae Diehl, A and Moylan, CA (2018) Whole-exome sequencing study of extreme phenotypes of nafld. *Hepatol Commun.* 2l, 1021-1029.

Klopotowska, D, Matuszyk, J and Wietrzyk, J (2019) Steroid hormone calcitriol and its analog tacalcitol inhibit mir-125b expression in a human breast cancer mcf-7 cell line. *Steroids.* 141l, 70-75.

Kmiec, Z (2001) Cooperation of liver cells in health and disease. *Adv Anat Embryol Cell Biol.* 161l, III-XIII, 1-151.

Kogiso, T, Moriyoshi, Y, Shimizu, S, Nagahara, H and Shiratori, K (2009) High-sensitivity c-reactive protein as a serum predictor of nonalcoholic fatty liver disease based on the akaike information criterion scoring system in the general japanese population. *J Gastroenterol.* 44l, 313-321.

Komagata, S, Nakajima, M, Takagi, S, Mohri, T, Taniya, T and Yokoi, T (2009) Human cyp24 catalyzing the inactivation of calcitriol is post-transcriptionally regulated by mir-125b. *Mol Pharmacol.* 76l, 702-709.

Koo, BK, Joo, SK, Kim, D, Bae, JM, Park, JH, Kim, JH and Kim, W (2018) Additive effects of pnpla3 and tm6sf2 on the histological severity of non-alcoholic fatty liver disease. *J Gastroenterol Hepatol.* 33l, 1277-1285.

Korgavkar, K, Xiong, M and Weinstock, MA (2014) Review: Higher vitamin d status and supplementation may be associated with risks. *Eur J Dermatol.* 24l, 428-434.

Korpal, M and Kang, Y (2008) The emerging role of mir-200 family of micrornas in epithelial-mesenchymal transition and cancer metastasis. *RNA Biol.* 5l, 115-119.

Kosgei, VJ, Coelho, D, Guéant-Rodriguez, RM and Guéant, JL (2020) Sirt1-ppars cross-talk in complex metabolic diseases and inherited disorders of the one carbon metabolism. *Cells.* 9l.

Kozlitina, J, Smagris, E, Stender, S, Nordestgaard, BG, Zhou, HH, Tybjærg-Hansen, A, Vogt, TF, Hobbs, HH and Cohen, JC (2014) Exome-wide association study identifies a tm6sf2 variant that confers susceptibility to nonalcoholic fatty liver disease. *Nat Genet.* 46l, 352-356.

Kozlitina, J, Stender, S, Hobbs, HH and Cohen, JC (2018) Hsd17b13 and chronic liver disease in blacks and hispanics. *N Engl J Med.* 379l, 1876-1877.

Krawczyk, M, Liebe, R and Lammert, F (2020) Toward genetic prediction of nonalcoholic fatty liver disease trajectories: Pnpla3 and beyond. *Gastroenterology.* 158l, 1865-1880 e1861.

Krawczyk, M, Rau, M, Schattenberg, JM, Bantel, H, Pathil, A, Demir, M, Kluwe, J, Boettler, T, Lammert, F, Geier, A and Group, NCS (2017) Combined effects of the pnpla3 rs738409, tm6sf2 rs58542926, and mboat7 rs641738 variants on nafld severity: A multicenter biopsy-based study. *J Lipid Res.* 58l, 247-255.

Krycer, JR, Sharpe, LJ, Luu, W and Brown, AJ (2010) The akt-srebp nexus: Cell signaling meets lipid metabolism. *Trends Endocrinol Metab.* 21l, 268-276.

Kumarswamy, R, Volkmann, I and Thum, T (2011) Regulation and function of mirna-21 in health and disease. *RNA Biol.* 8l, 706-713.

Kunst, RF, Niemeijer, M, van der Laan, LJW, Spee, B and van de Graaf, SFJ (2020) From fatty hepatocytes to impaired bile flow: Matching model systems for liver biology and disease. *Biochem Pharmacol.* 180l, 114173.

Kwok, RM, Torres, DM and Harrison, SA (2013) Vitamin d and nonalcoholic fatty liver disease (nafld): Is it more than just an association? *Hepatology.* 58l, 1166-1174.

Langi, G, Szczerbinski, L and Kretowski, A (2019) Meta-analysis of differential mirna expression after bariatric surgery. *J Clin Med.* 8l.

Latorre, J, Moreno-Navarrete, JM, Mercader, JM, Sabater, M, Rovira, Gironès, J, Ricart, W, Fernández-Real, JM and Ortega, FJ (2017a) Decreased lipid metabolism but increased fa biosynthesis are coupled with changes in liver micrornas in obese subjects with nafld. *International Journal of Obesity.* 41l, 620-630.

Latorre, J, Moreno-Navarrete, JM, Mercader, JM, Sabater, M, Rovira, Ò, Gironès, J, Ricart, W, Fernández-Real, JM and Ortega, FJ (2017b) Decreased lipid metabolism but increased fa biosynthesis are coupled with changes in liver micrornas in obese subjects with nafld. *Int J Obes (Lond).* 41l, 620-630.

Latorre, J, Ortega, FJ, Liñares-Pose, L, Moreno-Navarrete, JM, Lluch, A, Comas, F, Oliveras-Cañellas, N, Ricart, W, Höring, M, Zhou, Y, Liebisch, G, Nidhina Haridas, PA, Olkkonen, VM, López, M and

Fernández-Real, JM (2020) Compounds that modulate ampk activity and hepatic steatosis impact the biosynthesis of micrornas required to maintain lipid homeostasis in hepatocytes. *EBioMedicine.* 53l, 102697.
Lawlor, DA, Harbord, RM, Sterne, JA, Timpson, N and Davey Smith, G (2008) Mendelian randomization: Using genes as instruments for making causal inferences in epidemiology. *Stat Med.* 27l, 1133-1163.
Lee, HJ, Muindi, JR, Tan, W, Hu, Q, Wang, D, Liu, S, Wilding, GE, Ford, LA, Sait, SN, Block, AW, Adjei, AA, Barcos, M, Griffiths, EA, Thompson, JE, Wang, ES, Johnson, CS, Trump, DL and Wetzler, M (2014a) Low 25(oh) vitamin d3 levels are associated with adverse outcome in newly diagnosed, intensively treated adult acute myeloid leukemia. *Cancer.* 120l, 521-529.
Lee, J, Kim, Y, Friso, S and Choi, SW (2017a) Epigenetics in non-alcoholic fatty liver disease. *Mol Aspects Med.* 54l, 78-88.
Lee, JH, Friso, S and Choi, SW (2014b) Epigenetic mechanisms underlying the link between non-alcoholic fatty liver diseases and nutrition. *Nutrients.* 6l, 3303-3325.
Lee, JY, Cho, HK and Kwon, YH (2010) Palmitate induces insulin resistance without significant intracellular triglyceride accumulation in hepg2 cells. *Metabolism.* 59l, 927-934.
Lee, YS, Kim, SY, Ko, E, Lee, JH, Yi, HS, Yoo, YJ, Je, J, Suh, SJ, Jung, YK, Kim, JH, Seo, YS, Yim, HJ, Jeong, WI, Yeon, JE, Um, SH and Byun, KS (2017b) Exosomes derived from palmitic acid-treated hepatocytes induce fibrotic activation of hepatic stellate cells. *Sci Rep.* 7l, 3710.
Leti, F, Malenica, I, Doshi, M, Courtright, A, Van Keuren-Jensen, K, Legendre, C, Still, CD, Gerhard, GS and DiStefano, JK (2015) High-throughput sequencing reveals altered expression of hepatic micrornas in nonalcoholic fatty liver disease-related fibrosis. *Transl Res.* 166l, 304-314.
Li, B, Zhang, Z, Zhang, H, Quan, K, Lu, Y, Cai, D and Ning, G (2014) Aberrant mir199a-5p/caveolin1/pparα axis in hepatic steatosis. *J Mol Endocrinol.* 53l, 393-403.
Li, F, Zhang, A, Shi, Y, Ma, Y and Du, Y (2015) 1α,25-dihydroxyvitamin d3 prevents the differentiation of human lung fibroblasts via microrna-27b targeting the vitamin d receptor. *Int J Mol Med.* 36l, 967-974.
Li, J, Zhao, Y, Zhang, H, Hua, W, Jiao, W, Du, X, Rui, J, Li, S, Teng, H, Shi, B, Yang, X and Zhu, L (2021) Contribution of rs780094 and rs1260326 polymorphisms in gckr gene to non-alcoholic fatty liver disease: A meta-analysis involving 26,552 participants. *Endocr Metab Immune Disord Drug Targets.* 21l, 1696-1708.
Li, JZ, Huang, Y, Karaman, R, Ivanova, PT, Brown, HA, Roddy, T, Castro-Perez, J, Cohen, JC and Hobbs, HH (2012) Chronic overexpression of pnpla3i148m in mouse liver causes hepatic steatosis. *J Clin Invest.* 122l, 4130-4144.
Li, R, Guo, E, Yang, J, Li, A, Yang, Y, Liu, S, Liu, A and Jiang, X (2017) 1,25(oh)(2) d(3) attenuates hepatic steatosis by inducing autophagy in mice. *Obesity (Silver Spring).* 25l, 561-571.
Li, S, Chen, X, Zhang, H, Liang, X, Xiang, Y, Yu, C, Zen, K, Li, Y and Zhang, CY (2009) Differential expression of micrornas in mouse liver under aberrant energy metabolic status. *J Lipid Res.* 50l, 1756-1765.

Li, X, Liu, Y, Zheng, Y, Wang, P and Zhang, Y (2018) The effect of vitamin d supplementation on glycemic control in type 2 diabetes patients: A systematic review and meta-analysis. *Nutrients.* 10l.

Li, X, Zhang, S, Blander, G, Tse, JG, Krieger, M and Guarente, L (2007) Sirt1 deacetylates and positively regulates the nuclear receptor lxr. *Mol Cell.* 28l, 91-106.

Li, Y, Luan, Y, Li, J, Song, H, Li, Y, Qi, H, Sun, B, Zhang, P, Wu, X, Liu, X, Yang, Y, Tao, W, Cai, L, Yang, Z and Yang, Y (2020) Exosomal mir-199a-5p promotes hepatic lipid accumulation by modulating mst1 expression and fatty acid metabolism. *Hepatol Int.* 14l, 1057-1074.

Li, Y, Reddy, MA, Miao, F, Shanmugam, N, Yee, JK, Hawkins, D, Ren, B and Natarajan, R (2008) Role of the histone h3 lysine 4 methyltransferase, set7/9, in the regulation of nf-kappab-dependent inflammatory genes. Relevance to diabetes and inflammation. *J Biol Chem.* 283l, 26771-26781.

Liang, ZR, Qu, LH and Ma, LM (2020) Differential impacts of charcoal-stripped fetal bovine serum on c-myc among distinct subtypes of breast cancer cell lines. *Biochem Biophys Res Commun.* 526l, 267-272.

Liangpunsakul, S and Chalasani, N (2011) Serum vitamin d concentrations and unexplained elevation in alt among us adults. *Dig Dis Sci.* 56l, 2124-2129.

Liebe, R, Esposito, I, Bock, HH, Vom Dahl, S, Stindt, J, Baumann, U, Luedde, T and Keitel, V (2021) Diagnosis and management of secondary causes of steatohepatitis. *J Hepatol.* 74l, 1455-1471.

Lin, Q, Gao, Z, Alarcon, RM, Ye, J and Yun, Z (2009) A role of mir-27 in the regulation of adipogenesis. *Febs j.* 276l, 2348-2358.

Liu, CH, Ampuero, J, Gil-Gómez, A, Montero-Vallejo, R, Rojas, Á, Muñoz-Hernández, R, Gallego-Durán, R and Romero-Gómez, M (2018) Mirnas in patients with non-alcoholic fatty liver disease: A systematic review and meta-analysis. *J Hepatol.* 69l, 1335-1348.

Liu, J, Lin, B, Chen, Z, Deng, M, Wang, Y, Wang, J, Chen, L, Zhang, Z, Xiao, X, Chen, C and Song, Y (2020a) Identification of key pathways and genes in nonalcoholic fatty liver disease using bioinformatics analysis. *Arch Med Sci.* 16l, 374-385.

Liu, PT, Wheelwright, M, Teles, R, Komisopoulou, E, Edfeldt, K, Ferguson, B, Mehta, MD, Vazirnia, A, Rea, TH, Sarno, EN, Graeber, TG and Modlin, RL (2012a) Microrna-21 targets the vitamin d-dependent antimicrobial pathway in leprosy. *Nat Med.* 18l, 267-273.

Liu, RH, Ning, B, Ma, XE, Gong, WM and Jia, TH (2016a) Regulatory roles of microrna-21 in fibrosis through interaction with diverse pathways (review). *Mol Med Rep.* 13l, 2359-2366.

Liu, T, Wang, P, Cong, M, Xu, Y, Jia, J and You, H (2013) The cyp2e1 inhibitor ddc up-regulates mmp-1 expression in hepatic stellate cells via an erk1/2- and akt-dependent mechanism. *Biosci Rep.* 33l.

Liu, T, Xu, L, Chen, FH and Zhou, YB (2020b) Association of serum vitamin d level and nonalcoholic fatty liver disease: A meta-analysis. *Eur J Gastroenterol Hepatol.* 32l, 140-147.

Liu, W, Hu, J, Fang, Y, Wang, P, Lu, Y and Shen, N (2021a) Vitamin d status in mainland of china: A systematic review and meta-analysis. *EClinicalMedicine.* 38l, 101017.

Liu, WY, Zhang, X, Li, G, Tang, LJ, Zhu, PW, Rios, RS, Zheng, KI, Ma, HL, Wang, XD, Pan, Q, de Knegt, RJ, Valenti, L, Ghanbari, M and Zheng, MH (2021b) Protective association of klotho rs495392 gene polymorphism against hepatic steatosis in non-alcoholic fatty liver disease patients. *Clin Mol Hepatol.*

Liu, XL, Pan, Q, Cao, HX, Xin, FZ, Zhao, ZH, Yang, RX, Zeng, J, Zhou, H and Fan, JG (2020c) Lipotoxic hepatocyte-derived exosomal microrna 192-5p activates macrophages through rictor/akt/forkhead box transcription factor o1 signaling in nonalcoholic fatty liver disease. *Hepatology.* 72l, 454-469.

Liu, XL, Pan, Q, Zhang, RN, Shen, F, Yan, SY, Sun, C, Xu, ZJ, Chen, YW and Fan, JG (2016b) Disease-specific mir-34a as diagnostic marker of non-alcoholic steatohepatitis in a chinese population. *World J Gastroenterol.* 22l, 9844-9852.

Liu, Y, Han, X, Bian, Z, Peng, Y, You, Z, Wang, Q, Chen, X, Qiu, D and Ma, X (2012b) Activation of liver x receptors attenuates endotoxin-induced liver injury in mice with nonalcoholic fatty liver disease. *Dig Dis Sci.* 57l, 390-398.

Liu, YL, Patman, GL, Leathart, JB, Piguet, AC, Burt, AD, Dufour, JF, Day, CP, Daly, AK, Reeves, HL and Anstee, QM (2014a) Carriage of the pnpla3 rs738409 c >g polymorphism confers an increased risk of non-alcoholic fatty liver disease associated hepatocellular carcinoma. *J Hepatol.* 61l, 75-81.

Liu, YL, Reeves, HL, Burt, AD, Tiniakos, D, McPherson, S, Leathart, JB, Allison, ME, Alexander, GJ, Piguet, AC, Anty, R, Donaldson, P, Aithal, GP, Francque, S, Van Gaal, L, Clement, K, Ratziu, V, Dufour, JF, Day, CP, Daly, AK and Anstee, QM (2014b) Tm6sf2 rs58542926 influences hepatic fibrosis progression in patients with non-alcoholic fatty liver disease. *Nat Commun.* 5l, 4309.

Liu, Z, Que, S, Zhou, L, Zheng, S, Romeo, S, Mardinoglu, A and Valenti, L (2017) The effect of the tm6sf2 e167k variant on liver steatosis and fibrosis in patients with chronic hepatitis c: A meta-analysis. *Sci Rep.* 7l, 9273.

Loh, PR, Kichaev, G, Gazal, S, Schoech, AP and Price, AL (2018) Mixed-model association for biobank-scale datasets. *Nat Genet.* 50l, 906-908.

Loh, PR, Tucker, G, Bulik-Sullivan, BK, Vilhjalmsson, BJ, Finucane, HK, Salem, RM, Chasman, DI, Ridker, PM, Neale, BM, Berger, B, Patterson, N and Price, AL (2015) Efficient bayesian mixed-model analysis increases association power in large cohorts. *Nat Genet.* 47l, 284-290.

Lonardo, A, Bellentani, S, Argo, CK, Ballestri, S, Byrne, CD, Caldwell, SH, Cortez-Pinto, H, Grieco, A, Machado, MV, Miele, L and Targher, G (2015) Epidemiological modifiers of non-alcoholic fatty liver disease: Focus on high-risk groups. *Dig Liver Dis.* 47l, 997-1006.

Long, MD, Thorne, JL, Russell, J, Battaglia, S, Singh, PK, Sucheston-Campbell, LE and Campbell, MJ (2014) Cooperative behavior of the nuclear receptor superfamily and its deregulation in prostate cancer. *Carcinogenesis.* 35l, 262-271.

Long, MT, Gurary, EB, Massaro, JM, Ma, J, Hoffmann, U, Chung, RT, Benjamin, EJ and Loomba, R (2019) Parental non-alcoholic fatty liver

disease increases risk of non-alcoholic fatty liver disease in offspring. *Liver Int.* 39l, 740-747.

Loomba, R, Friedman, SL and Shulman, GI (2021) Mechanisms and disease consequences of nonalcoholic fatty liver disease. *Cell.* 184l, 2537-2564.

Loomba, R, Rao, F, Zhang, L, Khandrika, S, Ziegler, MG, Brenner, DA and O'Connor, DT (2010) Genetic covariance between gamma-glutamyl transpeptidase and fatty liver risk factors: Role of beta2-adrenergic receptor genetic variation in twins. *Gastroenterology.* 139l, 836-845, 845.e831.

Loomba, R, Schork, N, Chen, CH, Bettencourt, R, Bhatt, A, Ang, B, Nguyen, P, Hernandez, C, Richards, L, Salotti, J, Lin, S, Seki, E, Nelson, KE, Sirlin, CB, Brenner, D and Genetics of, NiTC (2015) Heritability of hepatic fibrosis and steatosis based on a prospective twin study. *Gastroenterology.* 149l, 1784-1793.

Lopez-Campistrous, A, Adewuyi, EE, Williams, DC and McMullen, TPW (2021) Gene expression profile of epithelial-mesenchymal transition mediators in papillary thyroid cancer. *Endocrine.* 72l, 452-461.

López-Riera, M, Conde, I, Quintas, G, Pedrola, L, Zaragoza, Á, Perez-Rojas, J, Salcedo, M, Benlloch, S, Castell, JV and Jover, R (2018a) Non-invasive prediction of nafld severity: A comprehensive, independent validation of previously postulated serum microrna biomarkers. *Scientific Reports.* 8l, 1-15.

López-Riera, M, Conde, I, Quintas, G, Pedrola, L, Zaragoza, Á, Perez-Rojas, J, Salcedo, M, Benlloch, S, Castell, JV and Jover, R (2018b) Non-invasive prediction of nafld severity: A comprehensive, independent validation of previously postulated serum microrna biomarkers. *Sci Rep.* 8l, 10606.

López-Riera, M, Conde, I, Tolosa, L, Zaragoza, Á, Castell, JV, Gómez-Lechón, MJ and Jover, R (2017) New microrna biomarkers for drug-induced steatosis and their potential to predict the contribution of drugs to non-alcoholic fatty liver disease. *Front Pharmacol.* 8l, 3.

Lorvand Amiri, H, Agah, S, Mousavi, SN, Hosseini, AF and Shidfar, F (2016) Regression of non-alcoholic fatty liver by vitamin d supplement: A double-blind randomized controlled clinical trial. *Archives of Iranian medicine.* 19l, 631-638.

Lorvand Amiri, H, Agah, S, Tolouei Azar, J, Hosseini, S, Shidfar, F and Mousavi, SN (2017) Effect of daily calcitriol supplementation with and without calcium on disease regression in non-alcoholic fatty liver patients following an energy-restricted diet: Randomized, controlled, double-blind trial. *Clinical nutrition (Edinburgh, Scotland).* 36l, 1490-1497.

Loyer, X, Paradis, V, Hénique, C, Vion, AC, Colnot, N, Guerin, CL, Devue, C, On, S, Scetbun, J, Romain, M, Paul, JL, Rothenberg, ME, Marcellin, P, Durand, F, Bedossa, P, Prip-Buus, C, Baugé, E, Staels, B, Boulanger, CM, Tedgui, A and Rautou, PE (2016) Liver microrna-21 is overexpressed in non-alcoholic steatohepatitis and contributes to the disease in experimental models by inhibiting pparα expression. *Gut.* 65l, 1882-1894.

Lü, B, Xu, J, Chen, J, Yu, J, Xu, E and Lai, M (2008) Taqman low density array is roughly right for gene expression quantification in colorectal cancer. *Clin Chim Acta.* 389l, 146-151.

Lukenda Zanko, V, Domislovic, V, Trkulja, V, Krznaric-Zrnic, I, Turk-Wensveen, T, Krznaric, Z, Filipec Kanizaj, T, Radic-Kristo, D, Bilic-Zulle, L, Orlic, L, Dinjar-Kujundzic, P, Poropat, G, Stimac, D, Hauser, G and Mikolasevic, I (2020) Vitamin d for treatment of non-alcoholic fatty liver disease detected by transient elastography: A randomized, double-blind, placebo-controlled trial. *Diabetes Obes Metab.* 22l, 2097-2106.

Luukkonen, PK, Nick, A, Holtta-Vuori, M, Thiele, C, Isokuortti, E, Lallukka-Bruck, S, Zhou, Y, Hakkarainen, A, Lundbom, N, Peltonen, M, Orho-Melander, M, Oresic, M, Hyotylainen, T, Hodson, L, Ikonen, E and Yki-Jarvinen, H (2019) Human pnpla3-i148m variant increases hepatic retention of polyunsaturated fatty acids. *JCI Insight.* 4l.

Luukkonen, PK, Tukiainen, T, Juuti, A, Sammalkorpi, H, Haridas, PAN, Niemela, O, Arola, J, Orho-Melander, M, Hakkarainen, A, Kovanen, PT, Dwivedi, O, Groop, L, Hodson, L, Gastaldelli, A, Hyotylainen, T, Oresic, M and Yki-Jarvinen, H (2020) Hydroxysteroid 17-beta dehydrogenase 13 variant increases phospholipids and protects against fibrosis in nonalcoholic fatty liver disease. *JCI Insight.* 5l.

Luukkonen, PK, Zhou, Y, Hyotylainen, T, Leivonen, M, Arola, J, Orho-Melander, M, Oresic, M and Yki-Jarvinen, H (2016) The mboat7 variant rs641738 alters hepatic phosphatidylinositols and increases severity of non-alcoholic fatty liver disease in humans. *J Hepatol.* 65l, 1263-1265.

Luukkonen, PK, Zhou, Y, Nidhina Haridas, PA, Dwivedi, OP, Hyotylainen, T, Ali, A, Juuti, A, Leivonen, M, Tukiainen, T, Ahonen, L, Scott, E, Palmer, JM, Arola, J, Orho-Melander, M, Vikman, P, Anstee, QM, Olkkonen, VM, Oresic, M, Groop, L and Yki-Jarvinen, H (2017) Impaired hepatic lipid synthesis from polyunsaturated fatty acids in tm6sf2 e167k variant carriers with nafld. *J Hepatol.* 67l, 128-136.

Ma, Y, Belyaeva, OV, Brown, PM, Fujita, K, Valles, K, Karki, S, de Boer, YS, Koh, C, Chen, Y, Du, X, Handelman, SK, Chen, V, Speliotes, EK, Nestlerode, C, Thomas, E, Kleiner, DE, Zmuda, JM, Sanyal, AJ, Kedishvili, NY, Liang, TJ and Rotman, Y (2019) 17-beta hydroxysteroid dehydrogenase 13 is a hepatic retinol dehydrogenase associated with histological features of nonalcoholic fatty liver disease. *Hepatology.* 69l, 1504-1519.

Macfarlane, LA and Murphy, PR (2010) Microrna: Biogenesis, function and role in cancer. *Curr Genomics.* 11l, 537-561.

Maestro, MA, Molnar, F, Mourino, A and Carlberg, C (2016) Vitamin d receptor 2016: Novel ligands and structural insights. *Expert Opin Ther Pat.* 26l, 1291-1306.

Mahdessian, H, Taxiarchis, A, Popov, S, Silveira, A, Franco-Cereceda, A, Hamsten, A, Eriksson, P and van't Hooft, F (2014) Tm6sf2 is a regulator of liver fat metabolism influencing triglyceride secretion and hepatic lipid droplet content. *Proc Natl Acad Sci U S A.* 111l, 8913-8918.

Mahesh, G and Biswas, R (2019) Microrna-155: A master regulator of inflammation. *J Interferon Cytokine Res.* 39l, 321-330.

Mahmoudi, L, Asadi, S, Al-Mousavi, Z and Niknam, R (2021) A randomized controlled clinical trial comparing calcitriol versus cholecalciferol

supplementation to reduce insulin resistance in patients with non-alcoholic fatty liver disease. *Clin Nutr.* 40l, 2999-3005.

Makkonen, J, Pietilainen, KH, Rissanen, A, Kaprio, J and Yki-Jarvinen, H (2009) Genetic factors contribute to variation in serum alanine aminotransferase activity independent of obesity and alcohol: A study in monozygotic and dizygotic twins. *J Hepatol.* 50l, 1035-1042.

Maldonado, EM, Fisher, CP, Mazzatti, DJ, Barber, AL, Tindall, MJ, Plant, NJ, Kierzek, AM and Moore, JB (2018) Multi-scale, whole-system models of liver metabolic adaptation to fat and sugar in non-alcoholic fatty liver disease. *NPJ Syst Biol Appl.* 4l, 33.

Mancina, RM, Dongiovanni, P, Petta, S, Pingitore, P, Meroni, M, Rametta, R, Boren, J, Montalcini, T, Pujia, A, Wiklund, O, Hindy, G, Spagnuolo, R, Motta, BM, Pipitone, RM, Craxi, A, Fargion, S, Nobili, V, Kakela, P, Karja, V, Mannisto, V, Pihlajamaki, J, Reilly, DF, Castro-Perez, J, Kozlitina, J, Valenti, L and Romeo, S (2016) The mboat7-tmc4 variant rs641738 increases risk of nonalcoholic fatty liver disease in individuals of european descent. *Gastroenterology.* 150l, 1219-1230 e1216.

Manco, M, Ciampalini, P and Nobili, V (2010) Low levels of 25-hydroxyvitamin d(3) in children with biopsy-proven nonalcoholic fatty liver disease. *Hepatology.* 51l, 2229; author reply 2230.

Manning, BD and Toker, A (2017) Akt/pkb signaling: Navigating the network. *Cell.* 169l, 381-405.

Manousaki, D, Dudding, T, Haworth, S, Hsu, YH, Liu, CT, Medina-Gómez, C, Voortman, T, van der Velde, N, Melhus, H, Robinson-Cohen, C, Cousminer, DL, Nethander, M, Vandenput, L, Noordam, R, Forgetta, V, Greenwood, CMT, Biggs, ML, Psaty, BM, Rotter, JI, Zemel, BS, Mitchell, JA, Taylor, B, Lorentzon, M, Karlsson, M, Jaddoe, VVW, Tiemeier, H, Campos-Obando, N, Franco, OH, Utterlinden, AG, Broer, L, van Schoor, NM, Ham, AC, Ikram, MA, Karasik, D, de Mutsert, R, Rosendaal, FR, den Heijer, M, Wang, TJ, Lind, L, Orwoll, ES, Mook-Kanamori, DO, Michaëlsson, K, Kestenbaum, B, Ohlsson, C, Mellström, D, de Groot, L, Grant, SFA, Kiel, DP, Zillikens, MC, Rivadeneira, F, Sawcer, S, Timpson, NJ and Richards, JB (2017) Low-frequency synonymous coding variation in cyp2r1 has large effects on vitamin d levels and risk of multiple sclerosis. *Am J Hum Genet.* 101l, 227-238.

Manousaki, D, Mitchell, R, Dudding, T, Haworth, S, Harroud, A, Forgetta, V, Shah, RL, Luan, J, Langenberg, C, Timpson, NJ and Richards, JB (2020) Genome-wide association study for vitamin d levels reveals 69 independent loci. *Am J Hum Genet.* 106l, 327-337.

Mao, Y, Chen, W, Wu, H, Liu, C, Zhang, J and Chen, S (2020) Mechanisms and functions of mir-200 family in hepatocellular carcinoma. *Onco Targets Ther.* 13l, 13479-13490.

Mariani, S, Fiore, D, Basciani, S, Persichetti, A, Contini, S, Lubrano, C, Salvatori, L, Lenzi, A and Gnessi, L (2015) Plasma levels of sirt1 associate with non-alcoholic fatty liver disease in obese patients. *Endocrine.* 49l, 711-716.

Matsuda, S, Inoue, T, Lee, HC, Kono, N, Tanaka, F, Gengyo-Ando, K, Mitani, S and Arai, H (2008) Member of the membrane-bound o-acyltransferase (mboat) family encodes a lysophospholipid

acyltransferase with broad substrate specificity. *Genes Cells.* 13l, 879-888.
Matsuda, S, Kobayashi, M and Kitagishi, Y (2013) Roles for pi3k/akt/pten pathway in cell signaling of nonalcoholic fatty liver disease. *ISRN Endocrinol.* 2013l, 472432.
Mazzoccoli, G, Vinciguerra, M, Oben, J, Tarquini, R and De Cosmo, S (2014) Non-alcoholic fatty liver disease: The role of nuclear receptors and circadian rhythmicity. *Liver Int.* 34l, 1133-1152.
McCollum, EV and Davis, M (1913) The necessity of certain lipins in the diet during growth. *Journal of Biological Chemistry.* 15l, 167-175.
Mendell, JT and Olson, EN (2012) Micrornas in stress signaling and human disease. *Cell.* 148l, 1172-1187.
Mendes, MM, Darling, AL, Hart, KH, Morse, S, Murphy, RJ and Lanham-New, SA (2019) Impact of high latitude, urban living and ethnicity on 25-hydroxyvitamin d status: A need for multidisciplinary action? *J Steroid Biochem Mol Biol.* 188l, 95-102.
Merlo, A, Herman, JG, Mao, L, Lee, DJ, Gabrielson, E, Burger, PC, Baylin, SB and Sidransky, D (1995) 5' cpg island methylation is associated with transcriptional silencing of the tumour suppressor p16/cdkn2/mts1 in human cancers. *Nat Med.* 1l, 686-692.
Meroni, M, Dongiovanni, P, Longo, M, Carli, F, Baselli, G, Rametta, R, Pelusi, S, Badiali, S, Maggioni, M, Gaggini, M, Fracanzani, AL, Romeo, S, Gatti, S, Davidson, NO, Gastaldelli, A and Valenti, L (2020a) Mboat7 down-regulation by hyper-insulinemia induces fat accumulation in hepatocytes. *EBioMedicine.* 52l, 102658.
Meroni, M, Longo, M, Rustichelli, A and Dongiovanni, P (2020b) Nutrition and genetics in nafld: The perfect binomium. *Int J Mol Sci.* 21l.
Miao, F, Gonzalo, IG, Lanting, L and Natarajan, R (2004) In vivo chromatin remodeling events leading to inflammatory gene transcription under diabetic conditions. *J Biol Chem.* 279l, 18091-18097.
Michaelsson, K, Wolk, A, Byberg, L, Mitchell, A, Mallmin, H and Melhus, H (2017) The seasonal importance of serum 25-hydroxyvitamin d for bone mineral density in older women. *J Intern Med.* 281l, 167-178.
Mirhosseini, N, Vatanparast, H, Mazidi, M and Kimball, SM (2018) Vitamin d supplementation, glycemic control, and insulin resistance in prediabetics: A meta-analysis. *J Endocr Soc.* 2l, 687-709.
Mitsumoto, K, Watanabe, R, Nakao, K, Yonenaka, H, Hashimoto, T, Kato, N, Kumrungsee, T and Yanaka, N (2017) Time-course microarrays reveal early activation of the immune transcriptome in a choline-deficient mouse model of liver injury. *Life Sci.* 184l, 103-111.
Miyaaki, H, Ichikawa, T, Kamo, Y, Taura, N, Honda, T, Shibata, H, Milazzo, M, Fornari, F, Gramantieri, L, Bolondi, L and Nakao, K (2014) Significance of serum and hepatic microrna-122 levels in patients with non-alcoholic fatty liver disease. *Liver Int.* 34l, e302-307.
Mohri, T, Nakajima, M, Takagi, S, Komagata, S and Yokoi, T (2009) Microrna regulates human vitamin d receptor. *Int J Cancer.* 125l, 1328-1333.
Moldovan, L, Batte, KE, Trgovcich, J, Wisler, J, Marsh, CB and Piper, M (2014) Methodological challenges in utilizing mirnas as circulating biomarkers. *J Cell Mol Med.* 18l, 371-390.
Moore, JB (2010) Non-alcoholic fatty liver disease: The hepatic consequence of obesity and the metabolic syndrome. *Proc Nutr Soc.* 69l, 211-220.

Moore, JB (2019a) From sugar to liver fat and public health: Systems biology driven studies in understanding non-alcoholic fatty liver disease pathogenesis. *Proc Nutr Soc.* 78l, 290-304.
Moore, JB (2019b) From sugar to liver fat and public health: Systems biology driven studies in understanding non-alcoholic fatty liver disease pathogenesis. *Proceedings of the Nutrition Society.* 78l, 290-304.
Mori, MA, Ludwig, RG, Garcia-Martin, R, Brandão, BB and Kahn, CR (2019) Extracellular mirnas: From biomarkers to mediators of physiology and disease. *Cell Metab.* 30l, 656-673.
Morvaridzadeh, M, Nachvak, SM, Mohammadi, R, Moradi, S, Mostafai, R, Pizarro, AB and Abdollahzad, H (2021) Probiotic yogurt fortified with vitamin d can improve glycemic status in non-alcoholic fatty liver disease patients: A randomized clinical trial. *Clin Nutr Res.* 10l, 36-47.
Mosmann, T (1983) Rapid colorimetric assay for cellular growth and survival: Application to proliferation and cytotoxicity assays. *J Immunol Methods.* 65l, 55-63.
Mraz, M, Malinova, K, Mayer, J and Pospisilova, S (2009) Microrna isolation and stability in stored rna samples. *Biochem Biophys Res Commun.* 390l, 1-4.
Mukhopadhyay, P, Horvath, B, Rajesh, M, Varga, ZV, Gariani, K, Ryu, D, Cao, Z, Holovac, E, Park, O, Zhou, Z, Xu, MJ, Wang, W, Godlewski, G, Paloczi, J, Nemeth, BT, Persidsky, Y, Liaudet, L, Hasko, G, Bai, P, Boulares, AH, Auwerx, J, Gao, B and Pacher, P (2017) Parp inhibition protects against alcoholic and non-alcoholic steatohepatitis. *J Hepatol.* 66l, 589-600.
Müller, FA and Sturla, SJ (2019) Human in vitro models of nonalcoholic fatty liver disease. *Current Opinion in Toxicology.* 16l, 9-16.
Munafò, MR, Tilling, K, Taylor, AE, Evans, DM and Davey Smith, G (2018) Collider scope: When selection bias can substantially influence observed associations. *Int J Epidemiol.* 47l, 226-235.
Murphy, SK, Yang, H, Moylan, CA, Pang, H, Dellinger, A, Abdelmalek, MF, Garrett, ME, Ashley-Koch, A, Suzuki, A, Tillmann, HL, Hauser, MA and Diehl, AM (2013) Relationship between methylome and transcriptome in patients with nonalcoholic fatty liver disease. *Gastroenterology.* 145l, 1076-1087.
Myung, JK, Jeong, JB, Han, D, Song, CS, Moon, HJ, Kim, YA, Kim, JE, Byun, SJ, Kim, WH and Chang, MS (2011) Well-differentiated liposarcoma of the oesophagus: Clinicopathological, immunohistochemical and array cgh analysis. *Pathol Oncol Res.* 17l, 415-420.
Naderi, M, Pazouki, A, Arefian, E, Hashemi, SM, Jamshidi-Adegani, F, Gholamalamdari, O, Soudi, S, Azadmanesh, K, Mirab Samiee, S, Merat, S, Gholami Fesharaki, M, Mondanizadeh, M, Vasei, M and Soleimani, M (2017) Two triacylglycerol pathway genes, ctdnep1 and lpin1, are down-regulated by hsa-mir-122-5p in hepatocytes. *Arch Iran Med.* 20l, 165-171.
Nair, R and Maseeh, A (2012) Vitamin d: The "sunshine" vitamin. *J Pharmacol Pharmacother.* 3l, 118-126.
Nam, JW, Rissland, OS, Koppstein, D, Abreu-Goodger, C, Jan, CH, Agarwal, V, Yildirim, MA, Rodriguez, A and Bartel, DP (2014) Global analyses of the effect of different cellular contexts on microrna targeting. *Mol Cell.* 53l, 1031-1043.

Namakin, K, Hosseini, M, Zardast, M and Mohammadifard, M (2021) Vitamin d effect on ultrasonography and laboratory indices and biochemical indicators in the blood: An interventional study on 12 to 18-year-old children with fatty liver. *Pediatr Gastroenterol Hepatol Nutr.* 24l, 187-196.

Namjou, B, Lingren, T, Huang, Y, Parameswaran, S, Cobb, BL, Stanaway, IB, Connolly, JJ, Mentch, FD, Benoit, B, Niu, X, Wei, WQ, Carroll, RJ, Pacheco, JA, Harley, ITW, Divanovic, S, Carrell, DS, Larson, EB, Carey, DJ, Verma, S, Ritchie, MD, Gharavi, AG, Murphy, S, Williams, MS, Crosslin, DR, Jarvik, GP, Kullo, IJ, Hakonarson, H, Li, R, e, MN, Xanthakos, SA and Harley, JB (2019) Gwas and enrichment analyses of non-alcoholic fatty liver disease identify new trait-associated genes and pathways across emerge network. *BMC Med.* 17l, 135.

National Institute for Health and Care Excellence (2016) Non-alcoholic fatty liver disease: Assessment and management. *NICE guideline NG49*

Negri, M, Gentile, A, de Angelis, C, Montò, T, Patalano, R, Colao, A, Pivonello, R and Pivonello, C (2020) Vitamin d-induced molecular mechanisms to potentiate cancer therapy and to reverse drug-resistance in cancer cells. *Nutrients.* 12l.

NHC. 2020. *Method for vitamin d deficiency screening.* National Health Commission of the People's Republic of China.

Nobili, V, Giorgio, V, Liccardo, D, Bedogni, G, Morino, G, Alisi, A and Cianfarani, S (2014) Vitamin d levels and liver histological alterations in children with nonalcoholic fatty liver disease. *Eur J Endocrinol.* 170l, 547-553.

Noetel, A, Kwiecinski, M, Elfimova, N, Huang, J and Odenthal, M (2012) Microrna are central players in anti- and profibrotic gene regulation during liver fibrosis. *Front Physiol.* 3l, 49.

Nunez Lopez, YO, Pittas, AG, Pratley, RE and Seyhan, AA (2017) Circulating levels of mir-7, mir-152 and mir-192 respond to vitamin d supplementation in adults with prediabetes and correlate with improvements in glycemic control. *J Nutr Biochem.* 49l, 117-122.

O-Sullivan, I, Zhang, W, Wasserman, DH, Liew, CW, Liu, J, Paik, J, DePinho, RA, Stolz, DB, Kahn, CR, Schwartz, MW and Unterman, TG (2015) Foxo1 integrates direct and indirect effects of insulin on hepatic glucose production and glucose utilization. *Nat Commun.* 6l, 7079.

O'Brien, J, Hayder, H, Zayed, Y and Peng, C (2018a) Overview of microrna biogenesis, mechanisms of actions, and circulation. *Front Endocrinol (Lausanne).* 9l, 402.

O'Brien, KM, Sandler, DP, Shi, M, Harmon, QE, Taylor, JA and Weinberg, CR (2018b) Genome-wide association study of serum 25-hydroxyvitamin d in us women. *Front Genet.* 9l, 67.

Ohara, M, Ohnishi, S, Hosono, H, Yamamoto, K, Fu, Q, Maehara, O, Suda, G and Sakamoto, N (2018) Palmitoylethanolamide ameliorates carbon tetrachloride-induced liver fibrosis in rats. *Front Pharmacol.* 9l, 709.

Okamoto, K, Koda, M, Okamoto, T, Onoyama, T, Miyoshi, K, Kishina, M, Kato, J, Tokunaga, S, Sugihara, T-A, Hara, Y, Hino, K and Murawaki, Y (2016) A series of microrna in the chromosome 14q32.2 maternally imprinted region related to progression of non-alcoholic fatty liver disease in a mouse model. *PLOS ONE.* 11l, e0154676.

Okamoto, K, Koda, M, Okamoto, T, Onoyama, T, Miyoshi, K, Kishina, M, Matono, T, Kato, J, Tokunaga, S, Sugihara, T, Hiramatsu, A, Hyogo, H, Tobita, H, Sato, S, Kawanaka, M, Hara, Y, Hino, K, Chayama, K, Murawaki, Y and Isomoto, H (2020) Serum mir-379 expression is related to the development and progression of hypercholesterolemia in non-alcoholic fatty liver disease. *PLOS ONE.* 15l, e0219412.

Oses, M, Margareto Sanchez, J, Portillo, MP, Aguilera, CM and Labayen, I (2019) Circulating mirnas as biomarkers of obesity and obesity-associated comorbidities in children and adolescents: A systematic review. *Nutrients.* 11l.

Oura, K, Morishita, A and Masaki, T (2020) Molecular and functional roles of micrornas in the progression of hepatocellular carcinoma-a review. *Int J Mol Sci.* 21l.

Pacifico, L, Osborn, JF, Bonci, E, Pierimarchi, P and Chiesa, C (2019) Association between vitamin d levels and nonalcoholic fatty liver disease: Potential confounding variables. *Mini Rev Med Chem.* 19l, 310-332.

Pan, YZ, Gao, W and Yu, AM (2009) Micrornas regulate cyp3a4 expression via direct and indirect targeting. *Drug Metab Dispos.* 37l, 2112-2117.

Papapostoli, I, Lammert, F and Stokes, CS (2016) Effect of short-term vitamin d correction on hepatic steatosis as quantified by controlled attenuation parameter (cap). *J Gastrointestin Liver Dis.* 25l, 175-181.

Park, SL, Li, Y, Sheng, X, Hom, V, Xia, L, Zhao, K, Pooler, L, Setiawan, VW, Lim, U, Monroe, KR, Wilkens, LR, Kristal, BS, Lampe, JW, Hullar, M, Shepherd, J, Loo, LLM, Ernst, T, Franke, AA, Tiirikainen, M, Haiman, CA, Stram, DO, Le Marchand, L and Cheng, I (2020) Genome-wide association study of liver fat: The multiethnic cohort adiposity phenotype study. *Hepatol Commun.* 4l, 1112-1123.

Park, TJ, Hwang, JY, Go, MJ, Lee, HJ, Jang, HB, Choi, Y, Kang, JH, Park, KH, Choi, MG, Song, J, Kim, BJ and Lee, JY (2013) Genome-wide association study of liver enzymes in korean children. *Genomics Inform.* 11l, 149-154.

Pastuszak-Lewandoska, D, Domańska-Senderowska, D, Kiszałkiewicz, J, Szmigielska, P, Snochowska, A, Ratkowski, W, Spieszny, M, Klocek, T, Godlewski, P, Cięszczyk, P, Brzeziańska-Lasota, E, September, AV and Laguette, MJ (2020) Expression levels of selected cytokines and micrornas in response to vitamin d supplementation in ultra-marathon runners. *Eur J Sport Sci.* 20l, 219-228.

Patel, YA, Henao, R, Moylan, CA, Guy, CD, Piercy, DL, Diehl, AM and Abdelmalek, MF (2016) Vitamin d is not associated with severity in nafld: Results of a paired clinical and gene expression profile analysis. *Am J Gastroenterol.* 111l, 1591-1598.

Pedersen, AW, Holmstrøm, K, Jensen, SS, Fuchs, D, Rasmussen, S, Kvistborg, P, Claesson, MH and Zocca, MB (2009) Phenotypic and functional markers for 1alpha,25-dihydroxyvitamin d(3)-modified regulatory dendritic cells. *Clin Exp Immunol.* 157l, 48-59.

Peng, X, Vaishnav, A, Murillo, G, Alimirah, F, Torres, KE and Mehta, RG (2010) Protection against cellular stress by 25-hydroxyvitamin d3 in breast epithelial cells. *J Cell Biochem.* 110l, 1324-1333.

Pessin, JE and Saltiel, AR (2000) Signaling pathways in insulin action: Molecular targets of insulin resistance. *J Clin Invest.* 106l, 165-169.

Peter, ME (2010) Targeting of mrnas by multiple mirnas: The next step. *Oncogene.* 29l, 2161-2164.
Pickett-Blakely, O, Young, K and Carr, RM (2018) Micronutrients in nonalcoholic fatty liver disease pathogenesis. *Cell Mol Gastroenterol Hepatol.* 6l, 451-462.
Pierce, BL, Ahsan, H and Vanderweele, TJ (2011) Power and instrument strength requirements for mendelian randomization studies using multiple genetic variants. *Int J Epidemiol.* 40l, 740-752.
Pillai, SS, Lakhani, HV, Zehra, M, Wang, J, Dilip, A, Puri, N, O'Hanlon, K and Sodhi, K (2020) Predicting nonalcoholic fatty liver disease through a panel of plasma biomarkers and micrornas in female west virginia population. *Int J Mol Sci.* 21l.
Pingitore, P, Dongiovanni, P, Motta, BM, Meroni, M, Lepore, SM, Mancina, RM, Pelusi, S, Russo, C, Caddeo, A, Rossi, G, Montalcini, T, Pujia, A, Wiklund, O, Valenti, L and Romeo, S (2016) Pnpla3 overexpression results in reduction of proteins predisposing to fibrosis. *Hum Mol Genet.* 25l, 5212-5222.
Pingitore, P, Pirazzi, C, Mancina, RM, Motta, BM, Indiveri, C, Pujia, A, Montalcini, T, Hedfalk, K and Romeo, S (2014) Recombinant pnpla3 protein shows triglyceride hydrolase activity and its i148m mutation results in loss of function. *Biochim Biophys Acta.* 1841l, 574-580.
Pingitore, P and Romeo, S (2019) The role of pnpla3 in health and disease. *Biochim Biophys Acta Mol Cell Biol Lipids.* 1864l, 900-906.
Pirazzi, C, Valenti, L, Motta, BM, Pingitore, P, Hedfalk, K, Mancina, RM, Burza, MA, Indiveri, C, Ferro, Y, Montalcini, T, Maglio, C, Dongiovanni, P, Fargion, S, Rametta, R, Pujia, A, Andersson, L, Ghosal, S, Levin, M, Wiklund, O, Iacovino, M, Borén, J and Romeo, S (2014) Pnpla3 has retinyl-palmitate lipase activity in human hepatic stellate cells. *Hum Mol Genet.* 23l, 4077-4085.
Pirola, CJ, Fernández Gianotti, T, Castaño, GO, Mallardi, P, San Martino, J, Mora Gonzalez Lopez Ledesma, M, Flichman, D, Mirshahi, F, Sanyal, AJ and Sookoian, S (2015) Circulating microrna signature in non-alcoholic fatty liver disease: From serum non-coding rnas to liver histology and disease pathogenesis. *Gut.* 64l, 800-812.
Pirola, CJ, Flichman, D, Dopazo, H, Fernández Gianotti, T, San Martino, J, Rohr, C, Garaycoechea, M, Gazzi, C, Castaño, GO and Sookoian, S (2018) A rare nonsense mutation in the glucokinase regulator gene is associated with a rapidly progressive clinical form of nonalcoholic steatohepatitis. *Hepatol Commun.* 2l, 1030-1036.
Pirola, CJ, Garaycoechea, M, Flichman, D, Arrese, M, San Martino, J, Gazzi, C, Castano, GO and Sookoian, S (2019) Splice variant rs72613567 prevents worst histologic outcomes in patients with nonalcoholic fatty liver disease. *J Lipid Res.* 60l, 176-185.
Pirola, CJ, Gianotti, TF, Burgueño, AL, Rey-Funes, M, Loidl, CF, Mallardi, P, Martino, JS, Castaño, GO and Sookoian, S (2013) Epigenetic modification of liver mitochondrial DNA is associated with histological severity of nonalcoholic fatty liver disease. *Gut.* 62l, 1356-1363.
Pludowski, P, Holick, MF, Pilz, S, Wagner, CL, Hollis, BW, Grant, WB, Shoenfeld, Y, Lerchbaum, E, Llewellyn, DJ, Kienreich, K and Soni, M (2013) Vitamin d effects on musculoskeletal health, immunity, autoimmunity, cardiovascular disease, cancer, fertility, pregnancy,

dementia and mortality-a review of recent evidence. *Autoimmun Rev.* 12l, 976-989.

Podolska, A, Kaczkowski, B, Litman, T, Fredholm, M and Cirera, S (2011) How the rna isolation method can affect microrna microarray results. *Acta Biochim Pol.* 58l, 535-540.

Potter, JJ, Liu, X, Koteish, A and Mezey, E (2013) 1,25-dihydroxyvitamin d3 and its nuclear receptor repress human alpha1 (i) collagen expression and type i collagen formation. *Liver Int.* 33l, 677-686.

Pritchard, CC, Cheng, HH and Tewari, M (2012) Microrna profiling: Approaches and considerations. *Nat Rev Genet.* 13l, 358-369.

Pritchard, JK and Przeworski, M (2001) Linkage disequilibrium in humans: Models and data. *Am J Hum Genet.* 69l, 1-14.

Provvisiero, DP, Negri, M, de Angelis, C, Di Gennaro, G, Patalano, R, Simeoli, C, Papa, F, Ferrigno, R, Auriemma, RS, De Martino, MC, Colao, A, Pivonello, R and Pivonello, C (2019) Vitamin d reverts resistance to the mtor inhibitor everolimus in hepatocellular carcinoma through the activation of a mir-375/oncogenes circuit. *Sci Rep.* 9l, 11695.

Puck, TT, Cieciura, SJ and Robinson, A (1958) Genetics of somatic mammalian cells. Iii. Long-term cultivation of euploid cells from human and animal subjects. *J Exp Med.* 108l, 945-956.

Purushotham, A, Schug, TT, Xu, Q, Surapureddi, S, Guo, X and Li, X (2009) Hepatocyte-specific deletion of sirt1 alters fatty acid metabolism and results in hepatic steatosis and inflammation. *Cell Metab.* 9l, 327-338.

Rafiee, S, Mohammadi, H, Ghavami, A, Sadeghi, E, Safari, Z and Askari, G (2021) Efficacy of resveratrol supplementation in patients with nonalcoholic fatty liver disease: A systematic review and meta-analysis of clinical trials. *Complement Ther Clin Pract.* 42l, 101281.

Raza, S, Tewari, A, Rajak, S and Sinha, RA (2021) Vitamins and non-alcoholic fatty liver disease: A molecular insight(small star, filled). *Liver Res.* 5l, 62-71.

Reddy, YK, Marella, HK, Jiang, Y, Ganguli, S, Snell, P, Podila, PSB, Maliakkal, B and Satapathy, SK (2020) Natural history of non-alcoholic fatty liver disease: A study with paired liver biopsies. *J Clin Exp Hepatol.* 10l, 245-254.

Reeder, SB and Sirlin, CB (2010) Quantification of liver fat with magnetic resonance imaging. *Magn Reson Imaging Clin N Am.* 18l, 337-357, ix.

Revez, JA, Lin, T, Qiao, Z, Xue, A, Holtz, Y, Zhu, Z, Zeng, J, Wang, H, Sidorenko, J, Kemper, KE, Vinkhuyzen, AAE, Frater, J, Eyles, D, Burne, THJ, Mitchell, B, Martin, NG, Zhu, G, Visscher, PM, Yang, J, Wray, NR and McGrath, JJ (2020) Genome-wide association study identifies 143 loci associated with 25 hydroxyvitamin d concentration. *Nat Commun.* 11l, 1647.

Rezaei, S, Tabrizi, R, Nowrouzi-Sohrabi, P, Jalali, M, Shabani-Borujeni, M, Modaresi, S, Gholamalizadeh, M and Doaei, S (2021) The effects of vitamin d supplementation on anthropometric and biochemical indices in patients with non-alcoholic fatty liver disease: A systematic review and meta-analysis. *Front Pharmacol.* 12l, 732496.

Rezaei, T, Amini, M, Hashemi, ZS, Mansoori, B, Rezaei, S, Karami, H, Mosafer, J, Mokhtarzadeh, A and Baradaran, B (2020) Microrna-181 serves as a dual-role regulator in the development of human cancers. *Free Radic Biol Med.* 152l, 432-454.

Rhee, EJ, Kim, MK, Park, SE, Park, CY, Baek, KH, Lee, WY, Kang, MI, Park, SW, Kim, SW and Oh, KW (2013) High serum vitamin d levels reduce the risk for nonalcoholic fatty liver disease in healthy men independent of metabolic syndrome. *Endocr J.* 60l, 743-752.

Ricchi, M, Odoardi, MR, Carulli, L, Anzivino, C, Ballestri, S, Pinetti, A, Fantoni, LI, Marra, F, Bertolotti, M, Banni, S, Lonardo, A, Carulli, N and Loria, P (2009) Differential effect of oleic and palmitic acid on lipid accumulation and apoptosis in cultured hepatocytes. *J Gastroenterol Hepatol.* 24l, 830-840.

Rich, NE, Oji, S, Mufti, AR, Browning, JD, Parikh, ND, Odewole, M, Mayo, H and Singal, AG (2018) Racial and ethnic disparities in nonalcoholic fatty liver disease prevalence, severity, and outcomes in the united states: A systematic review and meta-analysis. *Clin Gastroenterol Hepatol.* 16l, 198-210 e192.

Rinella, ME and Sanyal, AJ (2016) Management of nafld: A stage-based approach. *Nat Rev Gastroenterol Hepatol.* 13l, 196-205.

Rissin, DM, López-Longarela, B, Pernagallo, S, Ilyine, H, Vliegenthart, ADB, Dear, JW, Díaz-Mochón, JJ and Duffy, DC (2017) Polymerase-free measurement of microrna-122 with single base specificity using single molecule arrays: Detection of drug-induced liver injury. *PLoS One.* 12l, e0179669.

Rodrigues, PM, Afonso, MB, Simão, AL, Carvalho, CC, Trindade, A, Duarte, A, Borralho, PM, Machado, MV, Cortez-Pinto, H, Rodrigues, CM and Castro, RE (2017) Mir-21 ablation and obeticholic acid ameliorate nonalcoholic steatohepatitis in mice. *Cell Death Dis.* 8l, e2748.

Romeo, S, Kozlitina, J, Xing, C, Pertsemlidis, A, Cox, D, Pennacchio, LA, Boerwinkle, E, Cohen, JC and Hobbs, HH (2008) Genetic variation in pnpla3 confers susceptibility to nonalcoholic fatty liver disease. *Nat Genet.* 40l, 1461-1465.

Romero-Gomez, M, Zelber-Sagi, S and Trenell, M (2017) Treatment of nafld with diet, physical activity and exercise. *J Hepatol.* 67l, 829-846.

Ross, AC (2011) The 2011 report on dietary reference intakes for calcium and vitamin d. *Public Health Nutr.* 14l, 938-939.

Rotman, Y, Koh, C, Zmuda, JM, Kleiner, DE, Liang, TJ and Nash, CRN (2010) The association of genetic variability in patatin-like phospholipase domain-containing protein 3 (pnpla3) with histological severity of nonalcoholic fatty liver disease. *Hepatology.* 52l, 894-903.

Rottiers, V and Näär, AM (2012) Micrornas in metabolism and metabolic disorders. *Nat Rev Mol Cell Biol.* 13l, 239-250.

Rupaimoole, R and Slack, FJ (2017) Microrna therapeutics: Towards a new era for the management of cancer and other diseases. *Nat Rev Drug Discov.* 16l, 203-222.

Saberi, B, Dadabhai, AS, Nanavati, J, Wang, L, Shinohara, RT and Mullin, GE (2018) Vitamin d levels do not predict the stage of hepatic fibrosis in patients with non-alcoholic fatty liver disease: A prisma compliant systematic review and meta-analysis of pooled data. *World J Hepatol.* 10l, 142-154.

SACN. 2016. *Vitamin d and health report.* [Online]: London: Public Health England.

Safari, Z and Gerard, P (2019) The links between the gut microbiome and non-alcoholic fatty liver disease (nafld). *Cell Mol Life Sci.* 76l, 1541-1558.

SAHM (2013) Recommended vitamin d intake and management of low vitamin d status in adolescents: A position statement of the society for adolescent health and medicine. *J Adolesc Health.* 52l, 801-803.

Sakpal, M, Satsangi, S, Mehta, M, Duseja, A, Bhadada, S, Das, A, Dhiman, RK and Chawla, YK (2017) Vitamin d supplementation in patients with nonalcoholic fatty liver disease: A randomized controlled trial. *JGH open.* 1l, 62-67.

Salvoza, NC, Klinzing, DC, Gopez-Cervantes, J and Baclig, MO (2016) Association of circulating serum mir-34a and mir-122 with dyslipidemia among patients with non-alcoholic fatty liver disease. *PLoS ONE.* 11l.

Sapkota, BR, Hopkins, R, Bjonnes, A, Ralhan, S, Wander, GS, Mehra, NK, Singh, JR, Blackett, PR, Saxena, R and Sanghera, DK (2016) Genome-wide association study of 25(oh) vitamin d concentrations in punjabi sikhs: Results of the asian indian diabetic heart study. *J Steroid Biochem Mol Biol.* 158l, 149-156.

Sarafin, K, Durazo-Arvizu, R, Tian, L, Phinney, KW, Tai, S, Camara, JE, Merkel, J, Green, E, Sempos, CT and Brooks, SP (2015) Standardizing 25-hydroxyvitamin d values from the canadian health measures survey. *Am J Clin Nutr.* 102l, 1044-1050.

Schleicher, RL, Sternberg, MR, Looker, AC, Yetley, EA, Lacher, DA, Sempos, CT, Taylor, CL, Durazo-Arvizu, RA, Maw, KL, Chaudhary-Webb, M, Johnson, CL and Pfeiffer, CM (2016) National estimates of serum total 25-hydroxyvitamin d and metabolite concentrations measured by liquid chromatography-tandem mass spectrometry in the us population during 2007-2010. *J Nutr.* 146l, 1051-1061.

Schulze, RJ, Schott, MB, Casey, CA, Tuma, PL and McNiven, MA (2019) The cell biology of the hepatocyte: A membrane trafficking machine. *J Cell Biol.* 218l, 2096-2112.

Schwenger, KJP, Bolzon, CM, Li, C and Allard, JP (2018) Non-alcoholic fatty liver disease and obesity: The role of the gut bacteria. *Eur J Nutr.*

Schwer, B and Verdin, E (2008) Conserved metabolic regulatory functions of sirtuins. *Cell Metab.* 7l, 104-112.

Schwimmer, JB, Celedon, MA, Lavine, JE, Salem, R, Campbell, N, Schork, NJ, Shiehmorteza, M, Yokoo, T, Chavez, A, Middleton, MS and Sirlin, CB (2009) Heritability of nonalcoholic fatty liver disease. *Gastroenterology.* 136l, 1585-1592.

Scientific, TF (2014) Real-time pcr handbook. *Nueva York, Estados Unidos de Amrica: ThermofisherScientific.*

Sekula, P, Del Greco, MF, Pattaro, C and Kottgen, A (2016) Mendelian randomization as an approach to assess causality using observational data. *J Am Soc Nephrol.* 27l, 3253-3265.

Shan, MY, Dai, Y, Ren, XD, Zheng, J, Zhang, KB, Chen, B, Yan, J and Xu, ZH (2021) Berberine mitigates nonalcoholic hepatic steatosis by downregulating sirt1-foxo1-srebp2 pathway for cholesterol synthesis. *J Integr Med.* 19l, 545-554.

Shang, L, Hosseini, M, Liu, X, Kisseleva, T and Brenner, DA (2018) Human hepatic stellate cell isolation and characterization. *J Gastroenterol.* 53l, 6-17.

Sharifi, N, Amani, R, Hajiani, E and Cheraghian, B (2014) Does vitamin d improve liver enzymes, oxidative stress, and inflammatory biomarkers in adults with non-alcoholic fatty liver disease? A randomized clinical trial. *Endocrine.* 47l, 70-80.

Sharifi, N, Amani, R, Hajiani, E and Cheraghian, B (2016) Women may respond different from men to vitamin d supplementation regarding cardiometabolic biomarkers. *Experimental biology and medicine (Maywood, N.J.).* 241l, 830-838.

Shidfar, F, Agah, S, Ekhlasi, G, Mohammadi, RK, Zarrati, M and Hosseini, AF (2019a) Do symbiotic and vitamin e supplementation have favorite effects in nonalcoholic fatty liver disease? A randomized, double-blind, placebo-controlled trial. *Journal of gastroenterology and hepatology.* 34l, 150-.

Shidfar, F, Mousavi, SN, Agah, S, Hoseini, S and Hajimiresmail, SJ (2019b) Reduction of some atherogenic indices in patients with non-alcoholic fatty liver by vitamin d and calcium co-supplementation: A double blind randomized controlled clinical trial. *Iranian Journal of Pharmaceutical Research.* 18l, 496-505.

Sikora, MJ, Johnson, MD, Lee, AV and Oesterreich, S (2016) Endocrine response phenotypes are altered by charcoal-stripped serum variability. *Endocrinology.* 157l, 3760-3766.

Smagris, E, BasuRay, S, Li, J, Huang, Y, Lai, KM, Gromada, J, Cohen, JC and Hobbs, HH (2015) Pnpla3i148m knockin mice accumulate pnpla3 on lipid droplets and develop hepatic steatosis. *Hepatology.* 61l, 108-118.

Smith, GD and Ebrahim, S (2003) 'Mendelian randomization': Can genetic epidemiology contribute to understanding environmental determinants of disease? *Int J Epidemiol.* 32l, 1-22.

Sodum, N, Kumar, G, Bojja, SL, Kumar, N and Rao, CM (2021) Epigenetics in nafld/nash: Targets and therapy. *Pharmacol Res.* 167l, 105484.

Sookoian, S, Castano, GO, Scian, R, Mallardi, P, Fernandez Gianotti, T, Burgueno, AL, San Martino, J and Pirola, CJ (2015) Genetic variation in transmembrane 6 superfamily member 2 and the risk of nonalcoholic fatty liver disease and histological disease severity. *Hepatology.* 61l, 515-525.

Sookoian, S, Flichman, D, Garaycoechea, ME, Gazzi, C, Martino, JS, Castano, GO and Pirola, CJ (2018) Lack of evidence supporting a role of tmc4-rs641738 missense variant-mboat7- intergenic downstream variant-in the susceptibility to nonalcoholic fatty liver disease. *Sci Rep.* 8l, 5097.

Sookoian, S and Pirola, CJ (2011) Meta-analysis of the influence of i148m variant of patatin-like phospholipase domain containing 3 gene (pnpla3) on the susceptibility and histological severity of nonalcoholic fatty liver disease. *Hepatology.* 53l, 1883-1894.

Sookoian, S, Rosselli, MS, Gemma, C, Burgueno, AL, Fernandez Gianotti, T, Castano, GO and Pirola, CJ (2010) Epigenetic regulation of insulin resistance in nonalcoholic fatty liver disease: Impact of liver methylation of the peroxisome proliferator-activated receptor gamma coactivator 1alpha promoter. *Hepatology.* 52l, 1992-2000.

Soret, PA, Magusto, J, Housset, C and Gautheron, J (2020) In vitro and in vivo models of non-alcoholic fatty liver disease: A critical appraisal. *J Clin Med.* 10l.

Sparsø, T, Andersen, G, Nielsen, T, Burgdorf, KS, Gjesing, AP, Nielsen, AL, Albrechtsen, A, Rasmussen, SS, Jørgensen, T, Borch-Johnsen, K, Sandbaek, A, Lauritzen, T, Madsbad, S, Hansen, T and Pedersen, O (2008) The gckr rs780094 polymorphism is associated with elevated fasting serum triacylglycerol, reduced fasting and ogtt-related insulinaemia, and reduced risk of type 2 diabetes. *Diabetologia.* 51l, 70-75.

Speliotes, EK, Yerges-Armstrong, LM, Wu, J, Hernaez, R, Kim, LJ, Palmer, CD, Gudnason, V, Eiriksdottir, G, Garcia, ME, Launer, LJ, Nalls, MA, Clark, JM, Mitchell, BD, Shuldiner, AR, Butler, JL, Tomas, M, Hoffmann, U, Hwang, SJ, Massaro, JM, O'Donnell, CJ, Sahani, DV, Salomaa, V, Schadt, EE, Schwartz, SM, Siscovick, DS, Voight, BF, Carr, JJ, Feitosa, MF, Harris, TB, Fox, CS, Smith, AV, Kao, WH, Hirschhorn, JN and Borecki, IB (2011) Genome-wide association analysis identifies variants associated with nonalcoholic fatty liver disease that have distinct effects on metabolic traits. *PLoS Genet.* 7l, e1001324.

Staley, JR, Blackshaw, J, Kamat, MA, Ellis, S, Surendran, P, Sun, BB, Paul, DS, Freitag, D, Burgess, S, Danesh, J, Young, R and Butterworth, AS (2016) Phenoscanner: A database of human genotype-phenotype associations. *Bioinformatics.* 32l, 3207-3209.

Steensels, S, Qiao, J and Ersoy, BA (2020) Transcriptional regulation in non-alcoholic fatty liver disease. *Metabolites.* 10l.

Steg, A, Wang, W, Blanquicett, C, Grunda, JM, Eltoum, IA, Wang, K, Buchsbaum, DJ, Vickers, SM, Russo, S, Diasio, RB, Frost, AR, LoBuglio, AF, Grizzle, WE and Johnson, MR (2006) Multiple gene expression analyses in paraffin-embedded tissues by taqman low-density array: Application to hedgehog and wnt pathway analysis in ovarian endometrioid adenocarcinoma. *J Mol Diagn.* 8l, 76-83.

Sticht, C, De La Torre, C, Parveen, A and Gretz, N (2018) Mirwalk: An online resource for prediction of microrna binding sites. *PLOS ONE.* 13l, e0206239.

Stock, JH, Wright, JH and Yogo, M (2002) A survey of weak instruments and weak identification in generalized method of moments. *Journal of Business & Economic Statistics.* 20l, 518-529.

Stockert, JC, Horobin, RW, Colombo, LL and Blazquez-Castro, A (2018) Tetrazolium salts and formazan products in cell biology: Viability assessment, fluorescence imaging, and labeling perspectives. *Acta Histochem.* 120l, 159-167.

Stokowy, T, Eszlinger, M, Świerniak, M, Fujarewicz, K, Jarząb, B, Paschke, R and Krohn, K (2014) Analysis options for high-throughput sequencing in mirna expression profiling. *BMC Res Notes.* 7l, 144.

Su, D, Nie, Y, Zhu, A, Chen, Z, Wu, P, Zhang, L, Luo, M, Sun, Q, Cai, L, Lai, Y, Xiao, Z, Duan, Z, Zheng, S, Wu, G, Hu, R, Tsukamoto, H, Lugea, A, Liu, Z, Pandol, SJ and Han, YP (2016) Vitamin d signaling through induction of paneth cell defensins maintains gut microbiota and improves metabolic disorders and hepatic steatosis in animal models. *Front Physiol.* 7l, 498.

Su, Q, Kumar, V, Sud, N and Mahato, RI (2018) Micrornas in the pathogenesis and treatment of progressive liver injury in nafld and liver fibrosis. *Adv Drug Deliv Rev.* 129l, 54-63.

Su, W, Wang, Y, Jia, X, Wu, W, Li, L, Tian, X, Li, S, Wang, C, Xu, H, Cao, J, Han, Q, Xu, S, Chen, Y, Zhong, Y, Zhang, X, Liu, P, Gustafsson, J and Guan, Y (2014) Comparative proteomic study reveals 17β-hsd13 as a pathogenic protein in nonalcoholic fatty liver disease. *Proc Natl Acad Sci U S A.* 111l, 11437-11442.

Sudlow, C, Gallacher, J, Allen, N, Beral, V, Burton, P, Danesh, J, Downey, P, Elliott, P, Green, J, Landray, M, Liu, B, Matthews, P, Ong, G, Pell, J, Silman, A, Young, A, Sprosen, T, Peakman, T and Collins, R (2015) Uk biobank: An open access resource for identifying the causes of a wide range of complex diseases of middle and old age. *PLoS Med.* 12l, e1001779.

Sumida, Y, Nakajima, A and Itoh, Y (2014) Limitations of liver biopsy and non-invasive diagnostic tests for the diagnosis of nonalcoholic fatty liver disease/nonalcoholic steatohepatitis. *World J Gastroenterol.* 20l, 475-485.

Sun, C, Fan, JG and Qiao, L (2015a) Potential epigenetic mechanism in non-alcoholic fatty liver disease. *Int J Mol Sci.* 16l, 5161-5179.

Sun, C, Huang, F, Liu, X, Xiao, X, Yang, M, Hu, G, Liu, H and Liao, L (2015b) Mir-21 regulates triglyceride and cholesterol metabolism in non-alcoholic fatty liver disease by targeting hmgcr. *Int J Mol Med.* 35l, 847-853.

Sun, C, Zhang, F, Ge, X, Yan, T, Chen, X, Shi, X and Zhai, Q (2007) Sirt1 improves insulin sensitivity under insulin-resistant conditions by repressing ptp1b. *Cell Metab.* 6l, 307-319.

Sun, J (2018) Dietary vitamin d, vitamin d receptor, and microbiome. *Curr Opin Clin Nutr Metab Care.* 21l, 471-474.

Tabrizi, R, Moosazadeh, M, Lankarani, KB, Akbari, M, Heydari, ST, Kolahdooz, F, Samimi, M and Asemi, Z (2017) The effects of vitamin d supplementation on metabolic profiles and liver function in patients with non-alcoholic fatty liver disease: A systematic review and meta-analysis of randomized controlled trials. *Diabetes Metab Syndr.* 11 Suppl 2l, S975-S982.

Taghvaei, T, Akha, O., Mouodi, M., Fakheri, H.T., Kashi, Z., Maleki, I. & Mohammadpour, R. (2018) Effects of vitamin d supplementation on patients with non-alcoholic fatty liver disease (nafld). *Acta Medica Mediterranea.* 34l, 415-422.

Takaki, Y, Saito, Y, Takasugi, A, Toshimitsu, K, Yamada, S, Muramatsu, T, Kimura, M, Sugiyama, K, Suzuki, H, Arai, E, Ojima, H, Kanai, Y and Saito, H (2014) Silencing of microrna-122 is an early event during hepatocarcinogenesis from non-alcoholic steatohepatitis. *Cancer Sci.* 105l, 1254-1260.

Tan, SC and Yiap, BC (2009) DNA, rna, and protein extraction: The past and the present. *J Biomed Biotechnol.* 2009l, 574398.

Tan, Y, Ge, G, Pan, T, Wen, D and Gan, J (2014) A pilot study of serum micrornas panel as potential biomarkers for diagnosis of nonalcoholic fatty liver disease. *PLoS ONE.* 9l, e105192.

Tang, B, Lei, B, Qi, G, Liang, X, Tang, F, Yuan, S, Wang, Z, Yu, S and He, S (2016) Microrna-155-3p promotes hepatocellular carcinoma formation by suppressing fbxw7 expression. *J Exp Clin Cancer Res.* 35l, 93.

Tang, H, Tan, X, Zhu, L, Qin, K, Gao, H and Bai, H (2019) Swimming prevents nonalcoholic fatty liver disease by reducing migration inhibitory factor through akt suppression and autophagy activation. *Am J Transl Res.* 11l, 4315-4325.

Taniguchi, CM, Emanuelli, B and Kahn, CR (2006) Critical nodes in signalling pathways: Insights into insulin action. *Nat Rev Mol Cell Biol.* 7l, 85-96.

Targher, G, Bertolini, L, Scala, L, Cigolini, M, Zenari, L, Falezza, G and Arcaro, G (2007) Associations between serum 25-hydroxyvitamin d3 concentrations and liver histology in patients with non-alcoholic fatty liver disease. *Nutr Metab Cardiovasc Dis.* 17l, 517-524.

Targher, G, Byrne, CD and Tilg, H (2020) Nafld and increased risk of cardiovascular disease: Clinical associations, pathophysiological mechanisms and pharmacological implications. *Gut.* 69l, 1691-1705.

Team, RC (2014) R: A language and environment for statistical computing.

Testa, U, Pelosi, E, Castelli, G and Labbaye, C (2017) Mir-146 and mir-155: Two key modulators of immune response and tumor development. *Noncoding RNA.* 3l.

Tian, XF, Ji, FJ, Zang, HL and Cao, H (2016) Activation of the mir-34a/sirt1/p53 signaling pathway contributes to the progress of liver fibrosis via inducing apoptosis in hepatocytes but not in hscs. *PLoS One.* 11l, e0158657.

Tilg, H, Adolph, TE and Moschen, AR (2021) Multiple parallel hits hypothesis in nonalcoholic fatty liver disease: Revisited after a decade. *Hepatology.* 73l, 833-842.

Tran, M, Lee, S-M, Shin, D-J and Wang, L (2017a) Loss of mir-141/200c ameliorates hepatic steatosis and inflammation by reprogramming multiple signaling pathways in nash. *JCI Insight.* 2l.

Tran, M, Lee, SM, Shin, DJ and Wang, L (2017b) Loss of mir-141/200c ameliorates hepatic steatosis and inflammation by reprogramming multiple signaling pathways in nash. *JCI Insight.* 2l.

Tripkovic, L, Lambert, H, Hart, K, Smith, CP, Bucca, G, Penson, S, Chope, G, Hypponen, E, Berry, J, Vieth, R and Lanham-New, S (2012) Comparison of vitamin d2 and vitamin d3 supplementation in raising serum 25-hydroxyvitamin d status: A systematic review and meta-analysis. *Am J Clin Nutr.* 95l, 1357-1364.

Tryndyak, VP, Han, T, Muskhelishvili, L, Fuscoe, JC, Ross, SA, Beland, FA and Pogribny, IP (2011) Coupling global methylation and gene expression profiles reveal key pathophysiological events in liver injury induced by a methyl-deficient diet. *Mol Nutr Food Res.* 55l, 411-418.

Tsai, WC, Hsu, SD, Hsu, CS, Lai, TC, Chen, SJ, Shen, R, Huang, Y, Chen, HC, Lee, CH, Tsai, TF, Hsu, MT, Wu, JC, Huang, HD, Shiao, MS, Hsiao, M and Tsou, AP (2012) Microrna-122 plays a critical role in liver homeostasis and hepatocarcinogenesis. *J Clin Invest.* 122l, 2884-2897.

Tsuchida, T and Friedman, SL (2017) Mechanisms of hepatic stellate cell activation. *Nat Rev Gastroenterol Hepatol.* 14l, 397-411.

Tu, C, Fiandalo, MV, Pop, E, Stocking, JJ, Azabdaftari, G, Li, J, Wei, H, Ma, D, Qu, J, Mohler, JL, Tang, L and Wu, Y (2018) Proteomic analysis of

charcoal-stripped fetal bovine serum reveals changes in the insulin-like growth factor signaling pathway. *J Proteome Res.* 17l, 2963-2977.
Udomsinprasert, W and Jittikoon, J (2019) Vitamin d and liver fibrosis: Molecular mechanisms and clinical studies. *Biomed Pharmacother.* 109l, 1351-1360.
Ullah, R, Rauf, N, Nabi, G, Ullah, H, Shen, Y, Zhou, YD and Fu, J (2019) Role of nutrition in the pathogenesis and prevention of non-alcoholic fatty liver disease: Recent updates. *Int J Biol Sci.* 15l, 265-276.
Valenti, L, Alisi, A and Nobili, V (2012) Unraveling the genetics of fatty liver in obese children: Additive effect of p446l gckr and i148m pnpla3 polymorphisms. *Hepatology.* 55l, 661-663.
van Meerloo, J, Kaspers, GJ and Cloos, J (2011) Cell sensitivity assays: The mtt assay. *Methods Mol Biol.* 731l, 237-245.
Van Peer, G, Lefever, S, Anckaert, J, Beckers, A, Rihani, A, Van Goethem, A, Volders, PJ, Zeka, F, Ongenaert, M, Mestdagh, P and Vandesompele, J (2014) Mirbase tracker: Keeping track of microrna annotation changes. *Database (Oxford).* 2014l.
Vega-Badillo, J, Gutiérrez-Vidal, R, Hernández-Pérez, HA, Villamil-Ramírez, H, León-Mimila, P, Sánchez-Muñoz, F, Morán-Ramos, S, Larrieta-Carrasco, E, Fernández-Silva, I, Méndez-Sánchez, N, Tovar, AR, Campos-Pérez, F, Villarreal-Molina, T, Hernández-Pando, R, Aguilar-Salinas, CA and Canizales-Quinteros, S (2016) Hepatic mir-33a/mir-144 and their target geneabca1are associated with steatohepatitis in morbidly obese subjects. *Liver International.* 36l, 1383-1391.
Vieth, R (2020) Vitamin d supplementation: Cholecalciferol, calcifediol, and calcitriol. *Eur J Clin Nutr.* 74l, 1493-1497.
Vilar-Gomez, E and Chalasani, N (2018) Non-invasive assessment of non-alcoholic fatty liver disease: Clinical prediction rules and blood-based biomarkers. *J Hepatol.* 68l, 305-315.
Wagner, CL, Greer, FR, American Academy of Pediatrics Section on, B and American Academy of Pediatrics Committee on, N (2008) Prevention of rickets and vitamin d deficiency in infants, children, and adolescents. *Pediatrics.* 122l, 1142-1152.
Wang, B, Cruz Ithier, M, Parobchak, N, Yadava, SM, Schulkin, J and Rosen, T (2018a) Vitamin d stimulates multiple micrornas to inhibit crh and other pro-labor genes in human placenta. *Endocr Connect.* 7l, 1380-1388.
Wang, B, Howel, P, Bruheim, S, Ju, J, Owen, LB, Fodstad, O and Xi, Y (2011) Systematic evaluation of three microrna profiling platforms: Microarray, beads array, and quantitative real-time pcr array. *PLoS One.* 6l, e17167.
Wang, C, Li, Y, Li, H, Zhang, Y, Ying, Z, Wang, X, Zhang, T, Zhang, W, Fan, Z, Li, X, Ma, J and Pan, X (2020a) Disruption of fgf signaling ameliorates inflammatory response in hepatic stellate cells. *Front Cell Dev Biol.* 8l, 601.
Wang, DR, Wang, B, Yang, M, Liu, ZL, Sun, J, Wang, Y, Sun, H and Xie, LJ (2020b) Suppression of mir-30a-3p attenuates hepatic steatosis in non-alcoholic fatty liver disease. *Biochem Genet.*
Wang, G, Tam, LS, Kwan, BC, Li, EK, Chow, KM, Luk, CC, Li, PK and Szeto, CC (2012a) Expression of mir-146a and mir-155 in the urinary

sediment of systemic lupus erythematosus. *Clin Rheumatol.* 31l, 435-440.

Wang, G, Tam, LS, Li, EK, Kwan, BC, Chow, KM, Luk, CC, Li, PK and Szeto, CC (2010a) Serum and urinary cell-free mir-146a and mir-155 in patients with systemic lupus erythematosus. *J Rheumatol.* 37l, 2516-2522.

Wang, J, Thingholm, LB, Skieceviciene, J, Rausch, P, Kummen, M, Hov, JR, Degenhardt, F, Heinsen, FA, Ruhlemann, MC, Szymczak, S, Holm, K, Esko, T, Sun, J, Pricop-Jeckstadt, M, Al-Dury, S, Bohov, P, Bethune, J, Sommer, F, Ellinghaus, D, Berge, RK, Hubenthal, M, Koch, M, Schwarz, K, Rimbach, G, Hubbe, P, Pan, WH, Sheibani-Tezerji, R, Hasler, R, Rosenstiel, P, D'Amato, M, Cloppenborg-Schmidt, K, Kunzel, S, Laudes, M, Marschall, HU, Lieb, W, Nothlings, U, Karlsen, TH, Baines, JF and Franke, A (2016a) Genome-wide association analysis identifies variation in vitamin d receptor and other host factors influencing the gut microbiota. *Nat Genet.* 48l, 1396-1406.

Wang, J, Wu, Z, Li, D, Li, N, Dindot, SV, Satterfield, MC, Bazer, FW and Wu, G (2012b) Nutrition, epigenetics, and metabolic syndrome. *Antioxid Redox Signal.* 17l, 282-301.

Wang, JK, Wang, Z and Li, G (2019) Microrna-125 in immunity and cancer. *Cancer Lett.* 454l, 134-145.

Wang, JM, Qiu, Y, Yang, Z, Kim, H, Qian, Q, Sun, Q, Zhang, C, Yin, L, Fang, D, Back, SH, Kaufman, RJ, Yang, L and Zhang, K (2018b) Ire1α prevents hepatic steatosis by processing and promoting the degradation of select microrna s. *Sci Signal.* 11l.

Wang, L, Zhang, N, Wang, Z, Ai, D-M, Cao, Z-Y and Pan, H-P (2016b) Decreased mir-155 level in the peripheral blood of non-alcoholic fatty liver disease patients may serve as a biomarker and may influence lxr activity. *Cellular Physiology and Biochemistry.* 39l, 2239-2248.

Wang, L, Zhang, N, Wang, Z, Ai, DM, Cao, ZY and Pan, HP (2016c) Decreased mir-155 level in the peripheral blood of non-alcoholic fatty liver disease patients may serve as a biomarker and may influence lxr activity. *Cell Physiol Biochem.* 39l, 2239-2248.

Wang, M, Zhang, R, Wang, M, Zhang, L, Ding, Y, Tang, Z, Wang, H, Zhang, W, Chen, Y and Wang, J (2021) Genetic polymorphism of vitamin d family genes cyp2r1, cyp24a1, and cyp27b1 are associated with a high risk of non-alcoholic fatty liver disease: A case-control study. *Front Genet.* 12l, 717533.

Wang, N, Chen, C, Zhao, L, Chen, Y, Han, B, Xia, F, Cheng, J, Li, Q and Lu, Y (2018c) Vitamin d and nonalcoholic fatty liver disease: Bi-directional mendelian randomization analysis. *EBioMedicine.* 28l, 187-193.

Wang, TJ, Zhang, F, Richards, JB, Kestenbaum, B, van Meurs, JB, Berry, D, Kiel, DP, Streeten, EA, Ohlsson, C, Koller, DL, Peltonen, L, Cooper, JD, O'Reilly, PF, Houston, DK, Glazer, NL, Vandenput, L, Peacock, M, Shi, J, Rivadeneira, F, McCarthy, MI, Anneli, P, de Boer, IH, Mangino, M, Kato, B, Smyth, DJ, Booth, SL, Jacques, PF, Burke, GL, Goodarzi, M, Cheung, CL, Wolf, M, Rice, K, Goltzman, D, Hidiroglou, N, Ladouceur, M, Wareham, NJ, Hocking, LJ, Hart, D, Arden, NK, Cooper, C, Malik, S, Fraser, WD, Hartikainen, AL, Zhai, G, Macdonald, HM, Forouhi, NG, Loos, RJ, Reid, DM, Hakim, A, Dennison, E, Liu, Y, Power, C, Stevens, HE, Jaana, L, Vasan, RS, Soranzo, N, Bojunga, J,

Psaty, BM, Lorentzon, M, Foroud, T, Harris, TB, Hofman, A, Jansson, JO, Cauley, JA, Uitterlinden, AG, Gibson, Q, Jarvelin, MR, Karasik, D, Siscovick, DS, Econs, MJ, Kritchevsky, SB, Florez, JC, Todd, JA, Dupuis, J, Hypponen, E and Spector, TD (2010b) Common genetic determinants of vitamin d insufficiency: A genome-wide association study. *Lancet.* 376l, 180-188.

Wang, X, Gocek, E, Liu, CG and Studzinski, GP (2009) Micrornas181 regulate the expression of p27kip1 in human myeloid leukemia cells induced to differentiate by 1,25-dihydroxyvitamin d3. *Cell Cycle.* 8l, 736-741.

Wang, X, He, Y, Mackowiak, B and Gao, B (2020c) Micrornas as regulators, biomarkers and therapeutic targets in liver diseases. *Gut.*

Wang, X, Li, W, Zhang, Y, Yang, Y and Qin, G (2015) Association between vitamin d and non-alcoholic fatty liver disease/non-alcoholic steatohepatitis: Results from a meta-analysis. *Int J Clin Exp Med.* 8l, 17221-17234.

Wang, X, Ma, Y, Yang, LY and Zhao, D (2020d) Microrna-20a-5p ameliorates non-alcoholic fatty liver disease via inhibiting the expression of cd36. *Front Cell Dev Biol.* 8l, 596329.

Wang, Y, Zeng, Z, Guan, L and Ao, R (2020e) Grhl2 induces liver fibrosis and intestinal mucosal barrier dysfunction in non-alcoholic fatty liver disease via microrna-200 and the mapk pathway. *J Cell Mol Med.* 24l, 6107-6119.

Wang, Y, Zhu, J and DeLuca, HF (2012c) Where is the vitamin d receptor? *Arch Biochem Biophys.* 523l, 123-133.

Wang, Y, Zhu, K, Yu, W, Wang, H, Liu, L, Wu, Q, Li, S and Guo, J (2017) Mir-181b regulates steatosis in nonalcoholic fatty liver disease via targeting sirt1. *Biochem Biophys Res Commun.* 493l, 227-232.

Weber, JA, Baxter, DH, Zhang, S, Huang, DY, Huang, KH, Lee, MJ, Galas, DJ and Wang, K (2010) The microrna spectrum in 12 body fluids. *Clin Chem.* 56l, 1733-1741.

Willner, IR, Waters, B, Patil, SR, Reuben, A, Morelli, J and Riely, CA (2001) Ninety patients with nonalcoholic steatohepatitis: Insulin resistance, familial tendency, and severity of disease. *Am J Gastroenterol.* 96l, 2957-2961.

Wilson, LR, Tripkovic, L, Hart, KH and Lanham-New, SA (2017) Vitamin d deficiency as a public health issue: Using vitamin d2 or vitamin d3 in future fortification strategies. *Proc Nutr Soc.* 76l, 392-399.

Wittenbecher, C, Ouni, M, Kuxhaus, O, Jahnert, M, Gottmann, P, Teichmann, A, Meidtner, K, Kriebel, J, Grallert, H, Pischon, T, Boeing, H, Schulze, MB and Schurmann, A (2019) Insulin-like growth factor binding protein 2 (igfbp-2) and the risk of developing type 2 diabetes. *Diabetes.* 68l, 188-197.

Wu, DB, Wang, ML, Chen, EQ and Tang, H (2018) New insights into the role of vitamin d in hepatocellular carcinoma. *Expert Rev Gastroenterol Hepatol.* 12l, 287-294.

Wu, H, Ng, R, Chen, X, Steer, CJ and Song, G (2016) Microrna-21 is a potential link between non-alcoholic fatty liver disease and hepatocellular carcinoma via modulation of the hbp1-p53-srebp1c pathway. *Gut.* 65l, 1850-1860.

Xin, S, Zhan, Q, Chen, X, Xu, J and Yu, Y (2020) Efficacy of serum mirna test as a non-invasive method to diagnose nonalcoholic steatohepatitis: A systematic review and meta-analysis. *BMC Gastroenterol.* 20l, 186.

Xu, J, Wang, Y, Zhang, Y, Dang, S and He, S (2018) Astemizole promotes the anti-tumor effect of vitamin d through inhibiting mir-125a-5p-meidated regulation of vdr in hcc. *Biomed Pharmacother.* 107l, 1682-1691.

Xu, L, Hui, A, Albanis, E, Arthur, M, O'byrne, S, Blaner, W, Mukherjee, P, Friedman, S and Eng, F (2005) Human hepatic stellate cell lines, lx-1 and lx-2: New tools for analysis of hepatic fibrosis. *Gut.* 54l, 142-151.

Xu, Y, Zalzala, M, Xu, J, Li, Y, Yin, L and Zhang, Y (2015) A metabolic stress-inducible mir-34a-hnf4α pathway regulates lipid and lipoprotein metabolism. *Nat Commun.* 6l, 7466.

Yaghooti, H, Ghanavati, F, Seyedian, SS, Cheraghian, B and Mohammadtaghvaei, N (2021) The efficacy of calcitriol treatment in non-alcoholic fatty liver patients with different genotypes of vitamin d receptor foki polymorphism. *BMC Pharmacol Toxicol.* 22l, 18.

Yamada, H, Suzuki, K, Ichino, N, Ando, Y, Sawada, A, Osakabe, K, Sugimoto, K, Ohashi, K, Teradaira, R, Inoue, T, Hamajima, N and Hashimoto, S (2013) Associations between circulating micrornas (mir-21, mir-34a, mir-122 and mir-451) and non-alcoholic fatty liver. *Clin Chim Acta.* 424l, 99-103.

Yamada, T, Imaoka, S, Kawada, N, Seki, S, Kuroki, T, Kobayashi, K, Monna, T and Funae, Y (1997) Expression of cytochrome p450 isoforms in rat hepatic stellate cells. *Life Sci.* 61l, 171-179.

Yao, R, Ma, YL, Liang, W, Li, HH, Ma, ZJ, Yu, X and Liao, YH (2012) Microrna-155 modulates treg and th17 cells differentiation and th17 cell function by targeting socs1. *PLoS One.* 7l, e46082.

Ye, D, Zhang, T, Lou, G, Xu, W, Dong, F, Chen, G and Liu, Y (2018a) Plasma mir-17, mir-20a, mir-20b and mir-122 as potential biomarkers for diagnosis of nafld in type 2 diabetes mellitus patients. *Life Sci.* 208l, 201-207.

Ye, D, Zhang, T, Lou, G, Xu, W, Dong, F, Chen, G and Liu, Y (2018b) Plasma mir-17, mir-20a, mir-20b and mir-122 as potential biomarkers for diagnosis of nafld in type 2 diabetes mellitus patients. *Life Sciences.* 208l, 201-207.

Yin, H, Hu, M, Liang, X, Ajmo, JM, Li, X, Bataller, R, Odena, G, Stevens, SM, Jr. and You, M (2014) Deletion of sirt1 from hepatocytes in mice disrupts lipin-1 signaling and aggravates alcoholic fatty liver. *Gastroenterology.* 146l, 801-811.

Younossi, Z, Anstee, QM, Marietti, M, Hardy, T, Henry, L, Eslam, M, George, J and Bugianesi, E (2018) Global burden of nafld and nash: Trends, predictions, risk factors and prevention. *Nat Rev Gastroenterol Hepatol.* 15l, 11-20.

Younossi, ZM, Koenig, AB, Abdelatif, D, Fazel, Y, Henry, L and Wymer, M (2016) Global epidemiology of nonalcoholic fatty liver disease-meta-analytic assessment of prevalence, incidence, and outcomes. *Hepatology.* 64l, 73-84.

Yu, ZJ, Zeng, L, Luo, XQ, Geng, XR, Xu, R, Chen, K, Yang, G, Luo, X, Liu, ZQ, Liu, ZG, Liu, DB, Yang, PC and Li, HB (2017) Vitamin d3 inhibits

micro rna-17-92 to promote specific immunotherapy in allergic rhinitis. *Sci Rep.* 7l, 546.

Yuan, BY, Chen, YH, Wu, ZF, Zhuang, Y, Chen, GW, Zhang, L, Zhang, HG, Cheng, JC, Lin, Q and Zeng, ZC (2019) Microrna-146a-5p attenuates fibrosis-related molecules in irradiated and tgf-beta1-treated human hepatic stellate cells by regulating ptpra-src signaling. *Radiat Res.* 192l, 621-629.

Yuan, S and Larsson, SC (2022) Inverse association between serum 25-hydroxyvitamin d and nonalcoholic fatty liver disease. *Clin Gastroenterol Hepatol.*

Zarrinpar, A, Gupta, S, Maurya, MR, Subramaniam, S and Loomba, R (2016) Serum micrornas explain discordance of non-alcoholic fatty liver disease in monozygotic and dizygotic twins: A prospective study. *Gut.* 65l, 1546-1554.

Zeljic, K, Supic, G and Magic, Z (2017) New insights into vitamin d anticancer properties: Focus on mirna modulation. *Mol Genet Genomics.* 292l, 511-524.

Zenata, O and Vrzal, R (2017) Fine tuning of vitamin d receptor (vdr) activity by post-transcriptional and post-translational modifications. *Oncotarget.* 8l, 35390-35402.

Zeng, X, Zhu, M, Liu, X, Chen, X, Yuan, Y, Li, L, Liu, J, Lu, Y, Cheng, J and Chen, Y (2020) Oleic acid ameliorates palmitic acid induced hepatocellular lipotoxicity by inhibition of er stress and pyroptosis. *Nutr Metab (Lond).* 17l, 11.

Zeybel, M, Hardy, T, Robinson, SM, Fox, C, Anstee, QM, Ness, T, Masson, S, Mathers, JC, French, J, White, S and Mann, J (2015) Differential DNA methylation of genes involved in fibrosis progression in non-alcoholic fatty liver disease and alcoholic liver disease. *Clin Epigenetics.* 7l, 25.

Zhang, HB, Su, W, Xu, H, Zhang, XY and Guan, YF (2021a) Hsd17b13: A potential therapeutic target for nafld. *Front Mol Biosci.* 8l, 824776.

Zhang, L, Wang, W, Li, X, He, S, Yao, J, Wang, X, Zhang, D and Sun, X (2016) Microrna-155 promotes tumor growth of human hepatocellular carcinoma by targeting arid2. *Int J Oncol.* 48l, 2425-2434.

Zhang, M, Sun, W, Zhou, M and Tang, Y (2017) Microrna-27a regulates hepatic lipid metabolism and alleviates nafld via repressing fas and scd1. *Sci Rep.* 7l, 14493.

Zhang, Q, Yu, K, Cao, Y, Luo, Y, Liu, Y and Zhao, C (2021b) Mir-125b promotes the nf-κb-mediated inflammatory response in nafld via directly targeting tnfaip3. *Life Sci.* 270l, 119071.

Zhang, R, Wang, M, Wang, M, Zhang, L, Ding, Y, Tang, Z, Fu, Z, Fan, H, Zhang, W and Wang, J (2021c) Vitamin d level and vitamin d receptor genetic variation were involved in the risk of non-alcoholic fatty liver disease: A case-control study. *Front Endocrinol (Lausanne).* 12l, 648844.

Zhang, T, Duan, J, Zhang, L, Li, Z, Steer, CJ, Yan, G and Song, G (2019a) Lxrα promotes hepatosteatosis in part through activation of microrna-378 transcription and inhibition of ppargc1β expression. *Hepatology.* 69l, 1488-1503.

Zhang, T, Hu, J, Wang, X, Zhao, X, Li, Z, Niu, J, Steer, CJ, Zheng, G and Song, G (2019b) Microrna-378 promotes hepatic inflammation and fibrosis via modulation of the nf-κb-tnfα pathway. *J Hepatol.* 70l, 87-96.
Zhang, T, Yang, Z, Kusumanchi, P, Han, S and Liangpunsakul, S (2020) Critical role of microrna-21 in the pathogenesis of liver diseases. *Front Med (Lausanne).* 7l, 7.
Zhang, Y, Szustakowski, J and Schinke, M (2009) Bioinformatics analysis of microarray data. *Methods Mol Biol.* 573l, 259-284.
Zhang, Z, Moon, R, Thorne, J and Moore, J (2021d) Nafld and vitamin d: Evidence for intersection of microrna regulated pathways. *Nutrition Research Reviews.* 1-52.
Zhang, Z, Thorne, JL and Moore, JB (2019c) Vitamin d and nonalcoholic fatty liver disease. *Curr Opin Clin Nutr Metab Care.* 22l, 449-458.
Zhang, ZC, Liu, Y, Xiao, LL, Li, SF, Jiang, JH, Zhao, Y, Qian, SW, Tang, QQ and Li, X (2015) Upregulation of mir-125b by estrogen protects against non-alcoholic fatty liver in female mice. *J Hepatol.* 63l, 1466-1475.
Zheng, J, Baird, D, Borges, MC, Bowden, J, Hemani, G, Haycock, P, Evans, DM and Smith, GD (2017) Recent developments in mendelian randomization studies. *Curr Epidemiol Rep.* 4l, 330-345.
Zheng, J, Wang, W, Yu, F, Dong, P, Chen, B and Zhou, MT (2018) Microrna-30a suppresses the activation of hepatic stellate cells by inhibiting epithelial-to-mesenchymal transition. *Cell Physiol Biochem.* 46l, 82-92.
Zhu, S, Wang, Y, Luo, F, Liu, J, Xiu, L, Qin, J, Wang, T, Yu, N, Wu, H and Zou, T (2019a) The level of vitamin d in children and adolescents with nonalcoholic fatty liver disease: A meta-analysis. *Biomed Res Int.* 2019l, 7643542.
Zhu, X, Zhu, Y, Li, C, Yu, J, Ren, D, Qiu, S, Nie, Y, Yu, X, Xu, X and Zhu, W (2019b) 1,25-dihydroxyvitamin d regulates macrophage polarization and ameliorates experimental inflammatory bowel disease by suppressing mir-125b. *Int Immunopharmacol.* 67l, 106-118.
Zmuda, JM, Cauley, JA and Ferrell, RE (2000) Molecular epidemiology of vitamin d receptor gene variants. *Epidemiol Rev.* 22l, 203-217.
Zou, Y, Li, S, Li, Z, Song, D, Zhang, S and Yao, Q (2019) Mir-146a attenuates liver fibrosis by inhibiting transforming growth factor-β1 mediated epithelial-mesenchymal transition in hepatocytes. *Cell Signal.* 58l, 1-8.
Zumaraga, MP, Medina, PJ, Recto, JM, Abrahan, L, Azurin, E, Tanchoco, CC, Jimeno, CA and Palmes-Saloma, C (2017) Targeted next generation sequencing of the entire vitamin d receptor gene reveals polymorphisms correlated with vitamin d deficiency among older filipino women with and without fragility fracture. *J Nutr Biochem.* 41l, 98-108.